Utvrđivanje ravnotežnih uvjeta taloženja karbonata u Postojnskoj jami s mogućom primjenom u paleoklimatologiji

Mandić, Magda

Doctoral thesis / Disertacija

2013

Degree Grantor / Ustanova koja je dodijelila akademski / stručni stupanj: **University of Zagreb, Faculty of Science / Sveučilište u Zagrebu, Prirodoslovno-matematički fakultet**

Permanent link / Trajna poveznica: https://urn.nsk.hr/urn:nbn:hr:217:136652

Rights / Prava: In copyright / Zaštićeno autorskim pravom.

Download date / Datum preuzimanja: **2024-04-20**

Repository / Repozitorij:

Repository of the Faculty of Science - University of Zagreb

University of Zagreb

FACULTY OF SCIENCE

MAGDA MANDIĆ

DETERMINATION OF EQUILIBRIUM CONDITIONS OF CARBONATE PRECIPITATION IN POSTOJNA CAVE WITH POSSIBLE APPLICATION TO PALEOCLIMATOLOGY

DOCTORAL THESIS

Zagreb, 2013

Sveučilište u Zagrebu

PRIRODOSLOVNO-MATEMATIČKI FAKULTET

MAGDA MANDIĆ

UTVRĐIVANJE RAVNOTEŽNIH UVJETA TALOŽENJA KARBONATA U POSTOJNSKOJ JAMI S MOGUĆOM PRIMJENOM U PALEOKLIMATOLOGIJI

DOKTORSKI RAD

Zagreb, 2013.

University of Zagreb

FACULTY OF SCIENCE

MAGDA MANDIĆ

DETERMINATION OF EQUILIBRIUM CONDITIONS OF CARBONATE PRECIPITATION IN POSTOJNA CAVE WITH POSSIBLE APPLICATION TO PALEOCLIMATOLOGY

DOCTORAL THESIS

Supervisors:
dr. sc. Ines Krajcar Bronić
dr. sc. Albrecht Leis

Zagreb, 2013

Sveučilište u Zagrebu

PRIRODOSLOVNO-MATEMATIČKI FAKULTET

MAGDA MANDIĆ

UTVRĐIVANJE RAVNOTEŽNIH UVJETA TALOŽENJA KARBONATA U POSTOJNSKOJ JAMI S MOGUĆOM PRIMJENOM U PALEOKLIMATOLOGIJI

DOKTORSKI RAD

Mentori:
dr. sc. Ines Krajcar Bronić
dr. sc. Albrecht Leis

Zagreb, 2013.

Samples for this thesis have been collected in Postojna Cave under supervision of dr. sc. Andrej Mihevc, research advisor at the Karst Research Institute, Postojna, Slovenia. Measurements of stable isotope composition have been supervised by dipl. chem. dr. sc. Albrecht Leis in Laboratory Centre for Isotope Hydrology and Environmental Analytics, Joanneum Research, RESOURCES - Institute for Water, Energy and Sustainability, Graz, Austria, and interpretation of data has been supervised by dr. sc. Ines Krajcar Bronić, senior scientist at the Ruđer Bošković Institute, Zagreb.

BASIC DOCUMENTATION CARD

University of Zagreb
Faculty of Science
Department of Physics

Doctoral thesis

DETERMINATION OF EQUILIBRIUM CONDITIONS OF CARBONATE PRECIPITATION IN POSTOJNA CAVE WITH POSSIBLE APPLICATION TO PALEOCLIMATOLOGY

MAGDA MANDIĆ

Department of Physics
University of Rijeka

The contents of stable carbon and oxygen isotopes, ^{13}C and ^{18}O, in secondary precipitated carbonates (speleothems) of caves in karst areas can provide important information about paleoclimatic conditions of the area if the speleothems are formed at equilibrium conditions, i.e., if the isotopic composition of speleothems depends only on the deposition temperature. The purpose of this study was to determine areas within Postojna Cave with isotopic equilibrium conditions of carbonate precipitation where future paleoclimate research may be conducted. Environmental factors (temperature, concentration of atmospheric CO_2), chemical composition of drip water, isotopic composition of water, CO_2 and deposited carbonates were monitored during one year at nine locations. Difference between $\delta^{13}C$ in modern carbonates and in DIC was compared with the equilibrium fractionation factor ε. Fractionation factor α was determined from measured $\delta^{18}O$ values of drip water and carbonates and compared to its equilibrium value α_{eq}. Although environmetal and chemical parameters pointed to the fulfillment of preconditions for isotopic equilibrium precipitation of carbonates, specially at inner locations, isotopic composition of carbonates, both $\delta^{13}C$ and $\delta^{18}O$, did not show equilibrium precipitation at most of the studied locations. Only locations 06 – Stebrišče and 09 – Zgornji Tartar have the potential for future paleoclimatic studies. It was also shown that recent carbonate precipitated on watch glasses did not reflect the isotopic composition of speleothems at the same location. Process of prior calcite precipitation was identified at location Podrti kapnik.

(204 pages, 119 figures, 17 tables, 233 references, original in English language)

Thesis deposited in the Central Physics Library at Faculty of Science, University of Zagreb, The National and University Library in Zagreb and at the University of Zagreb

Keywords: stable isotopes, oxygen, carbon, carbonate, isotopic equilibrium, DIC, speleothems, Postojna Cave, cave climate, paleoclimatology;

First supervisor: dr. sc. Ines Krajcar Bronić, senior scientist, Ruđer Bošković Institute, Zagreb

Second supervisor: dipl. chem. dr. sc. Albrecht Leis, Laboratory Centre for Isotope Hydrology and Environmental Analytics, Joanneum Research, RESOURCES - Institute for Water, Energy and Sustainability, Graz, Austria

Reviewers: dr. sc. Bogomil Obelić, Academician prof. dr. sc. Nikola Kallay, dr. sc. Albrecht Leis, prof. dr. sc. Tihomir Marjanac, dr. sc. Ines Krajcar Bronić

Thesis accepted on 8th January 2013

TEMELJNA DOKUMENTACIJSKA KARTICA

Sveučilište u Zagrebu
Prirodoslovno-matematički fakultet
Fizički odsjek

Doktorski rad

UTVRĐIVANJE RAVNOTEŽNIH UVJETA TALOŽENJA KARBONATA U POSTOJNSKOJ JAMI S MOGUĆOM PRIMJENOM U PALEOKLIMATOLOGIJI

MAGDA MANDIĆ

Odjel za fiziku
Sveučilište u Rijeci

Sadržaj stabilnih izotopa ugljika i kisika, ^{13}C i ^{18}O, u sekundarno taloženim karbonatima (sigama) u špiljama krškog područja može dati važne informacije o paleoklimatskim uvjetima na tom području ako su sige nastale u uvjetima izotopne ravnoteže, tj, ako je izotopni sastav siga ovisan samo o temperaturi taloženja. Cilj ovog istraživanja bio je odrediti područja unutar Jame s ravnotežnim izotopnim uvjetima stvaranja siga na kojima bi se mogla provoditi buduća paleoklimatska istraživanja primjenom izotopnih tehnika. Pratili su se okolišni uvjeti (temperatura, koncentracija CO_2), kemijski sastav prokapne vode, te izotopni sastav vode, CO_2 i taloženih karbonata na devet lokacija tijekom jedne godine. Razlika između $\delta^{13}C$ u suvremenom karbonatu i u DIC-u usporedila se s ravnotežnim faktorom ε. Fraktionacijski faktor α određen je iz izmjerenih vrijednosti $\delta^{18}O$ prokapne vode i karbonata te je uspoređen s ravnotežnom vrijednošću α_{eq}. Iako okolišni i kemijski parametri upućuju na postojanje preduvjeta za taloženje karbonata u izotopnoj ravnoteži, pogotovo na unutarnjim lokacijama, izotpni sastav karbonata, $\delta^{13}C$ i $\delta^{18}O$, ukazuje na odstupanja od izotopne ravnoteže na većini lokacija. Jedino lokacije 06 – Stebrišče i 09 – Zgornji Tartar i pokazuju potencijal za buduća paleoklimatska istraživanja. Istraživanja su također pokazala da recentni karbonat istaložen na satnim staklima ne odražava izotopni sastav karbonata. Utvrđen je proces prethodnog taloženja karbonata u šupljinama nadsloja na lokaciji 05 – Podrti kapnik.

(204 stranica, 119 slika, 17 tablica, 233 literaturna navoda, jezik izvornika: engleski)

Rad je pohranjen u Središnjoj knjižnici za fiziku Prirodoslovno-matematičkog fakulteta Sveučilišta u Zagrebu, Nacionalnoj i sveučilišnoj knjižnici u Zagrebu te pri Sveučilištu u Zagrebu

Ključne riječi: stabilni izotopi, kisik, ugljik, karbonat, DIC, sige, Postojnska jama, okolišni uvjeti, paleoklimatologija, izotopna ravnoteža

Prvi mentor: dr. sc. Ines Krajcar Bronić, znanstvena savjetnica, Institut "Ruđer Bošković"
Drugi mentor: dipl. kem. dr. sc. Albrecht Leis, Laboratory Centre for Isotope Hydrology and Environmental Analytics, Joanneum Research, RESOURCES - Institute for Water, Energy and Sustainability, Graz, Austria

Ocjenitelji: dr. sc. Bogomil Obelić, Akademik prof. dr. sc. Nikola Kallay,
dr. sc. Albrecht Leis, prof. dr. sc. Tihomir Marjanac, dr. sc. Ines Krajcar Bronić

Rad prihvaćen 08. 01. 2013. na zajedničkoj sjednici Vijeća fizičkog i geofizičkog odsjeka

Acknowledgments

First and foremost I would like to express my deep and sincere gratitude to my supervisor, dr. sc. Ines Krajcar Bronić, senior scientist at the Ruđer Bošković Institute, Zagreb. Her wide knowledge, unselfish guidance and her logical way of thinking have been of great and invaluable experience for me, making each step of work enjoyable and precious. She provided insightful discussions and suggestions about the research. Her understanding, encouraging and personal guidance have provided a good basis for the present thesis.

I am deeply grateful to dr. sc. Andrej Mihevc, research advisor at the Karst Research Institute, Postojna, Slovenia, for his guidance through the "darkness" of Postojna Cave corridors and for enlightening the beauty in the world of karst.

I wish to express warm and sincere thanks to my supervisor Dipl. Chem. Dr. sc. Albrecht Leis, Head of Laboratory Centre for Isotope Hydrology and Environmental Analytics, Joanneum Research Institute, Graz, Austria, for unselfish help and supervision in laboratory work.

I also express my gratitude to my supervisor, full professor dr. sc. Dubravka Kotnik Karuza, Head of the Department of Physics, University of Rijeka, for believing in me in every step of the way. Her strong encouragement and professional guidance have been of great importance during my work.

I thank to all colleagues at the Physics Department for their support and encouragement.

My thanks go out to the people at the Karst Research Institute in Postojna: dr. sc. Mitja Prelovšek for help and friendship during sampling and for providing data from data logger monitoring; dr. sc. Franci Gabrovšek for his unpublished data from data logger monitoring; Jurij Hajna and Franjo Drole for company during field trips; the secretary of Karst Research Institute, Sonja Stamenković, for help in handling courier post deliveries of samples.

I am also grateful for the hospitality and support of people in Laboratory for Measurement of Low-Level Radioactivities, Ruđer Bošković Institute: dr. sc. Bogomil Obelić, dr. sc. Nada Horvatinčić, dr. sc. Jadranka Barešić, dr. sc. Andreja Sironić and Anita Rajtarić. I deeply appreciate the welcome and encouragement I have received.

Thanks to dr. sc. Polona Vreča and dr. sc. Sonja Lojen from Jožef Stefan Institute, Ljubljana, for giving me their unpublished data of stable isotope composition of precipitation at locations Zalog pri Postojni and Ljubljana. Special thanks to Polona for support and friendship.

Many thanks to dr. sc. Wolfgang Dreybrodt for discussions on modeling approaches, to dr. sc. Christopher Spötl for his valuable advices on sampling and data interpretation, and to Tyler B. Coplen, US Geological Survey, for his advices for usage of LIMS (Laboratory Information Management System) for light stable isotopes. Professor emeritus Derek Ford, McMaster University, is thanked for sharing his knowledge and experience about work in Karst and Postojna Cave.

I wish to thank my former teacher, and now colleague and friend, mr. sc. Branka Milotić, for her understanding and support during difficult times. Her words gave me hope and strength for the next day. She supported me with love and Lord's wisdom from the first day.

I owe my loving thanks to my husband Luka, my sons Sven and Vito. During my research we have all been in a new life situation. Without their encouragement and understanding it would be impossible for me to finish this work.

My special gratitude goes to my mother and father for taking care of Sven and Vito during one year of most intensive writing work and for all their support and encouragement.

Thanks!

Zahvale

Prije svega želim izraziti iskrenu i duboku zahvalnost mojoj mentorici dr. sc. Ines Krajcar Bronić, znanstvenoj savjetnici na Institutu Ruđer Bošković, Zagreb, u Zavodu za eksperimentalnu fiziku, Laboratoriju za mjerenje niskih radioaktivnosti. Njeno bogato znanje, logika razmišljanja i usmjeravanje, te savjeti i pristup radu predstavljali su za mene neprocjenjivo iskustvo. Iscrpne diskusije i konstruktivne sugestije doprinijele su kvaliteti rada.
Zahvaljujem idejnom začetniku rada dr. sc. Andreju Mihevcu, znanstvenom savjetniku na Institutu za istraživanje krša iz Postojne, Slovenija, na vodstvu kroz "tamu" Postojnske jame i na osvjetljavanju puta u svijet Krša. Svojim oduševljenjem i nadahnućem davao mi je nadu kada je bilo najteže.
Zahvaljujem mentoru dipl. kem. dr. sc. Albrechtu Leisu, voditelju Laboratorija za izotopnu hidrologiju i analizu okoliša na institutu Joanneum u Grazu, Austrija, na nesebičnoj pomoći i savjetima u zahtjevnom laboratorijskom radu.
Također želim izraziti svoju zahvalnost red. prof. dr. sc. Dubravki Kotnik Karuza, pročelnici Odjela za fiziku Sveučilišta u Rijeci, što je vjerovala u mene na svakom koraku. Njezina čvrsta ruka te ohrabrujuće vodstvo su bili od velike važnosti za vrijeme izrade rada.
Zahvaljujem i svim kolegama Odjela za fiziku na potpori i podršci u radu.
Zahvaljujem se suradnicima na Institutu za istraživanje krša iz Postojne, osobito dr. sc. Mitji Prelovšeku na pomoći i prijateljstvu za vrijeme uzorkovanja kao i na podatcima dobivenim monitoringom temperature u Postojnskoj jami. Dr. sc. Franci Gabrovšek je ustupio neobjavljene podatke praćenja temperature i tlaka CO_2 u Postojnskoj jami na čemu sam zahvalna. Gospoda Jurij Hajna i Franjo Drole bili su ugodno društvo u terenskom radu, na čemu im zahvaljujem. Gospođi Sonji Stamenković zahvaljujem na pomoći pri slanju uzoraka.
Na gostoprimstvu i podršci zahvaljujem članovima Laboratorija za mjerenje niskih radioaktivnosti Instituta Ruđer Bošković i to dr. sc. Bogomilu Obeliću, dr. sc. Nadi Horvatinčić, dr. sc. Jadranki Barešić, dr. sc. Andreji Sironić i Aniti Rajtarić.
Svoje neobjavljene podatke o izotopnom sastavu kisika ^{18}O u kišnicama sa lokacija Ljubljana i Zalog pri Postojni ustupile su dr. sc. Polona Vreča i dr. sc. Sonja Lojen s Instituta Jožef Stefan iz Ljubljane na čemu sam im zahvalna. Posebna hvala Poloni na podršci i prijateljstvu.
Dr. sc. Wolfgang Dreybrodt pridonio je kvaliteti rada posebno u dijelu koji se odnosi na taloženje karbonata na čemu mu zahvaljujem. Dr. sc. Christopher Spötl je svojim komentarima i uputama o uzorkovanju te interpretaciji podataka znatno pridonio radu. Tyler B. Coplen je konstruktivnim savjetima i uputama o korištenju Laboratorijskog sustava za praćenje i validaciju mjerenja stabilnih izotopa (LIMS) upotpunio moje znanje u laboratorijskom radu. Profesor emeritus Derek Ford je svojim iskustvom o procesima u kršu i poznavanjem sustava Postojnske jame rasvijetlio neke nedoumice u interpretaciji podataka.
Zahvaljujem se svojoj bivšoj profesorici, a sada kolegici i prijateljici mr. sc. Branki Milotić na razumijevanju i pomoći u teškim vremenima. Njene su mi riječi davale snagu i osvjetljavale nadolazeće dane. Od prvoga dana me je podržavala svojom ljubavlju i Božanskom mudrošću.
Posebno sam zahvalna svojoj obitelji - Luki, Svenu i Viti. Izrada ove doktorske radnje unijela je u živote svih nas puno promjena. Bez vaše podrške i razumijevanja sve bi bilo puno teže.
Posebno se zahvaljujem svojim roditeljima na svoj pruženoj pomoći, a posebno na čuvanju Svena i Vite u zadnjoj godini najintenzivnijeg rada.

Hvala!

TABLE OF CONTENTS / SADRŽAJ

PROŠIRENI SAŽETAK ..... **I**
I. UVOD ..... **I**
II. STABILNI IZOTOPI ..... **III**
III. PREGLED LITERATURE ..... **VI**
IV. PODRUČJE ISTRAŽIVANJA ..... **VIII**
V. METODE UZORKOVANJA I MJERENJA ..... **IX**
VI. REZULTATI ..... **X**
VII. DISKUSIJA ..... **XI**
VIII. ZAKLJUČAK ..... **XX**

1 INTRODUCTION **1**
1.1 Scope of the thesis 1
1.2 Outline of the thesis 3
2 STABLE ISOTOPES **6**
2.1 Isotopes 6
2.2 Abundance and delta value 8
2.3 Fractionation 9
2.3.1 Equilibrium and kinetic fractionation 12
2.4 Distribution of carbon and oxygen isotopes 13
2.4.1 Distribution of ^{13}C 13
2.4.2 Distribution of ^{18}O 19
2.5 Stable isotope measurements 23
2.5.1 Mass spectrometers 23
2.5.2 Inlet systems and gas flow 23
2.5.3 Ion source 27
2.5.4 The analyzer 28
2.5.5 Collector system 29
2.5.6 Corrections 30
2.5.7 Standards and quality assurance of stable isotope measurements 31
3 LITERATURE OVERVIEW **34**
3.1 Water chemistry in karst processes 34
3.2 Speleothems 37
3.2.1 Morphology of speleothems 37
3.2.2 Stalagmite formation 38
3.3 $\delta^{13}C$ in speleothems 39
3.4 $\delta^{18}O$ values of drip water and speleothem carbonate 41
3.5 Speleothems as paleothermometers 42
3.6 Dating of speleothems 48
3.7 Previous investigations 49
3.7.1 Paleoclimate 49
3.7.2 Cave environmental conditions 54
3.7.3 Previous studies on Postojna Cave 57
4 SITE DESCRIPTION **62**
4.1 Geology of Postojna Karst 62
4.2 Climate of Postojna area 66
4.3 Cave atmosphere, air circulation and temperature 71
5 SAMPLING AND MEASUREMENT METHODS **78**
5.1 General information on sampling locations 78
5.2 Location description 78
Location 01 – Slonova glava 81

Location 02 – Biospeleološka postaja ... 82
Location 03 – Vodopad ... 83
Location 04 – Kongresna dvorana ... 83
Location 05 – Podrti kapnik ... 83
Location 06 – Stebrišče ... 84
Location 07 – Čarobni vrt ... 85
Location 08 – Vrh Velike gore ... 86
Location 09 – Zgornji Tartar ... 87
Location 10 – Pivka River inside ... 88
Location 11 – Pivka River outside ... 88
5.3 Sampling and field work ... 89
5.3.1 Carbonate samples ... 89
5.3.2 Precipitation sampling ... 92
5.3.3 Drip water and air sampling ... 94
5.4 Handling data and results ... 95
5.5 Sampling diary ... 95
5.6 Sample preparation and measurements ... 96
5.7 Chemical analyses of water samples ... 99
6 RESULTS ... 100
6.1 Cave environment and drip water ... 100
6.1.1 Piper digram ... 121
6.2 Precipitation ... 121
6.3 Carbonates ... 123
7 DISCUSSION ... 131
7.1 Figure description ... 131
7.2 Temperature ... 132
7.3 Drip water and precipitation ... 136
7.4 Water chemistry ... 142
7.4.1 Calcium and magnesium concentration ... 142
7.4.2 Bicarbonate concentration and $\delta^{13}C$ ... 146
7.4.3 Conductivity ... 147
7.4.4 pH, aqueous CO_2 and saturation index ... 151
7.5 CO_2 in cave air ... 153
7.6 Special case of location 05 – Podrti kapnik ... 160
7.7 Recent carbonates ... 164
7.7.1 “Soda-straw” and watch-glass carbonates ... 164
7.7.2 The "peculiar" speleothems types ... 171
7.8 Old carbonates ... 172
7.8.1 Flowstones ... 172
7.8.2 Stalactites ... 175
7.8.3 Drilled core speleothems ... 177
7.8.4 $\delta^{18}O$ and $\delta^{13}C$ in vertical profiles of stalagmites ... 180
7.9 Assessment of isotopic equilibrium conditions in Postojna Cave ... 185
8 CONCLUSION ... 189
References ... 193

A. Appendix I ... v
B. Appendix II ... xxxvii
Biography ... xlix
Životopis ... l
Bibliography /Popis radova ... li

PROŠIRENI SAŽETAK

I. UVOD

Istraživanje klimatskih uvjeta u prošlosti pomoću siga započelo je tijekom 1960-ih i 1970-ih godina pionirskim radovima Broecker et al. (1960), Hendy i Wilson (1968), Dupplessy et al., (1970), Emiliani (1971) i Hendy (1971). U tim se istraživanjima koristi izotopni sastav kisika ($\delta^{18}O$) iz siga koje nastaju u stabilnom špiljskom okolišu, temperatura kojeg odražava srednju godišnju temperaturu u tom području. Broj studija koje obuhvaćaju proučavanje siga i drugih sekundarnih karbonata kao svjedoka proteklih klimatskih i ekoloških promjena povećao se dramatično tijekom posljednja dva desetljeća (Horvatinčić et al, 2003; Frisia et al., 2003; McDermott, 2004; Wang et al., 2004; 2005; Griffiths et al., 2009; Cheng et al., 2009, Surić et al., 2010). Studije o klimatskim promjenama iz cijelog svijeta omogućuju rekonstrukciju prostornih i vremenskih promjena klime prošlosti (Andrews et al., 1994; Dorale et al., 1998; Burns et al., 2001; Johnson et al., 2001; Cheng et al., 2009).

Razvoj mikroanalitičkih tehnika također doprinosi kvaliteti istraživanja (Spötl i Mattey, 2006). Uzorkovanje i mjerne tehnike omogućuju visoku razlučivost rasta siga, osiguravajući time proučavanje godišnjih, pa čak i sezonskih promjena (npr. Johnson et al., 2006; Mattey et al., 2008), koje se nadalje povezuju s rezultatima datiranja (npr., Horvatinčić et al., 2000; Fairchild et al., 2000; Cheng et al., 2009).

Općenito, sige nastaju taloženjem kalcijevog karbonata u procesu isplinjavanja CO_2 iz prokapne vode (Dreybrodt, 1980). Izotopni sastav kisika ($\delta^{18}O$) u prokapnoj vodi odražava izotopni sastav oborina, koji je određen temperaturom zraka na tom području. Izotopni sastav kisika u istaloženom karbonatu određen je izotopnim sastavom prokapne vode i temperaturom na kojoj se odvija taloženje, pod uvjetom da se proces taloženja odvija u izotopnoj ravnoteži. U studijama paleoklimatskih uvjeta pretežno se koriste stalagmiti zbog njihovog oblika

(geometrije), relativno brzog rasta, te karakteristike da uglavnom talože u izotopnoj ravnoteži s prokapnom vodom. Brojne studije okolišnih uvjeta u špiljama ukazuje na prostorne i vremenske varijacije čak i unutar iste špilje, a rezultirale su modernim pristupom proučavanju koji počinje praćenjem uvjeta okoliša (Spötl et al., 2005; Baldini et al., 2006; Surić et al., 2010; Mattey et al., 2010; Tremain et al., 2011). Specifičnost okolišnih uvjeta u svakoj pojedinoj špilji upućuje na potrebu razumijevanja svih mjernih podataka kao i načina nastajanja stalagmita prije uporabe izotopnih zapisa u tumačenju paleoklime (Fairchild et al., 2007; Baldini et al., 2008; Mattey et al., 2010). Da bi se neka siga mogla koristiti u paleoklimatskim istraživanjima, prema suvremenom pristupu, potrebno je proučavati sljedeće uvjete: 1) postojanje izotopne ravnoteže pri taloženju sige (za moderne i drevne sige), 2) okolišne uvjete u špilji pri taloženju siga, 3) kemiju prokapne vode, i 4) izotopni sastav prokapne vode te njegov odnos prema izotopnom sastavom oborinske vode. U ravnotežnim izotopnim uvjetima, $\delta^{18}O$ vrijednost u karbonatima ovisi o dva parametra: $\delta^{18}O$ prokapne vode i temperaturi špilje.

U ovom radu izloženo je sveobuhvatno znanstveno istraživanje Postojnske jame sa ciljem utvrđivanja uvjeta u kojima nastaju sige. Poseban naglasak u radu dan je istraživanju sadržaja stabilnih izotopa kisika i ugljika u sigama, prokapnoj vodi i zraku te okolišnim uvjetima (temperatura, koncentracija CO_2 u zraku u špilji). Mjereni su kemijski parametri prokapne vode kao i njen izotopni sastav. Mjeren je izotopni sastav ugljičnog dioksida u zraku. Jednogodišnje praćenje uvjeta okoliša provedeno je na devet lokacija unutar špilje koje su izabrane pod pretpostavkom da su neke od njih pogodne za paleoklimatka istraživanja, tj. da su se stalagmiti taložili pod stabilnim uvjetima okoliša i u uvjetima izotopne ravnoteže. Konačni zaključci doneseni su na temelju rezultata monitoringa, statističke analize kao i primjene paleotemperaturnih jednadžba.

Je li karbonat taložen u uvjetima izotopne ravnoteže može se provjeriti na nekoliko načina. 1) Iz izotopnog sastava kisika ($\delta^{18}O$) u karbonatu i vodi može se izračunati temperatura taloženja primjenom različitih jednadžba (Epstein i Mayeda, 1953; Craig, 1965; Shackleton, 1974; Grossman, 1982; Andrews, 1994, 1997; Mulitza et al., 2003; Leng i Marshall, 2004). Ako su izračunata i izmjerena temperatura jednake ili slične može se zaključiti da se karbonat taložio u ravnotežnim uvjetima. 2) Iz izmjerenih vrijednosti $\delta^{18}O$ u karbonatu i vodi mogu se odrediti vrijednosti frakcionacijskog faktora α te usporediti s vrijednošću α_{eq} za ravnotežne uvjete (O'Neil et al., 1969; Friedman i O'Neil, 1977; Kim i O'Neil, 1997; Kim et al., 2007; Coplen, 2007; Horita i Clayton, 2007; Chacko i Deines; 2008; Tremaine et al., 2011). Ako je $\alpha \approx \alpha_{eq}$

može se govoriti o taloženju u ravnotežnim uvjetima. 3) Razlike izmjerenih vrijednosti $\delta^{13}C$ u DIC-u i karbonatu ($\Delta = \delta^{13}C_{carb} - \delta^{13}C_{DIC}$) mogu se usporediti s ravnotežnim vrijednostima koeficijenta frakcionacije ε za izmjerenu temperaturu. Ukoliko je $\Delta \approx \varepsilon$, može se govoriti o taloženju u izotopnoj ravnoteži. Ako svi nabrojeni pristupi ukazuju na ravnotežne uvjete taloženja karbonata, može se zaključiti da se lokacija može smatrati pogodnom za daljnja paleoklimatska istraživanja.

Ova je dizertacija podijeljena na nekoliko poglavlja. Osnovni pojmovi i definicije vezani uz stabilne izotope, te raspodjela stabilnih izotopa ugljika i kisika u prirodi opisani su u poglavlju 2 (Stabilni izotopi). Spektrometrija masa, metoda korištena u ovom radu za određivanje izotopnog sastava tvari, također je opisana u tom poglavlju. U trećem poglavlju (Pregled literature) prikazan je pregled relevantne literature vezane uz problematiku rada. Geološke i klimatske karakteristike područja oko Postojnske jame dane su u poglavlju 4 (Područje istraživanja). Detaljan opis lokacija na kojima su provodena uzorkovanja, kao i postupci mjerenja primjenjeni u terenskom radu, laboratorijskim mjerenjima i analizi podataka predstavljeni su u poglavlju 5 (Metode uzorkovanja i mjerenja). Rezultati mjerenja s deskriptivnom statistikom prikazani su u poglavlju 6 (Rezultati), a diskusija rezultata prezentirana je u poglavlju 7 (Diskusija). Tu su prikazani rezultati računanja paleotemperature i usporedba s današnjom izmjerenom temperaturom. Na kraju poglavlja 7 je dana procjena jesu li zadovoljeni uvjeti za taloženje karbonata u izotopnoj ravnoteži za svaku lokaciju i sve vrste karbonata. Zaključci istraživanja sistematizirani su u poglavlju 8, koje završava planom budućih istraživanja. Popis korištenih literaturnih navoda dan je prije priloga. U Prilogu I dane su tablice sa svim numeričkim rezultatima istraživanja, dok Prilog II sadrži fotografije lokacija i uzorkovanja.

II. STABILNI IZOTOPI

Izotopi koji imaju stabilnu jezgru, tj. ne podliježu radioaktivnom raspadu, nazivaju se stabilnim izotopima. U prirodnim procesima najčešće su istraživani prirodni izotopi kisika (^{18}O), ugljika (^{13}C), dušika (^{15}N), sumpora (^{34}S) i vodika (^{2}H).

Svaka vrsta uzorka u prirodi ima svoj specifični izotopni sastav, kao otisak prsta, zbog čega se isti koristi za dokazivanje porijekla, tj. izvorišta supstancije. Tehnikama spektrometrije masa određuje se omjer zastupljenosti težeg izotopa u odnosu na lakši izotop (jednadžba 2.2). Zbog male zastupljenosti stabilnih izotopa od interesa, umjesto apsolutne vrijednosti određuje se relativno odstupanje zastupljenosti izotopa u uzorku u odnosu na referentni materijal, a

veličina se naziva delta vrijednost (δ) (jednadžba 2.3) i izražava se u promilima (‰). Za pozitivnije δ vrijednosti kaže se da je uzorak obogaćen težim izotopima u odnosu na standard (Coplen et al., 2002).

Izotopna frakcionacija (odjeljivanje izotopa) je process obogaćenja ili osiromašenja jednim izotopom u odnosu na drugi u nekom fizičkom ili kemijskom procesu, kao što su isparavanje, kondenzacija, taloženje ili fotosinteza (Mickler et al., 2006; Wiedner et al., 2008). Uzroci frakcionacije mogu se naći u termodinamičkim i kvantnomehaničkim svojstvima molekula koje se razlikuju po masama odnosno energijama vezanja. Veličina izotopne frakcionacije opisuje se frakcionacijskim faktorom α, odnosno omjerom izotopnih sastava tvari poslije i prije određenog procesa (jednadžba 2.8). U većini slučajeva bezdimenzionalni frakcionacijski faktor α je približno jednak jedinici, što govori da je promjena izotopnog sastava tvari u navedenim procesima vrlo mala. Stoga je uvedena nova veličina ε, koja se također naziva frakcionacijski faktor, a definirana je kao razlika δ vrijednosti nakon i prije promatranog procesa (jednadžba 2.11) i izražava se u ‰.

Proces frakcionacije može biti karakteriziran kao ravnotežni ili kinetički. Ravnotežna frakcionacija je proces u kojem dolazi do djelomičnog razdvajanja izotopa između dvije ili više tvari koje se nalaze u termodinamičkoj ravnoteži. Proces je temperaturno ovisan te je izraženiji na nižim temperaturama. U ravnotežnim uvjetima izotopna frakcionacija ovisi samo o temperaturi te zbog toga predstavlja osnovu za izotopnu paleotermometriju (Chacko et al., 2001).

Kinetička frakcionacija je proces karakteriziran brzim i nepotpunim prijelazima između faza. Procesi karakterizirani kinetičkom frakcionacijom su difuzija, isparavanje i kondenzacija, kinetički efekti koji dolaze do izražaja zbog različitih disocijacijskih energija, te metabolički procesi (fotosinteza).

Ugljik u prirodi ima dva stabilna izotopa, ^{12}C i ^{13}C. Njihova zastupljenost je 98,93 % i 1,07 %. ^{14}C je radioaktivni izotop ugljika koji se nalazi u atmosferi i biosferi, a zastupljen je sa svega 10^{-10} %. Vrijeme poluživota mu je 5730 godina.

Izotopni sastav ugljika svojstven određenoj vrsti materijala prikazan je na Slici 2.3. U ovome radu detaljnije će se obrađivati atmosferski CO_2, ugljik u biljkama, biogeni ugljični dioksid iz tla, DIC u vodi i taloženi sekundarni karbonati.

Atmosferski CO_2 glavni je izvor ugljika za biosferu, a koncentracija CO_2 u atmosferi se kreće od 380 ppmv do 400 ppmv (IPCC, 2001), uz moguće lokalne efekte. Sustavna mjerenja koncentracije ugljičnog dioksida u atmosferi provodi NOAA (National Oceanic and Atmospheric Administration), a istraživanja pokazuju da se koncentracija CO_2 povećala za 20 % u posljednjih 50 godina. Primijećen je pad $\delta^{13}C$ vrijednosti s povećanjem koncentracije CO_2, što se objašnjava povećanim izgaranjem fosilnih goriva u tom razdoblju. Koncentracija $\delta^{13}C$ u zraku izmjerena 2000. godine je -8,0 ‰ (Verburg, 2007).

$\delta^{13}C$ vrijednost u biljkama varira od -38 do -8 ‰, ovisno o procesu fotosinteze (Slika 2.3). Morski karbonati imaju $\delta^{13}C$ vrijednost ~0 ‰, u intervalu od -2 do +3 ‰, ovisno o starosti i fazi mineralizacije (McDermott et al., 2006). Karbonatni minerali imaju značajan doprinos u DIC-u (Dissolved Inorganic Carbon) u vodama zajedno s atmosferskim CO_2 i/ili CO_2 sadržanim u tlu (Genty et al., 2001a). DIC je naziv za različite anorganske ugljikove spojeve otopljene u vodi. Izotopni sastav ugljika u sigama i ostalim sekundarnim karbonatima koji nastaju taloženjem iz vode prezasićene karbonatom određen je prije svega izotopnim sastavom DIC-a u vodi, kao i samim procesom taloženja. Npr., $\delta^{13}C$ jezerskog sedimenta na Plitvičkim jezerima malo varira oko vrijednosti -9 ‰, dok je raspon $\delta^{13}C$ vrijednosti u sedrama s tog područja veći, od -10 do -6,5 ‰ (Horvatinčić et al., 2003). $\delta^{13}C$ u sigama iz Slovenije i Hrvatske varira između -12 i +3 ‰ (Urbanc et al., 1984; Horvatinčić et al., 2003).

Kisik je najzastupljeniji element na Zemlji. Ima tri izotopa (^{16}O, ^{17}O, ^{18}O) od kojih se u istraživanjima okoliša najčešće koristi izotop ^{18}O izražen kao omjer $^{18}O/^{16}O$, odnosno $\delta^{18}O$. U različitim fazama kruženja vode u prirodi $\delta^{18}O$ vode ima karakteristične vrijednosti (Slika 2.5). Podaci o izotopnom sastavu kisika ^{18}O (i vodika ^{2}H) u oborinama cijelog svijeta pohranjeni su u međunarodnoj bazi podataka GNIP/IAEA (Global Network of Isotopes in Precipitation/ International Atomic Energy Agency). Odnos između izotopnog sastava kisika ^{18}O i vodika ^{2}H naziva se Globalnom linijom oborinske vode (GMWL) (Slika 2.6).

U proučavanju siga važno je odrediti odnos izotopnog sastava oborina i prokapne vode, kako bi se mogao pratiti put vode od površine do mjesta prokapljavanja, kao i poznavati procese izotopne frakcionacije kisika i ugljika između prokapne vode i istaloženog karbonata za proučavanje paleoklimatskih uvjeta (Darling et al., 2006).

Spektrometrija masa

Sustav za određivanje koncentracije stabilnih izotopa sastoji se od jedinice za pripremu uzoraka i spektrometra masa (Slika 2.7). Ovisno o vrsti uzorka, jedinice za pripremu uzoraka su različite. Za određivanje koncentracija stabilnih izotopa $\delta^{13}C$ i $\delta^{18}O$ u uzorcima karbonata koristi se sustav *Gas Bench* (Slika 2.9), dok se za određivanje koncentracija izotopa $\delta^{18}O$ u vodama koristi HDO ekvilibratorska jedinica (Slika 5.18). Spektrometrom masa se kvantitativno određuje zastupljenost izotopa u tvari. Osnovni su mu dijelovi ionski izvor (Slika 2.13), analizator (Slika 2.14) i detektor (Slika 2.15). Svim procesima upravlja se iz centralnog računala. Rezultati dobiveni mjerenjem izraženi su kao δ vrijednosti u promilima (‰) relativno prema međunarodnom standardu VSMOW za vode i VPDB za karbonate (Tablica 2.3).

III. PREGLED LITERATURE

Oborinska voda sadrži otopljeni atmosferski CO_2, a pri prolasku kroz tlo koncentracija CO_2 u vodi se povećava zbog otapanja CO_2 iz tla. Koncentracija CO_2 u tlu je i do dva reda veličine viša nego u atmosferi. CO_2 otopljen u vodi stvara ugljičnu kiselinu (jednadžba 3.2) koja pri prolasku kroz tlo otapa vapnenačke stijene (jednadžba 3.6). Nakon tih procesa u špilju dolazi prokapna voda zasićena s CO_2 u odnosu na špiljski zrak te dolazi do procesa isplinjavanja pri čemu se taloži sekundarni karbonat (sige), jednadžba 3.13.

Klasifikacija istaloženog karbonata napravljena je prema nekim specifičnim oblicima. Sige se dijele na stalaktite, stalagmite i sigovinu, te neke druge, manje česte oblike.

Izotopni sastav ugljika $\delta^{13}C$ u sigama ovisi o izotopnom sastavu $\delta^{13}C_{DIC}$ koji je određen izotopnim sastavom otopljenog CO_2 (atmosferski i/ili iz tla) i karbonatnih stijena. Ovisi također i o načinu otapanja stijena (otvoreni i zatvoreni sustav), te o isplinjavanju CO_2 u špilji (Slika 3.4).

Izotopni sastav kisika $\delta^{18}O$ u prokapnoj vodi ovisi o izotopnom sastavu oborina iznad špilje, te najčešće pokazuje srednju godišnju $\delta^{18}O$ vrijednost oborina. Unutar iste špilje do razlike u izotopnom sastavu prokapne vode na različitim lokacijama može doći zbog specifičnih uvjeta okoliša na promatranoj lokaciji, zbog razlike u putevima kojima voda prolazi kroz tlo, te razlike u vremenu zadržavanja vode u tlu (Mattey et al., 2010).

Sige se mogu koristiti za istraživanje paleotemperature ako su taložene u stabilnoj špiljskoj atmosferi koja je karakterizirana malim kolebanjima temperature od ±1 °C oko srednje godišnje temperature koja odgovara srednjoj godišnjoj temperaturi zraka izvan špilje, te relativnom vlagom

zraka koja je približno jednaka 100 %. Također mora biti zadovoljen uvjet da su $\delta^{18}O$ vrijednosti prokapne vode i istaloženog karbonata u izotopnoj ravnoteži, te da je ugljik koji se taloži na vrhu stalagmita u izotopnoj ravnoteži s karbonatom otopljenim u prokapnoj vodi. Postoje različite empirijske i teorijske jednadžbe za određivanje paleotemperature (Tablica 3.1). Različite paleotemperaturne jednadžbe iz literature sistematizirane se u dva osnovna tipa. Jednadžbe tipa A povezuju temperaturu stvaranja siga (izraženu u ºC) i $\delta^{18}O$ vrijednosti vode (relativno prema VSMOW) i karbonata (relativno prema VPDB). Jednadžbe tipa B povezuju frakcionacijski faktor α i temperaturu taloženja karbonata (izraženu u K), pri čemu su obje vrijednosti $\delta^{18}O$ izražene relativno prema VSMOW. Određivanjem starosti siga, tj. datiranjem, dolazimo do podatka o vremenu kada je siga nastala.

Paleoklimatska istraživanja uporabom $\delta^{18}O$ iz siga počinju 60-tih i 70-tih godina 20. stoljeća (Broecker et al., 1960; Hendy i Wilson, 1968; Duplessy et al., 1970; Emiliani, 1971; Hendy, 1971). Od tada su istraživanja napredovala, kako zbog razvoja i usavršavanja mjernih tehnika tako i zbog mnogobrojnih novih saznanja dobivenih praćenjem uvjeta unutar špilje. U praćenju uvjeta okoliša važno je odrediti odražava li klima špilje sadašnje atmosferske prilike, postoji li cirkulacija zraka odnosno ventilacija u špilji, kako se geokemijski i izotopni parametri u prokapnoj vodi odražavaju u izotopnom sastavu suvremenih siga. Praćenje uvjeta unutar špilje potrebno je provoditi najmanje jednu godinu radi promatranja sezonskih promjena u geokemiji voda, temperaturi zraka, koncentraciji CO_2 u zraku te u izotopnom sastavu zraka, vode i recentnog karbonata (Bar-Matthews et al., 1996; Spötl et al., 2005; Baldini et al., 2008).

Postojnska jama je, kao najveća špilja u ovom dijelu Europe, budila znatiželju znanstvenika u različitim poljima znanosti, pa su provedena mnogobrojna geološka istraživanja (Gospodarič, 1981; Ikeya et al., 1982; Gospodarič, 1988; Šebela i Sasowsky, 1999; Čar i Šebela, 1998; Šušteršič, 2006), biospeleološka (Pipan i Brancelj, 2004) i hidrološka istraživanja (Kogovšek et al., 2004), a pratili su se i neki okolišni parametri: koncentracija CO_2 u zraku (Gams, 1974a), tlak zraka i temperatura (Šebela i Turk, 2011), kao i koncentracija radona (Vaupotič i Kobal, 2004: Bezek et al., 2012). Gams i Kogovšek (1998) su procijenili brzinu rasta karbonata u Postojnskoj jami na 0,11 mm godišnje. Stabilni izotopi kisika i ugljika su korišteni za procjenu mogućnosti primjene siga i njihovog izotopnog sastava u paleoklimatskim istraživanjima (Urbanc et al., 1984, 1987) i za proučavanje kretanja ugljika kroz krški teren (Vokal, 1999; Vokal et al., 1999). Mjerenja fizičkih, kemijskih i izotopnih

parametara u prokapnoj vodi provedena su na tri lokacije u Postojnskoj jami u razdoblju od jedne godine (lipanj 1996. – lipanj 1997.) (Vokal, 1999). Vanjska temperatura zraka u tom razdoblju je iznosila 9,1 ºC, a temperatura zraka unutar špilje na lokaciji Pisani rov iznosila je 7,8 ± 0,1 ºC. Temperatura prokapne vode se kretala od 8,2 ± 0,4 ºC (Pisani rov) do 10,4 ± 0,7 ºC (lokacija Briljant). Vrijednost pH prokapne vode bila je 7,8 ± 0,2, a indeks zasićenja I_{sat} varirao je od 0,5 do 6. Srednja vrijednost koncentracije Ca^{2+} iznosila je od 55,5 do 79,9 mg/L, a koncentracija bikarbonata od 165,2 do 232,8 mg/L. Na lokaciji Briljant zabilježene su najniže koncentracije. Provodnost je varirala od 301 do 424 µS/cm. Vrijeme zadržavanja vode u sloju tla iznad špilje procijenjeno je na 1 – 2 mjeseca. Procijenjena je i brzina rasta karbonata na 0,13 – 0,20 mm/god. Određen je izotopni sastav CO_2 u tlu ($\delta^{13}C$ vrijednosti na dvije lokacije -21,7 i -20,5 ‰, uz sezonske varijacije do 7,3 ‰), organske tvari u tlu ($\delta^{13}C$ = -26,7 ‰) i DIC-a u prokapnoj vodi ($\delta^{13}C$ varira od -14,7 do -10,2 ‰). Vrijednost $\delta^{18}O$ u prokapnoj vodu se kretala od -8,8 ‰ do -8,3 ‰, a vrijednosti $\delta^{2}H$ od -54 ‰ do -57 ‰. Uzorkovan je i stalagmit kojem je po vertikalnom profilu određen izotopni sastav: izmjeren je raspon vrijednosti $\delta^{18}O$ od -7,49 do -6,05 ‰ , te raspon vrijednosti $\delta^{13}C$ od -10,18 do -9,31 ‰.

IV. PODRUČJE ISTRAŽIVANJA

Špilja Postojnska jama nalazi se u području Dinarskog krša (Slika 4.1). Ulaz u Postojnsku jamu nalazi se na 529 metara nadmorske visine. Važnu ulogu u izgledu i geomorfologiji Postojnske jame ima rijeka Pivka koja ponire u nju, 18 m ispod ulaza. Reljefna karta površine iznad Postojnske jame zajedno sa skicom špiljskih prolaza prikazana je na Slici 4.3.

Na klimatske karakteristike područja postojnskog krša utječe mediteranska klima sjevernog Jadrana te kontinentalna klima Slovenije (Gospodarič et al., 1976). Srednja godišnja temperatura zraka u proteklih trideset godina iznosi 9,2 °C, dok je srednja godišnja količina oborine u istom razdoblju 1573 mm (Slike 4.4, 4.5 i 4.6). U posljednjih deset godina vidljiv je trend porasta temperature (0,06 ºC godišnje, Slika 4.7), kao i učestalija pojava ekstremno kišnih i/ili sušnih godina (Slika 4.8).

Temperatura i smjer strujanja zraka, te relativna vlaga praćeni su instrumentima za automatsko skupljanje podataka (podaci od Gabrovšek, Mihevc, Prelovšek) na različitim lokacijama u špilji i u različitim vremenskim razdobljima, a sve od 2006. do 2011. godine (Slika 4.10, Tablica 4.1). Pokazuje se da između promatranih lokacija postoje male razlike, no na pojedinoj lokaciji mjerena temperatura je stalna (Slika 4.11). Ustanovljeno je također da

postoje sezonska strujanja zraka u špilji te da se razlikuju načini ljetnog (Slika 4.12) i zimskog (Slika 4.13) kruženja zraka. U ljetnom razdoblju zrak izlazi iz špilje, dok u zimskom razdoblju hladniji vanjski zrak ulazi u špilju. Smjer strujanja zraka naznačen je pozitivnim i/ili negativnim predznacima za iznos brzine (Slika 4.14).

V. METODE UZORKOVANJA I MJERENJA

Lokacije na kojima su u ovom radu bile mjerne stanice te osnovni podaci o njima navedeni su u Tablici 5.1. Lokacije su prikazane na karti (Slika 5.1), te na poprečnom presjeku Postojnske jame (Slika 5.2). Lokacije su nazvane prema njihovim tradicionalnim imenima: lokacija 01 – Slonova glava, lokacija 02 – Biospeleološka postaja, lokacija 03 – Vodopad, lokacija 04 – Kongresna dvorana, lokacija 05 – Podrti kapnik, lokacija 06 – Stebrišče, lokacija 07 – Čarobni vrt, lokacija 08 – Vrh Velike gore, lokacija 09 – Zgornji Tartar. Lokacija 10 – Pivka River inside, nalazi se na rijeci Pivki 2500 m od ulaza/ponora, dok se lokacija 11 – Pivka River outside nalazi se na rijeci ispod samog ulaza u špilju. Imena lokacija se na isti način navode i u engleskom tekstu.

Dozvola za uzorkovanje karbonata zatražena je i dobivena od nadležnog ministarstva, odnosno Zavoda Republike Slovenije za zaštitu prirode (Prilog I, Slika A.2). Karbonatni uzorci sakupljani na lokacijama unutar špilje podijeljeni su po grupama: recentni karbonati i karbonati prikupljani na satnim stakalcima te stari karbonati. Nazivom stari karbonati obuhvaćene su sige koje su i danas aktivne, a nastajale su i u prošlosti. U grupu starih karbonata spada sigovina, bušene jezgre stalagmita te stalaktiti, dok u grupu recentnih karbonata pripadaju tzv. slamčice i tzv. uzorci čudnovatih oblika.

Uzorci slamčica su prikupljeni na lokacijama 01, 02, 03, 06, 07, 08 i 09. Satna stakalca su postavljena na svih devet lokacija, ali je uspješno uzorkovanje bilo na lokacijama 01, 02, 03, 04, 05, 06 i 09. Uzorci čudnovatih oblika sakupljeni su na lokacijama 01 i 09. Na lokacijama 06, 07 i 08 bušene su jezgre stalagmita, sigovina je sakupljena na lokacijama 04, 05 i 06, a stalaktiti na lokacijama 02, 04 i 09.

Oborinska voda sakupljana je na krovu Instituta za istraživanje krša u Postojni koji je od ulaza u špilju udaljen ~500 m.

Na terenu je mjerena temperatura zraka i prokapne vode ili rijeke Pivke, pH i električna provodnost prokapne vode, učestalost kapanja prokapne vode (na lokacijama 01 – 09) te koncentracija CO_2 (pCO_2) u atmosferi. Na svakoj lokaciji unutar špilje prikupljana je

prokapna ili riječna voda za kemijske i izotopne analize. U svim uzorcima voda odmah nakon uzorkovanja, u laboratoriju, mjerene su koncentracije Ca^{2+}, Mg^{2+}, i HCO_3^-, dok su koncentracije Na^+, K^+, Cl^-, SO_4^{2-}, NO_3^- mjerene samo dva puta tijekom razdoblja promatranja, budući da ti ioni predstavljaju manjinske elemente u krškim vodama. Uzorkovan je i zrak za izotopne analize. Sve izotopne analize provedene su u Laboratorijskom centru za izotopnu hidrologiju i analitiku okoliša na Joanneum Research Resources – Institutu za vodu, energiju i održivost, Graz, Austrija, dok su kemijske analize vode rađene na Nastavnom zavodu za javno zdravstvo u Rijeci. Priprema uzoraka za mjerenje i mjerenja odvijali su se prema certificiranim metodama.

Svaki je uzorak prilikom prikupljanja dobio jedinstveno ime oblika: **L – DDMMYYYY – S,** gdje L predstavlja broj lokacije (od 01 do 11), DDMMYYYY predstavlja datum uzorkovanja (dan mjesec godina), a S predstavlja vrstu uzorka: voda (W), zrak (A), ili karbonat (C).

Svi su podaci o uzorcima i mjerenjima pohranjeni u bazu podataka radi jednostavnije obrade podataka i osiguranja kvalitete rada. Dnevnik uzorkovanja prikazan je u Tablici 5.2.

VI. REZULTATI

Numeričke vrijednosti mjerenih parametara: temperatura zraka i vode, pH, brzina kapanja vode, električna provodnost i pCO_2 prikazane su u Tablici A.3 u Prilogu I. Rezultati kemijskih analiza prokapne vode, te izračunat indeks zasićenja kalcijevim karbonatom (I_{sat}) i koncentracija otopljenog ugljičnog dioksida u vodi $pCO_2(aq)$ nalaze se u Tablici A.4 Priloga I. Neki najvažniji kemijski i izotopni parametri za svaku lokaciju prikazani su grafički na Slikama 6.1 te 6.3 do 6.12, a Slika 6.2 prikazuje raspodjelu učestalosti prokapavanja prokapne vode za lokacije 01 – 09. Koncentracije aniona i kationa u vodama prikazane su i u ternarnom Piperovom dijagramu (Slika 6.13) na kojem se uočavaju razlike u porijeklu prokapne vode u Postojnskoj jami i rijeke Pivke.

Podaci dobiveni mjerenjem koncentracija stabilnih izotopa u DIC-u ($\delta^{13}C_{DIC}$), CO_2 u zraku ($\delta^{13}C_{air}$) i prokapnoj, odnosno riječnoj vodi ($\delta^{18}O_{water}$) dani su u Tablici A.5 Priloga I. Za svaku lokaciju su izračunate korelacijske matrice između najvažnijih kemijskih i izotopnih parametara (Tablica A.6, Prilog I). U Tablici A.7 Priloga I nalaze se podaci o izotopnom sastavu ($\delta^{18}O_p$) oborina iz Postojne, te Zaloga pri Postojni i Ljubljane koji su dobiveni iz Instituta Jožef Stefan u Ljubljani.

Podaci o izotopnom sastavu ugljika i kisika u slamčicama nalaze se u Tablici A.8 Priloga I, a podaci za uzorke čudnovatog rasta u Tablici A.9. Tablica A.10 sadrži podatke o $\delta^{13}C$ i $\delta^{18}O$ karbonata taloženog na satnim stakalcima.

Slika 6.15 daje pregled $\delta^{13}C$ i $\delta^{18}O$ vrijednosti recentnih karbonata na raznim lokacijama. Vrijednosti $\delta^{13}C$ variraju od -7,84 ‰ na lokaciji 01 do -10,58 ‰ na lokaciji 03. Najveća vrijednost za $\delta^{18}O$ je na lokaciji 03, -4,96 ‰, a najniža na lokaciji 06, -7,84 ‰. Vrijednosti $\delta^{13}C$ karbonata taloženog na satnom staklu variraju od -9,95 ‰ na lokaciji 05 do -12,37 ‰ na lokaciji 01. $\delta^{18}O$ vrijednosti za iste uzorke variraju od -3,08 ‰ na lokaciji 01 do -4,64 ‰ na lokaciji 04 (Slika 6.16). Vrijednosti $\delta^{13}C$ na satnim staklima su niže od vrijednosti $\delta^{13}C$ izmjerenih na slamčicama, te su slične $\delta^{13}C_{DIC}$ vrijednostima. $\delta^{18}O$ vrijednosti karbonata na satnim staklima razlikuju se od onih u prokapnim vodama, i pozitivnije su od $\delta^{18}O$ vrijednosti slamčica. Ovakav izotopni sastav karbonata na satnim staklima objašnjen je brzim, gotovo trenutnim taloženjem karbonata iz vodene otopine (Mickler et al., 2004). Pri tako brzom taloženju karbonata ne dolazi do uspostavljanja izotopne ravnoteže, već istaloženi karbonat odražava izotopni sastav DIC-a. To vrijedi za $\delta^{13}C$, ali i za $\delta^{18}O$. Mjerenje vrijednosti $\delta^{18}O$ u bikarbonatu, kao većinskoj sastavnici DIC-a, nije jednostavno i nije provedeno u ovom radu, a pretpostavlja se da je $\delta^{18}O$ u HCO_3^- do 6 ‰ pozitivniji od $\delta^{18}O$ u karbonatu (Mickler et al., 2004), što odgovara prikazanim izmjerenim vrijednostima $\delta^{18}O$ u.

Rezultati izotopnog sastava sigovine i stalaktita, uz kratak opis pojedinog sloja, nalaze se u Tablici A.11 Priloga I. Izotopni sastav kisika ^{18}O i ugljika ^{13}C u slojevima bušenih jezgri stalagmita s kratkim opisom slojeva te podatkom o udaljenosti sloja od vrha stalagmita prikazan je u Tablici A.12. Izmjerene $\delta^{13}C$ i $\delta^{18}O$ vrijednosti u uzorcima starih karbonata prikazane su na slikama 6.18, 6.19 i 6.20. Rezultati pokazuju širok raspon vrijednosti $\delta^{13}C$ (od -7,95 do -0,78 ‰ za sigovinu i od -9,91 do -1,15 ‰ za stalaktite) i $\delta^{18}O$ (od -6,66 do -3,38 ‰ za sigovinu i od -6,39 do -4,09 ‰ za stalaktite). $\delta^{13}C$ i $\delta^{18}O$ vrijednosti za jezgre bušenih stalagmita kreću se za $\delta^{13}C$ od -9,67 do -1,65 ‰, te za $\delta^{18}O$ od -12,11 do -3,59 ‰ (Slika 6.20).

VII. DISKUSIJA

Temperatura zraka

Srednja temperatura zraka, mjerena na svih devet lokacija unutar Postojnske jame iznosi 10,7 ± 0,6 °C, pri čemu je na lokaciji 03 izmjerena najniža 9,7 ± 1,6 °C, a na lokaciji 08 najviša

srednja temperatura zraka 11,6 ± 0,8 °C. (Slika 7.2). Unutarnje lokacije 05, 06, 07, 08 i 09 pokazuju manja sezonska kolebanja temperature nego lokacije bliže ulazu 01, 02, 03 i 04. Srednja temperature zraka na unutarnjim lokacijama (11,1 ± 0,5 °C) je viša nego na onima bliže ulazu (9,9 ± 0,3 °C). Srednja vanjska temperatura zraka za razdoblje od 6 godina (2006. – 2011.) iznosi 9,9 °C, iz čega se može zaključiti da srednja temperatura zraka unutar špilje odgovara srednjoj godišnjoj temperaturi vanjskog zraka.

Srednja temperatura prokapne vode slijedi temperature zraka (Slika 7.3), pa za lokacije 01, 02, 03 i 04 blizu ulaza špilju iznosi u prosjeku 9,7 ± 0,4 °C dok je za unutarnje lokacije 05, 06, 07, 08 i 09, 11,1 ± 0,5 °C. Srednja temperatura prokapne vode za lokacije blizu ulaza u Postojnsku jamu također predstavlja srednju godišnju temperaturu zraka. Temperatura prokapne vode pokazuje manje varijacije od temperature rijeke Pivke. Srednja temperatura prokapne vode je najveća na lokaciji 08, 11,9 ± 1,3 °C, gdje je i najviša srednja temperatura zraka. Lokacije 04, 05, 06, 07 i 09 pokazuju mala kolebanja oko srednje temperature vode i ove lokacije možemo smatrati zonama koje su karakterizirane stalnom temperaturom (Slika 7.3 i 7.4).

Prokapna voda i oborine

Najniža učestalost prokapljavanja vode (Slika 7.5) mjerena je u ljetnim mjesecima (kolovoz 2010). Ljetni mjeseci imaju ujedno i najmanju količinu oborina. Na lokacijama 01, 04, 07, 08 i 09 u studenom 2010. izmjerena je viša učestalost prokapljavanja kao posljedica obilnih oborina u rujnu te godine (Slika 7.8a). Srednja vrijednost učestalosti prokapljavanja i njene promjene izražene koeficijentom varijabilnosti prikazane su na Slici 7.6 i pokazuje se da sve prokapne vode unutar Postojnske jame pripadaju istoj grupi voda koje karakterizira curenje (eng. *seepage flow*), a što se očekivalo na osnovi malih sezonskih varijacija pojedinih kemijskih komponenata. Vrijednosti $\delta^{18}O$ u prokapnoj vodi, rijeci Pivki i oborinskoj vodi prikazane su na Slici 7.7. Godišnje amplitude $\delta^{18}O$ u oborinama Ljubljane i Zaloga pri Postojni (7,66 ‰, odnosno 5,45 ‰) su puno veće nego u prokapnoj vodi (od 0,12 do 2,00 ‰, Tablica 7.2). Najmanje sezonske varijacije u $\delta^{18}O$ u prokapnoj vodi opažene su na lokacijama 04, -8,86 ± 0,04 ‰, i 06, -8,73 ± 0,07 ‰. Razlog malom kolebanju oko srednje vrijednosti $\delta^{18}O$ je dugo vrijeme zadržavanja vode u tlu, 5 – 7 godina. Najveće varijacije $\delta^{18}O$ opažene su na lokacijama 08, -9,69 ± 0,66 ‰, i 02, -9,49 ± 0,65 ‰. Na ove dvije lokacije, kao i na 01 i 03, vrijeme zadržavanja vode u tlu je kratko, od nekoliko mjeseci do 1 godine. Za lokacije 05, 07 i 09 je procijenjeno vrijeme zadržavanja vode u tlu od 1 do 2 godine.

Koncentracije iona kalcija i magnezija u prokapnoj vodi

Najveće varijacije u koncentraciji kalcija (Slika 7.9) opažene su na lokaciji 01, 89 ± 16 mg/L, a najmanje na lokaciji 08, 82 ± 3 mg/L. Na lokacijama blizu ulaza (01 – 04) prosječna koncentracija kalcija (87,6 ± 1,5 mg/L) je visa nego na unutarnjim lokacijama 06 – 09 (77,8 ± 3,5 mg/L). Najniža koncentracija kalcija je izmjerena na lokaciji 05 – Podrti kapnik, 65 ± 12 mg/L (Slika 7.9). Rijeka Pivka ima koncentraciju kalcija 72 ± 4 mg/L. Male varijacije u koncentraciji kalcija u rijeci Pivki mogu se objasniti činjenicom da voda prolazi istim koritom bez iznenadnih dotoka vode koje može prouzročiti kiša. Koncentracija iona magnezija u svim prokapnim vodama je vrlo niska (Slika 7.10), sa srednjom vrijednošću 0,85 ± 0,18 mg/L, a u rijeci Pivki je znatno viša (3,8, odnosno 3,7 mg/L na lokacijama 10 i 11). Razlog tome može biti razlika u geologiji tla: dok su iznad Postojnske jame stijene vapnenačke, stijene na području prihranjivanja rijeke Pivke sadrže veće primjese dolomita. Omjer magnezija i kalcija kreće se u prokapnoj void od 0,006 na lokaciji 08 do 0,013 na lokaciji 01, dok je u rijeci Pivki 0,05 (Slika 7.11).

Koncentracije bikarbonata i $\delta^{13}C_{DIC}$

Koncentracija bikarbonata (HCO_3^-) kreće se od 200 ± 19 mg/L (lokacija 07) do 273 ± 52 mg/L na lokaciji 01, a izrazito je niža na lokaciji 05, 153 ± 28 mg/L (Slika 7.14). Na lokaciji 01 izmjerena je najveća vrijednost 365 mg/L u studenom 2010. Srednja vrijednost na lokacijama 01 – 04 bliže ulazu je viša (255 ± 12 mg/L) od srednje vrijednosti na unutarnjim lokacijama 06 – 09 (222 ± 18 mg/L).

Vrijednosti $\delta^{13}C_{DIC}$ prokapnih voda su između -12,3 ± 0,3 ‰ na lokaciji 07 i -13,3 ± 0,3 ‰ na lokaciji 01 (Slika 7.15) i ne pokazuju razlike između lokacija bliže ulazu i unutarnjih lokacija. Na lokaciji 05 $\delta^{13}C_{DIC}$ vrijednosti su najpozitivnije -9,9 ± 2,3 ‰, sa najnižom vrijednošću -11,78 ‰ i najvišom -5,64 ‰. Odstupanja za lokaciju 05 – Podrti kapnik bit će posebno objašnjena. $\delta^{13}C$ vrijednost u DIC-u za rijeku Pivku jednake su unutar (-12,4 ± 2,0 ‰) i izvan špilje (-12,4 ± 2,2 ‰).

Električna provodnost

Srednja vrijednost za električnu provodnost na lokacijama 01 – 04 iznosi 423 ± 25 μS/cm dok za lokacije 06 – 09 iznosi 358 ± 15 μS/cm. (Slika 7.16). Na lokaciji 05 izmjerena je niža provodnost, 277 ± 42 μS/cm, sukladno nižim koncentracijama Ca^{2+} i HCO_3^-. Provodnost je niža na lokacijama s većom učestalošću prokapljavanja, lokacije 06 – 09, (R^2 = 0,51 za

linearnu regresiju) (Slika 7.18). Koncentracije bikarbonata i kalcija su u korelaciji ($R^2 = 0,94$, Slika 7.17) u skladu s klasičnom teorijom okršavanja. Visoka koncentracija bikarbonata u prokapnoj vodi znači i visoku koncentraciju otopljenih minerala, što u slučaju vapnenca znači kalcija. U Postojnskoj jami su ioni kalcija i bikarbonata u prokapnoj vodi najzastupljeniji ioni (Slika 6.13).

pH, otopljeni CO_2 i indeks zasićenja

pH vrijednosti uzorkovanih prokapnih voda nalaze se između 7,0 i 8,4 što je ujedno i karakteristika vapnenačkog i dolomitskog terena. pH vrijednosti su više tijekom hladnijeg razdoblja. Najveće pH vrijednosti prokapne vode (Slika 7.19) mjerene su u ožujku 2010. na lokacijama 04 (8,22), 05 (8,38) i 06 (8,33). Na lokacijama 01 i 02 izmjerene su najniže pH vrijednosti prokapne vode 7,10 u kolovozu 2010. Najniža pH vrijednost svih mjerenih uzoraka vode (7,08) izmjerena je na rijeci Pivki (lokacija 11) u rujnu 2010, što je posljedica obilnih kiša. Izračunate su vrijednosti za $pCO_2(aq)$ i I_{sat}. Srednje koncentracije otopljenog CO_2 u prokapnoj vodi ($pCO_2(aq)$, Slika 7.20) kreću se od 2100 μatm na lokaciji 05 do 10 400 μatm na lokaciji 01. Srednja vrijednost $pCO_2(aq)$ na lokacijama 01 – 04 bliže ulazu, 6950 ± 3500 μatm, viša je srednje vrijednosti za unutarnje lokacije, 3465 ± 226 μatm, što je posljedica viših koncentracija CO_2 u tlu iznad lokacija 01 – 04. Više koncentracije $pCO_2(aq)$ uzrokuju i intenzivnije otapanje vapnenačkih stijena, pa je i koncentracija iona Ca^{2+} i HCO_3^-, kao i vodljivost, viša na lokacijama 01 – 04 nego na lokacijama 06 – 09. Srednja vrijednost indeksa zasićenja kalcijevim karbonatom I_{sat} (Slika 7.21) je na svim lokacijama >1, a najviša pojedinačna vrijednost opažena je na lokaciji 04 u veljači 2011. Odnos I_{sat} i pH prikazan je na Slici 7.22b: što je viši pH, to je viši I_{sat}.

CO_2 u špiljskom zraku

Koncentracija CO_2 u zraku mjerena je ispred i unutar špilje (Slika 7.23). Najniža koncentracija i najmanje varijacije (396 ± 46 ppmv) izmjerene su na lokaciji 11, izvan špilje, koja odražava vanjsku atmosferu. Srednja vrijednost pCO_2 u atmosferi mjerena na Mauna Loa (Hawaii), koja se smatra referentnom globalnom vrijednošću, u razdoblju 2010. – 2011. je 390 ppmv. Lokacija s najvećim varijacijama je lokacija 07 (1578 ± 885 ppmv) gdje je najniža vrijednost od 750 ppmv izmjerena u ožujku 2010, a najviša od 2940 ppmv u rujnu 2010. Najmanje varijacije od lokacija unutar špilje izmjerene su na lokaciji 04 (783 ± 300 ppmv). Sve lokacije pokazuju slične sezonske varijacije, s najnižim vrijednostima pCO_2 u ožujku 2010. ili veljači 2011. (Slika 7.23.), a najvišima od kolovoza do listopada 2010. Srednja

vrijednost pCO_2 na lokacijama 01 – 04, 794 ± 31 ppmv, značajno je niža nego na unutarnjim lokacijama 05 – 09, 1180 ± 245 ppmv. Unutar špilje je pCO_2 viši nego izvan šplje zbog procesa isplinjavanja CO_2 iz prokapne vode, a različite vrijednosti na lokacijama unutar špilje posljedica su različitog intenziteta ventilacije.

Vrijednost $\delta^{13}C_{air}$ u špiljskom zraku na svim lokacijama pokazuje također izrazite sezonske varijacije (Slika 7.24). Najniže vrijednosti izmjerene su na svim lokacijama u rujnu 2010, i to od -21,64 ‰ (lokacija 07) do -18,39 ‰ (lokacija 01). Najviše $\delta^{13}C_{air}$ vrijednosti na svim lokacijama izmjerene su u veljači 2011. i to između -6,35 ‰ na lokaciji 04 i -13,19 ‰ na lokaciji 08. Najmanje varijacije izmjerene su na lokaciji 07, -18,0 ± 2,0 ‰, dok su najveće varijacije -14,6 ± 4,9 ‰ mjerene na lokaciji 10. Vrijednosti za $\delta^{13}C_{air}$ slične su za lokacije 01 – 04 (Slika 7.25), sa srednjom vrijednošću -13,2 ± 0,6 ‰, a drugu grupu čine lokacije 05 – 09 sa srednjom vrijednošću -16,7 ± 1,0 ‰. Lokacije bliže ulazu imaju pCO_2 bliži atmosferskom. Na lokaciji 09 razlog relativno niskom pCO_2 je blizina drugog ulaza (Stara apnenca). Lokacije 07 i 08 s najvišim vrijednostima pCO_2 izolirane su od turističkih posjeta i glavnog špiljskog prolaza, te ne podliježu izrazitom strujanju zraka.

Koncentracije ugljikovih izotopa ^{13}C i ^{14}C u špiljskom zraku nisu do sada bile sustavno proučavane. Vrijednosti $\delta^{13}C_{air}$ i aktivnosti ^{14}C u CO_2 u zraku pokazale su da su obje vrijednosti niže unutar špilje (-9,3 ± 0,2 ‰ i 102,6 ± 1,6 pMC) od vanjskih vrijednosti (-8,0 ± 0,2 ‰ i 109,5 ± 1,1 pMC) (Horvatinčić et al., 1998; Vokal, 1999). Razlika se objasnila isplinjavanjem CO_2 iz prokapne vode, ali daljnja kvantitativna analiza nije bila moguća jer pCO_2 nije bio mjeren.

Konstantno jednogodišnje praćenje pCO_2 od srpnja 2010. do srpnja 2011. provedeno je na lokaciji 03 (Slika 7.26, neobjavljeni podaci F. Gabrovšeka). Vidljive su sezonske varijacije: od studenog 2010. do svibnja 2011. trenutne vrijednosti pCO_2 su niže od srednje vrijednosti (600 ppmv), dok su više vrijednosti izmjerene u toplijem dijelu godine, a u rujnu 2010. su bile najviše (>1200 ppmv). Srednja vrijednost pCO_2, 600 ± 210 ppmv, se dobro slaže s vrijednošću iz ovog rada, 770 ± 320 ppmv, ako uzmemo u obzir preklapanje u samo jednom dijelu promatranog razdoblja i činjenici da podaci iz ovog rada predstavljaju točkaste podatke. Slike 7.24 i 7.25. prikazuju da izotopni sastav ugljika u špiljskom zraku varira obrnuto proporcionalno s pCO_2. Dobra korelacija (R = 0,72) nađena je između $1/pCO_2$ i $\delta^{13}C_{air}$ u zraku (Slika 7.27) i predstavlja mješanje ugljičnog dioksida iz dvaju izvora. U jednostavnom modelu mješanja CO_2 iz dvaju izvora pretpostavlja se da je atmosferski CO_2 s $\delta^{13}C_{air}$ = -7,8 ‰ i

koncentracijom od 398 ppmv jedan izvor, dok je drugi izvor izotopno lakši CO_2 nastao razgradnjom organske tvari. Model binarnog mješanja opisan je jednadžbom 7.1. $\delta^{13}C$ vrijednosti izvora izotopno lakšeg CO_2 iznose -23,3 ± 0,7 ‰, što se može vidjeti u tzv. Keelingovom grafikonu (Slika 7.27). Izotopni sastav ugljika ($\delta^{13}C$) organske tvari iz tla na dvije mjerne točke iznad Postojnske jame iznosi -26,7 ‰ (Vokal, 1999), što je u skladu s C3 grupom biljaka u području krša Hrvatske i Slovenije. CO_2 iz tla nastao raspadom organske tvari i respiracijom korijenja bilja pokazuje za 2 do 4 ‰ pozitivniju $\delta^{13}C$ vrijednost zbog frakcionacije i difuzije (Amundson et al., 1998). Srednji $\delta^{13}C$ ugljikovog dioksida iz tla iznad Postojnske jame je -21,7 ‰ i -20,5 ‰ (Vokal, 1999), dakle nekoliko promila pozitivniji nego $\delta^{13}C$ organske tvari. Može se zaključiti da povišenim koncentracijama špiljskog pCO_2 doprinosi isplinjavanje otopljenog CO_2 iz prokapne vode.

Na Slici 7.29 prikazan je odnos između izračunate koncentracije vodnog CO_2 i izmjerenih pCO_2 u špiljskom zraku na različitim lokacijama. Iako je koncentracija vodnog CO_2 visoka (i do 30 000 μatm) na lokacijama 01 – 04, pCO_2 u špiljskom zraku ne prelazi 1300 ppmv i ne ovisi o koncentraciji vodnog CO_2. To se može objasniti cirkulacijom zraka, odnosno ventilacijom na lokacijama blizu ulaza u špilju, pri čemu se CO_2 nastao isplinjavanjem odnosi zračnim strujama s mjesta nastanka. Na unutarnjim lokacijama 05 – 09 niža koncentracija vodnog CO_2 (<10 000 μatm) rezultira višim pCO_2 u zraku. Izmjerene su vrijednosti pCO_2 do 3000 ppmv i što je veći $pCO_2(aq)$, veći je i pCO_2 u špiljskom zraku. Ovakav rezultat objašnjava se neefikasnom špiljskom ventilacijom na unutarnjim lokacijama. U razdoblju visokog pCO_2 u špiljskom zraku proces isplinjavanja iz prokapne vode može biti usporen ili zaustavljen, čime bi bio zaustavljen i proces formiranja siga, odnosno arhiviranje izotopnih podataka u sigama. Odnos između I_{sat} i pCO_2 prikazan je na Slici 7.30. I_{sat} ima visoke vrijednosti na nižim pCO_2 kad je razlika u koncentracijama vodnog i atmosferskog CO_2 velika, te intenzivno isplinjavanje CO_2 dovodi do visokog I_{sat} i taloženja kalcita. Kada je pCO_2 u špiljskom zraku visok, isplinjavanje je sporije i I_{sat} je niži. No, I_{sat} postaje manji od 1 samo u rijetkim slučajevima, pa se može zaključiti da u Postojnskoj jami rijetko dolazi do prestanka taloženje karbonata.

Posebni slučaj lokacije 05 – Podrti kapnik

Lokacija 05 – Podrti kapnik je često spominjana kao iznimka u usporedbi s ostalim lokacijama. Ističe se po niskim koncentracijama kalcija i bikarbonata te niskoj provodnosti, dok je srednja vrijednost $\delta^{13}C_{DIC}$ u prosjeku za 2 ‰ pozitivnija nego na ostalim lokacijama. Ova odstupanja imaju za posljedicu da su različite korelacije između parametara dobre za

ostale lokacije, dok za lokaciju 05 to nije slučaj (Slike 6.6, 6.16, 7.9, 7.11, 7.13, 7.14, 7.15 i 7.16). Temperature zraka i vode, učestalost prokapljavanja, pH, koncentracija magnezija i $\delta^{18}O$ u prokapnoj vodi imaju slične vrijednosti kao na ostalim lokacijama. Neki od parametara prikazanih na Slici 6.6 pokazuju neobično ponašanje, tj. ponašaju se drugačije nego na ostalim lokacijama. Na primjer, u veljači 2011. izmjerena je neobično niska koncentracija kalcija i bikarbonata, dok je koncentracija magnezija nepromijenjena. Tada je izmjerena i vrlo niska provodnost, kao i niska učestalost prokapljavanja, niski $pCO_2(aq)$, visoki $\delta^{13}C_{DIC}$ i $\delta^{13}C_{air}$. Ovakve karakteristike prokapne vode objašnjene su procesom prethodnog taloženja u nekoj šupljini na koju je voda naišla na svom putu prema lokaciji 05. Ta se pojava naziva "*prior calcite precipitation*" (PCP). PCP se objašnjava taloženjem kalcita u šupljinama nadsloja špilje pri prolasku vode prema mjestu prokapljavanja. PCP je uočljiv kada je prokapljavanje slabog intenziteta i tada je vrijednost $\delta^{13}C_{DIC}$ u prokapnoj vodi 2 do 7 ‰ pozitivnija nego kada nema PCP-a (Fairchild i Treble, 2009).

Na lokaciji 05 je srednja vrijednost $\delta^{13}C_{DIC}$ (-9,9 ± 2,3 ‰) za 2,4 do 4 ‰ viša nego srednje vrijednosti na ostalim lokacijama (od -12,3 do -13,9 ‰) (Slika 7.15). Tu je najniža vrijednost $\delta^{13}C_{DIC}$ -11,78 ‰, a najviša -5,64 ‰, te je tako njihova razlika 6 ‰. Budući da u PCP dolazi samo do taloženja kalcita, koncentracija magnezija ostaje nepromijenjena, što dovodi do većeg omjera koncentracija magnezija prema kalciju. Slika 7.31 prikazuje odnos između $pCO_2(aq)$ i $\delta^{13}C_{DIC}$ za sva pojedinačna mjerenja. Unatoč vrlo velikom rasponu vrijednosti $pCO_2(aq)$ (400 – 30 000 μatm), $\delta^{13}C_{DIC}$ na svim ostalim lokacijama ima raspon od -11,8 do -14 ‰ i nema korelacije između tih veličina. Na lokaciji 05 niže vrijednosti $pCO_2(aq)$ imaju pridružene više $\delta^{13}C_{DIC}$ vrijednosti. Jedino u studenome 2010. $\delta^{13}C_{DIC}$ iznosi -11,78 ‰, što je usporedivo s podacima mjerenim na ostalim lokacijama, a tada je opažena visoka učestalost prokapljavanja kao posljedica obilnih oborina u rujnu, što znači da su šupljine u nadsloju bile ispunjene vodom i nije moglo doći do isplinjavanja i PCP-a. Na slici 7.32 prikazan je odnos između $\delta^{13}C_{DIC}$ i koncentracije bikarbonata u prokapnoj vodi. Koncentracija bikarbonata ima raspon od 160 do 370 mg/L, dok $\delta^{13}C_{DIC}$ varira od -14 do -12 ‰ na svim lokacijama osim 05 gdje je koncentracija bikarbonata niža, a $\delta^{13}C_{DIC}$ viši. Sniženje koncentracije bikarbonata uz istovremeno povišenje $\delta^{13}C_{DIC}$ vrijednosti je još jedan dokaz u prilog tezi o taloženju kalcita zbog isplinjavanja izotopno lakšeg CO_2 u šupljinama nadsloja.

Recentni karbonati

Slamčice i kalcit taložen na satnom staklu

Kao prvi korak u procjeni uvjeta izotopne ravnoteže, razlika između $\delta^{13}C_{DIC}$ i $\delta^{13}C$ karbonata (Δ, jednadžba 7.2) uspoređuju se s teorijskim frakcionacijskim faktorom ε za izmjerene temperature. U poglavlju 2.4 (Slika 2.4) pokazano je da frakcionacijski faktor ε ima vrijednost 2,2 ‰ na temperaturi ~10 ºC. Ako je $\Delta \approx \varepsilon$, može se zaključiti da se karbonat taložio u izotopnoj ravnoteži (Tablica 7.2). Vrijednosti Δ za slamčice su samo na lokacijama 03 i 07 približno jednake ravnotežnom frakcionacijskom faktoru ($\varepsilon < \Delta < 3$ ‰), a na svim ostalim lokacijama $\Delta > 3$ ‰. Za karbonate taložene na satnom staklu vrijedi $\Delta < \varepsilon$ zbog brzog, gotovo trenutnog taloženja karbonata. Temperature izračunate prema jednadžbama tipa A (Tablica 3.1) su puno niže od izmjerenih temperatura (Slika 7.35) i ne ovise značajno o primijenjenoj jednadžbi. Izračunate temperature su usporedive s izmjerenima samo na lokaciji 06. Prema jednadžbama tipa B (Tablica 3.1) izračunate su vrijednosti frakcionacijskog faktora α. Vrijednosti α su za sve karbonate sa satnih stakalaca veće od ravnotežne vrijednosti α_{eq} za danu temperaturu, što odgovara opažanju da su izračunate temperature niže od izmjerenih. To vrijedi i za uzorke slamčica sa svih lokacija osim sa lokacije 06 (Tablica 7.4).

Uzorci siga neobičnog rasta sa lokacija 01 i 09 pokazuju različite promjene u $\delta^{13}C$ i $\delta^{18}O$ (Slika 6.17). Na lokaciji 01 povišene su i $\delta^{13}C$ i $\delta^{18}O$ vrijednosti zbog intenzivne cirkulacije zraka, te je $\Delta > \varepsilon$ (Tablica 7.6) i $\alpha > \alpha_{eq}$ (Tablica 7.4), a izračunate temperature (tip A) niže su od izmjerenih. Na lokaciji 09 vrijednost Δ ne ukazuje na ravnotežne uvjete, ali zbog načina taloženja koji utječe samo na obogaćenje u ^{13}C dok $\delta^{18}O$ ostaje nepromijenjen, na ovoj lokaciji vrijedi $\alpha \approx \alpha_{eq}$ (Tablica 7.4), a izračunata temperature je usporediva s izmjerenom (Tablica 7.6).

Uzorci starih karbonata

Izotopni sastav starih siga uspoređuje se s ravnotežnim frakcionacijskim faktorima (α, ε) na isti način kao kod recentnih karbonata. Treba napomenuti da su te sige nastajale tijekom dugog razdoblja u kojemu je moglo doći do promjena u temperaturi i vegetaciji. Vrijednosti Δ za sigovinu (Tablica 7.7) veće su od očekivanih za ravnotežne uvjete, što ukazuje na taloženje u kinetičkim uvjetima. Izračunate temperature jednadžbama tipa A (Tablica 3.1) su dosta niže od izmjerenih temperatura u špilji (Tablica 7.7), a sukladno tome vrijedi $\alpha > \alpha_{eq}$. Procjena

ravnotežnih uvjeta taloženja karbonata napravljena je i za stalaktite za koje je $\Delta > \varepsilon$ na svim lokacijama (Tablica 7.8) ukazujući na neravnotežne uvjete taloženja stalaktita. Izračunate temperature jednadžbama tipa A (Tablica 3.1) su puno niže od izmjerenih temperatura, a sukladno tome vrijedi $\alpha > \alpha_{eq}$ (Slika 7.38).

Vrijednosti Δ vrijednosti za bušene jezgre stalagmita imaju širok raspon, od 2,6 do 11,4 ‰, a prosječne vrijednosti za svaku jezgru su veće od ε (Tablica 7.9). Temperature izračunate jednadžbama tipa A su znatno niže od izmjerenih za stalagmite s lokacija 07 i 08, za koje je i $\alpha > \alpha_{eq}$ (Slika 7.38). Za stalagmit s lokacije 06 vrijedi $\alpha \approx \alpha_{eq}$, a izračunate temperature su usporedive s današnjima.

Na osnovi svih prikazanih rezultata može se napraviti pregled okolišnih i izotopnih uvjeta na svakoj lokaciji u Postojnskoj jami te provjeriti jesu li ti uvjeti sukladni preduvjetima za taloženje karbonata u izotopnoj ravnoteži. Tablica 7.10 prikazuje pregled takvih uvjeta. Gotovo sve lokacije u špilji (osim lokacije 01 najbliže ulazu) zadovoljavaju uvjet konstantne temperature i visoke relativne vlažnosti zraka. Na lokacijama bliže ulazu u špilju opaženo je jače strujanje zraka koje može uzrokovati kinetičke efekte izotopne frakcionacije tijekom taloženja karbonata iz prokapne vode. Na lokacijama udaljenijim od ulaza i/ili izoliranima od zračnih strujanja izmjerene su sezonske varijacije pCO_2 i I_{sat}. Na većini lokacija $\delta^{18}O$ prokapne vode ima konstantnu vrijednost tijekom godine s vrlo malim varijacijama.

Usporedba izotopnog sastava ^{13}C u DIC-u i istaloženom karbonatu može ukazivati na postojanje ravnotežnih izotopnih uvjeta ako je razlika $\Delta = \delta^{13}C_{carb} - \delta^{13}C_{DIC}$ usporediva s ε (ravnotežnim frakcionacijskim faktorom). Taj je uvjet ($\Delta \sim \varepsilon$) zadovoljen samo djelomično za recentne karbonate "slamčice" s dvije lokacije (03 i 07), dok za sve ostale vrste karbonata nije ispunjen. Unatoč tome, temperature taloženja izračunate iz $\delta^{18}O$ prokapne vode i karbonata primjenom različitih paleotemperaturnih jednadžbi barem približno odražavaju srednje temperature na unutrašnjim (07, 08, 09) i izoliranim lokacijama (02). Na lokaciji 06 – Stebrišče izračunata temperatura taloženja recentnog karbonata odgovara izmjerenoj temperaturi, kao i na lokaciji 09 – Zgornji Tartar.

VIII. ZAKLJUČAK

Cilj ovog rada bio je istražiti postojanje uvjeta izotopne ravnoteže u procesu formiranja siga u Postojnskoj jami, te pokazati mogućnost korištenja izotopnog sastava kisika, $\delta^{18}O$, u sigama za primjenu u paleoklimatskim studijama. Sukladno modernom pristupom istraživanja nastajanja siga, koji zahtijeva utvrđivanje sadašnjeg stanja geokemijskih i izotopnih uvjeta taloženja karbonata tijekom jednog hidrološkog ciklusa na nekoliko lokacija unutar iste špilje, provedeno je praćenje raznih parametara na 11 lokacija u Postojnskoj jami, Slovenija, u razdoblju od ožujka 2010. do travnja 2011. godine. Jedna od lokacija bila je izvan špilje kako bi se dobile referentne vanjske vrijednosti.

Glavni zaključci ovog interdisciplinarnog i sveobuhvatnog istraživanja geokemijskih i fizičkih uvjeta okoline su:

- Temperatura zraka u Postojnskoj jami (10,6 ± 0,7 °C, srednja vrijednost na svim lokacijama) je približno jednako srednjoj temperaturi vanjskog zraka izmjerenoj na meteorološkoj postaji tijekom posljednjih 6 godina (9,9 ± 0,4 °C). Temperatura prokapne vode (10,4 ± 0,8 °C, srednja vrijednost na svim lokacijama) odgovara temperaturi zraka.
- Prema kemijskom sastavu, sve prokapne vode pripadaju istoj vrsti voda ($Ca - HCO_3$). Prema učestalosti prokapljavanja sve prokapne vode pokazuju karakteristike curenja (*seepage flow*). Vrijednosti $\delta^{18}O$ prokapne vode kreću se između -10 i -8 ‰, bez izrazitih sezonskih varijacija. Procijenjeno vrijeme zadržavanje vode je od nekoliko mjeseci do nekoliko godina, ovisno o lokaciji.
- pCO_2 u špiljskom zraku pokazuje sezonske varijacije s višim koncentracijama u kasno ljeto i ranu jesen. Varijacije su izraženije na lokacijama udaljenijim od ulaza nego na lokacijama blizu ulaza, podložnijim cirkulaciji zraka. Sezonske varijacije u pCO_2 praćene su sezonskim varijacijama u izotopnom sastavu ugljika u zraku $\delta^{13}C_{air}$: što je viši pCO_2, to su niže vrijednosti $\delta^{13}C_{air}$. Dobra korelacija između pCO_2 i $\delta^{13}C_{air}$ pokazuje da je „suvišak“ CO_2 u špiljskom zraku rezultat isplinjavanja CO_2 porijeklom iz tla s vrijednošću $\delta^{13}C = -23,3 \pm 0,7$ ‰.
- Lokacije 01 – 04 blizu ulaza u špilju u nekim se karakteristikama razlikuju od udaljenijih lokacija 06 – 09. Na vanjskim lokacijama opažena je viša provodnost, više koncentracije Ca^{2+}, Mg^{2+} i HCO_3^-, niže temperature zraka i prokapne vode, niži pCO_2 i više vrijednosti $\delta^{13}C_{air}$, viši $pCO_2(aq)$ i više učestalosti prokapljavanja. Razlike se mogu objasniti višim koncentracijama CO_2 u tlu iznad lokacija 01 – 04, što ima za posljedicu intenzivnije otapanje karbonata iz

stijena, kao i izraženijom cirkulacijom zraka (ventilacijom) na lokacijama bliže ulazu. Lokacije se ne mogu grupirati prema vrijednostima $\delta^{18}O$ u prokapnoj vodi, srednjem vremenu zadržavanja vode, omjeru koncentracija Mg/Ca i vrijednostima $\delta^{13}C_{DIC}$.

- Lokacija 05 – Podrti kapnik se razlikuje od drugih lokacija po nižim koncentracijama kalcijevih iona i bikarbonata, kao i po nižoj provodnosti, dok je $\delta^{13}C_{DIC}$ vrijednost viša. Te razlike ukazuju na pojavu taloženja kalcita u šupljinama nadsloja tijekom prolaska vode kroz nadsvod špilje (PCP – *prior calcite precipitation*). Ostali mjereni parametri (temperatura vode i zraka, učestalost kapanja i $\delta^{18}O$ prokapne vode, pH i koncentracija magnezijevih iona, pCO_2 i $\delta^{13}C$ špiljskog zraka) ne pokazuju razlike u usporedbi s ostalim lokacijama.
- Vrijednosti $\delta^{13}C$ modernih „slamčica“ pokazuju varijacije od -10,6 do -7,8 ‰, a $\delta^{18}O$ od -7,8 do -4,8 ‰. Vrijednosti $\delta^{13}C$ karbonata taloženog na satnim staklima niže su za oko 2‰ od vrijednosti $\delta^{13}C$ slamčica i slične vrijednostima $\delta^{13}C_{DIC}$, dok su $\delta^{18}O$ vrijednosti više. Takve su vrijednosti objašnjene brzim, gotovo trenutnim taloženjem karbonata na satnim staklima pri čemu izotopni sastav karbonata odražava izotopni sastav $\delta^{13}C$ i $\delta^{18}O$ DIC-a.
- Vrijednosti $\delta^{13}C$ modernih karbonata uspoređene su s ravnotežnim frakcionacijskim faktorom ε kako bi se utvrdilo je li do taloženja došlo u izotopnoj ravnoteži. Razlika $\Delta = \delta^{13}C_{carb} - \delta^{13}C_{DIC}$ je za većinu uzoraka slamčica veća od ε, a samo nekoliko uzoraka slamčica sa lokacija 03 i 07 ima Δ vrijednosti usporedive s ε ukazujući na izotopnu ravnotežu. Vrijednosti Δ za sve karbonate taložene na satnom staklu su niže od ε.
- Na osnovi vrijednosti $\delta^{18}O$ vode i karbonata, izračunata je temperatura taloženja karbonata i frakcionacijski faktor α primjenom različitih paleotemperaturnih jednadžbi. Izračunate temperature su općenito niže od izmjerenih temperatura i slabo ovise o primijenjenoj jednadžbi. Izračunati faktor α je sukladno tome viši od vrijednosti ravnotežnog frakcionacijskog faktora α_{eq} ukazujući na nepostojanje ravnotežnih uvjeta taloženja. Izračunate temperature se slažu s mjerenima i vrijednost α je usporediva s α_{eq} samo za uzorke slamčica s lokacije 06 – Stebrišče.
- Za dvije skupine uzoraka čudnovatog rasta izračunate vrijednosti Δ su veće od ε ukazujući na neravnotežne izotopne uvjete taloženja. Izračunata temperature na lokaciji 01 – Slonova glava je čak 12 ºC niža od izmjerene temperature vjerojatno zbog brzog isplinjavanja CO_2 uslijed intenzivne cirkulacije zraka na lokaciji blizu ulaza u špilju. Izračunata temperatura na lokaciji 09 – Zgornji Tartar je usporediva s mjerenom temperaturom (10,7 ± 0,7 ºC), a vrijedi i $\alpha \approx \alpha_{eq}$. Čudnovati oblici na ovoj lokaciji vjerojatno nastaju sporim

isplinjavanjem CO_2 koje uzrokuje obogaćenje karbonata u $\delta^{13}C$, dok $\delta^{18}O$ ostaje nepromijenjen zbog čega je $\Delta\delta^{13}C/\Delta\delta^{18}O$ visok.

- Vrijednosti Δ za sigovine, stalaktite i bušene jezgre stalagmita veće su od ε, što znači da se karbonat taložio pod kinetičkim uvjetima. Ove vrste siga su taložene tijekom dužeg vremenskog razdoblja u kojem se temperatura mogla mijenjati, kao i vegetacija u tom području. Izračunate temperature taloženja ne odgovaraju današnjim izmjerenim temperaturama, ali se zaključak o promjeni temperature u prošlosti ne može izvesti ako nije pokazano da se danas taloženje karbonata odvija u uvjetima izotopne ravnoteže.

Cilj ovog istraživanja bio je odrediti dijelove Postojnske jame u kojima bi se mogla provesti buduća paleoklimatska istraživanja primjenom mjerenja sadržaja stabilnih izotopa ugljika i kisika. Promatrane veličine (temperatura, vlažnost, cirkulacija zraka, vrijednosti $\delta^{18}O$ prokapne vode) ukazuju na zadovoljavanje okolišnih preduvjeta za taloženje karbonata u izotopnoj ravnoteži, pogotovo na unutrašnjim lokacijama, tj., lokacijama udaljenima od ulaza. Međutim, izotopni sastav karbonata, $\delta^{13}C$ i $\delta^{18}O$, ne ukazuje na izotopno ravnotežno taloženje na većini promatranih lokacija. To se pogotovo odnosi na ulazni dio Postojnske jame u kojem je opažena cirkulacija zraka, odnosno provjetravanje. Temperature taloženja karbonata izračunate iz mjerenih vrijednosti $\delta^{18}O$ prokapne vode i istaloženog karbonata primjenom različitih paleotemperaturnih jednadžbi ne odgovaraju izmjerenim temperaturama, već su dosta niže. Sukladno tome, izračunate vrijednosti frakcionacijskog faktora α znatno su veće od ravnotežne vrijednosti α_{eq}. Izračunate temperature su usporedive s mjerenima, te vrijedi $\alpha \approx \alpha_{eq}$, samo za uzorke čudnovatih oblika na lokaciji 09 i za slamčice na lokaciji 06. Stoga se zaključuje da jedino lokacije 06 – Stebrišče i 09 – Zgornji Tartar pokazuju potencijal za buduća paleoklimatska istraživanja.

Osim ovog glavnog zaključka koji odgovara cilju istraživanja prikazanog u ovom radu, mogu se izvesti još sljedeći važni zaključci:

- Razlike u kemijskom i izotopnom sastavu prokapne vode na lokaciji 05 – Podrti kapnik u odnosu na prokapne vode s drugih lokacija objašnjene su pojavom prethodnog taloženja kalcita u šupljinama nadsvoda špilje, tzv. procesom PCP (*prior calcite precipitation*). Taj je proces često opisan u recentnoj literaturi u različitim špiljskim sustavima, ali dosad još nije opisan i dokazan u Dinarskom kršu.

- Recentni karbonati istaloženi na satnim stakalcima ne odražavaju izotopni sastav siga na danoj lokaciji, pa se ova vrsta umjetne podloge (satna stakla) ne mogu koristiti u proučavanju suvremenih uvjeta taloženja karbonata u špiljama.
- Različite raspodjele vrijednosti $\delta^{13}C$ i $\delta^{18}O$ u dubinskim profilima bušenih jezgri stalagmita s tri lokacije pokazuju da izotopni sastav siga može odražavati i promjene u okolišnim uvjetima špilje, a ne samo promjene temperature. Zaključeno je da je za paleoklimatska istraživanja potrebno pronaći i analizirati više stalagmita slične starosti i slične izotopne raspodjele kako bi se izmjereni izotopni podaci mogli interpretirati kao pouzdani zapisi paleotemperaturnih i paleookolišnih uvjeta i njihovih promjena.

Daljnja istraživanja

- Sustavno prikupljanje mjesečnih oborina sa ciljem određivanja izotopnog sastava vodika (δ^2H) i kisika ($\delta^{18}O$) radi definiranja lokalne linije oborinske vode (LMWL) na području Postojne. Također bi trebalo detaljnije odrediti vrijeme zadržavanja prokapnih voda u nadsvodu jame.
- Kontinuirano praćenje špiljskih uvjeta okoliša (pCO_2, prokapne vode, temperature zraka i vode te vlažnost) na više lokacija u špilji.
- Nastaviti eksperiment s taloženjem karbonata na umjetnim predlošcima. Trajanje eksperimenta trebali bi prilagoditi praćenju sezonskih promjena u taloženju karbonata. Lokacije na kojima bi trebalo nastaviti s praćenjem su unutarnje lokacije s višim varijacijama pCO_2.
- Mineraloška i kristalografska istraživanja različitih vrsta špiljskih karbonata.
- Datiranje profila starih siga U-Th metodom.
- Na nekoliko lokacija odrediti aktivnost ^{14}C modernih siga radi određivanja početne aktivnosti ^{14}C, i time omogućiti ^{14}C datiranje siga mlađih od 50 000 godina.
- Odrediti koncentracije elemenata u tragovima, s posebnim naglaskom na magnezij i stroncij (Mg-Sr) u prokapnim vodama i sigama. Informacije o njihovim udjelima koriste se kao dodatni alat u paleoklimatskim istraživanjima.
- Pratiti koncentraciju radona od ulaza do unutrašnjosti i usporediti s pCO_2 na istim lokacijama radi potpunijeg razumijevanje kruženja zraka u jami.
- Usporediti $\delta^{18}O_{carb}$ u Postojni s nekim drugim špiljama u regiji (Austrija, Italija i Hrvatska) radi povezivanja spoznaja o klimatskim promjenama na regionalnoj i globalnoj razini.

1 INTRODUCTION

1.1 Scope of the thesis

Interest in speleothem (secondary cave carbonates) as recorders of past climate started during 1960's and 1970's with pioneering works of Broecker et al. (1960), Hendy and Wilson (1968), Dupplessy et al. (1970), Emiliani (1971) and Hendy (1971). As the basic assumption for a possible use of $\delta^{18}O$ of speleothems served an observation that cave environments are quite stable and reflect the mean annual temperature of the region. The number of studies, which involved speleothems and other secondary carbonate deposits as records of past climatic and environmental changes, has increased dramatically during the last two decades (Frisia et al., 2003; Wang et al., 2004; McDermott, 2004; Wang et al., 2005; Griffiths et al., 2009; Cheng et al., 2009). Study of a climate archives, i.e. natural systems being capable of environmental information storage, from all over the globe allows to resolve spatial and temporal distributions of former climate changes (Andrews et al., 1994; Dorale et al., 1998; Burns et al., 2001; Johnson et al., 2001; Cheng et al., 2009).

The interest has been underpinned by analytical advances in microanalytical techniques (Spötl and Mattey, 2006). Sampling and measurement techniques enable extraction of high-resolution records from samples of sufficient growth rate, providing results for intra-annual variability in proxy data to be characterized (eg. Johnson et al., 2006; Mattey et al., 2008), and this is coupled with the dating results (e.g. Fairchild, 2000; Horvatinčić et al., 2000; Cheng et al., 2009). Generally, speleothems are deposited slowly by degassing of drip water in caves (Dreybrodt, 2008), where drip water represents average characteristics of meteoric water (precipitation). Most studies utilize stalagmites, rather than stalactites or flowstones, because of their geometry, relatively rapid growth rates, and their tendency to precipitate in isotope equilibrium with the cave drip water. However, the increased number of related studies of

environmental cave conditions revealed spatial and time variations even within the same cave, and resulted in modern approach to speleothem studies that starts with monitoring of environmental, geochemical and isotopic parameters within each specific cave (Spötl et al., 2005; Baldini et al., 2006; Mattey et al., 2010; Surić et al., 2010; Tremain et al., 2011). Due to specific climate conditions, signals from drip water are not transmitted to speleothem in a straightforward manner. Signals are often site-specific due to the karst hydrology and the host cave environment (Fairchild et al., 2000; Spötl et al., 2005; Mattey et al., 2010). Recent research has emphasized the need to understand these sources of signal modification prior to retrieving and interpreting proxy data (Fairchild et al., 2000; Baldini et al., 2008; Mattey et al., 2010; Morandi et al., 2010). Moreover, oxygen isotope records from stalagmites reflect a range of atmospheric phenomena, which affect the isotopic composition of the rainfall received at a given cave site (Baldini et al., 2010). With better understanding of the processes responsible for conveying climate signals to speleothem, and with continuing refinements to methodologies, proxy data from speleothem will be suitable for integration to general picture.

Therefore, when exploring the possibility of the use of speleothem in paleoclimatic research, according to modern approach, one must study: 1) the existence of equilibrium isotope effects in speleothem deposition (for modern speleothem as well as for ancient), 2) cave environment conditions of the speleothem deposition, 3) drip water chemistry, and 4) drip water isotopic composition and its relation to isotopic composition of precipitation (i.e., determine $\delta^{18}O$ – climate calibration). Under equilibrium conditions, the $\delta^{18}O$ value of speleothem carbonate is related to two parameters only: the $\delta^{18}O$ of drip water and the cave temperature. If equilibrium deposition is documented in modern speleothems for present-day conditions, then the assumption is made that fossil/old speleothem material in the same cave was also deposited under equilibrium conditions. Meaningful paleoclimatic information can only be retrieved from speleothem calcite deposited under conditions of isotopic equilibrium (Fairchild et al., 2007 and references therein).

The study described in this work presents the comprehensive and extensive scientific investigation of speleothem formation using stable isotopes of carbon and oxygen that is conducted in Postojna Cave, the largest known cave in Europe and most visited cave in Slovenia. The aim of the study is to elucidate our understanding about how the stable isotope composition of speleothems, i.e. deposited carbonate, is influenced by variety of environmental factors (temperature, airflow, humidity and concentration of cave-air CO_2), chemical and isotopic composition of the drip water, and the isotopic composition of CO_2. At

nine locations one year monitoring was conducted in order to determine areas with the environmental conditions eligible for carbonate deposition in past and recent times. The selection of the nine micro locations in Postojna cave was based on assumption that some of them have stable environmental conditions for carbonate precipitation. Assessment of locations suitable for reconstruction of paleoclimate is done based on monitoring results, statistical analysis and application of paleotemperature equations.

Relationships between various measured parameters will be shown. For example, the dependence of temperature and concentration of CO_2 in the cave air on distance from the entrance, or the dependence of isotopic composition of different types of carbonate samples on isotopic composition of dissolved inorganic carbon in water samples. Knowledge of isotopic composition of carbonates, water and cave air will allow the assessment of process (equilibrium or kinetic) of precipitation for modern carbonates, which can be done in several ways.

1. Temperature of carbonate precipitation can be calculated in terms of isotopic equilibrium based on the isotopic ^{18}O composition of carbonate and water. Several equations described in literature will be applied (Epstein and Mayeda, 1953; Craig, 1965; Schackleton, 1974; Grossman, 1982; Mulitza et al., 2003; Leng and Marshall, 2004; Andrews et al., 1994; 1997). If the calculated and measured temperatures are equal or at least similar, it may be concluded that carbonate precipitation occurs under equilibrium conditions.

2. Fractionation factor (α) for ^{18}O will be calculated from the measured values of $\delta^{18}O$ in water and carbonate. Obtained α value will be compared with the theoretical value of the fractionation equilibrium factor α_{eq} for the measured temperature (O'Neil et al., 1969; Friedman and O'Neil, 1977; Kim and O'Neil, 1997; Kim et al., 2007; Coplen, 2007; Horita and Clayton, 2007; Chacko and Deines, 2008; Tremaine et al., 2011).

3. Measured difference in $\delta^{13}C$ in DIC and carbonate will be compared with the theoretical fractionation ε value for measured temperature.

If all the approaches indicate equilibrium condition of carbonate precipitation, one can conclude that the speleothems from monitored location may be used in paleoclimate research.

1.2 Outline of the thesis

The main part of this thesis is based on stable isotope composition of speleothems and various other materials related to speleothem formation. This specific field has some characteristic

definitions and quantities, therefore the next chapter (2. Stable isotopes) contains basic data on stable isotopes in general, gives definitions of specific quantities and symbols (e.g., δ, ε and α values), presents distribution of carbon isotope ^{13}C and oxygen isotope ^{18}O in natural environment, and describes the mass spectrometric measurement technique.

Chapter 3 (Literature overview) presents the overview of karst area research, especially studies of cave environmental conditions with emphasis on speleothem formation and various approaches of determination of temperature of speleothem formation, i.e. the use of speleothems as paleothermometers. The results of previous investigations performed in the Postojna Cave are also presented.

The following Chapter 4 (Site description) describes the study area – its geology and climatic characteristics of both the external area and the cave interior related to this study. Chapter 5 describes characteristics of sampling sites, field measurements and sampling procedures, as well as laboratory measurements and data handling.

Chapter 6 (Results) contains results of cave monitoring and laboratory measurements with addition of descriptive statistics. Discussion of the results, relations between different environmental parameters, as well as comparison of various cave locations, is presented in Chapter 7 (Discussion). A special case of location Podrti kapnik is discussed. Stable isotope composition of speleothems is compared with the equilibrium fractionation factors for both $\delta^{13}C$ and $\delta^{18}O$ values. The temperature of deposition of various types of modern speleothems, including carbonate precipitated on watch glasses, is calculated according to various approaches and compared to the measured temperature. Measured $\delta^{13}C$ values of all types of carbonates and of the corresponding DIC are compared with the equilibrium fractionation ε value, while measured $\delta^{18}O$ values of drip water and carbonates are used for determination of fractionation factor α, which is then compared with the equilibrium α_{eq} value. Discussion on isotope composition of old speleothems (stalactites, flowstone and drilled speleothem cores) is also presented, but interpretation about climate changes is not attempted. An assessment of equilibrium isotopic composition at different locations in the Postojna Cave is given at the end of Chapter 7. Various environmental parameters (temperature, humidity, air circulation) and characteristics of drip waters (drip rate, saturation index, isotopic composition of drip water) that contribute to isotopic equilibrium deposition are compared with the requirements for establishment of equilibrium conditions.

Finally, conclusions are summarized in Chapter 8. The main conclusion refers to determination of locations within Postojna Cave where carbonate precipitation occurs under isotopic equilibrium conditions. However, the obtained data presented in this work has lead to several additional important conclusions which are also presented. At the end of the thesis references are given.

Throughout the thesis, figure and table captions are written in both English and Croatian language.

Appendix I contains numerical data from field and laboratory measurements, calculated chemical parameters, correlation matrix between different geochemical and isotopic parameters for each location, and data on stable isotope composition of all measured samples (water, carbonates, and air). There are also tables containing data from National Meteorological Service of Slovenia (meteo.si), data of isotopic composition of precipitation obtained from the Jožef Stefan Institute, Ljubljana, and the permission for speleothem sampling obtained from the Institute for Nature Conservation of the Republic of Slovenia. Appendix II presents photographs from investigated locations and sampling field trips.

2 STABLE ISOTOPES

2.1 Isotopes

Experiment of Thomson (1897) showed that measurement charge to mass (q/m) ratio is constant number. Rutherford (1911) has concluded that atoms have small (ca. 10^{-14} m) but massive and positively charged nucleus, surrounded by spherical electron cloud ca. 10^{-10} m in diameter and Chadwick (1932) confirmed existence of a neutron. All these findings lead to the definition of isotopes as atoms of the same element containing the same number of protons but different number of neutrons (Beiser, 1973).

Number of protons in an atom is called atomic number (Z) and is equal to the number of the electrons surrounding the nucleus. The sum of protons and neutrons (N) in nucleus is called mass number (A):

$$A = Z + N \qquad 2.1$$

With these numbers the nucleus of each element (X) can be described as ${}^{A}_{Z}X_{N}$.

Two groups of isotopes can be distinguished regarding the stability of their nuclei: stable and unstable (radioactive). After some time nucleus of radioactive isotope starts to decay spontaneously and the decay is characterized by the half-life specific for each radioactive isotope. Stable nuclide has never been observed to decay against the natural background. In other words, these elements have half-lives too long to be measured by any means, direct or indirect. As of December, 2010, there were a total of 253 known "stable" nuclides. Stable isotopes of oxygen, carbon, nitrogen, hydrogen and sulfur have been under investigation for many years in order to study processes of isotope fractionation in natural systems (Emiliani, 1971; Hendy, 1971; Schwarcz, 1986; Harmon et al., 1978; Lauritzen and Lundberg 1999; Fleitmann et al., 2008). Advances in mass spectrometry techniques (i.e. multiple-collector inductively coupled plasma mass spectrometry techniques (MC ICP-MS), secondary

ionization MS (SIMS), laser-related MS systems, fast atom bombardment MS (FAB-MS) or nuclear activation analysis (NAA)) now enable the measurement of heavier stable isotopes, such as iron, copper, zinc, molybdenum, strontium etc. (de Groot, 2009). Stable isotopes are herein studied in more detail, especially stable isotopes of oxygen and carbon.

The stability of the nucleus can be described by the symmetry rule and by the Oddo-Harkins rule (Petrucci et al., 2007). The symmetry rule states that nuclei with low atomic number Z have approximately the same the number of protons as the number of neutrons. In the case of high Z the electrostatic Coulomb repulsion force is also raising. Stability is maintained with raising number of neutrons in nucleus (Figure 2.1). The Oddo-Harkins rule claims that more abundant are nuclides of even atomic number then those with odd atomic numbers (Figure 2.1) (Olmsted III and Gregory, 2006).

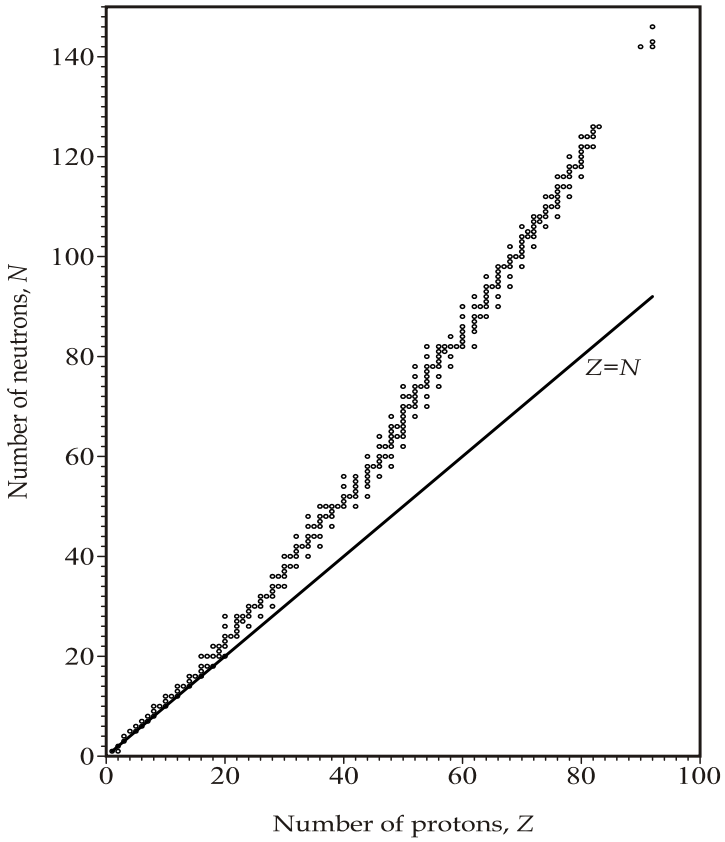

Figure 2.1 Relation between number of protons, Z, and number of neutrons, N, in nuclei. Dots present band of stable nuclei in nature.

Slika 2.1 Odnos broja protona, Z, i broja neutrona, N, u jezgrama. Stabilne jezgre (točke) nalaze se u području oko tzv. linije stabilnosti.

Table 2.1 Types of Z-N combinations of stable nuclides and their numbers of occurrence

Tablica 2.1 Moguće kombinacije broja protona, Z, i broja neutrona, N, u stabilnim jezgrama, te njihova učestalost

Z – N combination	Number of stable nuclides
Even – even	160
Even – odd	56
Odd – even	50
Odd – odd	5

2.2 Abundance and delta value

Each specimen in natural environment has its characteristic isotopic signature, and therefore can be used as a natural tracer. The principal isotopes in environmental investigation are those of elements occurring in hydrological, geological and biological systems (Clark and Fritz, 1997; Criss, 1999), namely oxygen, hydrogen, nitrogen, carbon and sulphur. Natural abundances of their stable isotopes are presented in Table 2.2.

Table 2.2 Natural abundances of environmental stable isotopes

Tablica 2.2 Prirodna zastupljenost nekih stabilnih izotopa iz okoliša

Element	Symbol	Abundance (%)
Hydrogen	^{1}H	99.988
	^{2}H (D)	0.115
Carbon	^{12}C	98.892
	^{13}C	1.108
Nitrogen	^{14}N	99.632
	^{15}N	0.368
Oxygen	^{16}O	99.759
	^{17}O	0.037
	^{18}O	0.204
Sulphur	^{32}S	94.93
	^{33}S	0.76
	^{34}S	4.29
	^{36}S	0.02

With mass spectrometry analytical techniques isotope ratio R is determined. Ratio of isotopes (R) is defined as the ratio of abundances of a heavier and a lighter, usually most abundant, isotope, i.e. as the ratio of rare to common isotope:

$$R \equiv \frac{\text{abundance of heavy isotope}}{\text{abundance of light isotope}} \qquad 2.2$$

This ratio usually contains information about processes and sources in physical and chemical environment of observed specimen. Because of small absolute abundance of each isotope in particular material, the composition of stable isotopes is expressed as relative difference of the ratios R of the sample and the reference (McKinney et al., 1950; Epstein and Mayeda 1953). Therefore a new quantity is introduced and it is called the delta (δ) value. It is defined as a relative difference of isotopes ratios R in a sample and in the international standard.

$$\delta_{\text{sample-standard}} = \frac{R_{\text{sample}} - R_{\text{standard}}}{R_{\text{standard}}} \qquad 2.3$$

The δ value is expressed in per mil (‰), and positive values mean that the sample is enriched with heavier isotope with respect to the standard (Coplen et al., 2002).

The reasons for reporting stable isotope composition in terms of relative δ values instead of absolute R values can be found in different fields dealing with stable isotopes:

a) A measurement technique allows high sensitivity of very low natural abundances.
b) International and inter-laboratory measurement of the same sample have to be mutually comparable
c) Because of low natural abundances of rare isotopes, the numbers of reported ratios R would have five to six digits
d) Absolute ratios R are less important than the changes in ratios during phase transitions

2.3 Fractionation

Isotope fractionation is enrichment of one isotope relative to another in a chemical or physical process. Two isotopes of an element have different masses but equal chemical properties. Chemical properties are determined by the number of electrons. However, subtle chemical effects do result from the difference in mass of isotopes. Isotope fractionation is a consequence also of physical processes, such as evaporation, condensation and transpiration. Process of photosynthesis also causes isotope fractionation (Mickler et al., 2006; Wiedner et al., 2008).

Cause of fractionation can be found in thermodynamic and quantum mechanical properties of molecules with different masses, i. e. different binding energy.

Translational kinetic energy E_k of a molecule with mass m is determined by thermodynamic temperature T as:

$$E_k = \frac{3}{2}kT \qquad 2.4$$

where k is the Boltzmann constant. Root-mean-square particle velocity v_{rms} is then given by:

$$v_{rms} = \sqrt{\frac{3kT}{m}} \qquad 2.5$$

Obviously, heavier molecules in a mixture will have lower diffusion velocity. Collision frequency, which is the primary condition for chemical reaction rate, is therefore also lower for heavier molecules, i.e. these molecules react slower.

Quantum mechanical process of fractionation arises from molecular binding energies. Interaction of two atoms in diatomic molecule can be represented by potential energy curve like Morse potential (Morse, 1929; Herzberg, 1950) shown in Figure 2.2. This potential is of great importance in theoretical considerations, although real potentials may slightly differ in shape. The equilibrium distance r_e is internuclear distance value defined by the minimum E_w of potential well (Figure 2.2). However, diatomic molecule is a quantum mechanical system and cannot be hold in this position. It rather vibrates around the equilibrium position, even at absolute zero temperature T_0. Such system can only have specified discrete values of total energy in bound state that can be obtained by solving the Schrödinger equation for a given system. For simplicity in finding properties of a ground state, the Morse potential can be approximated by the harmonic potential, for which the Schrödinger equation can be exactly solved, giving the term

$$E_0 = \frac{\hbar}{2}\sqrt{\frac{k}{\mu}} \qquad 2.6$$

for ground state energy, measured from the potential energy minimum. Here, ħ is reduced Planck's constant, $\underline{k}$ is interaction constant (analog to strength of string holding two balls at equilibrium distance), and μ is the reduced mass of the system:

$$\mu = \frac{m_1 m_2}{m_1 + m_2} \qquad 2.7$$

Reduced mass in system with two equal m_0 masses, like H_2 molecule, is then given by $\mu(H_2) = m_0/2$. If one of the H atoms is replaced by heavier isotope, deuterium (D), having mass $2m_0$ then reduced mass becomes larger, $\mu(HD) = 2\ m_0/3$, which in the same interaction frame

causes lowering of the energy level of bound state ($E'_0 < E_0$) defined by eq. 2.6. Lower energy level of a bound state means larger dissociation energy ($E'_d > E_d$) which has important role in the chemical reactions when isotope behavior is of interest. The same conclusion could be obtained, but involving much more of mathematical work, for higher related bound states, characteristic for other temperatures $T > T_0$.

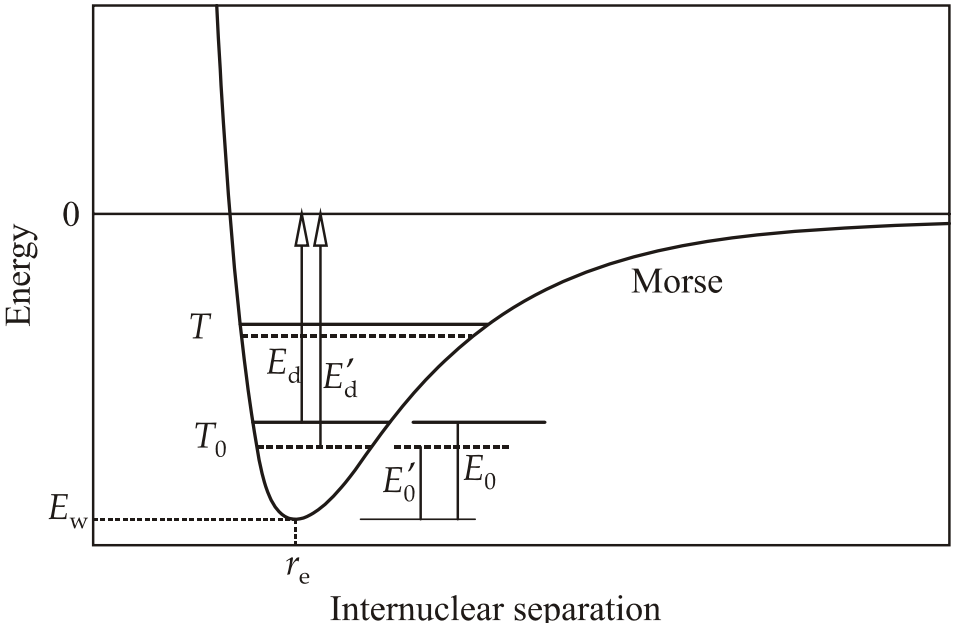

Figure 2.2 Schematic representation of the Morse potential energy for interaction of two atoms in a molecule. Ground energy levels are shown for lighter (—) and heavier compound (– –) respectively, as well as associated dissociation energies E_d and E'_d.

Slika 2.2 Shematski prikaz Morseove potencijalne energije za međudjelovanje dvaju atoma u molekuli. Prikazani su osnovni energijski nivoi E_0 i E'_0 za "lakšu" (—) i "težu" (– –) molekulu, kao i pridružene energije disocijacije E_d i E'_d.

The consequence of different isotope composition in physicochemical characteristic is called isotope fractionation. Mathematically it is described by fractionation factor α:

$$\alpha = \frac{R_B}{R_A} \qquad 2.8$$

It represents the portioning of isotopes between two phases (A and B), or between two parts of a system (A and B) where transition is from A → B (Craig, 1957).

In most cases fractionation factor α has the value close to 1. The value $\alpha = 1$ indicates that the isotopes are distributed evenly between A and B, with no isotopic fractionation, $\alpha > 1$ indicates that the stable isotope of interest is concentrated in substance B, and $\alpha < 1$ indicates

its concentration in substance A. The dimensionless fractionation factor α can be expressed by the previously defined δ values:

$$\alpha_{B/A} = \frac{1000 + \delta_B}{1000 + \delta_A} \qquad 2.9$$

Again for the convenience, a new parameter ε, called also fractionation factor, is defined as:

$$\varepsilon_{B/A} = \alpha_{B/A} - 1 = \frac{R_B}{R_A} - 1 \qquad 2.10$$

It can be also expressed by δ values:

$$\varepsilon_{B/A} \approx \delta_B - \delta_A \qquad 2.11$$

Therefore, ε is expressed in per mil (‰) and directly compares two δ values of interest. The value $\varepsilon > 0$ means that the final product B of the transition A → B is enriched in the heavy isotope comparing to the initial product A.

2.3.1 Equilibrium and kinetic fractionation

Characteristics of transitions from state A to state B can be described as equilibrium or kinetic (non-equilibrium) fractionation.

Partial separation of isotopes between two or more substances in chemical equilibrium is called equilibrium isotope fractionation. The effect depends on temperature and is the largest at low temperatures and therefore forms the basis for isotopic paleothermometers (Chacko et al., 2001). Equilibrium fractionation is also known as reversible process.

In a reaction occurring in two or more phases containing the same element, the fractionation process is due to quantum mechanical processes of atomic movement (rotation, translation and vibration). The larger fractionations are measured for lighter elements/ molecules (molecules that have lower atomic mass). Isotopic fractionations attributed to equilibrium processes have been observed in many elements, from hydrogen (D/H) to uranium ($^{238}U/^{235}U$). In general, the light elements (especially hydrogen, boron, carbon, nitrogen, oxygen and sulfur) are most susceptible to fractionation, and their isotopes tend to be separated to a greater degree than those of heavier elements.

Kinetic fractionation is known as irreversible process characterized by its dynamics (fast) and/or incompleteness. In this processes $\alpha_{kin} > \alpha_{eq}$ and $\varepsilon_{kin} > \varepsilon_{eq}$. Few different processes can contribute to this effect:

1. Diffusion can cause differences in abundance because of diversity of masses in specific molecules. The example of this is gas diffusion through small opening (smaller than

mean free path of molecules). Due to the average kinetic energy two molecules with different masses have different velocities. The faster molecule will be the one with smaller mass (lighter isotope) and will leave the system trough opening. The gas left in the system will become enriched with heavier isotopes.

2. Evaporation - condensation process is caused by difference in vapor pressure of isotopic compounds (usually between liquid and gas phases). The vapor is usually enriched with lighter isotopes, i.e. depleted with heavier isotopes. Enrichment decreases with temperature increase.
3. Kinetic isotope effect is raising from differences in the dissociation energies of isotopes. The dissociation or vibration energy is smaller for lighter isotopes.
4. Metabolic effect is caused by processes like breathing and photosynthesis. Example of different way of incorporation of ^{13}C in plants is given in the next section 2.4.
5. Chemical composition and crystal structure - Chemical composition of a specimen depends on nature of the chemical bond within. Differences in crystal structure are due to the chemical composition. The heavier isotopes are concentrated in more close structure geometrically nice balanced. For example, the fractionation factor ε between aragonite and calcite is 0.5 ‰, while ε of 10 ‰ is observed between graphite and diamond.

Although most non-equilibrium/kinetic processes tend to increase fractionation, i.e., $\varepsilon_{kin} > \varepsilon_{eq}$, there are studies on isotope ^{13}C showing that fast precipitation can result in $\varepsilon_{kin} < \varepsilon_{eq}$ and this will be described in section 2.4.1.

2.4 Distribution of carbon and oxygen isotopes

2.4.1 Distribution of ^{13}C

Carbon has two stable isotopes, ^{12}C and ^{13}C with the abundances 98.93 % and 1.07 %, respectively (Rosman et al., 1998). It also has a radioactive isotope ^{14}C that is present in contemporary atmosphere and biosphere in relative abundance of 10^{-10} %. It is a cosmogenic radioisotope with half life of 5730 years.

Due to the processes of isotopic fractionation in various physical, chemical and biological processes occurring in natural geochemical and biological carbon cycle, various carbon-containing compounds have distinct and characteristic carbon isotope content, as shown in Figure 2.3. Several carbon reservoirs important for the topic of this thesis (atmospheric CO_2,

marine carbonate minerals, plant material, biogenic soil CO_2, DIC in freshwaters, secondary carbonates) are discussed below.

Atmospheric CO_2 is the main source of carbon for biosphere. Its present concentration in the global atmosphere is about 380 – 400 ppmv (IPCC 2001). The CO_2 concentration can be influenced by local effects, e.g. winter concentrations can be as high as 447 ppmv in comparison with summer concentrations of 337 – 400 ppmv, due to various degree of fossil fuel combustion during winter (Górka et al., 2011). A network of stations for monitoring concentration in air was established by NOAA (National Oceanic and Atmospheric Administration) and the stations show continuous increase of CO_2 concentration. Since 2004 measured concentration of atmospheric CO_2 has increased to 380 ppmv, rising by 20 % in the past 50 years. Stable isotopic composition of atmospheric CO_2, $\delta^{13}C_{air}$, has been also monitored, and a decrease in $\delta^{13}C_{air}$ was observed with the increase of CO_2 concentration from about -6.3 ‰ in 1700 AD to -6.6 ‰ in 1900, -6.9 ‰ 1950, -7.5‰ in 1985 (Mook et al., 1985) and finally to about -8.0 ‰ in 2000 (Verburg, 2007). The decrease of isotopic value of $\delta^{13}C$ is due to the fossil fuel burning (Keeling, 1979; Keeling et al., 1980; Keeling et al., 1995). In the previously used example (Górka et al., 2011), the $\delta^{13}C_{air}$ during winter went down to -14.4 ‰. The change in the abundances of carbon isotopes (^{12}C, ^{13}C, ^{14}C) in any reservoir of the carbon cycle owing to anthropogenic activities is called the Suess effect (Verburg, 2007).

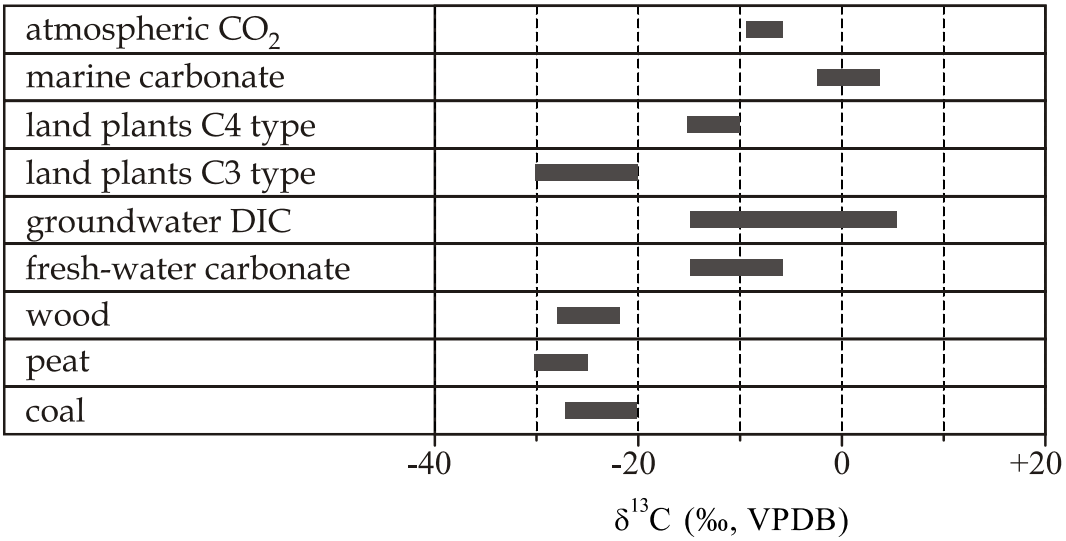

Figure 2.3 The $\delta^{13}C$ ranges in some natural materials

Slika 2.3 Rasponi $\delta^{13}C$ vrijednosti u nekim prirodnim tvarima

Measurement of the atmospheric CO_2 concentration and $\delta^{13}C$ over the ocean (Longinelli et al., 2010) helped to improve various models of carbon sinks and sources over oceans and continents. The main results are: 1) mean yearly growth of the CO_2 concentration in the

atmosphere over Indian ocean is 1.9 ppmv/yr (1996 – 2007) in good agreement with land stations (NOAA), and 2) change in $\delta^{13}C$ follows the change in CO_2 concentration and is in the observed period equal to -0.034 ‰/yr over Indian ocean, and -0.026 ‰/yr at land stations.

Historically, concentrations of atmospheric CO_2 within 20 ky BP have been lower than present day values. Atmospheric CO_2 concentration has been changing during glacial and interglacial transitions (Ford and Williams, 2007). During Last Glacial Maximum, i.e. ~20 ky BP, concentrations of atmospheric CO_2 varied from 180 to 200 ppmv (Pettit et al., 1999) and $\delta^{13}C$ was about -6.7 ‰ (Indermuhle et al., 1999). During interglacial conditions by the process of photosynthesis $^{12}CO_2$ is removed from the atmosphere (Ford and Williams, 2007) and atmosphere is enriched by $^{13}CO_2$. This influenced also $\delta^{13}C$ of plants (Feng and Epstein, 1995).

Plant material $\delta^{13}C$ value ranges from -38 to -8 ‰, depending on photosynthetic pathway (Figure 2.3). In C3 plants the $\delta^{13}C$ ranges from -38 ‰ to -22 ‰ and from -15 ‰ to -8 ‰ in C4 group of plants, and from -30 ‰ to -13 ‰ for CAM plants (Deines, 1980; Ye and Wang, 2001). The C3 pathway (Calvin cycle) is characteristic for terrestrial ecosystems in temperate and high-latitude region. The C4 pathway (Hatch-Slach cycle) is predominant in tropical and savannah grasses. The CAM (Crassulacean acid metabolism) cycle occurs mostly in succulents in arid ecosystems and evolves diurnal switching between C3 and C4 pathways. Average value of $\delta^{13}C$ in soil is -26 ‰ to -20 ‰ (McDermott et al., 2006) due to C3 plants, and due to the C4 plants is -16 ‰ to -10 ‰ (Cerling, 1984). In the area of research presented in the thesis, C3 plants dominate (Krajcar Bronić et al., 1986; Vokal, 1999; Šturm et al., 2012).

Marine carbonates have value ~0 ‰, with the range -2 ‰ to +3 ‰ (Figure 2.3) depending on age and mineral phase (McDermott et al., 2006 and references therein). Carbonate minerals are important contributor to Dissolved Inorganic Carbon (DIC) in terrestrial waters together with atmospheric and/or soil CO_2 (Genty et al., 2001a). DIC is a common term for various carbon-containing species in water solution, as will be described later in detail (section 3.1): CO_2 dissolved and aqueous, HCO_3^- and CO_3^{2-}. It is a result of dissolution of CO_2 in water, and then dissolution of carbonate bedrock by the carbonic acid. DIC is presented in environmental waters (stream, lakes, and groundwater) at concentrations of up to 10 mmol/L. The $\delta^{13}C$ of DIC in groundwaters can have a wide range of values (Figure 2.3). Factors that determine carbon concentration in water are, except origin, temperature and pH of the depositional environment (Clark and Friz, 1997) which is described later.

Under favorable conditions a secondary calcium carbonate in form of speleothem (from drip waters in caves), tufa (from fresh water in surface streams or lakes) or lake sediments, can precipitate in super-saturated waters. Isotopic composition of deposited secondary carbonate depends on the isotopic composition of DIC (Figure 2.3) (Horvatinčić et al., 2003; Lojen et al., 2004). For example, lake sediments from karstic Plitvice lakes (Croatia) have relatively narrow range of $\delta^{13}C$ of app. -9 ‰ (-8.6 ± 0.1 ‰ in Lake Prošće, -8.9 ± 0.2 ‰ in Lake Kozjak), while tufa from the same region have wider range of $\delta^{13}C$ values, between -10 and -6.5 ‰, with some exceptionally higher values at waterfalls (Horvatinčić et al., 2003). $\delta^{13}C$ values of speleothems from various karst caves in Croatia and Slovenia range from -12 ‰ to +3 ‰ (Urbanc et al., 1984; Horvatinčić et al., 2003), in good correlation with the theoretically predicted range from -16 ‰ to +3 ‰ (Dulinski and Rozanski, 1990). The individual $\delta^{13}C$ value is determined by temperature, chemical and isotopic parameters of the initial solutions and the actual precipitation process.

Knowledge of isotopic fractionations is essential for relating $\delta^{13}C$ in a proxy indicator of paleoclimate or paleoenvironment to the precursor carbon source (Darling et al., 2006). Its magnitude between various chemical species of dissolved and gaseous carbon is generally determined by carbon bond strength and phase transformation. Under equilibrium conditions the degree of isotope fractionation depends on the temperature only. Knowledge of the magnitude of these isotope fractionations is essential for the interpretation of the isotope variations of C and O in natural calcium carbonate. Gaseous or aqueous CO_2 in equilibrium with dissolved carbonate ions gives raise to the fractionation towards light isotope ratio between different chemical species. Solid carbonate is isotopically heavier than DIC with which it is in chemical equilibrium. Figure 2.4 summarizes equilibrium fractionation factors ε between various carbon-containing species (solid, bicarbonate, dissolved and gaseous forms of carbon).

The extent to which $^{13}C/^{12}C$ fractionation is affected by carbonate precipitation kinetics varies for different environmental conditions of a natural system. There were numerous studies concerning equilibrium fractionation and some of the results are presented here. The experimental results for ε between HCO_3^- and solid carbonate is ε = 1.85 ± 0.23 ‰ at 20 ºC, and dε/dT = (-0.035 ± 0.013) ‰/ºC (Emrich et al., 1970), leading to ε value of ~(2.2 ± 0.2) ‰ at 10ºC. However, (Turner, 1982) observed that fractionation between HCO_3^- and solid carbonate in some freshwater lakes that precipitate carbonate under presumably equilibrium conditions was higher than reported in work of Emrich (1970). It was suggested earlier

(McCrea, 1950) that the isotopic composition of precipitated carbonate depends on precipitation rate and that an instantaneously precipitated carbonate would have an isotopic composition identical to its aqueous carbon reservoir. In the later experiments, rapid carbonate precipitation resulted in small ε values, of about 0.3 ‰, while slower precipitation resulted in ε value of 2.26 ‰, which is considered to be the equilibrium value (Turner, 1982). In some experiments kinetic fractionation decreases as precipitation rate increases and in other cases (Romanek et al., 1992; Jimenez Lopez et al., 2001), fractionation is independent of precipitation rate as shown also in work of Mickler et al. (2004).

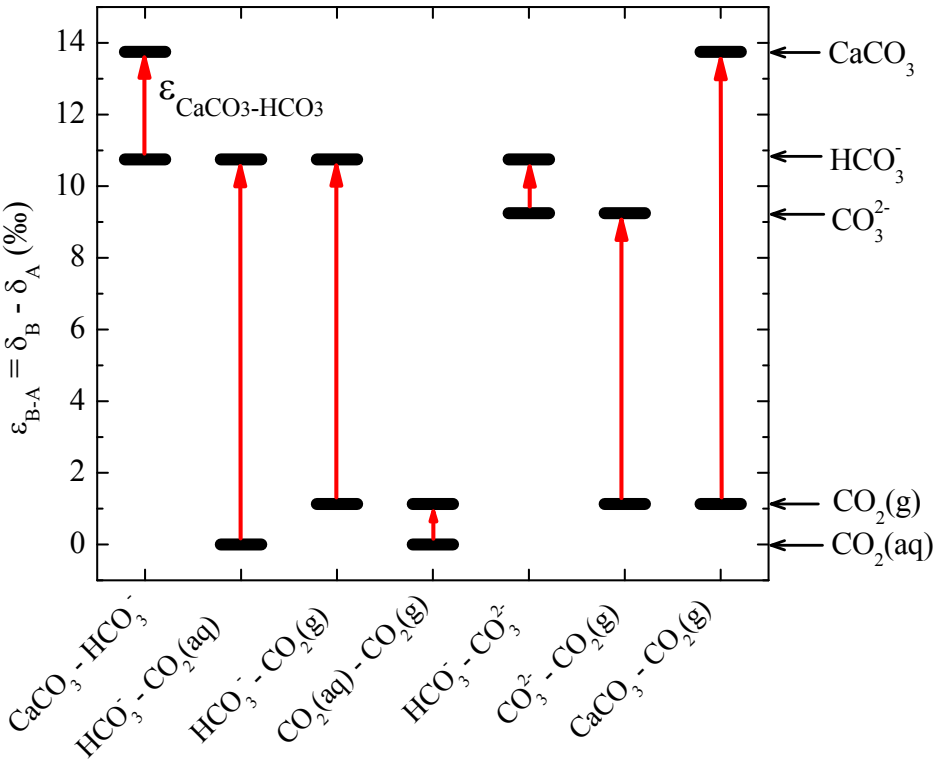

Figure 2.4 Equilibrium fractionation factor ε (in ‰) between different phases of carbon, i.e. gas, aquatic, solid. Among showed carbonaceous species, CO_2(aq) has the most negative $\delta^{13}C$ value, and $CaCO_3$ the most positive. Modified from Darling et al., 2006.

Slika 2.4 Ravnotežni frakcionacijski faktor ε (u ‰) između različitih faza i tvari koje sadrže ugljik: plinoviti, otopljen u vodi i u čvrstom stanju. Među prikazanim tvarima, najnižu (nejnegativniju) $\delta^{13}C$ ima CO_2(aq), a najvišu $CaCO_3$. Prema Darling et al, 2006.

Factors that cause kinetic fractionation during carbonate precipitation are outgassing of CO_2 and evaporation (Spötl, 2005; Baldini et al., 2006; Dreybrodt and Scholtz, 2011). However, most calcite is in isotopic equilibrium with DIC, but rapid CO_2 degassing may cause ^{13}C enrichment in the speleothem precipitated from water (Mickler et al., 2004).

Therefore, speleothem precipitated under high humidity conditions from relatively slow steady drips are expected to have the highest potential for precipitation in O and C isotopic equilibrium with their corresponding drip water. Also, calcite deposited from drips at low super-saturation may be the best for representing isotopic equilibrium conditions (Frisia et al., 2000; Lachniet et al., 2004). High humidity conditions limit evaporative ^{18}O enrichment in the drip water and may limit kinetic isotope effects caused by large variations in drip rates. In high humidity environments, CO_2 degassing from drip water is a more significant factor than evaporation in driving $CaCO_3$ precipitation.

Prior to identifying paleoenvironmental or climatic proxy information from the stable isotope data, it is essential to evaluate the degree of equilibrium conditions during speleothem growth (e.g., Mickler et al., 2004; Mickler et al., 2006; Meyer et al., 2012). For ancient speleothems an alternative approach is suggested: equilibrium versus kinetic fractionation during calcite precipitation (Meyer et al., 2012) is evaluated by analysing the correlation between $\delta^{13}C$ and $\delta^{18}O$ values of samples along the core, and the results suggest that isotopic composition of the different calcite fabrics reflect non-equilibrium isotope effects (i.e., by kinetic fractionation due to rapid CO_2 degassing and evaporation) to different degrees. Kinetic fractionation due to CO_2 degassing causes enrichment in ^{13}C in deposited carbonate, while $\delta^{18}O$ is generally less affected because of the buffering effect of the water reservoir (Mickler et al., 2006). Experimentally it was determined that in case of fast degassing $\delta^{13}C$ and $\delta^{18}O$ increase together with a slope $\Delta\delta^{13}C / \Delta\delta^{18}O = 1.4 \pm 0.6$, and that slow degassing causes enrichment with ^{13}C in carbonates (more positive $\delta^{13}C$) and no change in $\delta^{18}O$, therefore the slope tends to infinity (Meyer et al., 2012). Cave ventilation can also enhance degassing and thus kinetic fractionation (Spötl et al., 2005).

The conclusion of many recent studies of speleothems from various locations resulted in the following approach to their application in paleoclimatic studies. The direct comparison of the $\delta^{18}O$ and $\delta^{13}C$ values of modern speleothems with the values for their corresponding drip waters is done in order to assess the degree to which isotopic equilibrium is achieved during calcite precipitation. If modern speleothems can be demonstrated to precipitate in isotopic equilibrium, then ancient speleothems are suitable for paleoclimatic studies. If modern speleothems are precipitated out of isotopic equilibrium, then the magnitude and direction of the C and O isotopic offsets may allow specific kinetic and/or equilibrium isotopic fractionation mechanisms to be identified.

2.4.2 Distribution of ^{18}O

Oxygen is the most abundant element on the Earth. It has three stable isotopes with the following abundances: ^{16}O: 99.757 %, ^{17}O: 0.038 % and ^{18}O: 0.205 % (Rosman and Taylor, 1998). Because of the mass difference and the higher abundance the ratio of $^{18}O/^{16}O$ is determined and used in environmental research as the $\delta^{18}O$ value. Measurement results can be expressed in VPDB scale or in VSMOW scale. Conversion equations of $\delta^{18}O$ (VPDB) to $\delta^{18}O$ (VSMOW) and vice versa are given by Coplen et al. (1983):

$$\delta^{18}O\ (VSMOW) = 1.03091\ \delta^{18}O\ (VPDB) + 30.91 \qquad 2.12$$

and

$$\delta^{18}O\ (VPDB) = 0.97002\ \delta^{18}O\ (VSMOW) - 29.98 \qquad 2.13$$

In global water cycle abundance of oxygen isotopes is different in different species (Figure 2.5). The global (hydrological) water cycle starts with evaporation of seawater leading to cloud formation. With temperature decrease, rainout occurs. The different pathway determines way of water to get back to oceans (surface runoff of subsurface discharge, evaporation from lakes, and transpiration from vegetation).

Vertical profiles of water vapor, up to 40 km altitude, have been investigated since early 1960's (Craig and Gordon, 1965; Ehhalt, 1974; Johnson et al., 2001). The changes in isotopic composition of water and water moisture with altitude are consequences of two major processes. One is isotope fractionation associated with cloud formation and rainout process, leading to preferential removal of heavier isotopes, and the second is turbulent mixing of air masses with isotopically different moisture source. Isotopically heavier moisture can originate also from evapotranspiration (Jacob and Sonntag, 1991; Bariac et al., 1991), upward advection and subsequent evaporation of ice crystals (Keith, 2002), and methane oxidation (Johnson et al., 2001).

Changes of isotopic composition of moisture have been measured near ground level. Large short-term variability of isotopic composition has been observed at mid-latitude continental sites (Longinelli and Selmo, 2003), where they have the same magnitude as seasonal changes connected with different rainout events.

The primary source from which precipitation (clouds) is formed is water vapor. The investigations show that the isotopic composition of monthly precipitation collected worldwide reflects mean isotopic status of atmospheric vapor within planetary boundary (IAEA/GNIP, 1953 - 2012). Processes controlling water vapor are isotopic composition of ocean surface, sea-

surface temperature, relative humidity of atmosphere, and wind regime. Water vapor from the ocean is isotopically depleted in comparison with the oceanic water. The $\delta^{18}O$ in the surface sea layer is uniform, varying from +0.5 ‰ to -0.5 ‰ (Epstein and Mayeda, 1953). In tropical region changes in ^{18}O are caused by strong evaporation. In the Mediterranean region variations/deviations are approximately 2 ‰. In polar regions changes to more negative values originate from ice and snow melting. Ocean vapor have average $\delta^{18}O$ value of -12 ‰ to -13 ‰.

Moisture is transported horizontally and vertically until saturation conditions are reached and cloud formation starts. Isotopic depletion of vapor continues with raindrops leaving the cloud. Isotopic re-equilibration with air moisture occurs and isotopic composition of precipitation is in equilibrium with near-ground water vapor. The degree of re-equilibration depends on size of raindrops, height of the cloud base and relative humidity of atmosphere beneath the cloud. Solid precipitation (snow, hail) is more depleted in heavy isotopes, reflecting equilibrium at lower in-cloud temperatures.

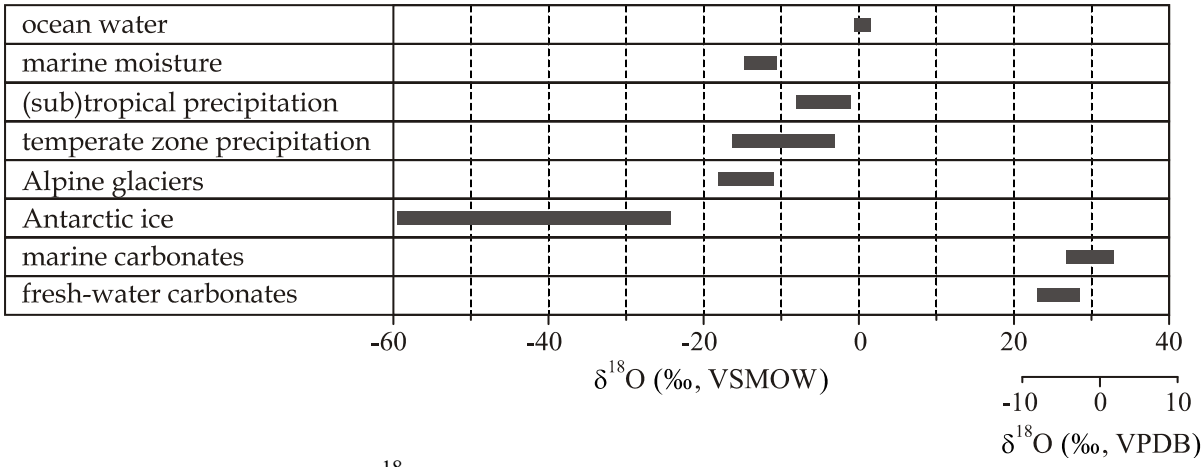

Figure 2.5 Typical range of $\delta^{18}O$ in various types of water and carbonates. For all materials the scale is relative to VSMOW, only for marine and fresh-water carbonates $\delta^{18}O$ can be expressed relative to VPDB (additional scale).

Slika 2.5 Karakterističan raspon $\delta^{18}O$ vrijednosti u različitim vodama i u karbonatima. Za sve tvari skala $\delta^{18}O$ izražena je prema standardu VSMOW, a $\delta^{18}O$ za karbonate se može izraziti i prema standardu VPDB.

Global Network of Isotopes in Precipitation (GNIP) is the network constituted of stations collecting precipitation on monthly basis at global and regional scale. It is operated by International Atomic Energy Agency (IAEA) and the World Meteorological Organization (WMO). Isotopic composition of precipitation on the global scale has been systematically reviewed (Dansgaard, 1953; Yurtsever and Gat, 1981; Rozanski et al., 1993). IAEA-WMO database helped in defining several “effects” that influence global distribution of isotopes in precipitation: the latitude, altitude and continental effects relate isotopic composition of

precipitation at different locations, while the temperature, amount and source effects are related to precipitation at a single location.

Relation between long-term annual means of oxygen $\delta^{18}O$ and hydrogen $\delta^{2}H$ in precipitation is known as Global Meteoric Water Line (GMWL) shown in Figure 2.6 (Craig, 1961).

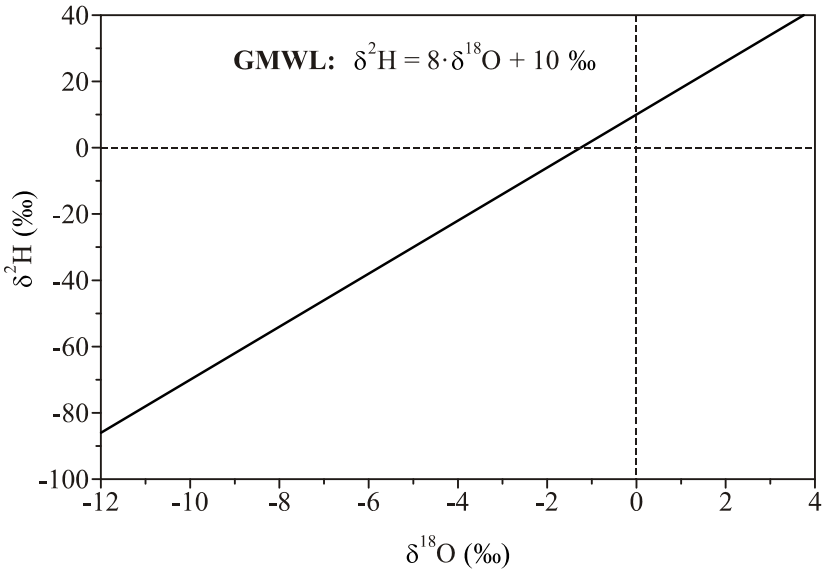

Figure 2.6 Global Meteoric Water Line (GMWL) shows relation between long term annual means of oxygen $\delta^{18}O$ and hydrogen $\delta^{2}H$ isotope composition of precipitation.

Slika 2.6 Globalna linija oborinske vode (GMWL) pokazuje odnos između dugogodišnjih srednjih vrijednosti $\delta^{18}O$ i $\delta^{2}H$ u oborinama.

Deviations from GMWL have been found in many regions (Rozanski et al., 1993) and for many regions Local Meteoric Water Lines (LMWL) have been constructed (Barešić et al., 2006; Vreča et al., 2006). Before precipitation gets to the soil, re-evaporation accompanied by isotopic fractionation can happen in leaves (Gat and Tzur, 1967; DeWalle and Swistock, 1994; Dawson, 1993). If the system is recharged from surface water (lakes, river) solar energy enhances evaporation also accompanied by isotope fractionation. Once the water passes through the soil into unsaturated zone it becomes recharge to the underlying aquifer. In karst terrain the water usually finds way to caves where it contributes to speleothem formation which is described in detail later.

The temperature effect of isotopic composition of precipitation at middle and high latitudes was first summarized by Dansgaard (1953) as

$$\delta^{18}O = 0.69\ T_{meas} - 13.6\ (‰\ SMOW) \qquad 2.14$$

where the slope of 0.69 is actually the temperature gradient $d\delta^{18}O_{precipitation}/dT$ determined from measured isotope data. However, later it was found that $d\delta^{18}O_{precipitation}/dT$ slope may vary substantially in different regions, being higher in colder regions (Rozanski and Sonntag, 1982). Monitoring of isotope in precipitation in Croatia and Slovenia since 1976 (Krajcar Bronić et al., 1998; Horvatinčić et al., 2005; Vreča et al., 2006; Barešić et al., 2006; Vreča et al., 2011) resulted in temperature gradient of about 0.3 ‰/ºC for continental stations (Zagreb, Ljubljana) and lower for maritime stations along the Adriatic coasts of Slovenia and Croatia. No amount effect was observed, and the altitude effect for the region was determined to be 0.28 ‰/100 m. The isotope data showed that the majority of precipitation is of Atlantic origin, and only the small part of the Mediterranean origin, and that the contribution of Mediterranean precipitation increases from North Adriatic (10 %) towards south (14 %) (Vreča et al., 2006).

All these processes are not the topic of this thesis. However, it is important to know the climatic conditions in the area (temperature, amount of precipitation) and isotopic composition of precipitation since precipitation is the main input for drip water. For speleothem studies, the local meteoric water line (LMWL) should be established – it is important to paleoclimatic studies because it allows the evaluation of soil and/or drip water relative to precipitation and constraining the seasonal precipitation contribution to drip water.

In addition, understanding of drip water transit time is important for the interpretation of speleothem $\delta^{18}O$ time series. A system with a shorter residence time will be more suitable for capturing rapid, high-frequency climatic events. A very slow transit time with substantial mixing will be more suited for constraining long-term climatic change (Lachniet, 2009). The transit time of water within the vadose zone may be estimated via lag times of $\delta^{18}O$ of drip water relative to rainfall, delay in drip response to rainfall events, with chemical variation, etc.

2.5 Stable isotope measurements

2.5.1 Mass spectrometers

Basic purpose of a mass spectrometer is to make a quantitative assessment of various isotopes in a given sample (Brandt, 1995; Brandt, 2004; Horita and Kendall, 2004; Vaughn et al., 2004).

Investigated samples can exist in different physical phases: liquid, gas and solid. Because of low abundances and measurement convenience, all samples are transferred into the gas phase with application of different chemical procedures and available periphery units, attached to the mass spectrometer (Figure 2.7). Transformation of a sample to the gas phase allows easier manipulation with the sample during the rest of measurement process. A stable isotope ratio mass spectrometer (IRMS) consists of an ion source, an analyzer for ion separation and ion detector. Various inlet systems, equilibrator(s), etc, as periphery units complete the mass spectrometer (de Groot, 2004).

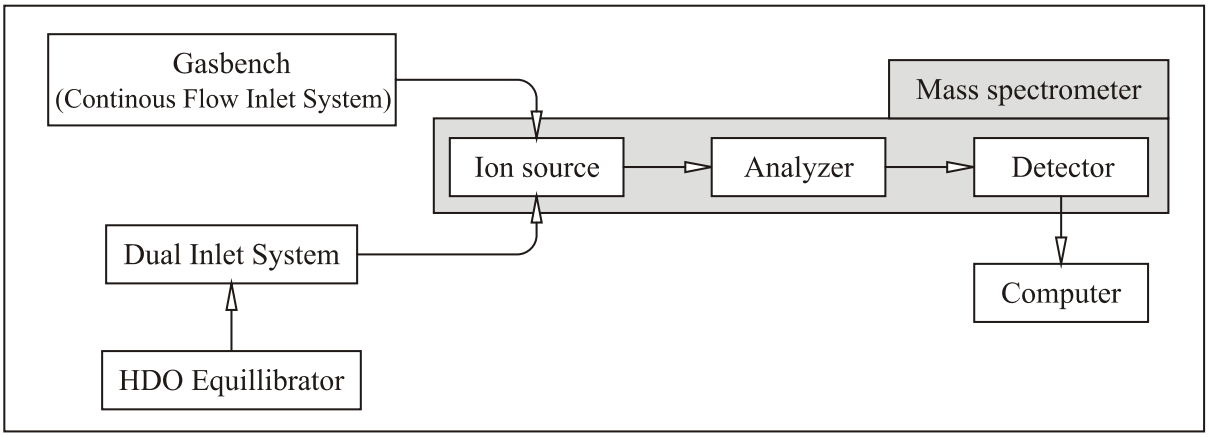

Figure 2.7 Schematic view of an experimental setup of a mass spectrometer with periphery units

Slika 2.7 Shema eksperimentalnog postava spektrometra masa s vanjskim jedinicama

2.5.2 Inlet systems and gas flow

There are two general types of gas inlet systems characterized by different types of gas flows into the mass spectrometer, namely a dual inlet system and a continuous flow system. Description of both is given in this work because they were both used in stable isotope analysis. Because of better precision, dual inlet system was used for measurement of oxygen isotopes in water samples, and continuous flow system was used for carbonate and air samples.

Dual inlet system. The gases that have to be analyzed are introduced into the inlet system through system of capillaries (Figure 2.8). The gas flow through capillaries is viscous and can be adjusted by crimps. By thin capillaries gases are carried to the change over valve. The main task of the changeover valve is to switch from one gas to another without mixing them. By automatically opening and closing different valves in the change over valve, independent introduction of two different gases (usually a standard gas and a gas from unknown sample) into the ion source is possible. Measurement is done by direct comparison of a sample gas to the calibrated reference gas. While the one gas is flowing into the ion source, the other is going to vacuum pump (waste). The vacuum system consists of turbo molecular or oil-diffusion pumps, backed by rotary vane pumps.

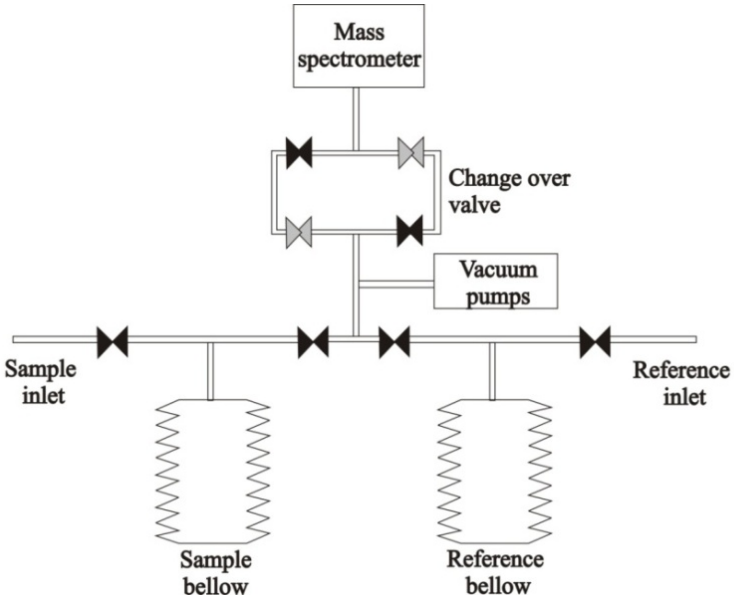

Figure 2.8 Schematic representation of Dual inlet system

Slika 2.8 Shema sustava dvojnog ulaza

The capillaries that lead the gas to the change over valve are thin, around 1 mm in diameter, with length of 1m. This assures uninterrupted gas flow in viscous flow conditions characterized by small free path length of molecule, meaning that collision of molecules is frequent and that gas flowing in the changeover valve is well mixed. Gas pressure in capillaries is required to be around 15 to 20 mbar (1.5 to 2 kPa).

Before the sample inlet system, an additional unit is used for sample preparation. Here, HDO unit is used for water equilibration. Procedure of measurement is described later.

Continuous flow inlet system. There are many periphery units characterized by continuous flow gas inlet systems. Here a principle of Gas Bench (Figure 2.9) operation is described

because it is the one used in stable isotope measurements in this work ($\delta^{18}O$ and $\delta^{13}C$ in carbon and air).

A sample is introduced in the borosilicate vials. They are placed in temperature controlled metal block - tray. For analysis in a mass spectrometer, each sample has to be transferred into the gas phase. For analysis of carbonate or DIC in water sample, a chemical reaction is activated by adding a few drops of phosphoric acid into a vial. With a double-hole needle (Figure 2.10) the produced CO_2 is extracted.

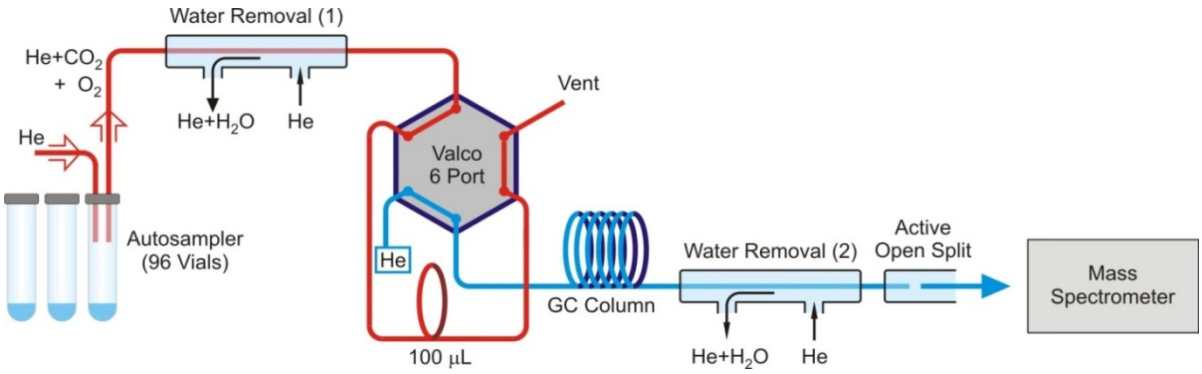

Figure 2.9 Schematic representation of a Gas Bench inlet system

Slika 2.9 Shema sustava *Gas Bench*

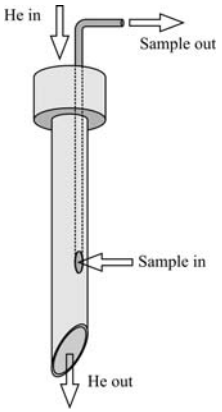

Figure 2.10 Double-hole sampling needle

Slika 2.10 Igla za uzorkovanje s dvije rupice

Through a hole (on the top of Figure 2.10) the helium gas with the flow rate of 0.5 mL/min is introduced into the sample vial and through the other hole (on Figure 2.10 marked "Sample in") sample gas is pushed into the Gas Bench system ("Sample out" on Figure 2.10). Water from the sample gas is removed with Nafion tube and inserted in the Valco valve (Figure 2.9).

This valve allows rotation of the ports in use by which insertion of gas component is precise. Afterwards the sample gas is inserted into the gas chromatograph column where separation of gas components is made. Another process of water removal follows and then the gas is introduced into the mass spectrometer. The signal height can be adjusted with an open split system (Figure 2.11). If the signal from the mass spectrometer is too high, above 50 V, the dilution with helium gas is turned on, as shown in Figure 2.11.b.

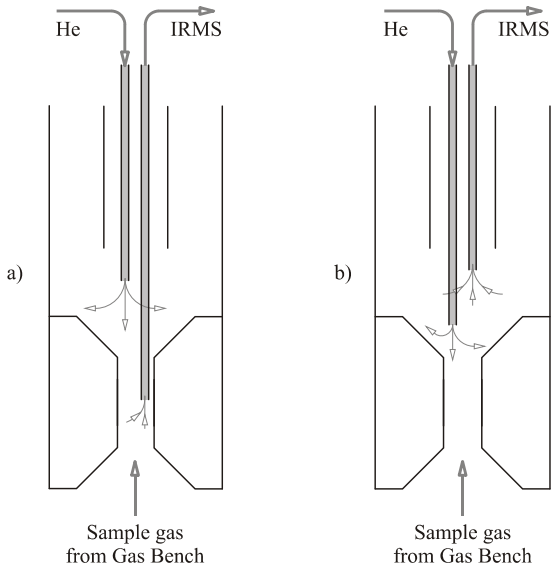

Figure 2.11 Different positions of the capillary in open split allow dilution with helium. a) Dilution with helium is not influencing sample gas from the Gas Bench. b) Dilution with helium is influencing sample gas from the Gas Bench

Slika 2.11 Različiti položaji kapilara u otvoru omogućavaju razrjeđenje uzorka helijem. a) Razrjeđenje helijem ne utječe na CO_2 od uzorka iz sustava *Gas Bench*. b) Plin iz uzorka iz sustava *Gas Bench* je razrijeđen helijem.

With introduction of the reference gas into the mass spectrometer rectangular shaped peaks are recorded (Figure 2.12Figure 2.). They have the same intensity due to the constant gas flow of the reference gas from the gas reservoir with pressure controlled and constant intensity. Number of reference peaks can be adjusted in mass spectrometer operating software.

Different peaks are recorded when a sample gas is introduced (Figure 2.12). The difference in the peaks' shapes is due to different amount of gas introduced into the system. For sample peak the pressure and intensity are controlled with the amount of gas extracted from the vial. Peak height of a sample decreases because the amount of a sample gas decreases with each extraction.

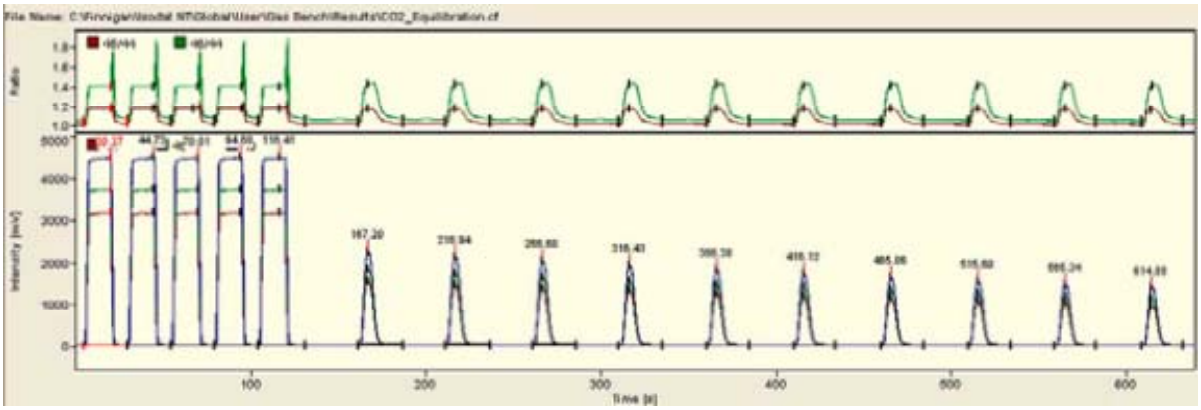

Figure 2.12 Gas Bench chromatogram. Rectangular shaped peaks represent reference gas peaks, followed by the sample peaks

Slika 2.12 Kromatogram *Gas Bench* sustava. Vrhovi pravokutnog oblika potječu od refentnog plina, nakon kojih slijede vrhovi koji potječu od uzorka

2.5.3 Ion source

The molecules (M) of a gas sample are introduced from the inlet system to an ion source of a mass spectrometer (Figure 2.13). Ionization by electrons (e^-) (electron impact, EI) occurs.

$$M + e^- \rightarrow M^+ + 2e^- \qquad 2.15$$

Source of electrons is a heated filament made of tungsten or rhenium. The energy of accelerated electrons before entering the source ionization chamber is between 50 and 150 eV. Because of low molecule velocity ($3 \cdot 10^2$ m/s) with respect to the velocity of electrons, ($6 \cdot 10^6$ m/s at 100 eV), the molecules seem to be motionless.

A homogeneous magnetic field assures spiral pathway of electrons and efficient ionization of a sample gas. Afterwards, electrons are collected by an electron trap. The current of the trap is regulated by emission current applied on a filament.

After ionization process molecular ions are extracted from the ion source by extraction lenses, and accelerated through the ion slit into the analyzer.

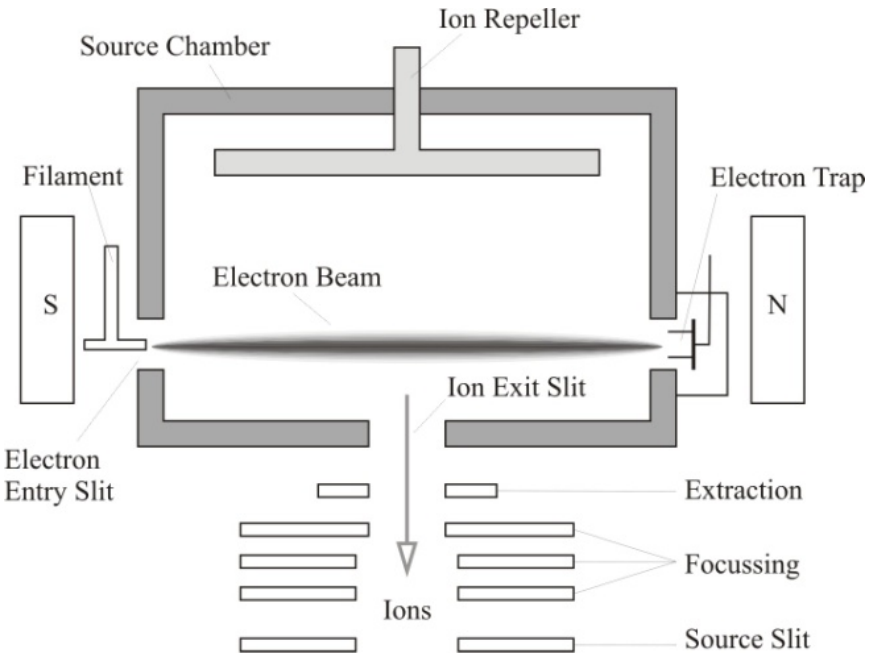

Figure 2.13 Schematic representation of an ion source of an Isotope Ratio Mass Spectrometer

Slika 2.13 Shema ionskog izvora u spektrometru masa

2.5.4 The analyzer

An analyzer of a mass spectrometer is a place where separation and detection of ions is occurring. Separation of ions of different masses is performed by applying homogeneous magnetic field (Figure 2.14).

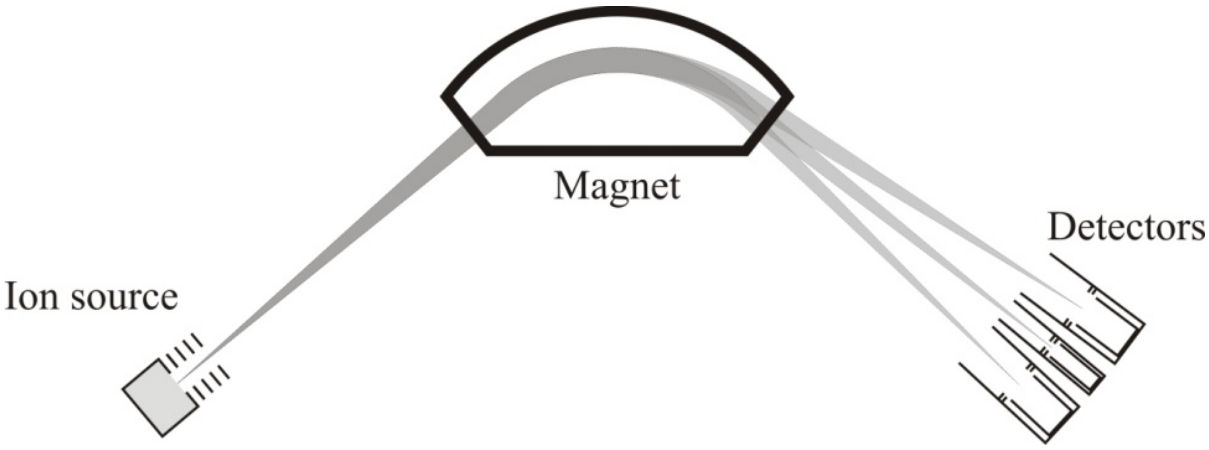

Figure 2.14 Schematic view of an ion separation in magnetic field of a mass spectrometer

Slika 2.14 Shema separatora (odjeljivača) iona u magnetskom polju spektrometra masa

The ion entering homogeneous magnetic field is deflected perpendicular to its flight direction and magnetic field. Ion motion is described by the Lorentz force:

$$\vec{F} = q\vec{v} \times \vec{B} \qquad 2.16$$

where: $\vec{F}$ is the vector of the Lorenz force, q is charge, $\vec{\mathbf{v}}$ is velocity of ion and $\vec{B}$ is magnetic induction.

In this environment the ion is moving in curved, circular path. Centripetal force is given by:

$$F = \frac{mv^2}{r} \qquad 2.17$$

where r is radius of the ion motion. Centripetal force equals to the Lorentz force

$$\frac{mv^2}{r} = qvB. \qquad 2.18$$

The kinetic energy of ion

$$E_{kin} = \frac{1}{2}mv^2 \qquad 2.19$$

is equal to the work (W) done by electrostatic field that accelerates ion having charge q through potential difference V

$$W = qV \qquad 2.20$$

After considering equation 2.17 – 2.20, the radius of ion movement can be described as:

$$r = \frac{1}{B}\sqrt{\frac{2mV}{q}} \qquad 2.21$$

It can be seen that radius of a molecule motion path depends on ion mass, which is used in ion separation process.

Two types of magnets can be used in magnet deflection mass spectrometers: permanent magnets and electromagnets. When permanent magnet is used, mass selection in analyzer is done by changing accelerating voltages (maximum is 5 kV), and in electromagnets altering current allows scanning a broad band of masses with decreased rate of sensitivity.

2.5.5 Collector system

A collector system in the mass spectrometers consists of multiple Faraday cup detectors, i.e. MEMCO (Miller Electric Manufacturing COmpany) collectors. They enable simultaneous detection of isotopes with different masses.

Each detector channel is fitted with ohmic resistor according to the isotope abundance in the nature. The Faraday cups are positioned along the focal plane of the instrument. Because of nonlinear peak width, collectors are constructed in the way that outer cups are wider than the middle one (Figure 2.15). This figure shows the Faraday cups settings in isotope ratio (IR) mass spectrometer Delta ^{plus}XP produced by Thermo Scientific. Molecules having different

atomic mass number (isotopomers) are detected at the same magnetic field. Molecule of oxygen (O_2) can have different atomic mass numbers depending on oxygen atom mass: ^{32}M: $^{16}O^{16}O$, ^{33}M: $^{16}O^{17}O$, ^{34}M: $^{16}O^{18}O$. Similarly, atomic mass numbers ^{44}M, ^{45}M, and ^{46}M can be obtained by various combinations of O and C isotopes in the carbon dioxide molecule: ^{44}M: $^{16}O^{12}C^{16}O$; ^{45}M: $^{16}O^{13}C^{16}O$ or $^{17}O^{12}C^{16}O$, ^{46}M: $^{18}O^{12}C^{16}O$ or $^{17}O^{13}C^{16}O$ or $^{17}O^{12}C^{17}O$.

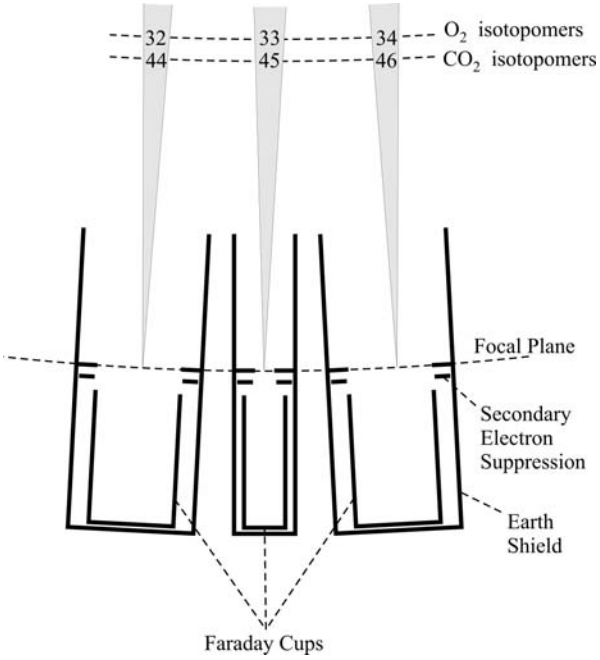

Figure 2.15 Faraday cups settings in IR mass spectrometer Delta^{plus} XP (Thermo Scientific)
Slika 2.15 Položaj Faradayevih čaša u spektrometru masa Delta ^{plus} XP (Thermo Scientific)

2.5.6 Corrections

During the measurement (in an ideal case) there is no fluctuation of ion current due to the filament temperature changes, no electron beam instability during long period of time, the magnet field and accelerating voltage remains constant during the measurement.

Even though mass spectrometer hardware enables high precision and accuracy during the measurements, some parameters still require corrections. For different isotopes variety of corrections is applied. In this thesis only those concerning measured stable isotopes (carbon and oxygen) will be described.

Linearity correction is used when the pressure in changeover valve is not the same during switch from sample to standard gas. This can be due to the process of sample preparation, drop of sensitivity in the ion source etc.

Background correction refers to electronic offset of a mass spectrometer representing the ion current of the ion source when there is no gas. The good background determination should

make no difference between different gases. Background correction for standard or sample measurement should be the same.

Memory effect is a result of mixing of two isotopic components i.e. different δ values. The final δ of a measured sample has contribution of an ion current of a previous sample. The correction for the memory effect is done by instrument.

Isobaric interferences can be discussed when ion current in Faraday cup of one sample is influenced by current signal of the other isotopic species contained in the same sample (Buhay et al., 1995).

2.5.7 Standards and quality assurance of stable isotope measurements

Results of mass spectrometry measurements are defined as delta (δ) value, equation 2.3. However, during measurement process internal laboratory standards (i.e. laboratory reference material calibrated against international standards) are used and the δ values are obtained as:

$$\delta_{\text{sample-reference}} = \frac{R_{\text{sample}} - R_{\text{reference}}}{R_{\text{reference}}} \qquad 2.22$$

However, for reporting results of measurements it is necessary to convert all values of the type 2.22 to the δ values relative to international standards (2.3) by transformation:

$$\delta_{X-A} = \left[\left(\frac{\delta_{B-A}}{10^3} + 1\right)\left(\frac{\delta_{X-B}}{10^3} + 1\right) - 1\right] \qquad 2.23$$

where X represents unknown sample, A represents the international standard and B represents internal laboratory standard (i.e. reference material).

International standard materials with defined isotopic values used for measurement of carbon and oxygen stable isotopes are presented in Table 2.3. In 2007 the amounts of international standards VSMOW and SLAP were exhausted, and their new names are now VSMOW2 and SLAP2. The consistency of reporting scale has stayed the same (Lin et al., 2010).

Each standard has to fulfill certain requirements: it has to be homogeneous, available in fairly large amount, easy to handle during preparation of measurement. The δ value of the standard must not diverse a lot from the δ values of the samples to be measured because of calibration and evaluation process that follows afterwards. Internal laboratory standards have to be correctly calibrated against international standards every two years, and it is necessary to do inter-laboratory calibration as often as it is possible (at least every six months) (Coplen, 1994).

Table 2.3 International reference materials with their isotopic values
Tablica 2.3 Međunarodni referentni materijali i njihov izotopni sastav

Standard	Material	$\delta^{18}O$ (‰)	$\delta^{13}C$ (‰)
VPDB*	Calcite	0 (by definition)	0 (by definition)
NBS - 18	Carbonitite (igneous carbonate)	-23.0 VPDB*	-5.03 VPDB*
NBS - 19	TS limestone (marble ring)	-2.20 VPDB*	1.95 VPDB*
VSMOW2**	Water	0 (combined standard uncertainty 0.02 ‰)	-
SLAP2**	Water	-55.50 VSMOW2 (combined standard uncertainty 0.02 ‰)	-

* "Stable oxygen and hydrogen isotopic ratios are normally reported relative to the SMOW standard ("Standard Mean Ocean Water" (Craig, 1961)) or the virtually equivalent VSMOW (Vienna-SMOW) standard. Carbon stable isotope ratios are reported relative to the PDB (for Pee Dee Belemnite) or the equivalent VPDB (Vienna PDB) standard." from http://wwwrcamnl.wr.usgs.gov/isoig/res/funda.html

** "The $\delta^{18}O$ value of VSMOW2 is identical to that of VSMOW within the uncertainty of the measurements performed The $\delta^{18}O$ value of SLAP2 is identical to that of SLAP within the uncertainty of measurements performed." from http://nucleus.iaea.org/rpst/Documents/VSMOW2_SLAP2.pdf

In each measurement performance, basic and routine procedures have to be checked and taken in the consideration before reporting final data. If the mass spectrometer is working properly, which can be checked by predefined tests (background test measurement, linearity test, etc.), measured raw data should be in the everyday range. If differences from the defined values are larger, the cause can be by external factors during chemical preparation of samples (amount and homogeneity of sample, contamination of sample because of imperfect sample handling), memory effect, drift of data because of day lasting measurements, etc. Usually all these imperfections can be recognized and corrected, but the results are still not comparable with the measurements of the same samples in other laboratories. The same value obtained in all laboratories, within acceptable uncertainty, is received after normalization calculation with values of internal laboratory standards calibrated against the international standards.

During everyday measurements two or more standards are measured between the samples. The measurement spreadsheet usually begins and ends with in-house standards. In this way shifts during the measurement can be noticed and measurement performance can be evaluated. One of the standards can be omitted during the process of every day calibration and can be used as quality control sample (QC) of laboratory performance (Brandt, 1995)

Uncertainty of an analytical laboratory measurement usually is a value calculated from several components. To estimate laboratory uncertainty of a measurement one has to identify possible sources of uncertainties and quantify them by estimation standard deviation of each, and then by combining them together (Mook, 2000).

Prior to numerical expression of laboratory measurement uncertainty it is necessary to establish standard operation procedure (SOP) (Ellison et al., 2000). In this procedure all possible mistakes have to be taken in the account, with additional care of clarifying contributions. The sources of uncertainties are: sampling, storage conditions, purity of chemicals used in analysis, measurements uncertainties and computational effects, blank effects, operator effect and random effect.

Final uncertainty of the measurement can be tested through the longer period of quality assurance sample measurement.

3 LITERATURE OVERVIEW

3.1 Water chemistry in karst processes

The dynamic equilibrium between CO_2 (gas) ↔ CO_2 (aqueous) ↔ H_2CO_3 (liquid) ↔ HCO_3^- (liquid) ↔ CO_3^{2-} (liquid) ↔ CO_3^{2-} (sediment) (Figure 3.1) is characteristic of karst system and processes in karst (Ford and Williams, 2007).

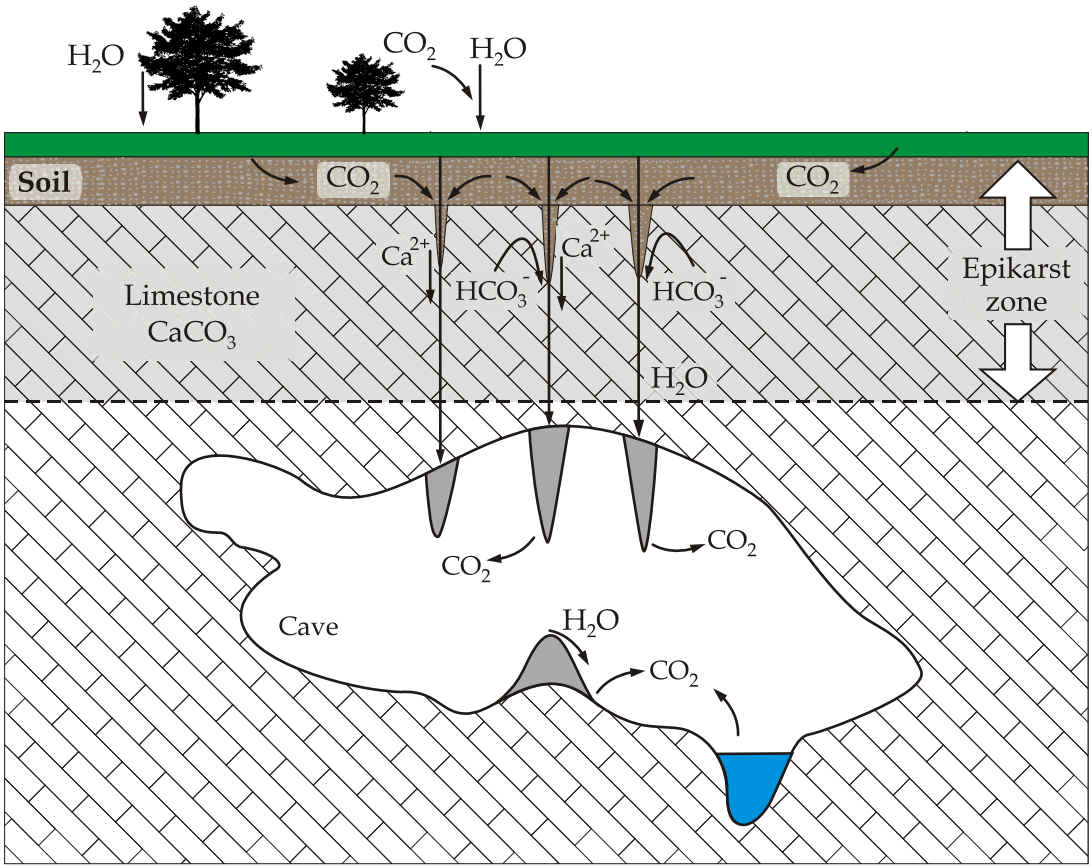

Figure 3.1 Cave evolution in karst terrain.

Slika 3.1 Razvoj špilja u krškom terenu.

The amount of dissolved CO_2 in water depends on partial pressure of CO_2 (pCO_2)[1] in atmosphere and temperature. For example, rain water at 25°C and at atmospheric pressure (containing 0.038 % or 380 ppm of CO_2) can dissolve 52 mg/L $CaCO_3$ (Stumm and Morgan, 1996). With microorganisms and bacterial activity, root respiration and organic matter decomposition, the amount of CO_2 in soil increases and can be higher than atmospheric CO_2 concentration by 1 – 2 orders of magnitude, reaching 0.1 to 10 % (Baldini et al., 2006; Fairchild et al., 2000).

CO_2 is transferred from gaseous to aquatic state:

$$CO_2(g) \leftrightarrow CO_2\ (aq) \qquad 3.1$$

In aquatic state, CO_2 forms carbonic acid:

$$CO_2(aq) + H_2O \leftrightarrow H_2CO_3. \qquad 3.2$$

Carbonic acid dissociates in two steps:

$$H_2CO_3 \leftrightarrow H^+ + HCO_3^- \qquad 3.3$$

and

$$HCO_3^- \leftrightarrow H^+ + CO_3^{2-} \qquad 3.4$$

Summarizing 3.1 to 3.4, the following carbon-containing species are present in water solution: $CO_2(aq)$, H_2CO_3, HCO_3^- and CO_3^{2-}, and they are together called total dissolved inorganic carbon (TDIC or simply DIC).

Concentration of $CO_2(aq)$ is difficult to be measured but can be calculated by using (e.g., Tremaine, 2011)

$$[CO_2\ (aq)] = [HCO_3^-]\frac{[H^+]^2}{\left(H^+ + 2K_2'\right)\cdot K_1'} \qquad 3.5$$

where K_1' and K_2' are dissociation constants ($K_1' = 6.187 \cdot 10^{-7}\text{Mol/L}$ and $K_2' = 2.525 \cdot 10^{-10}\text{Mol/L}$).

As water containing DIC passes through epikarst, or sometimes called vadose zone (Figure 3.1), it dissolves carbonate from limestone bedrock and the dissolution can be generally described as:

$$H_2O + CO_2 + CaCO_3 \leftrightarrow Ca^{2+} + 2\ HCO_3^- \qquad 3.6$$

Dissolution of carbonate in thermodynamic equilibrium is given by:

[1] pCO_2 is in fact volume fraction of CO_2 in the atmosphere. It is expressed in ppmv (volume part per million). 1 ppmv corresponds to 10^{-6} bar.

$$CaCO_3 \leftrightarrow Ca^{2+} + CO_3^{2-} \quad 3.7$$

The equilibrium constant for this process, K_C, at given pressure is defined as:

$$K_c = \gamma_{Ca^{2+}}[Ca^{2+}] \cdot \gamma_{CO_3^{2-}}[CO_3^{2-}] \quad 3.8$$

Its dependence on temperature can be expressed as

$$\log K_c = 13.870 - 0.04035 \cdot T - 3059/T; \quad 3.9$$

In eq 3.8, $[Ca^{2+}]$ and $[CO_3^{2-}]$ are equilibrium concentrations of Ca^{2+} and CO_3^{2-} ions, respectively, while $\gamma_{Ca^{2+}}$ and $\gamma_{CO_3^{2-}}$ are their respective coefficients of ionic activities.

Dissolution of carbonate rock increases concentration of Ca^{2+} ions in solution. The saturation index (I_{sat}) with respect to calcium carbonate is defined as (Langmuir, 1971):

$$I_{sat} = \frac{IAP}{K_c} \quad 3.10$$

where IAP is product of ionic activities:

$$IAP = (\gamma_{Ca^{2+}}[Ca^{2+}] \cdot \gamma_{HCO_3^-}[HCO_3^-] \cdot K_3)/[H^+] \quad 3.11$$

where $[H^+]$ and $[HCO_3^-]$ are ionic concentrations, and $\gamma_{HCO_3^-}$ is HCO_3^- ionic activity coefficient. K_3 in eq. 3.11 represents second order dissociation constant of H_2CO_3 which is temperature dependent and can be calculated as:

$$K_3 = 6.498 - 0.02379 \cdot T - 2902.39/T^{2.6} \quad 3.12$$

When a mineral is in equilibrium with the aqueous solution, then $I_{sat} = 1$. Aqueous solution is undersaturated with respect to a mineral when $I_{sat} < 1$, and supersaturated when $I_{sat} > 1$.

Fractional amounts of ionic species in a carbonate solution depend on pH of the solution (Figure 3.2). At pH between 7.5 and 8.5, which is characteristic of waters in karst, concentrations of all ion species can be neglected except that of HCO_3^-. In such cases DIC is approximated by HCO_3^- concentration.

When percolation water reaches the cave opening it is supersaturated with respect to CO_2 (free CO_2 species and CO_2 as hydrogen bicarbonate). Because of the difference in pCO_2 between cave air and water, a process of CO_2 degassing starts.

$$Ca^{2+} + 2\ HCO_3^- + CO_2(aq) \rightarrow H_2O + CaCO_3 + CO_2(gas) \quad 3.13$$

Degassing of CO_2 changes/moves the chemical equilibrium of the solution and secondary carbonate starts to precipitate.

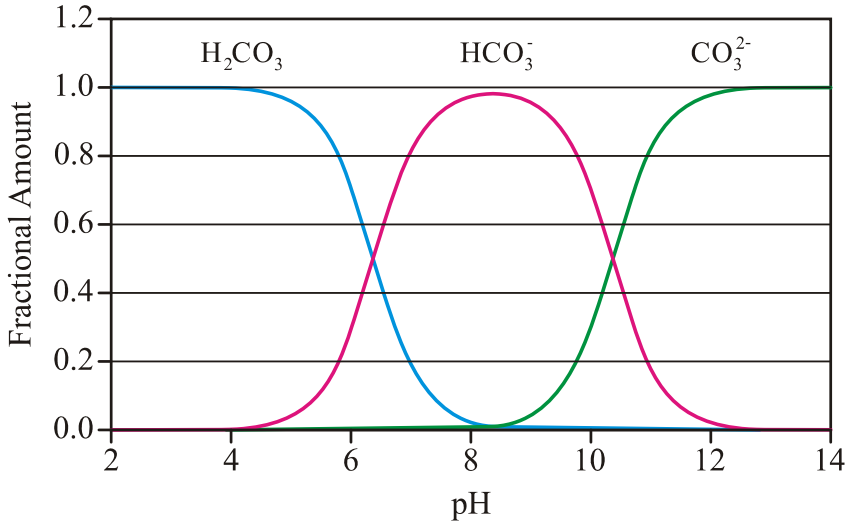

Figure 3.2 Fractional amounts of different carbon-bearing species in the solution vs. pH of the solution

Slika 3.2. Ovisnost udjela različitih ugljikovih spojeva u otopini o pH otopine

3.2 Speleothems

3.2.1 Morphology of speleothems

Calcareous speleothems (cave precipitates) in limestone caves are secondary deposited carbonate minerals, usually calcite. Speleothems are precipitated from drip water (Sasowsky and Mylroie, 2007). Calcareous speleothems are divided in groups (flowstones, stalagmites and stalactites) due to their shape (Franke, 1965).

Flowstone is term for laminated deposits on the floor or walls of caves with parallel carbonate layers that are formed from sheets of flowing water derived from relatively strong water flows from fissures or conduits. Although they have large surface, which allows sampling at more places (e.g. Hellstrom et al., 1998; Meyer et al., 2012), complex internal stratigraphy is disadvantage for paleoclimate studies. Flowstones are characterized with non-uniform calcite growth rates across the surface (Baker and Smart, 1995) and flow-switching behavior.

Stalactites are often associated with seepage zones on cave ceilings. Their growth begins with water flow through central canal which forms thin film on the stalactite outside surface. Special case are hollow cylindrical soda straw stalactites. They are usually very fragile and record the youngest few decades of a cave environmental conditions (Moore, 1962; Huang et al., 2001). Massive stalactites have conical growth from cave ceilings which display an internal growth layering parallel to the surface. In some studies stalactites, sliced parallel to or perpendicular to their length have been used in the highly successful paleoclimate work at Soreq

and other caves in Israel (e.g. Bar-Matthews et al., 2003), and their use is favored for conservation reasons.

Stalagmites grow upwards from the cave floor, particularly cylindrical types. They have relatively simple growth geometry and are usually used for paleoclimate investigations. The shape and diameter of a stalagmite depends on water flow rate (narrower for low flows), water supersaturation (more supersaturated waters may tend to precipitate more irregularly), and drop fall height (diameter increases with fall height). Various modeling studies and approaches have been used to suggest that variations in growth conditions could be deduced from speleothem shape (Kaufmann and Dreybrodt, 2004; Dreybrodt, 2011; Baker, 2012). In practice changes in the water flow path, i.e. changes oft drip location could occur, particularly on the longer time scale, which is often shown in growth hiatuses (Fairchild et al., 2007).

3.2.2 Stalagmite formation

Stalagmite growth rates can vary significantly, usually 10 – 300 μm/year (Mariethoz et al., 2012) and are influenced by the mean annual air temperature at the site, drip–water availability and the calcium concentration of drip waters (Genty et al., 2001b; Polyak and Asmeron 2001; Fleitmann et al., 2004). The process of stalagmite growth can be described in several steps, as summarized in Figure 3.3.

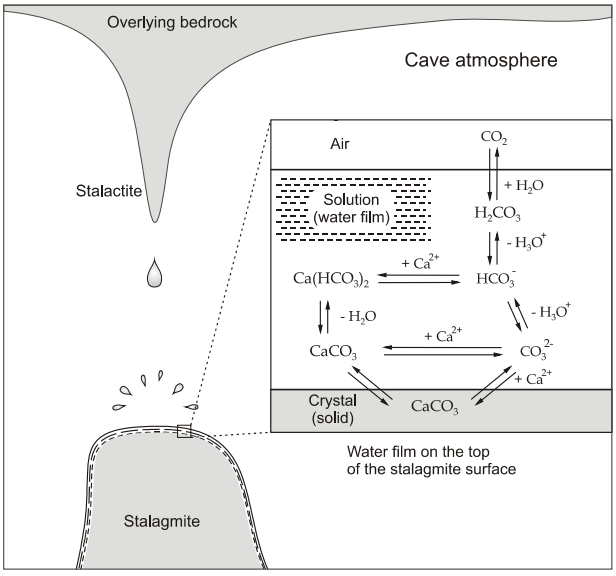

Figure 3.3 Reactions in the $CaCO_3 – CO_2 – H_2O$ system on the top of the stalagmite surface (modified from Dreybrodt, 1980)

Slika 3.3 Reakcije u sustavu $CaCO_3 – CO_2 – H_2O$ na vrhu stalagmita (modificirano prema Dreybrodt, 1980)

Growth of stalagmite starts with CO_2 evaporation from the thin water layer (~100 μm) from the apex of a stalagmite (Dreybrodt, 1980; Dixon and Hands, 1957). In this process CO_2 from water, enriched with respect to cave CO_2, is lost into the cave atmosphere until equilibrium with pCO_2 in cave air is achieved. Water film thickness is important for speleothem growth. Diffusion of CO_2 from the thin water film layer occurs within a few seconds (Dreybrodt, 2008), and depends on cave pCO_2. Evaporation and diffusion processes increase super-saturation with respect to calcite in solution, thus conditions for calcite precipitation are established.[1]

3.3 $\delta^{13}C$ in speleothems

The isotopic composition of carbon ($\delta^{13}C$) in speleothem (Figure 3.4) is determined by:

- concentration and isotopic composition of atmospheric CO_2,
- composition of soil above the cave and $\delta^{13}C$ of soil CO_2 gas
- way of transport of water through epikarst zone and aging of soil
- ratio of open to closed system, i.e. conditions of dissolution of overlying bedrock
- degassing of CO_2 in the cave

The $\delta^{13}C_{DIC}$ composition of percolation water is determined by interaction with ageing soil and pathway at which water dissolves the hostcaprock. Different patterns of dissolution of the host caprock can be described as open and closed system conditions. Close system conditions occur when percolation water looses contact with source of CO_2 limiting thus carbonate dissolution, and in open system percolation water continues to interact with CO_2 source, potentially generating higher DIC amount contained in water (Hendy, 1971; Krajcar Bronić et al., 1986; Baldini et al., 2006). However, water in nature usually experiences both open and closed systems, and such conditions are called the partially open system. Under open system conditions isotopic values $\delta^{13}C$ of DIC are more negative than under the closed-system. Also, in fully open systems, the cave seepage water is always in contact with an excess of soil CO_2.

[1] **Diffusion** is a process when molecules of one type move, in a random manner, from areas of higher concentration into areas of lower concentration. **Evaporation** occurs when the molecules of a substance in a liquid state leave the liquid state and move into the gaseous state. As this occurs, the gas molecules will diffuse into the gas already there until they reach an equilibrium state. Evaporation is a type of diffusion, as it is the random motion of molecules. However, diffusion usually means no change of state in the molecules moving through their medium

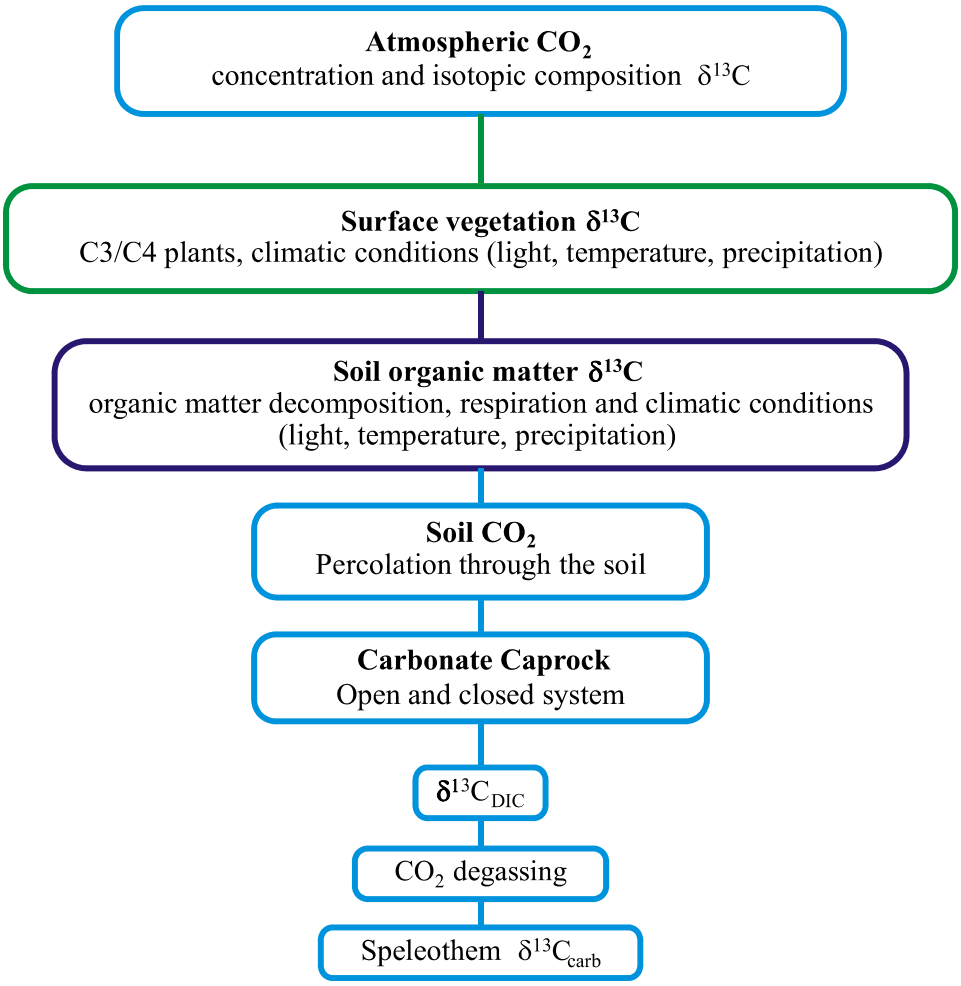

Figure 3.4 Factors determining $\delta^{13}C_{carb}$ in speleothems. Modified from Williams et al. (2004).
Slika 3.4 Čimbenici koji određuju $\delta^{13}C_{carb}$ vrijednost u sigama. Modificirano prema Williams et al. (2004.).

The expected $\delta^{13}C_{DIC}$ in systems overlain by C3 plants is from -14 to -18 ‰ (Hendy, 1971; Dulinski and Rozanski, 1990; Oster et al., 2012). In closed system seepage waters are isolated from soil CO_2 after entering the epikarst and $\delta^{13}C_{DIC}$ in is less negative, about -11 ‰. Value of $\delta^{13}C_{DIC}$ depends on pathways and flow through overlying bedrock, but also on residence time (Deines et al., 1974; Doctor et al., 2008). Water velocity through the overlying bedrock can vary from 2 cm s^{-1} (fast flow) to 0.001 cm s^{-1} (slow flow) (Kogovšek, 1997). Several components of flow are distinguished according to their mean residence time (MRT) (Bottrel and Atkinson, 1992): trough-flow or conduit flow with MRT of ~3 days, fracture flow with 30 to 60 days of storage, and a matrix seepage flow with long MRT of 160 and more days. When MRT or flushing rate is low, precipitation increases water velocity, and $\delta^{13}C_{DIC}$ decreases (Shopov, 1997).

3.4 $\delta^{18}O$ values of drip water and speleothem carbonate

Precipitation above the cave is the main source of cave drip water. Values of $\delta^{18}O$ in drip water are around mean annual $\delta^{18}O_p$ of precipitation in a region above the cave in low- and mid-latitude continental environments (Yonge et al., 1985), Figure 2.5. Seasonal variations of $\delta^{18}O$ in drip water are usually less pronounced than those in precipitation (O´Driscoll et al., 2005), because in the soil and epikarst zones precipitation waters are mixed with already present older waters However, in arid and warm semi-arid areas drip water can have different isotopic composition than precipitation reflecting seasonal recharge of epikarst waters (Bar-Matthews, 1996),. Differences in mean $\delta^{18}O$ values of drip water and precipitation can range from 1.1 to -1.9 ‰ (Harmon et al., 2004).

$\delta^{18}O$ values of drip water from different drip sites within a cave can vary significantly due to the differences in epikarstic flow routes and storage (Lauritzen and Ludberg, 1999; Ford and Williams, 2007). Pathways can be vertical, which indicates percolation through a network of interlinked voids, to horizontal. Water in dye tracing experiment reappeared 60 m horizontally from expected drip site (Mattey et al., 2010). Infiltrating water can follow bedding parallel fissures, up to 100 m and then percolate vertically down to the cave void. In short, water can be infiltrated to the cave system from any single point on the surface. Different $\delta^{18}O$ of drip waters at various locations within the same cave thus cause differences in carbonate $\delta^{18}O$ values (Serefiddin et al., 2004).

Factors that determine $\delta^{18}O$ composition of deposited speleothems are summarized in Figure 3.5. $\delta^{18}O$ signal of precipitation is modified by water percolation through the soil zone resulting in $\delta^{18}O$ of drip water. If there is no water, e.g., in arid and semi-arid areas where rain occurs seasonally, or in colder regions when the soil is frozen, speleothems cannot be deposited. Under favorable conditions speleothems can grow. Their growth rate is determined by degree of supersaturation and volume of seepage and their $\delta^{18}O$ value is determined by the $\delta^{18}O$ of drip water and temperature of deposition if the deposition occurs under isotopic equilibrium conditions. Therefore, $\delta^{18}O$ values of carbonates that grow in isotopic equilibrium with water contain information on cave temperature. However, before paleotemperature can be calculated for old speleothem, comprehensive study of each site has to be performed (Spötl et al., 2005).

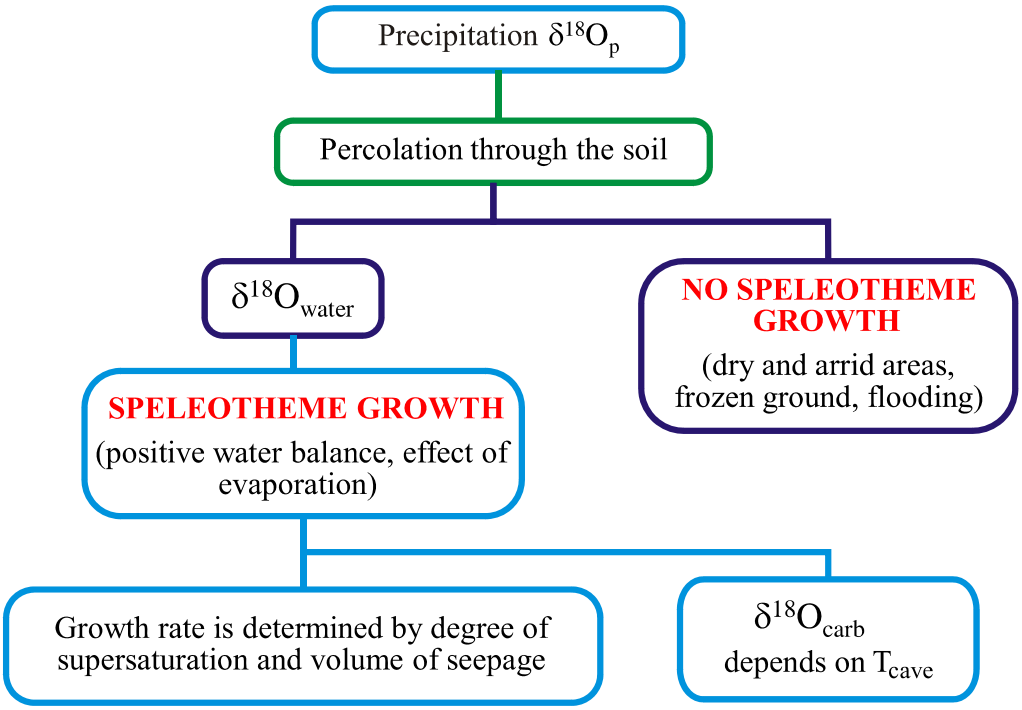

Figure 3.5 Factors determining $\delta^{18}O_{carb}$ in speleothems, from precipitation through the soil to the cave environment. Modified from Williams et al. (2004).

Slika 3.5 Čimbenici koji određuju vrijednost $\delta^{18}O_{carb}$ vrijednost u sigama. Modificirano prema Williams et al. (2004).

3.5 Speleothems as paleothermometers

The cave temperature is constant in most caves and invariant to annual temperature changes, but fluctuation on long term scale can reflect climatic changes (Clark and Friz, 1997). Caves can preserve insights in the paleoenvironment if they have stable climate interior. In stable conditions inside the cave temperature variation is ±1 ºC from the mean annual outside temperature. Relative humidity is close to 100 % (Ford and Williams, 2007).

Both stable isotopes ^{13}C and ^{18}O present in deposited carbonates could be used for paleotemperature studies. The temperature effects on $^{13}C/^{12}C$ fractionations between various DIC species and solid carbonate are rather low compared to the temperature effects that are propagated into the $\delta^{18}O$ of freshwater carbonates meaning that $\delta^{13}C$ of speleothems is rather insensitive to temperature changes. The temperature coefficient for $\delta^{13}C$ fractionation between calcite and DIC is only -0.05 ‰ per ºC (Bottinga 1968; Salomons and Mook, 1986) or even (-0.035 ± 0.013) ‰ per ºC (Emrich et al., 1970). The temperature coefficient for $\delta^{18}O$ fractionation between calcite and water is around -0.24 ‰ per ºC and the temperature dependent variation of $\delta^{18}O$ in meteoric water due to atmospheric liquid-vapor fractionation is

in the range 0.7 to 0.2 ‰ per ºC (eg. Rozanski et al., 1993, and described in section 2.4.2.). Moreover, the carbon cycle is far more complex than the water cycle because there are several sources of carbon (eg., atmospheric and/or soil CO_2, marine carbonates) in contrast to the single source of water (precipitation) (Darling et al., 2006). Therefore, for paleotemperature studies only ^{18}O in speleothems is considered.

As mentioned earlier in Chapter 2, each modern speleothem study starts with the relation of stable isotope composition of modern speleothems and modern cave environment. If carbon and oxygen isotopic equilibrium in modern speleothems can be demonstrated, then the stable isotopic composition of ancient speleothems from the same environment may be interpreted with greater confidence (Mickler et al., 2004). The study of glass plate calcite, i.e. calcite precipitated on glass plates, watch glasses or other artificial media, is a non-destructive method for modern calcite deposition studies (Luo et al., 2012; Tremaine et al., 2011; Lojen et al., 2004; Surić et al., 2010; Riechelmann, 2010). The use of glass plates enables a great number of speleothems sites to be studied in a defined time periods with no negative effect on the cave, such as breakage or drilling. Before speleothem collection for paleoclimate studies, the glass plate method allows assessment of the extent to which calcite achieves O and C isotopic equilibrium in the modern system. This allows identification of speleothems best suited for paleoclimatic studies, and last but not least, the glass plate method is a significant contribution to cave conservation/preservation (Mickler et al., 2004).

In order to retrieve information of paleoclimate from oxygen isotope record in speleothems, the following conditions have to be guaranteed (Dreybrodt and Scholtz, 2011):

- $\delta^{18}O$ values of the dissolved carbonate and drip water are in isotopic equilibrium
- calcite precipitated on the apex of the stalagmite is in isotopic equilibrium with carbonate dissolved in drip water

Isotopic equilibrium is disturbed if significant evaporation or rapid degassing occurs, if the relative humidity vitiates, if there is dominant air circulation (Ford and Williams, 2007). Also one has to consider if $\delta^{18}O_{calcite}$ is invariant to an increase of mean annual air temperature and if $d\delta^{18}O_p/dT$ is close to (-0.24 ‰/ºC), then changes in $d\delta^{18}O_p/dT$ are not be visible in $\delta^{18}O_{carb}/dT$ (McDermott et al., 2006).

Important for paleostudies are changes in seasonality, changes in $\delta^{18}O$ of the ocean in glacial/interglacial time scales due to ice volume effect (up to 1.2 ‰). Temperature gradient $d\delta^{18}O_p/dT$ was found to be 0.69 ‰/ºC on the global scale (Dansgaard, 1953), but it is site dependent and could be greater than, equal to, or less than the temperature dependence of

$\delta^{18}O_{calcite}$ deposited in speleothems ($d\delta^{18}O_{calcite}/dT$) which is approximately –0.24 ‰ ºC^{-1} at 25ºC (O'Neil et al., 1969). Reports have been published where the ($d\delta^{18}O_{calcite}/dT$) appears to be positive (Goede et al., 1990; Burns et al., 2001; Onac et al., 2002) and negative (Gascoyne 1992; Hellstrom et al., 1998; Frumkin et al., 1999a; 1999b).

Different approaches for calculation of paleotemperatures from stable isotope data, $\delta^{18}O_{carb}$ and $\delta^{18}O_{water}$ for various temperature ranges, for both organically and inorganically precipitated carbonate can be found in literature. Temperature dependence of $\delta^{18}O_{carb}$ is not linear and paleotemperature equations can be grouped into two different types (Table 3.1). Temperature range from 0 – 25 ºC of presented equations encompasses measured temperatures in this study.

The paleotemperature relation has the following form:

$$t\ (ºC) = a - b\ D + c\ D^2 \qquad 3.14$$

where

$$D = \delta^{18}O_{carb} - \delta^{18}O_{water} \qquad 3.15$$

$\delta^{18}O_{carb}$ is expressed relative to VPDB scale and $\delta^{18}O_{water}$ relative to VSMOW scale, t is temperature in °C. Coefficients a, b and c are calculated by fitting experimental results or measured field data.

The approach of type A (Table 3.1) has been proposed by Epstein and Mayeda (1953) after biogenically studying precipitated calcite of mollusk shells in the temperature range 0 – 25 ºC. Some other authors also studied organically precipitated carbonate in the same temperature range (Craig, 1965; Shackleton and Kennet, 1975, Mulitza et al., 2003). Similar paleotemperature equations have been proposed also for calcite precipitated inorganically (Grossman, 1982; Andrews et al., 1994, 1997; Leng and Marshall, 2004). Kim and O'Neil (1997) equation of type B was re-expressed in a more convenient form by Leng and Marshal (2004). This equation gives lower temperature than original Craig equation (McDermott et al., 2006, Figure 3.6)

Table 3.1 Overview of equations for paleotemperature determination from $\delta^{18}O$ of water and carbonates precipitated from water under isotopic equilibrium conditions

Tablica 3.1. Pregled jednadžbi za određivanje paleotemperature na osnovi $\delta^{18}O$ vrijednosti u vodi i u karbonatu istaloženom iz te vode u uvjetima izotopne ravnoteže

Type	Reference	Equation	t (°C)	Source
A $t(°C) = a - bD + cD^2$ $D = \delta^{18}O_{carb} - \delta^{18}O_{water}$ $\delta^{18}O_{carb}$ in VPDB, $\delta^{18}O_{water}$ in VSMOW	Epstein and Mayeda, 1953	$t(°C) = 16.5 - 4.3\ D + 0.14\ D^2$	0-25	organic
	Craig, 1965	$t(°C) = 16.9 - 4.2\ D + 0.13\ D^2$	0-25	organic
	Shackleton, 1974	$t(°C) = 16.9 - 4.38\ D + 0.10\ D^2$	0-25	organic
	Grossman, 1982	$t(°C) = 16.4 - 4.2\ D + 0.13\ D^2$	0-25	inorganic
	Mulitza et al., 2003	$t(°C) = 14.32 - 4.28\ D + 0.07\ D^2$	0-25	organic
	Leng and Marshall, 2004	$t(°C) = 13.8 - 4.58\ D + 0.08\ D^2$	0-25	inorganic
	Andrews, 1994, 1997	$t(°C) = 15.7 - 4.36 \times D + 0.12 \times D^2$	0-25	inorganic
B $1000 \ln\alpha = \frac{M \cdot 10^6}{T(K)^2} + \frac{N \cdot 10^3}{T(K)} - P$ $\alpha = \frac{1000 + \delta^{18}O_{carb}}{1000 + \delta^{18}O_{water}}$ $\delta^{18}O_{carb}$ and $\delta^{18}O_{water}$ in VSMOW	O'Neil et al., 1969	$1000 \ln\alpha = \frac{2.78 \times 10^6}{T(K)^2} - 3.4$	0-25	inorganic
	Friedman and O'Neil, 1977	$1000 \ln\alpha = \frac{2.78 \times 10^6}{T(K)^2} - 2.89$	0-25	inorganic
	Kim and O'Neil, 1997	$1000 \ln\alpha = \frac{18.03 \times 10^3}{T(K)} - 32.42$	0-25	inorganic
	Kim et al., 2007 – modified	$1000 \ln\alpha = \frac{18.03 \times 10^3}{T(K)} - 31.17$	25-75	inorganic/ laboratory reagent
	Coplen, 2007	$1000 \ln\alpha = \frac{17.4 \times 10^3}{T(K)} - 28.6$	34	inorganic
	Horita and Clayton, 2007	$10^3 \ln\alpha = \frac{0.9521 \times 10^6}{T(K)^2} + \frac{11.59 \times 10^3}{T(K)} - 21.56$	20	theoretical
	Chacko and Deines, 2008	$1000 \ln\alpha = \frac{2.5733 \times 10^6}{T(K)^2} - 0.869$	0-1000	theoretical
	Tremaine et al., 2011	$1000 \ln\alpha = \frac{16.1 \times 10^3}{T(K)} - 24.6$	18 – 25	inorganic

The second approach (type B in Table 3.1) has been suggested by O'Neil et al. (1969) and modified by Friedman and O'Neil (1977), Kim and O'Neil (1997), Kim et al. (2007), Coplen (2007), and Tremaine et al. (2011). Horita and Clayton (2007) and Chacko and Deines (2008) used statistical-mechanical calculation to obtain the temperature dependence of oxygen isotope fractionation. This type of equations relates the fractionation factor α and temperature, and can be generally written in the following form:

$$1000 \ln\alpha = \frac{M \cdot 10^6}{T^2} + \frac{N \cdot 10^3}{T} - P \qquad 3.16$$

where T is thermodynamic temperature expressed in kelvin (K), M, N, and P are parameters obtained by fitting experimental results. In some equations either M or N can have the value zero (Table 3.1).

For calculation of fractionation factor α expression (3.1) is used:

$$\alpha = \frac{1000 + \delta^{18}O_{carb}}{1000 + \delta^{18}O_{water}} \qquad 3.17$$

Both stable isotope values, $\delta^{18}O_{water}$ and $\delta^{18}O_{carb}$, should be referred relative to VSMOW scale.Both equation types are represented graphically in Figure 3.6, but not all equations are shown in Table 3.1. For more convenient and self-explanatory type of graphical presentation results from this work are presented on plot presented in Figure 3.7.

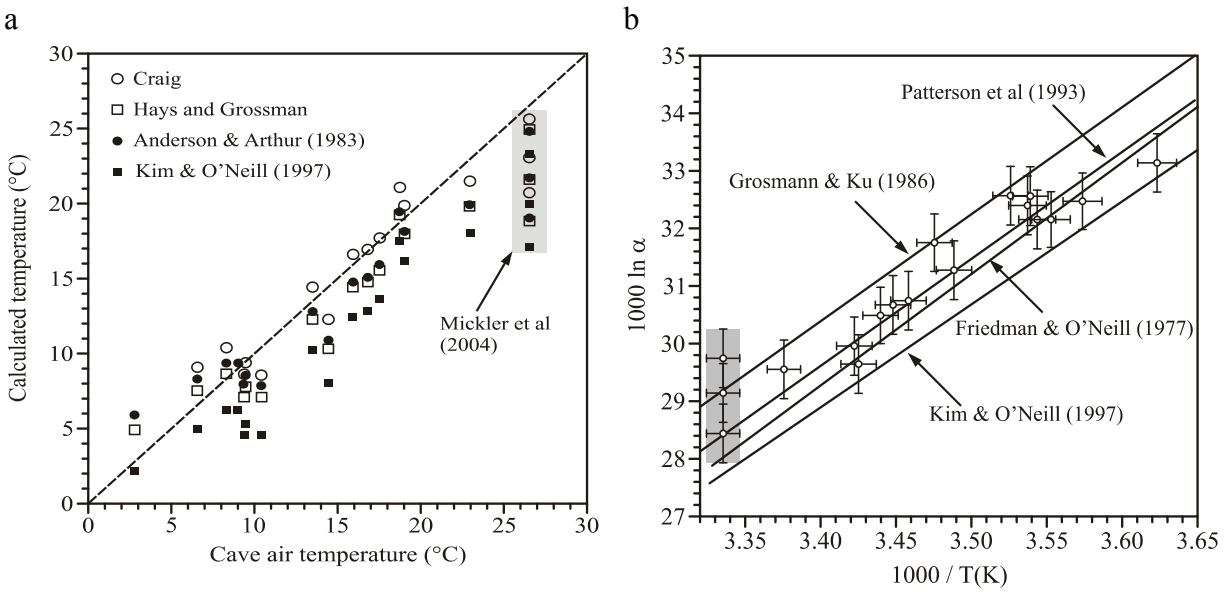

Figure 3.6 Comparison of measured cave air temperature and the temperature calculated by various approaches for a) paleotemperature equation of type A, and b) paleotemperature equation of type B from Table 3.1. From McDermott et al. (2006)

Slika 3.6 Usporedba izmjerenih temperatura zraka u špiljama i temperatura izračunatih prema paleotemperaturnim jednadžbama za a) oblik A i b) oblik B iz Tablice 3.1. Preuzeto iz McDermott et al. (2006)

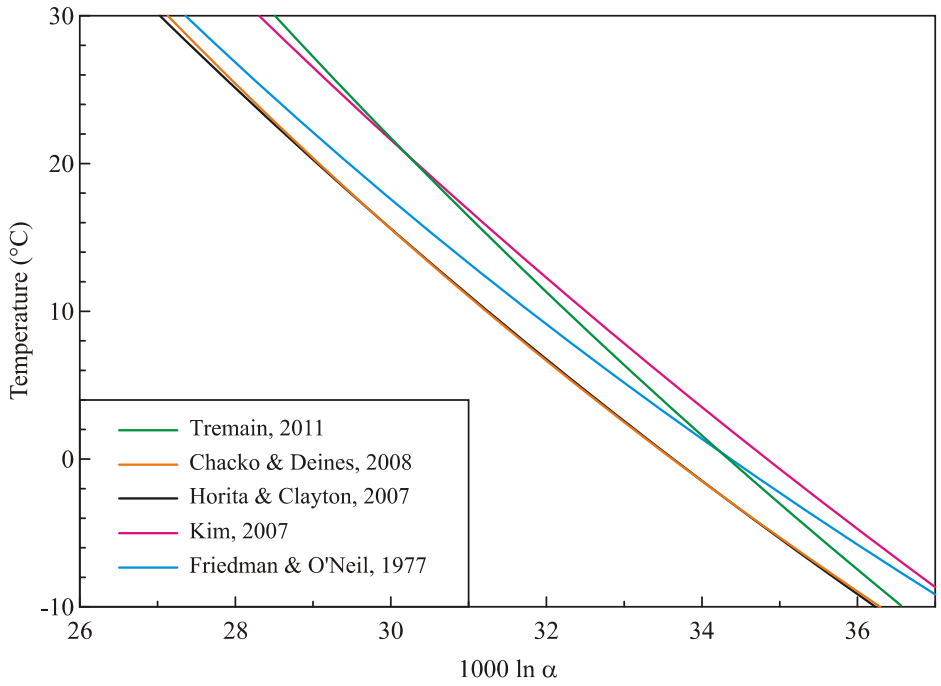

Figure 3.7 Comparison of various equations of type B (Table 3.1) for paleotemperature determination. Note different kind of graphical presentation of the equations of type B as compared to Figure 3.6b.

Slika 3.7 Usporedba raznih jednadžbi oblika B (Tablica 3.1) za određivanje paleotemperature. Treba primijetiti drugačiji grafički prikaz od prikaza istih jednadžbi na Slici 3.6b

3.6 Dating of speleothems

Information obtained from paleoclimate investigations has to be placed in a reliable chronological framework to assess the timing and rate of climate changes. In this context techniques of radiometric dating (e.g. uranium-series dating, radiocarbon dating) are applied.

Speleothems are protected from surface erosion and can form continuously for many millennia and bear the great advantage of being precisely and accurately datable using U-series techniques (Meyer et al., 2012). Clean calcite speleothems with low concentrations of detrital Th is preferable for U-Th chronology and this chronology in combination with $\delta^{18}O$ helps determine the timing and duration of major isotope-defined climatic events. This strategy results in atmospheric proxy signals ($\delta^{18}O$) that are accurately and precisely dated and can thus be supra-regionally correlated and compared (e.g. Wang et al., 2008). The $^{230}Th/^{234}U$ dating technique is a reliable method for precise dating of speleothems with several advantages over radiocarbon method, provided that the material has remained a close system to gain or loss of uranium and its decay products. It is important that the speleothems are free from contaminants and that the material contains sufficient uranium (Schwarz, 1986; Ford and Williams, 2007).

Radiocarbon (^{14}C*)* dating can be applied to speleothems younger than about 50000 yr. Due to geochemical processes involved in carbonate precipitation (section 3.1, equations 3.1 – 3.7), ^{14}C dating of speleothems, as well as lake sediment and tufa, is more complex than that of organic samples. The source of ^{14}C in speleothems is soil CO_2 dissolved in water that has ^{14}C activity approximately equal to that of the atmosphere and biosphere. The ^{14}C from soil CO_2 is mixed with ^{14}C-free carbon from limestone bedrock (section 3.1, equations 3.6), and as a result the ^{14}C activity of bicarbonate is lower than the atmospheric ^{14}C. This activity is usually known as the initial ^{14}C activity of the precipitated carbonate and it has to be determined for each carbonate system separately (Horvatinčić et al., 2003; Krajcar Bronić et al., 2010). Thus, the most important factor that affects the accuracy and reliability of the ^{14}C age of carbonate samples is the knowledge of the initial ^{14}C activity of the carbonate. If not known, the value of 85% is usually taken for karst areas (Horvatinčić et al., 2003).

3.7 Previous investigations

3.7.1 Paleoclimate

Caves are often treated as climate data information storage places on the geologic time scale. They are less prone to the changes caused by different environmental conditions and therefore can preserve unchanged information about climate over longer period of time. Important records are those kept in a secondary precipitated cave carbonates (stalactites, stalagmites, and flowstones). Employing investigations of stable isotopes, especially oxygen (^{18}O), in precipitated carbonate has been in main focus of paleoclimatic research. The great value of speleothem record is that they are continental records with high time resolution and the possibility of accurate dating. Enough data have been collected to show that the speleothem records very often agree well with other indicators of paleoclimate. A likely application of speleothem records will be to fill in much detail on the timing of climate shifts across continental masses where local climate can vary substantially over relatively short distances (White, 2007).

The use of stable oxygen isotope $\delta^{18}O$ values in speleothems as a paleoclimate proxy began in the 1960s and 1970s with benchmark studies of Broecker et al. (1960), Hendy and Wilson (1968), Duplessy et al. (1970), Hendy (1971) and Emiliani (1971). As the basic assumption for a possible use of $\delta^{18}O$ of speleothems served an observation that cave environments are quite stable and reflect the mean annual temperature of the region. Under equilibrium conditions, the $\delta^{18}O$ value of speleothem carbonate is related to two parameters (only): the $\delta^{18}O$ of drip water and the cave temperature. However, numerous later studies showed that the precipitation of speleothem calcite in O and C isotopic equilibrium with its corresponding drip water cannot be assumed, but must be carefully studied/checked (Lachniet, 2009).

If carbonate has been deposited in isotopic equilibrium conditions air temperature of the cave should stay constant and reflect mean annual outside temperature (±1 ºC) (Ford and Williams, 2007). Source for calcite deposition should be from saturated drip water entering the cave (Schwarz, 1986; Ford and Williams, 2007). If equilibrium deposition is documented in modern speleothems for present-day conditions, then the assumption is made that fossil/old speleothem material in the same cave was also deposited under equilibrium conditions. Meaningful paleoclimatic information can only be retrieved from speleothem calcite deposited under conditions of isotopic equilibrium (Harmon et al., 2007).

Depending on the growth rate of a speleothem (0.01 – 1.00 mm per year) different sampling techniques can be employed to get different time resolution of a climate changes (McDermott, 2004).

Study of influence of hydrological characteristics of precipitation on cave drip water lead to the conclusion that $\delta^{18}O$ of drip water should reflect weighted mean $\delta^{18}O$ value of precipitated rain above the cave (Smart and Friedrich, 1987). The problems may occur in water transport trough the soil surface because of evaporation (Bar-Matthews, 1996) and because of seasonal changes of pCO_2 and Ca concentration in the soil (Genty, 2001a; Genty, 2001b). With detailed site specific and seasonal monitoring, understanding of processes and environmental conditions should bring insights in easier interpretation of paleoclimate data.

Besides ^{18}O, a carbon isotope ^{13}C can also be used in paleoclimatic studies, however, $\delta^{13}C$ values in paleoclimate data interpretation should be taken with caution. Usage of speleothems $\delta^{13}C$ should be followed by trace elements and petrography to support processes predicted by mathematical models and field measurements (McDermott, 2004, and reference therein).

Origin of $\delta^{13}C$ in speleothems is influenced by dissolution of the overlying bedrock by percolation water. Different models for bedrock dissolution have been described in literature. For open systems continuous equilibration process occurs between percolation water and pCO_2 contained in soil (Hendy, 1971; Salomons et al., 1986). In these systems $\delta^{13}C$ of dissolved inorganic carbon (DIC) when saturated with respect to calcite, depends on pCO_2 and temperature, and in areas with prevailing C3 plants varies from -14 to -18 ‰. In closed system dissolution of carbonate rock is isolated from soil CO_2 and for the same C3 system value for DIC $\delta^{13}C$ is about -11 ‰ (Hendy, 1971; Salomons et al., 1986). Lighter $\delta^{13}C$ values (more negative) are due to larger biogenic production of the soil CO_2 that indicates warmer climate (Dulinski and Rozanski, 1990; Dorale et al., 1998; Genty et al., 2003).

Classic paleotemperature equation was given by Epstein and Mayeda (1953). It can be used either for paleoresearch, when it has 2 unknowns; T and $\delta^{18}O$ of water, or for assessing isotopic equilibrium for modern carbonate, when T is considered as unknown and calculated from measured $\delta^{18}O$ data and then compared to real cave temperature (Lachniet, 2009).

A significant contribution to speleothem-based climate studies is given by Mickler et al. (2004) who studied stable isotope composition of modern tropical speleothems and calcite precipitated on glass plates in Harrisons's Cave on Barbados. Three different locations in the same cave represented the range of microenvironment conditions in the cave, and samples collected recorded the sensitivity of speleothem to modern climatic and hydrologic variation.

They outlined new tests for O and C isotope equilibrium in modern speleothems and determined the magnitude and direction of offsets from equilibrium. Mechanism 1 results from the incorporation of HCO_3^-(aq) into calcite during rapid, almost instantaneous, mineral precipitation, such that isotopic fractionation is minimized (McCrea, 1950; Turner, 1982; Michaelis et al., 1985; Clark and Lauriol, 1992). As a result, $\delta^{13}C$ values of modern calcite differ from the predicted equilibrium values. They tend towards $\delta^{13}C$ values lower than the equilibrium values, and in some cases are equivalent to the carbon isotopic compositions of DIC. The $\delta^{18}O$ value of rapidly precipitated carbonate reflects the $\delta^{18}O$ composition of HCO_3^- from water. However, it is difficult to measure $\delta^{18}O$ of HCO_3^-. The difference between $\delta^{18}O$ of HCO_3^- and precipitated carbonate in equilibrium is about 6 ‰, but under rapid precipitation it is much lower and approaches 0 % (Mickler et al., 2004). Mechanism 2 starts with fast degassing of isotopically light CO_2 from the drip water into the cave environment with lower pCO_2. As degassing of ^{13}C (depleted) CO_2 progresses, the reservoir of HCO_3^-(aq) becomes isotopically heavier. The loss of isotopically heavy C trough $CaCO_3$ precipitation is not enough to offset the loss of the more ^{13}C-depleted carbon through CO_2 degassing. The final result is enrichment in both ^{13}C and ^{18}O as CO_2 degassing continues (Michaelis et al., 1985; Dulinski and Rozanski, 1990; Mickler et al., 2004).

Formation of alpine (high-altitude) speleothems preferentially occurs during warm interglacial and interstadial climatic conditions. However, they also precipitate during cooler and less favourable climatic periods if the cave is situated in a low or intermediate altitude range, where cessation of calcite precipitation due to cave freezing occurs only during the most severe cold events (Kempe et al., 2004; Spötl et al., 2007).

Review of age data of 660 speleothems and 140 tufa samples showed that formation of calcite (speleothem or tufa) was impossible if there was no water during extremely glacial or arid climates (Hennig et al., 1983). Rapid speleothem growth generally corresponds to exuberant flora on the cave-bearing rock, therefore Quaternary calcites contain climatic information that can be read out of pollen, paleofauna, morphology and stable isotope content. Thus, the U/Th dated Quaternary carbonates can be valuable sources of paleoclimatic information.

Histograms of speleothem ages for two climate regions, north and central Europe, and the Mediterranean show frequency distributions with increased number of age data within certain periods that reflect warm and humid climate (Hennig, et al., 1983). The absence of age data would possibly indicate glacial ages during which the speleothem growth ceased. Results show that the Holocene speleothem deposition in Central Europe begins at cca 15000 ± 3000 yr BP.

There are no speleothem data of ages between 30000 and 20000 yr BP in Northern Europe and similar climatic regions, which most likely reflects the maximum of the Würm glacial age.

Similarly, the age distributions of speleothems from various latitudes showed the absence of speleothem deposition in the mid- to high latitudes of the Northern Hemisphere during marine isotope stage MIS 2 from 24 ky to 11 ky (McDermott, 2004). The period is striking cold, consistent with results from previous compilations (Hennig, et al., 1983). By contrast, speleothem deposition appears to have been continuous through the glacial period at lower altitudes such as Soreq cave in Israel (Ayalon et al., 2002).

Detailed logging and outcrop mapping of Quaternary sediments in the region of Kvarner, South Velebit and in Northern Dalmatia gave evidence of widespread glacigenic sediments in the Adriatic and the Dinarides proving the far seawards extension of the Dinaric glaciation (Marjanac, 2012). However, no sufficient evidence was found for assumption that the Dinaric glaciation reached the Alps and for correlation with the Alpine glaciations.

Few terrestrial Holocene climate records exist for south-eastern Europe despite its important geographical position as a transitional climatic zone between the Mediterranean and mainland continental Europe (Rudzka et al., 2012). Modern meteorological and cave conditions have been monitored in Modrič Cave (Croatia) for 2 years to understand the links between climate variability and stable isotope time-series records in speleothems (Surić et al., 2010). Modern calcite from the tops of 2 stalagmites exhibits $\delta^{18}O$ values that are close to isotopic equilibrium with their respective drip water values. Radiocarbon dates have been used to constrain their chronology using a dead carbon correction. Both stalagmites were deposited during the late Holocene. Changes in stalagmite diameter during deposition were linked to $\delta^{13}C$ and $\delta^{18}O$ variations and indicated alternating periods of drier and wetter conditions (Rudzka et al., 2012). Both drip sites were classified as “seepage flow” drips (Smart and Friedrich, 1987). One of them indicated a greater fracture-controlled storage component. $\delta^{18}O$ value of dripwater was -5.8 ± 0.2 ‰ and that of modern speleothems varied from -3.58 to -5.66 ‰. For modern carbonates $\delta^{13}C$ ranged from -4.01 to -9.97 ‰. Measured cave temperature during monitoring period was 15.6 ± 0.1 ºC, and temperature calculated by equation of Craig (1961) was 15.2 ºC, thus pointing to isotopic equilibrium conditions of carbonate precipitation (Surić et al., 2010).

One of the earliest studies in Slovenia employing stable isotopes for investigation of recent speleothem and their applicability to paleoclimatic studies was performed by Urbanc et al. (1984). Stable isotope composition ($\delta^{13}C$ and $\delta^{18}O$) of recent speleothems in various karst caves in Slovenia, including Postojna Cave, was used for quantitative determination of climatic

conditions, and for determination of natural variability of stable isotope composition in both, recent and old speleothems. $\delta^{18}O$ values of recent speleothems from various caves ranged from -6.93 to -4.91 ‰, and $\delta^{18}O$ values of water from -7.2 to -9.90 ‰ (at altitude 1400 m). The temperatures calculated by using approaches of O'Neil et al. (1969) and Craig (1965) were in the range from 4.2 to 9.5 ºC, very close to the actually measured ones (5.3 to 10.0 ºC), although systematically lower by 0.5 to 3 ºC. Speleothems from low-altitude caves have $\delta^{13}C$ varying between -10 and -4 ‰, and $\delta^{18}O$ between -7.5 and -5 ‰. Positive correlation $\delta^{13}C$ vs. $\delta^{18}O$ was observed, although the samples were taken from deep unventilated locations with high humidity and small annual temperature variations. In the other group of samples from high-altitude (1400 m, Kamniška jama) $\delta^{13}C$ ranged from -3 to +2.2 ‰ and these values were explained as absence of biogenic (soil) CO_2 during speleothem formation. For several samples taken from the ventilated (windy) entrance region of Planinska jama, where humidity was not high and temperature variation were higher, the measured isotopic composition was much higher ($\delta^{13}C$ between -0.62 and +4.0 ‰, $\delta^{18}O$ between -2.17 and -2.91 ‰) indicating effects of evaporation of drip water. Speleothems from Postojna Cave (Pisani rov – Colorful gallery) had $\delta^{13}C$ in the range from -9.20 to -7.10 ‰, and $\delta^{18}O$ from -8.50 and -6.85 ‰.

As a continuation of this work, Urbanc et al. (1987) compared isotopic composition ($\delta^{13}C$, $\delta^{18}O$) and ^{14}C ages of speleothems from caves in Slovenian karst and tufa and lake sediment samples from the Plitvice Lakes in Croatia. Most of the $\delta^{13}C$ values of all types of samples were in the same range, from -11 to -5 ‰, and more pronounced differences observed in their $\delta^{18}O$ values (tufa and lake sediment from -10 to -8.5 ‰, speleothem from Divača cave about -5 ‰, from other caves, including Postojna Cave, -7 to -6 ‰) were explained by different $\delta^{18}O$ composition of waters from which they precipitated. Temperature of carbonate formation was calculated by using O'Neil et al. (1969) approach. The calculated temperature of speleothem formation were 0.5 to 3.2 ºC lower than the measured ones, while the calculated temperatures for tufa and lake sediment were higher (by 0.5 to 3.7 ºC) than the averaged water temperature measured for several past years. The $\delta^{18}O$ values of the 12-m-long sediment cores in two largest lakes of the Plitvice Lakes systems were very uniform (Srdoč et al., 1986) throughout the investigated sediment profile, indicating that no significant climatic changes occurred during the sedimentation, which lasted about 8000 years.

Vokal (1999) studied carbon transfer in karst area by applying geochemical and isotopic measurement of drip water and a stalagmite. Sampling was done in Postojna Cave. The

measured cave air temperature in a period of 1-year from June 1996 to June 1997 ranged from 7.8 ± 0.1 °C to 8.2 ± 0.4 ºC at different locations, and outside temperature was 10.4 ± 0.7 ºC. pH of drip water was 7.8 ± 0.2. No correlation between pH and drip rate was found. Mean Ca^{2+} concentration ranged from 55.5 mg/L to 79.9 mg/L while bicarbonate concentration ranged from 165.2 mg/L to 232.8 mg/L. Electrical conductivity varied from 301 µS/cm to 424 µS/cm. The delay between higher rain amount and change in drip rate was found to be 1 to 2 months. I_{sat} ranged from 0.5 to 6. The calculated growth rate ranged from 0.13 mm/yr to 0.20 mm/yr. Measured $\delta^{13}C$ of soil CO_2 was -21.7 and -20.5 ‰ with seasonal variations of up to 7.3 ‰, while the $\delta^{13}C$ of soil organic mater was -26.7 ‰. The isotopic composition of carbon, oxygen and hydrogen has been determined in drip water and in the River Pivka. Mean $\delta^{13}C$ value of DIC in drip water ranged from -14.7 to -10.2 ‰ and in the Pivka River it was -13.7 ‰. $\delta^{18}O$ value of drip water ranged from -8.8 to -8.3 ‰ and of the Pivka River $\delta^{18}O$ was -8.2 ‰. Values of deuterium concentration varied from -54 to -57 ‰ in drip water and -54 ‰ for the Pivka River. were Stable isotope composition was measured along the depth profile of an old stalagmite: $\delta^{18}O$ values ranged from -7.49 to -6.05 ‰ and $\underline{\delta}^{13}C$ from -10.18 ‰ to -9.31 ‰.

In summary, various and numerous studies of cave speleothems have reached the same conclusions: when exploring the possibility of the use of speleothems in paleoclimatic research, one must study: 1) the existence of equilibrium isotope effects in speleothem deposition, 2) drip water chemistry, 3) cave environment conditions of the speleothem deposition, and 4) drip water isotopic composition and its relation to isotopic composition of precipitation, i.e., to conduct so-called $\delta^{18}O$ – climate calibration.

3.7.2 Cave environmental conditions

Due to the sensitivity of interpretation data from speleothems as a paleoclimate proxy it is important to determine whether recent carbonate precipitation reflects recent climate conditions. Also it is important to explore different parameters in cave environment, such as cave ventilation dynamics. Different kinds of cave ventilations (chimney effect, convection, meteorologically driven patterns) can significantly influence speleothem precipitation (Fairchild et al., 2007). Influences of cave ventilation have been detected in $\delta^{18}O$ and $\delta^{13}C$ of precipitated carbonates as seasonal and intra-annual cycles (Bar-Matthews et al., 1996; Spötl et al., 2005; Baldini et al., 2008). Spötl et al. (2005) modeled impact of cave ventilation on geochemistry of drip water and found seasonal variations in electrical conductivity, alkalinity, pH and $\delta^{13}C$ of

DIC and cave air due to chemical modification of the groundwater by dynamic and bidirectional subsurface air circulation.

Influence of cave air circulation, temperature and pressure regarding cave internal geometry has been studied by Bourges et al. (2006), and the effects of distribution of pCO_2 on the complexity of carbonate precipitation has been studied by Baldini et al. (2006) and Whitaker et al. (2010). They showed that local differences in pCO_2 on specific sites within the cave influence speleothem growth. The changes in pCO_2 inside the cave dependent on the distance from the entrance, and also variations in the vertical profile have been found (Ek and Gewelt, 1985).

Seasonal variation in airflow at Obir (Spötl et al., 2005) results in low pCO_2 in cave air in winter, which is associated with higher $\delta^{13}C$ and pH of drip water. Enrichments in ^{13}C were found in winter growth of laminae. The winter season is associated with low pCO_2 which controls the pH of drip water by enhancing the degassing toward equilibrium. Seasonality observed in Obir Cave can be summarized as: 1) in winter pH rises (CO_2 lower), 2) $\delta^{13}C_{DIC}$ becomes 2 – 7 ‰ more positive (due to degassing of light CO_2), 3) modest decrease in Ca and HCO_3^- concentrations as well as in conductivity, which indicate PCP. Prior calcite precipitation (PCP) may occur in the vadose zone when downward-percolating water reaches a void in a caprock and becomes super saturated with calcium carbonate due to CO_2 degassing. Drip water that afterwards reaches the cave has consequently lower pCO_2, lower Ca and HCO_3^- concentrations as well as conductivity, higher Mg/Ca ratio and more positive $\delta^{13}C_{DIC}$ (Horvatinčić et al., 2003; Spötl et al., 2005; Fairchild, et al., 2007; 2010 and references therein).

In the area of Moravian Karst in the Czech Republic, Balcarka Cave and soil above the cave was studied with emphasis on CO_2 dynamics of the cave (Faimon et al., 2011). The CO_2 dynamics was visible in soil and cave sites with the autumn and spring periods. The values of CO_2 partial pressures in dripwater ($10^{-2.98}$ to $10^{-2.37}$ bar) exceeded the CO_2 partial pressures in the cave atmosphere ($10^{-3.25}$ to $10^{-2.55}$ bar), and predicted further CO_2 degassing from dripwater with supersaturation increase. No correlations between soil CO_2 levels and air temperature or humidity were found. The authors concluded that the detailed relations in the chain external conditions (temperature/humidity) – microbial activity – organic matter degradation (CO_2 production) wass complex and still poorly understood (Faimon et al., 2011).

Studies that employ several coeval stalagmites from the same cave are invaluable to asses the reliability of speleothems as paleo-climate recorders, as showh by comparison of $\delta^{18}O$ records of three different speleothems from the same cave at different locations (Linge et al., 2001a;

2001b). It seems that processes other than climate variability (e.g., variable seepage water routes, water mixing) can substantially affect the $\delta^{18}O$ values recorded in stagalmites. Therefore, stable isotope patterns should be confirmed from several samples before rigorous interpretations are made, and variations in percolation paths are sometimes very significant (Linge et al., 2001a; 2001b, McDermott, 2004). Even though the calcite is not deposited under isotopic equilibrium conditions, it can give information about environmental conditions at the time of deposition, vegetation and soil changes (Plagnes et al., 2002; Genty et al., 2003).

Similarly, Bar-Matthews et al. (1996) concluded that for successful interpretation of stable isotope composition of old/ancient speleothem (specially in semi-arid areas) it would be necessary to obtain fossil speleothem record from different types of contemporaneous deposit in order to fully characterize the $\delta^{18}O$ – $\delta^{13}C$ range representative of any climatic period. Additionally, they conclude also that the carbonate-water system in a cave needs to be calibrated for the present day variations in the isotopic composition of water and carbonates and for the relations between these values and the isotopic composition of the concurrent rainfall. One well-characterized cave system is preferable to studies in a diverse number of caves where the isotopic systems are not calibrated.

3.7.3 Previous studies on Postojna Cave

Postojna Cave is the most visited show cave in Slovenia with up to 500,000 tourist visits per year (Prelovšek et al., 2011). Due to its well-known beauty and diversities of karst phenomena and specific biota, the Cave has attracted attention of scientists from different scientific areas since its discovery until present days.

The oldest inscriptions in part of the cave called "Imenski rov" (en. old signature chamber) go back into 13th and 14th century. Inscriptions in the caves are important historic source especially if they are from historically known persons and from well described and documented explorations of caves (Kempe and Hubrich, 2011). Inscriptions have been used to calculate growth rate of a flowstone and accordingly to estimate the age of the cave formation (Kempe et al., 2006). Inscriptions in caves are also witnesses of stable cave climate (Shaw, 1992).

In Postojna Cave first investigations on biospeleology (biology of underground world) have been done. Representatives of cave-dwelling animals, many of them endemic species, have been discovered in Postojna Cave. The most famous is **olm**, or **proteus** (*Proteus anguinus*) also called the "human fish", and then beetle **drobnovratnik** (meaning "tiny necked"). Many species of copepods have been discovered and recorded (Pipan and Brancelj, 2004). The Postojna Cave is therefore considered to be the cradle of biospeleology.

Detailed maps at scale 1:500 and 1:2500 of some parts of Postojna Cave were made during Italian domination in 1933/34 (Gospodarič, 1976), and are in use since then. Some of these maps are used in this thesis for detailed description of sampling sites in Chapter 5.

Detailed and systematic studies of the diversity of the cave sediments showed connection of deposition phase and geological time with surface and undersurface processes during development of the Postojna Cave system (Brodar, 1966; Gospodarič, 1976).

Various studies reported different stages in geological history of the Postojna Cave (Gospodarič, 1981; Ikeya et al., 1982; Gospodarič, 1988). By the ESR (Electron Spin Resonance) and ^{14}C and U/Th dating methods a few "generations" of speleothems and sediments have been recognized: Holocene, Postglacial, Würm Interstadial and two Interglacial sinter generations of speleothems and sediments. First paleomagnetic dating of sediments in Postojna Cave indicated sediment ages between 0.73 to 0.90 Ma (Šebela and Sasowsky, 1999). Recently, much older cave sediments were dated in Postojna Cave and they showed that deposition of cave sediments occurred in periods from 5.4 to 4.1 Ma (Miocene – Pliocene), from 3.6 to 1.8 Ma (Pliocene) and in Quaternary (Zupan Hajna et al., 2008; 2010).

Tectonic and geological maps of surface above and in the cave can be found in Šebela (1998) and (Čar and Šebela, 1998). They found that karstification is not characteristics of all fault zones, but only of some of them due to specific tectonic mechanisms in the time of their formation. Basic geological map of the Postojna Cave system in shown in Figure 3.8.

Relations between faults, collapse dolines and collector channel formations have been described in Šušteršič (2006). For example, the Congress chamber (later in thesis location 04 – Kongresna dvorana) lies on the crossing of the tourist passage and fault. The thick flowstone ceiling above the location means that the ceiling has achieved stability. Another part of Postojna Cave described in the paper is Upper Tartarus (later in thesis location 09 – Zgornji Tartar) which was the continuation of the main ponor of the Pivka River in Otroška jama during Early Pleistocene (Gospodarič, 1976). After collapse of doline, known as Stara apnenca, the direction of the Pivka River flow changed. Fallen cave ceiling in Zgornji Tartar (Figure 22 in Appendix II) indicates a breakthrough point of the Pivka River.

To estimate mean residence time of water in the Postojna Cave system, transport through vadose zone was studied by trace experiment with uranin (flourescin sodium) dye (Kogovšek and Šebela, 2004). In the investigated area of Kristalni rov fast flow happens in the most conductive seep (21 to 43 hours) and the rest of the tracer is forced by precipitation with delay of 3 months. Subvertical tectonic fissures seem to be the best connection of the surface area and cave interior (Kogovšek and Šebela, 2004). Percolation of water goes trough fissured zones and dip direction of bedding planes.

Study of the environmental conditions associated with speleothem formation in the Postojna Cave is based on chemical and isotopic measurements during 1996-1997 at three different locations (Vokal et al., 1999). Measurements of the drip water chemistry have been done on two locations within Postojna cave and on Pivka River, and on spring Močilnik. The results have been presented in section 3.7.1.

Time required to grow a large stalagmite and carbonate precipitation rate was studied in the 34-year-long study, from 1963 to 1997, performed by Gams and Kogovšek (1998). Yearly precipitation growth rate of carbonate on a flowstone was determined to be 0.11 mm per year.

Natural hazards, like earthquakes, that affected Postojna cave are described by Perko (1929), Kempe (2004) and Šebela (2010).

Radon in show-caves was firstly studied because it was supposed that it affects human health, i.e. exposure to high level of radon concentration can provoke lung cancer. Since the Postojna Cave is a show-cave, monitoring of radon concentration was performed to estimate health risk for tourist guides. To study radon concentration in Postojna Cave radon detectors were placed at

two locations (Vaupotič and Kobal, 2004) and temperature and air humidity were monitored also. The temperature ranged between 13 and 15 ºC and relative humidity was around 100%. The radon concentration (C_{Rn}) and radon decay product (C_{RnDP}) concentration patterns revealed two different patterns of cave ventilation characteristic for summer and winter period of the year. Both C_{Rn} and C_{RnDP} values were lower in winter (1466 Bqm^{-3}, 736 Bqm^{-3}) than in summer (4089 Bqm^{-3}, 1367 Bqm^{-3}). to the changes were explained by the "chimney effect" (Vaupotič and Kobal, 2004). In winter period the cave temperature is higher than outside temperature and the air exits the cave through natural vertical channels. During the winter time chimney effect is dominant. During the summer the situation is opposite and there is almost no vertical circulation. During summer months effect of pressure difference of the cave air and outdoor air influences the cave atmosphere. Daily ventilation is dominant. When outdoor pressure starts to decrease, cave air becomes over-pressurized in respect to outside air and cave ventilation starts (Vaupotič and Kobal, 2004). Continuation of monitoring results was published in Gregorič et al. (2011) with addition of computational models that calculated delay of radon concentration from inside and outside the cave. The delay was calculated to be four days.

Concentration of CO_2 in the Postojna Cave has been studied by Gams (1974a), From two independent measurements of CO_2 concentration in 1963/64 and in 1972 conclusion is that tourists do not contribute to CO_2 concentration. CO_2 concentration was higher in summer (up to 2000 ppm) than in winter (400 – 600 ppm). The summer increase of pCO_2 was observed in both touristic and non-touristic parts of the cave.

The relation of external climate and cave temperature has been studied from different aspects. Gregorič et al. (2011) have investigated dependence of radon levels on outside temperature, Prelovšek et al. (2011) have described connection between number of tourists visit with the cave climate, and Šebela and Turk (2011) studied climate characteristic of the Postojna Cave during one year period (2009 - 2010) in connection to cave air pressure and cave temperature. They reported different microclimate characteristics (air temperature and pressure) in different (3) monitoring stations regarding known and possible unknown passages in vicinity. In Postojna Cave, many broken speleothems can be found. Explanation and possible determination of the cause of breaking (if not vandalism) may be used as the indication of natural and geological changes during the cave history (Perko, 1929; Kempe, 2004; Šebela, 2010). The processes of speleothem brakeage can be grouped into site-limited processes (mass-wasting, compaction, erosion, re-crystallization, vandalism), and processes of local impact (frost in entrance, in cold air traps and in caves at high altitudes, inundation, desiccation ice in the cave during glacial periods and earthquake) (Kempe, 2004).

Being aware that processes in cave interior development strongly depend on environmental conditions outside the cave, various monitoring studies were organized. The early study of climate and environmental conditions (temperatures outside and in the cave from 1932 to 1938) (Crestni and Anneli, 1939) resulted in observed temperature variations of 1 to 2 ºC.

Reconstruction of ^{14}C activity during last 50 years period in the Postojna Cave was enabled by well dated fire in the cave that left a black layer in the speleothem (Genty et al., 1998). Time resolution of 1 to 2 years was obtained by using AMS measurement technique. Studied stalagmites shows changes in ^{14}C activity that followed the ^{14}C activity of the atmosphere caused by so-called bomb-peak (Levin and Kromer, 1997; Krajcar Bronić et al., 1998). However, the ^{14}C peak in speleothem was delayed and damped in comparison with the atmospheric ^{14}C peak in 1963. Delay of the bomb peak was found to be 10 ± 5 years.

Horvatinčić et al. (2003) compared some basic parameters for tufa and speleothem precipitation from fresh water at Plitvice Lakes and from drip water in Postojna Cave, respectively, and concluded that these two types of calcareous deposits were formed under different environmental conditions. More stable conditions (physical and chemical parameters in parent waters, especially temperature and I_{sat}) accompany speleothem formation than tufa formation. The range of $\delta^{13}C$ of speleothem shows that speleothem formation is also possible from water poor in biogenic carbon (e.g., at high altitudes), while the biogenic carbon is more crucial in tufa formation.

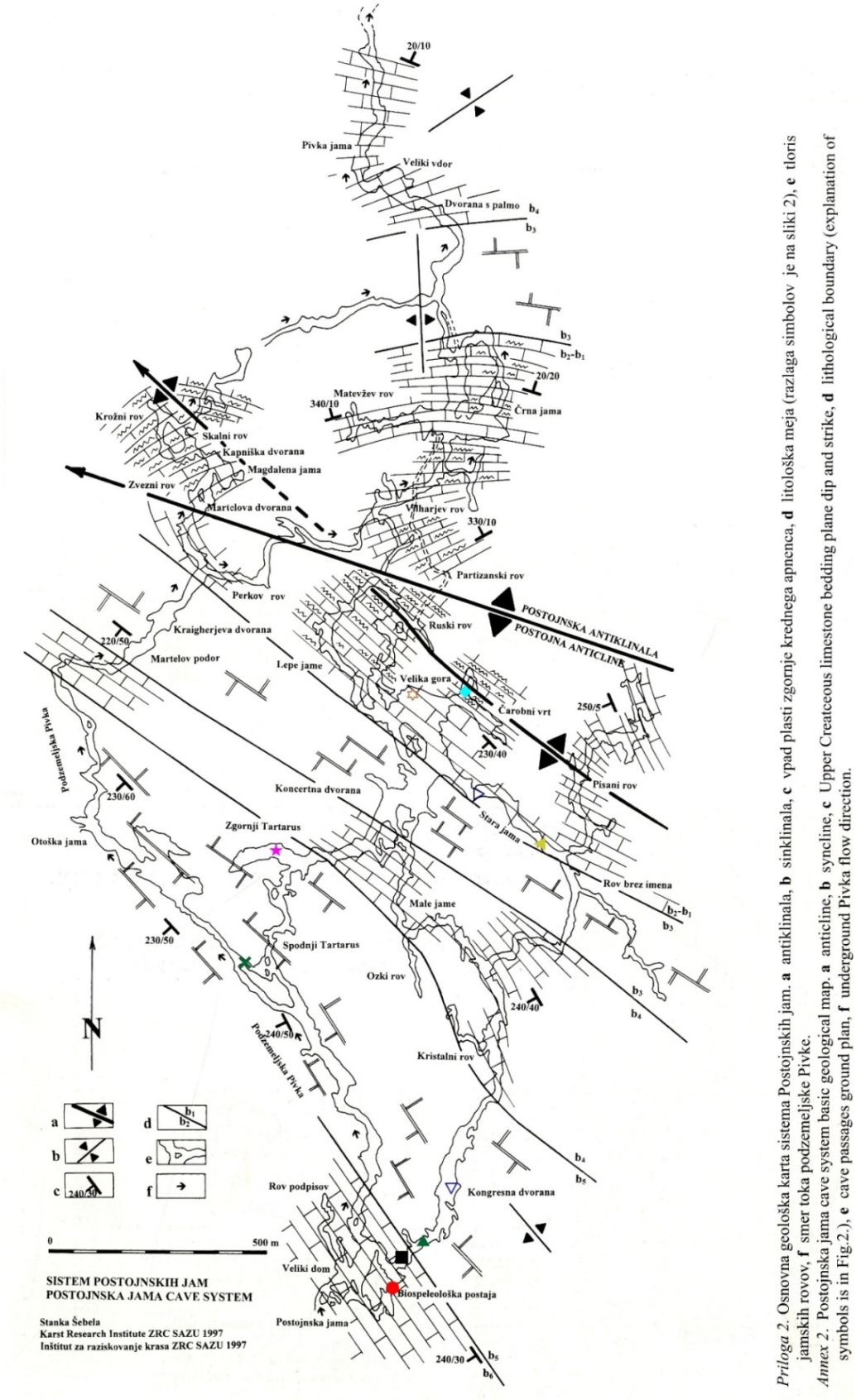

Priloga 2. Osnovna geološka karta sistema Postojnskih jam. **a** antiklinala, **b** sinklinala, **c** vpad plasti zgornje krednega apnenca, **d** litološka meja (razlaga simbolov je na sliki 2), **e** tloris jamskih rovov, **f** smer toka podzemeljske Pivke.

Annex 2. Postojnska jama cave system basic geological map. **a** anticline, **b** syncline, **c** Upper Createceous limestone bedding plane dip and strike, **d** lithological boundary (explanation of symbols is in Fig.2.), **e** cave passages ground plan, **f** underground Pivka flow direction.

Figure 3.8 Basic geological map of Postojna Cave system (from Šebela, 1998).
Slika 3.8 Osnovna geološka karta sustava Postojnske jame (preuzeto iz Šebela, 1998)

4 SITE DESCRIPTION

4.1 Geology of Postojna Karst

The word “karst” originates from “karra”, i.e. “gara” that means stone (Ford and Williams, 2007). It is a landscape characterized by rocks of high solubility with well developed secondary porosity and distinctive hydrology. The fundamental role in karst system development has dissolution of carbonate rocks. System of water underground network evolves over time, dissolute the rocks and forms surface and subterranean structures that are characteristic for karst areas. It is supposed that 12 % of a world land (uncovered by ice) is karst. The largest karstic areas in the world are in China (1 200 000 km^2) and Mexico (500 000 km^2). The largest karstic area in Europe is the area of Dinaric Karst (60 000 km^2), covering parts of Italy, Slovenia, Croatia, Bosnia and Herzegovina, Montenegro, Serbia and Albania.

Dinaric Karst is the largest continuous karst landscape in Europe. It is positioned between the Pannonian Basin in the northeast and the Adriatic Sea in the southwest. Border along the Alps in the north is determined by rivers Soča, Idrijica and Dolenjsko podolje in Slovenia. The border is Sava River valley and the eastern border form Kolubara and Morava River basins, Kosovo basin and Prokletije mountains. Figure 4.1 shows the border of the Dinaric Karst as defined by two different studies (Roglić, 1965; Gams, 1974b). Strike of the most relief features in Dinaric Karst is northwest – southeast, which is called the Dinaric strike. The main landforms are the mountains consisted of limestone and dolomites. The other characteristics of the relief are large leveled surfaces (poljes), plateaus and intermountain depressions. The Dinaric Karst is recognized as the geological “type region” for the definition of such relief characteristics worldwide. There are numerous caves located in Dinaric Karst, more than 7000 known in Slovenia and more than 6000 in Croatia, and many of them are rich in speleothems. There are also several regions of lakes and rivers where tufa is forming at

present, or where old tufa deposits can be found (Horvatinčić et al., 2003). The whole region has been a subject to considerable research interest and has a potential for paleoclimatic studies.

Figure 4.1 Dinaric karst borders after Roglić (1965) (—) and after Gams (1974b) (—). Black circle (●) denotes Postojna Karst area.

Slika 4.1 Granice dinarskog krša prema Roglić (1965) (—) i prema Gams (1974b) (—). Crni kružić (●) označava područje Postojnskog krša.

The Postojna Karst is situated on NW part of the Dinaric Karst in Slovenia (Figure 4.2). It is composed of mostly Cretaceous carbonate rocks (Figure 3.8), and Triassic and Jurassic dolomites appear on the northern and north-eastern side and of Eocen flysch on the western and south-western part. On the western and south-western side the Postojna Karst is in contact with non-carbonate Eocen flish rocks from where some rivers are flowing and sinking into the Postojna karst. More than 60 caves are known in Postojna Karst. The largest cave system is the Postojna Cave system, 20.5 km long, which consists of Podzemeljska Pivka (3128 m), Postojna Cave (10 399 m), Otroška Cave (713 m), Magdalena Cave (1427 m), Črna Cave (3225 m) and Pivka Cave (1874 m) (Šebela, 1997).

Important role in the formation of the Postojna Cave system has Pivka River that drains into the cave. The Pivka River basin is built-up of Eocene flysch rocks, which is in contrast to the

surface of Postojna Cave formed of Upper Cenomanian limestones (Buser et al., 1967). The Postojna Cave was formed by sinking Pivka River. There are two main levels of the cave passages: the upper, which is mostly dry and the lower where the river flows.

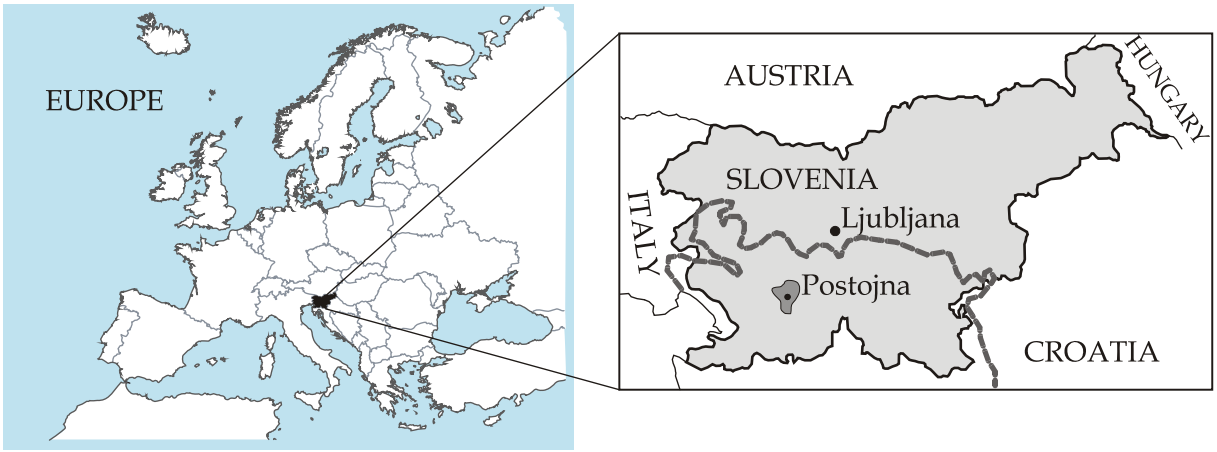

Figure 4.2 Map of Europe with position of Slovenia (left); (right) map of Slovenia with Postojna Karst area (darker shadowed area). The boundary of the Dinaric karst (- - -) by Gams (1974b) is shown.

Slika 4.2 Karta Europe s naznačenim položajem Slovenije (lijevo); (desno) karta Slovenije s označenim područjem Postojnskog krša (tamnije osjenčano) i granicom dinarskog krša (- - -) prema Gams (1974b).

The surface above the cave is dissected by numerous dolines and is about 50-100 m above the cave. This vertical development creates enough gradient for strong air circulations. Above the cave system there are numerous (17) collapse dolines (Šebela, 2001) characteristic for karst terrain. Some 150 years ago there was a bare pasture, meadow. The land area is now covered by forest.

Surface topography of Postojna Cave area is shown in Figure 4.3. A map of underground passages of the Postojna Cave with marked sampling sites is added to visualize geographical position of the Cave entrance of the Pivka River to Postojna Cave.

In addition to the Pivka River, bedding planes have large influence on orientation and formation of the cave passages (Čar and Šebela, 1998). The strike is in NW – SE Dinaric karst orientation, which is also the strike of Postojna anticline (Gospodarič, 1976; Šebela 1998).

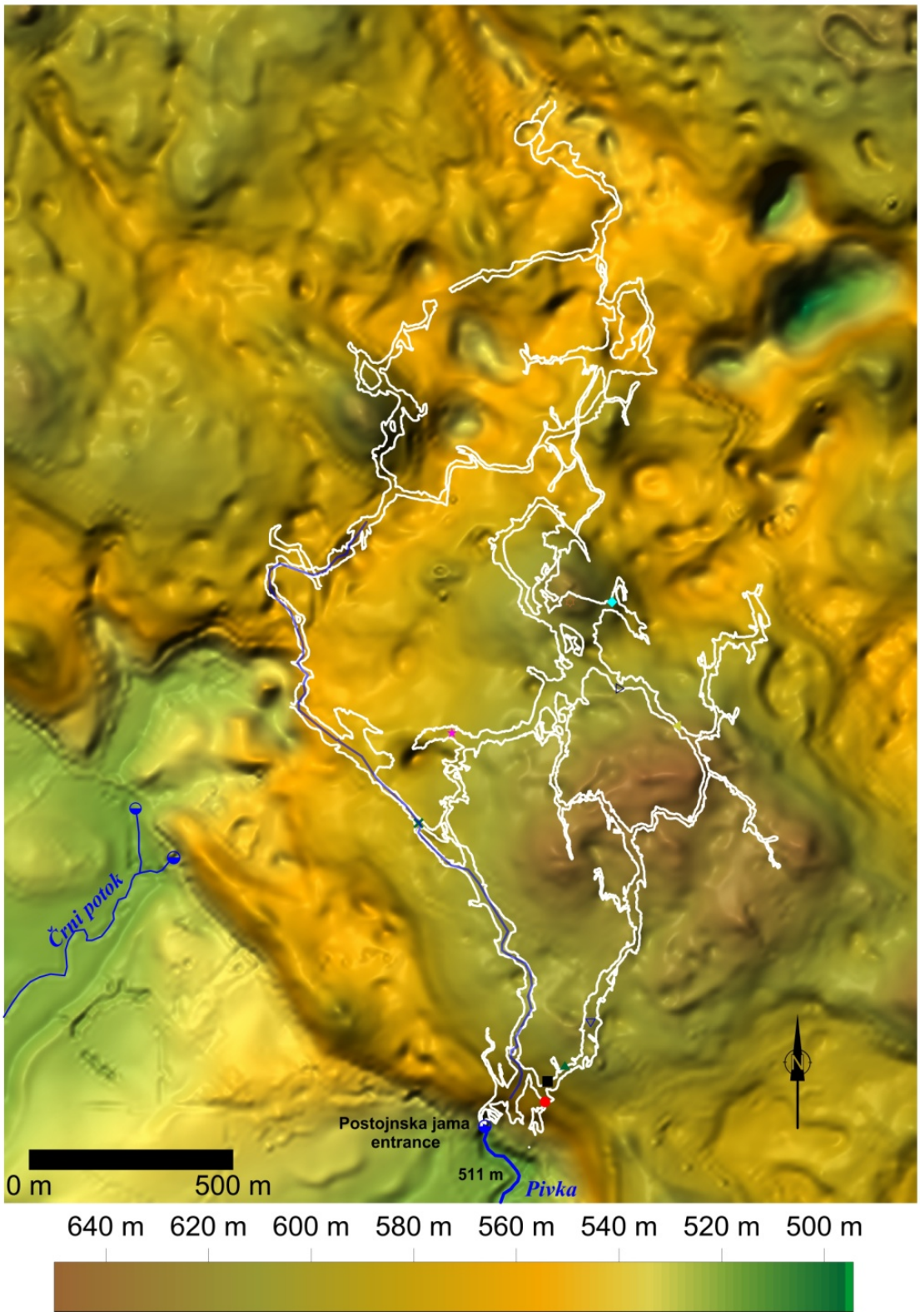

Figure 4.3 Superposition of Postojna Cave system network and surface area map (Mihevc, personal communication).

Slika 4.3 Karta (reljefna) površine iznad Postojnske jame kombinirana s kartom podzemnog sustava Postojnske jame i podzemnog toka rijeke Pivke (Mihevc, osobna komunikacija).

Modern entrance of the Postojna Cave is 529 m a.s.l. It is 18 m above the Pivka River sink-hole. The entrance leads to the upper level of cave passages and larger halls which are also connected with lower river passage. In the whole length crossection is rounded and shows leveled ceilings. On the walls and ceiling of the cave interior there are marks and remains of sediments, indicating that in the cave evolution there were cycles of filling and flushing out the cave passages during the past (Brodar, 1966).

Because of the construction of railway for tourist visits the natural floor was modified, i.e. it was covered with sand. Parts of passages where tourists are walking during the cave visit are covered with concrete. The whole cave is illuminated but the light is turned on only during the tourist visit, to prevent gestation of algae on cave ceiling and speleothems.

4.2 Climate of Postojna area

Postojna is located on the border of the sub-Mediterranean climate of the North Adriatic Sea and the continental climate of central Slovenia (Gospodarič and Habič, 1976). Contour plots in Figures 4.4 and 4.5 show overall yearly precipitation amount and mean yearly temperature, respectively, in the period 1971 – 2000 (ARS, 2006). Yearly precipitation amount in the period from 1971 to 2000 was 1587 mm and mean temperature was 8.7 ºC.

Monthly temperatures and mean yearly values in the period 1982 – 2011 in Postojna are shown in Table A.1 in Appendix I, and the monthly precipitation amounts and total yearly amounts of precipitation in the same period in Table A.2 in Appendix I. In this period the average yearly amount of precipitation was 1528 mm, which is slightly lower than in period from 1971 to 2000 (1587 mm). Mean temperature in period 1981 – 2010 is 9.2 ºC, what makes difference of 0.5 ºC comparing to the period 1971 – 2000. Mean temperature in each decade of 1981 – 2010 shows constant increase (Table A.1 in Appendix I, Figure 4.6) from 8.6 ºC (1982 – 1991) to 9.2 ºC (1992 – 2001) and to 9.7 ºC (2002 – 2011).

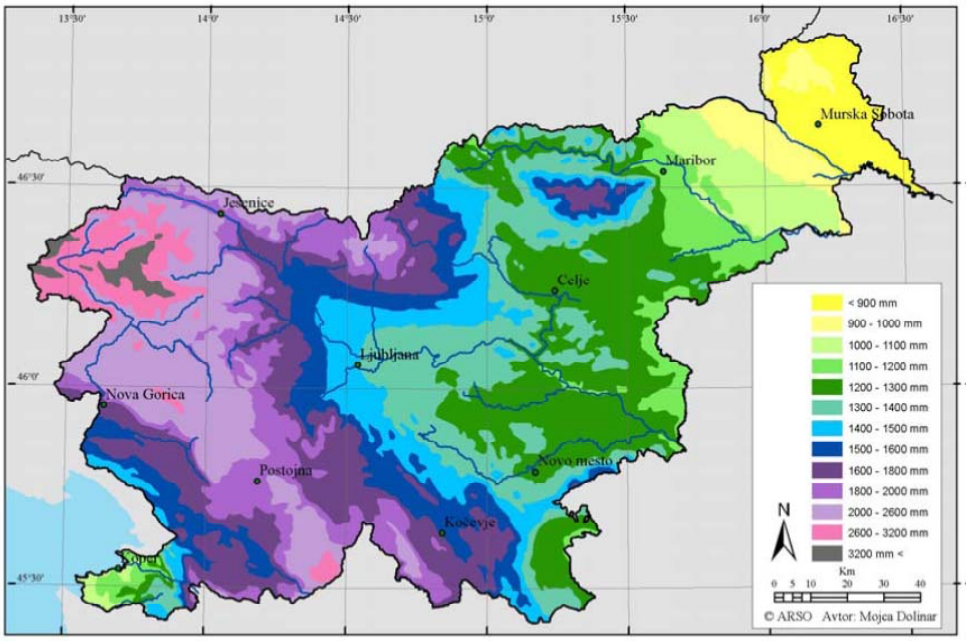

Figure 4.4 Averageyearly precipitation amount in the period from 1971 to 2000 in Slovenia. Plot from National Meteorological Service of Slovenia (meteo.si)

Slika 4.4. Srednja godišnja količina oborina u Sloveniji u razdoblju od 1971. do 2000. godine. Preuzeto sa stranica Državne meteorološke službe Republike Slovenije (meteo.si).

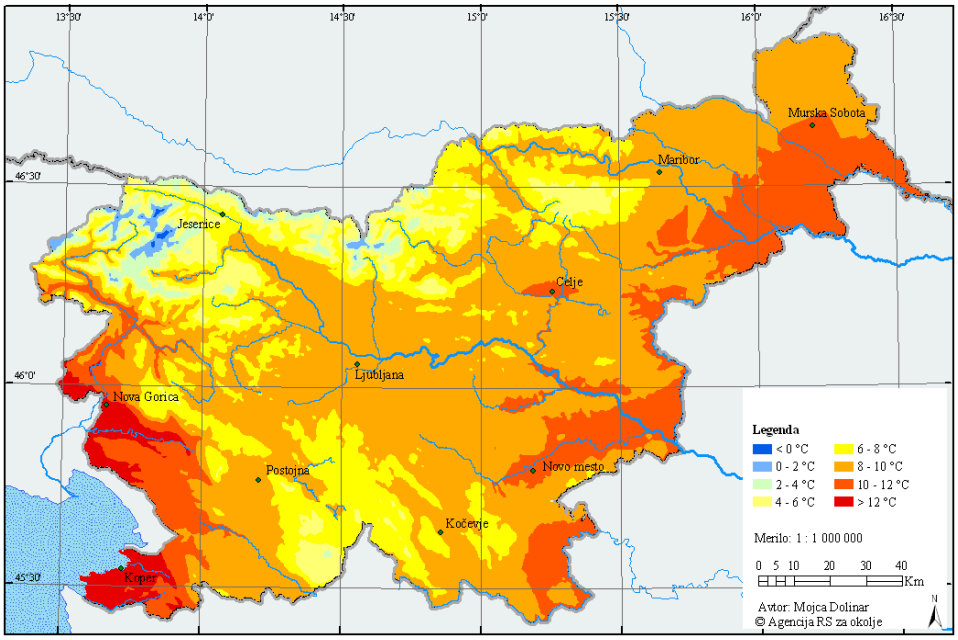

Figure 4.5 Average yearly temperature in period from 1971 to 2000. Plot from National Meteorological Service of Slovenia (meteo.si)

Slika 4.5 Srednja godišnja temperatura u razdoblju od 1971. do 2000. godine. Preuzeto sa stranica Državne meteorološke službe Republike Slovenije (meteo.si).

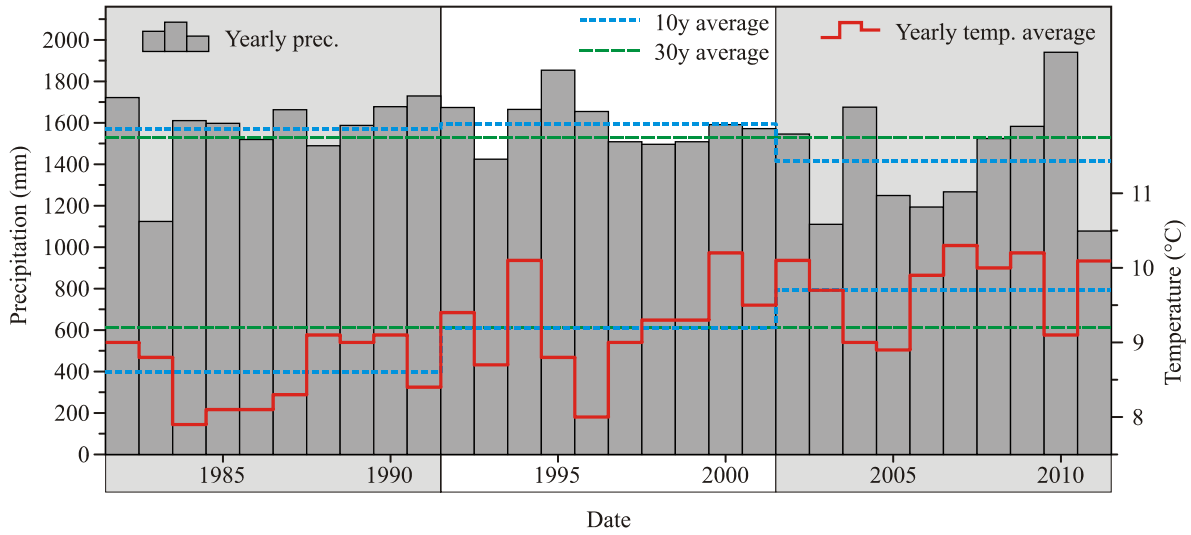

Figure 4.6 Yearly precipitation amount and temperature average in Postojna for period 1982 to 2011. Dashed lines (— — —) show 30-year average, while short-dashed-lines (- - -) show 10-year average in precipitation amount (higher) and temperature (lower). Data from National Meteorological Service of Slovenia (meteo.si).

Slika 4.6 Godišnja količina oborina i srednje godišnje temperature u Postojni u razdoblju 1982 . – 2011. Duge crtkane linije (— — —) prikazuju tridesetogišnje srednje vrijednosti, a kraće crtkane linije (- - -) desetogodišnje srednje vrijednosti količine oborina (gore) i temperature (dolje). Podaci od Državne meteorološke službe Republike Slovenije (meteo.si).

To explore the indicated increase in mean yearly temperature in Postojna, the trend of mean yearly temperatures in Postojna in the period 1982 – 2011 is presented in Figure 4.7. The slope of the linear regression line is 0.056 ± 0.011 ºC/yr and the correlation coefficient R is 0.67. This result is in agreement with the observed increasing trend of mean yearly temperatures in Zagreb of 0.06 ºC/yr (Barešić, 2009).

Therefore, the average temperature in the last thirty years (1982 to 2011) is 9.2 ± 0.6 ºC, while during the last decade it is 9.7 ± 0.5 ºC, and in the last period of six years (2006 – 2011) it is 9.9 ± 0.4 ºC. In last two years, 2010 and 2011, average air temperature is 9.7 ± 7.4 ºC, and in the sampling period (March 2010 – April 2011) it equals 10.3 ± 7.1 ºC. The average temperature during 2006 to 2011 (9.9 ± 0.4 ºC) is used in further discussion. Data from data loggers placed at several locations within Postojna Cave are also available for this period.

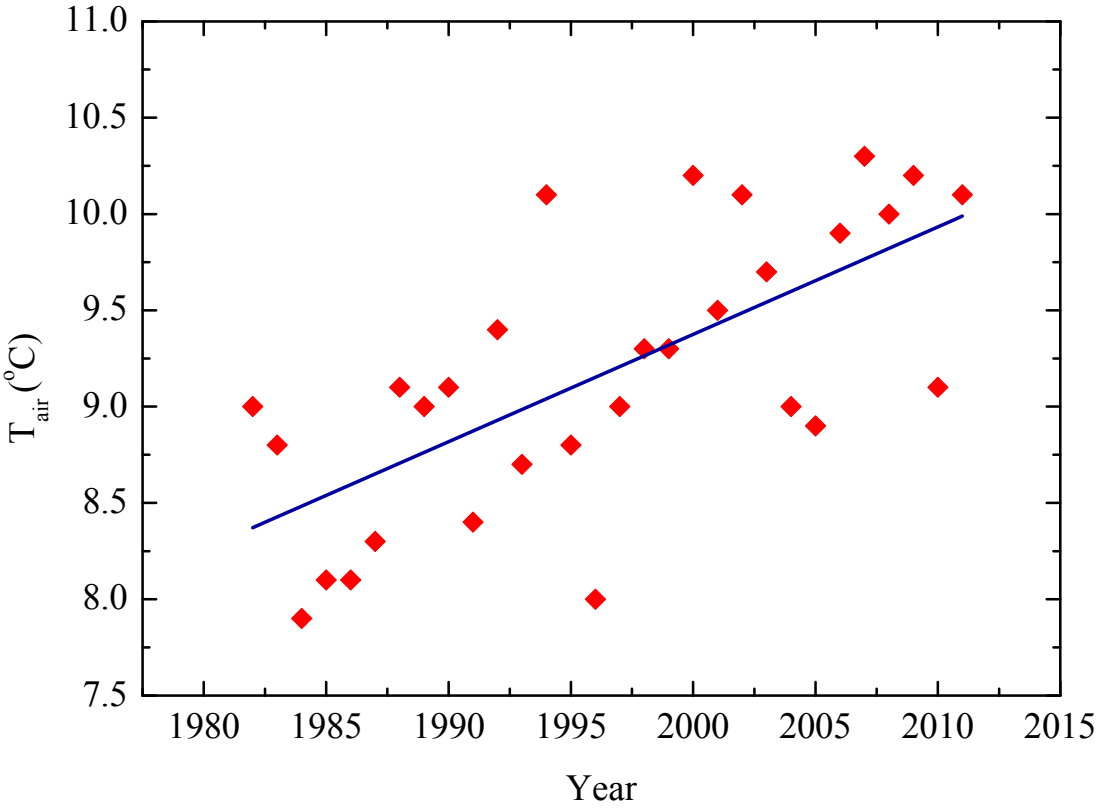

Figure 4.7 Mean yearly temperature in Postojna (◆) in the period 1982 – 2011. The slope of the linear regression line (——) is (0.056 ± 0.011) ºC/yr, R = 0.67. Data from National Meteorological Service of Slovenia (meteo.si).

Slika 4.7 Srednja godišnja temperature u Postojni (◆) u razdoblju 1982. – 2011. Nagib pravca linearne regresije (——) je (0,056 ± 0,011) ºC/god, a R = 0,67. Podaci od Državne meteorološke službe Republike Slovenije (meteo.si).

The total yearly amount of precipitation in Postojna in the same period (Figure 4.8) shows very weak negative trend (R = -0.17) with the slope of the linear regression line of (-6.0 ± 4.4) mm/yr. More important than the trend is the increase of variability of the yearly precipitation during the last decade, i.e., deviations from the trend line in both directions are more pronounced during the last decade than earlier indicating the alteration of very or extremely wet years with very or extremely dry years. The cave monitoring presented in this work has been performed in 2010 and 2011, and it should be noted that the year 2010 was extremely wet (1940 mm), the wettest year in the period 1982 – 2011, while 2011 was extremely dry (1078 mm), the driest year in the same period (Figures 4.6 and 4.8).

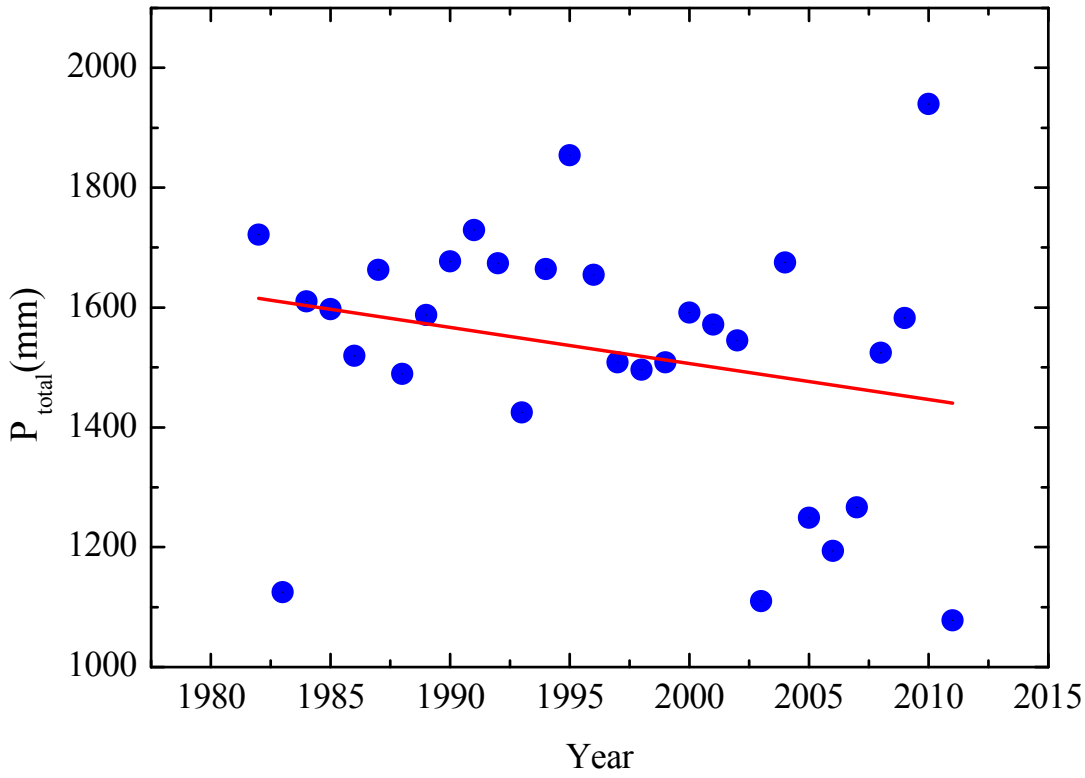

Figure 4.8 Total yearly amount of precipitation in Postojna (●) in the period 1982 – 2011. The slope of the linear regression line (—) is -6.0 ± 4.4 mm/yr, but the correlation coefficient R is low, -0.17. Data from National Meteorological Service of Slovenia (meteo.si).

Slika 4.8 Godišnja količina oborina u Postojni (●) u razdoblju 1982. – 2011. Nagib pravca linearne regresije (—) je -6,0 ± 4,4 mm/god, ali koeficijent korelacije R je samo -0,17. Podaci od Državne meteorološke službe Republike Slovenije (meteo.si).

To see the distribution of precipitation within a year, Figure 4.9 displays the monthly precipitation amount during the last decade. The highest monthly precipitation rate is observed in December 2009, when the precipitation (433.9 mm) is four times higher than average monthly precipitation (119 mm). The second next maximum of precipitation rate of 370.9 mm is observed in the sampling period, in September 2010. Minimum precipitation has been measured in April 2007 (0.5 mm) and November 2011 (3.1 mm). During the cave monitoring period the monthly average amount of precipitation is 119.2 mm.

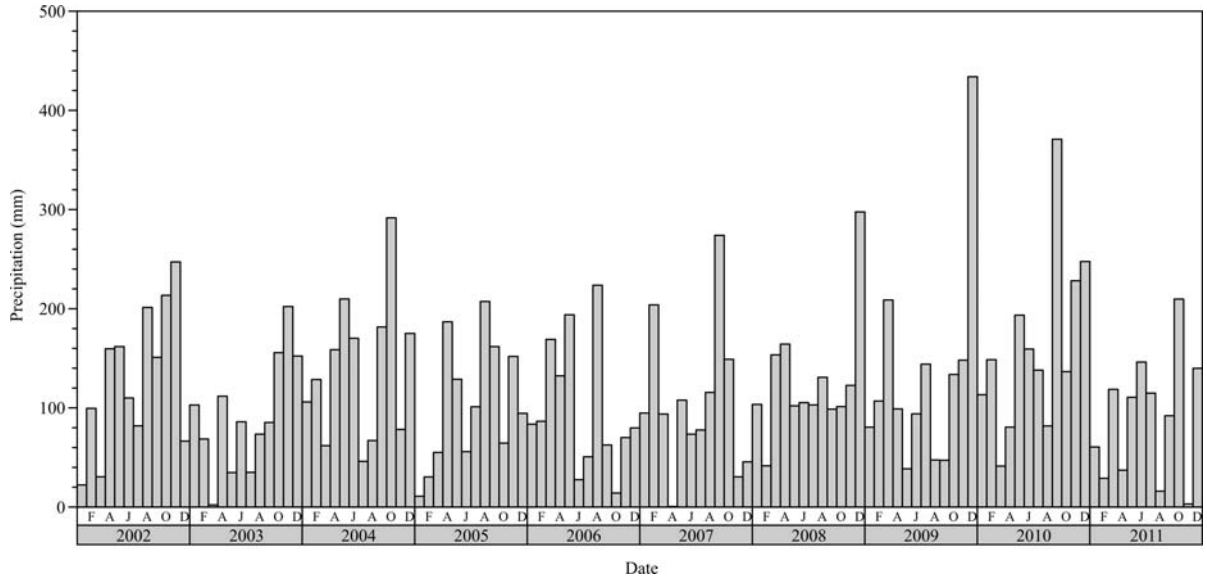

Figure 4.9 Monthly precipitation in Postojna during the last decade (2002 – 2011)
Slika 4.9 Mjesečna količina oborina u Postojni tijekom razdoblja 2002. – 2011.

4.3 Cave atmosphere, air circulation and temperature

Climate characteristics of the interior of Postojna Cave were monitored by data loggers of temperature from 2006 to 2011 (Personal communication M. Prelovšek; A. Mihevc; F. Gabrovšek, all from Karst Research Institute, Postojna). The periods of monitoring with data loggers at different locations are shown in Table 4.1. Sampling locations are presented in Figure 4.10 and they enable a detailed picture of Postojna cave temperature distribution. During the monitoring period from 2006 to 2011 data loggers were moved from one sampling locality to another. The locations Vodopad (03), Stebrišče (06) and Vrh Velike gore (08) are the same as locations 03, 06 and 08, respectively, of this work.

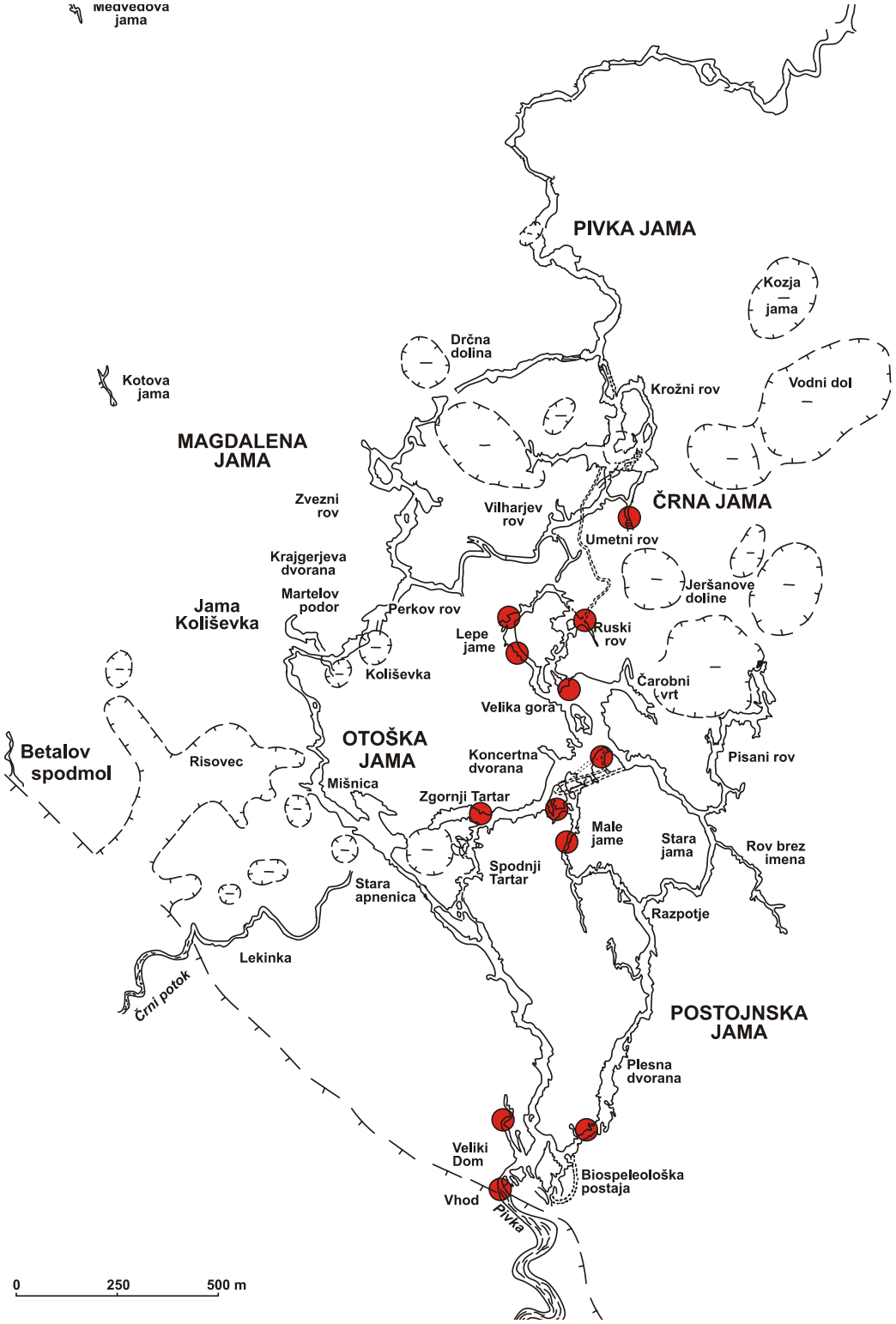

Figure 4.10 Locations of data loggers in Postojna Cave

Slika 4.10 Lokacije u Postojnskoj jami na kojima su postavljeni automatski instrumenti za mjerenje temperature i strujanja zraka

Table 4.1 Periods of monitoring by data loggers in Postojna Cave at locations shown in Figure 4.10. The locations Vodopad (03), Stebrišče (06) and Vrh Velike gore (08) are the same as locations 03, 06 and 08, respectively, of this work.

Tablica 4.1 Razdoblja u kojima su na pojedinim lokacijama (prikazane na Slici 4.10) bili postavljeni automatski instrumenti za mjerenje temperature i strujanja zraka. Lokacije Vodopad (03), Stebrišče (06) i Vrh Velike gore (08) odgovaraju lokacijama 03, 06 and 08 u ovom radu.

Location	Starting date	End date
Stebrišče (06)	30 December 2008	15 April 2009
	22 October 2009	13 December 2009
	24 March 2010	07 July 2010
Ruski most	5 March 2009	6 May 2009
Zrak pri vrtinah	20 March 2009	03 June 2009
Male jame	31 December 2008	06 May 2009
	22 October 2009	15 January 2010
	27 June 2010	27 September 2010
Vodopad (03)	18 February 2006	12 May 2006
	08 December 2006	27 June 2007
	03 June 2009	22 June 2009
	30 October 2009	16 November 2009
	18 January 2010	07 June 2010
Postojna Cave; entrance	03 July 2006	31 January 2007
	01 February 2007	15 February 2007
	11 April 2007	25 June 2007
	12 February 2008	15 March 2008
Vrh Velike gore (08)	06 July 2010	22 October 2010
Črna jama	27 July 2010	07 September 2010
Lepe jame		19 September 2010
Lepe jame – tunnel		20 August 2010
Partizanski rov		19 October 2010
Tartar - common passage		
Veliki Dom - above		07 September 2010

Figure 4.11 shows daily averages of temperatures measured by data loggers in fifteen-minute intervals and daily temperatures in Postojna city measured by National Meteorological Service of Slovenia (meteo.si). Mean daily temperatures in Postojna city vary from -12 °C in winter to 28 °C in summer months. The temperature measured at different locations in the cave is constant at each location (within ± 1 ºC), but is slightly different for various locations, e.g., 8.5 °C at Partizanski rov (no. 8 in Figure 4.11) and 11 °C Vrh Velike gore (no. 4 in Figure 4.11).

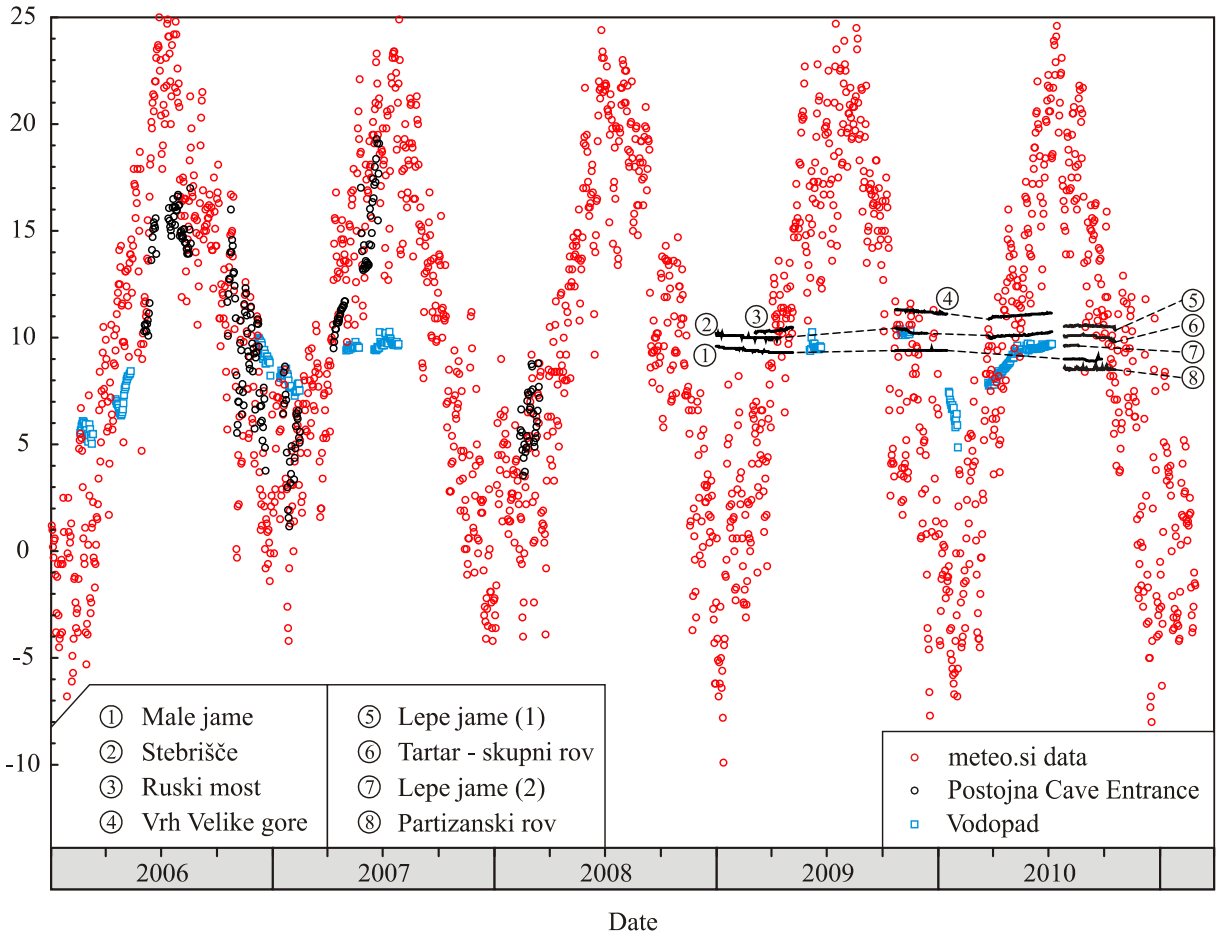

Figure 4.11 Temperatures in the interior of Postojna Cave measured by data loggers and data of outside air temperature measured by National Meteorological Service of Slovenia (meteo.si) for period 2006 – 2011.

Slika 4.11 Temperature mjerene unutar Postojnske jame automatskim instrumentima i vanjska temperature zraka (podaci od Državne meteorološke službe Republike Slovenije (meteo.si)) u razdoblju 2006. – 2011.

Mean annual temperature in the period 2006 – 2010, that coincides with the period of temperature monitoring by data loggers, varies from 9.1 ^{o}C to 10.3 ^{o}C (Table A.1 in Appendix

I), with the six-year average of 9.9 °C. The temperatures monitored in the Postojna Cave are within the range of six-year average of the external temperature. For example, mean temperature at Stebrišče is 10.12 ± 0.12 ºC, at Male jame 9.3 ± 0.2 ºC, at Vrh Velike gore 11.12 ± 0.11 ºC and at Ruski most 10.34 ± 0.07 ºC. The exception is location at the entrance of the Postojna Cave where the mean temperature is 10.6 ± 4.2 ºC. Maximum summer temperature of 19.3 ºC at the entrance is lower than data from National Meteorological Service of Slovenia (meteo.si) and can be explained by the summer-type air circulation, Figure 4.12. During summer months, the direction of the cave air circulation is from the interior towards out of the cave. The air on the entrance of the cave is thus cooled down by the cave air which reflects mean the yearly average temperature.

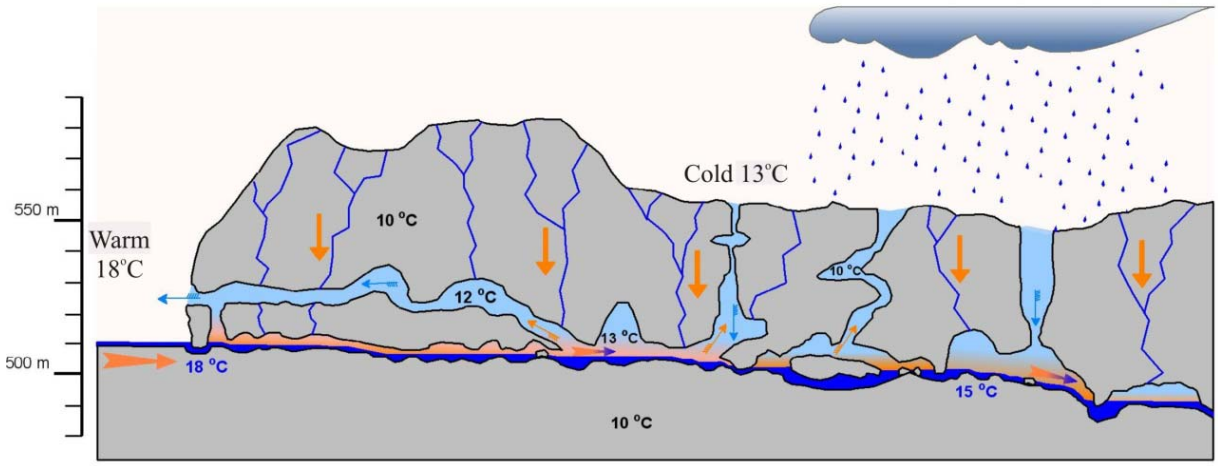

Figure 4.12 Summer-type of air circulation in Postojna Cave
Slika 4.12 Ljetni način cirkulacije zraka u Postojnskoj jami

Average minimum winter temperature, 1.16 ºC, is higher than temperature measured outside, -0.8 ºC. During the winter air circulation changes direction and outside air is influencing cave air (Figure 4.13). The cave entrance is mostly affected by this phenomenon. The effect of cooling is visible also at locations in the cave although less pronounced. The correlation between outside air and cave air temperatures is visible at Location 03 – Vodopad (Figure 4.11), which is closest to the cave entrance. Mean daily cave temperature on other locations (where data loggers have been placed) is not significantly influenced by changes in outside temperature. On some locations the cave air pressure changes are synchronous with those outside (Šebela and Turk, 2011).

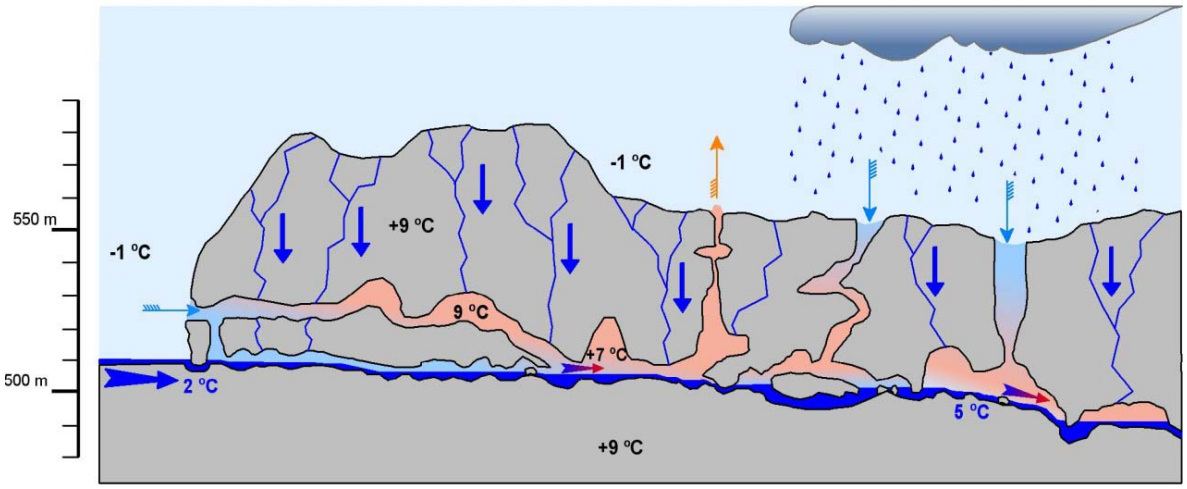

Figure 4.13 Winter-type air circulation in Postojna Cave
Slika 4.13 Zimski način cirkulacije zraka u Postojnskoj jami

Monitoring of wind velocity and wind direction is performed of the entrance of Postojna Cave and at Location 03 – Vodopad. Figure 4.14 presents average daily temperatures (calculated from 15-min intervals) from data loggers and average monthly temperatures from National Meteorological Service of Slovenia (meteo.si) in combination with the wind velocity data from data loggers at location 03 – Vodopad. Variations of temperature inside the cave at location 03 – Vodopad are much smaller than variation of the outside temperature. General direction of the wind velocity in winter periods has positive values in Figure 4.14, meaning that the direction is from outside into the cave, in accordance with prevailing winter-type circulation shown in Figure 4.13. It can also be observed that the intense wind in this winter-type circulation affects the temperature at location 03.

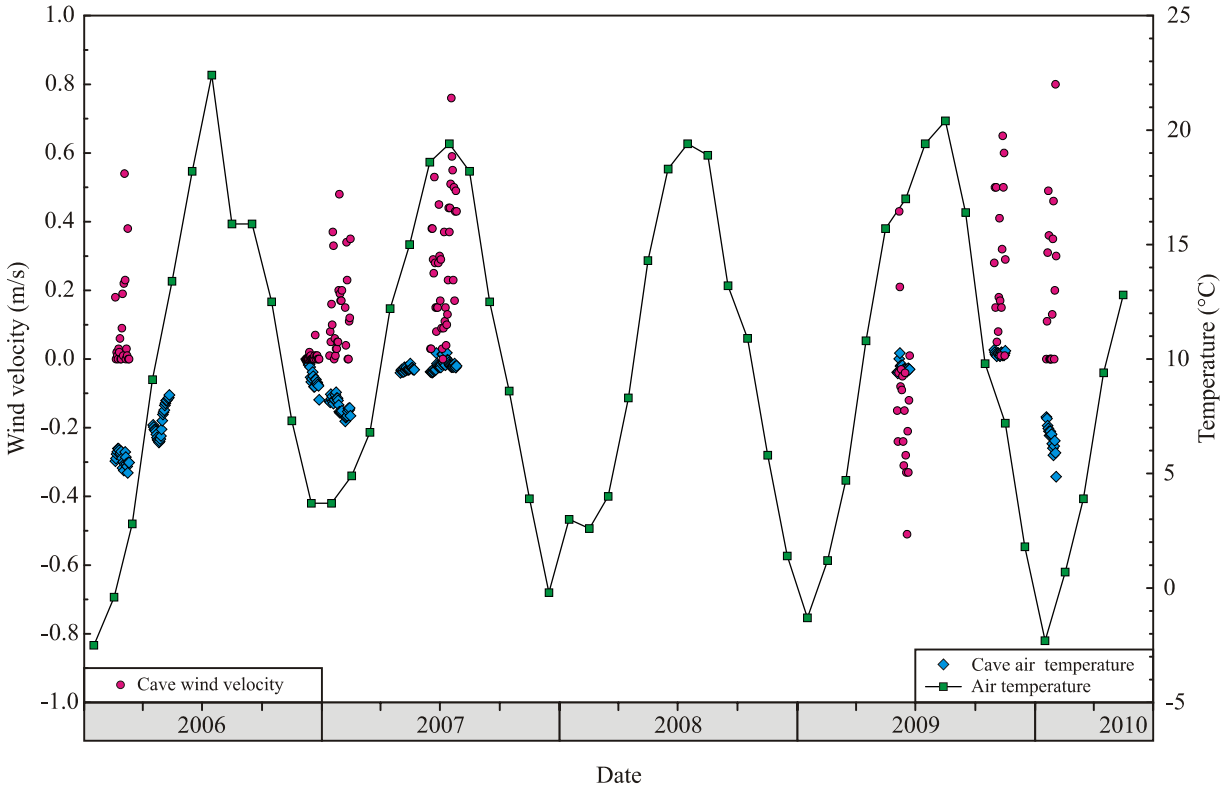

Figure 4.14 Air temperature (daily averages, ◆) and wind velocity (●) measured by data loggers at location 03 – Vodopad in Postojna Cave. For comparison, monthly averages of outside air temperature in Postojna (—■—, data from National Meteorological Service of Slovenia meteo.si) are also shown. Note. Negative (-) or positive (+) values of the wind velocities (left ordinate) denote the direction of the wind: negative values (-) - wind direction from the interior out of the cave, plus (+) - wind direction from outside into the cave.

Slika 4.14 Temperatura zraka (srednja dnevna vrijednost, ◆) i brzina vjetra (●) mjereni automatskim intrumentima na lokaciji 03 – Vodopad u Postojnskoj jami. Za usporedbu su prikazane srednje mjesečne temperature zraka u Postojni (—■—, podaci od Državne meteorološke službe Republike Slovenije (meteo.si). Negativne (-) ili positivne (+) vrijednosti brzine vjetra na lijevoj ordinati označavaju smjer vjetra: negativne vrijednosti (-) se odnose na smjer vjetra iz unutrašnjosti špilje prema van, a pozitivne (+) na smjer vjetra prema unutrašnjosti špilje.

5 SAMPLING AND MEASUREMENT METHODS

5.1 General information on sampling locations

Nine locations marked in Figures 5.1 and 5.2 at different distances from the entrance of Postojna Cave were chosen as monitoring stations. The locations are named: 01 – Slonova glava, 02 - Biospeleološka postaja, 03 - Vodopad, 04 – Kongresna dvorana, 05 – Podrti kapnik, 06 – Stebrišče, 07 – Čarobni vrt, 08 – Vrh Velike gore, 09 – Zgornji Tartar. Because of the importance of the Pivka River to the Postojna Cave evolution, two locations connected to Pivka River were chosen for observation; one outside the cave near the ponor of Pivka River, named location 11 – Pivka River outside and the other 2.5 km the cave entrance, named location 10 - Pivka River inside. Each location is described in more details in the following sections, while Table 5.1 summarizes some information on the sampling locations based on topographic maps of Republic of Slovenia in scale 1:5000, pages D2243, D222244, D2234, D2235. Schematic description of terms used in the table is shown in Figure 5.3.

5.2 Location description

A short description of each sampling location is presented in this section. The description contains data about physical appearance of a sampling location, its distance from the main entrance (or other entrances), admissibility of tourist visits to a location. Detailed maps at scale 1:500 and 1:2500, made during Italian domination in 1933/34 (Gospodarič, 1976), are used in description of each location (except of locations 04 – Kongresna dvorana and 06 Stebrišče) to point out a sampling locality at a specific location. On these “topographic” maps detailed positions of different speleothems are plotted as dots or circles. Some photographs of location chacteristics, field measurements and sampling at each location are given in Appendix II.

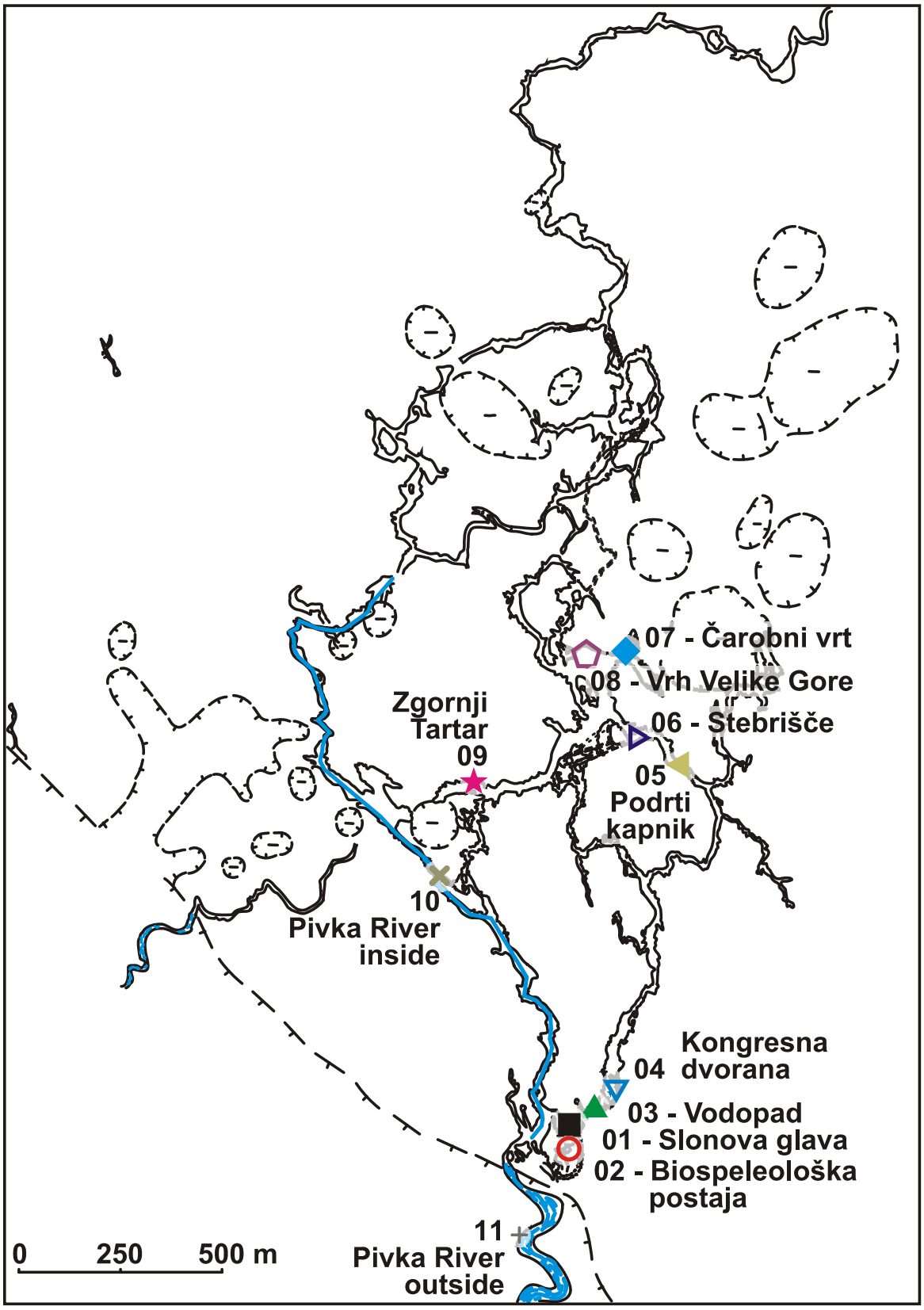

Figure 5.1 Sampling locations in Postojna Cave
Slika 5.1 Karta Postojnske jame s označenim lokacijama uzorkovanja

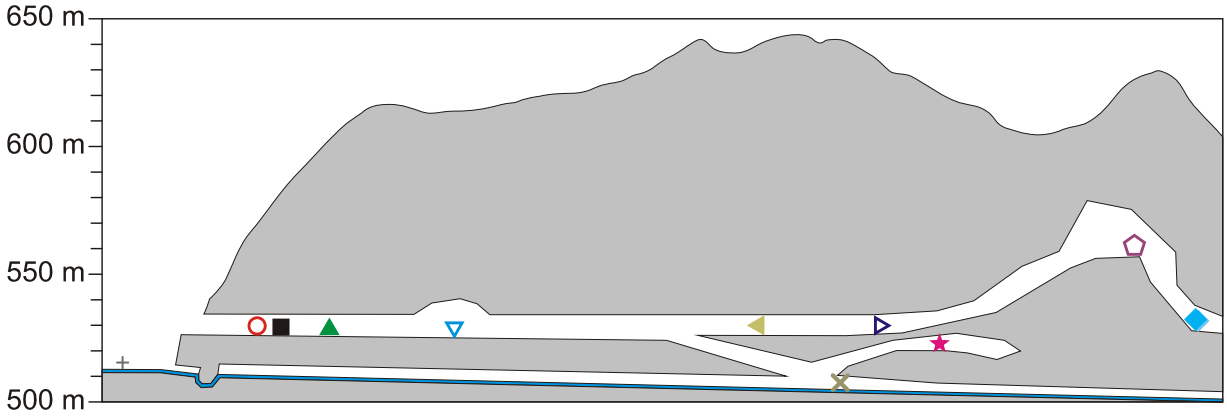

Figure 5.2 Schematic longitudinal section (profile) of the Postojna Cave. Symbols are the same as in Figure 5.1. Linear distances are not in scale.

Slika 5.2 Shematski profil Postojnske jame. Simboli lokacija kao na Slici 5.1. Linearne udaljenosti nisu proporcionalne.

Table 5.1 Physical characteristics of sampling locations

Tablica 5.1 Fizičke karakteristike lokacija uzorkovanja

Number and location name	**Surface altitude** (m a.s.l.)	**Altitude in cave** (m a.s.l.)	**Caprock thickness** (overburden) (m)	**Ceiling height above sampling site** (m)	**Distance from main entrance** (m)	**Distance from second entrance** (m)
01 – Slonova glava	585	529	56	1.5	240	
02 – Biospeleološka postaja	570	528	42	1.6	270	60
03 – Vodopad	605	531	74	1.5	330	
04 – Kongresna dvorana	617	528	89	7.5	540	
05 – Podrti kapnik	620	524	96	2	1 470	
06 – Stebrišče	607	524	83	6.4	1 666	
07 – Čarobni vrt	602	526	66	10	1 950	
08 – Vrh Velike gore	625	559	76	13	1 965	
09 – Zgornji Tartar	592	523	69	8.5	1 970	From Stare apnence 110
10 – Pivka River inside	592	505	87	4.3	2 500	
11 – Pivka River outside	511				0	

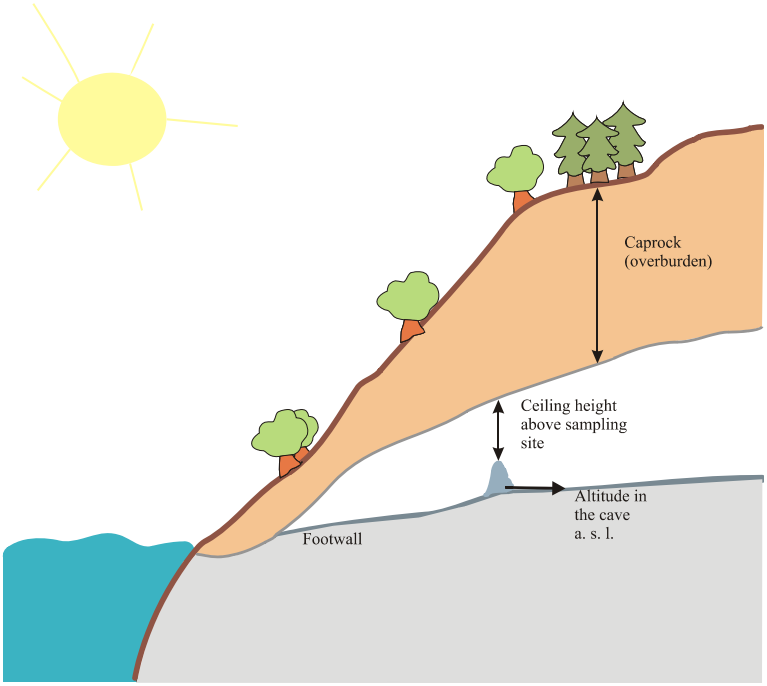

Figure 5.3 Schematic view of terms used in site description in Table 5.1.
Slika 5.3 Shematsko objašnjenje pojmova korištenih u Tablici 5.1.

Location 01 – Slonova glava

Location 01 – Slonova glava (eng. "Elephant head") is located 240 m from the main cave entrance, in a 10-m wide hall. Maximum ceiling height is 5 m. The color of the cave wall is dark to light gray with white soda straws growing on the ceiling (Appendix II, Figure B.1). Tourist railway is passing across the hall (Appendix II, Figure B.2). Few old speleothems are scattered on the modified cave floor. Seasonal cave "breathing" is noticeable on this location. It is wet during winter and dry during the summer season. The speleothem growth depends on this seasonality. Older stalactites have a kind of a bubbly surface. This is due to clogging of water inside of stalactite during the dry season (Mihevc, personal communication). In a wet season water from stalactites finds another way out. The sampling location (Figure 5.4) was chosen under the drip place where carbonate precipitation is visible (white spot on the floor sand, forming a recent stalagmite) (Appendix II, Figure B.3). It is located 3 m away from the railway. On this location the caprock thickness is 56 m and the ceiling height above the sampling site is 1.5 m.

Location 02 – Biospeleološka postaja

From the same hall where the first location is situated a small iron door leads to an old biospeleological room (Figure 5.4). Sampling locality is placed after approximately fifty meter long and narrow passage with low rounded ceiling. It is located 270 m from the main entrance. There is no railway at this location. The floor was modified because of the usage of the location for biospeleological investigations. A few stalagmites are found on the passage and many are visible at the lower part, near the walls (Appendix II, Figure B.5).

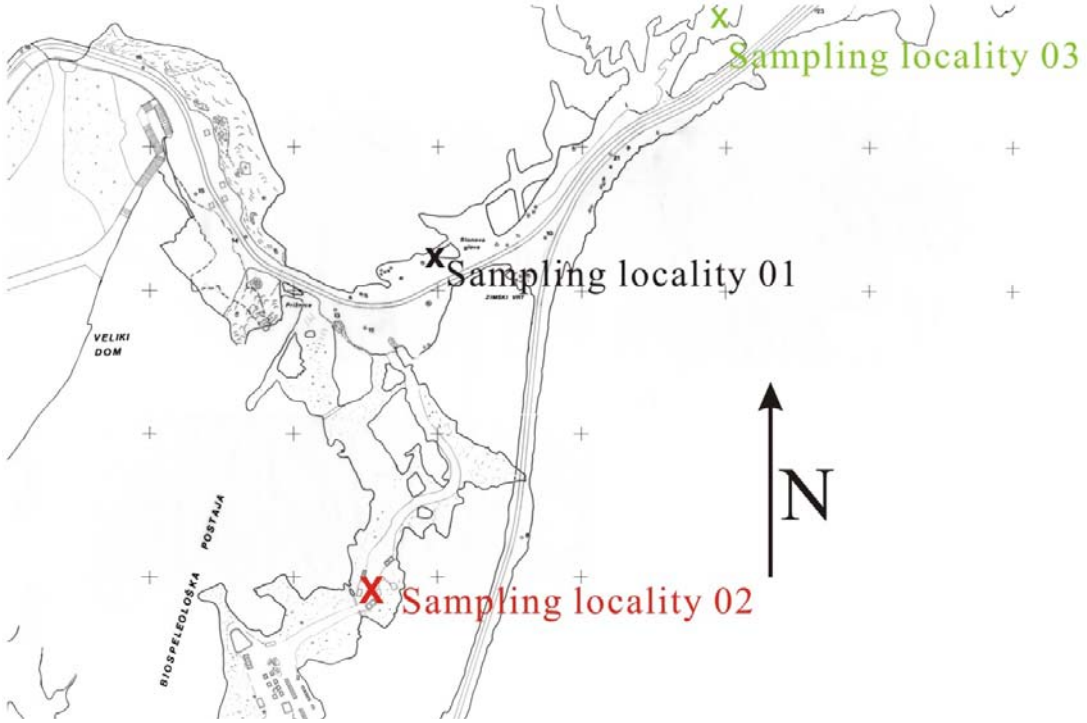

Figure 5.4 Detailed map of locations 01 – Slonova glava, 02 – Biospeleološka postaja and 03 – Vodopad with "x" signs marking the sampling sites

Slika 5.4. Detaljna karta lokacija 01 – Slonova glava, 02 – Biospeleološka postaja i 03 – Vodopad. Znak x označava točno mjesto uzorkovanja na svakoj lokaciji.

During 1960's there have been investigation of Pleistocene sediments (Brodar, 1966), and a small passage was made further into the cave interior. On the entrance to this artificial passage a metal door is placed. The hall where location 02 – Biospeleološka postaja is situated is small and low (Appendix II, Figure B.6). On the ceiling there are many "soda straws". The sampling place has been chosen under the drip where the white color of sand is visible. The ceiling height is in that place 1.6 m, with caprock of 42 m.

Location 03 – Vodopad

Location 03 – Vodopad (eng. "Waterfall") is a small semicircular passage located 2 m from the main passage (Figure 5.4), 330 m away from the cave entrance, near the railway. The location is named after the flowstone nearby, which resembles a waterfall. This is the location where anemometer and temperature data logger are placed for monitoring of wind velocity and air temperature (Appendix II, Figure B.7). It is expected that the wind velocity has the highest value at this location, because of the train passing and due to the cave morphology. The caprock is 74 m thick and the ceiling height above the drip site is 1.5 m. Under the drip site a stalagmite grows. Walls are rounded and of light gray color. There are only few "soda straws" hanging from the ceiling but dominant are white stripes of young precipitated carbonate (Appendix II, Figure B.8).

Location 04 – Kongresna dvorana

Location 04 – Kongresna dvorana (eng. "Congress hall") is named after Speleological congress held in 1965, but previously it was known as Plesna dvorana (eng."the dance room").The distance from the entrance is 540 m and the surface area of the hall is 75 m^2. The highest ceiling level is 12 m. The sampling place is chosen under the drip site on the right hand side from the entrance to the hall. The height of the ceiling above the drip site is 7.5 m. Surface of the hall ceiling and walls are rough and wrinkled. Because of floor modification there are almost no visible stalagmites. From the ceiling hang only few white stalactites (Appendix II, Figure B.9). The walls are in white and light gray in color but also yellow on the ceiling.

Location 05 – Podrti kapnik

In 1926 in Postojna area there was an earthquake that broke a large stalagmite (Šebela, 2010). Since then the broken stalagmite lays over the railway passage (Appendix II, Figure B.10). A few meters before it, near large flowstone, the sampling location 05 has been chosen, Figure 5.5 (Appendix II, Figure B.11). It is only two meters away from the main passage of the train. The distance from the cave entrance is 1470 meters and the ceiling thickness is 96 meters. The roof height where drip water is sampled is 2 m. The ceiling above the sampling site is white colored and flowstone color transforms from yellow to orange and brown. There are numerous stalactites hanging on the ceiling whereas the floor is modified due to the railway vicinity.

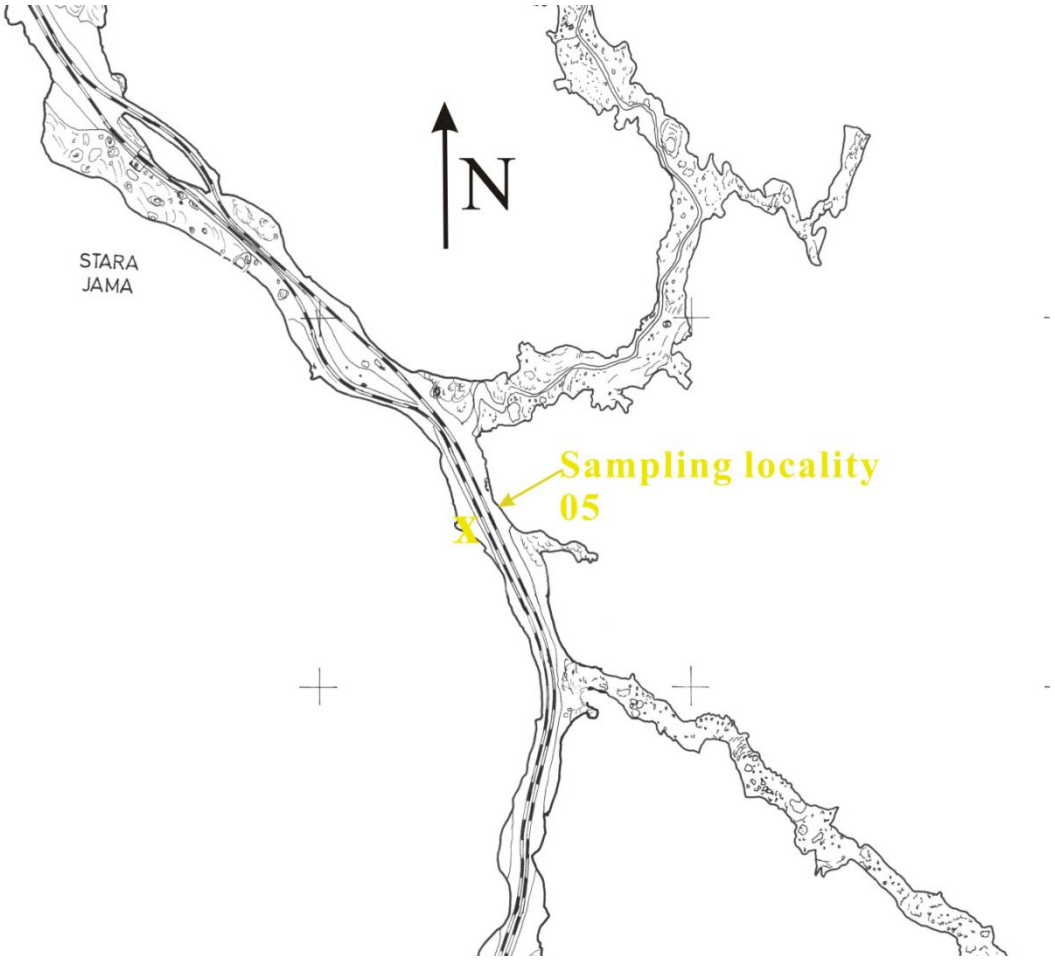

Figure 5.5 Detailed map of location 05 – Podrti kapnik with "x" sign marking the sampling site
Slika 5.5. Detaljna karta lokacije 05 – Podrti kapnik. Znak x označava točno mjesto uzorkovanja.

Location 06 – Stebrišče

About fifty meters before the end of the railway called Peron (eng. "platform"), 1666 m inside the cave, the location 06 – Stebrišče ("pillars place") is situated. It is located at the end of narrow passages where the volume of the Postojna cave interior is the largest. A part of the floor is transformed for railway, but there are numerous stalagmites near the cave walls and on the hills that surround the passage.

The sampling point is surrounded with flowstone (Appendix II, Figure B.13), and it is the point where a stalagmite is being formed, ten meters from the railway (Appendix II, Figure B.12). The caprock is 83 m, and the height of the ceiling above the drip site is 6.4 m. The flowstone color is white on the side where it is not facing the railway passage. On the opposite side the color changes from white to light gray.

Location 07 – Čarobni vrt

Čarobni vrt (eng. "the Magic garden") is located 1950 m from the cave entrance. To reach the location 07 – Čarobni vrt one has to climb the hill of Velika gora following the tourist route. On the right-hand side approximately 20 m before the top, there is a non-touristic 30 m downhill way across unfriendly cave environment (Appendix II, Figure B.14). It is worth of every step because it is, as the name says, magic garden where stalagmites grow (Appendix II, Figure B.16). Čarobni vrt is a location in the base of the biggest collapse doline in the Postojna Cave system. The entrance to this chamber is large (few tens of square meters) and elliptically shaped (Appendix II, Figure B.17). Way down is gray, but in side of chamber the color of the floor, the ceiling and the walls transforms from white to dark orange. Almost whole floor surface is covered with precipitated carbonate, where white headed stalagmites are raising up.

The sampling point (Figure 5.6) is placed eight meters from the entrance point to the chamber (Appendix II, Figure B.15). Under the drip site a flowstone is being formed and on it a young white stalagmite grows. The sampling point is on top of it. The ceiling is flat and is formed like stairs, along the bedding planes (Šebela, 1998). The caprock is 66 m and the drips are falling from 10 meters high ceiling (Appendix II, Figure B.18).

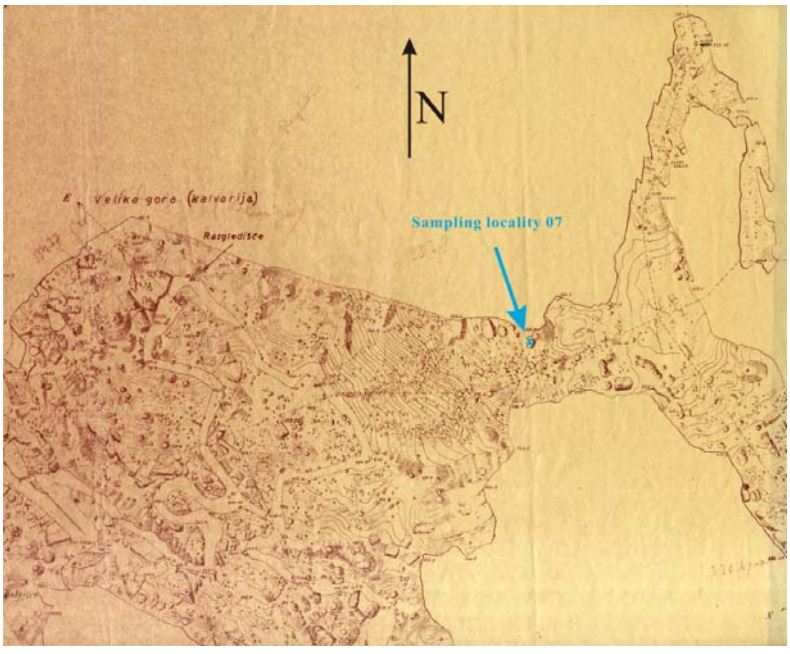

Figure 5.6 Detailed map of location 07 – Čarobni vrt with "x" sign the marking sampling site

Slika 5.6 Detaljna karta lokacije 07 – Čarobni vrt. Znak x označava točno mjesto uzorkovanja.

Location 08 – Vrh Velike gore

Location 08 – Vrh Velike gore is situated on the top of the Velika gora (eng. "Big" or "Large Mountain"). The other known name for this location is Kalvarija (eng. Calvary). Location is 1965 m far from the cave entrance, and the caprock is 76 m. Location is under the biggest collapse doline in Postojna Cave system (Šebela, 1998). The path uphill to the Velika Gora top was modified for tourist passage. Nowadays it is closed for tourist visits. The floor of Vrh Velike gore is covered with precipitated carbonates, with many presently growing stalagmites. The sampling site (Figure 5.7) is situated on the top of the white flowstone under 13 m high dripping place (Appendix II, Figure B.19). The color of the surrounding walls changes from white to gray and from yellow to dark orange and brown (Appendix II, Figure B.20). This is location at the highest altitude. The ceiling and surrounding walls are smooth and formed in a fault zone (Šebela, 1994).

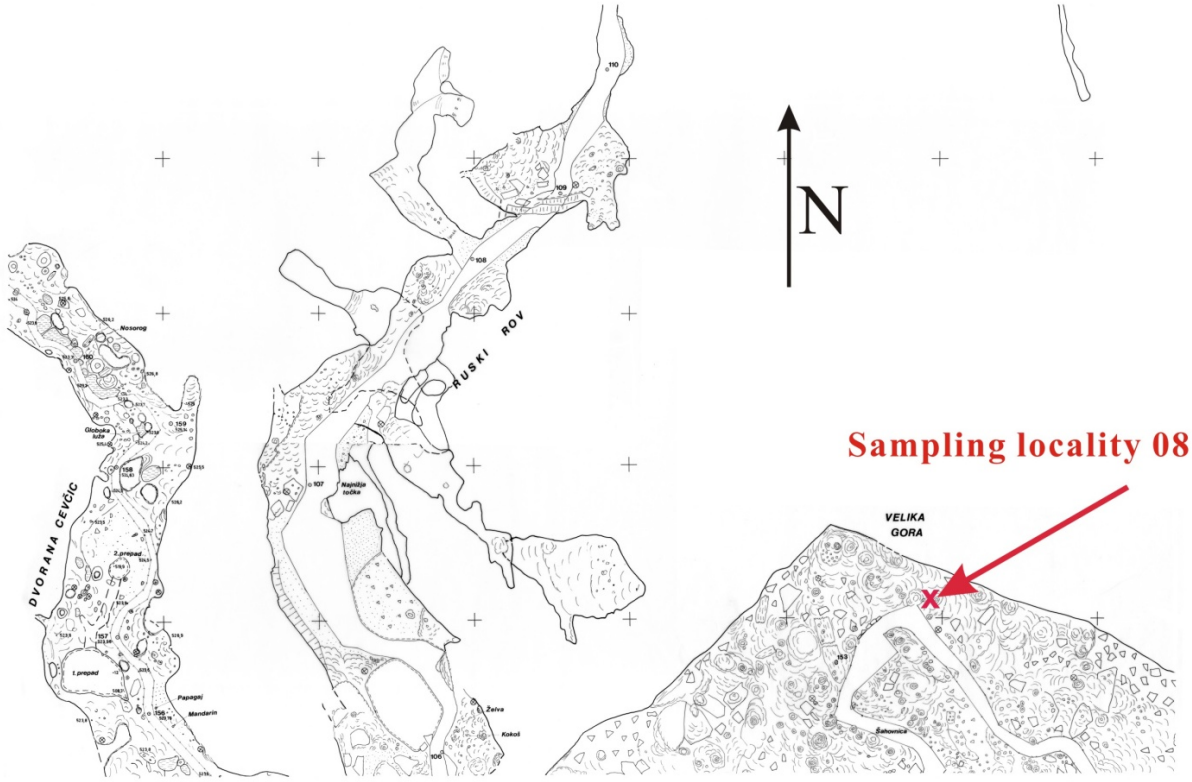

Figure 5.7 Detailed map of location 08 – Vrh Velike gore, "x" marking the sampling site
Slika 5.7 Detaljna karta lokacije 08 – Vrh Velike gore, x označava točno mjesto uzorkovanja.

Location 09 – Zgornji Tartar

Location 09 – Zgornji Tartar ("Upper Tartar" or Tartarus) is situated in the part of the Postojna Cave which is isolated from tourist visit. The sampling location (Figure 5.8) is in a vicinity of Stara apnenca collapse doline. Location 09 was in previous times under climatic influence of an opening which is nowadays closed by sediment (Gospodarič, 1976). Distance from this entrance is 110 m and from the main entrance to Postojna Cave is 1970 m. The sampling point is a freshly growing stalagmite situated on a larger flowstone. The ceiling height above the location is 8.5 m, and the caprock is 69 m. The floor in Zgornji Tartar was not modified and is partially filled with small-grained earth (during wet season the floor is muddy) and partially is rock. Few meters further from the drip site a place of collapse ceiling is visible. At the end of the ceiling, near the cave floor, (Appendix II, Figure B.22) there are numerous white stalactites (Appendix II, Figure B.23), but also fragile carbonate formations filled with air (cave corals).

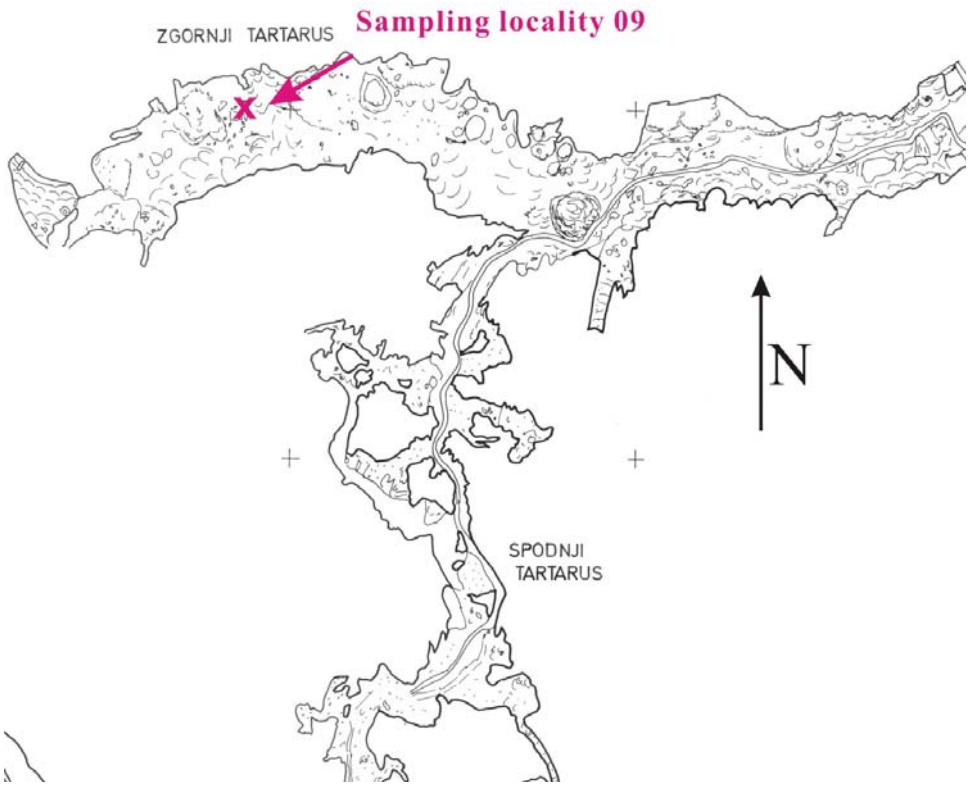

Figure 5.8 Detailed map of location 09 – Zgornji Tartar, "x" marking the sampling site
Slika 5.8 Detaljna karta lokacije 09 – Zgornji Tartar, x označava točno mjesto uzorkovanja.

Location 10 – Pivka River inside

The Pivka River is a sinking river that enters the Postojna Cave. The location 10 – Pivka River inside is located at the point where the river comes out in the interior of Postojna Cave. The location is isolated from tourist visits. At this location, Figure 5.9, sampling material is water from the Pivka River, not the percolation water. The caprock is 87 m. The floor is covered with small gravel and with material that the Pivka River brought inside. No speleothem formations are found on this location.

Figure 5.9 Detailed map of location 10 – Pivka River inside with "x" sign marking the sampling site

Slika 5.9 Detaljna karta lokacije 10 – Pivka River inside (Rijeka Pivka unutra), x označava točno mjesto uzorkovanja.

Location 11 – Pivka River outside

This location is different from all others because it is situated outside the Postojna Cave, 20 m from ponor of the Pivka River, under large parking lot. The altitude of this location is 511 m above the sea level.

5.3 Sampling and field work

5.3.1 Carbonate samples

Sampling of carbonates was peformed after obtained approval of the Ministry of Environment of the Republic of Slovenia, The Institute for Nature Conservation (Figure A.2 in Appendix I) in accordance with their requirements.

Carbonate samples are collected at each of nine locations (01 - 09) in the Postojna Cave. The carbonate samples can be grouped to recent and old carbonates. Recent carbonates include "soda straw" samples, modern carbonates precipitated on watch glasses and so-called speleothems of a peculiar shape. "Soda-straw" carbonates were of different lenght and masses (Table A.6 in Appendix I), and for stable isotope analysis only the top of the "soda straw" (the youngest part) is crumbled and homogenized in an agate mortar (Figure 5.10).

Figure 5.10 Recent carbonate samples and agate mortar for homogenization of a samples.
Slika 5.10 Uzorci recentnog karbonata i ahatni tarionik za homogenizaciju uzoraka.

Appart from classical forms of speleothems (stalactites, stalagmites, flowstone, "soda straws") some "peculiar" forms of speleothems are found in Postojna Cave. They are characterized by a specific, unusual shape and their occurrence is limited to specific locations. The stalactites with bubbly surface are found at location 01 – Slonova glava. They have specific growth because water channels are clogged and opened seasonally. During dry periods (summer) precipitated carbonate fills up channels in stalactites, while in wet periods (winter) water finds new fissures to come out into the cave (Mihevc, personal communication). At location 09 – Zgornji Tartar a part of cave ceiling is covered with white fragile carbonate formations (Figure 5.11.)

Figure 5.11 Speleothems from location 09 – Zgornji Tartar characterized by peculiar growth shapes: a) a place where a speleothem was sampled, and fragile speleothem formation b) inside and c) surface.

Sika 5.11 Uzorak sige specifičnog oblika s lokacije 09 – Zgornji Tartar, a) mjesto uzorkovanja, b) unutrašnjost uzorka i c) površina uzorka.

During the monitoring period, from September 15th 2010 to April 28th 2011, watch glass plates were placed at all sampling locations in Postojna Cave for collection of modern carbonate (Figure 5.12). After eight months of exposure watch glass plates were retrieved and precipitated carbonate was scraped off. Carbonate precipitated on watch glasses was collected successfully from locations 01 – 06 and 09, while at locations 07 and 08 they were moved from their initial position by strong drips.

Figure 5.12 A watch glass plate on a sampling site.

Slika 5.12. Satno stakalce postavljeno na mjestu uzorkovanja.

The group of old (fossil) carbonates consists of flowstones, stalactites and drilled cores speleothems. Samples of three flowstones (Figure 5.13) are taken from location 04 – Kongresna dvorana, 05 – Podrti kapnik and 06 – Stebrišče. Stalactites have been sampled at locations 02 – Biospeleološka postaja, 04 – Kongresna Dvorana and 09 – Zgornji Tartar (Figure 5.14). PROXON dentist drill in resolution of 1 mm and other laboratory tools are used for laboratory sub-sampling (Figure 5.15).

Figure 5.13 Flowstone samples from location 04 – Kongresna dvorana (a), 05 – Podrti kapnik (b) and 06 – Stebrišče (c).

Slika 5.13 Sigovina s lokacija 04 – Kongresna dvorana (a), 05 – Podrti kapnik (b) i 06 – Stebrišče (c).

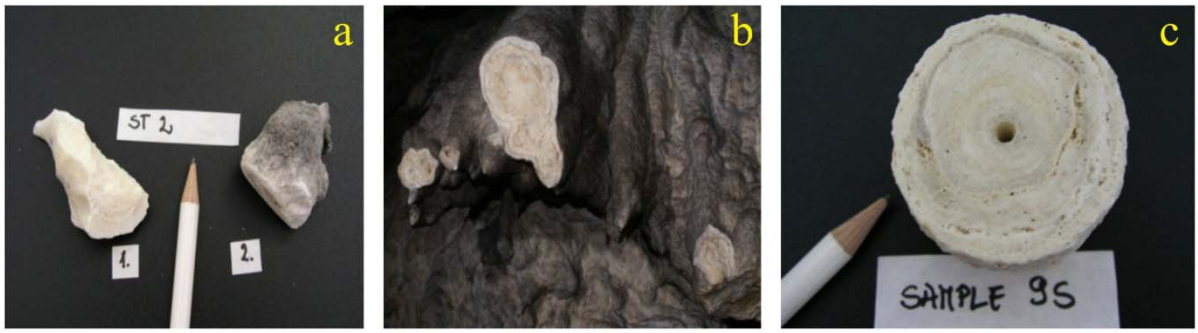

Figure 5.14 Stalactites sampled from locations 02 – Biospeleološka postaja (a), 04 – Kongresna dvorana (b) and 09 – Zgornji Tartar (c).

Slika 5.14 Stalaktiti s lokacija 02 – Biospeleološka postaja (a), 04 – Kongresna dvorana (b) and 09 – Zgornji Tartar (c).

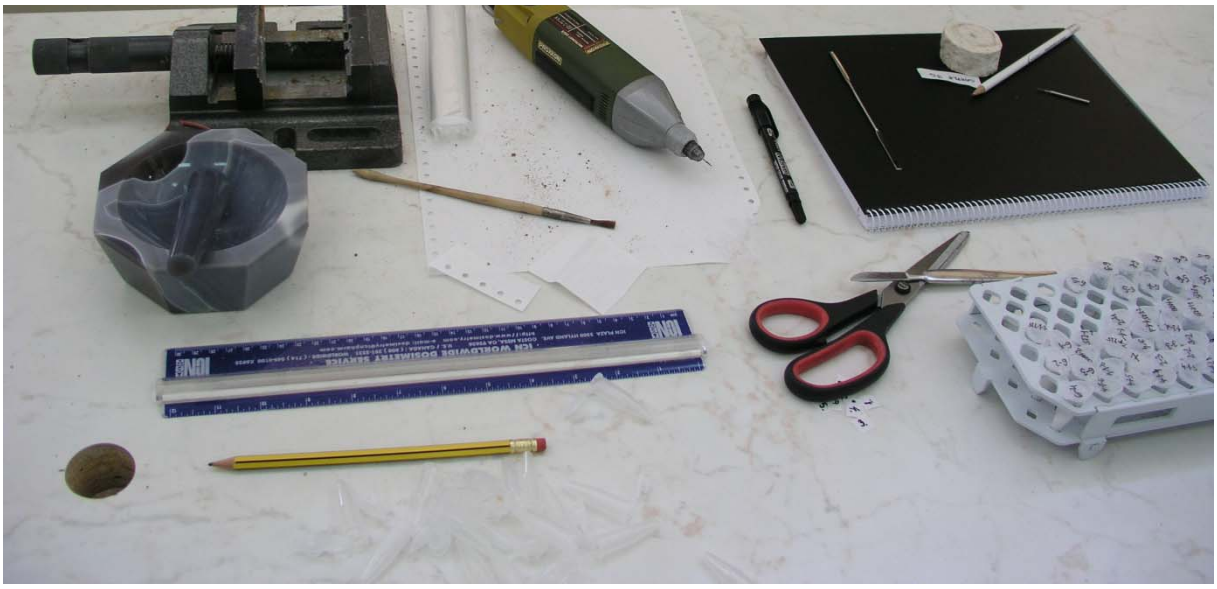

Figure 5.15 Tools for laboratory sub-sampling of carbonate samples.
Slika 5.15 Alat i pribor za obradu i pod-uzorkovanje karbonata u laboratoriju.

Drilling of the speleothems cores has been done on a few large stalagmites from largest collapsed doline Velika gora (Figure 5.16). The diameter of each drilled core, along the growth axis, is 2.5 cm. All samples were longitudinally cut by a diamond saw (Figure 5.17). One half is given for analysis and the other half is stored in the Karst Research Institute in Postojna. Stalagmite cores from locations 06 – Stebrišče, 07 – Čarobni vrt and 08 – Vrh Velike gore (in green circles in Figure 5.16) are taken for stable isotope analyses, while flowstone cores from locations Pred Peronom and Stara pot (red circles) are stored for later analysis. These locations have been chosen for stalagmite sampling in order to get profile of one large "hill" covered with speleothems. Further in the text location named Peron will be named as location 06 – Stebrišče, because of simplicity and convenience.

5.3.2 Precipitation sampling

Precipitation (rainfall) is sampled from June 2010 to February 2011 on the roof of the Karst Research Institute, which is 500 m away from the Postojna Cave entrance. Integrated monthly sample of the rain water is collected in a high-density polyethylene plastic (HDPE) canister (cca. 5 liter capacity), through a plastic funnel (IAEA, 1997). At the end of the month canister is replaced with the clean and empty one.

To avoid evaporation through paraffin oil has been added. Walls of the collector (plastic canister) are completely covered with aluminum foil and Styrofoam to achive temperature stability and to prevent growth of algae.

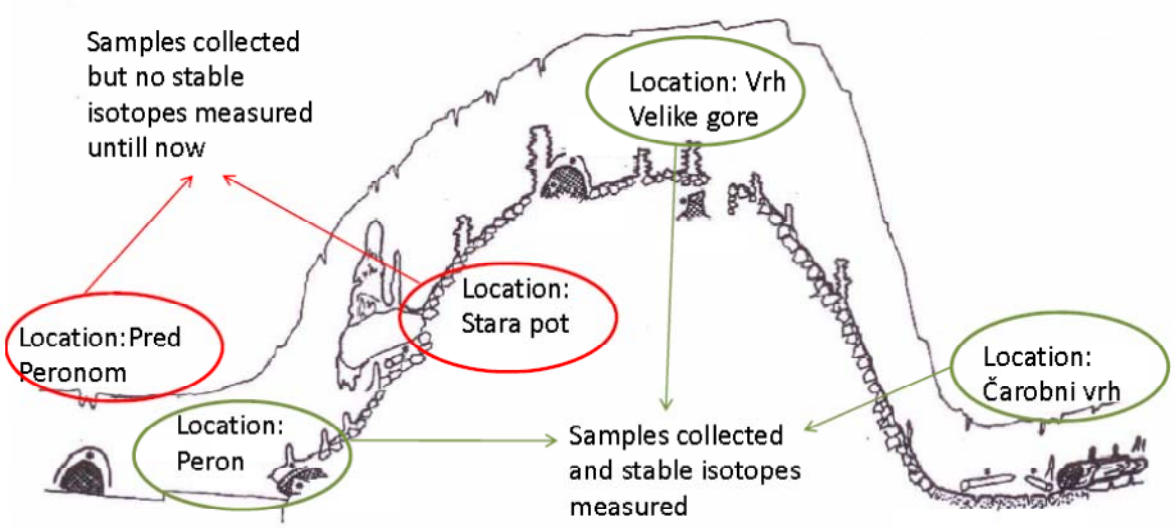

Figure 5.16 Locations where drilling of speleothems has been done (cross section). Samples from two locations, Pred Peronom and Stara pot, has not yet been analyzed.

Slika 5.16 Lokacije uzorkovanja (Peron, Vrh Velike gore i Čarobni vrt - zeleni krugovi). Uzorci s lokacija (Pred Peronom i Stara pot - crveni krugovi) još nisu analizirani.

Figure 5.17 Diamond saw for cutting the speleothems (left), and both halfs of a core drilled from an old stalagmite (right).

Slika 5.17 Dijamantna pila za rezanje siga (lijevo) i obje polovice prerezane jezgre bušenog stalagmita (desno).

5.3.3 Drip water and air sampling

A table for logging in measured values of physical and chemical parameters was prepared before going to the field trip. Instruments for chemical analyses were calibrated in the Karst Research Institute in Postojna by predefined procedures and with calibration standards. pH meter was calibrated by buffer solutions of pH 7 and 10, at 25 ºC.

Vials for sampling atmospheric CO_2 and dissolved inorganic carbon (DIC) for stable isotope analyses of were prepared in Joanneum Research in Graz (detailed description follows in section 5.6). Vials were then shipped by currier post to the Karst Research Institute.

Water samples were collected in narrow neck HDPE bottles of 50 mL and 1 L bottles. Bottles were sealed with double cap and taken for stable isotope and chemical analyses. Both bottles are filled with drip water to the top to prevent isotope fractionation between air and sample.

After arriving to a sampling location in the cave, measurement started. Concentration of CO_2 and air temperature were measured first. According to Baldini et.al. (2006) impact on cave atmosphere (CO_2 concentrations and air temperature) can be caused by human presence. CO_2 concentration and air temperature were measured with hand-held detector Vaisala Carbocap GM 70 and probe GMP 222. Prepared vial for CO_2 sample for $\delta^{13}C$ analysis was opened. Each vial was marked by sample name (date and location name). After a 1-2 minutes the vial wa closed and stored.

For drip water collection bottle with funnel was placed under the drip site. On each location water was always collected on the same place under the same drip. The drip rate, number of drops in one minute, was measured with stopwatch, and the mean value of ten 1-minute measurements was logged in.

For $^{13}C_{DIC}$ analysis an aliquot of 1 mL of water was placed in prepared vials with syringe and thin needle. Special attention has to be paid to insertion procedure of water into the vial. It is of utmost importance not to have bubbles of air mixed with water sample to avoid isotope fractionation between cave air and water.

After storing 50 mL bottles for stable isotope analysis, 1 L bottle was left to be filled with drip water and was collected on return from the last location in the cave. Before storing, the water sample physical (water temperature) and chemical parameters (pH, conductivity, both corrected to 25 ºC) were measured *in situ* with WTW multiline pH / Conductivity 340i Ph Meter.

Each sample is named and numbered. The same sample number is on each sample written twice on different places of the sample bottle, to enable proper identification of sample even if erasing one sample number.

The vials for $^{13}C_{DIC}$ and $^{13}C_{air}$ isotope analyses were sent back to Joanneum Research by currier mail as soon as possible after the sampling trip. It is important that stable isotope analysis is done within the next few days (Spötl, 2005).

5.4 Handling data and results

During each sampling trip 66 records of different parameters were recorded. It is important to mark these records as unique numbers connected to specific sample, to prevent their duplication. It is also important to have the results ready for further analysis without additional typing or other processes where typewriting errors are possible. That is the reason that data base is created in Access - Microsoft Office application program.

The primary purposes of the database are to store a large number of information about samples and enable easy data handling. The benefit of using computer database storage is to ensure efficiency of working with reduction of possible errors made by retyping data.The database consists of the following tables: Location, Samples, Field parameters, Water chemistry, $^{13}C_{DIC}$ and $^{13}C_{air}$, stable isotopes ^{13}C and ^{18}O of carbonates and water, and meteorological data. All records and data are uniquely linked to a sample number.

To each sample a unique sample number **(Sample ID)** is given. The Sample ID has the form: **L – DDMMYYYY – S,** where

- L represents a location code number (01 to 11, see Table 5.1),
- DDMMYYYY represents the sampling date, and
- S represents the sample medium type: water (W), air (A), or carbonate (C).

For example, ID 02 – 26112010 – W is a water sample taken at location 02 – Biospeleološka postaja on November 26th 2010. The database disables possibilityof ID duplication.

5.5 Sampling diary

Sampling diary is summarized in Table 5.2 where general remarks have been introduced after each field trip. Field trips and samplings were performed on the following days: 26th March 2010, 8th June 2010, 5th August 2010, 15th September 2010, 24th November 2010, 3rd February 2011 and 28th April 2011. In the column “Location” (Table 5.2) a comment is written if any of the locations was not visited (e.g., location 10 was flooded in November 2011 and no sample has been taken

from this location). Column "Medium" summarizes which types of samples were taken (W – water, A – air, C – carbonates). Other columns in table 5.2 contain details related to *in situ* measurement, water sampling, chemical analyses, sampling of water and air for $\delta^{13}C$ determination and pCO_2 measurements. Remark "Basic" in column "Chemistry" means that only Ca^{2+}, Mg^{2+} and HCO_3^- concentrations are going to be measured in laboratory and "All" means that chemical analyses includes measurement of Na^+, K^+, Cl^-, SO_4^- and NO_3^- concentrations. On 5th August 2010 drilling of speleothems was performed and because of that no samples for water chemical analyses and for stable isotope analyses were taken. Watch glasses were placed at each location in September 2010 and retrieved during the last sampling in April 2011.Field parameters were not measured in April 2011 because instruments were no available.

Total number of measured and calculated data presented in Appendix I is as follows: 820 data on *in situ* measurements (temperature of air and water, drip rate, pH, conductivity, pCO_2), 302 data on concentrations of various ions in water, and 130 calculated values of calcite saturation index (I_{sat}) and pCO_2(aq). There is also 200 data on isotopic composition of water ($\delta^{18}O_{water}$), CO_2 in air ($\delta^{13}C_{air}$) and DIC in water ($\delta^{13}C_{DIC}$), as well as 308 data on isotopic composition of carbonates ($\delta^{13}C$ and $\delta^{18}O$).

5.6 Sample preparation and measurements

Carbonate samples. Carbonate samples (250 μg to 450 μg) are loaded into borosilicate vials and sealed using rubber septa (Labco). For each sample three individual subsamples are needed. Together with 72 vials of samples 12 international standards (IAEA – CO - 8 and NBS - 19) are routinely loaded in the sample tray. Mass of standard samples is within the same range as that of samples, so that the linearity corrections of obtained results could be avoided (Werner and Brandt, 2001). The prepared vials are placed into heated aluminum tray. The tray temperature is kept constant at 75 ^oC (Spötl et al., 2003).

Exetainers are then flushed by a double-hole needle with helium 6.0 of flow-rate adjusted to 120 mL/min. Each vial is flushed for 10 minutes. Afterwards, 3-7 drops of phosphoric acid is manually added in each vial (McCrea, 1950). Reaction time of phosphoric acid and carbonate sample is around 85 minutes per sample. After that time, measurement starts.

Table 5.1 Sampling dates with details on *in situ* measured parameters on each field trip and samples taken for various parameters to be measured in laboratories.
Tablica 5.2 Dnevnik uzorkovanja: datum i posjećene lokacije, vrsta uzetih uzoraka, mjereni parametri na terenu, te uzorci uzeti za različita mjerenja u laboratorijima.

Sampling date	Location	Medium	Field parameters and water sampling	Chemistry	DIC	AirCO_2 for ^{13}C	pCO_2
26.03.2010.	All	A&W	All	01, 02, 04, 06, 07, 08, 09, 11 Basic	02, 04, 05, 07, 09	01, 02, 03, 05,06, 07, 08, 09, 11	02, 03, 04, 05, 06, 07, 08, 09, 11
08.06.2010	All	A&W	All	Basic	All	All	All
05.08.2010. Drilling of speleothems	All	A&W&C	All	No	No	No	All
15.09.2010. Watch glasses placed in all locations	All	A&W	All	All	All	All	All
24.11.2010.	Loc. 10 flooded	A&W	All except 10	Basic	All except 10	All except 10	All except 10
03.02.2011.	All	A&W	All	Basic	All	All	All
28.04.2011. Watch glasses retrieved	All	A&W&C	instruments not available; drip rate measured	All	All	All	instruments not available

Each measurement automatically starts with peak centering to get the best signal with electronic set up. Each sample measurement starts with rectangular peaks of CO_2 reference ^{18}O is 0.1 ‰ calculated on specific number of sample peaks. If the sample has too high CO_2 signal (higher than adjusted), then the auto diluter on open split is switched on automatically.

DIC samples. Before going to the field, 10 mL (Lobco) borosilicate vials are filled in the laboratory manually with five drops of phosphoric acid (ortho-Phosphoric acid 85%, Merck Chemicals). Vials are then caped with rubber septa, and flushed with Helium 6.0. Prepared vials were then shipped by courier mail to the Postojna Karst Research Institute and taken to the field site. Depending on the carbonate alkalinity the amount of water was introduced with syringe to the exetainer (Spötl, 2005). For samples from Postojna Cave having HCO_3^- concentrations of approximately 400 mg/L, the amount of water was 100 µL (Spötl, 2005). Reaction of sample and acid starts immediately. Samples were shipped back to the Joanneum Research soon after sampling. Within few days samples were set for final analysis.

Tray holder of CTC Combi – Pal autosampler was routinely loaded with DIC samples and with carbonate standards that are used because international (IAEA or NIST) standards for

DIC are not available. For replicate measurements of samples the overall reproducibility is < 0.1‰ (VPDB) for both $\delta^{13}C$ and $\delta^{18}O$ values (Kosednar-Legenstein et al., 2008). The software calculates raw delta values by taking average raw ratios of a sample peaks and comparing them with raw ratios of reference gas. The declared and overall precision of the method is 0.1 ‰ (Poberžnik et al., 2012).

Atmospheric CO_2 sampless. Before going to the field 10 mL borosilicate vials were capped by rubber septa, flushed with He gas 6.0, and then shipped by courier post to the sampling site. On each location one vial is opened and closed shortly after. After field trip the vials have been, together with other samples, sent back to the Joanneum Research. Analyses were made shortly after receiving the samples.

The measurement on the gas bench is nearly identical to that of DIC and carbonates. The exception is that dilution with helium gas (Chapter 2.5.2) is switched on automatically before CO_2 peak. The calibration is done to calcite reference material (Table 2.3) prepared the day before air sample measurement. The internal standard deviation for air samples is less than 0.3 ‰.

HDO equilibration unit is used for water equilibration. An aliquot of 5 mL of water is inserted in 20 mL flasks (Horita et al., 1989). Set of 48 bottles containing samples and reference water is placed on valves (normally opened) and put into water bath (Avak and Brandt, 1995). The temperature of water bath is controlled and held constant 20.0 ± 0.1 ºC (Figure 5.18).

Figure 5.18 Set of 48 bottles prepared for water equilibration in water bath at constant temperature.

Slika 5.18 Skup od 48 bočica pripremljenih za ekvilibraciju vode u vodenoj kupelji stabilne temperature.

The bottles (Figures 5.18 and 5.19) are flushed few times with CO_2 reference gas (Finnigan, 1997). After 45 minutes process of exchange of isotopic composition of water with CO_2 reference gas is finished, i.e., water is in isotopic equilibrium with CO_2 and measurement can start. Prior to the gas introduction to sample bellow of dual inlet system, equilibrated gas passes through cooling system at -72 °C for water vapor removal.

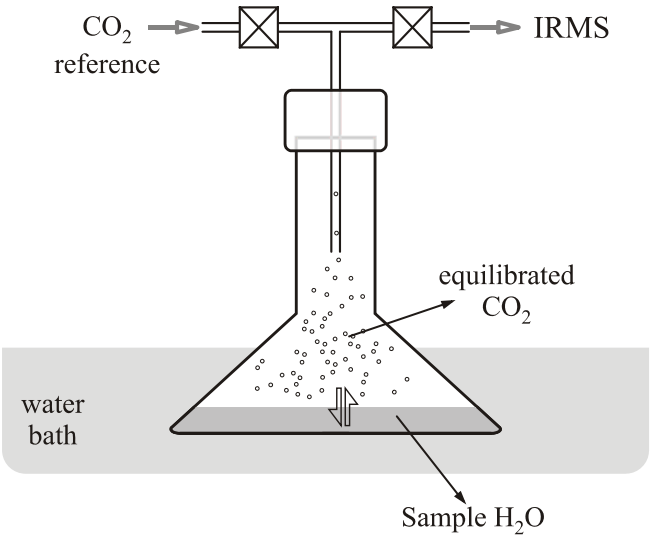

Figure 5.19 Schematic view of equilibration procedure in the HDO equilibration unit.
Slika 5.19 Shematski prikaz ekvilibracijske procedure u HDO jedinici za ekvilibraciju.

5.7 Chemical analyses of water samples

Chemical analysis of water was performed in the Institute for Public Health in Rijeka in the certificated laboratory for water quality examination. Concentrations of Ca^{2+}, Mg^{2+} and HCO_3^- were determined in all water samples. Analyses of Na^+, K^+, Cl^-, SO_4^{2-} and NO_3^- concentrations were performed only twice during the monitoring period, because of assumed minor abundance in a clean karst groundwater (Ford and Williams, 2007; Merkel and Planer-Friedrich, 2008). The method used for determination of Ca^{2+}, Mg^{2+}, Na^+, K^+ and HCO_3^- concentrations was HRN EN ISO 14911:2001 (Water quality - Determination of dissolved Li^+, Na^+, NH_4^+, HCO_3^-, K^+, Mn^{2+}, Ca^{2+}, Mg^{2+}, $Sr^{2+}$and Ba^{2+} using ion chromatography). Measurement of Cl^-, SO_4^{2-} and NO_3^- concentrations was performed according to the HRN EN ISO 10304-1:2009 method (Water quality - Determination of dissolved anions by liquid chromatography of ions - Part 1: Determination of bromide, chloride, fluoride, nitrate, nitrite, phosphate and sulfate).

6 RESULTS

Numerical values of field parameters: air temperature, water temperature, pH, drip rate, conductivity, and pCO_2 in cave air are listed in Table A.3 (Appendix I). Results of chemical analyses of drip water are listed in Table A.4 (Appendix I) together with calculated I_{sat} and pCO_2(aq) values. For all locations concentrations of Ca^{2+}, Mg^{2+}, and HCO_3^- in drip water have been measured each time after field sampling, and concentrations of Na^+, K^+, Cl^-, SO_4^{2-}, NO_3^- are measured twice during monitored period as they are minor elements in karst groundwater (Ford and Williams, 2007; Merkel and Planer-Friedrich, 2008). Stable isotope concentrations $\delta^{13}C_{DIC}$, $\delta^{13}C_{air}$ and $\delta^{18}O_{water}$ are listed in Tables A.5 (Appendix I). Table A.6 presents correlation matrices between chemical and isotopic parameters for each location.

Table A.7 (Appendix I) contains $\delta^{18}O$ values in precipitation, while in Tables A.8, A.9 and A.10 stable carbon $\delta^{13}C$ and oxygen $\delta^{18}O$ composition of recent carbonate samples ("soda straw", peculiar growth samples and carbonate precipitated on watch glasses, respectively) is presented. Table A.11 (Appendix I) shows data of stable carbon $\delta^{13}C$ and oxygen $\delta^{18}O$ composition of old carbonates (flowstones and stalactites) with description of lamina color for each subsample, while Table A.12 contains $\delta^{13}C$ and $\delta^{18}O$ data of drilled cores of stalagmites.

6.1 Cave environment and drip water

Location 01 – Slonova glava

On location 01 – Slonova glava (Figure 6.1) air temperature varies from 12 °C in August 2010 to 6 °C in February 2011, with mean value 9.8 ± 2.2 °C. Lowest water temperature is measured also in February 2011, 6.4 °C, and the highest of 11.2 °C in September 2010. Mean water temperature is 9.3 ± 2.0 °C. Concentration of CO_2 in the air is the lowest in February 2011 (400 ppmv) and the highest in August 2010 (1160 ppmv). The highest conductivity of

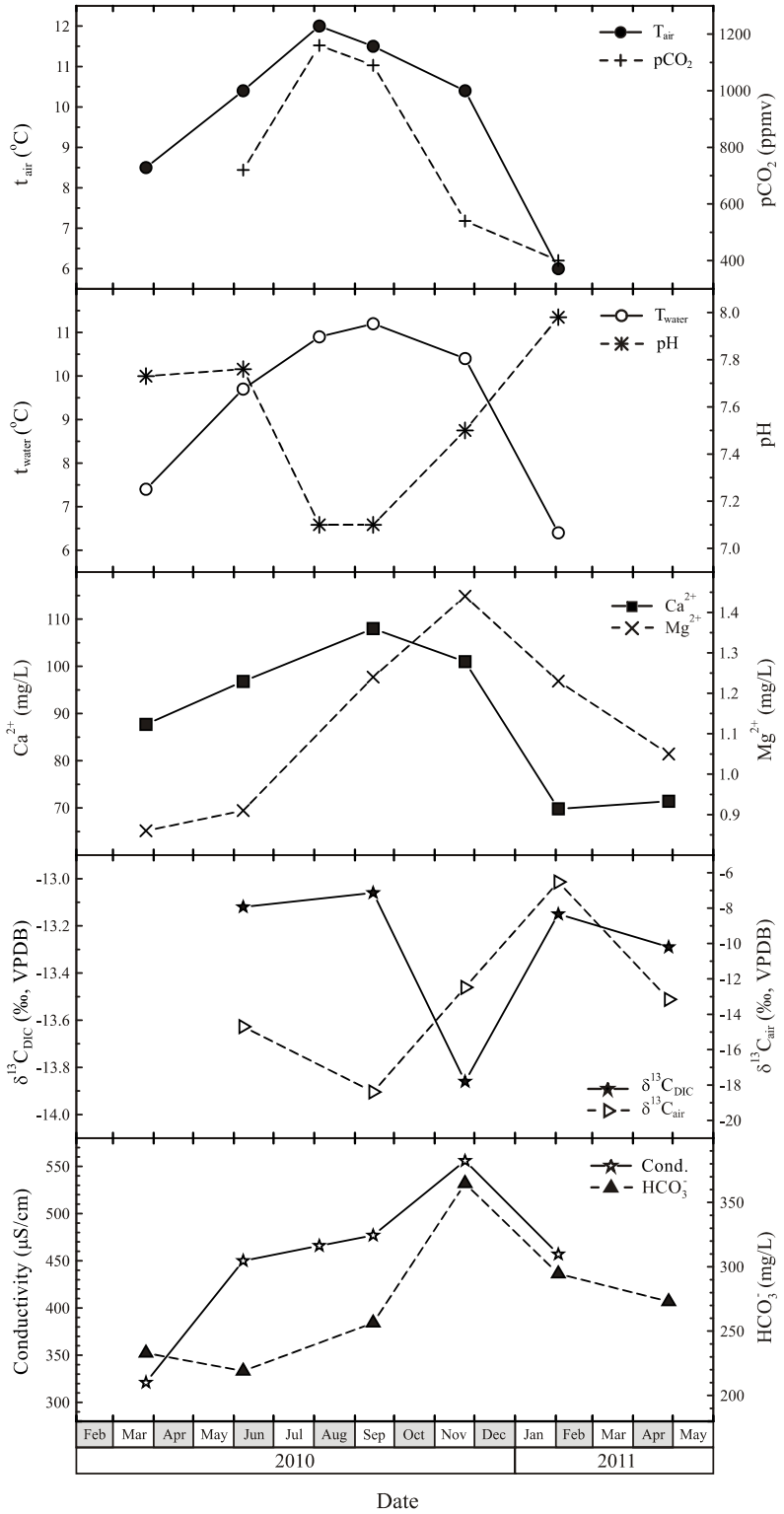

Figure 6.1 Time series of field measured parameters (air temperature, water temperature, pH, conductivity, and pCO_2), chemical parameters (Ca^{2+}, Mg^{2+}, and HCO_3^- concentrations) in drip water and stable isotope composition $\delta^{13}C_{DIC}$ and $\delta^{13}C_{air}$ for location 01 – Slonova glava.

Slika 6.1 Rezultati mjerenja na terenu (temperature zraka i prokapne vode, pH, vodljivosti i pCO_2), kemijskih parametara (koncentracije Ca^{2+}, Mg^{2+} i HCO_3^-) u prokapnoj vodi te izotopni sastav $\delta^{13}C_{DIC}$ i $\delta^{13}C_{air}$ na lokaciji 01 – Slonova glava.

556 µS/cm is measured in November 2010 and the lowest, 321 µS/cm, in March 2010. The pH value ranges from 7.10 in August and September 2010 to 7.98 in February 2011. The concentration of magnesium varies from 0.86 mg/L in March 2010 to 1.44 mg/L in November 2010. The Ca^{2+} concentration ranges from 69.8 mg/L in February 2011 to 108.0 mg/L in September 2010, and HCO_3^- concentration ranges from 219 mg/L in June 2010 to 364.8 mg/L in November 2010. The stable isotope value $\delta^{13}C$ in DIC has a narrow range of values, bezween -13.86 ‰ in November 2020 and -13.06 ‰ in September 2010. The $\delta^{13}C_{air}$ value varies from -6.52 ‰ in February 2011 to -18.39 ‰ in September 2010.

Drip rate varies from 13 to 165 drops per minute (Figure 6.2). The pronounced maximum is observed in Nov 2011, about two months after abundant precipitation (Sept 2010, Figure 4.9).

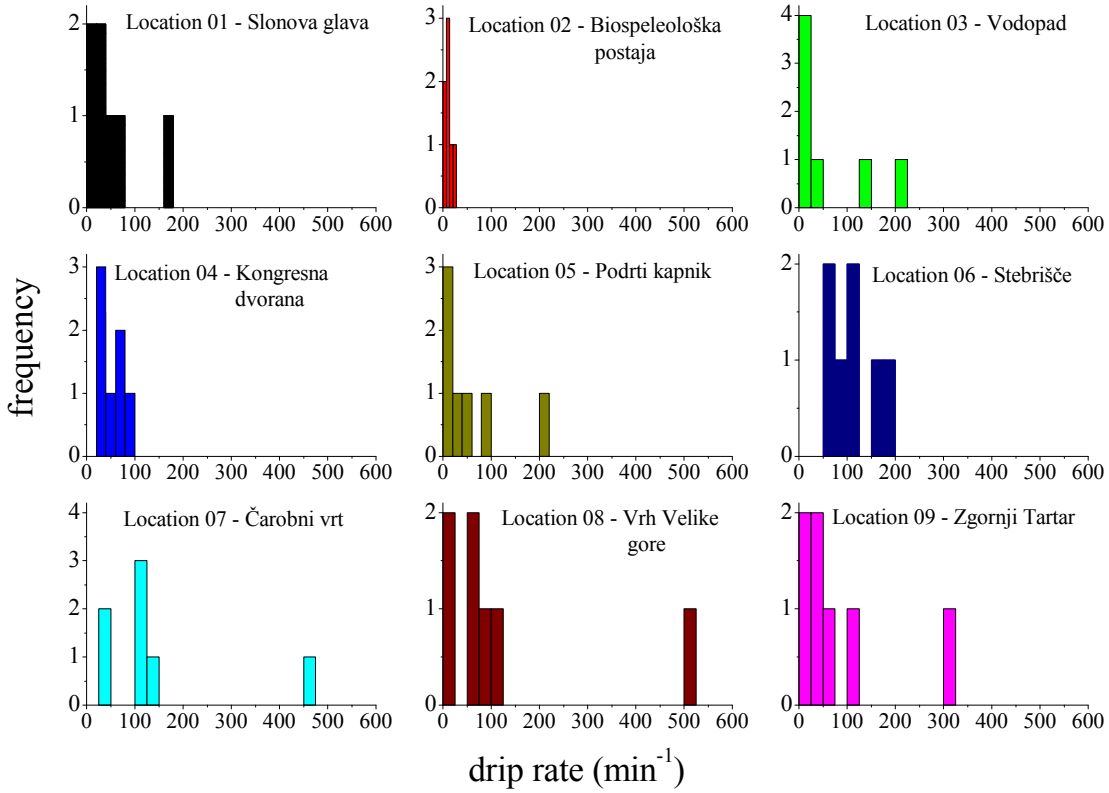

Figure 6.2 Histograms of measured drip rate.

Slika 6.2 Histogrami učestalosti prokapljavanja.

For measured and calculated parameters (conductivity, pH, concentrations of bicarbonates, calcium and magnesium, $\delta^{13}C_{DIC}$, pCO_2 in cave air, $\delta^{13}C_{air}$, pCO_2 (aq), I_{sat}) correlation matrix is made for each location separately. Correlation matrix is a diagonal matrix that contains correlation coefficients with perfect positive correlation (R = 1) values as diagonal elements, since this is correlation of a parameter with itself. The correlation matrix is also symmetric since the

correlation of parameter i with parameter j is the same as the correlation of parameter j with parameter i. The correlation matrices for all locations are presented in Table A.6 in Appendix I. In addition to correlation coefficients R, the table also contains p-values, i.e., statistical significance. The statistical significance of a result is the probability that the observed relationship occurred by pure chance. The higher the p-value, the less we can believe that the observed correlation is a reliable indicator of the relation between the respective variables in the population. The lower the p-value, the more reliable is the observed correlation. In many areas of research, the p-value of 0.05 is customarily treated as a "border-line acceptable" error level. However, the actual border-line of acceptance is rather arbitrary. For the purpose of interpretation of the present data, the border-line statistical significance (the p-value) is defined as 0.1 (Walpole, 2007)

Significant ($p < 0.1$) positive correlation ($R > 0$) is found between bicarbonate and magnesium concentrations, conductivity and magnesium concentration, pH and I_{sat}, and $pCO_2(aq)$ and pCO_2. Significant negative correlation ($R < 0$) is obtained between $\delta^{13}C_{DIC}$ and bicarbonate concentration, conductivity and drip rate. Calcium concentration is negatively correlated with pH and I_{sat}. pH is also negatively correlated with pCO_2 and $pCO_2(aq)$. pCO_2 is negatively correlated with I_{sat} and $\delta^{13}C_{air}$. $pCO_2(aq)$ is significantly negatively correlated with I_{sat}.

Location 02 – Biospeleološka postaja

The lowest air temperature (Figure 6.3) is measured in February 2011, 8.2 °C and highest value is 10.8 °C measured in August 2010. Mean air and water temperature are 9.9 ± 1.0 ºC and 10 ± 2 ºC, respectively. Lowest measured water temperature is measured in March 2010 8.6 °C and highest value is measured 12.4 °C in November 2010. Mean pH value is 7.57 ± 0.40. Lowest measured pH value is 7.10 in August and September 2010, and highest value of pH is 8.06 measured in February 2011. Conductivity varies from 370 µS/cm to 471 µS/cm in March and November 2010, respectively. The pCO_2 mean value is 840 ± 335 ppmv with the range from 420 ppmv in February 2011 to 1260 ppmv in September 2010. The lowest Ca^{2+} concentration 69.8 mg/L is measured in February 2011 and the highest 98.2 mg/L in April 2011. The Mg^{2+} concentration ranges from 0.72 mg/L in June 2010 to 1.34 mg/L in November 2010. Mean values for magnesium and calcium concentrations are 1.12 ± 0.22 mg/L and 89.1 ± 15.8 mg/L, respectively. Bicarbonate concentration 274± 53 mg/L varies from 183 mg/L in March 2010 to 327 mg/L in November 2010. The lowest stable isotope value $\delta^{13}C$ of DIC is -13.39 ‰ in April 2011 and the highest value -12.52 ‰ is measured in September 2010., showing thus a narrow range of values of less than 1 ‰. $\delta^{13}C$ values in air samples range from -7.58 ‰ in February 2011 to -19.12 ‰ in

September 2010. Mean values for $\delta^{13}C$ of DIC and $\delta^{13}C$ in cave-air samples are -12.84 ± 0.32 ‰ and -13.92 ± 4.50 ‰, respectively. Drip rate varies from 3 to 30 drops per minute (Figure 6.2) with the lowest mean drip rate of 14 ± 9 min^{-1} and mosta stable among all studied locations.

Positive correlation is found between bicarbonate concentration and conductivity, and also magnesium concentration. Magnesium concentration is positively correlated with conductivity, and pH is positively correlated with I_{sat}. Negative correlation is found between pH and pCO_2, as well as between pCO_2 and both $\delta^{13}C_{air}$ and I_{sat}.

Location 03 – Vodopad

At location 03 – Vodopad (Figure 6.4) mean air temperature is 9.7 ± 1.6 ºC and varies from 11.2 °C in August 2010 to 7.5 °C in February 2011. The lowest water temperature is measured also in February 2011, 7.5 °C, and the highest value of 11.8 °C in September 2010. Mean water temperature is 9.6 ± 1.7 ºC. The concentration of CO_2 in the air is the lowest in February 2011 (400 ppmv) and the highest in August 2010 (1100 ppmv). The highest conductivity of 458 µS/cm is measured in November 2010 and the lowest 372 µS/cm in March 2010. Mean values for CO_2 concentration and conductivity are 771 ± 321 ppmv and 406 ± 29 µS/cm, respectively. The drip rate 60 ± 79 min^{-1} varie from 5 to 210 drops per minute (Figure 6.2). The pH value 7.91 ± 0.41 ranges from 7.10 in September 2010 to 8.22 in June 2010. The minimum measured value for magnesium Mg^{2+} is 0.71 mg/L in June 2010 and maximum value is 1.20 mg/L in November 2010. For Ca^{2+} minimum is measured in June 2010, 81.7 mg/L, and maximum in September 2010, 93.9 mg/L. Minimum of bicarbonate content, HCO_3^- is measured in June 2010, 192 mg/L and maximum in November 2010, 292.8 mg/L. Mean values of magnesium, calcium and bicarbonate concentrations are 1.0 ± 0.2 mg/L, 89 ± 7 mg/L, and 249 ± 38 mg/L, respectively. $\delta^{13}C$ value in DIC -12.90 ± 0.29 ‰ has again narrow range of values from -13.20 ‰ in April 2011 to -12.44 ‰ in June 2010. The $\delta^{13}C$ measured in air samples varies from -6.35 ‰ in February 2011 to -18.75 ‰ in September 2010. Mean value of $\delta^{13}C$ in air is -13.2 ± 4.6 ‰.

Bicarbonate concentration is positively correlated with magnesium concentration (Table A.6). pH is negatively correlated with pCO_2 and pCO_2(aq), and positively correlated with I_{sat}. Significant negative correlation is found between pCO_2 and both $\delta^{13}C_{air}$ and I_{sat}. I_{sat} is negatively correlated with pCO_2(aq).

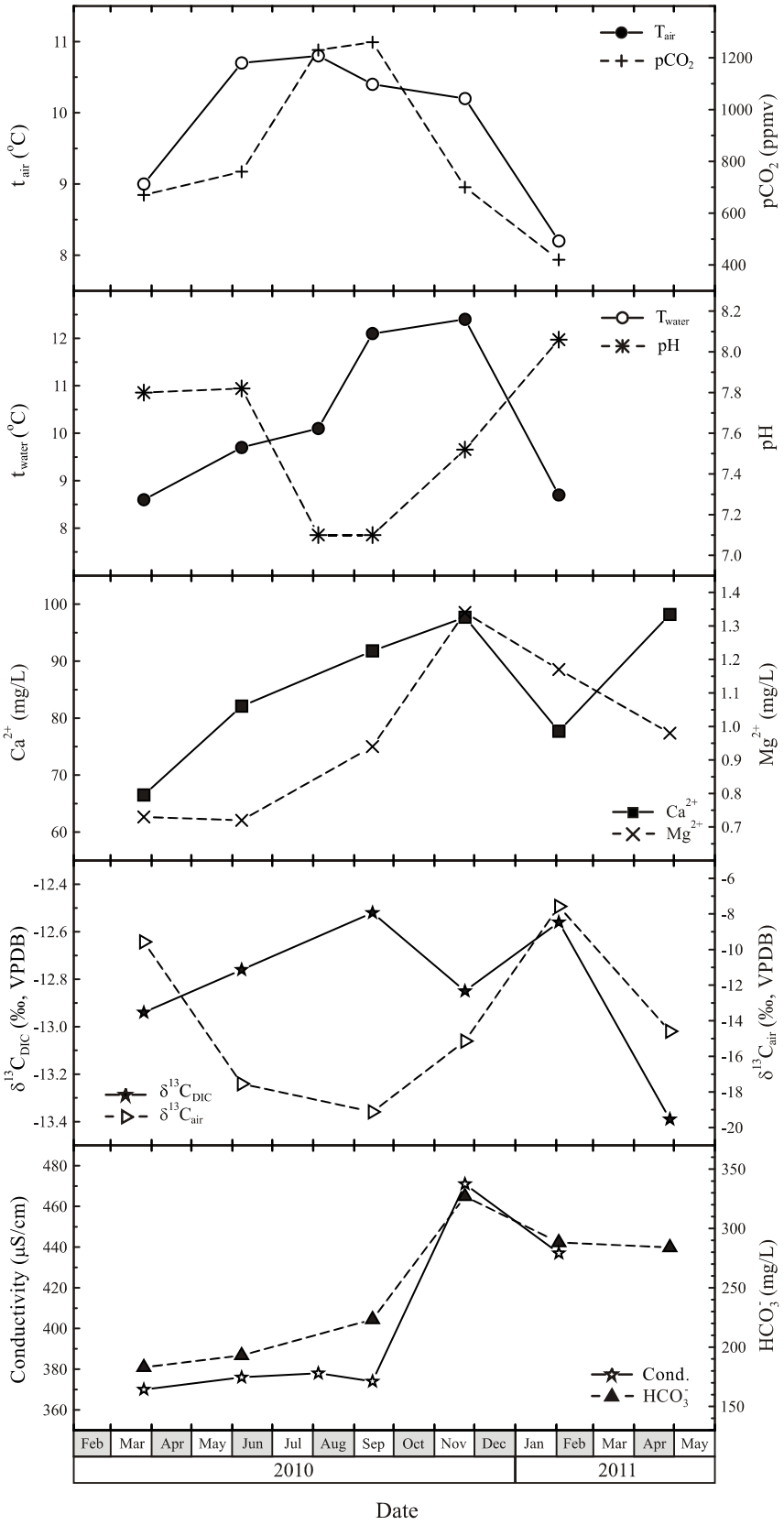

Figure 6.3 *Ibid* (6.1). Location 02 – Biospeleološka postaja

Slika 6.3 *Ibid* (6.1). Lokacija 02 – Biospeleološka postaja

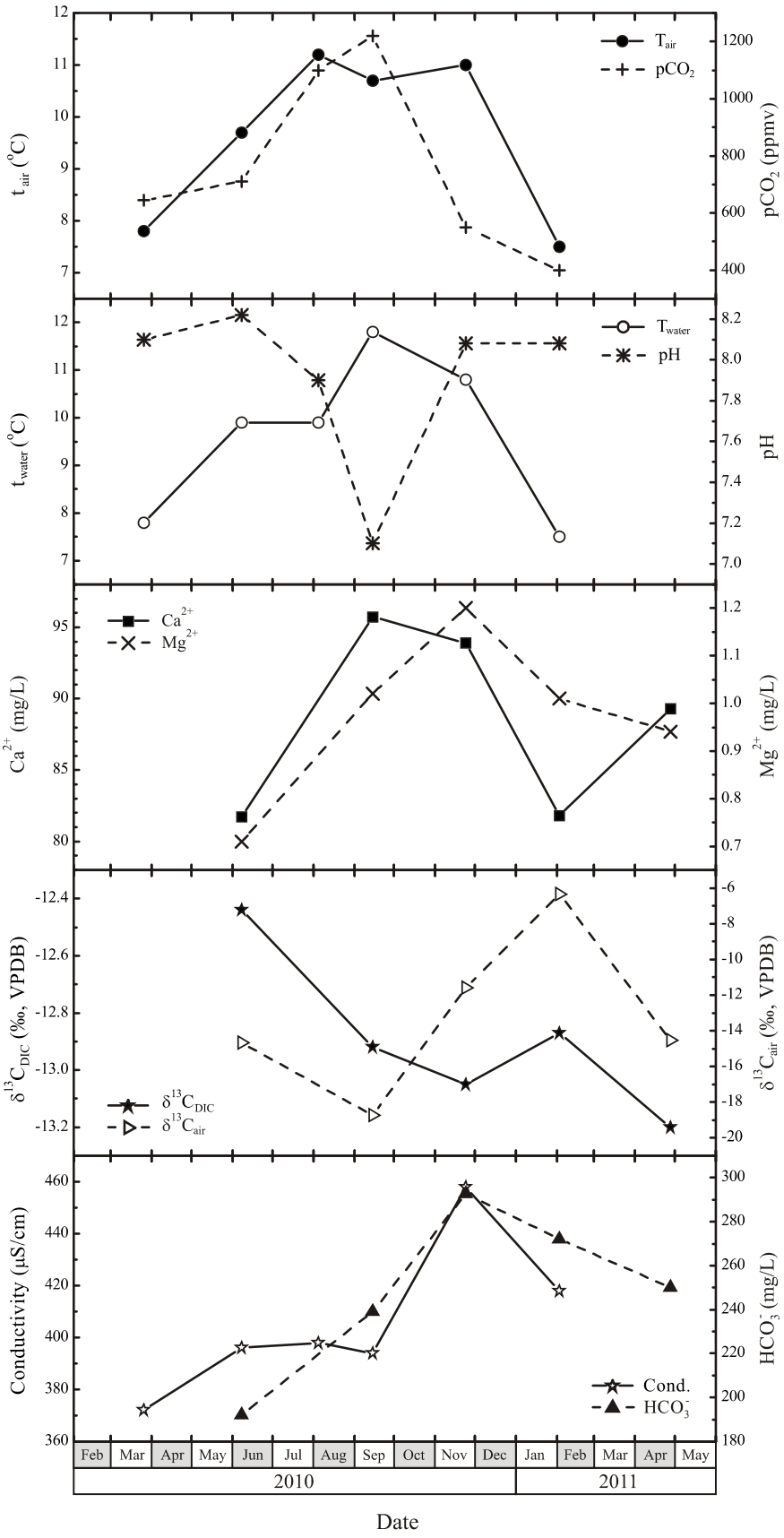

Figure 6.4 *Ibid* (6.1) Location 03 – Vodopad

Slika 6.4 *Ibid* (6.1) Lokacija 03 – Vodopad

Location 04 – Kongresna dvorana

Mean air temperature at location 04 – Kongresna dvorana is 10.3 ± 1.4 ºC, Figure 6.5. The lowest air temperature is measured in March 2010 8.5 °C and highest value is 12.7 °C measured in August 2010. Lowest water temperature is also measured in March 2010, 8.4 °C, and highest value (10.7 °C) in August 2010. Mean water temperature is 10 ± 1 °C. The lowest pH value is 7.58 in June 2010 and the highest 8.35 in March 2010. The conductivity values vary from 409 µS/cm to 476 µS/cm for September and June 2010, respectively. The lowest pCO_2 is 430 ppmv in February 2011 and the highest 1220 ppmv i in September 2010. Mean values for conductivity, pH, and pCO_2 are 429 ± 24 µS/cm, 8.04 ± 0.33, and 783 ± 300 ppmv, respectively. Ca^{2+} concentration ranges from 74.8 mg/L in March 2010 to 103 mg/L in June 2010. Mean concentrations of calcium and magnesium are 87 ± 13 mg/L and 1.0 ± 0.1 mg/L, respectively. The lowest Mg^{2+} concentration is 0.77 mg/L measured in March and November 2010 and the highest 1.05 mg/L in September 2010. Bicarbonate concentration 247 ± 24 mg/L varies from 209 mg/L in March 2010 to 269 mg/L in February 2011. Drip rate 50 ± 25 min^{-1} varies from 20 to 90 drops per minute without extreme values (Figure 6.2). The lowest $\delta^{13}C$ of DIC is -13.09 ‰ measured in June 2011 and the highest value -11.90 ‰ in March 2010. The $\delta^{13}C$ in air samples ranged between -6.41 ‰ in February 2011 and -18.61 ‰ in September 2010. Mean values for $\delta^{13}C$ of DIC and $\delta^{13}C$ in air samples are -12.4 ± 0.5 ‰ and -12.6 ± 4.5 ‰, respectively.

Negative correlation is found between conductivity and $\delta^{13}C_{DIC}$ (Table A.6). The pH is significantly positively correlated with I_{sat} and drip rate, and negatively correlated with $pCO_2(aq)$. pCO_2 is negatively correlated with $\delta^{13}C_{air}$. $pCO_2(aq)$ is negatively correlated with I_{sat} and drip rate. Between I_{sat} and drip rate positive correlation is found.

Location 05 – Podrti kapnik

At location 05 – Podrti kapnik, Figure 6.6, air temperature 11.1 ± 0.4 ºC varies from 11.6 °C in September 2010 to 10.5 °C in February 2011. Mean water temperature is 10.6 ± 0.6 and the lowest is measured in March 2010, 9.9 °C, and the highest 11.7 °C in September 2010. pCO_2 is lowest in February 2011 (430 ppmv) and highest in August 2010 (1530 ppmv). The highest conductivity of 318 µS/cm is measured in November 2010 and the lowest 197 µS/cm in February 2011. Mean values of conductivity and pCO_2 are 277 ± 42 µS/cm and 1162 ± 463 ppmv, respectively. The pH 9.0 ± 0.4 ranges from 7.46 in September 2010 to 8.38 in March 2010. The minimum magnesium (Mg^{2+}) concentration is 0.67 mg/L in June 2010 and

maximum value is 0.88 mg/L in February 2011. For Ca^{2+} minimum is measured in February 2011, 47.0 mg/L and maximum in November 2010, 76.3 mg/L. Minimal HCO_3^- concentration is measured in February 2011, 121.7 mg/L and maximum in November 2010, 194.2 mg/L. Mean values for magnesium, calcium and bicarbonate concentrations are 0.79 ± 0.08 mg/L, 65 ± 12 mg/L, and 153 ± 29 mg/L, respectively. $\delta^{13}C$ in DIC -10 ± 2 ‰ is highest measured in February 2011, -5.64 ‰, and lowest in November 2010, -11.78 ‰. When compared to other locations, the range of $\delta^{13}C$ values of DIC is larger. $\delta^{13}C$ in air samples -15 ± 4 ‰ varies from -9.32 ‰ in February 2011 to -19.16 ‰ in September 2010. Drip rate 56 ± 69 min^{-1} varies from 10 to 200 drops per minute (Figure 6.2).

Conductivity is significantly positively correlated with calcium concentration (Table A.6), and negatively correlated with $\delta^{13}C_{DIC}$. Bicarbonate and calcium concentrations are positively correlated. Calcium concentration is negatively correlated with $\delta^{13}C_{DIC}$ and $\delta^{13}C_{air}$. pH is found to be negatively correlated with pCO_2 and pCO_2(aq), and positively correlated with I_{sat} and drip rate. Negative correlation is found between pCO_2 and both $\delta^{13}C_{air}$ and I_{sat}. Negative correlation is found between pCO_2(aq) and I_{sat}.

Location 06 – Stebrišče

Mean air temperature at location 06 – Stebrišče is 11.3 ± 1.2 ºC, being lowest 10.2 °C in February 2011 and highest 13.5 °C in August 2010 (Figure 6.7). Mean water temperature is 11.0 ± 0.7 ºC. Lowest water temperature is in March and June 2010 (10.4 °C) and highest value (12.2 °C) in September 2010. pH ranges from 7.38 in August 2010 to 8.33 in March 2010. Mean conductivity value is 366 ± 17 µS/cm and varies from 338 µS/cm to 387 µS/cm for June and September 2010, respectively. The mean pCO_2 is 1038 ± 399 ppmv ranging from 510 ppmv in February 2011 to 1490 ppmv in August 2010. The lowest Ca^{2+} concentration is 68.3 mg/L in March 2010 and the highest value is 89.8 mg/L in April 2011. The mean concentrations of calcium and magnesium are 79 ± 8 mg/L and 0.9 ± 0.1 mg/L, respectively. Concentration of HCO_3^- is 232 ± 25 mg/L and ranges from 187 mg/L in March 2010 to 255 mg/L in November 2010. The mean $\delta^{13}C$ values of DIC and $\delta^{13}C$ in air are -13.1 ± 0.1 ‰ and -16.3 ± 3.7 ‰, respectively. The lowest $\delta^{13}C$ value of DIC is -13.17 ‰ measured in March 2010 and highest value -12.87 ‰ is measured in February 2011, showing a very narrow range of values. The $\delta^{13}C$ values in air range between -10.13 ‰ in February 2011 and -19.62 ‰ in September 2010. Drip rate 108 ± 48 varies from 50 to 180 drops per minute (Figure 6.2).

Bicarbonate and magnesium concentrations are significantly positively correlated (Table A.6). Bicarbonate concentration is also positively correlated with $\delta^{13}C_{DIC}$. Calcium concentration is found to be positively correlated with pCO_2 and negatively with $\delta^{13}C_{air}$ and I_{sat}. The pH is negatively correlated with magnesium concentration and pCO_2(aq), and positively correlated with I_{sat}. The magnesium concentration is positively correlated with $\delta^{13}C_{DIC}$. pCO_2 is negatively correlated with $\delta^{13}C_{air}$ and I_{sat}, and positively correlated with pCO_2(aq), while pCO_2(aq) is negatively correlated with I_{sat}.

Location 07 – Čarobni vrt

At location 07 – Čarobni vrt (Figure 6.8) the air temperature 10.7 ± 0.8 ºC varies from 9.6 °C in August 2010 to 11.7 °C in September 2010. Mean water temperature is 10.7 ± 0.9 ºC with the lowest value in March 2010, 9.5 °C, and the highest (11.8 °C) in September 2010. pCO_2 in the air is 1578 ± 885 ppmv ranging from 750 ppmv in March 2010 to 2940 ppmv in September 2010. Conductivity is 336 ± 30 µS/cm and ranges from 378 µS/cm in June 2010 to 301 µS/cm in February 2011. Mean pH value is 7.9 ± 0.3 and ranges from 7.35 in September 2010 to 8.17 in February 2011. The lowest magnesium concentration is 0.25 mg/L in September 2010 and the highest is 1.20 mg/L in June 2010. For Ca^{2+} minimum is measured in November 2010, 68.0 mg/L and maximum in September 2010, 90.3 mg/L. HCO_3^- concentration ranges from 167 mg/L in June 2010 to 216 mg/L in April 2011. Mean values of magnesium, calcium and bicarbonate concentrations are 0.9 ± 0.3 mg/L, 74 ± 9 mg/L, and 200 ± 19 mg/L, respectively. The $\delta^{13}C$ in DIC -12.3 ± 0.3 ‰ is highest in February 2011, -11.98 ‰, and lowest in April 2011, -12.66 ‰. $\delta^{13}C$ in air samples -18.0 ± 2.1 ‰ varies from -15.67 ‰ in February 2011, to -21.64 ‰ in September 2010. The highest drip rate is measured in November 2010, 450 min^{-1}, and lowest in August 2010, 35 min^{-1} (Figure 6.2). Mean drip rate is 144 ± 140 min^{-1}.

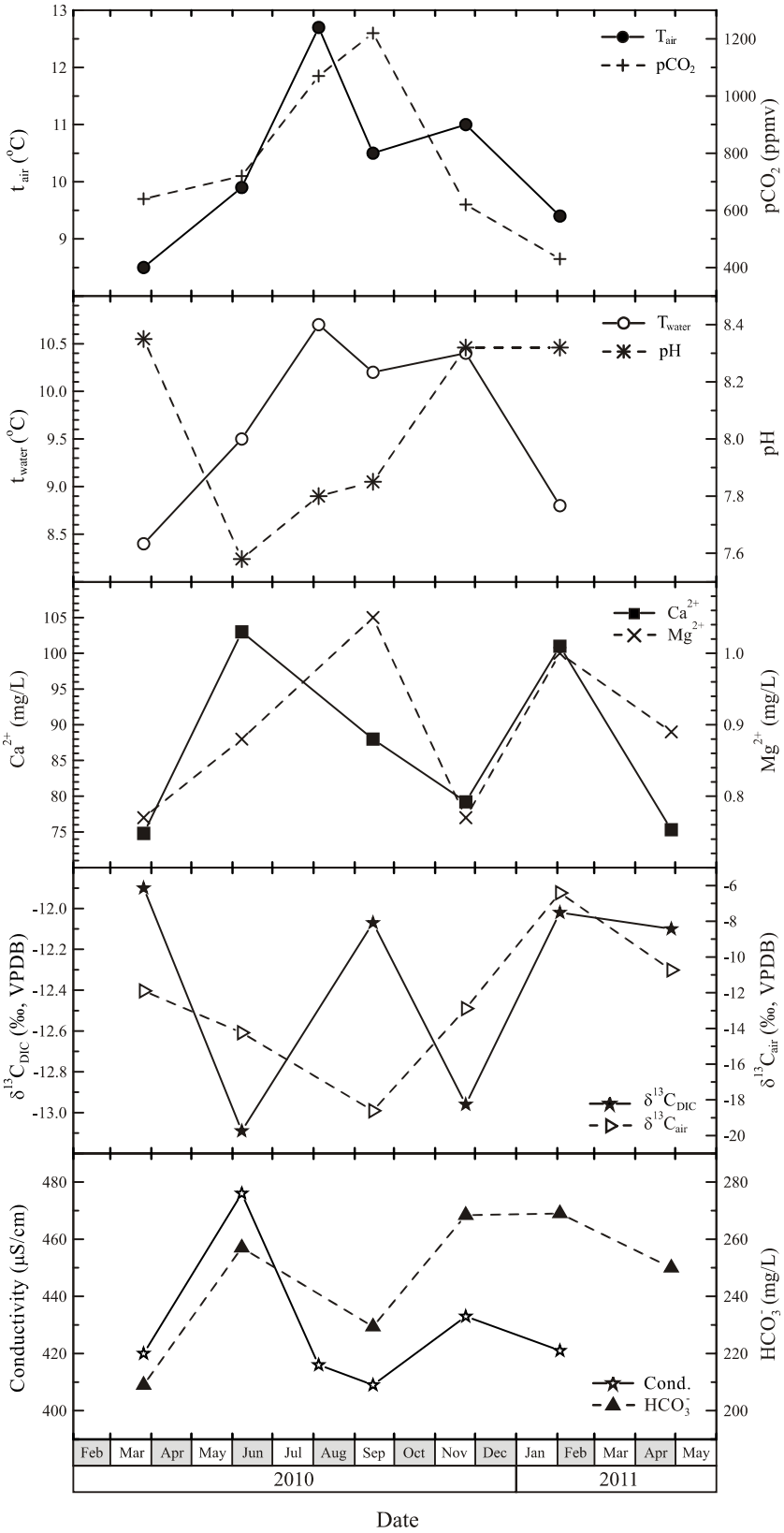

Figure 6.5 *Ibid* (6.1) Location 04 – Kongresna dvorana

Slika 6.5 *Ibid* (6.1) Lokacija 04 – Kongresna dvorana

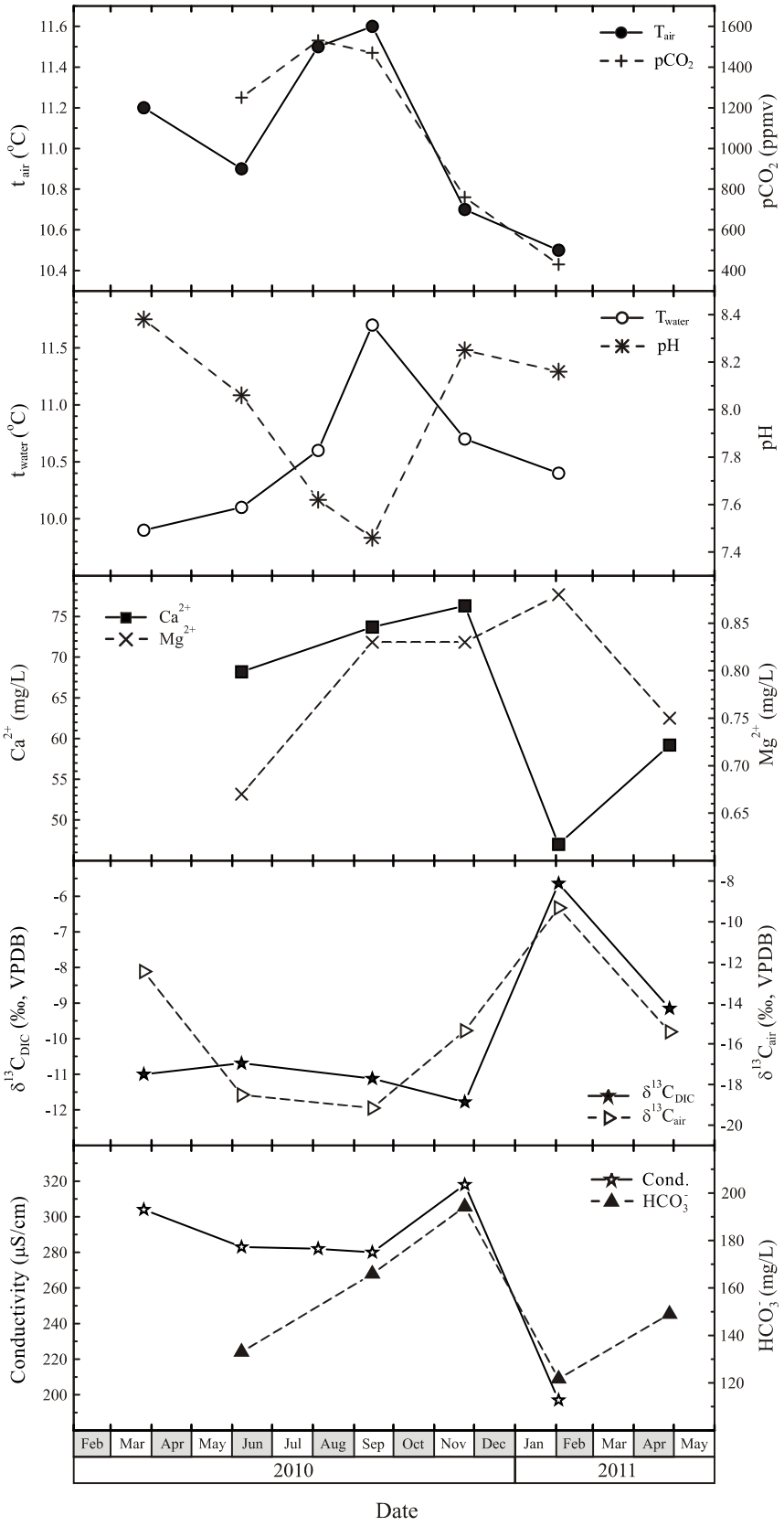

Figure 6.6 *Ibid* (6.1) Location 05 – Podrti kapnik
Slika 6.6 *Ibid* (6.1) Lokacija 05 – Podrti kapnik

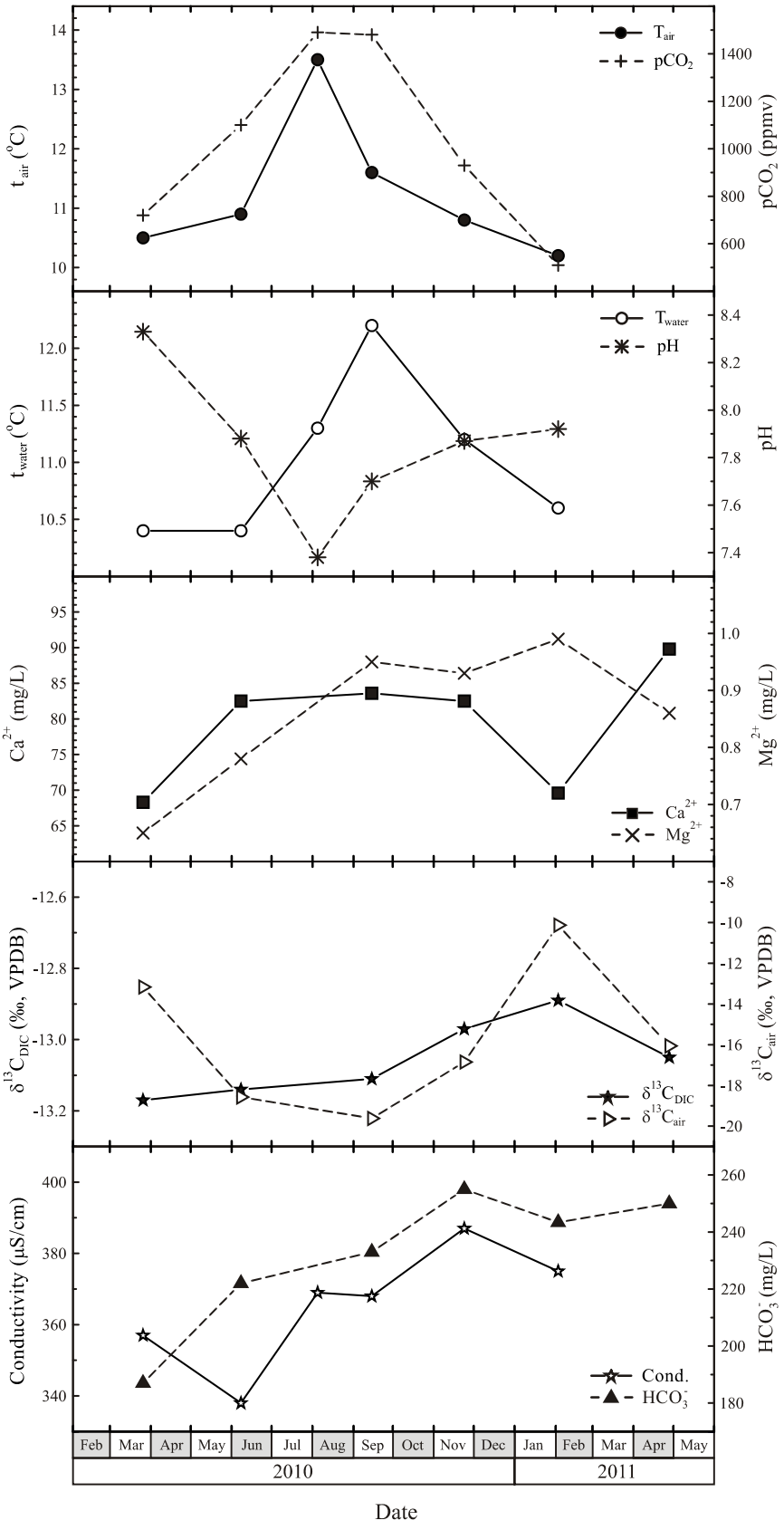

Figure 6.7 *Ibid* (6.1) Location 06 – Stebrišče
Slika 6.7 *Ibid* (6.1) Lokacija 06 – Stebrišče

Conductivity is negatively correlated with bicarbonate concentration (Table A.6). Calcium concentration is found to be negatively correlated with pH, magnesium concentration, and $\delta^{13}C_{air}$. The calcium concentration is significantly positively correlated with pCO_2 and pCO_2(aq). The pH is positively correlated with $\delta^{13}C_{air}$ and I_{sat}, and negatively correlated with pCO_2 and pCO_2(aq). Significant negative correlation is found between magnesium concentration and pCO_2(aq). pCO_2 is negatively correlated with $\delta^{13}C_{air}$ and I_{sat}, and positively correlated with pCO_2(aq). $\delta^{13}C_{air}$ is negatively correlated with pCO_2(aq), and positively correlated with I_{sat}. Significant negative correlation is obtained between pCO_2(aq) and I_{sat}.

Location 08 – Vrh Velike gore

Mean air temperature at location 08 – Vrh Velike gore is 11.6 ± 0.7 ºC, lowest air temperature is measured in March 2010, 11.0 °C and the highest, 13.0 °C, in August 2010. The water temperature 11.9 ± 1.3 ºC ranges from 10.9 °C in March 2010, to 14.3 °C in September 2010. The highest drip rate is measured in November 2011 (500 min^{-1}) and the lowest in September 2010 (4 min^{-1}) (Figure 6.2). The pH (7.8 ± 0.1) value ranges from 7.69 in August 2010 to 8.05 in February 2011. The conductivity values vary from 323 µS/cm to 431 µS/cm for June and November 2010, respectively. Mean conductivity is 369 ± 37 µS/cm. The lowest value for pCO_2 is 600 ppmv in February 2011 and the highest 1670 ppmv in August 2010, with the mean value 1187 ± 470 ppmv. The lowest Ca^{2+} concentration is 78.1 mg/L measured in June 2010 and highest is measured in February 2011, 86.5 mg/L. The lowest concentration for magnesium is 0.37 mg/L in March 2010, and highest value of 0.63 in September 2010. Bicarbonate concentration varies from 187 mg/L in June 2010 to 286.7 mg/L in November 2010. Mean values of magnesium, calcium and bicarbonate concentrations are 0.5 ± 0.1 mg/L, 82 ± 3 mg/L, and 241 ± 33 mg/L, respectively. The $\delta^{13}C_{DIC}$ -12.8 ± 0.4 ‰ ranges from -13.36 ‰ in November 2010 to -12.35 ‰ in February 2011. The $\delta^{13}C$ in air samples is -18 ± 3 ‰. Data are plotted in Figure 6.9.

Conductivity is positively correlated with bicarbonate concentration (Table A.6). Calcium concentration is positively correlated with pH and I_{sat}. pH is found to be negatively correlated with pCO_{2r} and pCO_2(aq), and positively correlated with $\delta^{13}C_{air}$ and I_{sat}. pCO_2 is significantly positively correlated with pCO_2(aq) and negatively correlated with $\delta^{13}C_{air}$. pCO_2(aq) is negatively correlated with $\delta^{13}C_{air}$.

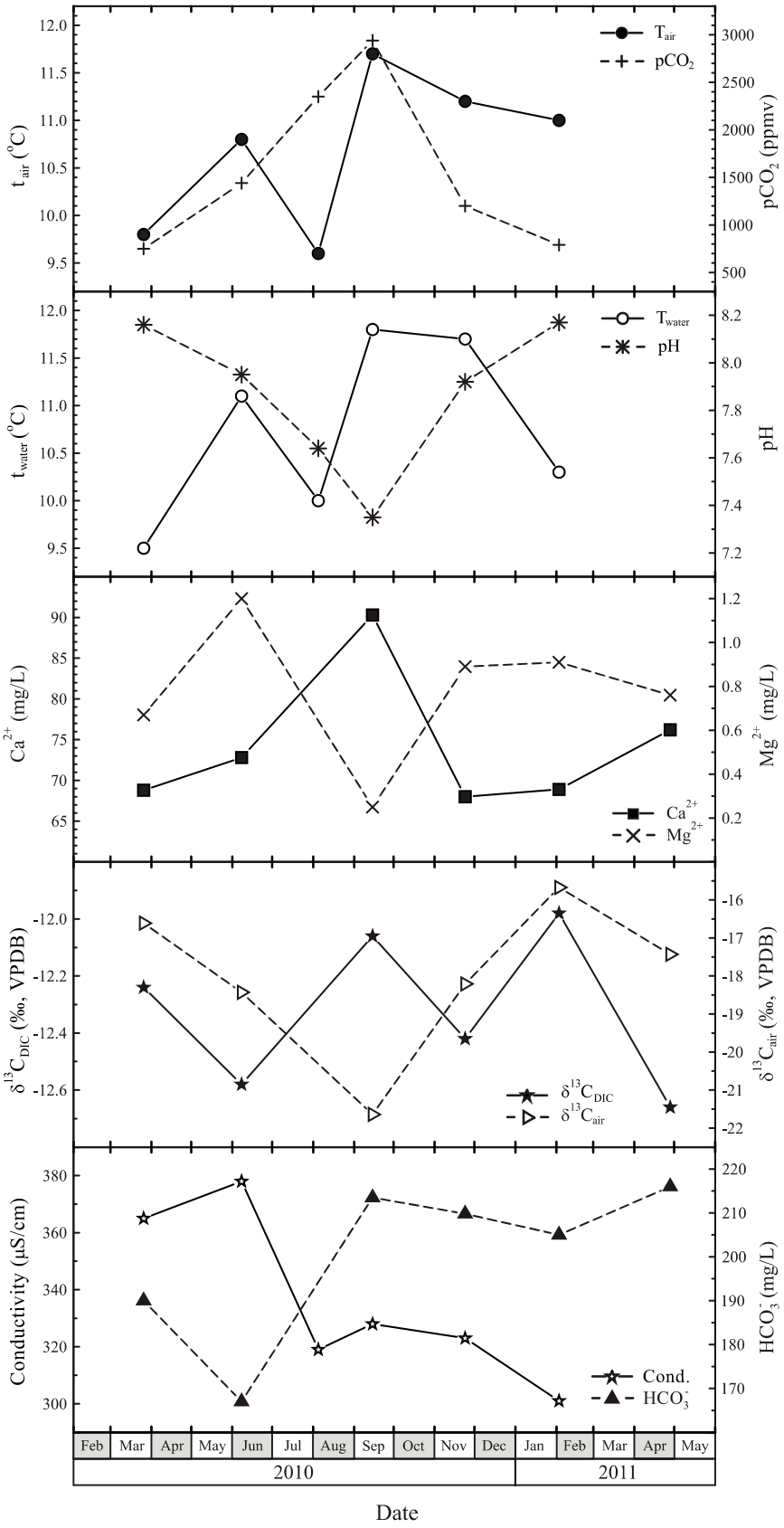

Figure 6.8 *Ibid* (6.1) Location 07 – Čarobni vrt

Slika 6.8 *Ibid* (6.1) Lokacija 07 – Čarobni vrt

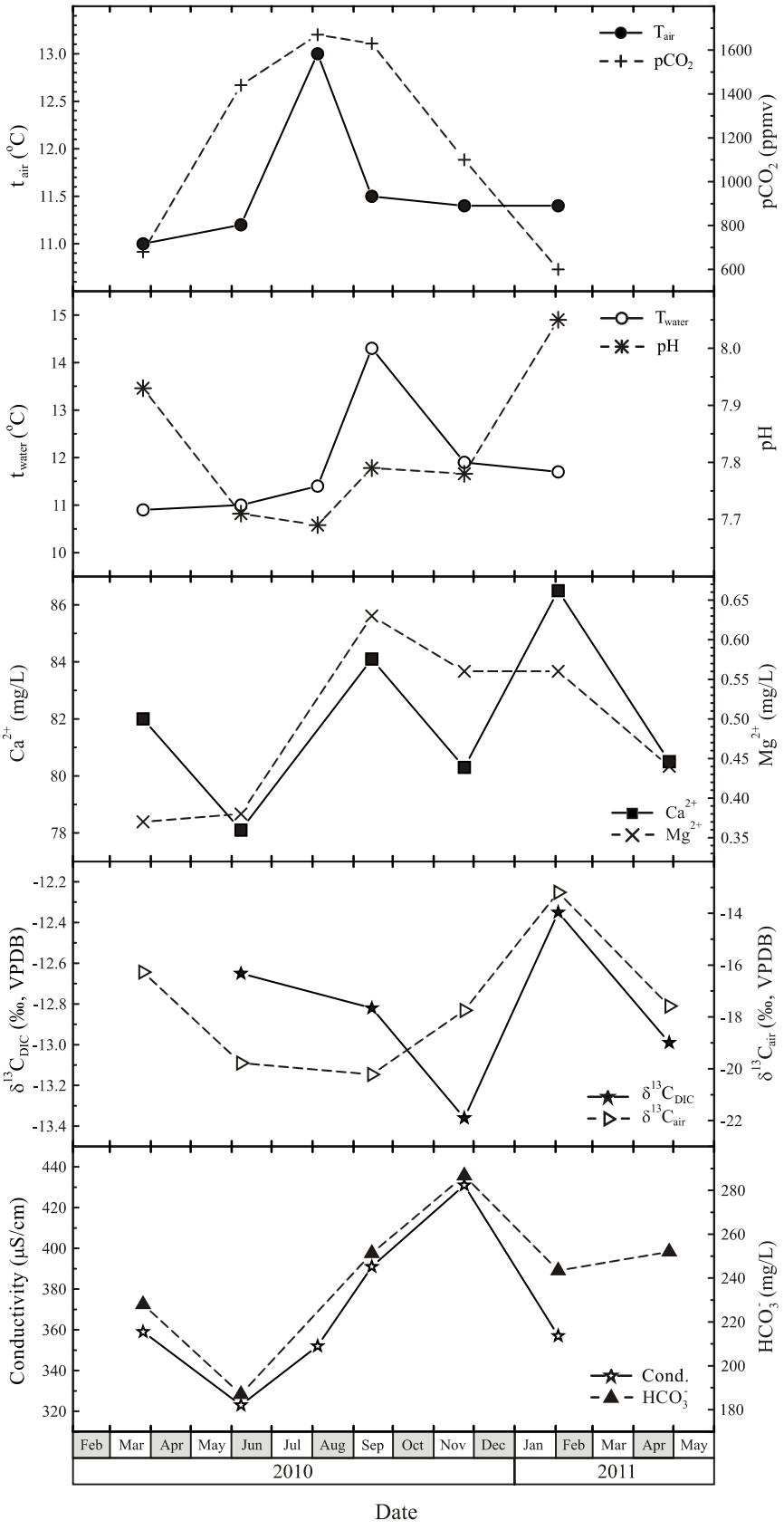

Figure 6.9 *Ibid* (6.1) Location 08 – Vrh Velike gore

Slika 6.9 *Ibid* (6.1) Lokacija 08 – Vrh Velike gore

Location 09 – Zgornji Tartar

Mean air temperature at location 09 – Zgornji Tartar is 10.7 ± 0.9 ºC varying from 9.1 °C in February 2011 to 11.7 °C in August 2010. The lowest water temperature is 9.8 °C in June 2010, and the highest 12.5 °C in September 2010. The mean water temperature is 10.9 ± 1.0 ºC. The drip rate 80 ± 103 min^{-1} varies from 19 to 300 min^{-1} (Figure 6.2). Mean pCO_2 is 937 ± 325 ppmv, and ranges from 480 ppmv in February 2011 to 1260 ppmv in September 2010. The highest conductivity of 389 µS/cm is measured in November 2010 and the lowest 65 µS/cm in August 2010. The pH value ranges from 7.36 in September 2010 to 8.13 in February 2011. Mean values of conductivity, pH, and pCO_2 are 313 ± 123 µS/cm, 7.8 ± 0.3, and 937 ± 325 ppmv, respectively. Minimum magnesium concentration is 0.62 mg/L in March and June 2010 and maximum value is 1.05 mg/L in November 2010. Calcium concentration is lowest in September 2010, 69.0 mg/L, and highest in March 2010, 80.1 mg/L. Lowest HCO_3^- concentration is measured in June 2010, 183 mg/L and highest 255 mg/L in November 2010. Mean values of magnesium, calcium and bicarbonate concentrations are 3.8 ± 0.6 mg/L, 76 ± 4 mg/L, and 215 ± 24 mg/L, respectively. The mean $\delta^{13}C$ values in DIC is -13.01 ± 0.75 ‰ being highest in September 2010 (-11.86 ‰) and lowest in November 2010 (-13.78 ‰). The $\delta^{13}C$ in air (-16.1 ± 3.2 ‰) ranges from -10.04 ‰ in February 2011 to -18.53 ‰ in September 2010. Data are plotted in Figure 6.10.

Conductivity is negatively correlated with $\delta^{13}C_{air}$ (Table A.6). Positive correlation is found between bicarbonate and magnesium concentrations. Negative correlation is found between pH and $pCO_2(aq)$, and positive correlation between pH and I_{sat}. pCO_2 is found to be negatively correlated with $\delta^{13}C_{air}$. Positive correlation is obtained between $\delta^{13}C_{air}$ and I_{sat}. $pCO_2(aq)$ and I_{sat} are negatively correlated.

Location 10 – Pivka River inside

The air temperature 11 ± 4 ºC range from 5.3 °C in February 2011 to 15.7 °C in August 2010, and water temperature 11.7 ± 5.5 ºC varies from 3.8 °C in February 2011 to 17.0 °C in August 2010. Mean pH value is 7.8 ± 0.2, the lowest 7.53 is measured in August 2010, and highest of 8.19 in February 2011. The conductivity 405 ± 59 µS/cm range from 351 µS/cm to 470 µS/cm in August 2010 and February 2011, respectively.The mean pCO_2 is 998 ± 345 ppmv, ranging from 480 ppmv in February 2011 to1250 ppmv in September 2010 (Figure 6.11).

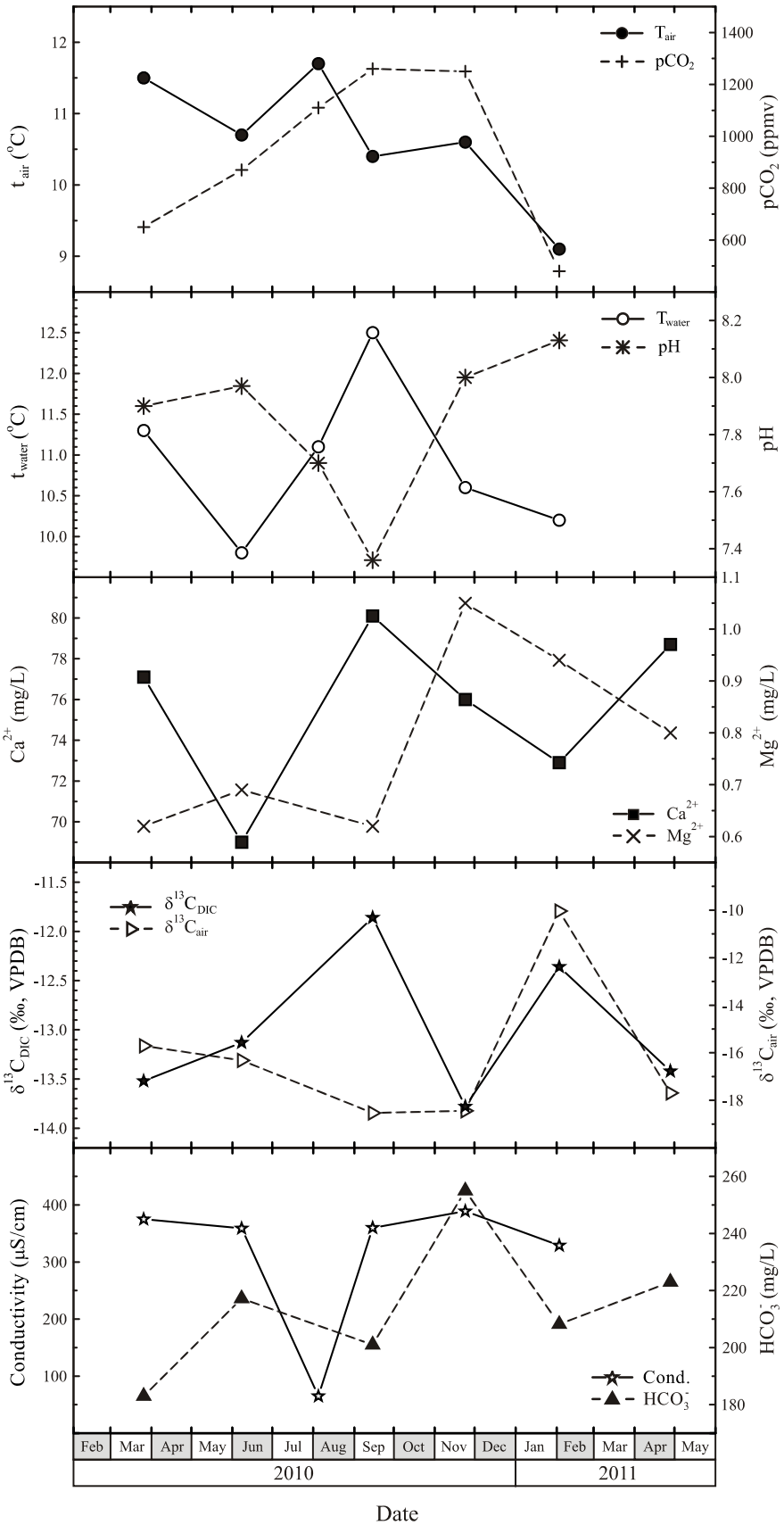

Figure 6.10 *Ibid* (6.1) Location 09 – Zgornji tartar
Slika 6.10 *Ibid* (6.1) Lokacija 09 – Zgornji tartar

The mean magnesium and calcium concentrations are 3.8 ± 0.6 mg/L and 77 ± 12 mg/L, respectively. The lowest Ca^{2+} value is 64.9 mg/L measured in September 2010 and the highest value is 91.8 mg/L measured in February 2011. The lowest concentration of Mg^{2+} is 3.06 mg/L, measured in September 2010, and the highest 4.48 mg/L is measured in February 2011. The mean bicarbonate concentration is 212 ± 35 mg/L and the values range from 179.3 mg/L in September 2010 to 259.4 mg/L in February 2011. The mean $\delta^{13}C_{DIC}$ value is -12.4 ± 2.0 ‰, and it ranges from -14.57 ‰ in September 2010 to -9.75 ‰ in April 2011. The mean value of $\delta^{13}C$ in air is -15 ± 5 ‰ having variations between -8.29 ‰ in February 2011 and -19.26 ‰ in September 2010. Data are plotted in Figure 6.11.

The conductivity is positively correlated with $\delta^{13}C_{DIC}$ and I_{sat}. For bicarbonate concentration, significant positive correlation is found with the pH, the magnesium concentration, and $\delta^{13}C_{air}$, and negative correlation with $pCO_{2,air}$. The pH is positively correlated with $\delta^{13}C_{air}$ and I_{sat}. Magnesium concentration is positively correlated with $\delta^{13}C_{air}$. Significant negative correlation is found between $pCO_{2,air}$ and $\delta^{13}C_{air}$.

Location 11 – Pivka River outside

At location 11 – Pivka River outside air temperature (12.1 ± 9.8ºC) varies from -1.0 °C in February 2011 to 27.0 °C in August 2010. Mean water temperature is 11.2 ± 6.6 ºC, and variations are from 1.3 °C in February 2011 to 18.0 °C in August 2010. pCO_2 has lowest value 350 ppmv in August 2010 and highest 480 ppmv in March 2010 with mean (398 ± 46 ppmv). Mean conductivity is 388 ± 32 µS/cm and the range is from 345 µS/cm, in August 2010 to 434 µS/cm in June 2010. The pH value (7.9 ± 0.4) varies from 7.08 in September 2010 to 8.27 in February 2011. Mg concentration ranges from 2.79 mg/L in June 2010 to 4.68 mg/L in February 2011 with the mean 3.7 ± 0.7 mg/L. Ca^{2+} concentration ranges from 67.2 mg/L in September 2010 to 78.7 mg/L in June 2010 with mean value 72 ± 4 mg/L. Bicarbonate concentration ranges from 197 mg/L in June 2010 to 256.2 mg/L in February 2011 having the mean of 221± 28 mg/L. Mean $\delta^{13}C$ in DIC is -12.4 ± 2.2 ‰ ranging from -8.75 ‰ in April 2011 to -14.39 ‰ in September 2010. Mean $\delta^{13}C$ value in air is (-7.7 ± 3.9 ‰), and varies from -4.35 ‰ in April 2011 to -15.5 ‰ in September 2010. Data are plotted in Figure 6.12.

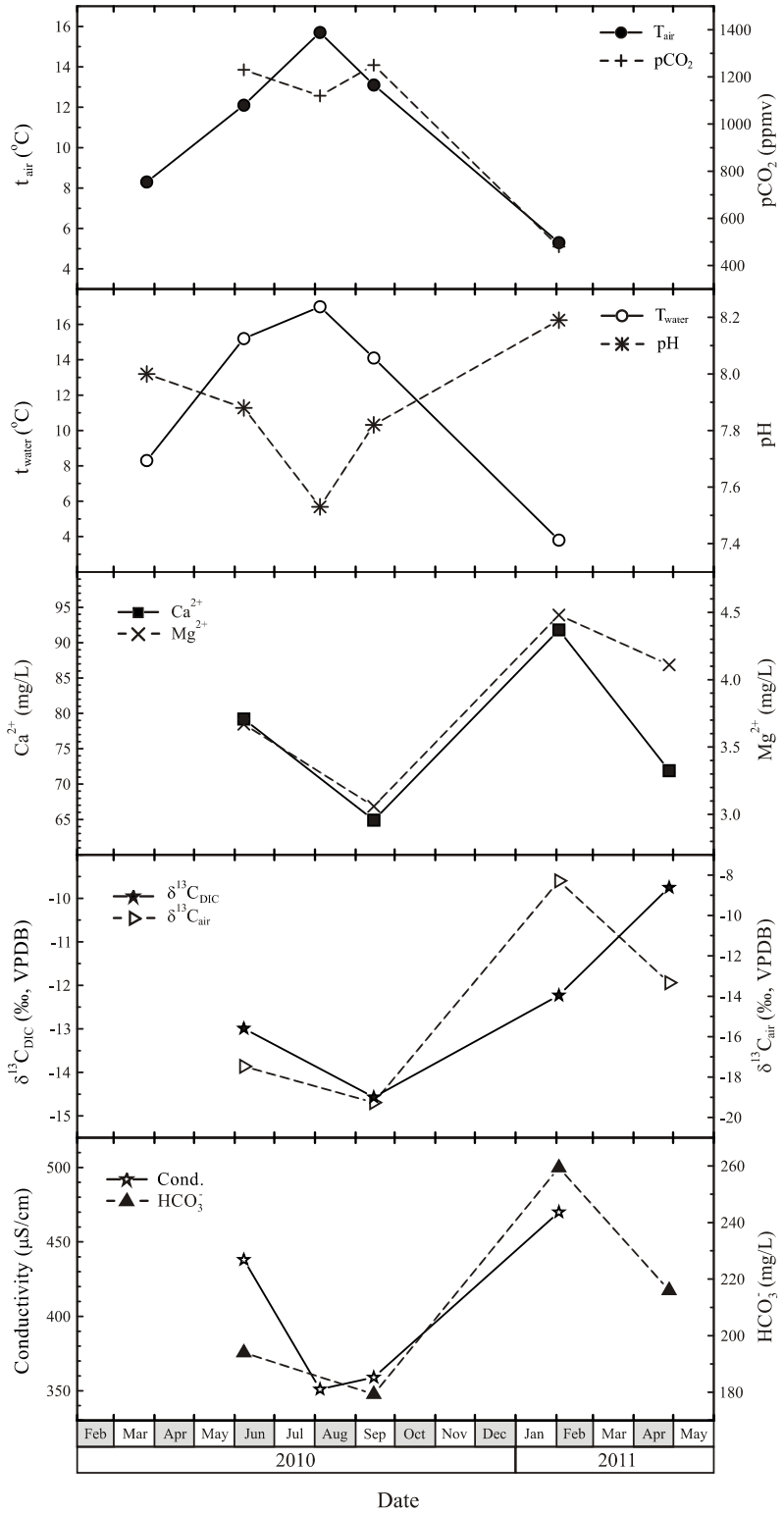

Figure 6.11 At location 10 – Pivka River inside field measured parameters are air temperature, water temperature, pH, conductivity, and pCO_2, chemical parameters are Ca^{2+}, Mg^{2+}, and HCO_3^- concentrations in river water and stable isotope composition $\delta^{13}C_{DIC}$ and $\delta^{13}C_{air}$.

Slika 6.11 Za lokaciju 10 – Rijeka Pivka mjereni parametri su temperatura zraka i riječne vode, pH, vodljivost i pCO_2, kemijski parametri su koncentracije Ca^{2+}, Mg^{2+} i HCO_3^- u riječnoj vodi, te koncentracija stabilnih izotopa u $\delta^{13}C_{DIC}$ i $\delta^{13}C_{air}$.

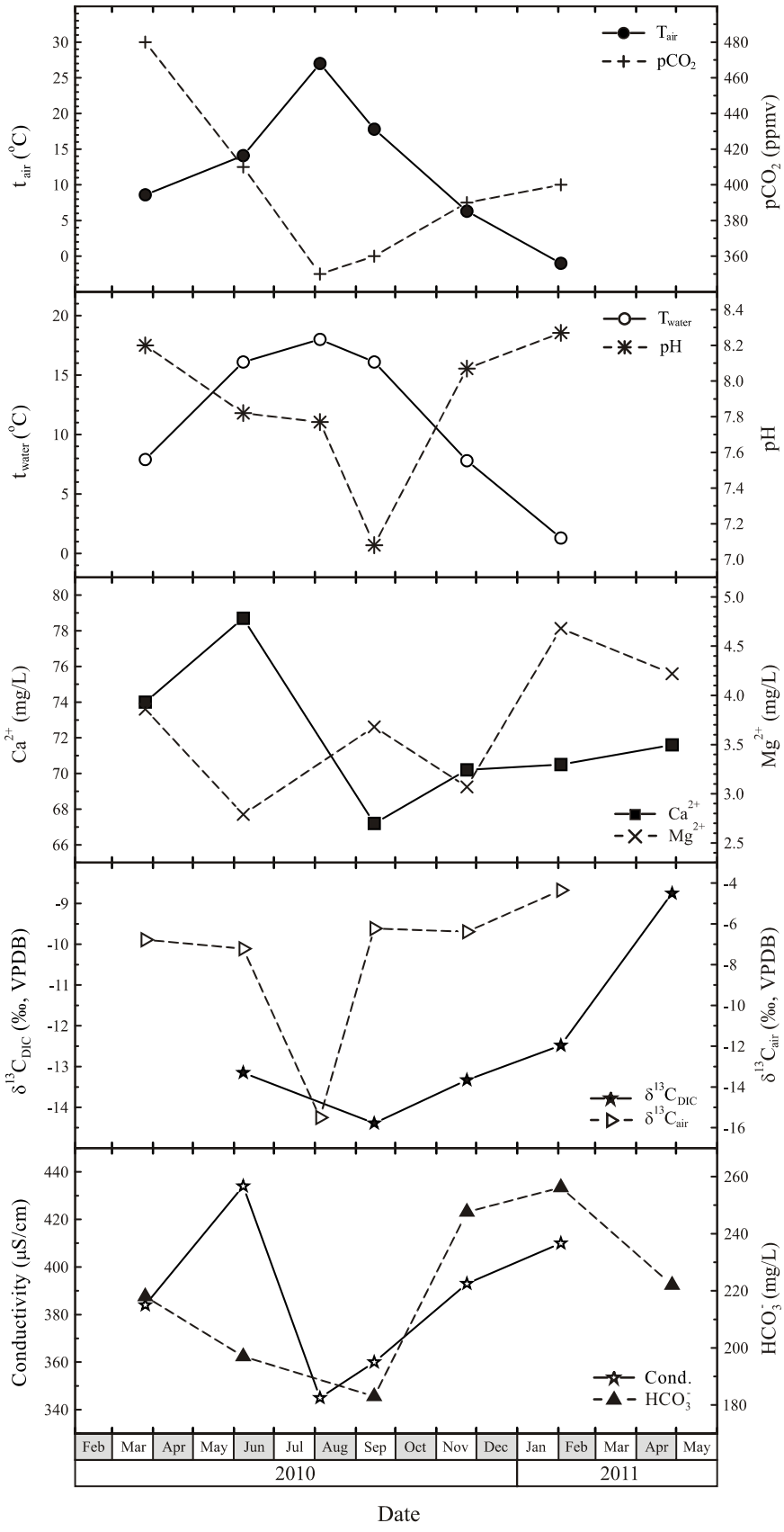

Figure 6.12 *Ibid* (6.11) Location 11 – Pivka River outside
Slika 6.12 *Ibid* (6.11) Lokacija 11 – Pivka River vani

Correlations between parameters for location 11 are the following (Table A.6). Bicarbonate concentration is significantly positively correlated with pH and I_{sat}. pH is positively correlated with $\delta^{13}C_{DIC}$ and I_{sat}, but also negatively correlated with pCO_2(aq). Magnesium concentration is positively correlated with $\delta^{13}C_{air}$. $\delta^{13}C_{DIC}$ is positively correlated with I_{sat}, and negatively with pCO_2(aq). pCO_2 is positively correlated with I_{sat}. Significant negative correlation is found between pCO_2(aq) and I_{sat}.

6.1.1 Piper digram

Chemical composition of drip and river water samples from Postojna Cave is shown in the Piper diagram (Figure 6.13). Here are included also concentrations of minor ions (Table A.4), that were measured twice during the sampling period. The Piper diagram identifies geologically and chemically similar waters, and defines the evolution in water chemistry along the flow path. With the piper diagram one can distinguish waters according to their geochemistry (Trudgill and Inkepen, 1993). The drip waters are clearly distinguished from the Pivka River water, Figure 6.13. All drip waters, (Figure 6.13 in red squares), have similar chemical properties because of the same geologic origin and belong to the Ca-HCO_3 type of waters. Samples from Pivka River, (Figure 6.13 in blue squares), have different origin and flow path and therefore different chemical composition – they have non-negligible concentration of Mg and other minor ions.

6.2 Precipitation

Precipitation is collected as described in Chapter 5.3.2. In integrated monthly precipitation samples concentration of $\delta^{18}O_p$ has been determined (Figure 6.14). The most negative value is -9.24 ‰ in December 2010 and the most positive value is determined in September 2010, -5.86 ‰. Calculated mean value is -7.40 ± 1.34 ‰, but this value cannot be taken as a representative value of mean annual $\delta^{18}O$ in precipitation since only data for 5 months are available. Therefore another data have been used for further discussion in chapter 7.3.

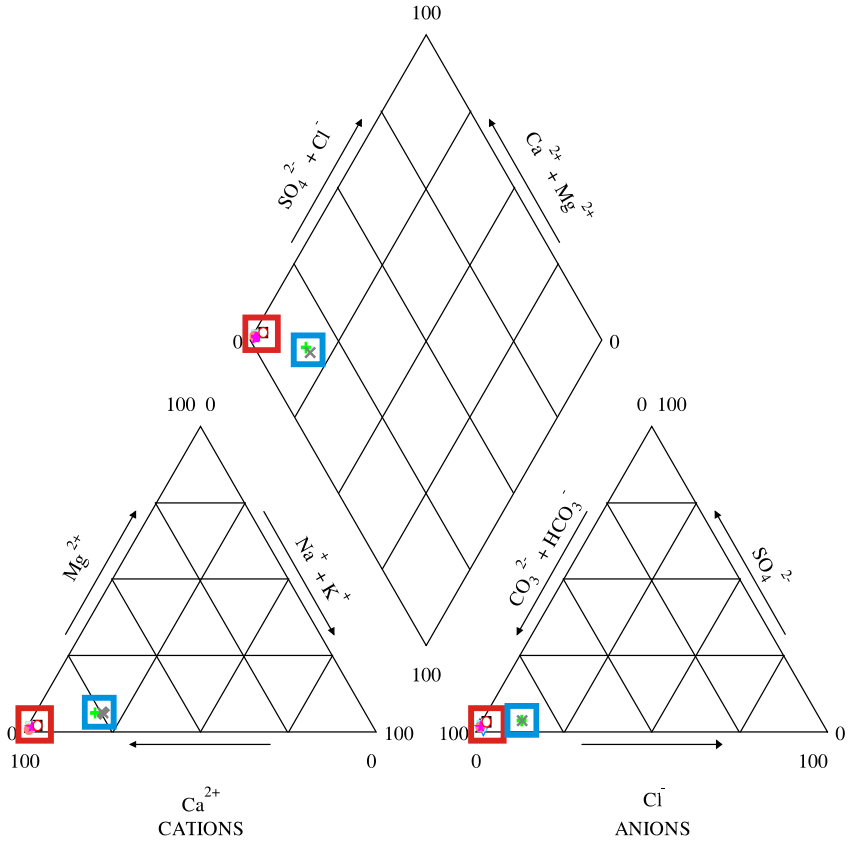

Figure 6.13 Piper diagram for sampled drip waters (in red squares) in Postojna Cave and Pivka River (in blue squares).

Slika 6.13 Piperov dijagram za prokapnu vodu (crveni kvadrati) i rijeku Pivku (plavi kvadrati)

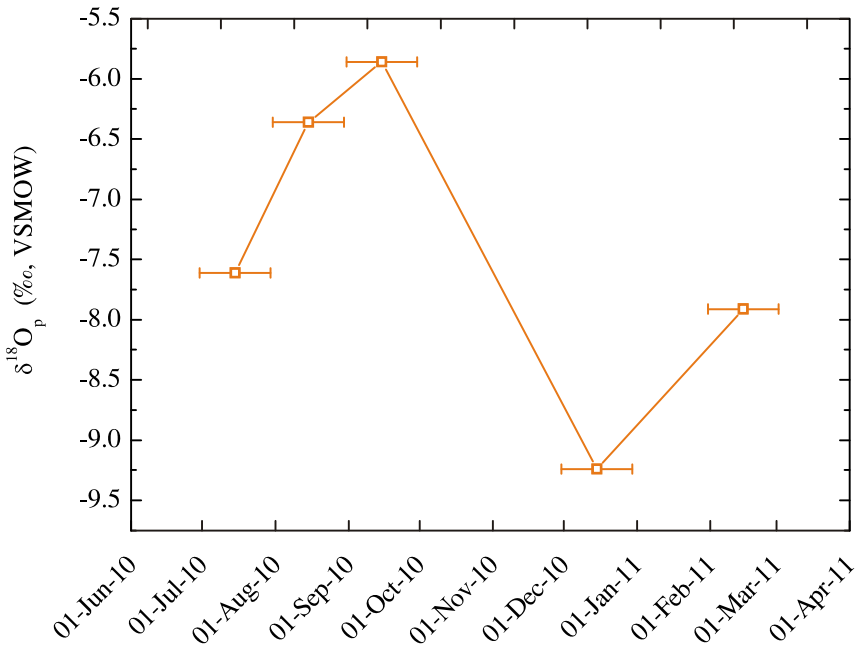

Figure 6.14 $\delta^{18}O$ in precipitation at Postojna in the period July 2010 – March 2011.

Slika 6.14 $\delta^{18}O$ u oborinama za Postojnu u razdoblju od srpnja 2010. do ožujka 2011.

6.3 Carbonates

Figure 6.15 summarizes $\delta^{13}C$ and $\delta^{18}O$ values of modern carbonates precipitated on watch glasses, described in section 5.3.1, and of "soda straws" from various locations.

The values of $\delta^{13}C$ for "soda straws" vary from -7.84 ‰ at location 01 – Slonova glava to -10.58 ‰ at location 03 – Vodopad (with an exceptionally high value -3.94 ‰ at location 02 – Biospeleološka postaja, sample 2-1). The highest value for $\delta^{18}O$ is at location 01 – Slonova glava (-4.84 ‰) and the lowest at location 06 – Stebrišče (-7.84 ‰).

$\delta^{13}C$ values of carbonates precipitated on watch glasses range from -9.95 ‰ at location 05 – Podrti kapnik to -12.37 ‰ at location 01 – Slonova glava, while their $\delta^{18}O$ values range from -3.07 ‰ (01 – Slonova glava) to –4.84 ‰ (04 – Kongresna dvorana). The $\delta^{18}O$ values of carbonates on watch glasses differ from $\delta^{18}O$ of drip water and are more positive/less negative than $\delta^{18}O$ of "soda straws" (Figure 6.15).

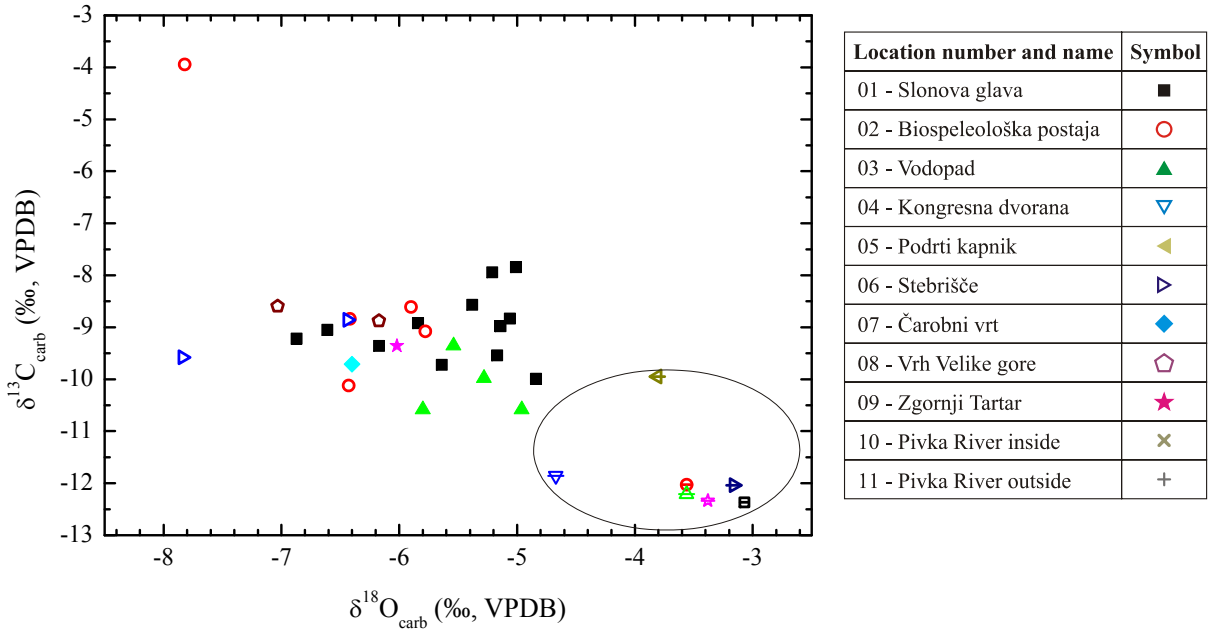

Figure 6.15 The $\delta^{13}C$ and the $\delta^{18}O$ in modern carbonates ("soda straws" and carbonate precipitated on watch glasses). Circle encompasses data of carbonates precipitated on watch glasses. Symbols referring to sampling locations have a stripe across.

Slika 6.15 $\delta^{13}C$ i $\delta^{18}O$ u modernim karbonatima (slamčicama i karbonatu taloženom na satnim staklima). Krug naglašava podatke za uzorke taložene na satnim staklima. Simboli za te uzorke su iste boje i oblika kao oni na prethodnim slikama, a radi lakšeg razlikovanja preko njih je povučena crta.

Distinctive difference in delta values between "soda straws" and carbonate precipitated on watch glass is observed. $\delta^{13}C_{WG}$ values of carbonates precipitated on watch glasses are lower by several permills than those of "soda straws" and are close to the corresponding $\delta^{13}C_{DIC}$ values (≈-12 to -13 ‰, Table A.5 in Appendix I), as shown in Figure 6.16. The $\delta^{13}C$ of DIC and carbonates precipitated on watch glasses at location 05 – Podrti kapnik, -9.90‰ and -9.95‰, respectively, differ significantly from the corresponding data at other locations (Figure 6.16). The special case of Podrti kapnik will be discussed in section 7.6.

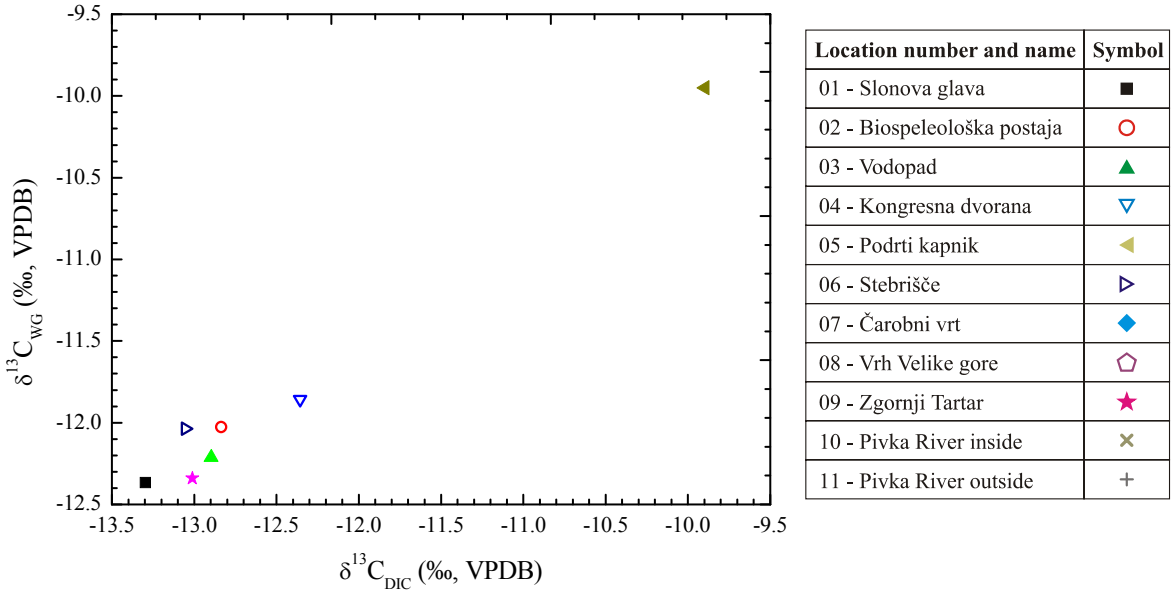

Figure 6.16 $\delta^{13}C$ isotopic composition of carbonates on watch glasses vs. $\delta^{13}C_{DIC}$.

Slika 6.16 Izotopni sastav karbonata taloženog na satnim staklima u ovisnosti o izotopnom sastavu $\delta^{13}C$ DIC-a.

The $\delta^{13}C$ and $\delta^{18}O$ composition of the two "peculiar" types of speleothems described in Section 5.3.1 is shown in Figure 6.17. It is obvious that they form two distinct groups and that the difference is more pronounced in their $\delta^{18}O$ values. At location 01 – Slonova glava the $\delta^{18}O$ values range from -4.39 to -3.39 ‰ and at location 09 – Zgornji Tartar from -7.09 to -6.53 ‰. The $\delta^{13}C$ values vary from -5.23 to -4.27 ‰ at location 01 – Slonova glava and from -7.50 to -5.52 ‰ at location 09.

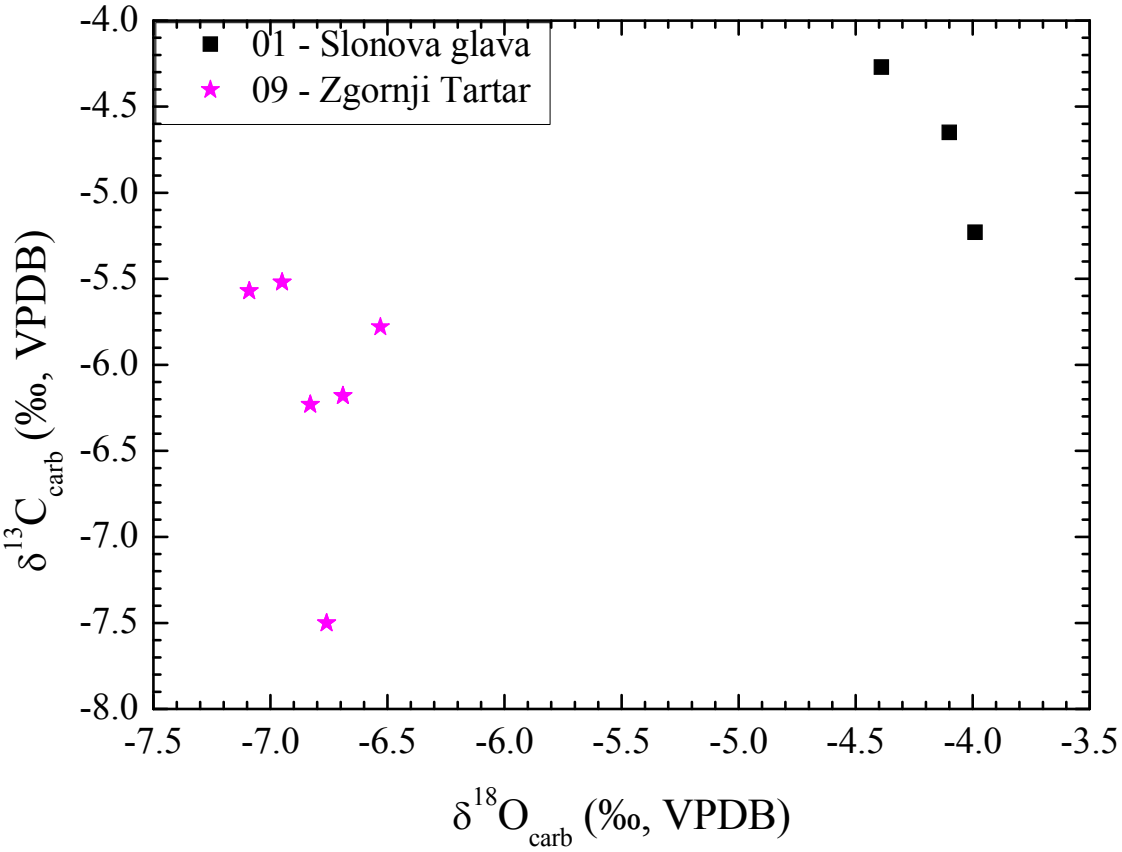

Figure 6.17 $\delta^{13}C$ and $\delta^{18}O$ values of "peculiar" type of growth speleothems from locations 01 – Slonova glava and 09 – Zgornji Tartar

Slika 6.17 $\delta^{13}C$ i $\delta^{18}O$ vrijednosti za karbonatne uzorke specifičnog oblika s lokacija 01 – Slonova glava i 09 – Zgornji Tartar

The $\delta^{13}C$ and $\delta^{18}O$ values of flowstones (Figure 6.18) range from -7.95 ‰ to -0.78 ‰ and from -6.66 ‰ to -3.38 ‰, respectively. Carbonate $\delta^{13}C$ at location 04 – Kongresna dvorana varies from -6.99 to -0.78 ‰ and $\delta^{18}O$ from -6.66 ‰ to -4.21‰. At location 05 – Podrti kapnik $\delta^{13}C$ ranges from -7.95 ‰ to -3.97 ‰ and $\delta^{18}O$ from -6.35 to -4.60 ‰. At location 06 – Stebrišče $\delta^{18}O$ ranges from -6.01 ‰ to -3.38‰ and $\delta^{13}C$ from -6.25 ‰ to -2.02 ‰. It can be noticed that $\delta^{18}O$ values of carbonate samples at location 05 – Podrti kapnik have smallest variation.

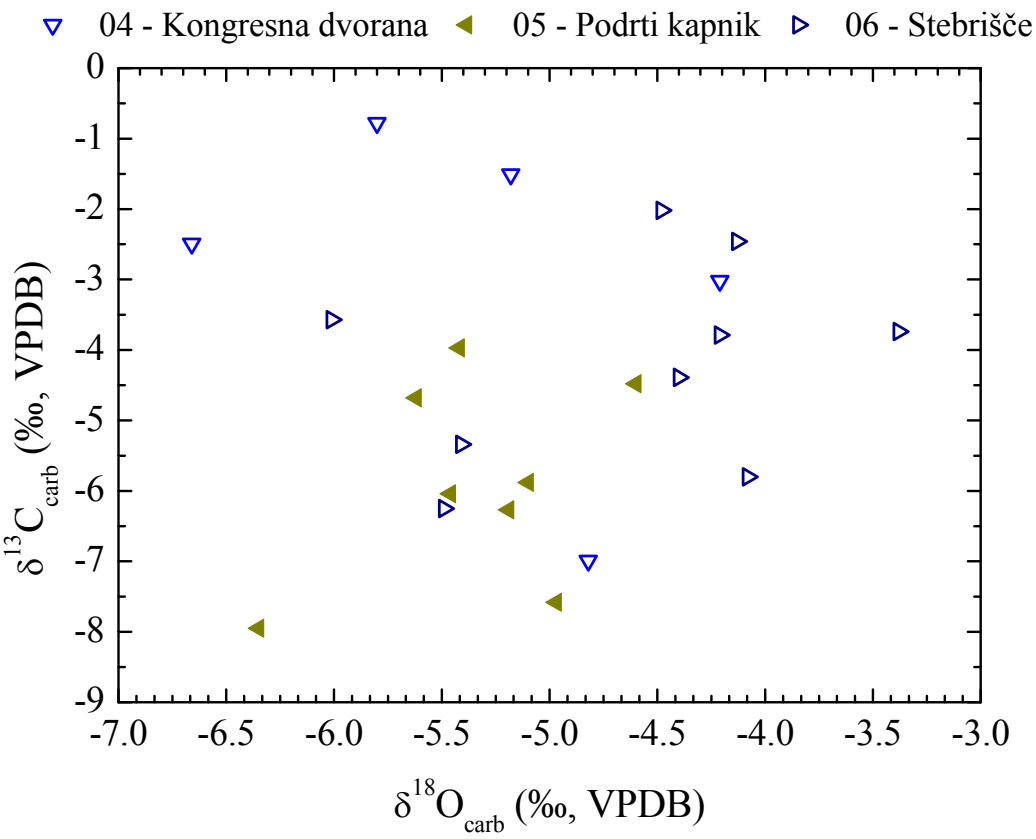

Figure 6.18 The $\delta^{13}C$ and $\delta^{18}O$ values of flowstones from locations 04 – Kongresna dvorana, 05 – Podrti kapnik and 06 – Stebrišče.

Slika 6.18. $\delta^{13}C$ i $\delta^{18}O$ vrijednosti sigovine sa lokacija 04 – Kongresna dvorana, 05 – Podrti kapnik i 06 – Stebrišče.

The $\delta^{13}C$ values of stalactites range from -9.91 to -1.15 ‰, and $\delta^{18}O$ from -10.35 to -4.09 ‰ (Figure 6.19). It can be noticed that the $\delta^{18}O$ value of -10.35 ‰ is an extremely negative value. If this point is omitted, the values for $\delta^{18}O$ range from -6.39 to -4.09 ‰. At location 02 – Biospeleološka postaja the $\delta^{13}C$ values range from -7.33 to -3.65 ‰, and the $\delta^{18}O$ values from -10.35 to -4.97 ‰. Stalactite $\delta^{18}O$ values at location 02 – Biospeleološka postaja are more negative than those from locations 04 – Kongresna dvorana and 09 – Zgornji Tartar. Values for $\delta^{18}O$ at locations 04 range from -5.52 to -4.23 ‰ and at location 09 from -5.16 to -4.09 ‰. $\delta^{13}C$ values at location 04 – Kongresna dvorana range from -5.36 to -1.15 ‰ and at location 09 – Zgornji Tartar from -9.91 to -1.52 ‰. The largest difference in $\delta^{13}C$ values is at location 09 – Zgornji Tartar 8.39 ‰ and for $\delta^{18}O$ 5.38 ‰ at location 02 – Biospeleološka postaja.

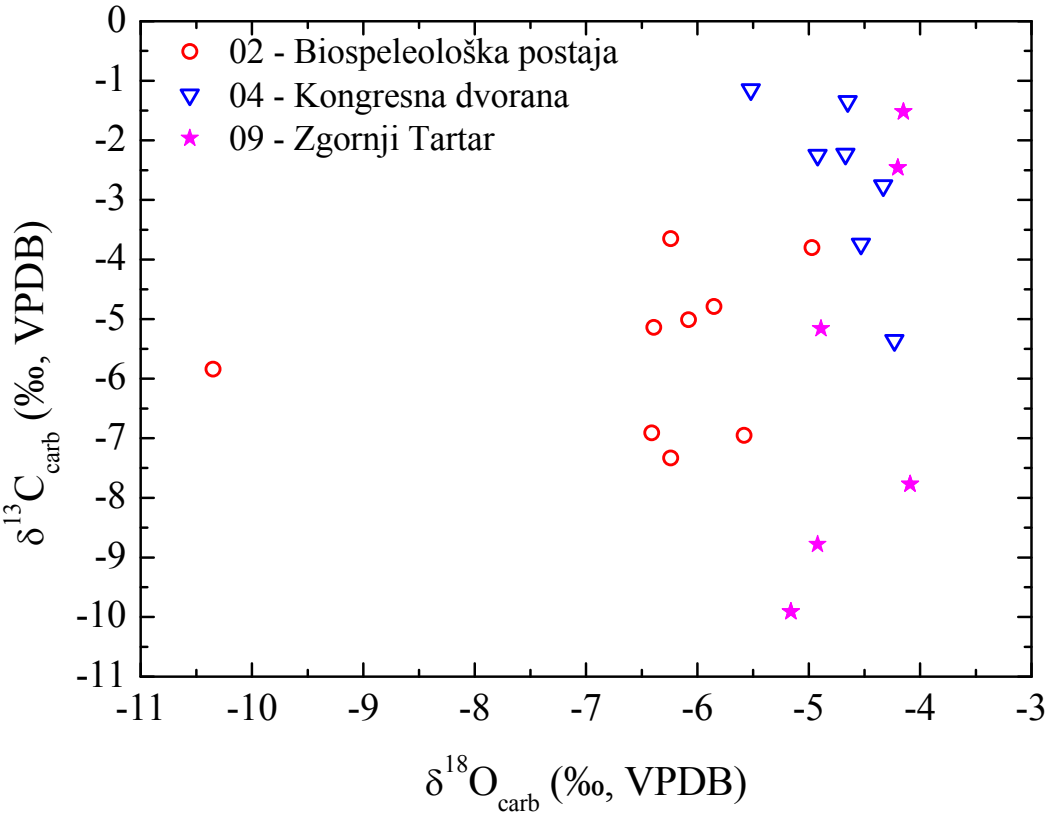

Figure 6.19 Stalactite $\delta^{13}C$ and $\delta^{18}O$ values from locations 02 – Biospeleološka postaja, 04 – Kongresna dvorana and 09 – Zgornji Tartar.

Slika 6.19 $\delta^{13}C$ and $\delta^{18}O$ vrijednosti za uzorke stalaktita s lokacija 02 – Biospeleološka postaja, 04 – Kongresna dvorana i 09 – Zgornji Tartar.

The $\delta^{13}C$ and $\delta^{18}O$ analyses have been performed on samples taken from drilled cores of speleothem from location Peron (~100 m from sampling location 06 – Stebrišče), location 07 – Čarobni vrt, and 08 – Vrh Velike gore (Section 5.3). For all locations values of $\delta^{13}C$ vary from -9.67 to -1.65 ‰, and for $\delta^{18}O$ from -12.11 to -3.59 ‰ (Figure 6.20). Majority of $\delta^{18}O$ values is in the interval -7.35 to -3.59 ‰. Three points with most negative values (-12.11, -8.76 and -8.86 ‰) belong to the core from location 06 Stebrišče, where $\delta^{18}O$ range from -12.11 to -4.34 ‰. At locations 07 – Čarobni vrt and 08 – Vrh Velike gore $\delta^{18}O$ values range from -6.91 to -3.77 ‰ and from -6.60 to -3.59 ‰, respectively. The values of $\delta^{13}C$ at location 06 – Stebrišče range from -8.55 to -1.65 ‰, at location 07 – Čarobni vrt from -9.67 to -4.54 ‰ and at location 08 – Vrh Velike gore from -9.56 to -1.79 ‰. From Figure 6.20 it can be noticed that values from $\delta^{18}O$ of locations 07 – Čarobni vrt and 08 – Vrh Velike gore overlap and that most of values measured from sample 06 – Stebrišče constitute another group with lower $\delta^{18}O$ values.

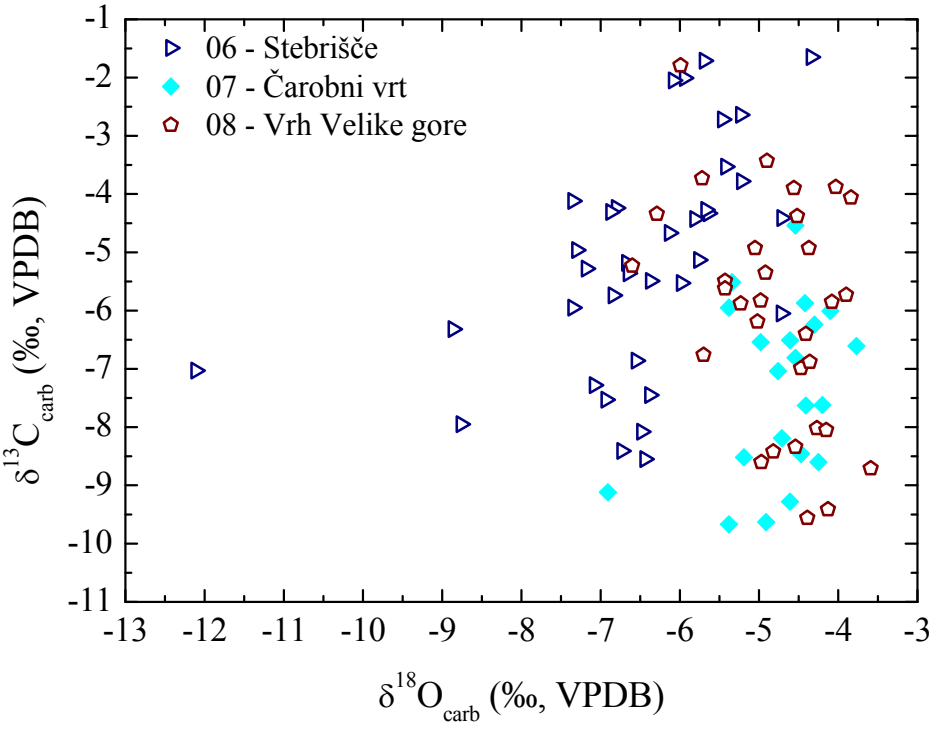

Figure 6.20 Speleothems drilled core $\delta^{13}C$ and $\delta^{18}O$ values from locations 06 – Stebrišče, 07 – Čarobni vrt and 08 – Vrh Velike gore.

Slika 6.20 $\delta^{13}C$ i $\delta^{18}O$ vrijednosti bušenih uzoraka s lokacija 06 – Stebrišče, 07 – Čarobni vrt i 08 – Vrh Velike gore.

All $\delta^{13}C$ and $\delta^{18}O$ values of carbonate samples are summarized in Figures 6.21 and 6.22, respectively. Only the results for "perculiar growth" type of samples are not presented (compare Figure 6.17).

Old speleothem groups in Figure 6.21and 6.22 encompasses data for old stalactites, flowstones and stalagmites (drilled cores). The ranges of both $\delta^{13}C$ and $\delta^{18}O$ of old speleothems are wider than those of recent/modern carbonates, i.e. from -0.78 to -7.95 ‰ and from -4.21 to -10.35 ‰, respectively.

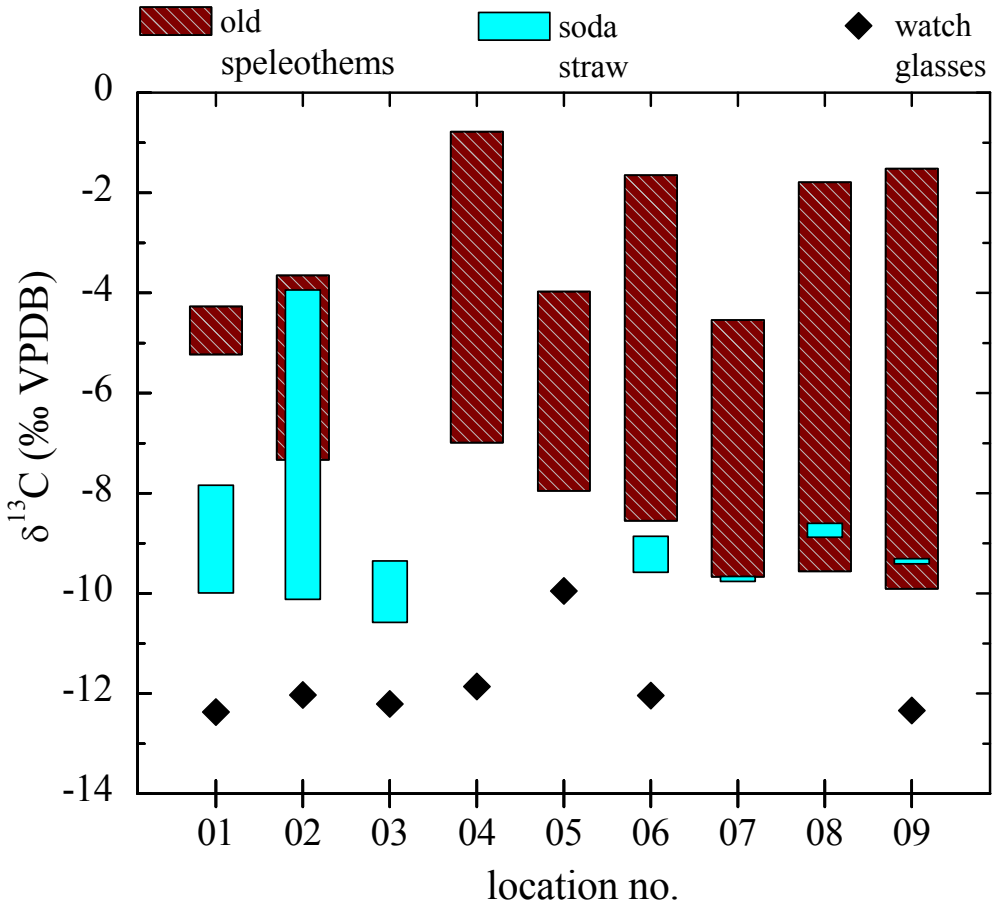

Figure 6.21 Measured $\delta^{13}C$ in various types of carbonates.

Slika 6.21 $\delta^{13}C$ u različitim uzorcima karbonata s lokacija u Postojnskoj jami.

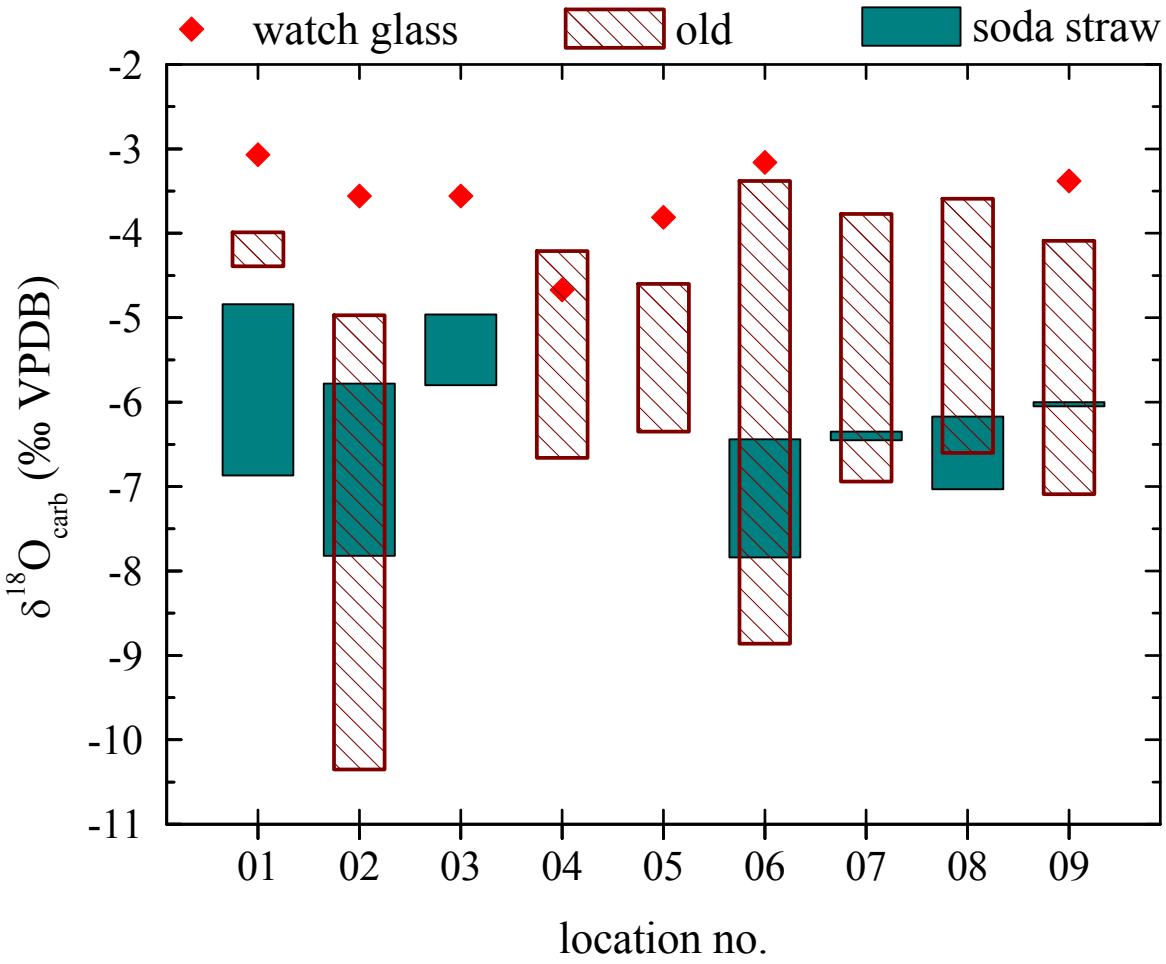

Figure 6.22 Measured $\delta^{18}O$ in various types of carbonates.

Slika 6.22 Mjerene koncentracije $\delta^{18}O$ u različitim uzorcima karbonata.

7 DISCUSSION

7.1 Figure description

Because of the diversity and large number of data to be presented in various types of figures, for reading simplification and better understanding, all parameters for a specific location are presented by the same symbol and color chacteristic for this location, as summarized in Table 7.1. If there is a need for introduction of additional colors and/or symbols for presentation of data of other authors or from various sources, figure captions contain additional explanations.

Table 7.1 Symbol and color used in the following figures for representing data from a specific location.

Tablica 7.1 Simboli i boje koji se koriste u sljedećim grafovima predstavljaju podatke s određene lokacije.

Location number and name	Symbol	Color
01 - Slonova glava	■	
02 - Biospeleološka postaja	○	
03 - Vodopad	▲	
04 - Kongresna dvorana	▽	
05 - Podrti kapnik	◀	
06 - Stebrišče	▷	
07 - Čarobni vrt	◆	
08 - Vrh Velike gore	⬠	
09 - Zgornji Tartar	★	
10 - Pivka River inside	×	
11 - Pivka River outside	+	

Figures presenting and comparing time series of various parameters at all locations contain two graphs. The left one shows different parameters in form of a time series. The right graph presents basic descriptive statistics of measured parameters for individual location. Basic statistical parameters are presented in form of box-plots (whisker plots). For each location

box-plot will maintain recognizable shape color from Table 7.1. Construction of the box-plot is given in Figure 7.1. Box-plot describes basic descriptive statistical parameters. The uppermost and lowermost sides of the box-plot mark maximum and minimum values, respectively. Rectangle in the middle shows second (Q_2) and third (Q_3) quartile, i.e., the lower one starts at 25% and the upper one ends at 75% of probability of occurrence of all data. They are separated by the line representing the median value (50% probability of occurrence). In the case where odd number of values is measured, median is exactly the value in the middle. Otherwise (even number of data in a series), median is defined as mean value of two central measured values, in data set sorted by magnitudes. Symbol (□) in the rectangle represents the mean value ($\bar{x}$) calculated as $\bar{x} = \frac{1}{n}\sum_{i=1}^{n} x_i$.

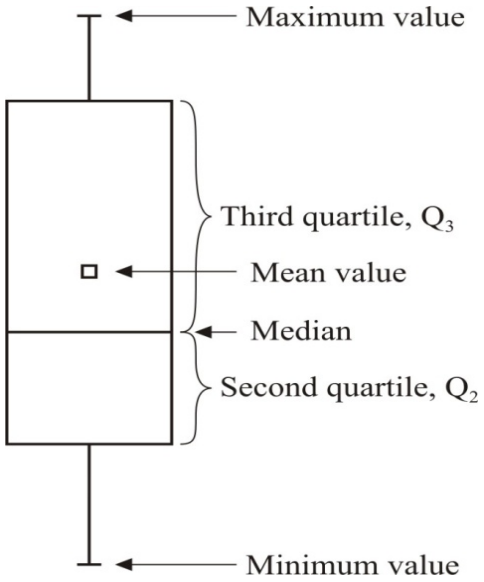

Figure 7.1 Box-plot representation of basic statistical parameters.
Slika 7.1 Pravokutni dijagram (box-plot) reprezentacija osnovnih statističkih parametara.

7.2 **Temperature**

Air temperature measured at sampling locations in the Postojna Cave, together with mean monthly air temperature for Postojna city from National Meteorological Service of Slovenia (meteo.si) are shown in Figure 7.2. Mean outside temperature from National Meteorological Service of Slovenia (meteo.si) is 9.35 ^{o}C during the sampling period. Mean temperatures in the cave show variations from 9.7 ^{o}C at location 03 – Vodopad to 11.58 ^{o}C at location 08 – Vrh Velike gore. Locations deep in the cave show smaller deviations from mean value, while locations placed closer to the entrance show larger variations, because of larger influence of

outside air temperature. Mean air temperature at location 03 – Vodopad is the lowest (9.7 ± 1.6 °C) of all temperatures even though locations 01 – Slonova glava and 02 – Biospeleološka postaja are closer to the entrance. We assume that lowest temperature at this location is due to the tourist train passage. The train is passing through this location twice, firstly when entering the cave and secondly on its way out. Through location 01 – Slonova glava the train is passing only once i.e. on his way out of the cave. Location 02 – Biospeleološka postaja is isolated from the railway.

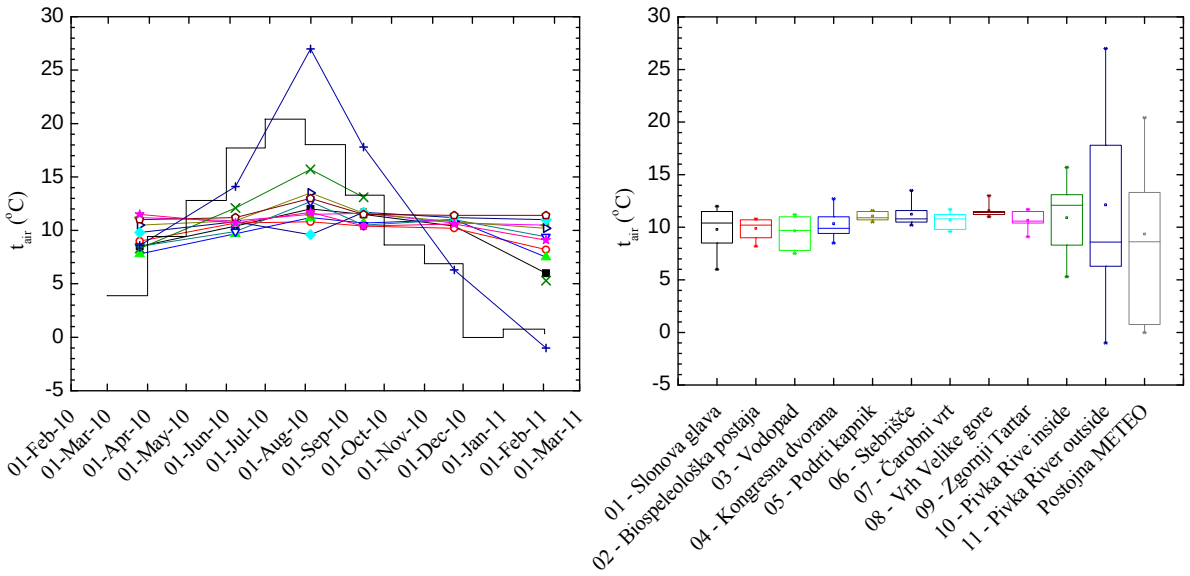

Figure 7.2 Air temperatures on sampling locations in Postojna cave, together with data from Slovenian meteorological survey for Postojna during sampling period from March 2010 to March 2011. Symbols and colors as defined in Table 7.1. Mean monthly temperatures for Postojna are calculated from daily temperatures from National Meteorological Service of Slovenia (meteo.si)

Slika 7.2. Temperatura zraka mjerena unutar postojnske jame, s podacima Slovenskog meteorološkog zavoda za Postojnu u period od ožujka 2010 do svibnja 2011. Simboli i boje definirani su u tabeli 7.1. Srednje vrijednosti temperature zraka za Postojnu računate su iz dnevnih temperatura državne meteorološke službe Republike Slovenije (meteo.si).

Location 04 – Kongresna dvorana with temperature of 10.3 ± 1.4 °C and location 05 – Podrti kapnik with temperature 11.1 ± 0.4 °C are locations within the cave but not isolated from the air circulation. Location 08 – Vrh Velike gore with highest mean temperature of 11.6 ± 0.7 °C is also the location with highest altitude (559 m a.s.l.). The temperature at location 09 – Zgornji Tartar (10.7 ± 0.9 °C) may be influenced by nearby location 10 – Pivka River inside (10.9 ± 4.1 °C).

Variations in temperatures at location 10 – Pivka River inside can be explained by variation in outside air temperature which has the strong influence on temperature of the Pivka River.

The temperature measured at location 11 – Pivka River outside (12.1 ± 9.8 ^{o}C) shows larger values than monthly averaged temperature of Slovenian meteorological survey because the measured temperature is "instant" temperature measured at the time of sampling, in particular time of the day, 6 times the sampling period. The average monthly temperature of Slovenian Meteo Survey (National Meteorological Service of Slovenia (meteo.si) is measured according to protocols of WMO (World Meteorological Organization): tree times in a day, at 7, 14 and 21 hours. Then, mean daily temperature is calculated. With all daily averages mean monthly temperature is calculated.

Mean air temperature of the Postojna cave measured on nine locations (01 - 09) within the Postojna Cave locations involved in study during period from March 2010 to February 2011 is 10.7 ^{o}C and mean monthly outside air temperature for period of 6 years (2006 - 2011) is 9.9 ^{o}C. It can be concluded that the mean temperature within the cave reflects average yearly temperature of outside air with difference between these two values of 0.8 ^{o}C. The location 10 – Pivka River inside is omitted from calculation of mean air temperature because of differences in environmental conditions which are incomparable to the other observed locations in the Cave.

The temperature of drip water shows smaller variation than water of the Pivka River (Figure 7.3). The locations close to the entrance of the cave 01 – Slonova glava, 02 – Biospeleološka postaja and 03 – Vodopad, show larger deviation in temperatures (around 2 ^{o}C), than inner locations (around 1 ^{o}C) (Figures 7.3 and 7.4). The mean water temperature at locations close to the exit is 9.7 ± 0.5 ^{o}C and for inner location mean water temperature is 10.4 ± 0.8 ^{o}C. This temperature reflects mean air temperature for all sampling locations, with exception of both locations of Pivka River, in period from March 2010 to February 2011, (10.5 ± 0.7 ^{o}C).

At the entrance of the cave mean drip water temperatures are 9.3 ± 1.9 ^{o}C at location 01 – Slonova glava, 10.3 ± 1.6 ^{o}C at location 02 – Biospeleološka postaja and 9.6 ± 1.6 ^{o}C at location 03 – Vodopad. Because of the cave entrance vicinity this differences in water temperatures are attributed to the seasonal temperature changes of air temperature, classified like heterothermic zone (Luetscher and Jeannin, 2004). The mean drip water temperature at Location 08 – Vrh Velike gore is the highest 11.9 ±1.3 ºC of all study locations within the cave.

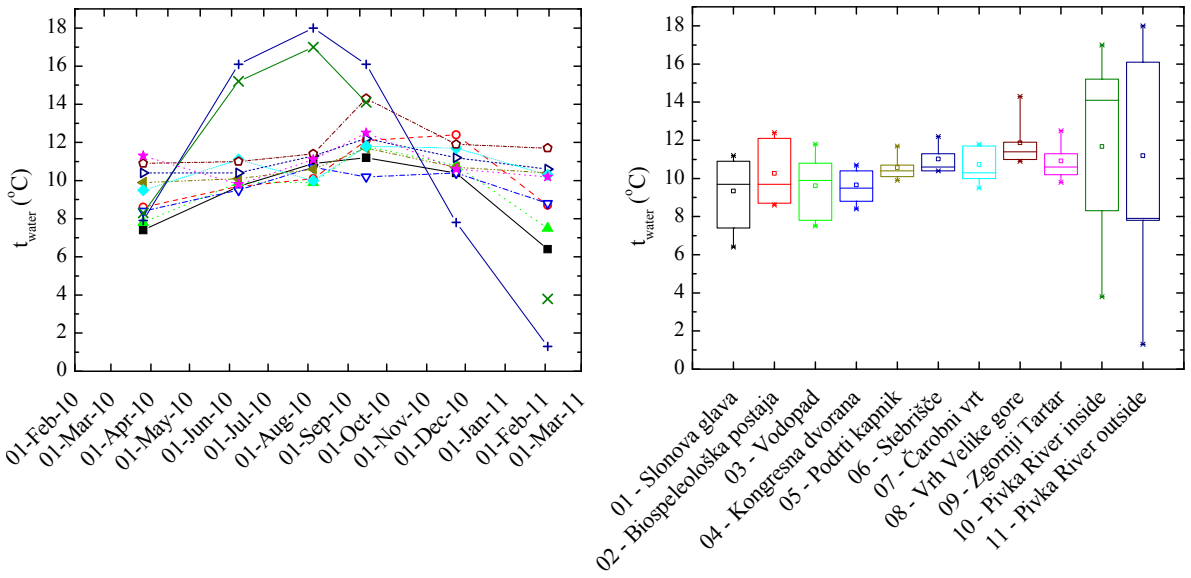

Figure 7.3 Temperature of drip water and Pivka River on sampling locations in Postojna Cave in time series and their variations on specific location.

Slika 7.3 Temperatura pokapne vode i rijeke Pivke na lokacijama uzorkovanja i njihove varijacije.

Locations 04, 05, 06, 07 and 09 show small deviations with mean temperature of 10.6 ± 0.5 ºC. These locations can be treated like zones with homothermic conditions, characterised by high temperature stability.

Temperture od the Pivka rivers shows larger variations than drip water temperature (Figures 7.3 and 7.4). Temperatures of both locations of Pivka River inside (10) and outside (11) of the Cave reflect mean air temperatures. The highest water temperature was measured at location 11 – Pivka River outside (18 °C) in August 2010. Mean monthly air temperature in August 2010 is also 18 °C. Lowest value of measured temperature at this location is 1.3 °C in February 2011, when the lowest mean monthly temperature of 0.3 °C was observed by National Meteorological Service of Slovenia (meteo.si). At the same time, variations of temperatures at location 10 – Pivka River inside are lower, from 3.8 °C in February 2011 to 17.0 °C in August 2010. Passing through a 2.5 km long cave interior, the Pivka River becoms warmer during winter and colder during summer so that the temperature variations are smaller at location 10 than at location 11. Variation of the Pivka River water temperature are much higher than of the drip water (Figure 7.3 and 7.4). Pivka River reflects mean outside temperature and shows large seasonal fluctuations. In summer at location 10 the River is colder than at location 11, while in winter it is warmer. Air temperature at location 10 shows larger variations than other parts of the cave, but smaller than location 11 (Figure 7.4).

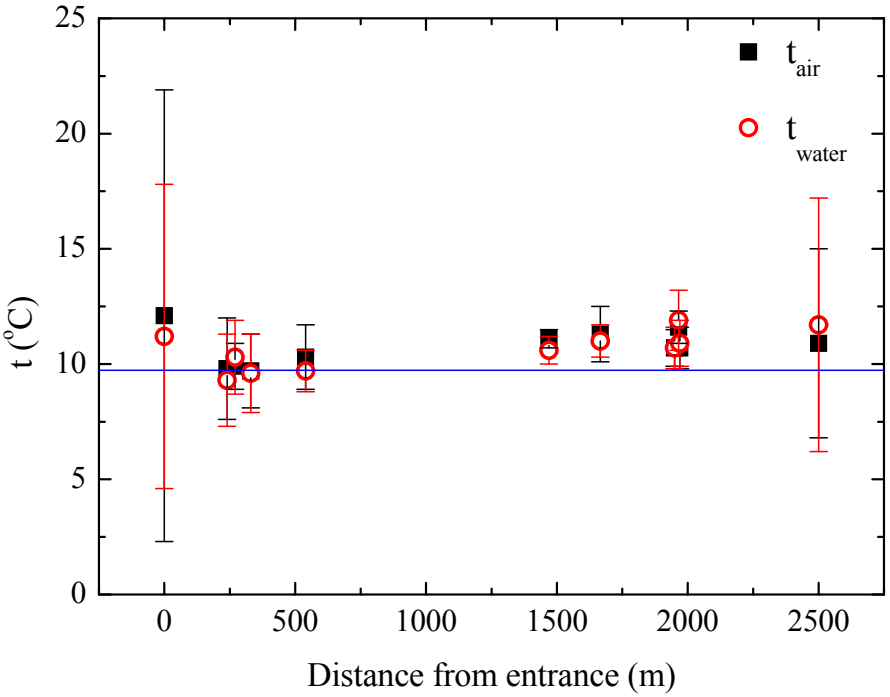

Figure 7.4 Mean temperatues of water (○) and air (■) vs. distance from entrance. Blue line marks mean monthly outside air temperature in the period of 6 years (2006 - 2011).

Slika 7.4 Srednje temperature vode (○) i zraka (■) u ovisnosti o udaljenosti od ulaza. Plava linija označava srednju vrijednost temperature zraka za razdoblje od šest godina (2006. – 2011.).

7.3 Drip water and precipitation

The interest in measurement of drip rates is to improve our knowledge of seepage dynamics in karst terrains (Genty and Deflandre, 1998). Therefore, the drip rate measured on all locations during the sampling period are presented in Figure 7.5. The histogram of measured drip rates is presented in Figure 6.2. The lowest drip rates are measured in August 2010. Summer months are also the months with small amount or no rain events.

The largest drip rate is measured in November 2010, namely: at location 01 – Slonova glava 165 drips per minute (mean on this location during the whole period is 50 min^{-1}), at location 04 – Kongresna dvorana 60 min^{-1} (mean is 50 min^{-1}), at location 07 – Čarobni vrt 450 min^{-1} (mean 145 min^{-1}), at location 08 – Vrh Velike gore 500 min^{-1} (mean 128 min^{-1}) and at location 09 – Zgornji Tartar 300 min^{-1} with mean value of 74 min^{-1}. Smaller variations are observed at location 02 – Biospeleološka postaja, where the lowest drip rate 3 min^{-1} is measured,. The largest differences in drip rate are measured at location 08 – Vrh Velike gore where also maximum drip rate is measured (Figure 7.5, Table A.3 in Appendix AI).

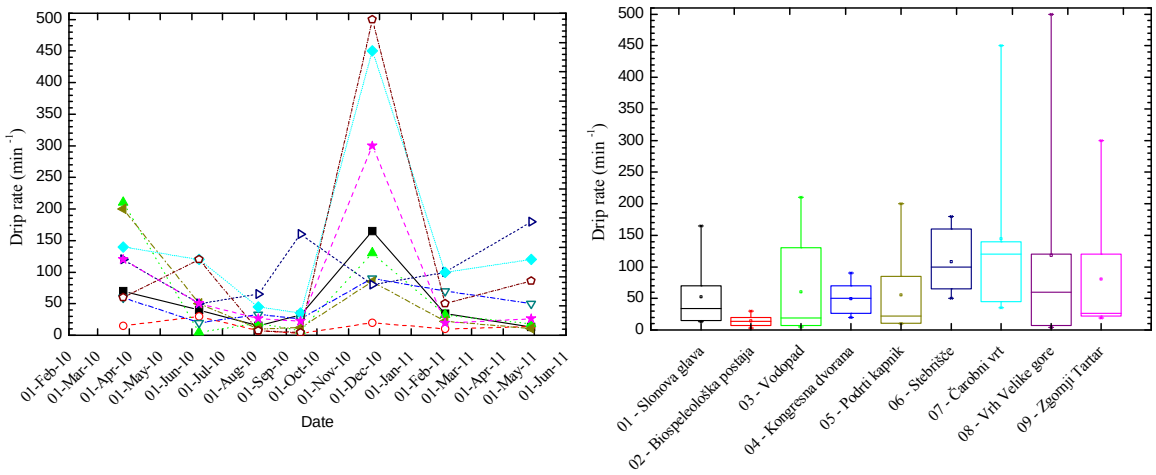

Figure 7.5 Drip rate in Postojna cave sampling sites through sampling period from March 2010 to May 2011.

Sika 7.5 Učestalost kapljanja na lokacijama u Postojnskoj jami tijekom razdoblja uzorkovanja.

The mean values of drip rate and their variabilities, expressed as coefficient of variability, defined as the ratio of the standard deviation and the mean drip rate, can be presented in a diagram first introduced by Smart and Friedrich (1987) (Figure 7.6). The diagram relates the absolute flow of drip water and the variations in discharge, and groups various flow types together. Discharge at a drip site (L/d) is obtained from measured drip rate (drops per minute) and a drop volume of 0.14 mL (Genty et al., 1998). All drip waters from the Postojna Cave belong to the seepage flow group, as expected from small seasonal variations in various chemical components. This is true for the mean drip rates at each locations, but also for the highest (individual) drip rates in the studied period, justifying the conclusion that in the case of the Postojna Cave all drip waters are of the seepage type and are relatively well mixed.

$\delta^{18}O$ values in drip water, Pivka River and precipitation from three stations are shown in Figure 7.7. The Largest variations are observed for precipitation stations Ljubljana, Zalog pri Postojni and Postojna. $\delta^{18}O$ in precipitation from Ljubljana varies from -12.71 ‰ in November 2010 to -5.05 ‰ in May 2010.

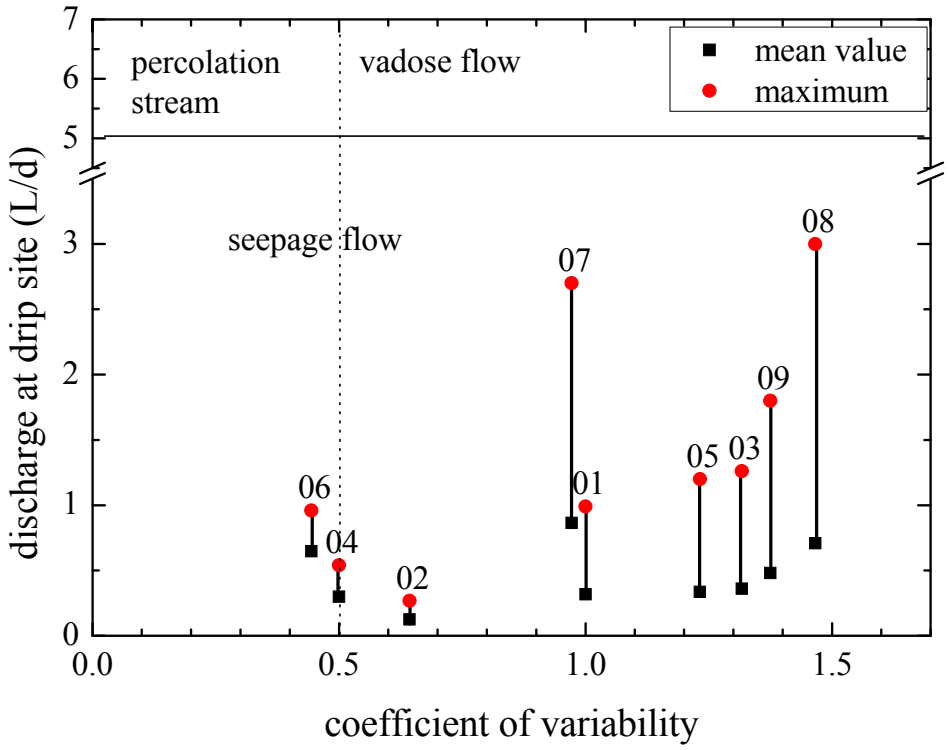

Figure 7.6 Average drip discharge versus coefficient of variability at locations in Postojna cave (denoted 01 – 09) within the vadose hydrology scheme of Smart and Friederich (1987).

Slika 7.6 Srednja vrijednost prokapljavanja u odnosu na koeficijent varijabilnosti za prokapnicu na lokacijama u Postojnskoj jami (oznake 01 do 09) po uzoru na dijagram iz Smart i Friederich (1987)

Even though there are differences in monthly $\delta^{18}O$ values, because of the local environmental conditions (Vreča et al., 2006), mean values are in approximately the same range from 7.40 ± 1.34 ‰ in Postojna, to 8.25 ± 2.34 ‰ in Ljubljana. Only Ljubljana has a 12-month set of data, while Zalog pri Postojni encompass only 10 months and for Postojna only 5 data are available.

At both locations of the Pivka River (inside and outside) $\delta^{18}O$ mean values are almost identical, -8.07 ± 0.69 ‰ and -8.06 ± 0.63 ‰, respectively. The Pivka River $\delta^{18}O$ values show similar seasonal variation behavior as precipitation $\delta^{18}O$ values, but less pronounced.

The drip water $\delta^{18}O$ values have smallest deviations at location 04 – Kongresna dvorana (-8.86 ± 0.04 ‰) and at location 06 – Stebrišče (-8.73 ± 0.07 ‰), followed by location 09 – Zgornji Tartar (-8.97 ± 0.23 ‰). The reason for small deviations from mean $\delta^{18}O$ value is long mean residence time (MRT). Highest variations in $\delta^{18}O$ values have location 08 – Vrh Velike gore (-9.69 ± 0.66 ‰) and location 02 – Biospeleološka postaja (-9.49 ± 0.65 ‰). At location 08 very strong changes in drip rate from 7 to 500 min^{-1} as a response to high

precipitation amount are observed, and one can conclude that the drip rate at location 08 – Vrh Velike gore is strongly affected by changes in precipitation amount.

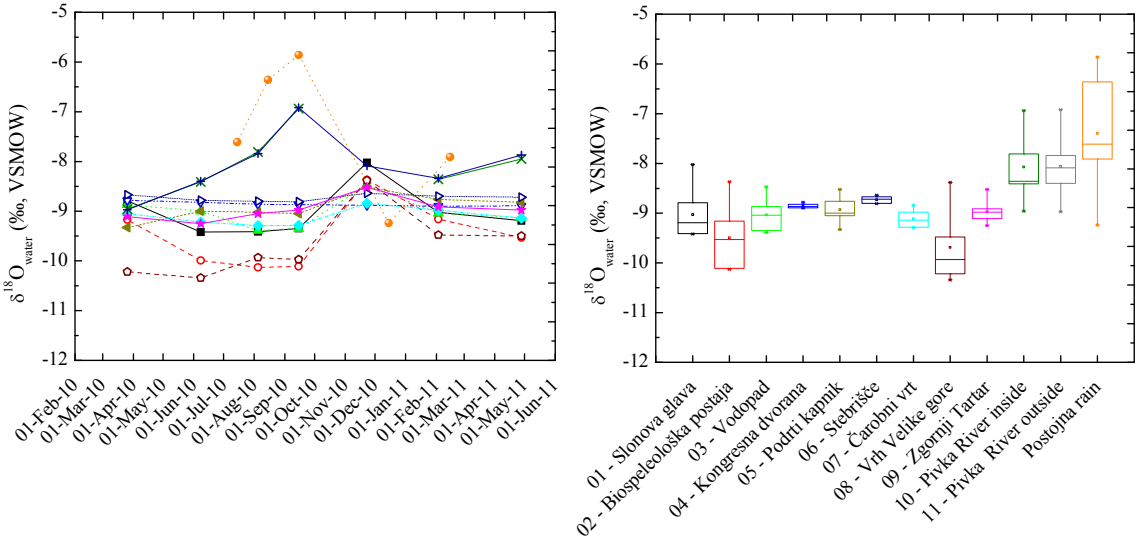

Figure 7.7 $\delta^{18}O$ in drip water, Pivka River and precipitation from Postojna (□), Ljubljana (□) and Zalog pri Postojni (□). Data for $\delta^{18}O$ in precipitation are obtained from the Jožef Stefan Institute, Ljubljana (dr. S. Lojen for station Zalog pri Postojni and dr. P. Vreča for Ljubljana).

Slika 7.7 $\delta^{18}O$ u prokapnoj vodi, rijeci Pivki i oborinama iz Postojne (□), Ljubljane (□) i Zaloga pri Postojni (□). Podaci o $\delta^{18}O$ za Ljubljanu i Zalog pri Postojni su dobiveni za korištenje iz Instituta Jožef Štefan u Ljubljani i to za Zalog pri Postojni od dr.sc. S. Lojen te za Ljubljanu od dr. sc. P. Vreča.

Mean residence time (MRT) can be estimated by aplying exponential mixing model of various ages of water in epikarst (Maloszewski et al. 1983),. The model compares yearly variations in $\delta^{18}O$ values in drip water and in precipitation, equation 7.1, under assumption of the complete mixing of water in epikarsts.

$$MRT = \omega^{-1} \cdot \left(\frac{A_{prec}^2}{A_{dw}^2} - 1\right)^{\frac{1}{2}} \qquad 7.1$$

where A_{prec} and A_{dw} are the amplitudes of $\delta^{18}O$ in precipitation and in drip water, respectively. The ω equals 2π/T where T represents period of seasonal variations. $\delta^{18}O$ show seasonal vatiations with period of 1 year therefore the optained MRT will be calculated in years. Amplitudes are calculated as a differences of minimum and maximum valuesof $\delta^{18}O$ of precipitation and dripwater. The obtained MRT's are presented in Table 7.2. As expected,

locations showing higher variations (e.g., locations 01, 02, 03 and 08, box plot in Figure 7.7) have short MRT of several months, locations 05, 07 and 09 have MRT between 1 and 2 years, while locations 04 and 06 show smallest seasonal variations (and the smallest coefficient of variability, Figure 7.6) and therefore have the longest MRT of 5 – 7 years.

Table 7.2 Mean residence time (MRT) for monitored locations

Tablica 7.2 Srednje vrijeme zadržavanja (MRT) vode u tlu

Location	A_{prec} (‰)	A_{dw} (‰)	MRT (yr)
01	5.45	1.40	0.60
02	5.45	1.76	0.47
03	5.45	0.90	0.95
04	5.45	0.12	7.23
05	5.45	0.80	1.07
06	5.45	0.16	5.42
07	5.45	0.44	1.97
08	5.45	2.00	0.40
09	5.45	0.72	1.19

Monthly amount of precipitation and drip rate are compared in Figure 7.8a. The highest drip rate is measured in winter (November 2010), and the lowest in summer (August 2010). During winter period (February 2011), preceded by two months of low precipitation, the drip rate is again low. The effect of low discharge in winter is observed because of snow cover during winter months, but also the low precipitation amount cannot be neglected. Prominent changes in drip rate are observed at locations 07 – Čarobni vrt, 08 – Vrh Velike gore and 09 – Zgornji Tartar in November 2010 after high monthly precipitation amounts in September 2010 and in spring (March 2010) and March 2011, probably after snow melting. The response of drip rate to the precipitation is delayed for about 2 months. Opposite to this conclusion are events monitored at location 02 – Biospeleološka postaja where response of a drip rate to precipitation amount is negligible (Figure 7.8a).

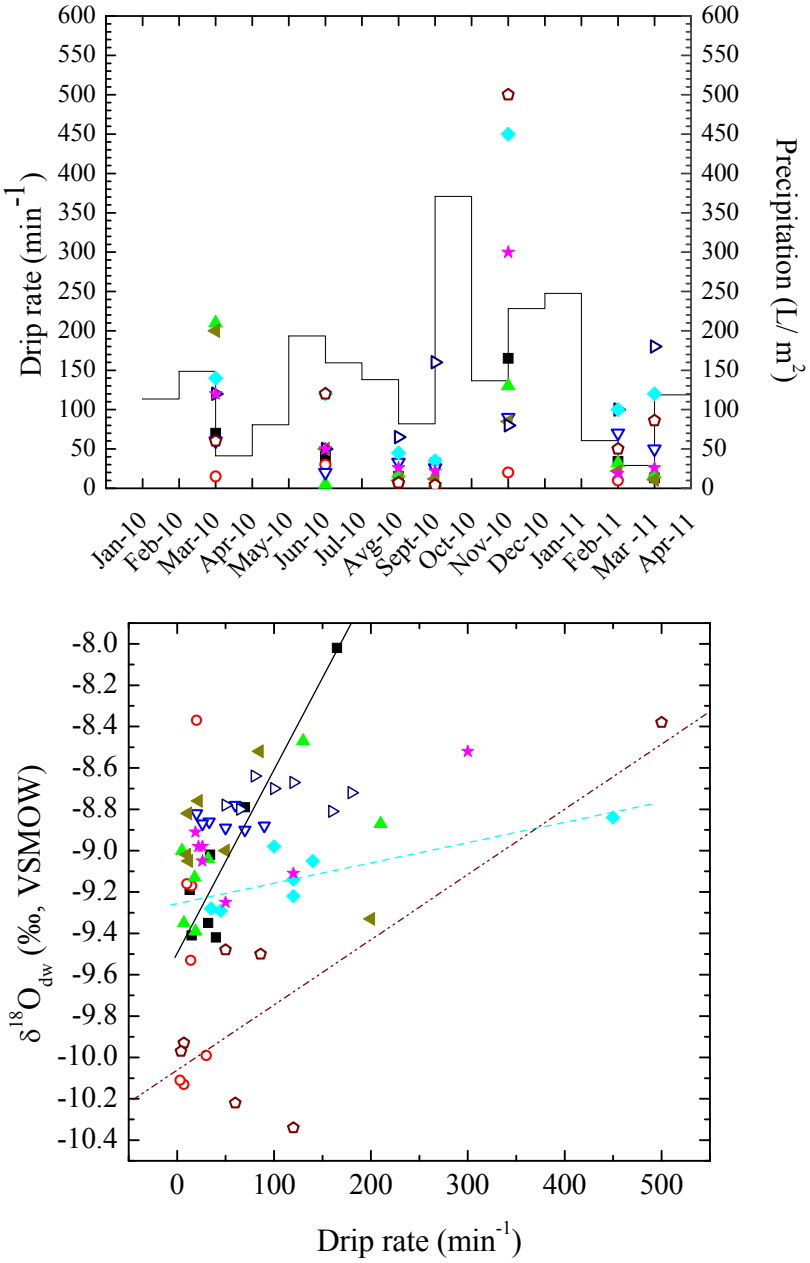

Location number and name	Symbol
01 - Slonova glava	■
02 - Biospeleološka postaja	○
03 - Vodopad	▲
04 - Kongresna dvorana	▽
05 - Podrti kapnik	◀
06 - Stebrišče	▷
07 - Čarobni vrt	◆
08 - Vrh Velike gore	⬠
09 - Zgornji Tartar	★
10 - Pivka River inside	×
11 - Pivka River outside	+

Figure 7.8 a) Monthly precipitation (—) and drip rate in the sampling period. b) $\delta^{18}O$ of drip water vs. drip rate. Linear regression lines are plotted only for locations with $R^2 > 0.8$.

Slika 7.8 a) Mjesečne oborine (—) i učestalost prokapljavanja u razdoblju uzorkovanja. b) $\delta^{18}O$ prokapne vode u ovisnosti o učestalosti prokapljavanja. Regresijski pravci prikazani su samo za lokacije s $R^2 > 0.8$.

By comparing of $\delta^{18}O$ of drip water and drip rate, shown in Figure 7.8b, it can be seen in what extent the older drip water is mixed with the fresh rain water. Good correlations between $\delta^{18}O$ of drip water and drip rate are obtained at locations 01 – Slonova glava ($R^2 = 0.94$, $p = 0.0016$), 07 – Čarobni vrt ($R^2 = 0.82$, $p = 0.0219$) and 08 – Vrh Velike gore ($R^2 = 0.82$, $p = 0.0226$) (Figure 7.8b). At these locations the drip rate increased significantly in November 2010, two months after

heavy precipitation in September 2010 (Figures 4.9 and 7.8). The higher drip rate is accompanied by an increase of 1 – 1.5 ‰ in $\delta^{18}O$,, because of more positive $\delta^{18}O$ value of rain water (-5.86 ‰, Table A.7 in Appendix I). Assuming that the increase in both $\delta^{18}O$ of drip water and drip rate is caused by rainfall from September 2010, the fraction of fresh rain is estimated to 0.38, 0.13 and 0.38 for locations 01, 07 and 08, respectively.

At locations 02 – Biospeleološka postaja drip rate is relatively constant and does not show a response to high amount of precipitation as locations 01, 07 and 08. However, the $\delta^{18}O$ of drip water shows similar increase and the fraction of fresh rain is 0.41, i.e. of the same magnitude as at locations 01 and 08, in accordance with similar MRT for these three locations (Table 7.2).

At location 05 – Podrti kapnik the highest drip rate is measured in March 2010. The $\delta^{18}O$ of drip water in March 2010 is more negative than in other months and it is probably a consequence of heavy rains in December 2009 (Figure 4.9, Table A.2 in Appendix I), when $\delta^{18}O$ of precipitation is low.

7.4 Water chemistry

7.4.1 Calcium and magnesium concentration

Largest variation from mean value for calcium concentration is found at location 01 – Slonova glava (89 ± 16 mg/L), and at location 08 – Vrh Velike gore deviation from mean value is minimal (82 ± 3 mg/L). The caprock thickness is for both locations approximately the same, 61 m and 66 m. Location 05 – Podrti kapnik has the lowest mean value (65 ± 12 mg/L), with the lowest measured calcium concentration in February 2011 (Figure 7.9).

Mean values of calcium concentration at location 11 – Pivka River outside is (72 ± 4 mg/L). Small variation in values for Pivka River can be explained with the fact that water is passing through the same area with no sudden infiltration that can be a consequence of strong showers, i.e. rain events.

Concentration of Mg^{2+} ion in all drip waters is very low (Figure 7.10). Mean value of all locations in the monitored period is 0.85 ± 0.18 mg/L. This can be due to limestone aquifer which differs from the Pivka River flow path. Smallest variations in Mg^{2+} concentration are observed at locations 03 – Vodopad and 08 – Podrti kapnik, while location 02 – Biospeleološka postaja has the largest variations (0.72 mg/L to 1.34 mg/L). The highest value is measured at location 01 – Slonova glava, 1.44 mg/L. Both sampling locations of the Pivka River show higher concentrations of magnesium ions and it is due to the Pivka River origin

and flow path. The highest value of 4.58 mg/L is measured at location 11 – Pivka River outside. Ratio of Mg/Ca (Figure 7.11) ranges between 0.006 at location 08 to 0.013 at location 01. Drip water at all location have the Mg/Ca ratio much lower than the waters of the Pivka River, as was already shown in the Piper diagram (Figure 6.13).

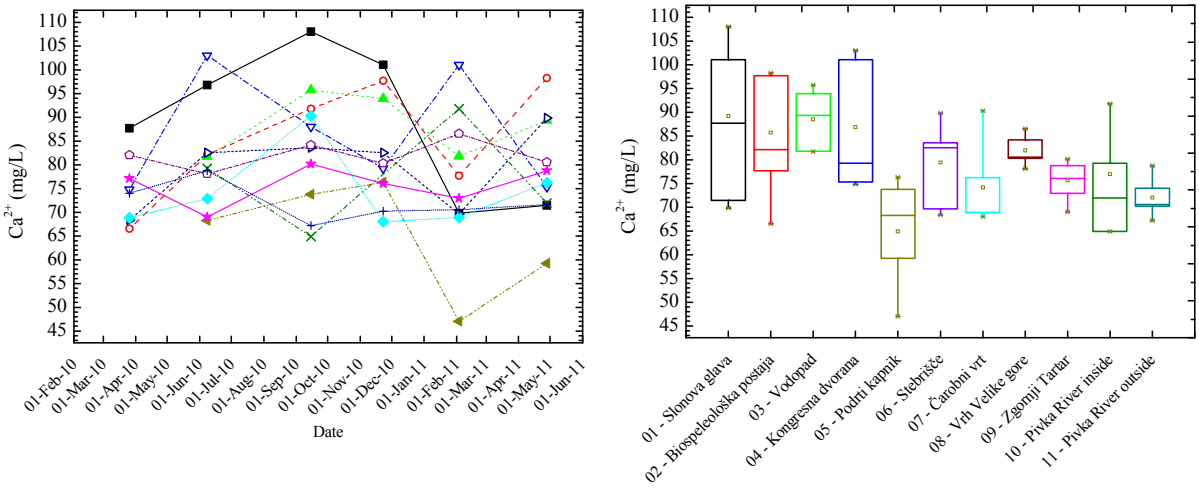

Figure 7.9 Calcium ion concentration in drip water and in Pivka River during sampling period

Slika 7.9 Koncentracija iona kalcija u prokapnoj vodi i rijeci Pivki.

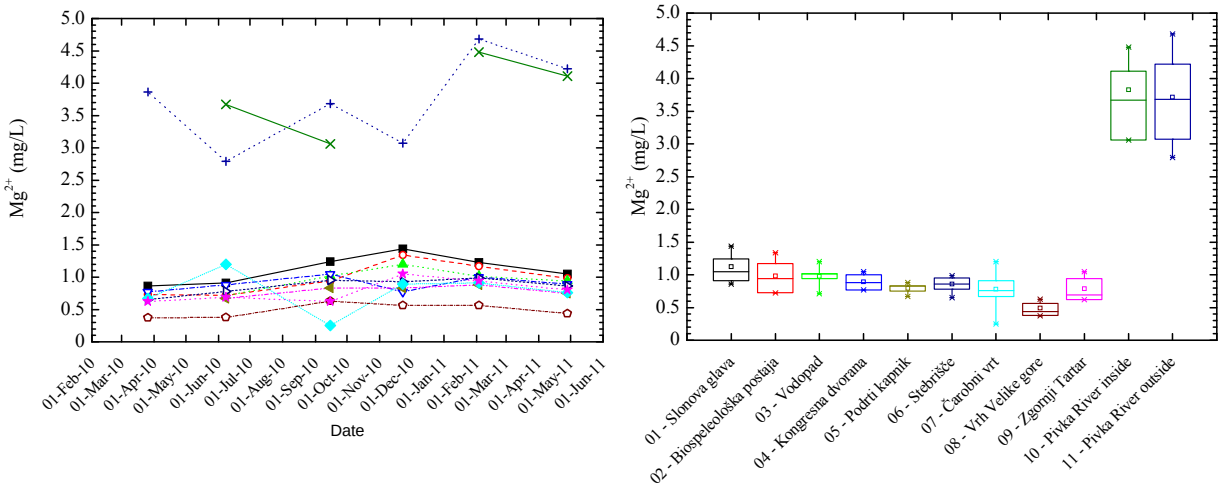

Figure 7.10 Magnesium ion concentration in drip water and in Pivka River during sampling period.

Slika 7.10 Koncentracija magnezija u prokapnoj vodi i rijeci Pivki tjekom perioda uzorkovanja.

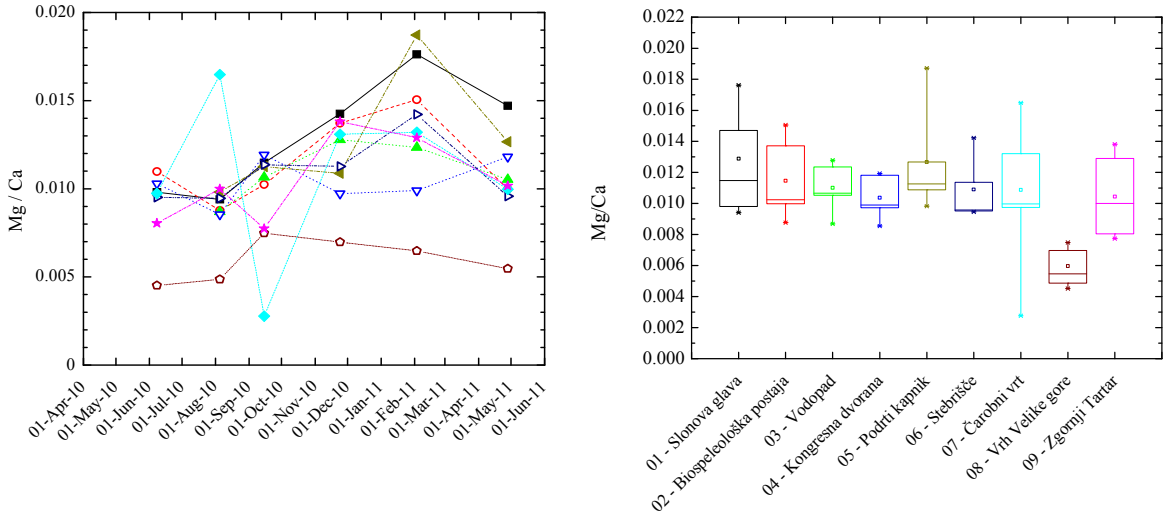

Figure 7.11 Mg/Ca ratio during monitoring period.
Slika 7.11 Omjer Mg/Ca tijekom razdoblja promatranja

Relation of calcium ion concentration with drip rate is different for different locations (Figure 7.12). Correlations between these sets of data is not significant at any locations, as shown in Table A.6. At locations where drip rate has variations from low (50 min^{-1}) to very high (500 min^{-1}) calcium concentration is stable. This is pronounced at locations 08 – Čarobni vrt, 07 – Vrh Velike gore and 09 – Zgornji Tartar. The larger variation of calcium ion concentration has been observed at location 02 – Biospeleološka postaja, where highest drip rate is 30 droplets per minute. The amount of precipitation strongly influences drip rate at some locations (Figure 7.8aFigure). At locations where response to precipitation rate is visible (07 – Čarobni vrt, 08 – Vrh Velike gore and 09 – Zgornji Tartar) in high drip rate, concentration of calcium ions is not affected. This is probsbly due to the high speed of water passing through karst terrain which decreases time for water – rock interaction during which rock minerals are dissolved in water.

In Figure 7.13 average concentration of calcium ions is plotted as a function of the caprock thickness. The highest calcium concentration (from 86 mg/L to 89 mg/L) is determined at locations 01, 02, 03 and 04, with caprock thickneses between 40 m and 90 m. At other locations (06, 07, 08, 09) with caprock thicknesses from 65 m to 85 m, calcium ion concentration shows variations from around 73 to 82 mg/L, therefore concentration of calcium ions in drip water is not determined by caprock thickness only, but also by geomorphology of the karst terrain itself, i.e. by the routes that drip water undergoes before reaching the drip site (Baker et al., 2000, Fairchild et al. 2000, Tooth and Fairchild, 2003). Most dissolution of limestone occurs in the epikarst zone (up to 60 m terrain depth) (Ford and Williams, 2007).

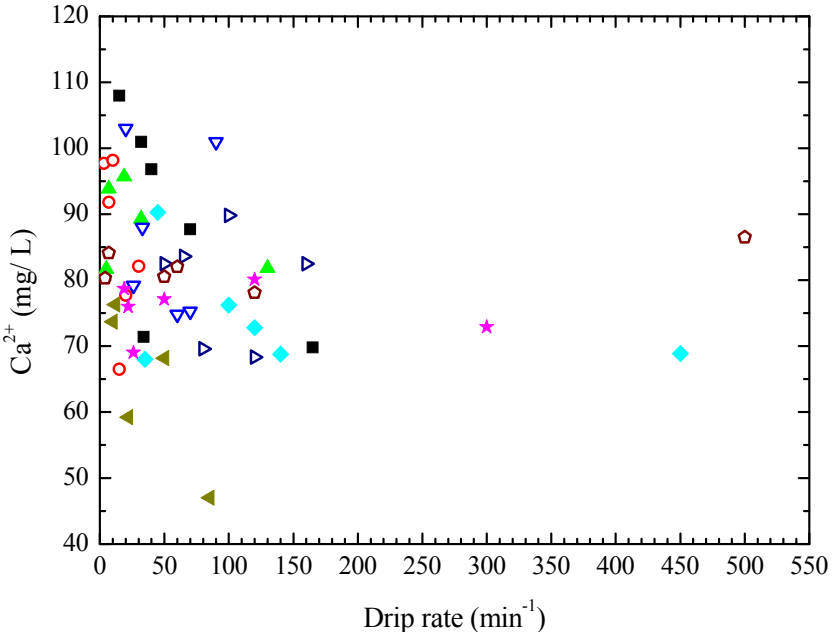

Location number and name	Symbol
01 - Slonova glava	■
02 - Biospeleološka postaja	○
03 - Vodopad	▲
04 - Kongresna dvorana	▽
05 - Podrti kapnik	◁
06 - Stebrišče	▷
07 - Čarobni vrt	◆
08 - Vrh Velike gore	⬠
09 - Zgornji Tartar	★
10 - Pivka River inside	×
11 - Pivka River outside	+

Figure 7.12 Dependence of calcium ion concentration on drip rate.

Slika 7.12 Ovisnost koncentracije kalcija o učestalosti porokapljavanja.

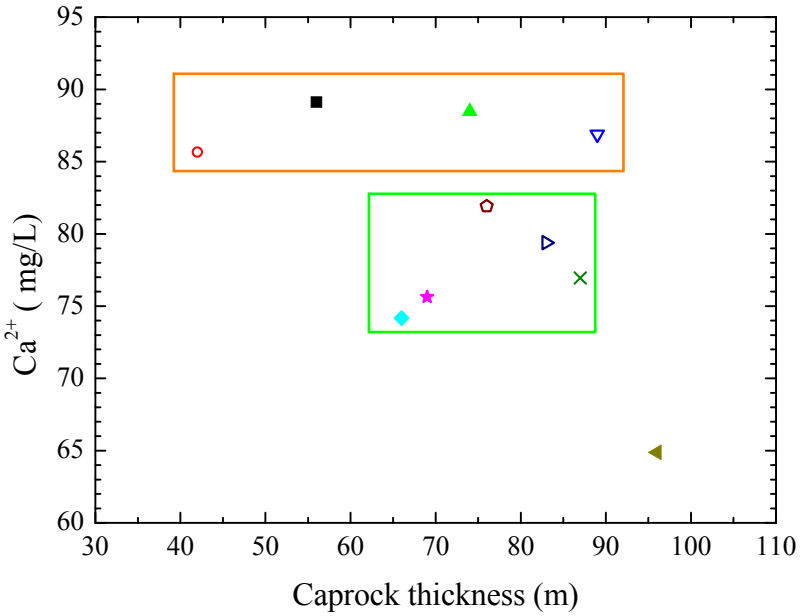

Location number and name	Symbol
01 - Slonova glava	■
02 - Biospeleološka postaja	○
03 - Vodopad	▲
04 - Kongresna dvorana	▽
05 - Podrti kapnik	◁
06 - Stebrišče	▷
07 - Čarobni vrt	◆
08 - Vrh Velike gore	⬠
09 - Zgornji Tartar	★
10 - Pivka River inside	×
11 - Pivka River outside	+

Figure 7.13 Mean values of calcium ion concentration and caprock thickness. There are two groups of locations. Read square points out outer ocations and green square inner locations. Location 05 does not belong to any of the two groups

Slika 7.13 Srednja vrijednost Ca^{2+} i debljina stropa. Crveni pravokutnik naglašava sličnost uutarnjih lokacija, dok zeleni pravokutnik ističe unutarnje lokacije. Lokacija 05 – Podrti kapnik ne pripada niti jednoj grupi

In Figure 7.13 location 11 – Pivka River inside is plotted only for comparison with drip water sites, although caprock at site 11 does not influence chemical composition of the river because of

absence of drip sites. Location 05 – Podrti kapnik is an exception and is not taken into consideration here. A special case of Podrti kapnik will be discussed later in section 7.6. Other chemical parameters are also not influenced by caprock thickness

Calcium concentration (mean 87.6 ± 1.5 mg/L) at locations 01, 02, 03 and 04 is higher than at locations 06, 07, 08, 09 (mean 77.8 ± 3.5 mg/L). Difference between these groups of locations is observed also in some other parameter that are discussed in the following sections. Mean values for groups of outer (01 – 04) and inner locations (06 – 09) are given in Tables A.3, A.4 and A.5 in Appendix I.

7.4.2 Bicarbonate concentration and $\delta^{13}C$

Concentration of hydrogen carbonates is measured during sampling period from March 2010 to May 2011 (Figure 7.14). The largest variation from the mean value is observed at location 02 – Biospeleološka postaja (250 ± 58 mg/L) and smallest at location 07 – Čarobni vrt (200 ± 19 mg/L). The location with maximum HCO_3^- value of 365 mg/L is location 01 – Slonova glava in November 2010, whereas minimum value of 122 mg/L is measured at location 05 – Podrti kapnik with mean value 153 ± 29 mg/L. For all locations except at location 04 – Kongresna dvorana and 07 – Čarobni vrt maximum bicarbonate value is measured in November 2010.

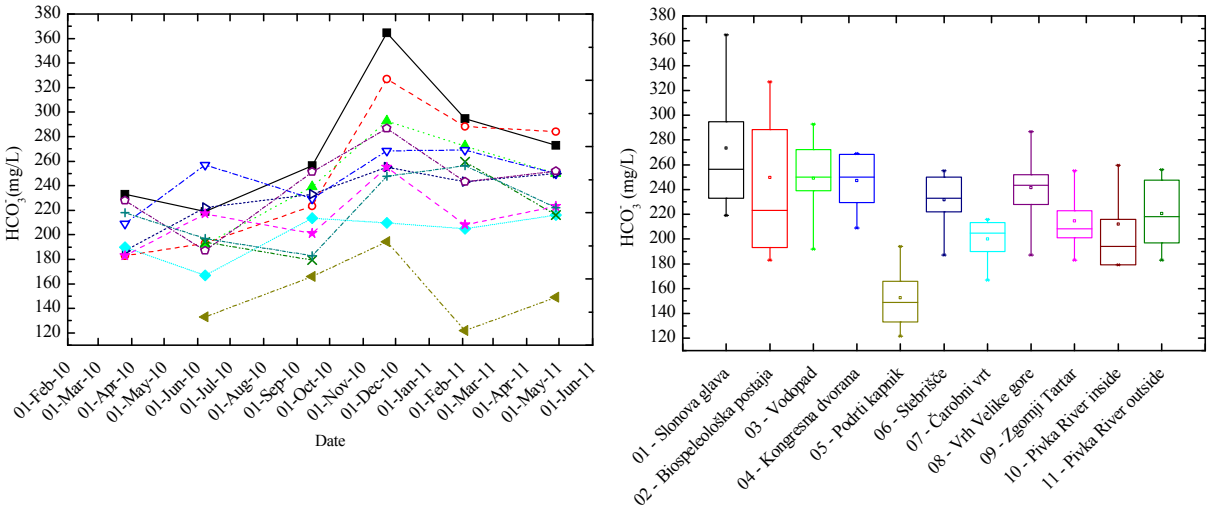

Figure 7.14 Bicarbonate concentration in drip water from different locations in the Postojna Cave and in Pivka River.

Slika 7.14 Koncentracija bikarbonata u prokapnici s različitih lokacija u Postojnskoj jami i u rijeci Pivki.

The $\delta^{13}C_{DIC}$ values in Pivka River water and in drip waters are shown in Figure 7.15. Mean values at location 10 – Pivka River inside and at location 11 – Pivka River outside are

approximately the same, i.e. -12.4 ± 2.0 ‰ and -12.4 ± 2.2 ‰, respectively. The drip water at location 05 – Podrti kapnik has more positive $\delta^{13}C_{DIC}$ values than other drip waters. Mean value at location 05 – Podrti kapnik is -9.90 ± 2.26 ‰ with minimum $\delta^{13}C_{DIC}$ of -11.78 ‰ and maximum -5.64 ‰. $\delta^{13}C_{DIC}$ values in other drip waters show relatively narrow range of values. Mean value range from -12.32 ± 0.28 ‰ at location Čarobni vrt to -13.30 ± 0.33 ‰ at location 01 – Slonova glava. Smallest variations have been measured at location 06 – Stebrišče (-13.06 ± 0.11) ‰.

HCO_3^- concentration at outer locations 01 – 04 is higher (255 ± 12 mg/L) than at inner locations (222 ± 18 mg/L), in accordance with the calcium contration mean values (section 7.4.1). There is no difference in $\delta^{13}C$ vaues of DIC at outer and inner locations, being -12.9 ± 0.4 ‰ and -12.8 ± 0.3 ‰, respectively.

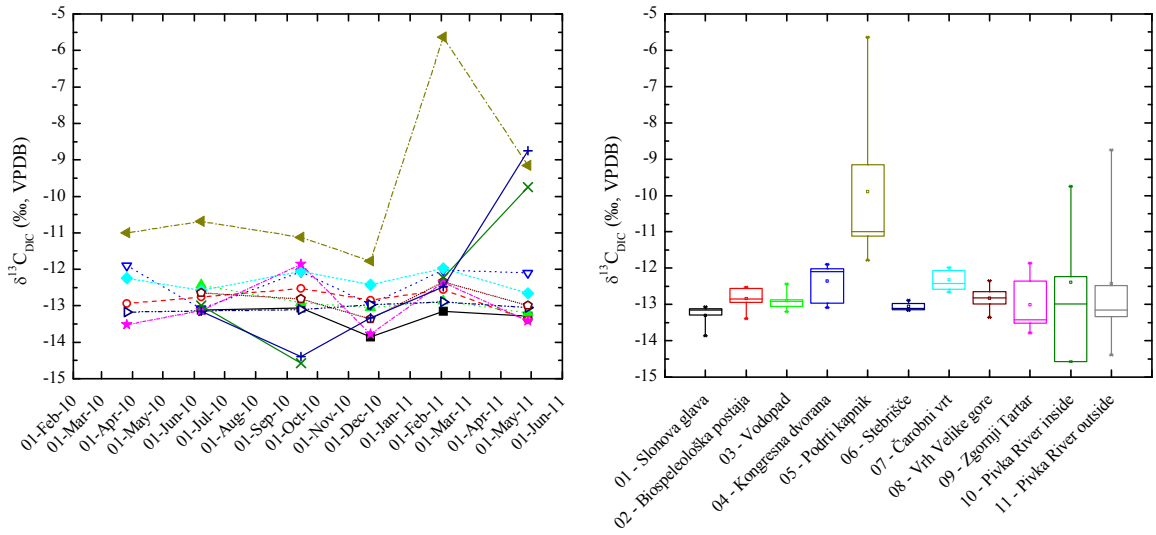

Figure 7.15 $\delta^{13}C_{DIC}$ in drip water and River Pivka.
Slika 7.15 $\delta^{13}C_{DIC}$ u prokapnoj vodi i rijeci Pivki.

7.4.3 Conductivity

Figure 7.16 shows electrical conductivity in drip water and the Pivka River in the monitored period. The highest average conductivity value has been measured at location 01 – Slonova glava (454 ± 76 µS/cm) with the maximum value of 556 µS/cm in November 2010. The lowest average value is found at location 05 – Podrti kapnik (277 ± 42 µS/cm), as well as the lowest conductivity value of 197 µS/cm in February 2011. At location 06 – Stebrišče minimum deviation from mean value is calculated 366 ± 17 µS/cm, i.e. location 06 – Stebrišče show most stable conductivity condition of all sampling locations. Form the statistical analysis of data, it can be noticed that

locations 01 – 04 have on average higher conductivity values of drip water (433 ± 25 µS/cm) than locations 06 – 09 (358 ± 15 µS/cm) and location 05

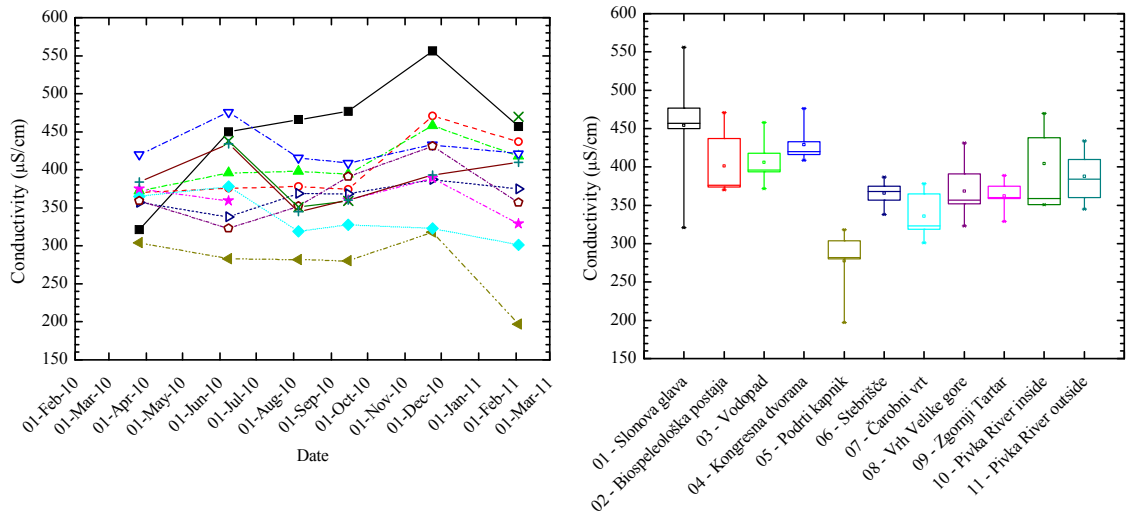

Figure 7.16 Electrical conductivity of drip waters from locations inside Postojna cave and of the Pivka River.

Slika 7.16 Električna provodnost prokapnice s lokacija unutar Postojnske jame i rijeke Pivke.

.

Conductivity is in direct correlation with concentration of dissolved minerals in the solution. Correlation between mean values of HCO_3^- and Ca^{2+} ions, which are the principal conducting ion species in drip waters of the Postojna Cave (Figure 6.13), is shown in Figure 7.17. Good correlation of these two ions with $R^2 = 0.94$ is in agreement with classical processes in karst where higher concentrations of bicarbonate HCO_3^- in drip water causes higher concentrations of dissolved minerals, in the case of limestone, the calcium minerals. Locations closer to the entrance of the cave (01 to 04, full line square on Figure 7.17) have higher concentration of HCO_3^- (255 ± 12 mg/L) and of Ca^{2+} ions (87.6 ± 1.5 mg/L), than the inner locations (06 to 09, dashed line square on Figure 7.17): 222 ± 18 mg/L (HCO3) and 77.8 ± 3.5 mg/L (Ca^{2+}), respectively. Location 05 – Podrti kapnik, where both Ca^{2+} and HCO_3^- concentrations have the lowest values, as well as lowest conductivity, will be discussed separately in Chapter 7.6. Locations 10 and 11 at the Pivka River are of different origin and are not comparable with drip water.

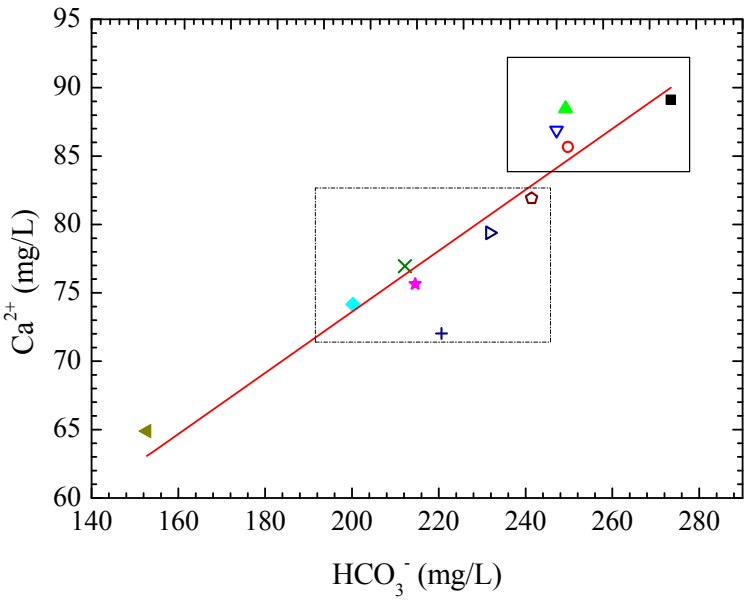

Location number and name	Symbol
01 - Slonova glava	■
02 - Biospeleološka postaja	○
03 - Vodopad	▲
04 - Kongresna dvorana	▽
05 - Podrti kapnik	◀
06 - Stebrišče	▷
07 - Čarobni vrt	◆
08 - Vrh Velike gore	⬠
09 - Zgornji Tartar	★
10 - Pivka River inside	×
11 - Pivka River outside	+

Figure 7.17 Correlation between mean values of HCO_3^- and Ca^{2+} ion concentration for all sampling locations. Locations 01 to 04 are grouped in full line square, and locations 06 to 11 in dashed square.

Slika 7.17 Korelacija između srednjih vrijednosti HCO_3^- i Ca^{2+} koncentracija na svim lokacijama. Lokacije 01 do 04 grupirane su punom crtom, a lokacije 06 do 09 isprekidanom crtom

Mean conductivity of drip waters and drip rate show linear correlation ($R^2 = 0.51$) (Figure 7.18). Locations 01 to 04 with lower drip rate (full-line square on Figure 7.18) have higher conductivity and locations 06 to 09 (dashed-line square on Figure 7.18) with higher drip rate have lower conductivity. Locations with higher mean drip rate show also stronger response to the rain events (Figure 7.8 and Figure 6.2). Location 05 with the lowest conductivity is omitted from linear fit. The reasons for low conductivity will be discussed in Chapter 7.6.

The analysis of data in this section has shown that several groups of locations can be distinguished. Locations 01 – 04, which are close to the entrance (“outer” locations), form the first group, and locations 06 – 09 (“inner” locations) are the second group. The Pivka River, locations 10 and 11, form a third group, while location 05 is a special case that will be discussed in Chapter 7.6.

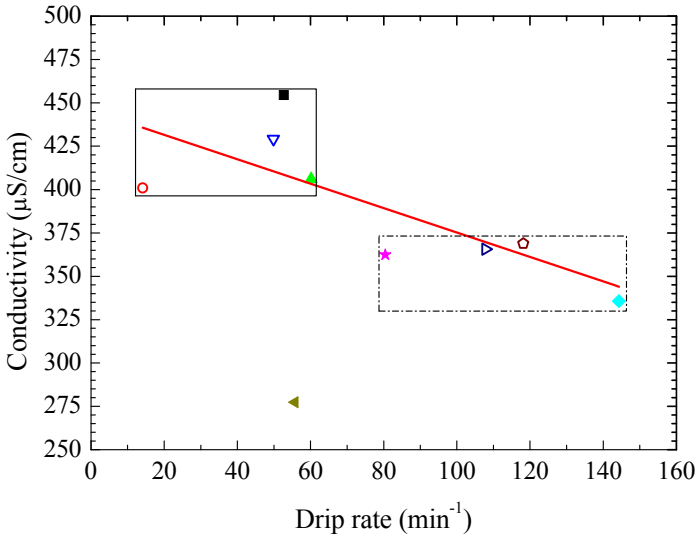

Location number and name	Symbol
01 - Slonova glava	■
02 - Biospeleološka postaja	○
03 - Vodopad	▲
04 - Kongresna dvorana	▽
05 - Podrti kapnik	◀
06 - Stebrišče	▷
07 - Čarobni vrt	◆
08 - Vrh Velike gore	⬠
09 - Zgornji Tartar	★

Figure 7.18 Correlations of mean annual conductivity and drip rate with linear fit (location 05 is omitted from the linear regression). Locations 01 to 04 are grouped in full-line square, and locations 06 to 09 in dashed-line square.

Slika 7.18 Korelacija između srednje godišnje provodnosti i učestalosti kapanja. Lokacije 01 do 04 grupirane su punom crtom, a lokacije 06 do 09 isprekidanom crtom

The inner and outer locations can be distinguished by their conductivity values, Ca^{2+} and HCO_3^- concentrations (Figures 7.9, 7.14, 7.17, 7.18), as well as by their air temperature (9.9 ± 0.3 °C and 11.1 ± 0.5 °C at outer and inner locations, respectively) and drip water temperature (9.7 ± 0.4 °C and 11.1 ± 0.5 °C, respectively), Mg^{2+} ion concentrations (1.0 ± 0.1 mg/L and 0.7 ± 0.2 mg/L, respectively), pCO_2 and $\delta^{13}C_{air}$ (Figure 7.25), pCO_2(aq) (Figures 7.20 and 7.29) and drip rate (Figures 7.5 and 7.18). The two groups of locations cannot be distinguished by the values of MRT (Table 7.2), $\delta^{18}O$ of drip water (Figure 7.7), $\delta^{13}C_{DIC}$ (Figure 7.15), and Mg/Ca ratio. The mean values of the mentioned parameters for locations 01 – 04 and 06 – 09 are presented in Tables A.3, A.4 and A.5 in Appendix I.

The differences in temperatures, pCO_2 and $\delta^{13}C_{air}$ can be explained by more pronounced ventilation at the outer location, closer to the cave entrance. Higher pCO_2(aq) at outer locations may be caused by higher concentration of CO_2 in soil above the cave which subsequently can dissolve more carbonate rocks and thus cause higher concentrations of Ca^{2+}, Mg^{2+} and HCO_3^- ions, as well as higher conductivity. However, $\delta^{13}C_{DIC}$ values are the same (12.9 ± 0.4 ‰ and 12.8 ± 0.3 ‰ at outer an inner locations, respectively, Table A.5) showing that the carbonate dissolution process is of the same type.

7.4.4 pH, aqueous CO_2 and saturation index

The pH values of sampled drip waters (Figure 7.19) are between 7.0 and 8.4 which is characteristic of a limestone and dolomite terrains (pH values usually fall between 6 and 9) (Merkel and Planer-Friedrich, 2008). Water from the Pivka River and all drip waters show typical limestone pH values which are higher during the cold season. The highest pH values of drip water (Figure 7.19) are measured in March 2010 at locations 04 – Kongresna dvorana (8.22), 05 – Podrti kapnik (8.38) and location 06 – Srebrišče (8.33). At locations 01 – Slonova glava and 02 – Biospeleološka postaja minimum value of pH is 7.10 measured in August 2010. The same pH of 7.10 is measured at locations 01 – Slonova glava, 02 – Biospeleološka postaja and 03 – Vodopad in September 2010. The lowest pH value is measured at location 11 – Pivka River outside (7.08) in September 2010. The largest difference in pH value of drip water is measured at Location 03 – Vodopad.

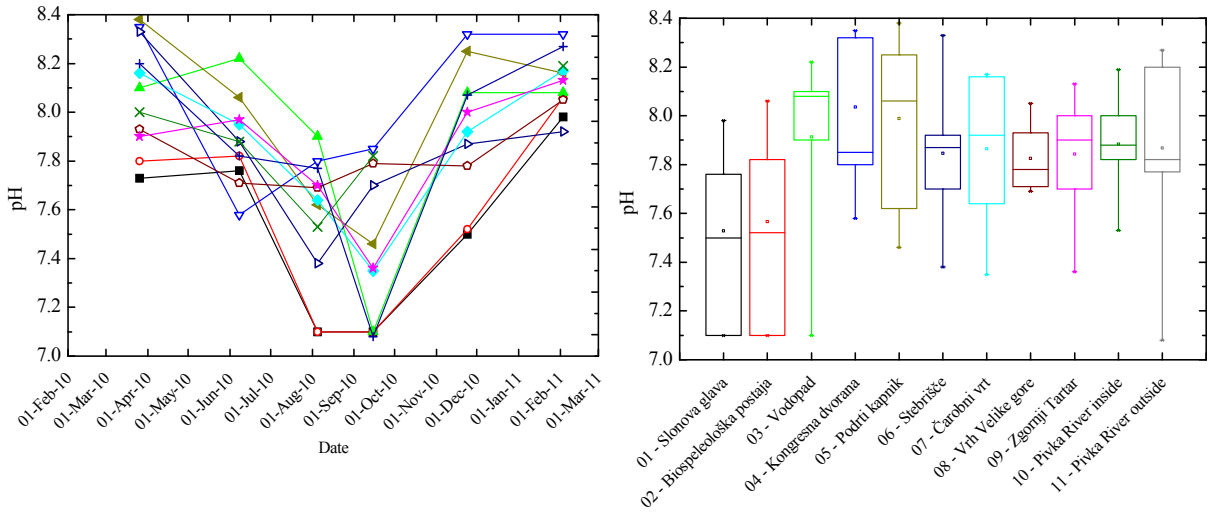

Figure 7.19 pH values measured in drip waters and in Pivka River, in the sampling
Slika 7.19 pH vrijednosti mjerene u prokapnici i rijeci Pivki u razdoblju uzorkovanja.

The pCO_2(aq) is calculated by equation (3.5) and is presented in Figure 7.20. The highest mean value is 10 379 ± 9715 µatm, calculated at location 01 – Slonova glava and minimum value is calculated for the location 05. The maximum values of pCO_2(aq) are calculated in November 2010 at locations 01, 02, 03 and 11. The highest value is found at location 01 (26141 µatm). The minimum value is calculated at location 05 – Podrti kapnik in March 2010 (850 µatm). The smalest variation in pCO_2 (aq) are noticed at location 08 – Vrh Velike gore (3387 ± 1037 µatm), and the highest in above mentioned location 01.

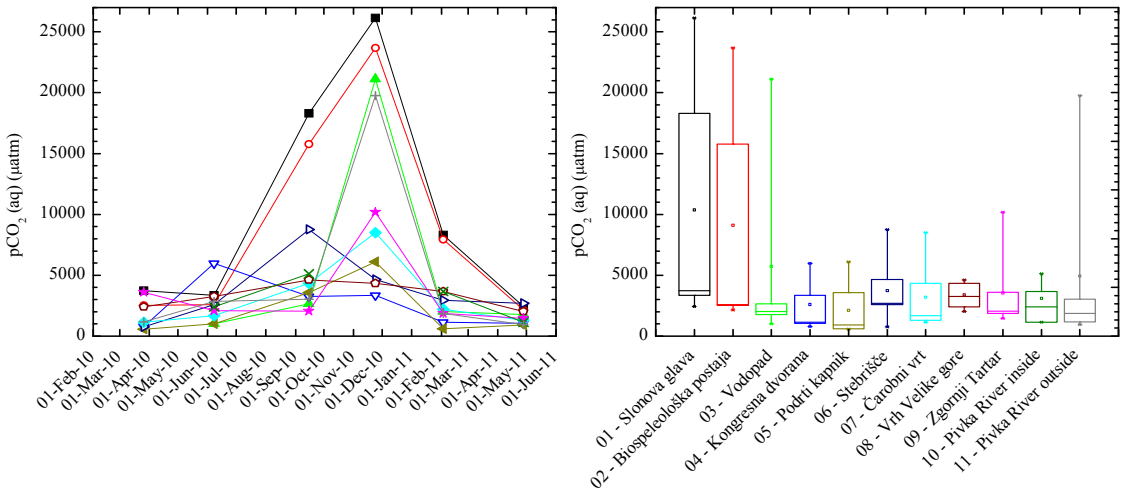

Figure 7.20 Calculated pCO_2(aq) in the sampling period.

Slika 7.20 Izračunati pCO_2(aq) tijekom razdoblja uzorkovanja.

Saturation index I_{sat} is calculated by equation 3.10 and varies from 1.94 ± 0.81 at location 01 – Slonova glava, to 6.19 ± 4.12 at location 04 – Kongresna dvorana. The highest value is calculated at location 04 (12.82) in February 2011, and the minimum value of I_{sat} is calculated at location 02 (0.58) (Figure 7.21).

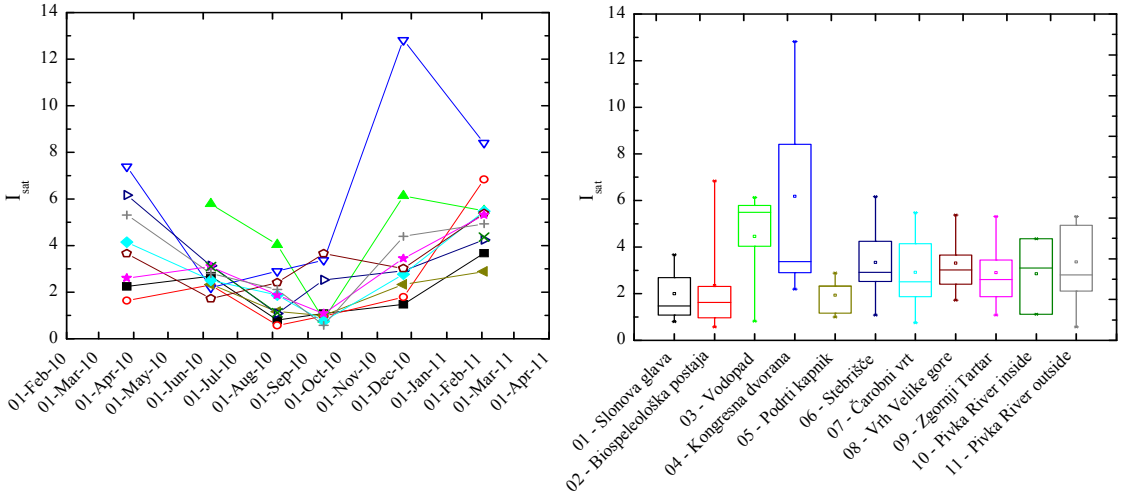

Figure 7.21 I_{sat} values calculated for drip waters and in Pivka River, in the sampling period

Slika 7.21 Vrijednosti I_{sat} računate za prokapnicu i Pivku tijekom perioda uzorkovanja.

Relation between pH and calcium concentration is plotted in Figure 7.22. Red line on the plot presents equilibrium solution, i.e. $I_{sat} = 1$ (Dreybrodt, 2011). The data points below the red line have $I_{sat} < 1$, with no possibility to precipitate carbonate. Above the line, $I_{sat} > 1$ and carbonate precipitates. The locations at which low pH is measured, are locations 01 and 02 in August and September 2010 and at locations 03, 07, 08 and 09 in September2010. The corresponding I_{sat} values are close to or slightly lower than 1.

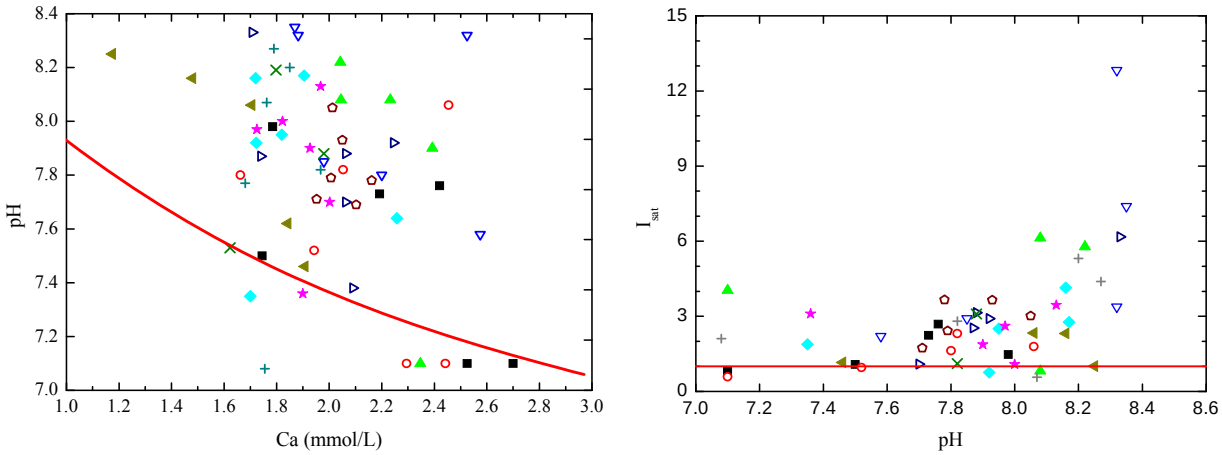

a b

Figure 7.22 Relation between pH and calcium concentration (a) and relation between I_{sat} and pH (b). Red line presents equilibrium solution, $I_{sat} = 1$. Datapoints below red line have $I_{sat} < 1$, and above the line $I_{sat} > 1$.

Slika 7.22 Odnos pH vrijednosti i koncentracije kalcija (a) i odnos između I_{sat} i pH (b). Crvena linija prikazuje kemijsku ravnotežu otopine obzirom na I_{sat}, $I_{sat} = 1$. Točke ispod linije imaju $I_{sat} < 1$, dok one iznad linije imaju $I_{sat} > 1$.

7.5 CO_2 in cave air

In the air outside the Postojna Cave and inside the Cave pCO_2 has been measured (Figure 7.23). Smallest variations have been measured outside the Postojna cave at location 11, 396 ± 46 ppmv. Mean monthly value for pCO_2 measured on Mauna Loa (Hawaii) in 2010 and 2011 is 390 ppmv (http://www.esrl.noaa.gov/gmd/ccgg/trends). Location with lagest variations in pCO_2 concentration is location 07 – Čarobni vrt, (1578 ± 885 ppmv), where minimum is measured in March 2010, 750 ppmv, and maximum in September 2010, 2940 ppmv. The smallest variation has been measured at location 04 – Kongresna dvorana, 783 ± 300 ppmv. Minimum is measured in February 2011 (430 ppmv) and maximum in September 2010 (1220 ppmv). The pCO_2 trend of high and low values for all locations are the same, minimum in March 2010 or February 2011 and maximum in August to October 2010. The differences in pCO_2 values from outside and inside the cave arise from the processes of drip water outgassing.

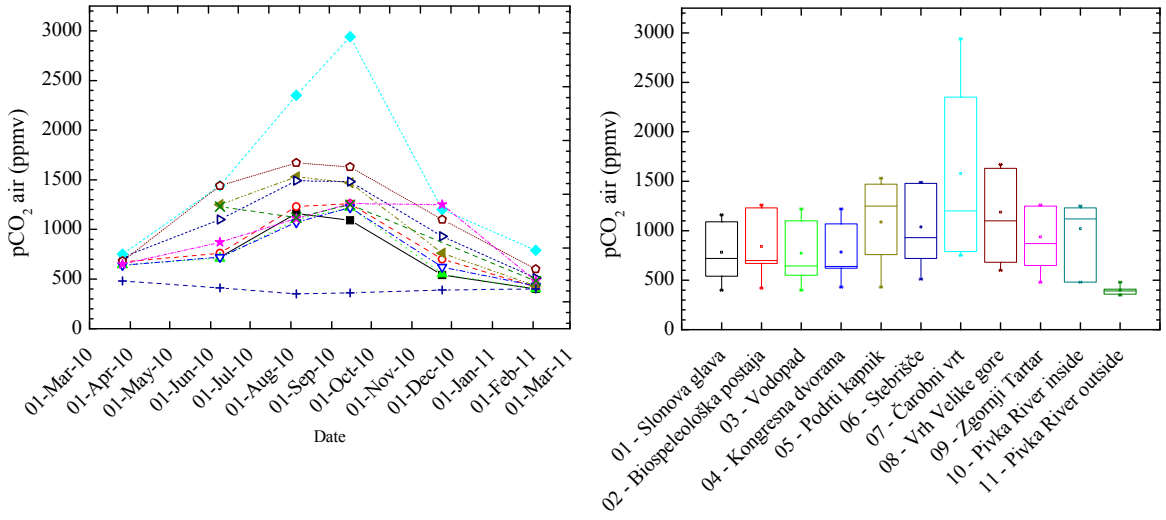

Figure 7.23 The pCO_2 values in air outside and inside the Postojna Cave.
Slika 7.23 pCO_2 u špiljskom zraku i zraku izvan Postojnske jame.

Values of $\delta^{13}C$ of the cave air at all locations inside the Postojna Cave have the same type of sesonality (Figure 7.24). The smallest variations in $\delta^{13}C$ have been measured at location 07 – Čarobni vrt (-18.00 ± 2.06 ‰), and the highest variations from mean value (-14.59 ± 4.88 ‰) was measured at location 10 – Pivka River inside. Minimum values for all locations was measured in September 2010 ranging from -21.64 ‰ to -18.39 ‰ at location 02 – Biospeleološka postaja.

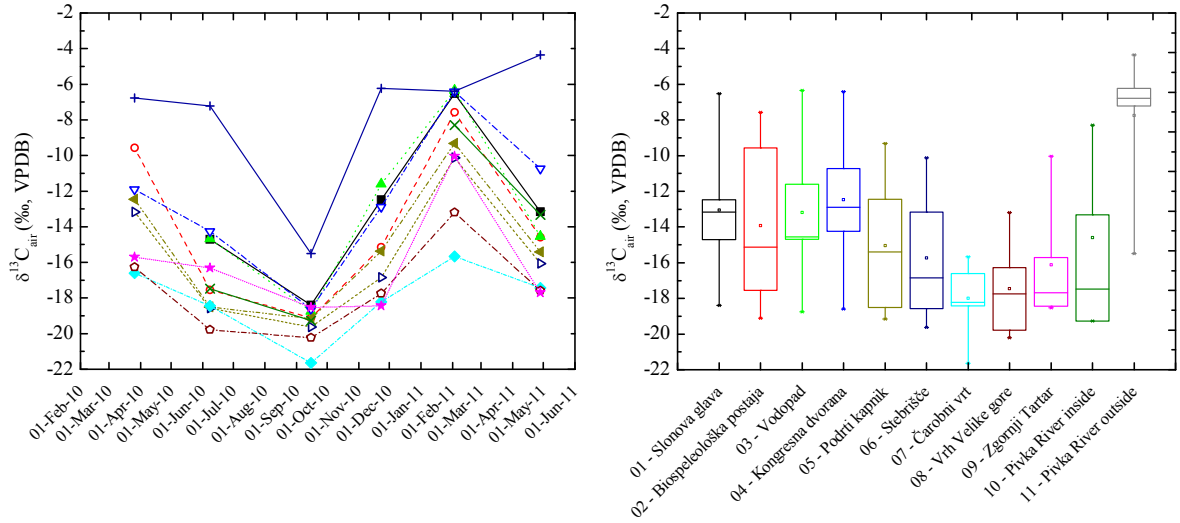

Figure 7.24 The $\delta^{13}C$ value on all sampling locations in Postojna Cave and air outside the Cave.
Slika 7.24 $\delta^{13}C$ vrijednosti u zraku na svim lokacijama unutar Postojnske jame i zraku izvan špilje.

The highest values on all locations have been measured in February 2011 with maximum measured at location 04 – Kongresna dvorana (-6.35 ‰) and minimum at location 08 – Vrh Velike gore (-13.19 ‰).

The mean pCO_2 and $\delta^{13}C$ concentrations in the cave air at the locations 01 – 04 range from 771 ppmv to 840 ppmv and from -12.58 ‰ to -13.92 ‰ respectively. The other group is formed by locations 05 – 09, where data for pCO_2 and $\delta^{13}C$ range from 937 ppmv to 1578 ppmv and from – 9.90 ‰ to -13.01 ‰ respectively. Two groups of data are shown in Figure 7.25. Locations closer to the entrance have pCO_2 closer to the atmospheric pCO_2. At location 09 – Zgornji Tartar pCO_2 is low because of the vicinity of the second entrance at Stara apnenca.

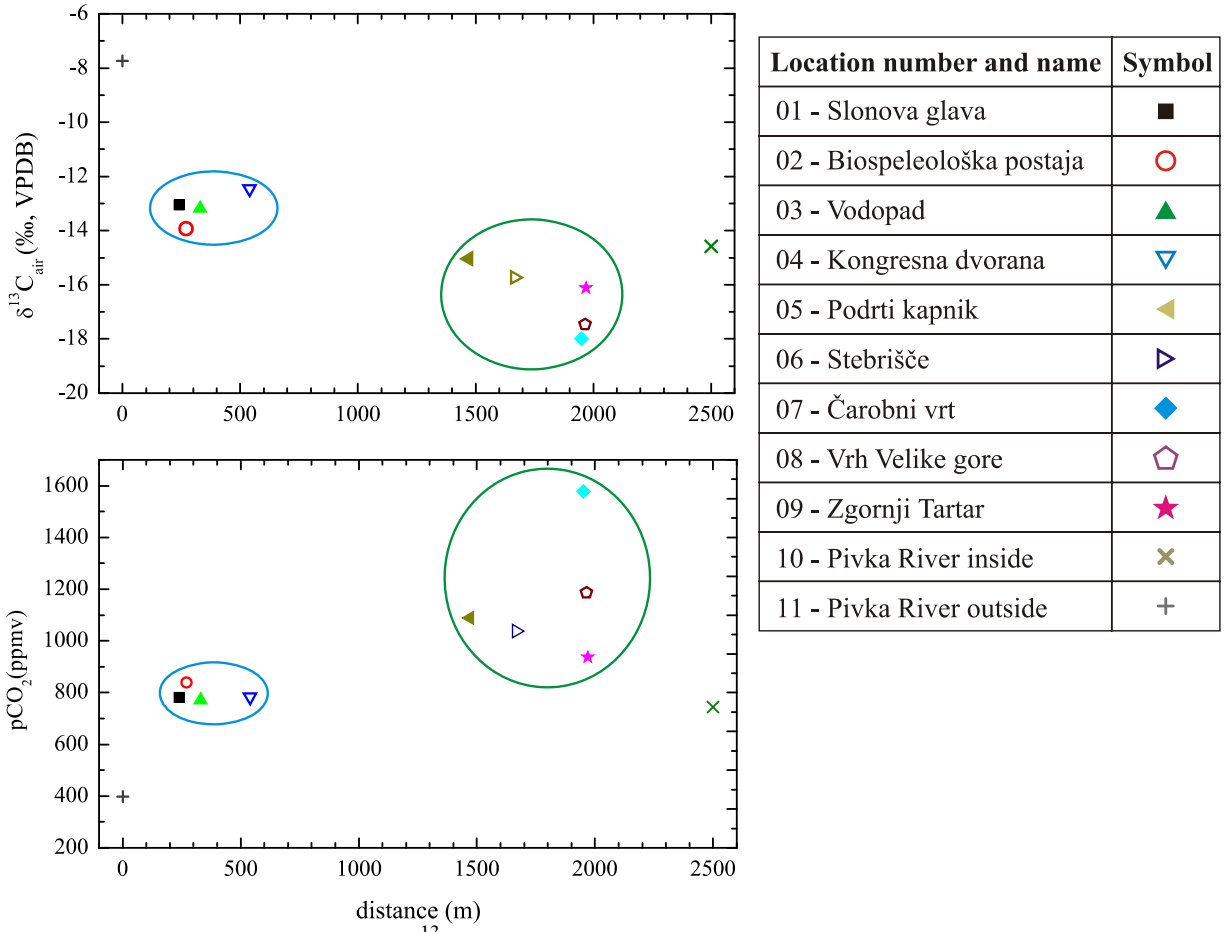

Figure 7.25 Concentrations of $\delta^{13}C_{air}$ and CO_2 in the cave air as a function of distance from the entrance.

Slika 7.25 $\delta^{13}C_{air}$ i CO_2 koncentracija u špiljskom zraku obzirom na udaljenost lokacije od ulaza.

Location 07 – Čarobni vrt, as described in chapter 0, is isolated from tourist visit and main cave passage, therefore it is not influenced with cave ventilation at location 08 – Vrh Velike gore which is in approximately the same distance from the main entrance as the location 07 – Čarobni vrt.

Carbon isotope composition (^{13}C and ^{14}C) of the cave air CO_2 has not been studied systematically in the past. Measured $\delta^{13}C$ and ^{14}C activity of CO_2 in the atmosphere outside

and in the cave air (at a single location) showed that $\delta^{13}C$ and $a^{14}C$[3] were lower inside the cave -9.3 ± 0.2 ‰ and 102.6 ± 1.6 pMC, respectively; than outside -8.0 ± 0.2 ‰ and 109.5 ± 1.1 pMC, and it was explained by contribution of soil CO_2 brought to the cave by drip water (Vokal, 1999; Horvatinčić et al., 1998). However, the soil CO_2 concentration was not measured so no further quantification was not possible.

A continuous one-year (July 2010 – July 2011) monitoring of pCO_2 at location 03 – Vodopad (Gabrovšek, unpublished, Figure 7.26) showed pronounced seasonal variation, with lower values (<600 ppmv) from Nov 2010 to May 2011, and higher in late summer (>1000 ppmv in Sept 2010). The mean pCO_2 was 600 ± 210 ppmv, in good agreement with our average values, having in mind only partially overlapping of monitoring periods, and the fact that our data present only several data in comparison to continuous monitoring of Gabrovšek.

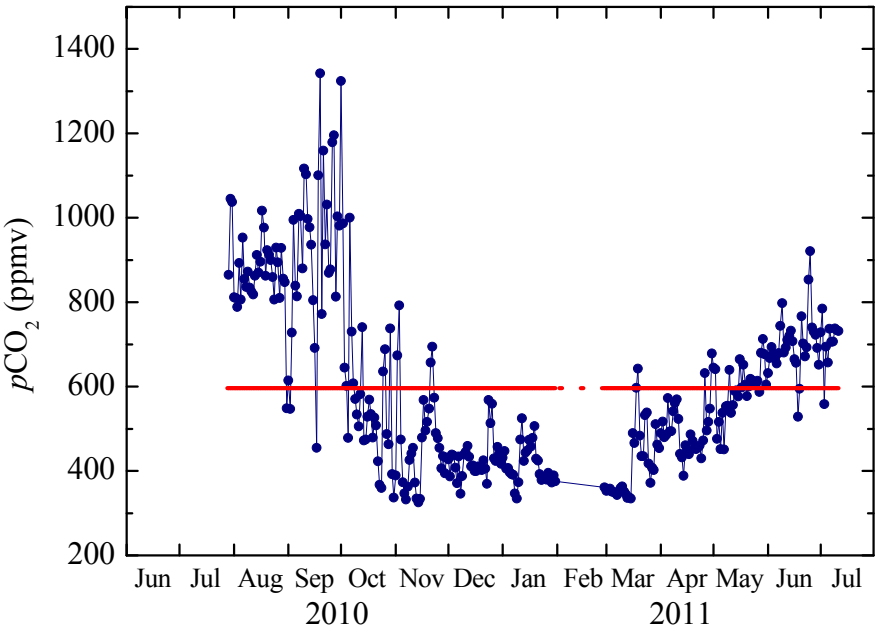

Figure 7.26 A continuous measurement of pCO_2 in period July 2010 – July 2011 at location 03 – Vodopad (Gabrovšek, unpublished).

Slika 7.26 Kontinuirano mjerenje pCO_2 u period od srpnja 2010 do srpnja 2011 na lokaciji 03 – Vodopad (neobjavljeni podaci, Gabrovšek).

[3] $a^{14}C$ is relative specific activity of ^{14}C. Specific activity of a sample, expressed in Bq/kg of carbon is divided by the specific activity of 226 Bq/kg C, which is supposed to be the specific activity of the atmosphere before anthropogenic influence in 20th century. $a^{14}C$ is a dimensionless quantity, but is usually expressed in percent, and such unit is called pMC, percet of Modern Carbon (Krajcar Bronić et al., 2010).

The data presented in Figures 7.22, 7.23 and 7.24 show that the carbon isotopic composition of cave-air CO_2 varies inversely with pCO_2. The relation between pCO_2 (in fact, $1/pCO_2$) and $\delta^{13}C$ is shown in Figure 7.27. A good correlation between the CO_2 concentration and its $\delta^{13}C$ value has been obtained indicating mixing of two sources of CO_2. In a simple mixing model with two sources of CO_2 it is assumed that the atmospheric CO_2 with $\delta^{13}C$ = -7.8 ‰ and pCO_2 of 398 ppmv (as determined here at location 11) is one source. The other source is isotopically lighter CO_2 produced by the decay of soil organic matter, as indicated by the regression shown in the Keeling plot (Figure 7.27). Carbon isotopic composition of soil organic matter and soil CO_2 was determined earlier by Vokal (1999) at two sampling locations above the Postojnska jama. Soil organic matter had average $\delta^{13}C$ value of -26.7 ‰, in accordance with the prevailing C3 plants in the karst region of Croatia and Slovenia (Krajcar Bronić et al., 1986, Vokal 1999, Šturm et al., 2012). Soil CO_2 is produced by decomposition of organic matter and by root respiration and its $\delta^{13}C$ differs by 2 – 4 ‰ from the $\delta^{13}C$ composition of the plant material from which it is produced (Clarck and Fritz, 1997, Amundson et al., 1998). The mean $\delta^{13}C$ values of CO_2 in soil above the Postojnska jama were -21.7 ‰ and -20.5 ‰ (Vokal, 1999).

Mathematically, the mixing model can be described as

$$p_{atm} \cdot \delta^{13}C_{atm} + (p_{meas} - p_{atm}) \cdot \delta^{13}C_x = p_{meas} \cdot \delta^{13}C_{air} \qquad 7.1$$

Here, p_{atm} and $\delta^{13}C_{atm}$ are the concentration (i.e., pCO_2 values) and stable isotope composition of atmospheric CO_2 (here, location 11), and p_{meas} and $\delta^{13}C_{meas}$ are the corresponding measured values for each location 01 to 09. The $\delta^{13}C_x$ is the carbon isotopic composition of the unknown end member, source of additional CO_2 inside the cave, which contributes to the difference between the measured pCO_2 and the atmospheric pCO_2. The $\delta^{13}C$ of the other end-member in the mixing equation is determined from the Keeling plot (Figure 7.27) and its value is -23.3 ± 0.7 ‰, in reasonable agreement with the measured $\delta^{13}C$ of soil CO_2 (Vokal, 1999), and therefore it may be concluded that inside the cave the soil CO_2 brought to the cave by drip water contributes to the CO_2 concentration in the cave. Figure 7.28 illustrates the relation between measured pCO_2 and $\delta^{13}C_{air}$ values (symbols) together with the $\delta^{13}C_{air}$ values of cave air calculated from equation 7.1 for variable $\delta^{13}C$ values of soil CO_2 between -20 and -30 ‰.

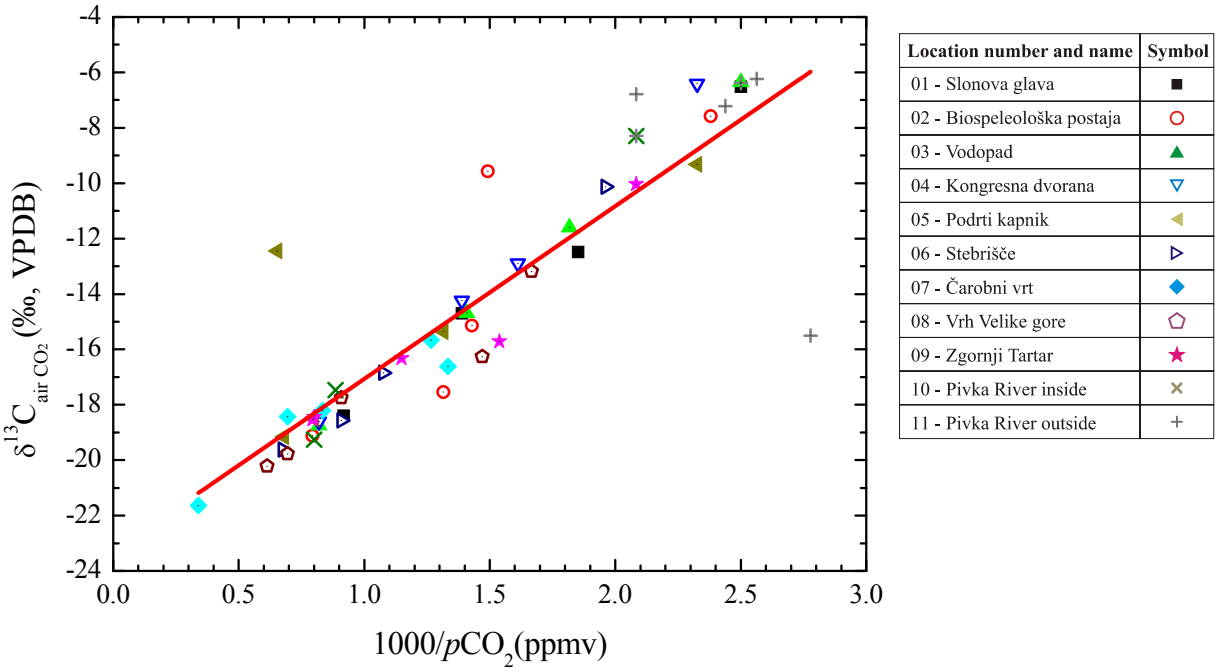

Figure 7.27 The Keeling plot of $\delta^{13}C$ in cave air vs. $1/pCO_2$

Slika 7.27 Odnos $\delta^{13}C$ u špiljskom zraku i recipročne vrijednosti pCO_2, tzv. Keelingov graf

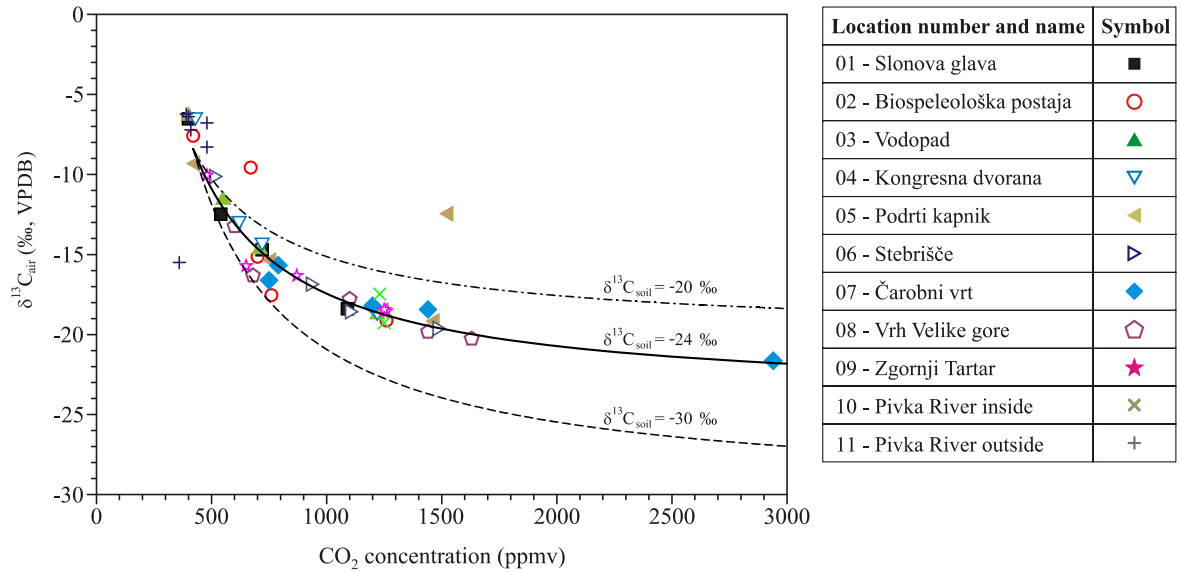

Figure 7.28 Relation between $\delta^{13}C_{air}$ and pCO_2 of individual measurements at all sampling locations. Lines represent the modeled $\delta^{13}C_{air}$ values (eq. 7.1) for different $\delta^{13}C$ of soil CO_2.

Slika 7.28 Odnos između različitih vrijednosti $\delta^{13}C_{air}$ i pCO_2 u pojedinačnim mjerenjima na različitim lokacijama. Linije predstavljaju modelirane $\delta^{13}C_{air}$ vrijednostizraka (jednadžba 7.1) za različite $\delta^{13}C$ vrijednosti CO_2 sadržanog u tlu.

As shown above, the main source of CO_2 in cave air is soil CO_2 brought to cave by drip water. Figure 7.29 shows the relation between the calculated concentration of aqueous CO_2 and pCO_2 in cave air at various locations. Even concentration/pressure of aqueous CO_2 is high

at locations 01 – 04, the pCO_2 in cave air is limited to about 1300 ppmv and does not depend on the concentration of aqueous CO_2. This may be explained by (efficient) air circulation/ ventilation at these locations close to the entrance. At inner locations 05 – 09, the concentration of aqueous CO_2 is generally lower but results in higher pCO_2 (up to 3000 ppmv) and the higher the CO_2 aq, the higher the pCO_2 in cave air. Significant correlation between pCO_2 and pCO_2(aq) with p > 0.08 is obtained only for locations 06, 07 and 08 (Table A.6 in Appendix). This effect can be explained by inefficient cave ventilation at inner locations.

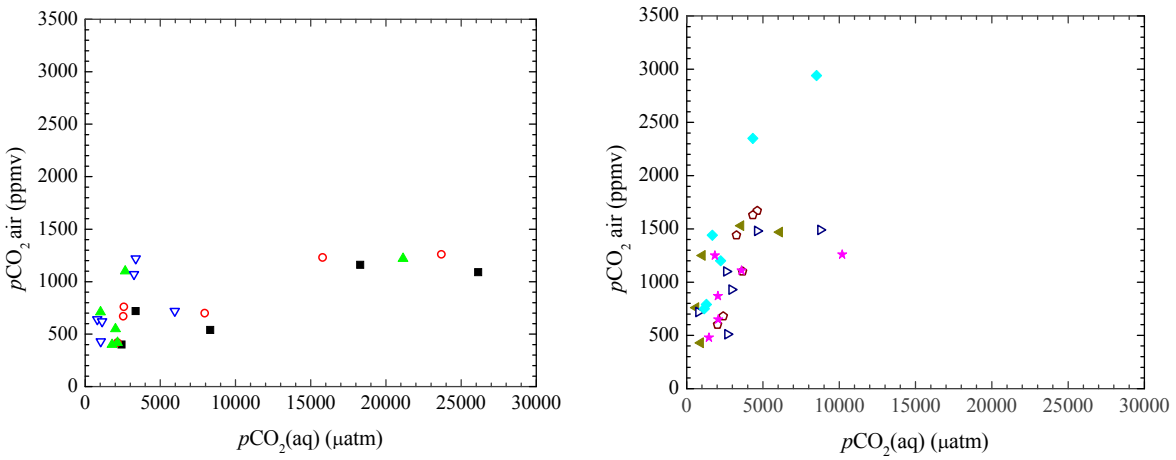

Figure 7.29 Calculated concentration of aqueous CO_2 and pCO_2 in cave air. Locations 01 – 04 on the left handside figure; locations 05 – 09 on right hand side figure.

Slika 7.29 Računata koncentracija pCO_2 (aq) i pCO_2 air Lokacije 01 – 04 prikazane su na lijevoj strani, dok su lokacije 05 – 09 prikazane na desnoj strani grafa.

In the period of high pCO_2 in cave air, the process of degassing CO_2 from drip water solution may be slowed down or even stopped (Spötl et al., 2005) and thus the speleothem formation may cease during such periods leading to the bias of the isotope record of speleothem towards growth season. To check if this situation is likely to occur in the Postojna cave, the relation between index of saturation I_{sat} and pCO_2 is shown for all sampling events in Figure 7.30. I_{sat} has higher values at low pCO_2 because then the gradient between the low pCO_2 in cave air and high pCO_2(aq) in drip water is high and degassing of CO_2 is intensive leading to high I_{sat} and calcite deposition. When the pCO_2 in cave air is high, the gradient is low and degassing is slower. However, I_{sat} becomes slightly <1 only exceptionally, and it may be concluded that calcite deposition is very seldom ceased in the Postojna Cave.

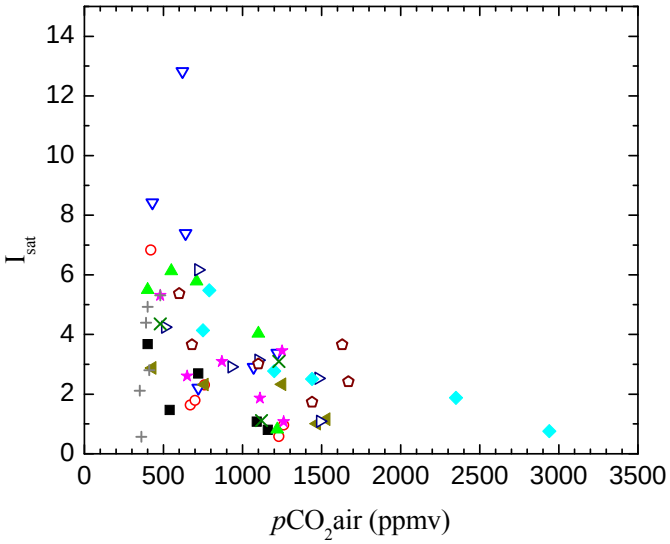

Location number and name	Symbol
01 - Slonova glava	■
02 - Biospeleološka postaja	○
03 - Vodopad	▲
04 - Kongresna dvorana	▽
05 - Podrti kapnik	◁
06 - Stebrišče	▷
07 - Čarobni vrt	◆
08 - Vrh Velike gore	⬠
09 - Zgornji Tartar	★
10 - Pivka River inside	×
11 - Pivka River outside	+

Figure 7.30 Relation between I_{sat} and pCO_2
Slika 7.30 Odnos između I_{sat} i pCO_2

Anthropogenic contribution to the excess of CO_2 concentration in the Postojna cave can not be completely neglected. Breathing of numerous tourists that visit the cave could increase the CO_2 concentration and change its $\delta^{13}C$ composition. The $\delta^{13}C$ of CO_2 in human breath reflects the source of organic matter that is used for food, and for Europeans it is in the range from -19.8 to -24.3 ‰ (Epstein and Zeiri, 1988). Therefore, the isotopic composition of human breath can not be distinguished from the $\delta^{13}C$ of soil CO_2 (-23.3 ± 0.7 ‰) determined by applying the binary mixing model (Figure 7.27). However, locations 01 – 04 that are mostly visited by the tourists have lower mean pCO_2 (794 ± 31 ppmv) and higher $\delta^{13}C_{air}$ values (-13.2 ± 0.6 ‰) than inner locations 05 – 09 (1185 ± 280 ppmv and -17.0 ± 0.9 ‰, respectively). Some of the inner locations (07, 08, 09) are even closed for tourists, and the highest mean pCO_2 values are determined at locations 07 and 08. Good correlation of pCO_2(aq) and pCO_2 is shown in Figure 7.29 for inner locations 05 – 09, while outer locations 01 – 04 do not show high pCO_2 although pCO_2(aq) is very high due to good ventilation of the area. All these facts lead to the conclusion that the athropogenic influence to pCO_2 in the cave is negligible.

7.6 Special case of location 05 – Podrti kapnik

Location 05 – Podrti kapnik has been often mentioned as an exception from all other locations by several characteristics: concentrations of Ca^{2+} and HCO_3^- are lower than at all other locations, as well as conductivity, while $\delta^{13}C$ of DIC is about 2 ‰ more positive. These discrepancies/deviations/exceptions have a consequence that various correlations between parameters are good for all other locations, while 05 is a special case (Ca concentration vs.

caprock thickness, conductivity vs. drip rate, $\delta^{13}C_{DIC}$ vs. pCO_2(aq), $\delta^{13}C_{DIC}$ vs. concentration of HCO_3^- (Figures 6.21, 7.8, 7.10, 7.12, 7.13, 7.14 and 7.15). Other characteristics are similar to other locations: temperature of water and cave air, drip rate, pH, Mg concentration, $\delta^{18}O$ of drip water.

Time series of measured parameters presented in Figure 6.6 show also some peculiar behavior. For example, in February 2011 exceptionally low concentrations of Ca^{2+} and HCO_3^- were measured, (470 mg/L and 121.7 mg/L, respectively) while Mg concentration did not change substantially, leading to higher Mg/Ca ratio (0.19). Consequently, low conductivity was also measured (197 μS/cm), as well as low drip rate, low pCO_2 (430 ppmv), high $\delta^{13}C_{DIC}$ (-5.64 ‰) and $\delta^{13}C$ of cave air (-9.32 ‰). Calculated value of I_{sat} is also low (1.94 ± 0.81).

Such a behavior of drip water parameters has been explained in literature by so-called prior calcite precipitation (PCP) (Section 3.7.2), i.e., the deposition of calcite in voids in the caprock during percolation of water to the drip site in the cave (Horvatinčić et al., 2003; Spötl et al., 2005; Fairchild et al., 2007; Fairchild, 2010 and references therein). The PCP is usually observed when the drip rate is low. The $\delta^{13}C_{DIC}$ in drip water after PCP is 2 ‰ – 7 ‰ more positive than without PCP (in case of drip water at 05 this enrichment is about 5 ‰), and a decrease in Ca^{2+} and HCO_3^-, as well as conductivity is expected. Since only calcite was deposited, concentration of Mg^{2+} remains the same as without PCP, leading to higher Mg/Ca ratio.

All these characteristics are observed at location 05 – Podrti kapnik. It is therefore justified to conclude that the reason for such an exceptional behaviour is the prior calcite precipitation in some voids or smaller caves in the caprock above the location 05. The effect is more pronounced during low drip rate, when the water level is low, and the voids are free of water.

Figure 7.31 shows the relation between aqueous pCO_2 and $\delta^{13}C_{DIC}$. In spite of relatively large range of aqueous pCO_2 values (400 – 30 000 μatm), there is no correlation of $\delta^{13}C_{DIC}$ at all locations other than 05. At location 05 the lower the pCO_2(aq), the higher the $\delta^{13}C_{DIC}$.

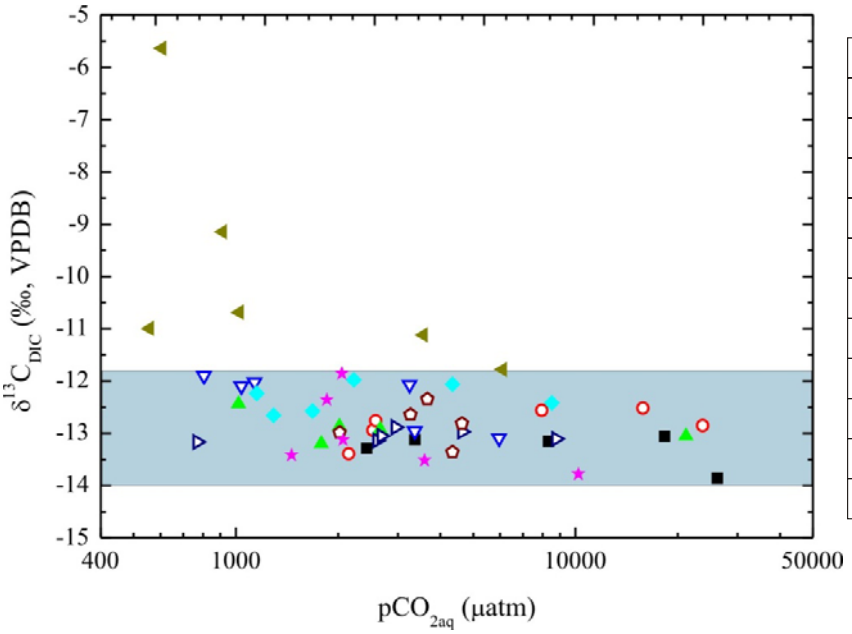

Location number and name	Symbol
01 - Slonova glava	■
02 - Biospeleološka postaja	○
03 - Vodopad	▲
04 - Kongresna dvorana	▽
05 - Podrti kapnik	◁
06 - Stebrišče	▷
07 - Čarobni vrt	◆
08 - Vrh Velike gore	⬠
09 - Zgornji Tartar	★
10 - Pivka River inside	×
11 - Pivka River outside	+

Figure 7.31 $\delta^{13}C_{DIC}$ vs. pCO_2(aq) values. Data at location 05 – Podrti kapnik show different behavior from data on other locations in blue area.

Slika 7.31 Odnos $\delta^{13}C_{DIC}$ i pCO_2(aq). Podaci za lokaciju 05 – Podrti kapnik razlikuju se od ostalih podataka mjerenih na drugim lokacijama (plavo područje vrijednosti).

The exception is $\delta^{13}C_{DIC}$ = -11.78 ‰ from 24 November 2010 when it is comparable to $\delta^{13}C_{DIC}$ of other locations. Drip rate in November 2010 (80 min^{-1}) was higher than mean drip rate of 56 min^{-1} (and higher than in February 2011, 22 min^{-1}), so it is reasonable to conclude that at that time water level was high enough to fill the voids with water and stop degassing of CO_2 and inhibiting PCP. Similar conclusions are valid also for correlation of $\delta^{13}C_{DIC}$ and pCO_2 in cave air (not shown).

Figure 7.32 present the relation between $\delta^{13}C_{DIC}$ and HCO_3^- concentration in drip waters. Although the range of individual HCO_3^- concentrations is rather wide, from 160 to 370 mg/L, the $\delta^{13}C$ values range from -14 ‰ to -12 ‰ at all locations except at 05, where HCO_3^- concentration is lower and $\delta^{13}C$ higher, even a correlation is relatively good (R = -0.76, p = 0.13, Table A.6). The reason for high $\delta^{13}C_{DIC}$ values may be degassing of isotopically light CO_2 in the voids, which turn the chemical equilibrium toward calcite deposition, and thus HCO_3^- and Ca^{2+} concentrations decrease while the remaining DIC has more positive $\delta^{13}C$ values, i.e., it remains heavier than before PCP occurred. The correlation between Ca^{2+} and $\delta^{13}C_{DIC}$ is also very good (R = -0.98, p = 0, Table A.6). In November 2010 during high water level (high drip rate) the $\delta^{13}C_{DIC}$ at location 05 is comparable with $\delta^{13}C_{DIC}$ at other locations, thus not showing PCP.

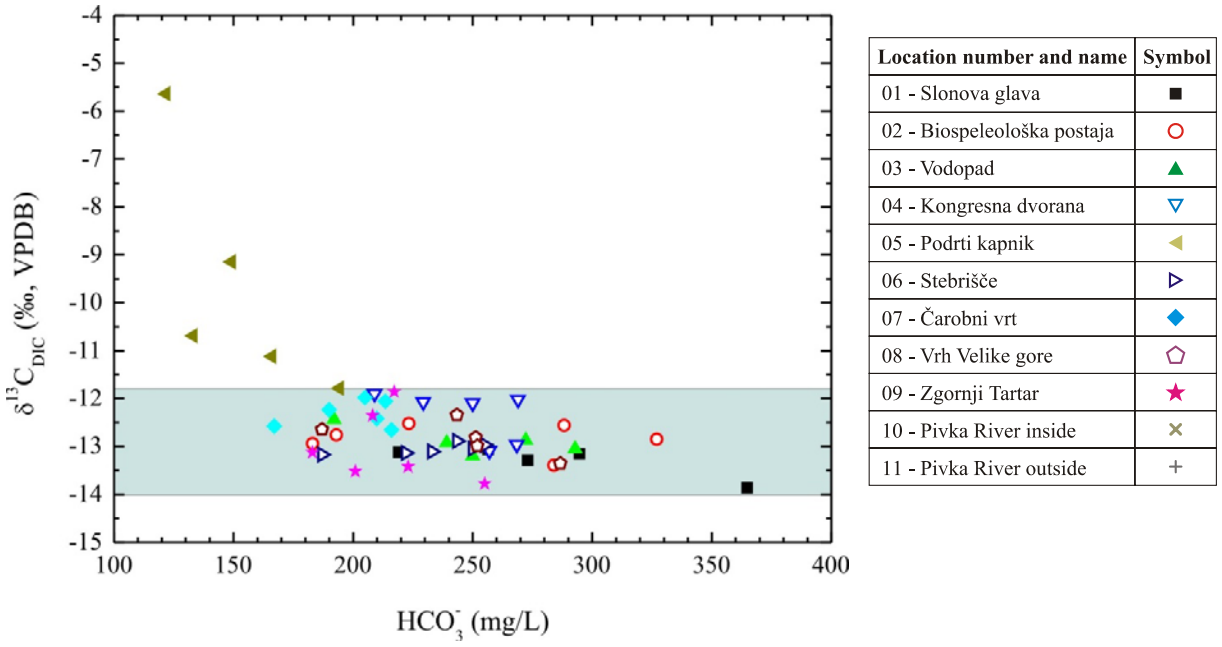

Figure 7.32 $\delta^{13}C_{DIC}$ vs. HCO_3^- values. Data at location 05 – Podrti kapnik show different behavior from data on other locations grouped in blue area.

Slika 7.32 Odnos $\delta^{13}C_{DIC}$ i HCO_3^-. Podaci za lokaciju 05 – Podrti kapnik razlikuju se od podataka mjerenih na drugim lokacijama (plavo područje vrijednosti).

At location Brilliant, that was studied by Vokal (1999), similar behaviour was observed. At location Brilliant concentration of Ca and HCO_3^- in drip water were lower (mean value 55.5 mg/L and 195.2 mg/L, respectively) than at locations Collorfull Gallery and Entrance (range 65.3 to 79.9 mg/L, and 194 to 233 mg/L, respectively. Conductivity was also lower 301 µS/cm at brilliant, 334 to 397 µS/cm at other locations) as well as I_{sat} (app. 1.3 compared to 2 – 3.2 otherwisde). However, the Mg/Ca ratio was higher (≈0.35) than at other locations 0.02), as well as $\delta^{13}C_{DIC}$ (-10.2 ‰ at Brilliant, from -12.7 to -14.7 ‰ other locations). While at other locations ratio Mg/Ca did not show seasonal variations, at Brilliant Mg/Ca ratio was lower during the rainfall when water level is high and higher during dry periods.Isotopic composition of water did not differ among the locations. All these characteristics are the same as the ones for location 05 – Podrti kapnik and can be explained by the prior calcite precipitation. However, such explanation was not given by Vokal (1999).

7.7 Recent carbonates

7.7.1 "Soda-straw" and watch-glass carbonates

As the first step in assessment whether the process of precipitation of modern carbonates occurs under isotopic equilibrium conditions, the difference in $\delta^{13}C$ in DIC and carbonate will be compared with the theoretical fractionation ε value for measured temperature. In section 2.4.1 and Figure 2.4 it was shown that the equilibrium fractionation factor ε between $\delta^{13}C_{DIC}$ and calcite that precipitates from DIC has the value of ~2.2 ‰ at temperature of about 10 ºC. In Figure 7.33 the expected range $\delta^{13}C$ values of carbonates in isotopic equilibrium with the $\delta^{13}C$ of the corresponding DIC is shown as green areas.

The Δ value, which will be compared with the equilibrium fractionation factor ε, is calculated as the difference between $\delta^{13}C$ values of the final and the initial products (equation 7.2), i.e., as the difference between the measured $\delta^{13}C$ of the precipitated carbonate and the $\delta^{13}C$ of the corresponding DIC:

$$\Delta = \delta^{13}C_{carb} - \delta^{13}C_{DIC} \qquad 7.2$$

If the Δ value is close to the ε value, it may be concluded that ^{13}C isotope indicates calcite deposition under isotopic equilibrium conditions. Table 7.3 contains calculated Δ values for carbonate samples deposited on watch glasses. Δ values range from -0.05 to 1.02 ‰ and are thus lower than the equilibrium ε value, as can be seen also from Figure 7.33.

Table 7.3 Δ values for samples of carbonates precipitated on watch glasses and calculated temperatures by using various approaches presented in Table 3.1

Tablica 7.3. Δ vrijednosti za uzorke karbonata taloženog na satnim staklima i temperature izračunate prema jednadžbama iz tablice 3.1

Location	$\Delta = (\delta^{13}C_{carb} - \delta^{13}C_{DIC})$ (‰)	Calculated temperatures (ºC)			
		Shackleton and Kennett, 1975	Grossman, 1982	Epstein and Mayeda, 1953	Craig, 1965
01	0.93	-5.6	-4.0	-4.1	-5.1
02	0.81	-5.6	-3.9	-4.1	-5.0
03	0.69	-4.1	-2.7	-2.9	-3.7
04	0.50	0.3	1.1	0.9	0.3
05	-0.05	-2.9	-1.7	-1.8	-2.6
06	1.02	-4.4	-3.0	-3.1	-4.0
09	0.69	-4.5	-3.0	-3.2	-4.0

Figure 7.33 illustrates $\delta^{13}C$ values of different carbonate samples, at different locations in Postojna Cave measured in this study compared with other data (Urbanc et al., 1987; Vokal, 1999; Horvatinčić et al., 2003). Sampling of the DIC (Vokal, 1999) was done at different locations than the ones monitored in this work. Locations are namely: Colorful gallery (C2), Entrance (C3) and Brilliant (C4). At location C1 – Biospeleoška postaja a stalagmite was sampled (Vokal, 1999). The lowest $\delta^{13}C_{DIC}$ value is measured at location Colorful gallery (C2), -14.4‰, while at C3 and C4 the $\delta^{13}C_{DIC}$ values are comparable with the present ones, C4 (Brilliant resembling location 05 – Podrti kapnik). The expected $\delta^{13}C$ values of carbonate that would precipitate from the DIC under isotopic equilibrium condition (green shapes) are calculated by using the equilibrium ε value of 2.2 ‰. If the $\delta^{13}C$ values of any type of the deposited carbonates overlap with the green rectangle, it would mean that the carbon isotopic composition of DIC and the carbonate are in isotopic equilibrium. The overlapping of equilibrium $\delta^{13}C$ value and soda straw $\delta^{13}C$ value is found at location 03, and at location 07 the overlap is almost achieved, while the gap between the equilibrium (green) and measured $\delta^{13}C$ of "soda straws" (blue) is observed at other location. $\delta^{13}C$ values of watch glass carbonates are lower than the equilibrium value and are close to $\delta^{13}C$ values of DIC.

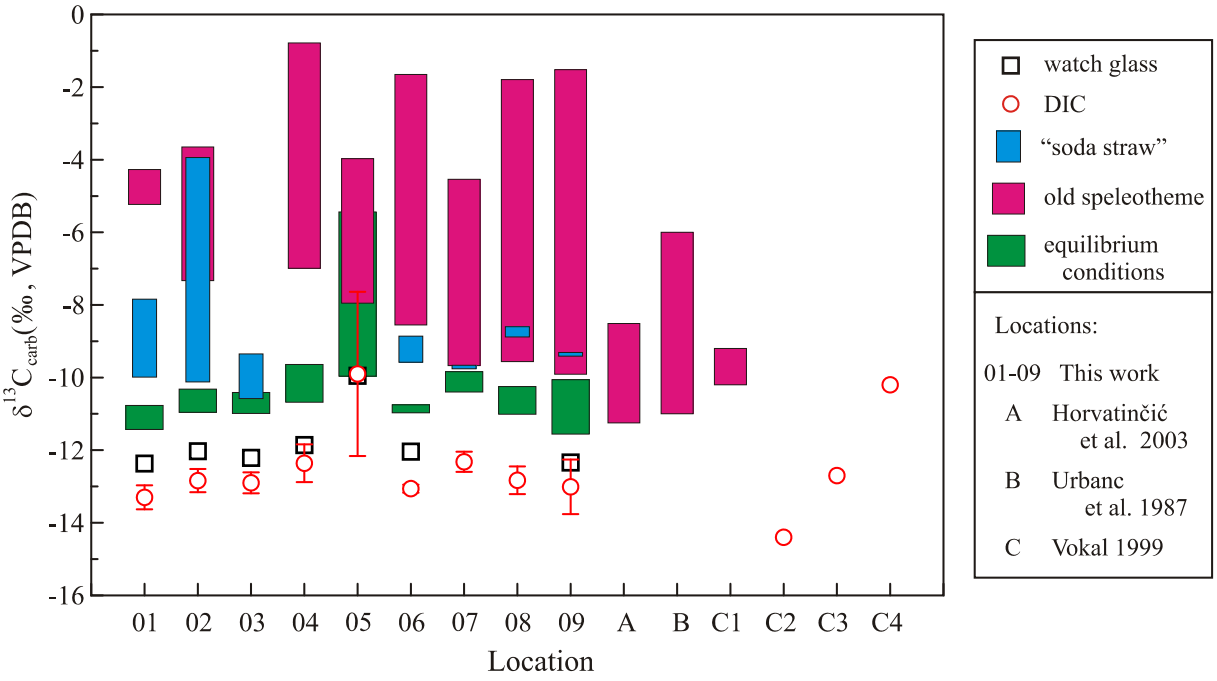

Figure 7.33 $\delta^{13}C$ values of DIC and various carbonate samples at different locations.
Slika 7.33 $\delta^{13}C$ vrijednosti za DIC i različite uzorke karbonata na raznim lokacijama u Postojnskoj jami. Usporedba s podacima iz literature.

Similarly, Figure Figure 7.34 presents values of $\delta^{18}O$ for water and different carbonate samples at various locations in Postojna Cave. There are two different scales, VPDB and VSMOW, for carbonate samples and drip water, respectively. Values of $\delta^{18}O$ of watch glass carbonates are the most positive, i.e., isotopically the haviest. On most locations $\delta^{18}O$ values of "soda straw" samples fall within the $\delta^{18}O$ range of old speleotheme samples. $\delta^{18}O$ values of drip water have similar range in this work and in Vokal (1999).

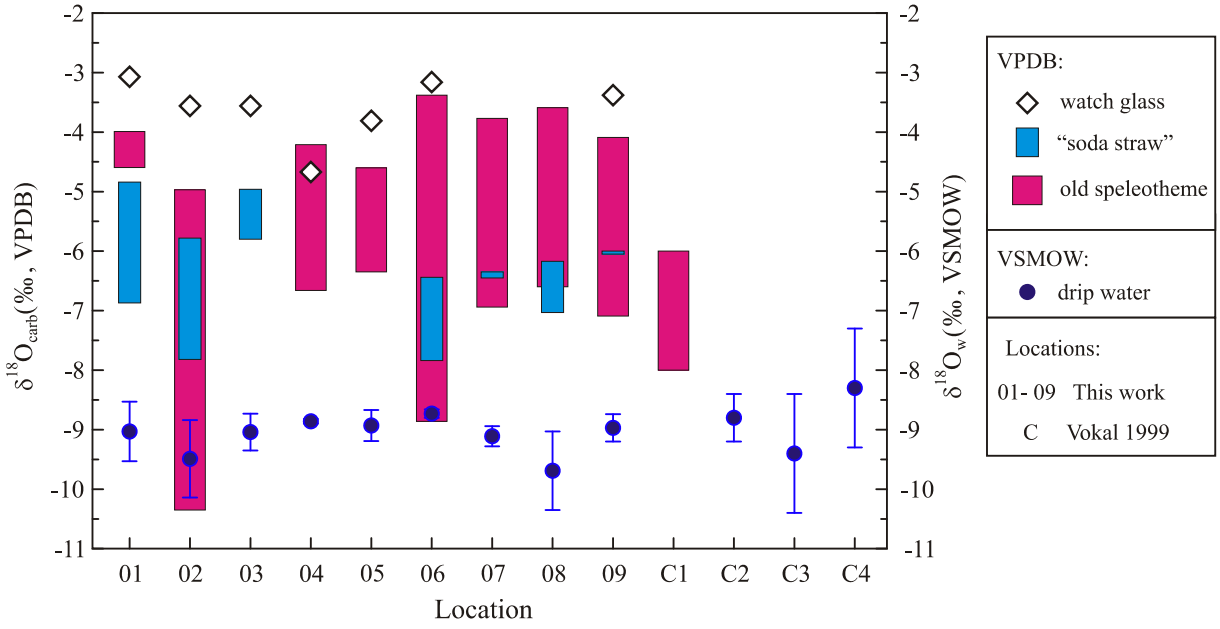

Figure 7.34 $\delta^{18}O$ of drip water and carbonates at different sampling locations.
Slika 7.34 $\delta^{18}O$ prokapnice i karbonata na raznim lokacijama lokacijama uzorkovanja.

How can the isotope composition of carbonate precipitated on watch glasses be explained? If carbonate precipitation on watch glasses had occurred under fast CO_2 degassing, i.e., kinetic fractionation conditions, both $\delta^{13}C$ and $\delta^{18}O$ of values should be shifted toward more positive values (Hendy, 1971; Gonfiantini et al., 1968; Horvatinčić et al., 2003; Mickler et al., 2004). However, the $\delta^{13}C_{WG}$ values are negative and close to the $\delta^{13}C_{DIC}$ values, while $\delta^{18}O_{WG}$ are enriched (more positive). The process causing such values is desribed as the incorporation of HCO_3^-(aq) into calcite during rapid, almost instantaneous, mineral precipitation, such that isotopic fractionation in both $\delta^{18}O$ and $\delta^{13}C$ is minimized (Michaelis et al., 1985; Clark and Lauriol, 1992; Mickler et al., 2004). As a result, $\delta^{13}C$ values of modern calcite differ from the predicted equilibrium values. They tend towards $\delta^{13}C$ values lower than the equilibrium values, and in some cases are equivalent to the carbon isotopic compositions of DIC. The $\delta^{18}O$ value of rapidly precipitated carbonate reflects the $\delta^{18}O$ composition of HCO_3^- from water, but it is difficult to measure this value. The difference between $\delta^{18}O$ of HCO_3^- and

precipitated carbonate in equilibrium is about 6 ‰, but under rapid precipitation it is much lower and approaches 0 % (Mickler et al., 2004). The use of glass plates as a non-destructive method for modern calcite deposition studies should enable a study of speleothem deposition conditions in a very defined time periods and assessment of the extent to which calcite achieves O and C isotopic equilibrium in the modern system. However, the isotopic composition of carbonate precipitated on watch glasses in Postojna cave was significantly different than the naturally deposited carbonates and the applications of watch glasses did not contribute to the assessment of equilibrium conditions probably because the artificial glass substrate changed the details of the calcite deposition process.

The values of fractionation factor α are calculated from measured $\delta^{18}O_{carb}$ and $\delta^{18}O_{water}$ values by using equation 3.17, where $\delta^{18}O_{carb}$ relative to VPDB scale where converted to values relative to VSMOW scale by using equation 2.12. The α values are then compared to the equilibrium values α_{eq} obtained from various equations of type B (Table 3.1). The results are shown in Table 7.4.

Table 7.4 Equilibrium α value (α_{eq}) calculated by different equations of type B (Table 3.1, Section 3.5) and by $\delta^{18}O$ for modern carbonates. Orange-shaded cells represent $\alpha = \alpha_{eq}$
Tablica 7.4 Ravnotežni faktor frakcionacije α izračunat iz jednadžbi tipa B (Tablica 3.1) i iz $\delta^{18}O$ za uzorke modernih karbonata. Narančasto obojene ćelije označavaju $\alpha = \alpha_{eq}$

		Equilibrium α values, α_{eq}						α values for recent carbonates in the Postojna Cave		
Location	t_{air} (°C)	O'Neil et al., 1969; Kim and O'Neil, 1997; Horita and Clayton, 2007	Friedman and O'Neil, 1977	Kim et al., 2007	Coplen, 2007	Chacko and Deines, 2008	Tremaine et al., 2011	"Soda straw"	Carbonate deposited on watch glasses	Peculiar growth types
01	9.8	1.0318	1.0323	1.0331	1.0334	1.0318	1.0328	1.0345	1.0371	1.0360
02	9.9	1.0318	1.0323	1.0331	1.0334	1.0317	1.0328	1.0341	1.0371	-
03	9.7	1.0318	1.0324	1.0331	1.0335	1.0318	1.0328	1.0347	1.0366	-
04	10.3	1.0317	1.0322	1.0330	1.0333	1.0317	1.0327	-	1.0353	-
05	11.1	1.0315	1.0320	1.0328	1.0332	1.0315	1.0326	-	1.0362	-
06	11.3	1.0314	1.0320	1.0327	1.0331	1.0314	1.0325	1.0326	1.0367	-
07	10.7	1.0316	1.0321	1.0329	1.0332	1.0316	1.0326	1.0337	-	-
08	11.6	1.0314	1.0319	1.0327	1.0330	1.0313	1.0325	1.0337	-	-
09	10.7	1.0316	1.0321	1.0329	1.0332	1.0316	1.0326	1.0341	1.0367	1.0332
	10.6	1.0316	1.0322	1.0329	1.0333	1.0316	1.0327	1.0340	1.0365	1.0346

For any applied equation the α_{eq} value decreases as temperature increases, demonstrating that isotopic fractionation is more pronounced at lower temperatures (section 2.3.1). For a given temperature, the lowest equilibrium α value is predicted by approhes of O'Neil et al. (1969); Kim and O'Neil (1997), Horita and Clayton (2007) and Chacko and Deines (2008), while the highest α_{eq} values are obtained by equations of Coplen (2007) and Kim et al. (2007).

The α values obtained for carbonate deposited on watch glasses are much higher than any equilibrium α value, indicating (strong) non-equilibrium conditions of deposition, and also suggest that the temperatures of carbonate deposition calculated by using equations of type A from Table 3.1 will be very low (much lower than the actually measured ones).

Estimation of equilibrium conditions from $\delta^{13}C$ values for soda straw samples is presented in Table 7.5. Some samples from location 02 – Biospeleološka postaja, 03 – Vodopad, and 07 – Čarobni vrt indicate equilibrium conditions, $\varepsilon < \Delta < 3$. Other Δ values range from 3.31 to 8.90 ‰ and are higher than equilibrium ε value.

The α values calculated from measured $\delta^{18}O$ values for soda straw samples are higher than the equilibrium α values at all sampling locations except at 06 – Stebrišče (Table 3.4). The α value for soda straws at location 06 – Stebrišče, 1.0326, agrees best with the equilibrium α value of 1.0325 (by using equation of Tremaine et al., 2011) and 1.0327 (Kim et al., 2007). Such values suggest that the only soda straws from location 06 are deposited under isotopic equilibrium conditions. The calculated a values are compared by α_{eq} in Figure 7.36.

Temperature of precipitation/formation of different speleothem shapes determined by various equations of type A is presented in Tables 7.2 to 7.7 for each shape separately are summarized in Figure 7.35. The calculated temperature at all locations is too low compared to the present measured air temperature. The lowest temperature 0.3 ºC is calculated by the Shackleton and Kennett (1975) and Craig (1957) paleotemperature equations at location 01 – Slonova glava and the highest temperature of 13.1 ºC is calculated after Shackleton and Kennett (1975) paleotemperature equation (Tabele 7.5).

The lines shown in Figure 7.35 represent the ideal case, i.e., if the calculated temperatures of carbonate precipitation is equal to the measured temperature. Different approaches applied to the same sample result in slightly different calculated temperatures, and among them the paleotemperature equation of Grossman (1982) gives the smallest deviation from the measured temperature, and that of Shackleton and Kennett (1975) the largest, but the differences among various equations are less than 1 ºC. The calculated temperatures by

applying any of the mentioned equations are mostly lower than the measured ones . Only a few “soda straw” samples give temperature similar to the measured one.

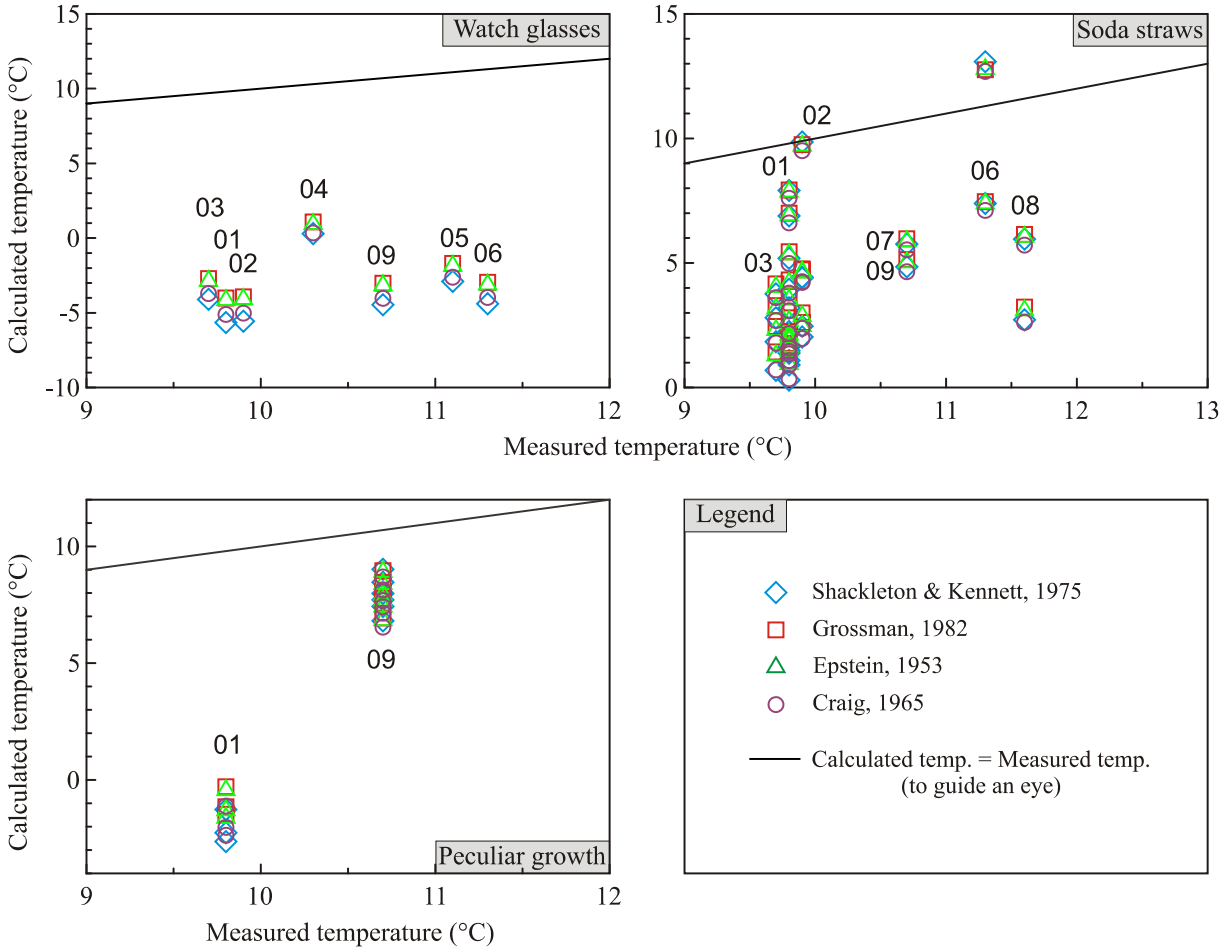

Figure 7.35 Calculated (equations of type A) and measured temperatures from different modern speleothem shapes. Strait line is plotted only to guide an eye and shows equal measured and calculated temperature.

Slika 7.35 Računate i izmjerene temperature različitih vrsta modernih karbonatnih uzoraka. Ravna linija predstavlja idealan slučaj kada je računata temperatura jednaka izmjerenoj temperaturi.

Table 7.5 Δ values for "soda straw" samples and calculated temperatures by using various approaches presented in Table 3.1
Tablica 7.5 Δ vrijednosti za uzorke slamčica i temperature izračunate prema jednadžbama iz Tablice 3.1

ID	$\Delta = (\delta^{13}C_{carb} - \delta^{13}C_{DIC})$ (‰)	Calculated temperatures (°C)						
		Epstein and Mayeda, 1953	Craig, 1965	Shackleton and Kennett, 1975	Grossman, 1982	Mulitza et al., 2003	Leng and Marshall, 2004	Andrews, 1994,1997
01 – Slonova glava								
1-1-a	4.38	4.2	3.8	3.9	4.3	1.4	0.0	3.0
1-1-b	4.73	2.7	2.2	2.2	2.8	-0.4	-1.9	1.4
1-1-c	5.36	2.1	1.6	1.6	2.3	-1.0	-2.5	0.8
1-1-d	4.25	6.9	6.6	6.9	7.0	4.4	3.2	5.9
1-2-a	4.32	1.9	1.4	1.4	2.0	-1.3	-2.8	0.6
1-2-b	3.76	2.0	1.5	1.5	2.1	-1.2	-2.7	0.7
1-2-c	5.46	1.5	0.9	0.9	1.6	-1.8	-3.3	0.1
1-2-d	3.94	5.3	5.0	5.2	5.5	2.7	1.4	4.2
1-3-a	3.58	3.5	3.1	3.2	3.7	0.6	-0.8	2.3
1-3-b	4.47	1.6	1.1	1.1	1.8	-1.6	-3.1	0.3
1-3-c	4.08	7.9	7.6	7.9	7.9	5.4	4.3	6.8
1-3-d	3.31	0.9	0.3	0.3	1.1	-2.4	-4.0	-0.5
mean	4.30	3.4	2.9	3.0	3.5	0.4	-1.0	2.1
02 – Biospeleološka postaja								
2-1	8.90	9.7	9.5	9.9	9.7	7.4	6.4	8.8
2-2	4.00	4.6	4.2	4.4	4.7	1.8	0.5	3.4
2-3	4.23	2.9	2.4	2.5	3.0	-0.1	-1.6	1.6
2-4	3.76	2.5	2.0	2.0	2.6	-0.6	-2.1	1.2
2-5	2.72	4.7	4.3	4.4	4.8	1.9	0.5	3.5
mean	4.72	4.9	4.5	4.6	5.0	2.1	0.7	3.7
03 – Vodopad								
3-1	2.32	1.3	0.7	0.7	1.4	-2.0	-3.6	-0.1
3-2	2.32	4.0	3.6	3.8	4.2	1.2	-0.2	2.8
3-3	2.92	2.3	1.8	1.8	2.4	-0.8	-2.3	1.0
3-4	3.55	3.2	2.7	2.8	3.3	0.2	-1.3	1.9
mean	2.78	2.7	2.2	2.3	2.8	-0.3	-1.8	1.4
06 – Stebrišče								
6-3	4.20	7.4	7.1	7.4	7.5	4.9	3.7	6.3
6-4	3.48	12.8	12.7	13.1	12.8	10.6	9.8	11.9
07 – Čarobni vrt								
7	2.61	5.9	5.5	5.8	6.0	3.2	2.0	4.8
08 – Vrh Velike gore								
8-1	4.23	6.1	5.7	6.0	6.1	3.4	2.2	5.0
8-2	3.95	3.1	2.6	2.7	3.2	0.1	-1.3	1.8
09 – Zgornji Tartar								
9	3.65	5.0	4.7	4.8	5.1	2.3	1.0	3.9

7.7.2 The "peculiar" speleothems types

The Δ values and temperatures of carbonate precipitation for these two types of speleothems are shown in Table 7.6. For both groups the Δ values are higher than ε, indicating the absence of isotopic equilibrium conditions. At the location 01 – Slonova glava calculated temperature values are all negative, due to the wind and outside air influence (Horvatinčić et al., 2003). Calculated temperatures are too low by as much as 12 ºC (Figure 7.40). At location 09 – Zgornji Tartar calculated temperatures are close to mean annual air temperature (10.7 ± 0.7 ºC), although Δ values indicated that there are no isotopic equilibrium conditions.

For samples of peculiar growth types at location 09 – Zgornji Tartar calculated α values agree with approach of Coplen (2007) (Table 7.4). At location 01 – Slonova glava all α values are higher indicating non equilibrium conditions.

Table 7.6 Δ values for two peculiar growth type samples and calculated temperatures by using various approaches of type A presented in Table 3.1
Tablica 7.6 Vrijednosti Δ za uzorke specifičnog oblika i temperature izračunate prema jednadžbama tipa A iz Tablice 3.1

ID	$\Delta = (\delta^{13}C_{carb}-\delta^{13}C_{DIC})$ (‰)	Calculated temperatures (ºC)			
		Shackleton and Kennett, 1975	Grossman, 1982	Epstein and Mayeda, 1953	Craig, 1965
01 – Slonova glava					
1a	9.03	-1.3	-0.3	-0.4	-1.1
1b	8.07	-2.6	-1.5	-1.6	-2.4
1c	8.65	-2.3	-1.1	-1.3	-2.0
mean	8.50	-2.1	-1.0	-1.1	-1.8
09 – Zgornji Tartar					
9OH1-U	7.23	6.8	6.9	6.8	6.5
9OH2-U	7.44	9.0	9.0	8.9	8.7
9OH3-U	7.49	8.5	8.4	8.4	8.1
mean	7.39	8.1	8.1	8.0	7.8
9OH1-V	6.83	7.4	7.5	7.4	7.1
9OH2-V	6.78	8.0	8.0	7.9	7.7
9OH3-V	5.51	7.7	7.8	7.7	7.4
mean	6.37	7.8	7.8	7.8	7.4

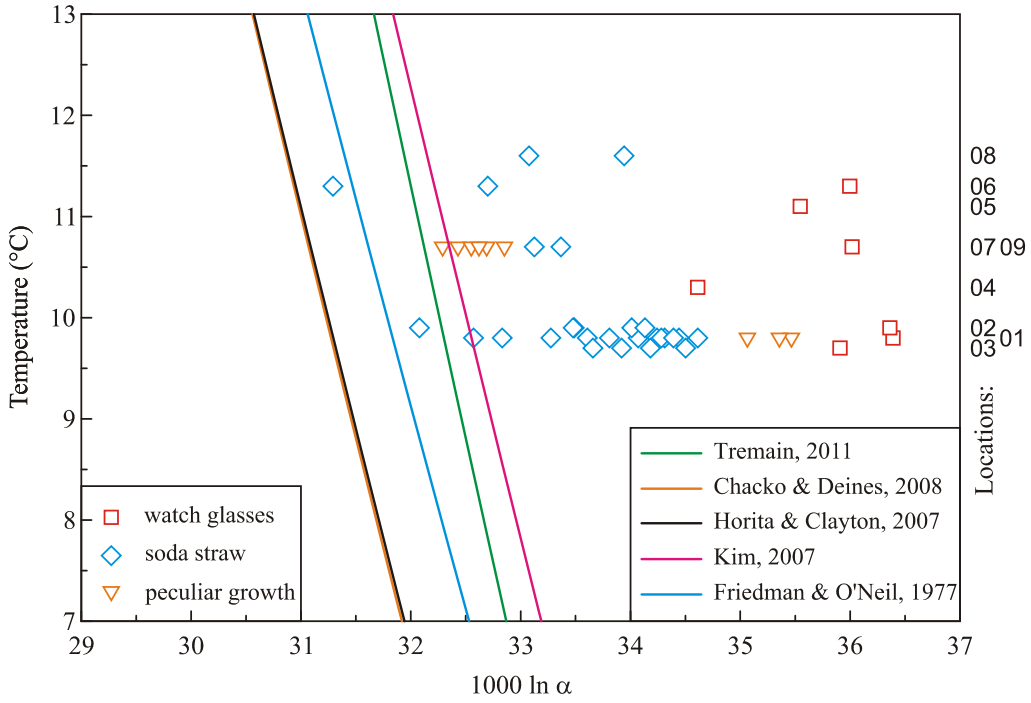

Figure 7.36 Fractionation factor 1000 ln α obtained from measured $\delta^{18}O$ values by various approaches of type B (from Table 3.1) for *in situ* measured temperature (symbols) and equilibrium 1000 ln α values obtained by various approaches (lines) for watch glasses, soda straw and peculiar growth type of samples.

Slika 7.36 Vrijednosti faktora frakcionacije (1000 ln α) izračunate iz mjerenih $\delta^{18}O$ vrijednosti i *in situ* mjerene temperature (simboli) uspoređene s ravnotežnim faktorom frakcionacije (linije) prema različitim jednadžbama tipa B (Tablica 3.1) za uzorke karbonata taloženog na satnim staklima, "slamčice" i uzorke čudnovatog rasta.

7.8 Old carbonates

Comparison of isotopic composition of various types of "old" speleothems (stalactites, flowstones, drilled core of stalagmites) described in chapters 5 and 6, with the equilibrium fractionation factors is performed in the same way as that for recent carbonates. Old speleothems have been deposited during unknown longer deposition period which can implicate differences in cave temperature, as well as in the vegetation in the area.

7.8.1 Flowstones

The difference between measured $\delta^{13}C_{DIC}$ and $\delta^{13}C_{carb}$ (Δ) is shown in Table 7.7. The mean $\delta^{13}C_{DIC}$ values from Table A.5 and $\delta^{13}C_{carb}$ from Tables A.11 and A.12 in Appendix I are used for calculation of Δ.

Table 7.7 Δ values for flowstone samples and calculated temperatures by using various approaches presented in Table 3.1
Tablica 7.7 Δ vrijednosti za stalaktite i temperature izračunate prema jednadžbama iz Tablice 3.1

ID	$\Delta = (\delta^{13}C_{carb} - \delta^{13}C_{DIC})$ (‰)	**Calculated temperatures** (°C)			
		Shackleton and Kennett, 1975	Grossman, 1982	Epstein and Mayeda,1953	Craig, 1965
04 – Kongresna dvorana					
4-2-1	5.37	0.8	1.6	1.4	2.1
4-2-2	9.34	-1.3	-0.3	-0.5	0.2
4-2-3	9.87	7.7	7.8	7.7	8.3
4-2-4	11.58	4.4	4.8	4.7	5.3
4-2-5	10.85	2.1	2.7	2.6	3.2
mean	9.40	1.7	3.3	3.2	3.8
05 – Podrti kapnik					
5-1	1.95	6.5	6.7	6.6	7.2
5-2	2.32	1.4	2.0	1.9	2.5
5-3	3.63	2.2	2.7	2.6	3.2
5-4	5.22	3.8	4.2	4.0	4.7
5-5	4.02	1.8	2.4	2.3	2.9
5-6	5.42	0.1	0.9	0.7	1.4
5-7	5.93	3.0	3.5	3.4	4.0
5-S	3.86	2.9	3.4	3.3	3.9
mean	4.04	2.7	3.2	3.1	3.7
06 – Stebrišče					
6-1r	7.72	3.5	3.9	3.8	4.4
6-2r	9.49	5.7	5.9	5.8	6.4
6-3r	6.81	3.8	4.2	4.0	4.7
6-4r	11.04	0.1	0.9	0.8	1.4
6-5r	9.27	-0.9	0.1	-0.1	0.6
6-6r	8.67	-0.2	0.7	0.5	1.2
6-7r	10.6	-1.1	-0.2	-0.3	0.3
6-8r	9.32	-3.7	-2.3	-2.5	-1.8
6-9r	7.26	-1.3	-0.3	-0.5	0.2
6-Sr	6.86	-0.4	0.5	0.3	1.0
mean	8.70	0.6	1.3	1.2	1.8

At location 04 – Kongresna dvorana the Δ values range from 11.58 to 5.37 ‰, at location 05 – Podrti kapnik from 8.39 to 3.86 ‰ and at location 06 – Stebrišče from 11.04 to 6.81 ‰. These differences are larger than if the carbonate precipitated under equilibrium conditions

and suggest that precipitation occurred under kinetic conditions. Under such conditions the temperature of precipitation calculated by using measured $\delta^{18}O$ values ($\delta^{18}O_{water}$ and $\delta^{18}O_{carb}$ from TablesA.5 and A.11 and A.12, Appendix I) and paleotemperature equations (section 3.5) would not reflect the measured cave temperature (Figures 7.37 aand 7.38). The results are shown in Table 7.5 for several paleotemperature equations. As expected, the obtained temperatures show a wide range of values, from -3.67 to 7.75 (8.29 ºC, by Craig (1965)), and all values are much lower than the present-day mean cave temperature of 10.7 ºC, or mean temperatures of 10.3 ºC, 11.1 ºC and 11.3 ºC at locations 04, 05 and 06, respectively (see Table 9.1 in Appendix I). On each locations the lowest values for (ed) temperatures have been calculated by Shackleton and Kennett (1975), from -1.3 to 7.7 ºC and the highest by Craig (1965), from 0.2 to 8.3 ºC.

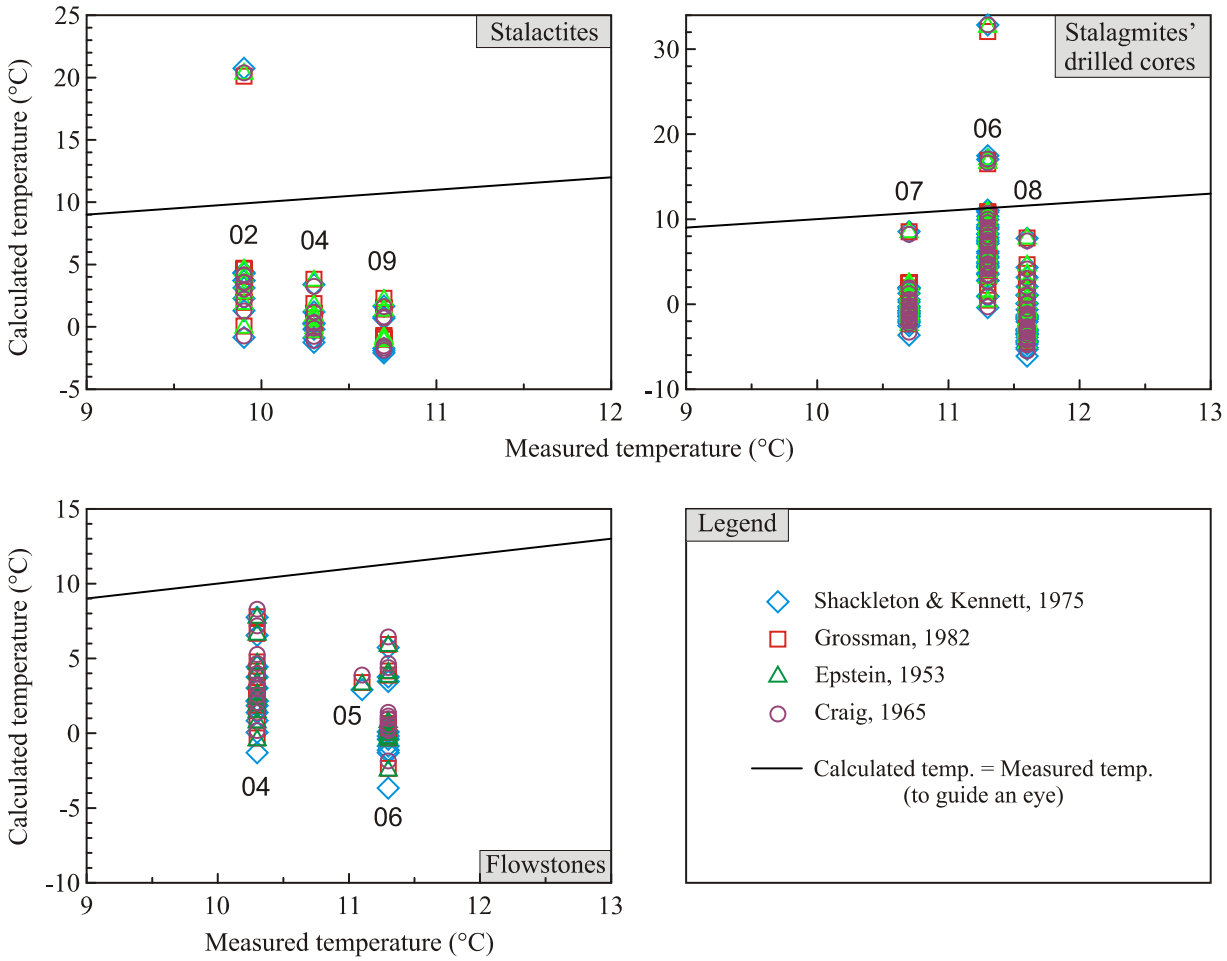

Figure 7.37 Calculated and measured temperatures from different old speleothem shapes described in previous sections. Strait line is plotted only to guide an eye and shows equal measured and calculated temperature.

Slika 7.37 Računate i mjerene temperature različitih vrsta siga opisanih u prijašnjem poglavlju. Ravna linija predstavlja idealan slučaj kada je mjerena temperatura jednaka računatoj temperaturi.

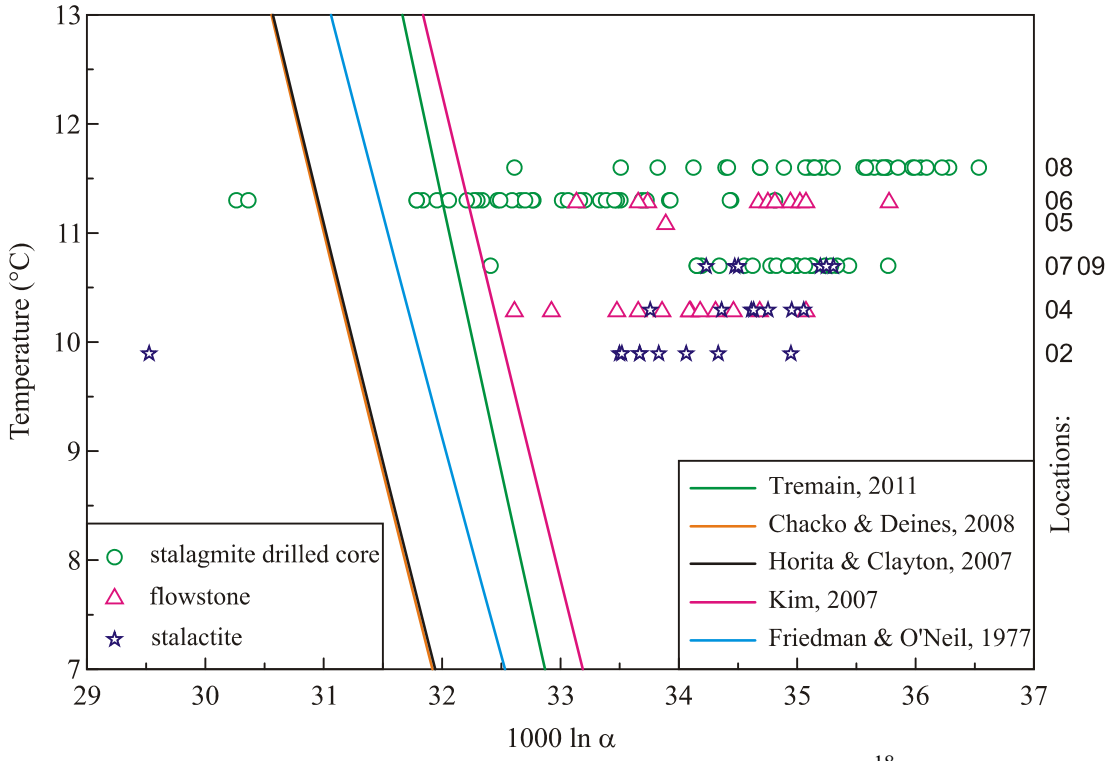

Figure 7.38 .Fractionation factor 1000 ln α obtained from measured $\delta^{18}O$ values by various approaches of type B (from table 3.1) for *in situ* measured temperature (symbols) and equilibrium 1000 ln α values obtained by various approaches (lines) for drilled speleothems, flowstone and stalactites.

Slika 7.38 Vrijednosti faktora frakcionacije (1000 ln α) izračunate iz mjerenih $\delta^{18}O$ vrijednosti i *in situ* mjerene temperature (simboli) uspoređene s ravnotežnim faktorom frakcionacije (linije) prema različitim jednadžbama tipa B (Tablica 3.1) za bušene stalagmite, sigovinu i stalaktite.

7.8.2 Stalactites

Estimation of equilibrium conditions for carbonate precipitation, calculation of Δ, gives large values ranging from 3.10 to 11.49 ‰ (Table 7.8). Both these values are found for sample from location 09 – Zgornji Tartar. Calculation of paleotemperature gives temperature in range from -2.1 to 4.4 ºC, with excursion value of 20.7 ºC for sample from location 02 – Biospeleološka postaja, which is obtained with -10.35 ‰ $\delta^{18}O$ value, commented previously.

The Δ values indicate non-equilibrium precipitation of stalactites (Table 7.6), and the calculated temperatures of carbonate precipitation are very low and do not agree with the measured temperature (Slika 7.43). These facts lead to the conclusion that neither of the stalactites could be used in paleotemperature studies.

Table 7.8 Δ values for stalactite samples and calculated temperatures by using various approaches presented in Table 3.1
Tablica 7.8 Δ vrijednosti za stalaktite i temperature izračunate prema jednadžbama iz Tablice 3.1

ID	$\Delta = (\delta^{13}C_{carb} - \delta^{13}C_{DIC})$ (‰)	Calculated temperature (°C)			
		Shackleton and Kennett, 1975	Grossman, 1982	Epstein and Mayeda, 1953	Craig, 1965
02 – Biospeleološka postaja					
ST2-1-1	9.19	3.7	4.1	4.0	3.6
ST2-1-2	9.04	-0.9	0.1	-0.1	-0.7
ST2-1-3	7.00	20.7	20.1	20.3	20.4
ST2-1-4	5.93	4.4	4.7	4.6	4.2
ST2-1-5	5.89	1.3	2.0	1.8	1.3
ST2-2-1	7.70	4.3	4.6	4.5	4.1
ST2-2-2	7.83	3.1	3.6	3.5	3.0
ST2-2-3	8.05	2.3	2.8	2.7	2.2
ST2-2-4	5.51	3.7	4.1	4.0	3.6
mean	7.35	4.7	5.1	5.0	4.6
04 – Kongresna dvorana					
Stalactite 1					
4b	9.60	-0.9	0.0	-0.1	-0.8
Stalactite 2					
4-1-1	7.00	-1.2	-0.3	-0.4	-1.1
4-1-2	10.13	0.3	1.1	0.9	0.3
4-1-3	8.62	-0.2	0.7	0.5	-0.1
4-1-4	11.21	3.4	3.8	3.7	3.3
4-1-5	11.01	0.2	1.0	0.9	0.3
4-1-6	10.11	1.2	1.9	1.7	1.2
mean	9.68	0.6	1.4	1.2	0.7
09 – Zgornji Tartar					
9S-1a	4.23	0.8	1.5	1.4	0.8
9S-1b	5.24	-2.1	-1.0	-1.1	-1.9
9S-2	3.10	1.7	2.3	2.1	1.6
9S-3	10.55	-1.7	-0.7	-0.8	-1.5
9S-4	11.49	-1.9	-0.8	-1.0	-1.7
9S-5S	7.85	0.7	1.4	1.3	0.7
mean	7.08	-0.42	0.45	0.3	0.3

7.8.3 Drilled core speleothems

The Δ and paleotemperature have been calculated for this group of samples (Table 7.7). There are only two Δ values that point out toward equilibrium conditions for carbonate precipitation, both at location 07 – Čarobni vrt (2.65 and 2.69 ‰), calculated temperatures are too low compared to mean temperature at this location, (10.1 ± 0.8) ºC (Table 7.9, Figure 7.43, 7.44).

Table 7.9 Δ values for drilled core samples and calculated temperatures by using various approaches presented in Table 3.1
Tablica 7.9 Δ vrijednosti za bušene uzorke i temperature izračunate prema jednadžbama iz Tablice 3.1

ID	$\Delta = (\delta^{13}C_{carb} - \delta^{13}C_{DIC})$ (‰)	**Calculated temperature** (°C)			
		Shackleton and Kennett, 1975	Grossman, 1982	Epstein and Mayeda, 1953	Craig, 1965
06 – Stebrišče					
6-1a	7.57	7.1	7.2	7.1	6.8
6-1b	8.73	4.3	4.7	4.5	4.1
6-1c	11.05	5.5	5.7	5.6	5.2
6-2-1	10.34	3.6	4.1	3.9	3.5
6-2-2-a	10.42	2.8	3.3	3.2	2.7
6-2-2-b	9.28	2.8	3.3	3.1	2.7
6-2-2-c	8.65	0.9	1.6	1.5	0.9
6-2-3	9.53	3.5	3.9	3.8	3.4
6-2-3-b	8.63	5.0	5.2	5.1	4.8
6-2-3-c	8.79	4.4	4.8	4.7	4.3
6-2-4	5.61	7.2	7.2	7.2	6.9
6-2-5	4.98	7.6	7.6	7.5	7.3
6-2-6	7.93	4.8	5.1	5.0	4.6
6-2-7	8.10	10.8	10.7	10.6	10.5
6-2-8a	7.78	10.4	10.2	10.2	10.0
6-2-8b	7.01	0.9	1.6	1.5	0.9
6-2-9	8.82	8.8	8.8	8.7	8.5
6-2-10a	7.32	9.0	8.9	8.9	8.6
6-2-10b	6.20	7.8	7.9	7.8	7.5
6-2-11	7.88	8.3	8.3	8.2	8.0
6-2-12	8.39	6.2	6.4	6.3	5.9
6-2-13	8.94	11.0	10.9	10.8	10.7
6-2-14	7.70	8.2	8.2	8.2	7.9
6-2-15	6.74	17.5	16.9	17.1	17.1
6-3-1	4.51	7.4	7.5	7.4	7.1

6-3-2	11.01	6.0	6.2	6.1	5.8
6-3-3	11.41	-0.4	0.5	0.3	-0.3
6-3-4	11.35	4.5	4.8	4.7	4.3
6-3-5	8.75	9.1	9.0	9.0	8.8
6-3-6	7.53	5.6	5.8	5.7	5.4
6-3-7a	7.11	11.0	10.9	10.8	10.7
6-3-7b	5.78	9.9	9.8	9.8	9.6
6-3-8a	6.03	32.8	32.1	32.6	32.9
6-3-8b	5.53	9.3	9.3	9.2	9.0
6-3-8c	5.11	17.0	16.5	16.6	16.6
6-3-8d	3.91	8.5	8.5	8.5	8.2
mean	7.90	7.8	7.9	7.8	7.5
07 – Čarobni vrt					
7-1	2.65	2.0	2.5	2.4	1.9
7-2	3.80	1.3	1.9	1.8	1.2
7-2a	7.78	-1.0	-0.1	-0.2	-0.9
7-3a	6.81	1.8	2.4	2.3	1.8
7-3b	6.37	2.0	2.5	2.4	1.9
7-4	5.71	-3.6	-2.3	-2.5	-3.3
7-5	6.08	-1.9	-0.8	-0.9	-1.7
7-6	6.31	-2.5	-1.4	-1.5	-2.3
7-7	5.51	-1.0	-0.1	-0.2	-0.9
7-8	4.69	-1.5	-0.5	-0.6	-1.3
7-9a	5.28	-0.3	0.6	0.4	-0.2
7-9b	5.78	0.5	1.3	1.1	0.5
7-9c	6.45	-1.4	-0.4	-0.6	-1.3
7-10	5.81	-0.8	0.1	0.0	-0.7
7-11a	4.13	-0.4	0.4	0.3	-0.3
7-11b	4.70	-2.2	-1.1	-1.2	-2.0
7-11c	3.86	-1.3	-0.3	-0.4	-1.1
7-12a	2.69	0.3	1.1	0.9	0.3
7-12b	3.04	-0.8	0.1	0.0	-0.7
7-13a	3.72	-2.0	-0.9	-1.1	-1.8
7-13b	3.71	7.7	7.8	7.7	7.4
mean	4.99	-0.2	0.6	0.5	-0.2
08 – Vrh Velike gore					
8-1a	6.98	-4.5	-3.1	-3.2	-4.1
8-1b	7.48	-1.7	-0.7	-0.8	-1.5
8-1c	7.00	-1.5	-0.5	-0.6	-1.3

8-2	8.93	-2.9	-1.7	-1.9	-2.7
8-3	8.49	3.2	3.6	3.5	3.0
8-4	9.40	-1.8	-0.7	-0.9	-1.6
8-5	9.10	1.1	1.8	1.6	1.1
8-6	11.04	2.1	2.6	2.5	2.0
8-7	8.77	-5.3	-3.7	-3.9	-4.8
8-8	8.95	-4.7	-3.2	-3.4	-4.2
8-9	8.45	-3.1	-1.8	-2.0	-2.8
8-10a	6.95	-0.6	0.3	0.1	-0.5
8-10b	6.07	1.0	1.7	1.6	1.0
8-11a	6.64	-1.4	-0.4	-0.5	-1.2
8-11b	7.34	0.1	0.9	0.7	0.1
8-11c	7.21	0.1	0.9	0.7	0.1
8-11d	7.60	4.3	4.7	4.5	4.1
8-12a	7.90	-1.3	-0.3	-0.4	-1.1
8-12b	7.90	-3.6	-2.3	-2.4	-3.2
8-13	7.10	-5.1	-3.6	-3.7	-4.6
8-14	6.43	-3.4	-2.2	-2.3	-3.1
8-15	5.84	-3.2	-2.0	-2.1	-2.9
8-16	5.95	-3.6	-2.3	-2.4	-3.3
8-17a	4.81	-3.9	-2.5	-2.7	-3.5
8-17b	4.49	-3.0	-1.8	-1.9	-2.7
8-17c	4.78	-4.3	-2.9	-3.0	-3.9
8-18a	4.12	-6.1	-4.4	-4.5	-5.5
8-18b	4.23	-1.5	-0.5	-0.7	-1.4
8-18c	3.42	-4.4	-2.9	-3.1	-3.9
8-19	3.27	-3.5	-2.2	-2.4	-3.2
8-20	4.41	-2.1	-1.0	-1.1	-1.8
mean	6.81	-2.2	-1.1	-1.2	-1.9

7.8.4 $\delta^{18}O$ and $\delta^{13}C$ in vertical profiles of stalagmites

For detailed analysis of drilled cores of stalagmites, and for planed U/Th dating analysis, stable isotopes of $\delta^{18}O$ and $\delta^{13}C$ along the vertical profiles are shown in Figures 7.46 – 7.48. The vertical profile represents direction of speleothem growth. Height of speleothem is measured from the top, i.e. from the present-day growing layer. Samples for stable isotope analysis have been taken from growth layers (perpendicular to the growth direction) of various colors and fabric types. In Table A.12 (Appendix I) data about estimated layer thickness are given, and it ranges from ~1 mm up to ~70 mm. Changes in $\delta^{18}O$ and $\delta^{13}C$ along the profiles show different trends for the 3 stalagmite samples.

Drilled core of the stalagmite from location 06 – Stebrišče is 42 cm long. The core has not been dated yet but its age can be estimated by taking the speleothem growth rate of either 0.1 mm/yr (Gams and Kogovšek, 1998) or 0.06 mm/yr (Horvatinčić et al., 2003), and assuming constant growth and deposition rate. Vokal (1999) modeled growth rate of speleothem (Dreybrodt, 1998) using measured Ca^{2+} concentration and water temperature. However, pCO_2 was not measured and it was assumed to be constant, 300 ppmv. The obtained growth rates have similar order of magnitude for all sampling sites (0.13 – 0.20 mm/yr). Under these assumption the maximal age of the Stebrišče core is between 4200 yr and 7000 yr, i.e., the whole length has been deposited during Holocene. Along the growth axis, different colors of layers, but also different types of materials are found. Density of sampling points, drilled with a 1-mm borer, depends on layer material and color diversity. For example, from 0 to 100 mm and from 200 to 400 mm the sampling frequency is low because of sample homogeneity in different layers, while from 120 to 200 cm and at the end of the core the sampling is more frequent (Figure 7.46). Orange, powder-like part is noticed at about 12 cm of the sample length, and around 24 cm of the sample length a clay layer is visible indicating hyatus in carbonate deposition, therefore the lower part od speleotheme can be older than estimated above. Most of the $\delta^{18}O$ values range from -7.35 to -4.34 ‰ (mean -6.17 ± 0.80 ‰) with two lower values of -8.8 % and one extremely low value of -12.11 ‰ for the gray/black lamina at 42 cm. The $\delta^{13}C$ values range from -8.55 to -1.65 ‰ and are not correlated with the $\delta^{18}O$ values.

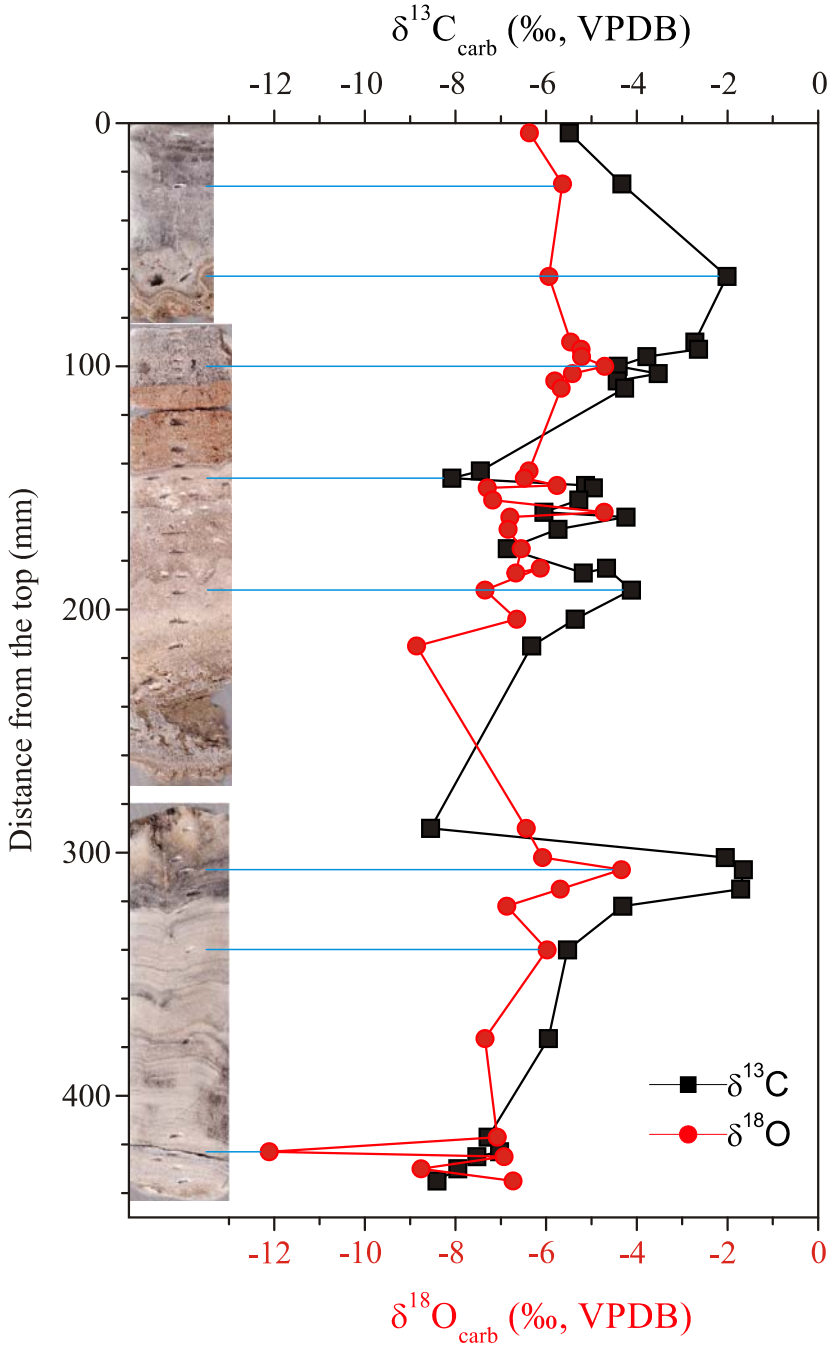

Figure 7.39 Stable isotope composition, $\delta^{13}C$ and $\delta^{18}O$, along the vertical profile of the drilled core of the stalagmite from location 06 – Stebrišče. Blue lines are plotted only to guide an eye, i.e. the connect place of drilling with measured stable isotope value.

Slika 7.39 Izotopni sastav $\delta^{13}C$ i $\delta^{18}O$ stalagmita uzorkovnog na lokaciji 06 – Stebrišče. Plave linije služe za lakše očitavanje vrijednosti.

The same drilling procedure has been applied on sample from location 07 – Čarobni vrt (Figure 7.40) that is 36 cm long (lowest part of the core, about 4 cm long, was broken and not scanned, but is available for further analysis). The estimated maximal age of the Čarobni vrt

stagmite is 3600 yr (according to Gams and Kogovšek, 1998) or 6000 yr (according to Horvatinčić et al., 2003). Again, both estimates result in a deposition during the Holocene.

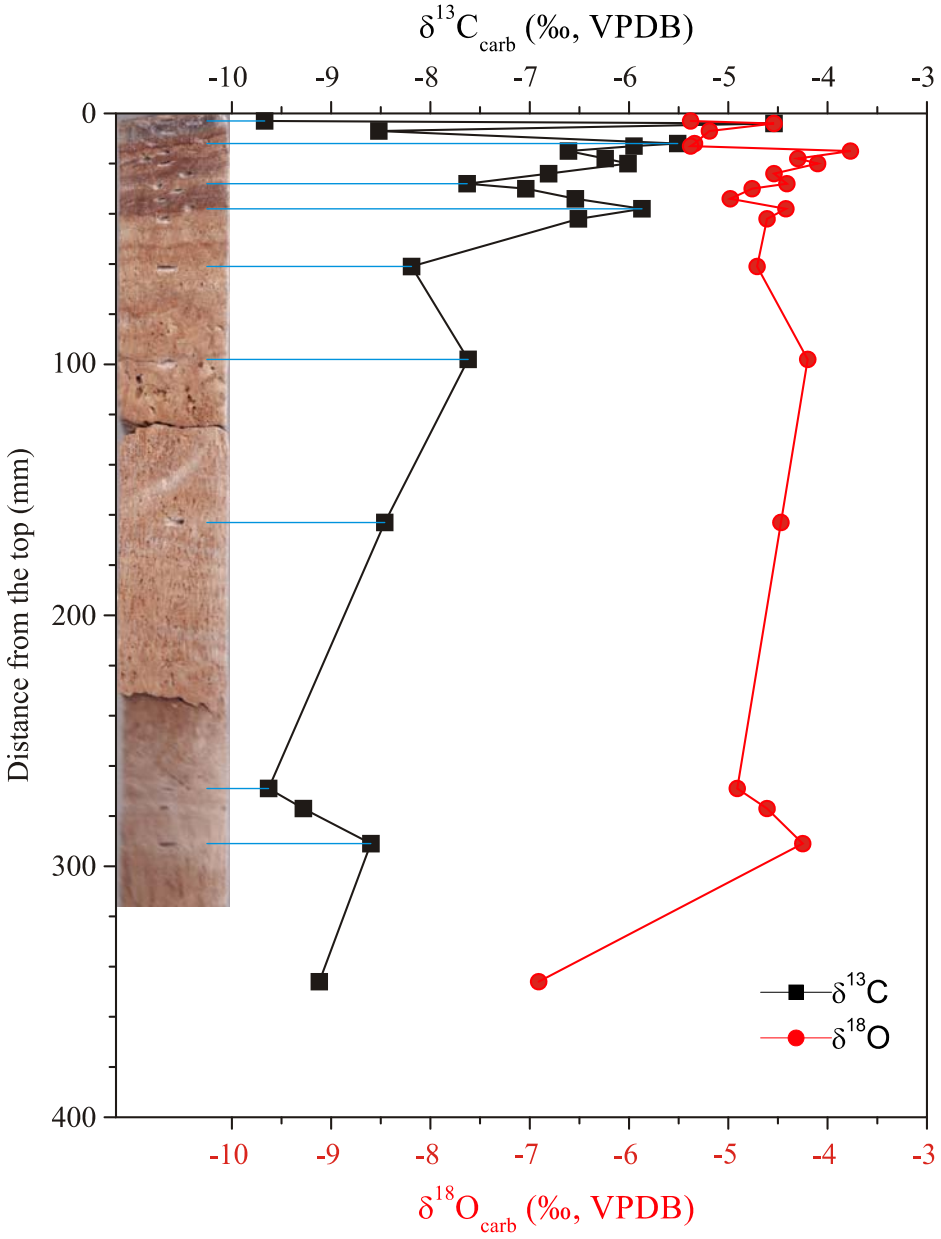

Figure 7.40 Stable isotope composition, $\delta^{13}C$ and $\delta^{18}O$, along the vertical profile of the drilled core of the stalagmite from location 07 – Čarobni vrt. Blue lines are plotted only to guide an eye i.e. connect place of drilling with measured stable isotope value.

Slika 7.40 Izotopni sastav $\delta^{13}C$ i $\delta^{18}O$ profila stalagmita uzorkovanog na lokaciji 07 – Čarobni vrt. Plave linije služe za lakše očitavanje vrijednosti.

Several different types of fabrics are observed along the profile. In the top 6 cm of the core, laminae of different colors are distinguished. The rest of the sample has different crystal

morphology, porous with numerous voids. Sampling is performed accordingly, i.e., more frequent sampling is done in the top 6 cm of the core than in the lower section.

The $\delta^{18}O$ values in the top 6 cm vary between -5.38 and -3.77 ‰, between 6 cm and 30 cm the variations in $\delta^{18}O$ are smaller, between -4.98 and -4.10 ‰, while the last sample has much more negative $\delta^{18}O$ value of -6.91 ‰. The variations in $\delta^{13}C$ value in the top 6 cm (estimated age 600 to 1000 yr) are even more pronounced than those in $\delta^{18}O$. The $\delta^{13}C$ varies between -9.67 and -4.54 ‰, but is not correlated with $\delta^{18}O$. Between 6 cm and 30 cm $\delta^{13}C$ values range from -8.12 to -9.63 ‰ , and their behavior can be correlated with the variations in $\delta^{18}O$ ($R = 0.70$, $p = 0.11$).

Drilled core of the stalagmite from location 08 – Vrh Velike gore is 20 cm long (Figure 7.41). The maximal estimated age is between 2000 yr and 3330 yr, so this is the youngest core of the three cores studied here. The top 4 cm of the core (the youngest part) is gray, while the rest of the sample is brown. At the beginning there are no laminas observed, while between 3 cm and 6 cm dense and thin laminae are visible, and further on laminae become thicker. Below 9 cm of the core different crystal morphology is observed with many voids and without laminae. The oldest part of sample is again laminated and dense. The most frequent sampling is done on laminated part of sample from 3 to 6 cm.

Variations in $\delta^{13}C$ values along the growth layers are more pronounced than those in $\delta^{18}O$ values. The $\delta^{18}O$ values range from -6.6 to -3.59 ‰, and there is no significant difference between the mean value in the laminated part of the core (0 – 9 cm, mean -4.95 ± 0.76 ‰) and that below 9 cm (-4.35 ± 0.43 ‰). On the contrary, the $\delta^{13}C$ values in the upper 9 cm (mean -5.11 ± 1.27 ‰, range from -6.99 ‰ to -1.79 ‰) are significantly different than those in the lower part (mean -8.64 ± 0.57 ‰, range from -9.56 to -8.02 ‰). The changes in $\delta^{18}O$ and $\delta^{13}C$ in the upper 9 cm seem to be in anticorrelation, i.e. increase in $\delta^{18}O$ is accompanied with decrease of $\delta^{13}C$ ($R = -0.19$, $p = 0.38$), while in the lower part there is no correlation ($R = -0.11$, $p = 0.78$). The drilled cores of the three stalagmites from different locations, but close to each other, are formed during the Holocene, as estimated by two growth rates from literature. However, they show different patterns of $\delta^{13}C$ and $\delta^{18}O$ values along the profiles. For more accurate interpretation of the isotope data, a precise dating of the cores is necessary.

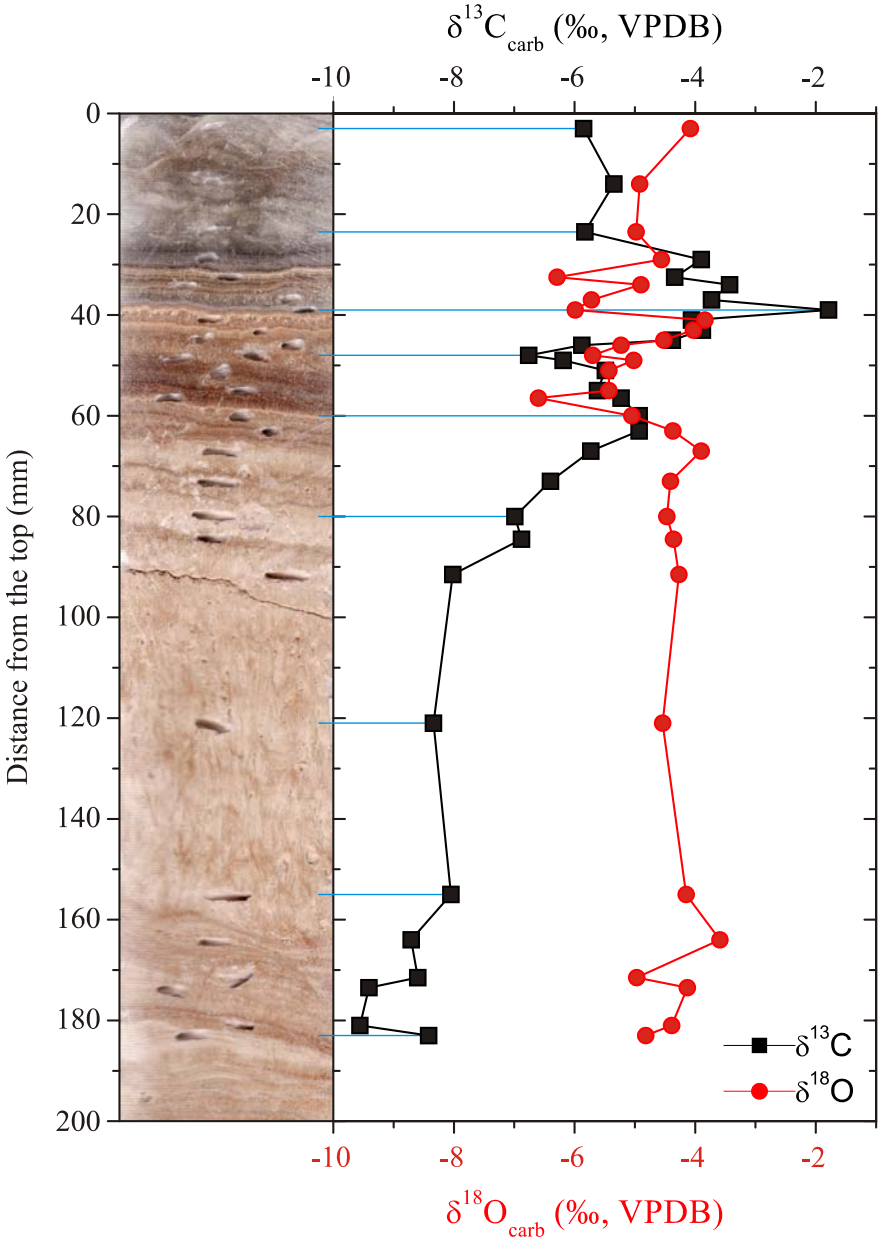

Figure 7.41 Stable isotope composition, $\delta^{13}C$ and $\delta^{18}O$, along the vertical profile of the drilled core of the stalagmite from location 08 – Vrh Velike gore. Blue lines are plotted only to guide an eye, i.e. connect place of drilling with measured stable isotope value

Slika 7.41 Izotopni sastav $\delta^{13}C$ i $\delta^{18}O$ profila stalagmita uzorkovanog na lokaciji 08 – Vrh Velike gore. Plave linije služe za lakše očitavanje vrijednosti.

Additional sampling/drilling at the same locations would also be advisable to obtain several coeval stalagmites confirming changes in isotope composition (Linge et al., 2001a,b, McDermott, 2004). The danger of relying on a single stalagmite $\delta^{18}O$ record is discussed by (Linge et al., 2001a,b) leading to the conclusion that processes other than climate variability (e.g., variable seepage water routes, water mixing) can substantially affect the $\delta^{18}O$ values recorded in stagalmites.

With data from U/Th dating, age of carbonate precipitation will be accompained by the stable isotope data for detailed paleclimate reconstruction.

7.9 Assessment of isotopic equilibrium conditions in Postojna Cave

Various requirements for deposition of speleothems under isotopic equilibrium conditions described in literature are presented in the literature overview of this work (sections 3.5 and 3.7). The requirements are summarized in Table 7.10, and the assessment of their fulfillment is given for each location (01 – 09) that was studied in this work. If a specific requirement is fulfilled at given location, a plus (+) mark is associated with the location. Consequently, a minus (–) mark is associated with the location if the requirement is not fulfilled. In some cases, a ± mark is associated with the location where a certain requirement is partially fulfilled, e.g., seasonal variation in air temperature just slightly larger than required for "+" mark.

The first requirement for achieving carbonate precipitation under isotopic equilibrium is stable temperature of the cave environment. Variations of temperature are usually allowed to be within ± 1 ºC. Air temperature at location 01 close to the entrance is 9.8 ± 2.2 ºC (section 6.1 and Table A.3 in Appendix I) and therefore location 01 does not satisfy this requirement. Variations of the mean air temperatures at locations 02, 05, 07, 08 and 09 are ± 1.0 ºC, ± 0.4 ºC, ± 0.8 ºC, ± 0.7 ºC, and ± 0.9 ºC, respectively. Thus, the requirement of variations lower than ± 1 ºC is fulfilled. At other three locations (03, 04 and 06), the temperature variation are slightly above + 1 ºC, namely ± 1.6 ºC, ± 1.4 ºC and ± 1.2 ºC, so the ± mark is associated with these locations for the stable temperature requirement (Table 7.10, first raw).

High and stable humidity is the next condition, and it is fulfilled at all studied locations, because the humidity is always and everywhere in the Postojna Cave close to 100 %.

The next parameter is "no ventilation", i.e. no strong air circulation that may induce kinetic isotopic effects. This condition may be quantified by the pCO_2 values (section 7.5 and table A.3 in Appendix I), and the limit of 1000 ppmv (mean value of pCO_2) was chosen. The condition of "no ventilation" is not satisfied (- mark) at locations 01 – 04 close to the entrance, where the mean pCO_2 is lower than 1000 ppmv. The mean pCO_2 at location 09 is 937 ± 325 ppmv, and the ± mark was associated with this locations. Locations 05 – 08 with mean $pCO_2 > 1000$ ppmv are marked by "+".

I_{sat} should have values between 1 and 3 (Frisia et al., 2000) and this conditions is at least partially satisfied at all locations. The mean I_{sat} at locations 01, 02, 05, 07 and 09 is lower than 3 and they are marked by +, while other location are marked by ± because the value of 3 lies

within the standard deviation of I_{sat}, e.g., saturation index at location 06 is 3.35 ± 1.72 (section 7.4.4 and Table A.4 in Appendix I).

Continuous deposition of carbonate is possible under continuous drip water supply. Steady drip rate is defined here as the drip rate for which standard deviation is smaller than the mean drip rate, i.e., for which the coefficient of variability is ≤ 1 (section 7.3 and Table A.3 in Appendix I). This condition is satisfied at locations 01, 02, 04, 06 and 07.

Stable $\delta^{18}O$ of drip water, without pronounced seasonal variations is an indication of long mean residence time of water in the epikarst zone, and this condition is defined as $\sigma < 0.3$ ‰. The standard deviation of $\delta^{18}O$ in drip water at locations 01, 02 and 08 is larger than 0.3 ‰ (section 7.3 and Table A.5 in Appendix I), and they are marked by the – mark. At location 03 the standard deviation is 0.31 ‰, i.e., just slightly above the predefined requirement, so this location is marked by ±. Locations associated with the + mark showing stable $\delta^{18}O$ of drip water have mean residence time (MRT) longer than 1 year (section 7.3).

All requirements discussed above refer to the cave environmental conditions and drip water conditions. The next set requirements refer to the isotopic composition ($\delta^{18}O$ and $\delta^{13}C$) of deposited carbonate.

Under isotopic equilibrium conditions, the difference $\Delta = \delta^{13}C_{carb} - \delta^{13}C_{DIC}$ should be $\varepsilon = 2.2$ ‰ (section 2.4.1). The temperature calculated by various paleotemperature equations (presented in section 3.5) should reflect the actual temperature at the site of carbonate deposition, or equivalently, the fractionation factor α obtained from the measured $\delta^{18}O$ values of water and the precipitated carbonate should be equal to the equilibrium fractionation factor α (section 3.5) at the depositional temperature.

For carbonates precipitated on watch glasses, the condition $\Delta \sim \varepsilon$ is not satisfied at any location, the calculated temperatures are different than the measured ones and α values deviate from the α values. The $\Delta \sim \varepsilon$ condition for soda straw samples is only partially satisfied ($\varepsilon < \Delta < 3$ ‰) at two locations (03 and 07), but the calculated temperature is close to the actual one at location 06, and within still acceptable limits at 4 locations more. The mark + is associated with location 06, where the temperature calculated by paleotemperature equations lies within $\pm \sigma$ of the measured air temperature, and mark ± is associated with the locations where the difference between the measured temperatures and those obtained from paleotemperature equations is lower than 6 ºC. α values calculated from $\delta^{18}O$ of carbonates and water (section 7.7.1) differ from equilibrium α values obtained from measured air temperature according to different equations (section 3.5).

Both peculiar types of speleothems at locations 01 and 09 also do not satisfy the condition $\Delta \sim \varepsilon$, but the temperatures calculated from fragile forms at location 09 are close to the measured ones. For peculiar types of speleothems $\alpha = \alpha_{eq}$ at location 09 (section 7.7.2).

None of the flowstones, stalactites and stalagmites (drilled cores) satisfy the $\Delta \sim \varepsilon$ condition for $\delta^{13}C$ values and the calculated temperature does not reflect the measured one, except partially at 02 (stalactite) and 06 (drilled stalagmite). However, these speleothems have been growing for an unknown period, and any conclusion about the temperature of deposition in the past is meaningless if the equilibrium conditions at present are not demonstrated.

Therefore, although the environmental requirements for isotopic equilibrium calcite deposition are mostly fulfilled at inner locations 05 – 09, the isotopic requirements are not. The calculated temperature, independent on the equations used, generally does not reproduce the actual temperature. Similarly, α values determined from the measured $\delta^{18}O$ values generally do not equal the equilibrium α_{eq} values at given temperatures. The location 06 – Stebrišče is the only location where the modern soda straw samples reproduce the modern temperature within the variation of the measured one, as well as the speleothems of "peculiar" growth from location 09 – Zgornji Tartar.

Table 7.10 Requirements for deposition of carbonates under isotopic equilibrium conditions and assessment of their fulfillment at the studied locations within Postojna Cave.

Tablica 7.10 Zahtjevi koji moraju zadovoljeni za taloženje karbonata u uvjetima izotopne ravnoteže i procjena njihovog ostvarenja na proučavanim lokacijama u Postojnskoj jami.

parameter		Location								
		01	02	03	04	05	06	07	08	09
stable t_{air} (σ < 1.0 ºC) *1		-	+	±	±	+	±	+	+	+
high humidity		+	+	+	+	+	+	+	+	+
no ventilation		-	-	-	-	+	+	+	+	±
1 > I_{sat} >3 *2		+	+	±	±	+	±	+	±	+
steady drip rate (σ < mean)		+	+	-	+	-	+	+	-	-
stable $\delta^{18}O_{dw}$ (σ < 0.3 ‰)		-	-	±	+	+	+	+	-	+
watch glasses	$\delta^{13}C$: $\Delta \sim \varepsilon$	-	-	-	-	-	-			-
	$\delta^{18}O$: $\alpha = \alpha_{eq}$	-	-	-	-	-	-			-
	$t_{calc} \approx t_{air}$	-	-	-	-	-	-			-
soda straw	$\delta^{13}C$: $\Delta \sim \varepsilon$ *3	-	-	±			-	±	-	-
	$\delta^{18}O$: $\alpha = \alpha_{eq}$	-	-	-			+	-	-	-
	$t_{calc} \approx t_{air}$ *4	-	±	-			+	±	±	±
peculiar	$\delta^{13}C$: $\Delta \sim \varepsilon$	-								-
	$\delta^{18}O$: $\alpha = \alpha_{eq}$	-								+
	$t_{calc} \approx t_{air}$	-								±
flowstone	$\delta^{13}C$: $\Delta \sim \varepsilon$				-	-	-			
	$\delta^{18}O$: $\alpha = \alpha_{eq}$				-	-	-			
	$t_{calc} \approx t_{air}$				-	-	-			
stalactites	$\delta^{13}C$: $\Delta \sim \varepsilon$		-		-					-
	$\delta^{18}O$: $\alpha = \alpha_{eq}$				-					-
	$t_{calc} \approx t_{air}$		±		-					-
stalagmites (drilled)	$\delta^{13}C$: $\Delta \sim \varepsilon$						-	-	-	
	$\delta^{18}O$: $\alpha = \alpha_{eq}$									
	$t_{calc} \approx t_{air}$						±	-	-	

*1 ± if 1 ºC < σ < 1.6 ºC
*2 ± if the value of 3 is within standard deviation,
*3 ± if $\varepsilon < \Delta < 3$
*4 + if $t_{calc,mean}$ is within ($t_{air} \pm \sigma$), and ± if $t_{calc,mean} - t_{air}$ < 6 ºC

8 CONCLUSION

The aim of this thesis was to explore existence of isotopic equilibrium conditions in the process of speleothem formation (stalagmites) in the Postojna Cave and to show the possibility of using isotopic composition of oxygen, $\delta^{18}O$, in speleothems for paleoclimatic studies. In accordance with a modern approach in speleothem studies that requires determination of present-day geochemical and isotopic conditions of speleothem formation at several locations within the same cave at least during one hydrological cycle, monitoring of various parameters at 11 locations in the Postojna Cave, Slovenia, was performed from March 2010 to April 2011 during 7 field trips. One of the locations was outside the cave to obtain referent external parameters.

The main conclusions of this interdisciplinary and comprehensive geochemical and isotopic investigation can be summarized as follows:

- Air temperature within the Postojna Cave (mean value at all monitored locations 10.6 + 0.7 °C) is close to the mean air temperature measured at the Postojna meteorological station during the last 6 years (9.9 + 0.4 °C). Drip water temperature (mean 10.4 + 0.8 °C) closely follows the air temperature.
- According to chemical composition, all drip waters belong to the same type (Ca – HCO_3). According to drip rate and their variability all drip waters belong to the seepage type. The $\delta^{18}O$ values of drip water vary between -10 and -8 ‰, with practically no seasonal variations. The estimated mean residence time of water is between several months to several years, depending on the location.
- The pCO_2 in cave air shows seasonal variations with higher values in late summer – early autumn. The variations are pronounced deeper in the cave than at locations close to the entrance and prone to ventilation. Seasonal variations in pCO_2 are accompanied by seasonal variation in $\delta^{13}C$ of cave air: the higher the pCO_2, the lower the $d^{13}C_{air}$. The excess pCO_2 in

the cave is a result of degassing of soil CO_2 with $\delta^{13}C$ value of -23.3 + 0.7 ‰ that was transported to the cave by drip water.

- Locations 01 – 04, close to the entrance, show some characteristics different from inner locations 06 – 09: higher conductivity values, higher Ca^{2+}, Mg^{2+} i HCO_3^- concentrations, lower air and drip water temperatures, lower pCO_2 and higher $\delta^{13}C_{air}$ values, higher pCO_2(aq) and higher drip rate. The two groups of locations cannot be distinguished by $\delta^{18}O$ values of drip water, MRT, $\delta^{13}C_{DIC}$ and Mg/Ca ratio. The differences can be explained higher concentration of CO_2 in soil above locations 01 – 04, which subsequently leads to more intense dissolution of carbonate rocks, as well as by more pronounced air circulation (ventilation) at the outer locations.
- Location 05 – Podrti kapnik differs from other locations by lower concentrations of Ca^{2+} ions and bicarbonates, as well as lower conductivity. The $\delta^{13}C_{DIC}$ is higher than at other locations. These differences indicate onset of prior calcite precipitation (PCP), i.e., the deposition of calcite in voids in the caprock during percolation of water to the drip site in the cave. Other parameters (water and cave air temperature, drip rate, $\delta^{18}O$ of drip water, pH, Mg^{2+} ion concentration, pCO_2 and $\delta^{13}C$ of cave air) do not differ significantly from the values at all other locations.
- $\delta^{13}C$ and $\delta^{18}O$ values of "soda straw" show variations from -10.6 to -7.8 ‰ VPDB and from -7.8 to -4.8 ‰, respectively. The $\delta^{13}C$ of carbonates on watch glasses are lower (by app. 2 ‰) and $\delta^{18}O$ are higher than the corresponding values for modern "soda straw" samples at the same location. The precipitation of carbonate on watch glasses can be explained by rapid mineral precipitation that results in isotopic composition that reflects isotopic composition of DIC, both $\delta^{13}C$ and $\delta^{18}O$.
- Measured $\delta^{13}C$ in modern carbonates was compared to equilibrium fractionation factor ε to determine if the carbonate precipitation occurred under isotopic equilibrium conditions. The difference $\Delta = \delta^{13}C_{carb} - \delta^{13}C_{DIC}$ was larger than ε for most "soda straw" samples, and only a few samples of from locations 03 – Vodopad and 07 – Čarobni vrt gave Δ comparable to ε indicating isotopic equilibrium. All Δ values for carbonates from watch glasses are lower than ε.
- For "soda straw" samples the temperature calculated from $\delta^{18}O$ of water and carbonate by using several paleotemperature equations is to low compared to the present day air temperature. Only at location 06 the calculated and measured temperatures are comparable.

Similar conclusion is obtained after comparison of fractionation factors α with the equilibrium α_{eq} values – only for soda straws at location 06 the α value is comparable with the α_{eq} value, while at other locations α is higher than α_{eq}.

- For both groups of peculiar growth types of speleothems the calculated Δ values are higher than ε indicating the absence of isotopic equilibrium conditions. Calculated temperatures at location 01 – Slonova glava are lower by as much as 12 ºC probably due to intensive cave ventilation (windy conditions) close to the entrance causing fast CO_2 degassing. At location 09 – Zgornji Tartar, however, the calculated temperatures are close to the mean annual air temperature (10.7 ± 0.7 ºC) and $\alpha \approx \alpha_{eq}$. Peculiar growth types of speleothems at location 09 are probably formed by slow CO_2 degassing that causes enrichment in carbon, while $\delta^{18}O$ remains unchanged leading to a large gradient $\Delta\delta^{13}C/\Delta\delta^{18}O$.
- The Δ values of flowstone, stalactites and drilled cores of stalagmites are larger than the equilibrium fractionation factor ($\Delta > \varepsilon$), suggesting that precipitation occurred under kinetic conditions. These speleothem types have been deposited during unknown longer time period during which the cave temperature could have been changed, as well as the vegetation in the area. Calculated temperatures are too low compared to the present-day mean temperature, but any conclusion about the change of deposition temperature in the past is meaningless if the equilibrium conditions at present are not demonstrated.

The purpose of this study was to determine areas where future paleoclimate research may be conducted. The presented parameters (temperature, humidity, air circulation, drip water $\delta^{18}O$) point to the fulfillment of the environmental preconditions for isotopic equilibrium precipitation of carbonates, specially at the inner locations. However, isotopic composition of carbonates, both $\delta^{13}C$ and $\delta^{18}O$, do not show equilibrium precipitation at most of the studied locations. The temperatures of calcite precipitation calculated from stable isotope data ($\delta^{18}O$ of drip water and of deposited carbonate) by using different equations generally do not agree with the measured temperatures at given locations – the calculated temperatures are lower. Accordingly, the fractionation factor α is larger than the equilibrium α_{eq} value. Comparable temperatures and $\alpha \approx \alpha_{eq}$ are obtained only for "fragile" formations from location 09 and some “soda-straw” samples from location 06. **Therefore, it is concluded that locations 06 – Stebrišče and 09 – Zgornji Tartar are the only ones that have potential for future paleoclimatic studies.**

In addition to this main conclusion that responds to the aim of the dissertation, three important conclusions can be identified:

- Differences in isotopic and chemical composition of drip water at location 05 – Podrti kapnik in comparison with all other cave locations are explained by the onset of the PCP process. The prior calcite precipitation is often described in recent literature in various cave systems, but in the Dinaric karst it has not yet been identified and proved.
- Recent carbonate precipitated on watch glasses does not reflect the isotopic compositin of speleothems at the same location, and therefore the type of artificial substrate (watch glass) cannot be used for studies of process of carbonate precipitation in caves.
- Different distributions of $\delta^{13}C$ and $\delta^{18}O$ along the depth profiles of drilled cores of 3 speleothems indicate that isotopic record of speleothems may reflect some changes in the cave environment, not only changes in temperature. For paleoclimatic studies several coeval stalagmites with similar isotopic distributions should be analyzed in order to interprete measured isotopic data as reliable records of paleoclimatic or paleoenvironmental changes.

Further plans

- Systematic collection of monthly precipitation for stable isotope composition of hydrogen ($\delta^{2}H$) and oxygen ($\delta^{18}O$) in order to define local meteoric water line (LMWL) for Postojna area and better determination of residence time of water.
- Continuous monitoring of cave environmental parameters (pCO_2, drip rate, air and water temperature and humidity) should be established at different locations.
- Collection of carbonate precipitates on various substrates should be continued. The time of carbonate precipitation is suggested to be sufficient to monitor seasonal effect (at least two sampling periods in a year) with emphasize on inner locations with stronger variations of pCO_2.
- Mineralogic and chrystalographic studies of various types of cave carbonates
- Dating of old speleothems profiles by U-Th method.
- On few locations ^{14}C activity of modern speleothems should be measured to determine initial ^{14}C activity enabling thus ^{14}C dating of speleothems younger than app. 50 000 years.
- Investigations of trace elements, with emphasis on magnesium and strontium (Mg-Sr) compositions in drip waters and speleothems, since they can be used as an additional tool in paleoclimate studies and/or dating
- Monitoring of radon concentration and its relation to pCO_2 in order to quantify and better understand cave air circulation.
- Relate $\delta^{18}O_{carb}$ in Postojna with some other caves in the region (Austria, Italy, and Croatia) to establish connections in regional and global climate change.

REFERENCES

Allison, C. E., Francey, R. J. and Meijer, H. A., 1995. Recommendations for the reporting of stable isotope measurements of carbon and oxygen in CO_2 gas. In *Reference and Intercomparison Materials for Stable Isotopes of Light Elements*, TECDOC 825, 155–162. IAEA, Vienna.

Amundson, R., Stern, L., Baisden, T. and Wang, Y., 1998. The isotopic composition of soil and soil-respired CO_2. *Geoderma* **82**(1), 83–114.

Andrews, J. E., Pedley, H. M. and Dennis, P. F., 1994. Stable isotope record of palaeoclimatic change in a British Holocene tufa. *The Holocene* **4**(4), 349–355.

Andrews, J. E., Riding, R. and Dennis, P. F., 1997. The stable isotope record of environmental and climatic signals in modern terrestrial microbial carbonates from Europe. *Palaeogeography, Palaeoclimatology, Palaeoecology* **129**, 171–189.

ARS, 2006. Podnebne razmere v Sloveniji (obdobje 1971-2000). Technical report, Agencija Republike Slovenije za okolje, Ljubljana.

Avak, H. and Brand, W. A., 1995. A fully automated H_2O/gas phase equilibration system for hydrogen and oxygen isotope analysis. Technical report, Finnigan MAT Application News. 11: 113, Bremen.

Ayalon, A., Bar-Matthews, M. and Kaufman, A., 2002. Climatic conditions during marine isotopic stage 6 in the Eastern Mediterranean region, as evident from the isotopic composition of speleothems; Soreq Cave, Israel. *Geology* **30**, 303–306.

Baker, A., Genty, D. and Fairchild, I. J., 2000. Hydrological characterisation of stalagmite dripwaters at Grotte de Villars, Dordogne, by the analysis of inorganic species and luminescent organic matter. *Hydrology and Earth System Sciences Discussions* **4**(3), 439–449.

Baldini, J. U. L., Baldini, L. M., McDermott, F. and Clipson, N., 2006. Carbon dioxide sources, sinks, and spatial variability in shallow temperate zone caves: Evidence from Ballynamintra Cave, Ireland. *Journal of Cave and Karst Studies* **68**(1), 4–11.

Baldini, J. U. L., McDermott, F., Hoffmann, D. L., Richards, D. A. and Clipson, N., 2008. Very high-frequency and seasonal cave atmosphere pCO_2 variability: Implications for stalagmite growth and oxygen isotope-based paleoclimate records. *Earth and Planetary Science Letters* **272**, 118–129.

Baldini, L. M., McDermott, F., Baldini, J. U. L., Fischer, M. J. and Möllhoff, M., 2010. An investigation of the controls on Irish precipitation $\delta^{18}O$ values on monthly and event timescales. *Climate Dynamics* **35**, 977–993.

Bar-Matthews, M., Ayalon, A., Matthews, A., Sass, E. and Halicz, L., 1996. Carbon and oxygen isotope study of the active watercarbonate system in a karstic Mediterranean Cave: implication for palaeoclimate research in semiarid regions. *Geochimica et Cosmochimica Acta* **60**(2), 337–347.

Barešić, J., 2009. *Primjena izotopnih i geokemijskih metoda u praćenju globalnih i lokalnih promjena u ekološkom sustavu Plitvička jezera*. Ph.D. thesis, Fakultet kemijskog inženjerstva i tehnologije, Zagreb.

Barešić, J., Horvatinčić, N., Krajcar Bronić, I., Obelić, B. and Vreča, P., 2006. Stable isotope composition of daily and monthly precipitation in Zagreb. *Isotopes in Environmental and Health Studies* **3**, 239–249.

Bariac, T., Deleens, E., Gerbaud, A. and Mariotti, A., 1991. La composition isotopique (^{18}O,^{2}H) de la vapeur d'eau transpiree: Etude en conditions asservies. *Geochimica et Cosmochimica Acta* **55**, 3391–3402.

Beiser, A., 1973. *Concepts of Modern Physics*. McGraw-Hill, NewYork.

Bezek, M., Gregorič, A., Kávási, N. and Vaupotič, J., 2012. Diurnal and seasonal variations of concen-

tration and size distribution of nano aerosols (10-1100 nm) enclosing radon decay products in the Postojna Cave, Slovenia. *Radiation Protection Dosimetry* **152**, 174–178.

Bottrel, S. H. and Atkinson, T. C., 1992. Tracer study and storage in the unsaturated zone of a karstic limestone aquifer. In Holtz, H. and Werner, A., eds., *Tracer hydrology*. Balkema, Rotterdam.

Bourges, F., Genthon, P., Mangin, A. and d'Hulst, D., 2006. Microclimates of l'Aven d'Orgnac. *International Journal of Climatology* **26**, 1651–1670.

Brandt, W., 1995. High precision isotope ratio monitoring techniques in mass spectrometry. *Journal of Mass Spectrometry* **31**, 225–235.

Brandt, W. A., 2004. Mass Spectrometer Hardware for Analyzing Stable Isotope Ratios. In *Handbook of Stable Isotope Analytical Techniques*, 835–856. Elsevier B.V, Amsterdam, The Netherlands.

Brodar, S., 1966. Pleistocenski sedimenti in paleolitska najdišča v Postojnski jami. *Acta carsologica* **4**, 57–138.

Broecker, W. S., Olson, E. A. and Orr, P. C., 1960. Radiocarbon measurements and annual rings in cave formations. *Nature* **185**, 93–94.

Buhay, W. M., Wolfe, B. B., Elgood, R. and Edwards, T. W. D., 1995. *Reference and Intercomparison Materials for Stable Isotopes of Light Elements*. IAEA-TECDOC-825, Vienna.

Burns, S. J., Fleitmann, D., Matter, A., Neff, U. and Mangini, A., 2001. Speleothem evidence from Oman for continental pluvial events during interglacial periods. *Geology* **29**, 623–626.

Buser, S., Grad, K. and Plencar, M., 1967. Osnovna geološka karta SFRJ, list Postojna, 1 : 100 000. Technical report, Savezni geološki zavod Beograd, Beograd.

Cerling, T. E., 1984. The stable isotopic composition of modern soil carbonate and its relationship to climate. *Earth and Planetary Science Letters* **71**, 229–240.

Chacko, T., Cole, D. R. and Horita, J., 2001. Equilibrium oxygen, hydrogen and carbon isotope fractionation factors applicable to geologic systems. *Mineralogy and geochemistry* **43**, 1–81.

Chacko, T. and Deines, P., 2008. Theoretical calculation of oxygen isotope fractionation factors in carbonate systems. *Geochimica et Cosmochimica Acta* **72**, 3642–3660.

Chadwick, J., 1932. Possible Existence of a Neutron. *Nature* **129**, 312.

Cheng, H., Edwards, R. L., Broecker, W. S., Denton, G. H., Kong, X. G., Wang, Y. J., Zhang, R. and Wang, X. F., 2009. Ice Age Terminations. *Science* **326**, 248–252.

Cigna, A. A., 2005. Radon in Caves. *International Journal of Speleology* **34**(1-2), 1–18.

Clark, I. D. and Friz, P., 1997. Environmental Isotopes in Hydrogeology. In Clark, I. D. and Friz, P., eds., *Environmental Isotopes ih Hydrogeology*, 328. Lewis Publishers, New York.

Clark, I. D. and Lauriol, B., 1992. Kinetic enrichment of stable isotopes in cryogenic calcites. *Chemical Geology* **102**, 217–228.

Coplen, T. B., 1994. Reporting of stable hydrogen, carbon, and oxygen isotopic abundances. *Pure and Applied Chemistry* **66**(2), 273–276.

Coplen, T. B., 2007. Calibration of the calcitewater oxygen-isotope geothermometer at Devils Hole, Nevada, a natural laboratory. *Geochimica et Cosmochimica Acta* **71**, 3948–3957.

Coplen, T. B., Bohlke, J. K., De Bievre, P., Ding, T., Holden, N. E., Hopple, J. A., Krouse, H. R., Lamberty, A., Peiser, H. S., Revesz, K., Rieder, S. E., Rosman, K. J. R., Roth, E., Taylor, P. D. P., Vocke, R. D. and Xiao, Y. K., 2002. Isotope-abundance variations of selected elements, IUPAC Technical report. *Pure and Applied Chemistry* **74**, 1987–2017.

Coplen, T. B., Kendall, C. and Hopple, J., 1983. Comparison of stable isotope reference samples. *Nature* **302**, 236–238.

Craig, H., 1957. Isotopic standards for carbon and oxygen and correction factors for mass-spectrometric analysis of carbon dioxide. *Geochimica et Cosmochimica Acta* **12**, 133–149.

Craig, H., 1961. Isotopic variations in meteoric water. *Science* **133**, 1702–1703.

Craig, H., 1965. The measurements of oxygen isotope paleotemperatures. In Tongiorgi, E., ed., *Stable Isotopes in Oceanographic Studies and Paleotemperatures*, 161–182. Laboratorio di Geologia Nucleare, Consiglio Nazionale Delle Ricerche, Pisa.

Craig, H. and Gordon, L. I., 1965. Deuterium and oxygen-18 variations in the ocean and the marine

atmosphere. In Tongiorgio, E., ed., *Stable isotopes in oceanographic studies and palaeotemperatures.*, volume 9-130. Spoleto Conference, Italy. Laboratorio di Geologia Nucleare, Pisa.

Crestani, G. and Anneli, F., 1939. *Ricerche di meteorologia ipogea nelle grotte di Postumia*, volume XVII. Istituto poligrafico della stato, Roma. Publicazione N. 143, Ministero dei lavori pubblici, Magistrato alle Acque, Ufficio idrografico, XVII, Roma, 1162.

Criss, R. E., 1999. *Principles of stable isotopes distribution*. Oxford University Press, Oxford.

Čar, J. and Šebela, S., 1998. Bedding planes, moved bedding planes, connective fissures and horizontal cave passages (examples from Postojnska jama system). *Acta carsologica* **5**, 75–95.

Dansgaard, W., 1953. The abundance of O^{18} in atmospheric water vapour. *Tellus* **5**, 461–469.

Darling, W. G., Bath, A. H., Gibson, J. J. and Rozanski, K., 2006. Isotopes in water. In Leng, M., ed., *Isotopes in paleoenvironmental research*. Springer.

Dawson, T. E., 1993. Water sources of plants as determined from xylem-water isotopic composition: perspectives on plant competition. In Ehleringer, J., Hall, A. and Farquhar, G., eds., *Stable Isotopes and Plant Carbon–Water Relations*, 465–496. Academic Press Inc., San Diego,.

de Groot, P. A., 2004. *Handbook of Stable isotope Analytical Techniques*, volume I. Elsevier, Amsterdam, The Netherlands.

de Groot, P. A., 2009. *Handbook of Stable isotope Analytical Techniques*, volume II. Elsevier, Amsterdam, The Netherlands.

Deines, P., 1980. The isotopic composition of reduced organic carbon. In Fritz, P. and Fontes, J., eds., *Handbook of Environmental Isotope Geochemistry*. Elsevier, Amsterdam.

Deines, P., Langmuir, D. and Harmon, R. S., 1974. Stable carbon isotope ratios and the existence of a gas phase in the evolution of carbonate ground waters. *Geochimica et Cosmochimica Acta* **38**, 1147–1164.

DeWalle, D. R. and Swistock, B. R., 1994. Differences in oxygen-18 content of throughfall and rainfall in hardwood and coniferous forests. *Hydrological Processes* **8**, 75–82.

Dietzel, M., Tang, J., Leis, A. and Köhler, S. J., 2009. Oxygen isotopic fractionation during inorganic calcite precipitation – Effects of temperature, precipitation rate and pH. *Chemical Geology* **268**, 107–115.

Dixon, B. E. and Hands, G. C., 1957. Desorption and absorption of gases by drops during impact. *Journal of Applied Chemistry* **7**, 342–348.

Doctor, D., Kendall, C., Sebestyen, S. D., Shaneley, J. B., Ohte, N. and Boyer, E. W., 2008. Carbon isotope fractionation of dissolved inorganic carbon (DIC) due to outgassing of carbon dioxide from a headwater stream. *Hydrological Processes* **22**, 2410–2423.

Dorale, J. A., Edwards, R. L., Ito, E. and Gonzalez, L. A., 1998. Climate and vegetation history of the midcontinent from 75 to 25 ka: a speleothem record from Crevice Cave, Missouri, USA. *Science* **282**, 1871–1874.

Dreybrodt, W., 1980. Deposition of calcite from thin films of natural calcareous solution and the growth of speleotems. *Chemical Geology* **29**, 89–105.

Dreybrodt, W., 1988. *Processes in Karst systems*. Springer Series in Springer Physical Environment., Heidelberg.

Dreybrodt, W., 2008. Evolution of the isotopic composition of carbon and oxygen in a calcite precipitating H_2O-CO_2-$CaCO_3$ solution and the related isotopic composition of calcite in stalagmites. *Geochimica et Cosmochimica Acta* **72**, 4712–4724.

Dreybrodt, W., 2011. Comments on processes contributing to the isotope composition on ^{13}C and ^{18}O in calcite deposited speleothems. *Acta carsologica* **40**, 233–238.

Dreybrodt, W. and Scholz, D., 2011. Isotope signals recorded in speleothems: From soil water to speleothem calcite. *Geochimica et Cosmochimica Acta* **75**, 734–752.

Dulinski, M. and Rozanski, K., 1990. Formation of $^{13}C/^{12}C$ isotope ratios in speleothems: a semi-dynamic model. *Radiocarbon* **32**, 7–16.

Duplessy, J. C., Labeyrie, J., Lalou, C. and Nguyen, H. V., 1970. Continental climatic variations between 130,000 and 90,000 years BP. *Nature* **226**, 631–633.

Ehhalt, D. H., Rohrer, F. and Fried, A., 2005. Vertical profiles of HDO/H_2O in the troposphere. *Journal*

of Geophysical Research **110**(D9), 13301.

Ek, C. and Gewelt, M., 1985. Carbon dioxide in cave atmospheres.New results in Belgium and comparison with some countries. *Earth Surface Processes and Landforms* **10**, 173–187.

Ellison, S., Rosslein, M. and Williams, A., 2000. Quantifying Uncertainty in Analytical Measurement. Guide.

Emiliani, C., 1971. Last interglacial paleotemperatures and chronology. *Science* **171**, 571–573.

Emrich, K., Ehhalt, D. H. and Vogel, J. C., 1970. Carbon isotope fractionation during the precipitation of calcium carbonate. *Earth and Planetary Science Letters* **8**, 363–371.

Epstein, S. and Mayeda, T. K., 1953. Variations of ^{18}O of waters from natural sources. *Geochimica et Cosmochimica Acta* **4**, 213–224.

Epstein, S. and Zeiri, L., 1988. Oxygen and carbon isotopic compositions of gases respired by humans. *Proceedings of the National Academy of Sciences* **85**(6), 1727–1731.

Fairchild, I. J., Borsato, A., Tooth, A. F., Frisia, S., Hawkesworth, C. J. and Huang, Y., 2000. Controls on trace element (Sr-Mg) compositions of carbonate cave waters: Implications for speleothem climatic records. *Chemical Geology* **166**, 255–269.

Fairchild, I. J., Frisia, S., Borsato, A. and Tooth, A. F., 2007. Speleothems. In Nash, D. and McLaren, S., eds., *Geochemical Sediments and Landscapes*. Wiley-Blackwell, Oxford.

Fairchild, I. J. and McMillan, E. A., 2007. Speleothems as indicators of wet and dry periods. *International Journal of Speleology* **36**, 69–74.

Fairchild, I. J., Smith, C. L., Baker, A., Fuller, L., Spötl, C., Mattey, D. and McDermott, F., 2006. Modification and preservation of environmental signals in speleothems. *Earth Science Reviews* **75**, 105–153.

Fairchild, I. J., Spötl, C., Frisia, S., Borsato, A., Susini, J., Wynn, P. M. and Cauzid, J., 2010. Petrology and geochemistry of annually laminated stalagmites from an Alpine cave (Obir, Austria): seasonal cave physiology. In Pedley, H. M. and Rogerson, M., eds., *Tufas and Speleothems: Unravelling the Microbial and Physical Controls*, volume 336, 295–321. Geological Society, London, special publication edition.

Fairchild, I. J. and Treble, P. C., 2009. Trace elements in speleothems as recorders of environmental change. *Quaternary Science Reviews* **28**, 449–468.

Feng, X. and Epstein, S., 1995. Carbon isotopes of trees from arid environments and implications for reconstructing atmospheric CO_2 concentration. *Geochimica et Cosmochimica Acta* **59**, 2599–2608.

Finnigan, 1997. Automated Water Isotope Analysis HDO Equilibrator. Technical report, Bremen.

Ford, D. and Williams, F., 2007. *Karst hydrogeology and geomorphology*. John Wiley and Sons, West Sussex.

Franke, H. W., 1965. Theory behind stalagmite shapes. *Studies in Speleology* **1**, 89–95.

Friedman, I. and O'Neil, J. R., 1977. *Compilation of stable isotope fractionation factors of geochemical interest*. US Geological Survey, Washington, DC, 6th edition.

Frisia, S., Borsato, A., Fairchild, I. J. and McDermott, F., 2000. Calcite fabrics, growth mechanisms and environments of formation in speleothems from the Italian Alps and southwestern Ireland. *Journal of Sedimentary Research* **70**, 1183–1196.

Frisia, S., Borsato, A., Preto, N. and McDermott, F., 2003. Late Holocene annual growth in three Alpine stalagmites records the influence of solar activity and the North Atlantic Oscillation on winter climate. *Earth and Planetary Science Letters* **216**(3), 411–424.

Frumkin, A., Carmi, I., Gopher, A., Tsuk, T., Ford, D. C. and Schwarcz, H. P., 1999. Holocene millenial-scale climatic cycle from Nahal Qanah Cave speleothem, Israel. *The Holocene* **9**, 677–682.

Frumkin, A., Ford, D. C. and Schwarcz, H. P., 1999. Continental Oxygen Isotopic Record of the Last 170,000 Years in Jerusalem. *Quaternary Research* **51**, 317–327.

Gams, I., 1974a. Koncentracija CO_2 v jamah v odvisnosti od zračne cirkulacije (na primeru Postojnske jame). In *Krasoslovni zbornik, VI /12*, 185–192. SAZU, Ljubljana.

Gams, I., 1974b. *Kras: zgodovinski, naravoslovni in geografski oris*. Slovenska matica, Ljubljana.

Gams, I. and Kogovšek, J., 1998. The dynamics of flowstone deposition in th caves Postojnska, Planinska, Taborska and Škocjanske, Slovenia. *Acta carsologica* **27**(1), 299–324.

Garrels, R. M. and Christ, C. L., 1965. *Solutions, minerals, and equilibria*. Harper & Row, New York.

Gascoyne, M., 1992. Palaeoclimate determination from cave calcite deposits. *Quaternary Science Reviews* **11**, 609–632.

Gascoyne, M., Schwarcz, H. P. and Ford, D. C., 1980. A paleotemperature record for the MidWisconsin in Vancouver Island. *Nature* **285**, 474–476.

Gat, J. R. and Tzur, Y., 1967. Modificationof the isotopic composition of rainwater by processes which occur before groundwater recharge. In *Isotopes in Hydrology (Proc. Symp. Vienna, 1966)*, 49–60. IAEA, Vienna.

Genty, D., Baker, A., Massault, M., Procter, C., Gilmour, M., Pons - Banchu, E. and Hamelin, B., 2001. Dead carbon in stalagmites carbonate bedrock paleodissolution vs. ageing of soil organic matter. Implications for ^{13}C variations in speleothems. *Geochimica et Cosmochimica Acta* **65**, 3443–3457.

Genty, D., Baker, A. and Vokal, B., 2001. Intra- and inter-annual growth rate of modern stalagmites. *Chemical Geology* **176**, 191–212.

Genty, D., Blamart, D., Ouahdi, R., Gilmour, M., Baker, A., Jouzel, J. and Van-Exter, S., 2003. Precise dating of Dansgaard–Oeschger climatic oscillations in western Europe from stalagmite data. *Nature* **421**, 833–837.

Genty, D. and Deflandre, G., 1998. Drip flow variations under a stalactite of the Père Noël cave (Belgium). Evidence of seasonal variations and air pressure constraints. *Journal of Hydrology* **211**, 208–232.

Genty, D., Vokal, B., Obelić, M. and Massault, M., 1998. Bomb ^{14}C time history recorded in two modern stalagmites - importance for soil organic matter dynamics and bomb ^{14}C distribution over continent. *Earth and Planetary Science Letters* **160**, 795–809.

Goede, A., Harmon, R. S., Atkinson, T. C. and Rowe, P. J., 1990. Pleistocene climatic change in Southern Australia and its effect on speleothem deposition in some Nullarbor caves. *Journal of Quaternary Science* **5**(1), 29–38.

Gonfiantini, R., Panichi, C. and Tongiorgi, E., 1968. Isotopic disequilibrium in travertine deposition. *Earth and Planetary Science Letters* **5**, 55–58.

Górka, M., Sauer, P. E., Lewicka-Szczebak, D. and Jędrysek, M.-O., 2011. Carbon isotope signature of dissolved inorganic carbon (DIC) in precipitation and atmospheric CO_2. *Environmental Pollution* **159**, 294–301.

Gospodarič, R., 1976. The Quaternary caves development between the Pivka basin and Polje of Planina. *Acta carsologica* **7**, 5–135.

Gospodarič, R., 1981. Geokronološko proučavanje sige v Postojnskem jamskem sistemu. *Naše jame* **22**.

Gospodarič, R., 1988. Paleoclimatic record of Cave sediments from Postojna karst. *Annales de la Societe geologique de Belgique* **111**, 91–95.

Gospodarič, R. and Habič, P., 1976. *Underground water tracing*. Institute for the Karst Research SAZU, Postojna.

Gregorič, A., Zidanšek, A. and Vaupotič, J., 2011. Dependence of radon level in Postojna Cave on outside temperature. *Natural Hazards and Earth System Sciences* **11**, 1523–1528.

Griffiths, M. L., Drysdale, R. N., Gagan, M. K., Zhao, J. X., Ayliffe, L. K., Hellstrom, J. C., Hantoro, W. S., Frisia, S., Feng, Y. X., Cartwright, I., Pierre, E. S., Fischer, M. J. and Suwargadi, B. W., 2009. Increasing Australian-Indonesian monsoon rainfall linked to early Holocene sea-level rise. *Nature Geoscience* **2**, 636–639.

Grossman, E. L., 1982. *Stable isotopes in live benthic foraminifera from the Southern California Borderland*. Ph.D. thesis, University of Southern California, Los Angeles.

Habič, P., Gospodarič, R. and Kogovšek, J., 1987. Raziskave kraških izvirov v Malnih pri Planini in zaledja vodnih virov v občini Postojna. Technical report, Karst Research Institute, Postojna.

Harmon, R. S. and Curl, R. L., 1978. Preliminary results on growth rate and paleoclimate studies of a stalagmite from Ogle Cave, New Mexico. *National Speleological Society Bulletin* **40**, 25–26.

Harmon, R. S., Schwarcz, H. P., Gascoyne, M., Hess, J. W. and Ford, D. C., 2004. Paleoclimate information from speleothems: the present as a guide to the past. In Sasowsky, I. and Mylroie, J., eds., *Studies of Cave Sediments*, 199–226. Kluwer Academic, New York, New York.

Harmon, R. S., Schwarcz, H. P., Gascoyne, M., Hess, J. W. and Ford, D. C., 2007. Paleoclimate information from speleothems: the present as a guid to the past. In Mylroie, J. and Sasowsky, I., eds., *Studies of Cave Sediments, Physical and Chemical Records of Paleoclimate*. Springer, Dordrecht, The Netherlands.

Hays, P. D. and Grossman, E. L., 1991. Oxygen isotopes in meteoric calcite cement as indicators of continental paleoclimate. *Geology* **19**, 441–414.

Hellstrom, J., McCulloch, M. and Stone, J., 1998. A detailed 31,000-year record of climate and vegetation change, from the isotope geochemistry of two New Zealand speleothems. *Quaternary Research* **50**, 167–178.

Hendy, C. H., 1971. The isotopic geochemistry of speleothems I. The calculation of the effects of different modes of formation on the isotopic composition of speleothems and their applicability as palaeoclimatic indicators. *Geochimica et Cosmochimica Acta* **35**, 801–824.

Hendy, C. H. and Wilson, A. T., 1968. Palaeoclimatic data from speleothems. *Nature* **219**, 48–51.

Hennig, G. J., Grün, R. and Brunnacker, K., 1983. Speleothems, travertines and paleoclimates. *Quaternary Research* **20**, 1–29.

Herzberg, G., 1950. *Molecular Spectra and Molecular Structure. I. Spectra of Diatomic Molecules*. Van Nostrand, New York.

Hoefs, J., 2004. *Stable isotope geochemistry*. Springer, New York.

Horita, J. and Clayton, R. N., 2007. Comment on the studies of oxygen isotope fractionation between calcium carbonates and water at low temperatures by Zhou and Zheng (2003, 2005). *Geochimica et Cosmochimica Acta* **71**, 3131–3135.

Horita, J. and Kendall, C., 2004. *Stable Isotope Analysis of Water and Aqueous Solutions by Conventional Dual-Inlet Mass Spectrometry*, volume I. Elsevier.

Horita, J., Ueda, A., Mizukami, K. and Takatori, I., 1989. Automatic δD and δ^{18}O analyses of multi-water samples using H_2- and CO_2-water equilibration methods with a common equilibration set-up. *Applied Radiation and Isotopes* **40**(9), 801–805.

Horvatinčić, N., Krajcar Bronić, I., Barešić, J., Obelić, B. and Vidič, S., 2005. Tritium and stable isotope distribution in the atmosphere at the coastal region of Croatia. In Gourcy, L., ed., *Isotopic composition of precipitation in the Mediterranean Basin in relation to air circulation patterns and climate*, TECDOC 1453, 37–50. IAEA, Vienna.

Horvatinčić, N., Krajcar Bronić, I. and Obelić, B., 2003. Differences in the ^{14}C age, δ^{13}C and δ^{18}O of Holocene tufa and speleothem in the Dinaric Karst. *Palaeogeography, Palaeoclimatology, Palaeoecology* **193**(1), 139–157.

Horvatinčić, N., Obelić, B., Krajcar Bronić, I. and Vokal, B., 1998. ^{14}C u atmosferi. In Obelić, B. and Franić, Z., eds., *Zbornik radova Četvrtog simpozija Hrvatskog društva za zaštitu od zračenja*, 213–218. HDZZ, Zagreb.

Horvatinčić, N., Čalić, R. and Geyh, M., 2000. Interglacial growth of tufa in Croatia. *Quaternary Research* **53**, 185–195.

IAEA, November 1997. Technical Procedure for cumulative monthly sampling of precipitation for isotopic analyses. Technical report, IAEA, Vienna.

Ikeya, M., Miki, T. and Gospodarič, R., 1982. ESR dating of Postojna Cave stalactite. *Acta carsologica* **11**, 117–130.

Indermuhle, A., Stocker, T. F. and Joos, F., 1999. Holocene carbon-cycle dynamics based on CO_2 trapped in ice at Taylor Dome, Antartica. *Nature* **398**, 121–126.

Jacob, S. and Sonntag, C., 1991. An 8-year record of the seasonal variation of ^{2}H and ^{18}O in atmospheric water vapour and precipitation at Heidelberg, Germany. *Tellus* **43**, 267–346.

Jimenez Lopez, C., Caballero, E., Huertas, F. J. and Romanek, C. S., 2001. Chemical, mineralogical and isotopic behaviour, and phase transformation during the precipitation of calcium carbonate minerals from intermediate ionic solution at 25°C. *Geochimica et Cosmochimica Acta* **65**, 3219–

3231.

Johnson, C. E., Stevenson, D. S., Collins, W. J. and Derwent, R. G., 2001. Role of climate feedback on methane and ozone studied with a coupled Ocean-Atmosphere-Chemistry model. *Geophysical Research Letters* **28**, 1723–1726.

Johnson, D. G., Jucks, K. W., Traub, W. A. and Chance, K. V., 2000. Isotopic composition of stratospheric ozone. *Journal of Geophysical Research* **105**, 9025–9031.

Johnson, K. R., Hu, C. Y., Belshaw, N. S. and Henderson, G. M., 2006. Seasonal trace-element and stable-isotope variations in a Chinese speleothem: The potential for high-resolution paleomonsoon reconstruction. *Earth and Planetary Science Letters* **244**, 394–407.

Kaufmann, G. and Dreybrodt, W., 2004. Stalagmite deposition and paleo-climate: an inverse approach. *Earth and Planetary Science Letters* **224**, 529–545.

Keeling, C. D., 1979. The Suess Effect: ^{13}Carbon-^{14}Carbon Interrelations. *Environment International* **2**, 229–300.

Keeling, C. D., Bacastow, R. B. and Tans, P. P., 1980. Predicted Shift in the $^{13}C/^{12}C$ Ratio of Atmospheric Carbon Dioxide. *Geophysical Research Letters* **7**, 505–508.

Keeling, C. D., Whorf, T. P., Wahlen, M. and van der Plicht, J., 1995. Interannual extremes in the rate of rise of atmospheric carbon dioxide since 1980. *Nature* **375**, 666–670.

Keith, D. W., 2000. Stratosphere-troposphere exchange: Inferences from the isotopic composition of water vapor. *J. Geophys. Res* **105**, 167–173.

Kempe, S., 2004. Natural speleothem damage in Postojnska jama (Slovenia), caused by glacial cave ice? A first assesment. *Acta carsologica* **18**, 265–289.

Kempe, S. and Hubrich, H. P., 2011. Inscriptions of some hystorically known persons in Postojnska jama. *Acta carsologica* **40**(2), 397–415.

Kempe, S., Hubrich, P. H. and Suckstorff, K., 2006. The history of Postojnska jama: the 1748 Joseph Anton Nagel inscriptions in Jama near Predjama and Postojnska jama. *Acta carsologica* **35**(2), 155–162.

Kim, S. T., Mucci, A. and Taylor, B., 2007. Phosphoric acid fractionation factors for calcite and aragonite between 25 and 75°C: Revisited. *Chemical Geology* **246**, 135–146.

Kim, S. T. and O'Neil, J. R., 1997. Equilibrium and nonequilibrium oxygen isotope effects in synthetic carbonates. *Geochimica et Cosmochimica Acta* **61**, 3461–3475.

Kogovšek, J., 1980. Distribution of some elements during sinter forming in the karst caves. *Acta carsologica* **9**, 111–128.

Kogovšek, J., 1997. Water tracing test in the vadose zone. In Kranjc, A., ed., *Tracer Hydrology*. Balkema, Rotterdam.

Kogovšek, J. and Habič, P., 1980. The study of vertical water percolation in the case of Postojna and Planina Caves. *Acta carsologica* **9**, 129–148.

Kogovšek, J. and Šebela, S., 2004. Water tracing through the vadose zone above Postojnska Jama, Slovenia. *Environmental Geology* **45**, 992–1001.

Kosednar-Legenstein, B., Dietzel, M., Leis, A. and Stingl, K., 2008. Stable carbon and oxygen isotope investigation in historical lime mortar and plaster – Results from field and experimental study. *Applied Geochemistry* **23**(8), 2425–2437.

Kossmat, F., 1897. Über die geologischen Verhältnisse der Umgebung von Adelsberg und Planina. *Vehr. Geol. R. A.* 78–84.

Krajcar Bronić, I., Horvatinčić, N. and Obelić, B., 1998. Two decades of environmental isotope record in Croatia: Reconstruction of the past and prediction of future levels. *Radiocarbon* **40**, 399–416.

Krajcar Bronić, I., Horvatinčić, N., Srdoč, D. and Obelić, B., 1986. On the initial ^{14}C activity in karst aquifers with short mean residence time. *Radiocarbon* **28**(2A), 436–440.

Krajcar Bronić, I., Obelić, B., Horvatinčić, N., Barešić, J., Sironić, A. and Minichreiter, K., 2010. Radiocarbon application in environmental science and archaeology in Croatia. *Nuclear Instruments and Methods in Physics Research A* **619**, 491–496.

Krajcar Bronić, I., Vreča, P., Horvatinčić, N., Barešić, J. and Obelić, B., 2006. Distribution of hydrogen, oxygen and carbon isotopes in the atmosphere of Croatia and Slovenia. *Arhiv za higijenu rada i*

toksikologiju **57**, 23–29.

Lachniet, M. S., 2009. Climatic and environmental controls on speleothem oxygen-isotope values. *Quaternary Science Reviews* **28**, 412–432.

Lachniet, M. S., Asmerom, Y., Burns, S. J., Patterson, W. P., Polyak, V. J. and Seltzer, G. O., 2004. Tropical Response to the 8200 yr B. P. Cold Event? Speleothem Isotopes Indicate a Weakend Early Holocene Monsoon in Costa Rica. *Geology* **32**, 957–960.

Langmuir, D., 1971. The geochemistry of some carbonate groundwaters in central Pennsylvania. *Geochimica et Cosmochimica Acta* **35**, 1023–1045.

Langmuir, D., 1997. *Aquaeous Environmental Geochemistry*. Prentice - Hall, New Jersey.

Lauritzen, S.-E. and Lundberg, J., 1999. Speleothems and climate. *The Holocene* **9**(6), 643–647.

Leng, M. J. and Marshall, J. D., 2004. Palaeoclimate interpretation of stable isotope data from lake sediment archives. *Quaternary Science Reviews* **23**, 811–831.

Lin, Y., Clayton, R. N. and Gröning, M., 2010. Calibration of delta(17)O and delta(18)O of international measurement standards - VSMOW, VSMOW2, SLAP, and SLAP2. *Rapid Communications in Mass Spectrometry* **24**(6), 773–776.

Lojen, S., Dolenec, T., Vokal, B., Cukrov, N., Mihelčič, G. and Papesch, W., 2004. C and O stable isotope variability in recent freshwater carbonates (River Krka, Croatia). *Sedimentology* **51**, 361–375.

Longinelli, A., Lenaz, R., Ori, C., Langone, L., Selmo, E. and Giglio, F., 2010. Decadal changes in atmospheric CO_2 concentration and $\delta^{13}C$ over two seas and two oceans: Italy to New Zealand. *Atmospheric Environment* **44**(34), 4303–4311.

Longinelli, A. and Selmo, E., 2003. Isotopic composition of precipitation in Italy: a first overall map. *Journal of Hydrology* **270**, 75–88.

Luetscher, M. and Jeannin, P.-Y., 2004. Temperature distribution in karst systems: the role of air and water fluxes. *Terra Nova* **16**, 344–350.

Mariethoz, G., Kelly, B. F. J. and Baker, A., 2012. Quantifying the value of laminated stalagmites for paleoclimate reconstructions. *Geophysical Research Letters* **39**, L05407.

Marjanac, Lj., 2012. *Pleistocene glacial and periglacial sediments of Kvarner, northern Dalmatia and southern Velebit Mts. - evidence of Dinaric glaciation*. Ph.D. thesis, Sveučilište u Zagrebu - Prirodoslovno-matematički fakultet.

Mattey, D. P., Fairchild, I. J., Atkinson, T. C., Latin, J.-P., Ainsworth, M. and Durell, R., 2010. Seasonal microclimate control of calcite fabrics, stable isotopes and trace elements in modern speleothem from St Michaels Cave, Gibraltar. In Pedley, H. M. and Rogerson, M., eds., *Tufas and Speleothems: Unravelling the Microbial and Physical Controls*, volume 336 of *GSL Special Publications*, 323–344. Geological Society of London.

Mattey, D. P., Lowry, D., Duffet, J., Fisher, R., Hodge, E. and Frisia, S., 2008. A 53 year seasonally resolved oxygen and carbon isotope record from a modern Gibraltar speleothem: Reconstructed drip water and relationship to local precipitation. *Earth and Planetary Science Letters* **269**, 80–95.

McCrea, J. M., 1950. On the isotopic chemistry of carbonates and a paleotemperatures scale. *Journal of Chemical Physics* **18**, 849–857.

McDermott, F., 2004. Paleo-climate recontruction from stable isotope variations in speleothems: a review. *Quaternary Science Reviews* **23**, 901–918.

McDermott, F., Schwarz, H. and Rowe, P. J., 2006. Isotopes in speleothems. In Leng, M. J., ed., *Isotopes in Paleoenvironmental studies*, 185–225. Springer, Dordecht, The Netherlands.

McKinney, R. C., McCrea, J. M., Epstein, S., Allen, H. A. and Urrey, H. C., 1950. Improvements in mass spectrometers for the measurement of small differences in isotopic abundance ratios. *Review of Scientific Instruments* **21**, 724–730.

Merkel, B. J. and Planer-Friedrich, B., 2008. *Groundwater Geochemistry: A Practical Guide to Modeling of Natural and Contaminated Aquatic Systems*. Springer, Heilderbeg.

Meyer, C. M., Spötl, C., Mangini, A. and Tessadri, R., 2012. Speleothem deposition at the glaciation threshold An attempt to constrain the age and paleoenvironmental significance of a detrital-rich flowstone sequence from Entrische Kirche Cave (Austria). *Palaeogeography, Palaeoclimatology,*

Palaeoecology **319-320**, 93–106.

Michaelis, J., Usdowski, E. and Menschel, G., 1985. Partitioning of ^{13}C and ^{12}C on the degassing of CO_2 and the precipitation of calcite-Rayleigh type fractionation and a kinetic model. *American Journal of Science* **285**, 318–327.

Mickler, P., Stern, L. A. and Banner, J. L., 2006. Large kinetic isotope effects in modern speleothems. *Geological Society of America, Bulletin* **118**, 65–81.

Mickler, P. J., Banner, J.-L., Stern, L., Asmerom, Y., Edwards, R. L. and Ito, E., 2004. Stable isotope variations in modern tropical speleothems: Evaluating equilibrium vs. kinetic isotope effects. *Geochimica et Cosmochimica Acta* **68**, 4381–4393.

Miorandi, R., Borsato, A., Frisia, S., Fairchild, I. J. and Richter, D. K., 2010. Epikarst hydrology and implications for stalagmite capture of climate changes at Grotta di Ernesto (NE Italy): results from long-term monitoring. *Hydrological Processes* **24**, 3101–3114.

Mook, W. G., 2000. *Environmental isotopes in the hydrological cycle: Principles and applications*. Unesco, International Hydrological Programme IHP-V., Paris.

Mook, W. G., Koopmans, M., Carter, A. F. and Keeling, C. D., 1985. Seasonal latitudinal and secular variations in the abundance and isotopic ratios of atmospheric carbon dioxide I. Results from land stations. *Journal of Geophysical Research* **88**, 10915–10933.

Morse, P. M., 1929. Diatomic Molecules According to the Wave Mechanics. II. Vibrational Levels. *Physical Review* **34**, 57–64.

Mulitza, S., Donner, B., Fischer, G., Paul, A., Pätzold, J., Rühlemann, C. and Segl, M., 2003. The South Atlantic oxygen isotope record of planktic foraminifera. In Wefer, G., Mulitza, S. and Ratmeyer, V., eds., *The South Atlantic in the Late Quaternary*, 121–142. Springer.

O'Driscoll, M. A., DeWalle, D. R., McGuire, K. J. and Gburek, W. J., 2005. Seasonal ^{18}O variations and groundwater recharge for three landscape types in central Pennsylvania, USA. *Journal of Hydrology* **303**, 108–124.

Olmsted III, J. and Gregory, M. W., 2006. *Chemistry*. John Wiley and Sons Inc.

Onac, B. P., Constantin, S., Lundberg, Y. and Lauritzen, S. E., 2002. Isotopic climate record in a Holocene stalagmite from Ursilor Cave (Romania). *Journal of Quaternary Science* **17**, 319–327.

O'Neill, J. R., Clayton, R. N. and Mayeda, T., 1969. Oxygen isotope fractionation in divalent metal carbonates. *Journal of Chemistry and Physics* **51**, 5547–5558.

Perko, A., 1929. *Die Adelsberg Grotte in Wort und Bild*. Mondaini.

Petrucci, R. H., Harwood, W. S., Herring, F. G. and Madura, J. D., 2007. *General Chemistry*. Pearson Education Inc.

Pettit, J. R., Jouzel, J. and Raynaud, D., 1999. Climate and atmospheric history of the past 420,000 years from the Vostok ice core, Antartica. *Nature* **399**, 429–436.

Pipan, T. and Brancelj, A., 2004. Distribution Patterns of Copepods (Crustacea: Copeopoda) in percolation water of the Postojnska Jama Cave System (Slovenia). *Zoological studies* **43**(2), 206–210.

Plagnes, V., Causse, C., Genty, D., Paterne, M. and Blamart, D., 2002. A discontinuous climatic record from 187 to 74 ka from a speleothem of the Clamouse Cave (south of France). *Earth and Planetary Science Letters* **201**, 87–103.

Plummer, L. N. and Busenberg, E., 1982. The solubilities of calcite, aragonite and vaterite in CO_2-H_2O solutions between 0 and 90°C, and an evaluation of the aqueous model for the system $CaCO_3$-CO_2-H_2O. *Geochimica et Cosmochimica Acta* **46**, 1011–40.

Plummer, L. N., Wigley, T. M. L. and Parkhurst, D. L., 1978. The kinetics of calcite dissolution in CO_2 -water systems at 5 degrees to 60 degrees C and 0.0 to 1.0 atm CO_2. *American Journal of Science* **278**, 179–216.

Poberžnik, M., Leis, A. and Lobnik, A., 2012. Use of a stable carbon isotope to assess the efficiency of a drinking water treatment method with CO_2. *Water Science & Technology* **65**(6), 983–988.

Prelovšek, M., Šebela, S. and Turk, J., 2011. Climate change in Postojnska jama in consequence to the massive tourism. In *Proceedings of International Scientific Symposium Man and Karst*. Center for Karst and Speleology, Medjugorje.

Renault, P., 1982. CO_2 atmospherique karstique et speleomorphologie. *Revue Belge de Geographie*

106, 121–130.

Riechelmann, D. F. C., Richter, D. K., Schröder Ritzau, A., Scholz, D. and Spötl, C., 2010. C/O - Isotopic composition and crystal morphology of recent calcite precipitates: Kinetic versus equilibrium. In Mangini, A. and Spötl, C., eds., *3rd Daphne workshop*. Innsbruck.

Rižnar, I., 1997. Geologija okolice Postojne. Technical report, Ljubljana.

Romanek, C. S., Grossman, E. L. and Morse, J. L., 1992. Carbon isotopic fractionation in synthetic aragonite and calcite: Effects of temperature and precipitation rate. *Geochimica et Cosmochimica Acta* **56**(1), 419–430.

Rosman, K. J. R. and Taylor, P. D. P., 1998. Isotopic compositions of the elements 1997. *Pure Appl Chem* **70**, 217–235.

Rozanski, K., Araguas-Araguas, L. and Gonfiantini, R., 1993. Isotope patterns in modern global precipitation. *Geophysical monograph* **78**, 1–35.

Rozanski, K. and Sonntag, C., 1982. Vertical distribution of deuterium in atmospheric water vapour. *Tellus* **34**, 135–141.

Rudzka, D., McDermott, F. and Surić, M., 2012. A late-Holocene climate record in stalagmites from Modrič Cave (Croatia). *Journal of Quaternary Science* **27**. U tisku.

Rutherford, E., 1911. The Scattering of $\alpha-$ and $\beta-$ Particles by Matter and the Structure of the Atom. *Philosophical Magazine* **21**, 669–688.

Salomons, W. and Mook, W. G., 1986. Isotope geochemistry of carbonates in the weathering zone. In Fritz, P. and Fontes, C., eds., *Handbook of Environmental Isotope Geochemistry*, volume 2. Elsevier, Amsterdam.

Sasowsky, I. D. and Mylroie, J., 2007. *Studies of Cave sediments, Physical and Chemical Records of Paleoclimate*. Springer, The Netherlands.

Schwarz, H. P., 1986. Geochronology and isotopic geochemistry of speleothems. In Fritz, P. and Fontes, J. C., eds., *Handbook of Environmental Isotope Geochemistry*, volume 239–270. Elsevier, Amsterdam.

Serefiddin, F., Schwartz, H. P., Ford, D. C. and Baldwin, S., 2004. Late Pleistocene paleoclimate in the Black Hills of South Dakota from isotopic records in speleothems. *Palaeogeography, Palaeoclimatology, Palaeoecology* **203**, 1–17.

Shackleton, N. J., 1974. Attainment of isotopic equilibrium between ocean water and the benthonic foraminifera genus Uvigerina: isotopic changes in the ocean during the last glacial. *Cent. Nat. Rech. Sci. Colloq. Int.* **219**, 203–209.

Sharp, Z., 2007. *Principles of Stable Isotope Geochemistry*. Pearson Prentice Hall, Upper Saddle River, NJ.

Shaw, T., 2009. Gassoil lamps in Postojnska jama in the 19th century. *Atti e memorie della commissione Grotte "E. Bogan"* **42**, 41–51.

Shopov, Y. Y., Tsankov, L. T., Yonge, C. J., Krouse, H. P. R. and Jull, A. J. T., 1997. Influence of the bedrock CO_2 on stable isotope records in cave calcites. In *Proceedings of the 12th International Congress of Speleology*, 65–68.

Smart, P. L. and Friedrich, H., 1987. Water movement and storage in the unsaturated zone of a naturally karstified aquifer unsaturated zone of a maturaly karstified aquifer, Mendip Hills, England. In *Zeitschrift fur Geomorphologie / Proceedings of Conference on Environmental Problems in Karst Terrains and their Solutions*, volume 59-87. National Water Well Association, Bowling Green, Kentucky.

Spötl, C., 2005. A robust and fast method of sampling and analysis of δ^{13}C of dissolved inorganic carbon in ground waters. *Isotopes in Environmental and Health Studies* **41**(3), 217–221.

Spötl, C., Fairchild, I. J. and Tooth, A. F., 2005. Cave air control on dripwater geochemistry, Obir Caves (Austria): Implications for speleothem deposition in dynamically ventilated caves. *Geochimica et Cosmochimica Acta* **69**, 2451–2468.

Spötl, C. and Mattey, D., 2006. Stable isotope microsampling of speleothems for palaeoenvironmental studies: a comparison of microdrill, micromill and laser ablation techniques. *Chemical Geology* **235**, 48–58.

Spötl, C. and Vennemann, T. W., 2003. Continuous-flow isotope ratio mass spectrometric analysis of carbonate minerals. *Rapid Communications in Mass Spectrometry* **17**, 1004–1006.

Srdoč, D., Obelić, B., Horvatinčić, N., Krajcar Bronić, I., Marčenko, E., Merkt, S. and Wong, H., 1986. Radiocarbon dating of lake sediments from two karstic lakes in Yugoslavia. *Radiocarbon* **28**, 495–502.

Stumm, W. and Morgan, J. J., 1996. *Aquatic Chemistry*. John Wiley & Sons, New York.

Surić, M., Roller-Lutz, Z., Mandić, M., Krajcar Bronić, I. and Juračić, M., 2010. Modern C, O, and H isotope composition of speleothem and dripwater from Modrič Cave, eastern Adriatic coast (Croatia). *International Journal of Speleology* **39**, 91–97.

Šebela, S., 1994. *Geološke osnove oblikovanja največje podorne dvorane v Postojnski jami - Velike gore*. Annals for Istrian and Mediterranean studies, Series historia naturalis, Postojna.

Šebela, S., 1998. *Tectonic structure of Postojnska jama Cave System*. ZRC SAZU, Postojna.

Šebela, S., 2001. Collapse dolines and passages of Postojnska jama Cave system. In *Proceedings of 13th International Congress of Speleology*, 157–162. Brasil DF.

Šebela, S., 2010. Effects of earthquakes in Postojna Cave system. *Acta carsologica* **39**(3), 597–604.

Šebela, S. and Sasowsky, I. D., 1999. Age and magneism of Cave sediments from Postojnska jama Cave system and Planinska jama Cave. *Acta carsologica* **28**(2), 293–305.

Šebela, S. and Turk, J., 2011. Postojna Cave climate, air temperature, and pressure monitoring. *Theoretical and Applied Climatology* **105**(3-4), 371–386.

Šturm, M., Vreča, P. and Krajcar Bronić, I., 2012. Carbon isotopic composition (δ^{13}C and ^{14}C activity) of plant samples in the vicinity of the Slovene nuclear power plant. *Journal of Environmental Radioactivity* **110**, 24–29.

Šušteršič, F., 2006. Relationship between deflector faults, collapse dolines and collector channel formation: some examples from Slovenia. *Journal of Speleology* **35**(1), 1–12.

Thomson, J. J., 1897. Cathode rays. *Philosophical Magazine* **44**, 293–316.

Tooth, A. F. and Fairchild, I. J., 2003. Soil and karst aquifer hydrological controls on the geochemical evolution of speleothem-forming drip waters, Crag Cave, southwest Ireland. *Journal of Hydrology* **273**, 51–68.

Tremaine, D. T., Froelich, P. N. and Wang, Y., 2011. Speleothem calcite farmed in situ: Modern calibration of δ^{18}O and δ^{13}C paleoclimate proxies in continuously-monitored natural cave system. *Geochimica et Cosmochimica Acta* **75**, 4929–4950.

Trudgill, S. T. and Inkepen, R., 1993. Impact of acid rain on karst environments. In Williams, P., ed., *Karst Terrains; Environmental Changes and Human Impacts*, volume 25, 199–218. Catena Supplement.

Turner, J. V., 1982. Kinetic fractionation of carbon-13 during calcium carbonate precipitation. *Geochimica et Cosmochimica Acta* **46**, 1183–1191.

Urbanc, J., Pezdič, J., Dolenec, T. and Perko, S., 1984. Isotopic composition of oxygen and carbon in cave water and speleothems of Slovenia. *Acta carsologica* **13**(4), 101–111.

Urbanc, J., Pezdič, J., Krajcar Bronić, I. and Srdoč, D., 1987. Comparison of isotopic composition of different forms of calcite precipitated from fresh water. In *Proceedings of the International Symposium on the Use of Isotope Techniques in Water Resources Development*, 783–787. IAEA, Vienna.

Vaughn, B. H., Miller, J., Ferretti, D. F. and White, J. W. C., 2004. *Stable isotope measurements of atmospheric CO_2 and CH_4*, volume I. Elsevier, Amsterdam, The Netherlands.

Verburg, P., 2007. The need to correct for the Suess effect in the application of δ^{13}C in sediment of autotrophic Lake Tanganyika, as a productivity proxy in the Anthropocene. *Journal of Paleolimnology* **37**(4), 591–602.

Vokal, B., 1999. *The carbon transfer in karst areas - an application to the study of environmental changes and paleoclimatic reconstruction*. Ph.D. thesis, Polytechnic, Nova Gorica.

Vokal, B., Obelić, B., Genty, D. and Kobal, I., 1999. Chemistry measurements of dripping water in Postojna Cave. *Acta carsologica* **28**(1), 305–321.

Vollweiler, N., Scholz, D., Mühlinghaus, C., Mangini, A. and Spötl, C., 2006. A precisely dated climate

record for the last 9 kyr from three high alpine stalagmites, Spannagel Cave, Austria. *Geophysical Research Letters* **33**, L20703.

Vreča, P., Krajcar Bronić, I., Horvatinčić, N. and Barešić, J., 2006. Isotopic characteristics of precipitation in Slovenia and Croatia: Comparison of continental and maritime stations. *Journal of Hydrology* **330**, 457–469.

Vreča, P., Krajcar Bronić, I. and Leis, A., 2011. Isotopic composition of precipitation in Portorož (Slovenia). *Geologija* **54**, 129–136.

Walpole, R. E., Myers, R. H., Myers, S. L. and Ye, K., 2001. *Probability and Statistics for Engineers and Scientists*. Prentice Hall, Lebanon, Indiana, USA, 7th edition.

Wang, X. F., Auler, A. S., Edwards, R. L., Cheng, H., Cristalli, P. S., Smart, P. L., Richards, D. A. and Shen, C. C., 2004. Wet periods in northeastern Brazil over the past 210 kyr linked to distant climate anomalies. *Nature* **432**, 740–743.

Wang, Y. J., Cheng, H., Edwards, R. L., He, Y. Q., Kong, X. G., An, Z. S., Wu, J. Y., Kelly, M. J., Dykoski, C. A. and Li, X. D., 2005. The Holocene Asian monsoon: Links to solar changes and North Atlantic climate. *Science* **308**, 854–857.

Werner, A. R. and Brandt, W. A., 2001. Referencing strategies and techniques in stable isotope ratio analysis. *Rapid Communications in Mass Spectrometry* **15**, 501–519.

Whitaker, T., Jones, D., Baldini, J. U. L. and Baker, A. J., 2010. A high-resolution spatial survey of cave air carbon dioxide concentrations in Scoska Cave (North Yorkshire, UK): implications for calcite deposition and re-dissolution. *Cave and Karst Science* **36**, 85–92.

White, W. B., 2007. Paleoclimate records from speleothes in limestone caves. In Mylroie, J. E. and Sasowsky, I., eds., *Studies of cave sediments; Physical and Chemical records of Paleoclimate*. Springer, Dordrecht, The Netherlands.

Wiedner, E., Scholz, D., Mangini, A., Polag, D., Mühlinghaus, C. and Segl, M., 2008. Investigation of the stable isotope fractionation in speleothems with laboratory experiments. *Quaternary International* **187**, 15–24.

Williams, P. W., King, D. N., Zhao, J.-X. and Collerson, K. D., 2004. Speleothem master chronologies: combined Holocene ^{18}O and ^{13}C records from the North Island of New Zealand and their palaeoenvironmental interpretation. *The Holocene* **14**(2), 194–208.

Ye, H. W. and Wang, W. M., 2001. Factors affecting the isotopic composition of organic matter. (1)Carbon isotopic composition of terrestrial plant materials. *Proceedings of the National Science Council* **25**, 137–147.

Yonge, C. J., Ford, D. C., Gray, J. and Schwarcz, H. P., 1985. Stable isotope studies of cave seepage water. *Chemical Geology* **58**, 97–105.

Yurtsever, Y. and Gat, J. R., 1981. Atmospheric water. In *Stable isotope Hydrology, Deuterium and Oxygen-18 in the water cycle*, volume 210, 339. IAEA Technical Report Series, Vienna.

Zupan Hajna, N., Mihevc, A., Pruner, P. and Bosak, P., 2010. Paleomagnetic research on karst sediments in Slovenia. *International Journal of Speleology* **39**(2), 47–60.

Zupan Hajna, N., Pruner, P., Mihevc, A., Schnabl, P. and Bosak, P., 2008. Cave sediments from the Postojnska - Planinska cave system (Slovenia): Evidence of multi - phase evolution in epiphreatic zone. *Acta carsologica* **37**(1), 63–86.

A. Appendix I

Table and figure captions:

Table A.1 Mean monthly air temperature (ºC) in Postojna during last 30 years (1982 - 2011). Data from National Meteorological Service of Slovenia (meteo.si)

Table A.2 Monthly amount of precipitation (mm) in Postojna during last 30 years (1982 - 2011). Data from National Meteorological Service of Slovenia (meteo.si)

Table A.3 *In situ* measured field parameters: air temperature, water temperature, pH of water, drip rate, conductivity and pCO_2. Mean values and standard deviations are given for each parameter.

Table A.4 Concentrations of Ca^{2+}, Mg^{2+}, HCO_3^-, Na^+, K^+, Cl^-, SO_4^{2-} and NO_3^- ions in drip water and calculated values of saturation index (I_{sat}) and aquatic CO_2 partial pressure. Mean values and standard deviations are calculated for parameters having more than 2 individual measurements.

Table A.5 Stable carbon composition of DIC in drip water ($\delta^{13}C_{DIC}$) and of CO_2 in air ($\delta^{13}C_{air}$) and stable oxygen composition of drip and river water ($\delta^{18}O_{water}$). Mean values and standard deviations are given for each parameter.

Table A.6 Correlation matrix between chemical and isotopic parameters for each location. R is correlation coefficient and p is statistical significance.

Table A.7 Oxygen composition ($\delta^{18}O_p$) of precipitation at sampling locations: Postojna, Zalog pri Postojni and Ljubljana.

Table A.8 Stable carbon $\delta^{13}C$ and oxygen $\delta^{18}O$ composition of soda straw samples. Length and mass of each sample is given.

Table A.9 Stable carbon $\delta^{13}C$ and oxygen $\delta^{18}O$ composition of carbonates of peculiar growth type.

Table A.10 Stable isotope composition $\delta^{13}C$ and $\delta^{18}O$ of modern carbonate precipitated on watch glasses.

Table A.11 Stable isotope composition $\delta^{13}C$ and $\delta^{18}O$ of old carbonate samples with description of each layer.

Table A.12 Stable isotope composition $\delta^{13}C$ and $\delta^{18}O$ of drilled cores from stalagmites with description of each layer.

Figure A.1 Letter with $\delta^{18}O_p$ in precipitation from Ljubljana (dr. Polona Vreča) and Zalog pri Postojni (dr. Sonja Lojen)

Figure A.2 Request for sampling in Postojna Cave and permission obtained from Slovenian Ministry of Environment, the Institute of the Republic of Slovenia for Nature Conservation.

Table A.1 Mean monthly air temperature (ºC) in Postojna during last 30 years (1982 – 2011). Data from National Meteorological Service of Slovenia (meteo.si)

Year / Month	1982	1983	1984	1985	1986	1987	1988	1989	1990	1991	Monthly average
1	-1.3	1.0	-0.8	-4.7	-0.8	-3.6	3.8	0.3	0.2	0.2	-0.6
2	-1.4	-2.3	-0.9	-2.0	-4.0	0.5	1.9	3.0	4.9	-1.5	-0.2
3	2.9	4.4	2.7	3.0	2.1	-0.4	3.2	6.1	6.5	6.3	3.7
4	6.2	8.8	7.0	7.0	7.7	8.5	7.9	8.5	6.9	6.9	7.5
5	12.9	12.6	10.1	12.8	14.7	10.9	13.2	12.3	13.0	9.3	12.2
6	16.8	16.0	14.7	14.5	15.3	15.3	14.9	14.2	15.1	15.5	15.2
7	19.0	20.6	16.7	19.2	17.4	18.9	19.5	17.8	17.6	19.5	18.6
8	17.4	17.6	16.3	18.0	17.8	16.5	18.2	17.2	17.3	18.5	17.5
9	16.4	14.0	12.8	14.6	12.8	16.6	13.2	13.6	12.4	15.4	14.2
10	10.0	9.4	10.6	8.9	9.4	10.5	10.4	8.6	10.4	7.9	9.6
11	5.8	2.4	5.2	2.0	5.6	4.6	1.4	3.5	5.1	4.6	4.0
12	2.7	0.7	0.9	3.8	-0.7	0.9	1.0	2.5	-0.1	-1.7	1.0
Yearly average	**9.0**	**8.8**	**7.9**	**8.1**	**8.1**	**8.3**	**9.1**	**9.0**	**9.1**	**8.4**	**8.6**
Year / Month	1992	1993	1994	1995	1996	1997	1998	1999	2000	2001	**Monthly average**
1	0.3	0.4	2.7	0.1	-1.1	-0.7	2.6	0.8	-2.0	1.1	0.4
2	1.6	-0.2	1.2	3.7	-1.6	3.0	4.1	-0.3	2.7	2.8	1.7
3	4.1	2.6	7.9	2.7	1.6	5.6	3.6	5.8	5.1	7.3	4.6
4	8.4	7.9	7.9	7.9	8.0	5.3	8.7	8.6	10.4	7.4	8.0
5	13.9	14.3	12.7	12.3	13.3	13.4	13.2	14.2	14.2	15.4	13.7
6	16.1	16.6	16.3	14.3	16.7	16.6	17.5	16.8	17.8	15.9	16.5
7	18.4	17.1	20.3	20.2	16.8	17.1	19.2	18.7	16.9	18.9	18.4
8	20.0	18.6	19.5	17.1	17.1	17.8	19.5	18.2	19.1	20.1	18.7
9	13.4	12.9	15	12.2	10.8	14.6	13.6	15.7	14.2	11.6	13.4
10	8.9	10.2	8.3	11.1	9.2	8.2	9.8	9.7	11.8	12.8	10.0
11	6.6	1.5	7.0	4.1	6.1	5.0	2.3	2.1	7.6	3.3	4.6
12	0.5	2.4	2.1	0.4	-1.2	2.3	-3.1	0.9	4.3	-2.1	0.7
Yearly average	**9.4**	**8.7**	**10.1**	**8.8**	**8.0**	**9.0**	**9.3**	**9.3**	**10.2**	**9.5**	**9.2**
Year / Month	2002	2003	2004	2005	2006	2007	2008	2009	2010	2011	**Monthly average**
1	-0.1	-1.0	-1.3	-0.7	-2.5	3.7	3.0	-1.3	-2.3	0.8	0.2
2	3.7	-2.4	0.5	-1.8	-0.4	4.9	2.6	1.2	0.7	0.3	1.6
3	7.1	5.0	3.0	3.3	2.8	6.8	4.0	4.7	3.9	4.9	4.5
4	7.9	7.8	8.5	8.0	9.1	12.2	8.3	10.8	9.4	10.5	10.0
5	13.7	15.1	11.4	14.3	13.4	15.0	14.3	15.7	12.8	14.5	14.3
6	18.3	20.6	16.5	17.9	18.2	18.6	18.3	17.0	17.7	17.9	18.0
7	19.1	20.2	18.4	19.6	22.4	19.4	19.4	19.4	20.4	18.7	19.9
8	17.8	21.6	18.3	16.8	15.9	18.2	18.9	20.4	18.0	20.2	18.6
9	12.7	13.1	14.2	14.6	15.9	12.5	13.2	16.4	13.3	17.5	14.8
10	10.2	7.7	12.0	10.5	12.5	8.6	10.9	9.8	8.6	8.9	9.9
11	8.8	7.0	5.2	4.2	7.3	3.9	5.8	7.2	6.9	3.9	5.8
12	1.4	1.7	1.0	-0.3	3.7	-0.2	1.4	1.8	0.0	3.1	1.6
Yearly average	**10.1**	**9.7**	**9.0**	**8.9**	**9.9**	**10.3**	**10.0**	**10.2**	**9.1**	**10.1**	**9.7**
							30 year average				**9.2**

Table A.2 Amount of precipitation (mm) in Postojna during last 30 years (1982 – 2011). Data from National Meteorological Service of Slovenia (meteo.si)

Year / Month	1982	1983	1984	1985	1986	1987	1988	1989	1990	1991	Monthly average
1	102.6	43.6	165.9	207.9	135.5	108.5	193.1	0.0	53.6	87.5	109.8
2	6.2	81.4	96.1	73.0	62.5	106.3	149.0	78.1	32.0	96.7	78.1
3	141.6	154.5	88.0	198.4	116.4	132.0	147.6	194.3	87.0	65.5	132.5
4	24.1	66.9	77.6	213.6	150.7	94.2	137.8	198.0	193.0	59.9	121.6
5	207.0	133.0	215.2	115.3	129.9	192.8	158.7	71.6	102.0	275.4	160.1
6	245.5	106.4	134.3	224.3	169.2	125.4	157.0	263.4	177.9	221.2	182.5
7	22.4	21.4	73.7	33.5	62.1	111.7	48.1	58.0	101.6	105.6	63.8
8	124.6	48.7	91.2	117.2	186.9	172.6	180.2	166.7	136.5	117.1	134.2
9	95.1	86.3	176.5	22.6	110.5	121.9	185.4	218.9	200.7	107.4	132.5
10	343.4	115.9	237.2	29.6	164.3	146.5	76.5	50.5	260.4	181.5	160.58
11	167.4	43.0	73.5	207.2	132.2	308.1	14.9	198.8	216.8	393.3	175.5
12	241.7	223.7	181.0	154.8	99.0	42.9	41.0	89.3	115.8	17.9	120.7
Yearly total	**1721.6**	**1124.8**	**1610.2**	**1597.4**	**1519.2**	**1662.9**	**1489.3**	**1587.6**	**1677.3**	**1729.0**	**1571.9**
Year / Month	1992	1993	1994	1995	1996	1997	1998	1999	2000	2001	**Monthly average**
1	35.0	6.6	144.7	132.5	83.7	163.3	34.4	58.2	4.2	287.3	95.0
2	52.6	7.4	89.3	291.0	116.6	26.0	1.9	119.9	4.1	26.4	73.5
3	166.4	49.0	39.4	205.9	12.4	28.9	33.3	94.1	149.0	273.5	105.2
4	140.9	71.3	170.1	22.3	158.7	68.5	282.0	286.5	102.1	82.8	138.5
5	75.3	24.7	180.0	136.6	167.7	78.0	62.7	95.1	96.9	52.0	96.9
6	121.3	147.1	209.1	203.7	146.5	149.7	106.0	138.4	74.9	111.4	140.8
7	130.3	54.2	63.4	59.1	114.3	153.9	150.4	106.8	158.7	159.8	115.1
8	57.9	77.0	160.2	212.2	80.9	86.7	150.0	68.0	24.3	14.9	93.2
9	86.8	331.9	160.1	232.0	203.6	26.4	172.0	139.4	138.7	382.0	187.3
10	512.9	324.9	234.6	42.4	185.5	143.1	287.9	98.3	192.5	53.5	207.6
11	141.0	160.9	99.4	109.6	218.5	367.5	183.1	103.2	455.2	76.7	191.5
12	153.2	169.7	113.8	207.0	166.0	216.4	32.5	200.8	153.8	51.1	146.4
Yearly total	**1673.6**	**1424.7**	**1664.1**	**1854.3**	**1654.4**	**1508.4**	**1496.2**	**1508.7**	**1591.3**	**1571.4**	**1594.7**
Year / Month	2002	2003	2004	2005	2006	2007	2008	2009	2010	2011	**Monthly average**
1	22.3	102.9	106.0	10.9	83.6	94.8	103.5	80.6	113.3	60.6	77.9
2	99.5	68.6	128.6	30.4	86.5	203.9	41.6	106.9	148.6	29.0	94.4
3	30.5	2.2	61.9	55.1	169.1	93.8	153.5	208.8	41.3	118.7	93.5
4	159.6	111.8	158.7	186.8	132.3	0.5	164.3	99.0	80.6	37.2	113.1
5	161.8	34.8	209.8	128.9	193.9	107.8	102.1	38.6	193.5	110.7	128.2
6	110.0	86.0	170.2	55.9	27.6	73.5	105.3	94.0	159.3	146.2	102.8
7	81.9	35.0	46.1	101.1	50.7	77.7	103.0	144.1	138.1	114.9	89.3
8	201.3	73.5	67.1	207.3	223.7	115.6	130.8	47.5	81.8	16.0	116.5
9	151.0	85.3	181.6	161.8	62.6	274.0	98.7	47.2	370.9	92.1	152.5
10	213.5	155.7	291.6	64.5	14.1	149.0	101.3	133.7	136.6	209.7	147.0
11	247.2	202.2	78.3	151.9	70.1	30.5	122.7	148.1	228.2	3.1	128.2
12	66.5	152.3	175.1	94.5	79.8	45.6	297.6	433.9	247.6	139.9	173.3
Yearly total	**1545.1**	**1110.3**	**1675.0**	**1249.1**	**1194.0**	**1266.7**	**1524.4**	**1582.4**	**1939.8**	**1078.1**	**1416.5**
							30 year average				**1527.7**

Table A.3 *In situ* measured field parameters: air temperature, water temperature, pH of water, drip rate, conductivity and pCO_2. Mean values and standard deviations are calculated for each parameter.

Date dd/mm/yyyy	**t_{air}** (°C)	**t_{water}** (°C)	**pH**	**Drip rate** (min^{-1})	**Conductivity** (µS/cm)	***p*CO₂** (ppmv)
Location 01 – Slonova glava						
26/03/2010	8.5	7.4	7.73	70	321	
08/06/2010	10.4	9.7	7.76	40	450	720
05/08/2010	12.0	10.9	7.10	15	466	1160
15/09/2010	11.5	11.2	7.10	32	477	1090
24/11/2010	10.4	10.4	7.5	165	556	540
03/02/2011	6.0	6.4	7.98	34	457	400
28/04/2011				13		
Mean	9.8	9.3	7.53	53	455	782
St. Dev.	2.2	2.0	0.36	53	76	334
Location 02 – Biospeleološka postaja						
26/03/2010	9.0	8.6	7.80	15	370	670
08/06/2010	10.7	9.7	7.82	30	376	760
05/08/2010	10.8	10.1	7.10	7	378	1230
15/09/2010	10.4	12.1	7.10	3	374	1260
24/11/2010	10.2	12.4	7.52	20	471	700
03/02/2011	8.2	8.7	8.06	10	437	420
28/04/2011				14		
Mean	9.9	10.3	7.57	14	401	840
St. Dev.	1.0	1.6	0.40	9	43	335
Location 03 – Vodopad						
26/03/2010	7.8	7.8	8.10	210	372	644
08/06/2010	9.7	9.9	8.22	5	396	710
05/08/2010	11.2	9.9	7.90	19	398	1100
15/09/2010	10.7	11.8	7.10	7	394	1220
24/11/2010	11.0	10.8	8.08	130	458	550
03/02/2011	7.5	7.5	8.08	32	418	400
28/04/2011				18		
Mean	9.7	9.6	7.91	60	406	771
St. Dev.	1.6	1.7	0.41	79	29	321
Location 04 – Kongresna dvorana						
26/03/2010	8.5	8.4	8.35	60	420	640
08/06/2010	9.9	9.5	7.58	20	476	720
05/08/2010	12.7	10.7	7.80	33	416	1070
15/09/2010	10.5	10.2	7.85	26	409	1220
24/11/2010	11.0	10.4	8.32	90	433	620
03/02/2011	9.4	8.8	8.32	70	421	430
28/04/2011				50		
Mean	10.3	9.7	8.04	50	429	783
St. Dev.	1.4	0.9	0.33	25	24	300

Date dd/mm/yyyy	**t_{air}** (°C)	**t_{water}** (°C)	**pH**	**Drip rate** (min^{-1})	**Conductivity** (µS/cm)	***p*CO_2** (ppmv)
Location 05 – Podrti kapnik						
26/03/2010	11.2	9.9	8.38	200	304	1530
08/06/2010	10.9	10.1	8.06	50	283	1250
05/08/2010	11.5	10.6	7.62	10	282	1530
15/09/2010	11.6	11.7	7.46	12	280	1470
24/11/2010	10.7	10.7	8.25	85	318	760
03/02/2011	10.5	10.4	8.16	22	197	430
28/04/2011				11		
Mean	11.1	10.6	7.99	56	277	1162
St. Dev.	0.4	0.6	0.37	69	42	463
Location 06 – Stebrišče						
26/03/2010	10.5	10.4	8.33	120	357	720
08/06/2010	10.9	10.4	7.88	50	338	1100
05/08/2010	13.5	11.3	7.38	65	369	1490
15/09/2010	11.6	12.2	7.70	160	368	1480
24/11/2010	10.8	11.2	7.87	80	387	930
03/02/2011	10.2	10.6	7.92	100	375	510
28/04/2011				180		
Mean	11.3	11.0	7.85	108	366	1038
St. Dev.	1.2	0.7	0.31	48	17	399
Location 07 – Čarobni vrt						
26/03/2010	9.8	9.5	8.16	140	365	750
08/06/2010	10.8	11.1	7.95	120	378	1440
05/08/2010	9.6	10.0	7.64	45	319	2350
15/09/2010	11.7	11.8	7.35	35	328	2940
24/11/2010	11.2	11.7	7.92	450	323	1200
03/02/2011	11.0	10.3	8.17	100	301	790
28/04/2011				120		
Mean	10.7	10.7	7.87	144	336	1578
St. Dev.	0.8	0.9	0.32	140	30	885
Location 08 – Vrh Velike gore						
26/03/2010	11.0	10.9	7.93	60	359	680
08/06/2010	11.2	11.0	7.71	120	323	1440
05/08/2010	13.0	11.4	7.69	7	352	1670
15/09/2010	11.5	14.3	7.79	4	391	1630
24/11/2010	11.4	11.9	7.78	500	431	1100
03/02/2011	11.4	11.7	8.05	50	357	600
28/04/2011				86		
Mean	11.6	11.9	7.83	118	369	1187
St. Dev.	0.7	1.3	0.14	173	37	470

Date dd/mm/yyyy	**t_{air}** (°C)	**t_{water}** (°C)	**pH**	**Drip rate** (min^{-1})	**Conductivity** (µS/cm)	***p*CO_2** (ppmv)
Location 09 – Zgornji Tartar						
26/03/2010	11.5	11.3	7.90	120	375	650
08/06/2010	10.7	9.8	7.97	50	359	870
05/08/2010	11.7	11.1	7.70	26	365	1110
15/09/2010	10.4	12.5	7.36	22	360	1260
24/11/2010	10.6	10.6	8.00	300	389	1250
03/02/2011	9.1	10.2	8.13	19	329	480
28/04/2011				26		
Mean	10.7	10.9	7.84	80	363	937
St. Dev.	0.9	1.0	0.28	103	20	325
Location 10 – Pivka River inside						
26/03/2010	8.3	8.3	8.00			
08/06/2010	12.1	15.2	7.88		438	1130
05/08/2010	15.7	17.0	7.53		351	1120
15/09/2010	13.1	14.1	7.82		359	1250
24/11/2010	-[a]	-[a]	-[a]		-[a]	-[a]
03/02/2011	5.3	3.8	8.19		470	480
28/04/2011						
Mean	10.9	11.7	7.88		405	995
St. Dev.	4.1	5.5	0.24		59	348
Location 11 – Pivka River outside						
26/03/2010	8.6	7.9	8.20		384	480
08/06/2010	14.1	16.1	7.82		434	410
05/08/2010	27.0	18.0	7.77		345	350
15/09/2010	17.8	16.1	7.08		360	360
24/11/2010	6.3	7.8	8.07		393	390
03/02/2011	-1.0	1.3	8.27		410	400
28/04/2011						
Mean	12.1	11.2	7.87		388	398
St. Dev.	9.8	6.6	0.43		32	46
Outer locations 01, 02, 03, 04						
Mean	9.9	9.7		44.3	422.8	794.0
St. Dev.	0.3	0.4		20.6	24.7	31.1
Iner locations 06, 07, 08, 09						
Mean	11.1	11.1		112.5	358.5	1185.0
St. Dev.	0.5	0.5		26.5	15.2	281.4

[a]Flood

Table A.4 Concentrations of Ca^{2+}, Mg^{2+}, HCO_3^-, Na^+, K^+, Cl^-, SO_4^{2-} and NO_3^- ions in drip water and calculated values of saturation index (I_{sat}) and aquatic CO_2 partial pressure. Mean values and standard deviations are calculated for parameters having more than 2 individual measurements.

Date	**Ca^{2+}** (mg/L)	**Mg^{2+}** (mg/L)	**HCO_3^-** (mg/L)	**Na^+** (mg/L)	**K^+** (mg/L)	**Cl^-** (mg/L)	**SO_4^{2-}** (mg/L)	**NO_3^-** (mg/L)	**I_{sat}**	**pCO_2,aq** (μatm)
Location 01 – Slonova glava										
26/03/2010	87.7	0.86	233.0						2.24	3737
08/06/2010	96.8	0.91	219.0						2.69	3363
15/09/2010	108.0	1.24	256.4	3.24	0.69	4.03	9.62	19.08	0.80	18294
24/11/2010	101.0	1.44	364.8						1.08	26141
03/02/2011	69.8	1.23	294.6						1.47	8315
28/04/2011	71.4	1.05	273.0	2.05	0.15	1.74	7.36	8.40	3.68	2426
Mean	89.1	1.12	273.5						1.99	10379
St. Dev.	15.8	0.22	52.3						1.09	9715
Location 02 – Biospeleološka postaja										
26/03/2010	66.5	0.73	183.0						1.63	2530
08/06/2010	82.1	0.72	193.0						2.31	2577
15/09/2010	91.8	0.94	223.3	1.64	0.38	1.02	5.22	0.92	0.58	15792
24/11/2010	97.7	1.34	327.0						0.96	23686
03/02/2011	77.7	1.17	288.2						1.79	7947
28/04/2011	98.2	0.98	284.0	1.14	0.15	0.80	4.02	0.51	6.83	2150
Mean	85.7	0.98	249.8						2.35	9114
St. Dev.	12.5	0.24	58.3						2.28	8864
Location 03 – Vodopad										
26/03/2010										
08/06/2010	81.7	0.71	192.0						5.78	1018
15/09/2010	95.7	1.02	239.1	1.45	0.15	1.16	6.59	9.92	4.04	2663
24/11/2010	93.9	1.20	292.8						0.82	21135
03/02/2011	81.8	1.01	272.2						6.13	2017
28/04/2011	89.3	0.94	250.0	1.08	0.15	1.07	5.54	5.51	5.50	1786
Mean	88.5	0.98	249.2						4.45	5724
St. Dev.	6.6	0.18	38.1						2.18	8635
Location 04 – Kongresna dvorana										
26/03/2010	74.8	0.77	209.0						7.39	805
08/06/2010	103.0	0.88	257.0						2.20	5963
15/09/2010	88.0	1.05	229.4	1.11	0.20	1.68	1.92	3.25	2.91	3249
24/11/2010	79.2	0.77	268.4						3.38	3367
03/02/2011	101.0	1.00	269.0						12.82	1136
28/04/2011	75.3	0.89	250.0	1.05	0.18	5.69	1.07	2.15	8.42	1037
Mean	86.9	0.89	247.1						6.19	2593
St. Dev.	12.6	0.12	23.7						4.12	2006

Date	Ca^{2+} (mg/L)	Mg^{2+} (mg/L)	HCO_3^- (mg/L)	Na^+ (mg/L)	K^+ (mg/L)	Cl^- (mg/L)	SO_4^{2-} (mg/L)	NO_3^- (mg/L)	I_{sat}	pCO_2,aq (μatm)
Location 05 – Podrti kapnik										
26/03/2010										556
08/06/2010	68.2	0.67	133.0						2.33	1024
15/09/2010	73.7	0.83	165.9	0.91	0.50	0.79	6.22	8.69	1.16	3558
24/11/2010	76.3	0.83	194.2						1.01	6098
03/02/2011	47.0	0.88	121.7						2.32	605
28/04/2011	59.2	0.75	149.0	0.93	0.17	0.74	5.70	5.19	2.88	912
Mean	64.9	0.79	152.8						1.94	2126
St. Dev.	11.9	0.08	28.5						0.81	2249
Location 06 – Stebrišče										
26/03/2010	68.3	0.65	187.0						6.17	770
08/06/2010	82.5	0.78	222.0						3.14	2605
15/09/2010	83.6	0.95	233.0	1.03	0.15	0.84	6.35	3.61	1.09	8767
24/11/2010	82.5	0.93	255.0						2.53	4633
03/02/2011	69.6	0.99	243.4						2.91	2950
28/04/2011	89.8	0.86	250.0	0.88	0.18	0.75	5.76	2.43	4.25	2681
Mean	79.4	0.86	231.7						3.35	3734
St. Dev.	8.5	0.13	24.9						1.72	2754
Location 07 – Čarobni vrt										
26/03/2010	68.8	0.67	190.0						4.14	1151
08/06/2010	72.8	1.20	167.0						2.51	1681
15/09/2010	90.3	0.25	213.5	0.86	0.15	0.65	4.86	0.25	1.88	4341
24/11/2010	68.0	0.89	209.8						0.76	8512
03/02/2011	68.9	0.91	205.0						2.77	2225
28/04/2011	76.2	0.76	216.0	0.70	0.15	0.70	4.11	0.20	5.48	1291
Mean	74.2	0.78	200.2						2.92	3200
St. Dev.	8.5	0.32	18.7						1.67	2850
Location 08 – Vrh Velike gore										
26/03/2010	82.0	0.37	228.0						3.65	2398
08/06/2010	78.1	0.38	187.0						1.73	3267
15/09/2010	84.1	0.63	251.3	1.04	0.15	0.91	4.28	1.48	2.42	4629
24/11/2010	80.3	0.56	286.7						3.66	4341
03/02/2011	86.5	0.56	243.4						3.01	3663
28/04/2011	80.5	0.44	252.0	0.77	0.15	0.66	3.54	0.44	5.37	2024
Mean	81.9	0.49	241.4						3.31	3387
St. Dev.	3.0	0.11	32.9						1.26	1037
Location 09 – Zgornji Tartar										
26/03/2010	80.1	0.62	201.0						1.87	3599
08/06/2010	77.1	0.62	183.0						2.61	2071
15/09/2010	69.0	0.69	217.2	1.20	0.15	0.75	3.90	1.23	3.10	2054
24/11/2010	76.0	1.05	255.0						1.08	10193
03/02/2011	72.9	0.94	208.2						3.45	1852
28/04/2011	78.7	0.80	223.0	0.94	0.15	0.76	3.53	1.04	5.31	1460
Mean	75.6	0.79	214.6						2.90	3538
St. Dev.	4.1	0.18	24.2						1.46	3341

Date	Ca^{2+} (mg/L)	Mg^{2+} (mg/L)	HCO_3^- (mg/L)	Na^+ (mg/L)	K^+ (mg/L)	Cl^- (mg/L)	SO_4^{2-} (mg/L)	NO_3^- (mg/L)	I_{sat}	pCO_2,aq (μatm)
Location 10 – Pivka River inside										
26/03/2010										
08/06/2010	79.2	3.67	194.0						3.09	2412
15/09/2010	64.9	3.06	179.3	14.0	4.11	14.8	9.99	4.98	1.11	5125
24/11/2010	-[a]	-[a]	-[a]							
03/02/2011	91.8	4.48	259.4							3653
28/04/2011	71.9	4.11	216.0	21.5	2.71	31.1	9.35	5.19	4.35	1149
Mean	77.0	3.83	212.2						2.85	3085
St. Dev.	11.5	0.61	34.9						1.63	1702
Location 11 – Pivka River outside										
26/03/2010	74.0	3.86	218.0						5.31	1182
08/06/2010	78.7	2.79	197.0						2.80	2847
15/09/2010	67.2	3.68	183.0	15.2	4.07	15.1	9.93	3.88	2.11	3043
24/11/2010	70.2	3.07	247.6						0.57	19753
03/02/2011	70.5	4.68	256.2						4.39	1879
28/04/2011	71.6	4.22	222.0	23.3	2.67	28.8	9.84	3.94	4.93	957
Mean	72.0	3.72	220.6						3.35	4943
St. Dev.	3.9	0.70	28.2						1.84	7304
Outer locations 01, 02, 03, 04										
Mean	87.6	1.0	254.9							6952.5
St. Dev.	1.5	0.1	12.5							3508.4
Inner locations 06, 07, 08, 09										
Mean	77.8	0.7	222.0							3464.8
St. Dev.	3.5	0.2	18.3							226.6

[a]Flood

Table A.5 Stable carbon composition of DIC in drip water ($\delta^{13}C_{DIC}$) and of CO_2 in air ($\delta^{13}C_{air}$) and stable oxygen composition of drip and river water ($\delta^{18}O_{water}$). Mean values and standard deviations are calculated for each parameter.

Date	**$\delta^{13}C_{DIC}$** (‰, VPDB)	**$\delta^{13}C_{air}$** (‰, VPDB)	**$\delta^{18}O_{water}$** (‰, VSMOW)
Location 01 – Slonova glava			
26/03/2010			-8.79
08/06/2010	-13.12	-14.70	-9.42
05/08/2010			-9.41
15/09/2010	-13.06	-18.39	-9.35
24/11/2010	-13.86	-12.48	-8.02
03/02/2011	-13.15	-6.52	-9.02
28/04/2011	-13.29	-13.16	-9.19
Mean	-13.30	-13.05	-9.03
St. Dev.	0.33	4.31	0.50
Location 02 – Biospeleološka postaja			
26/03/2010	-12.94	-9.57	-9.17
08/06/2010	-12.76	-17.54	-9.99
05/08/2010			-10.13
15/09/2010	-12.52	-19.12	-10.11
24/11/2010	-12.85	-15.14	-8.37
03/02/2011	-12.56	-7.58	-9.16
28/04/2011	-13.39	-14.59	-9.53
Mean	-12.84	-13.92	-9.49
St. Dev.	0.32	4.50	0.65
Location 03 – Vodopad			
26/03/2010			-8.87
08/06/2010	-12.44	-14.68	-9.00
05/08/2010			-9.39
15/09/2010	-12.92	-18.75	-9.35
24/11/2010	-13.05	-11.60	-8.47
03/02/2011	-12.87	-6.35	-9.04
28/04/2011	-13.20	-14.55	-9.13
Mean	-12.90	-13.19	-9.04
St. Dev.	0.29	4.59	0.31
Location 04 – Kongresna dvorana			
26/03/2010	-11.90		-8.78
08/06/2010	-13.09	-14.24	-8.82
05/08/2010			-8.86
15/09/2010	-12.07	-18.61	-8.87
24/11/2010	-12.96	-12.89	-8.88
03/02/2011	-12.02	-6.41	-8.90
28/04/2011	-12.10	-10.73	-8.89
Mean	-12.36	-12.58	-8.86
St. Dev.	0.52	4.49	0.04

Date	$\delta^{13}C_{DIC}$ (‰, VPDB)	$\delta^{13}C_{air}$ (‰, VPDB)	$\delta^{18}O_{water}$ (‰, VSMOW)
Location 05 – Podrti kapnik			
26/03/2010	-11.00	-12.45	-9.33
08/06/2010	-10.69	-18.51	-9.00
05/08/2010			-9.02
15/09/2010	-11.12	-19.16	-9.05
24/11/2010	-11.78	-15.36	-8.52
03/02/2011	-5.64	-9.32	-8.76
28/04/2011	-9.15	-15.41	-8.82
Mean	-9.90	-15.04	-8.93
St. Dev.	2.26	3.71	0.26
Location 06 – Stebrišče			
26/03/2010	-13.17		-8.67
08/06/2010	-13.14	-18.57	-8.78
05/08/2010			-8.80
15/09/2010	-13.11	-19.62	-8.81
24/11/2010	-12.97	-16.85	-8.64
03/02/2011	-12.89	-10.13	-8.70
28/04/2011	-13.05	-16.06	-8.72
Mean	-13.06	-16.25	-8.73
St. Dev.	0.11	3.69	0.07
Location 07 – Čarobni vrt			
26/03/2010	-12.24	-16.61	-9.05
08/06/2010	-12.58	-18.43	-9.22
05/08/2010			-9.29
15/09/2010	-12.06	-21.64	-9.28
24/11/2010	-12.42	-18.21	-8.84
03/02/2011	-11.98	-15.67	-8.98
28/04/2011	-12.66	-17.43	-9.14
Mean	-12.32	-18.00	-9.11
St. Dev.	0.28	2.06	0.17
Location 08 – Vrh Velike gore			
26/03/2010		-16.27	-10.22
08/06/2010	-12.65	-19.78	-10.34
05/08/2010			-9.93
15/09/2010	-12.82	-20.22	-9.97
24/11/2010	-13.36	-17.75	-8.38
03/02/2011	-12.35	-13.19	-9.48
28/04/2011	-12.99	-17.58	-9.50
Mean	-12.83	-17.47	-9.69
St. Dev.	0.38	2.56	0.66

Date	$\delta^{13}C_{DIC}$ (‰, VPDB)	$\delta^{13}C_{air}$ (‰, VPDB)	$\delta^{18}O_{water}$ (‰, VSMOW)
Location 09 – Zgornji Tartar			
26/03/2010	-13.52	-15.71	-9.11
08/06/2010	-13.13	-16.32	-9.25
05/08/2010			-9.05
15/09/2010	-11.86	-18.53	-8.98
24/11/2010	-13.78	-18.44	-8.52
03/02/2011	-12.36	-10.04	-8.91
28/04/2011	-13.42	-17.69	-8.98
Mean	-13.01	-16.12	-8.97
St. Dev.	0.75	3.19	0.23
Location 10 – Pivka River inside			
26/03/2010			-8.96
08/06/2010	-12.99	-17.47	-8.41
05/08/2010			-7.81
15/09/2010	-14.57	-19.26	-6.94
24/11/2010	-[a]	-[a]	-[a]
03/02/2011	-12.23	-8.29	-8.36
28/04/2011	-9.75	-13.33	-7.95
Mean	-12.39	-14.59	-8.07
St. Dev.	2.01	4.88	0.69
Location 11 – Pivka River outside			
26/03/2010		-6.78	-8.97
08/06/2010	-13.15	-7.22	-8.40
05/08/2010			-7.84
15/09/2010	-14.39	-15.5	-6.92
24/11/2010	-13.33	-6.23	-8.09
03/02/2011	-12.48	-6.39	-8.34
28/04/2011	-8.75	-4.35	-7.87
Mean	-12.42	-7.75	-8.06
St. Dev.	2.16	3.92	0.63
Outer locations 01, 02, 03, 04			
Mean	-12.9	-13.2	-9.1
St. Dev.	0.4	0.6	0.3
Inner locations 06, 07, 08, 09			
Mean	-12.8	-17.0	-9.4
St. Dev.	0.3	0.9	0.6

Table A.6 Correlation matrix between chemical and isotopic parameters for each location. R is correlation coefficient and p is statistical significance.

Shaded cells represent significantly good correlation ($p < 0.1$)

Location 01 – Slonova glava												
		Cond.	**HCO_3^-**	**Ca^{2+}**	**pH**	**Mg^{2+}**	**$\delta^{13}C_{DIC}$**	***p*CO_2 air**	**$\delta^{13}C_{air}$**	***p*CO_2 (aq)**	**I_{sat}**	**Drip rate**
Cond.	R	1.00	0.74	0.36	-0.32	0.86	-0.95	-0.24	-0.06	0.31	-0.29	0.39
	p	--	0.16	0.56	0.54	0.06	0.05	0.69	0.94	0.55	0.58	0.44
HCO_3^-	R		1.00	0.00	-0.08	0.89	-0.88	-0.51	0.40	0.01	-0.19	0.71
	p		--	1.00	0.89	0.02	0.05	0.49	0.51	0.99	0.76	0.11
Ca^{2+}	R			1.00	-0.87	0.23	-0.17	0.78	-0.76	0.70	-0.91	0.43
	p			--	0.05	0.67	0.79	0.22	0.14	0.19	0.03	0.39
pH	R				1.00	-0.36	0.05	-0.90	0.86	-0.94	0.95	0.14
	p				--	0.55	0.95	0.04	0.14	0.01	0.00	0.79
Mg^{2+}	R					1.00	-0.66	-0.19	0.18	0.38	-0.32	0.53
	p					--	0.23	0.81	0.78	0.53	0.60	0.28
$\delta^{13}C_{DIC}$	R						1.00	0.42	-0.16	0.20	0.34	-0.92
	p						--	0.58	0.79	0.80	0.66	0.03
***p*CO_2 air**	R							1.00	-0.93	0.86	-0.80	-0.49
	p							--	0.07	0.06	0.10	0.40
$\delta^{13}C_{air}$	R								1.00	-0.76	0.81	0.07
	p								--	0.24	0.19	0.91
***p*CO_2 (aq)**	R									1.00	-0.81	-0.28
	p									--	0.05	0.60
I_{sat}	R										1.00	-0.10
	p										--	0.84
Drip rate	R											1.00
	p											--

Location 02 – Biospeleološka postaja												
		Cond.	**HCO_3^-**	**Ca^{2+}**	**pH**	**Mg^{2+}**	**$\delta^{13}C_{DIC}$**	***p*CO_2 air**	**$\delta^{13}C_{air}$**	***p*CO_2 (aq)**	**I_{sat}**	**Drip rate**
Cond.	R	1.00	0.97	0.51	0.29	0.95	-0.02	-0.53	0.26	-0.41	0.46	0.15
	p	--	0.00	0.38	0.58	0.01	0.97	0.28	0.68	0.49	0.36	0.78
HCO_3^-	R		1.00	0.65	0.01	0.95	-0.16	-0.32	0.14	-0.34	0.39	-0.14
	p		--	0.16	0.99	0.00	0.76	0.59	0.80	0.66	0.52	0.79
Ca^{2+}	R			1.00	-0.65	0.54	-0.29	0.45	-0.63	0.35	-0.28	-0.07
	p			--	0.24	0.27	0.58	0.44	0.18	0.65	0.64	0.90
pH	R				1.00	-0.07	-0.25	-0.95	0.77	-0.59	0.78	0.53
	p				--	0.91	0.68	0.00	0.13	0.30	0.07	0.28
Mg^{2+}	R					1.00	0.11	-0.25	0.15	-0.21	0.35	-0.23
	p					--	0.84	0.69	0.78	0.79	0.57	0.66
$\delta^{13}C_{DIC}$	R						1.00	0.33	-0.03	0.64	0.40	-0.25
	p						--	0.59	0.95	0.36	0.51	0.64
***p*CO_2 air**	R							1.00	-0.82	0.63	-0.77	-0.49
	p							--	0.09	0.26	0.07	0.33
$\delta^{13}C_{air}$	R								1.00	-0.54	0.70	-0.14
	p								--	0.46	0.19	0.79
***p*CO_2 (aq)**	R									1.00	-0.36	-0.61
	p									--	0.55	0.28
I_{sat}	R										1.00	0.05
	p										--	0.93
Drip rate	R											1.00
	p											--

Location 03 – Vodopad												
		Cond.	**HCO_3^-**	**Ca^{2+}**	**pH**	**Mg^{2+}**	**$\delta^{13}C_{DIC}$**	***p*CO_2 air**	**$\delta^{13}C_{air}$**	***p*CO_2 (aq)**	**I_{sat}**	**Drip rate**
Cond.	R	1.00	0.83	0.28	0.18	0.76	-0.64	-0.40	0.50	-0.38	0.56	-0.02
	p	--	0.17	0.72	0.73	0.24	0.36	0.43	0.50	0.53	0.32	0.97
HCO_3^-	R		1.00	0.40	0.03	0.94	-0.74	-0.41	0.52	-0.11	0.18	0.76
	p		--	0.51	0.97	0.02	0.15	0.59	0.36	0.89	0.82	0.14
Ca^{2+}	R			1.00	-0.70	0.66	-0.60	0.60	-0.57	0.68	-0.58	0.38
	p			--	0.30	0.22	0.28	0.40	0.32	0.32	0.42	0.53
pH	R				1.00	-0.23	0.37	-0.77	0.68	-0.98	0.98	0.36
	p				--	0.77	0.63	0.07	0.32	0.00	0.00	0.49
Mg^{2+}	R					1.00	-0.72	-0.11	0.24	0.16	-0.07	0.77
	p					--	0.17	0.89	0.69	0.84	0.93	0.13
$\delta^{13}C_{DIC}$	R						1.00	0.00	-0.04	-0.29	0.22	-0.38
	p						--	1.00	0.95	0.71	0.78	0.53
***p*CO_2 air**	R							1.00	-0.93	0.70	-0.85	-0.43
	p							--	0.07	0.19	0.07	0.40
$\delta^{13}C_{air}$	R								1.00	-0.73	0.71	0.37
	p								--	0.27	0.29	0.54
***p*CO_2 (aq)**	R									1.00	-0.95	-0.32
	p									--	0.01	0.60
I_{sat}	R										1.00	0.49
	p										--	0.40
Drip rate	R											1.00
	p											--

Location 04 – Kongresna dvorana												
		Cond.	**HCO_3^-**	**Ca^{2+}**	**pH**	**Mg^{2+}**	**$\delta^{13}C_{DIC}$**	***p*CO_2 air**	**$\delta^{13}C_{air}$**	***p*CO_2 (aq)**	**I_{sat}**	**Drip rate**
Cond.	R	1.00	0.39	0.51	-0.46	-0.30	-0.82	-0.33	-0.02	0.65	-0.18	-0.24
	p	--	0.52	0.38	0.36	0.63	0.09	0.52	0.97	0.17	0.73	0.65
HCO_3^-	R		1.00	0.48	-0.02	0.11	-0.56	-0.46	0.42	0.10	0.35	0.33
	p		--	0.34	0.97	0.84	0.25	0.44	0.41	0.88	0.57	0.52
Ca^{2+}	R			1.00	-0.57	0.54	-0.32	-0.13	0.10	0.60	-0.51	-0.39
	p			--	0.32	0.27	0.54	0.84	0.85	0.28	0.38	0.44
pH	R				1.00	-0.37	0.45	-0.62	0.62	-0.97	0.87	0.91
	p				--	0.54	0.44	0.19	0.27	0.00	0.02	0.01
Mg^{2+}	R					1.00	0.36	0.46	-0.14	0.27	-0.51	-0.48
	p					--	0.49	0.44	0.80	0.66	0.38	0.33
$\delta^{13}C_{DIC}$	R						1.00	0.11	0.24	-0.55	-0.04	0.03
	p						--	0.87	0.65	0.34	0.94	0.95
***p*CO_2 air**	R							1.00	-0.93	0.45	-0.64	-0.68
	p							--	0.02	0.37	0.17	0.13
$\delta^{13}C_{air}$	R								1.00	-0.53	0.49	0.58
	p								--	0.36	0.40	0.23
***p*CO_2 (aq)**	R									1.00	-0.80	-0.85
	p									--	0.06	0.03
I_{sat}	R										1.00	0.99
	p										--	0.00
Drip rate	R											1.00
	p											--
Location 05 – Podrti kapnik												
		Cond.	**HCO_3^-**	**Ca^{2+}**	**pH**	**Mg^{2+}**	**$\delta^{13}C_{DIC}$**	***p*CO_2 air**	**$\delta^{13}C_{air}$**	***p*CO_2 (aq)**	**I_{sat}**	**Drip rate**
Cond.	R	1.00	0.82	0.97	0.06	-0.41	-0.97	0.51	-0.56	0.01	-0.44	0.48
	p	--	0.18	0.03	0.91	0.59	0.01	0.38	0.33	0.98	0.46	0.33
HCO_3^-	R		1.00	0.81	-0.08	0.20	-0.76	0.20	-0.39	0.19	-0.43	0.55
	p		--	0.10	0.92	0.74	0.13	0.80	0.51	0.81	0.57	0.34
Ca^{2+}	R			1.00	-0.31	-0.25	-0.98	0.67	-0.81	0.34	-0.65	0.52
	p			--	0.69	0.69	0.00	0.33	0.09	0.66	0.35	0.37
pH	R				1.00	-0.04	0.13	-0.83	0.65	-0.95	0.94	0.73
	p				--	0.96	0.84	0.08	0.24	0.00	0.02	0.10
Mg^{2+}	R					1.00	0.40	-0.55	0.60	0.17	0.03	-0.09
	p					--	0.51	0.45	0.28	0.83	0.97	0.89
$\delta^{13}C_{DIC}$	R						1.00	-0.69	0.71	-0.20	0.60	-0.41
	p						--	0.31	0.12	0.75	0.40	0.43
***p*CO_2 air**	R							1.00	-0.95	0.73	-0.89	-0.42
	p							--	0.05	0.16	0.04	0.49
$\delta^{13}C_{air}$	R								1.00	-0.58	0.76	0.29
	p								--	0.31	0.24	0.58
***p*CO_2 (aq)**	R									1.00	-0.90	-0.57
	p									--	0.04	0.24
I_{sat}	R										1.00	0.52
	p										--	0.37
Drip rate	R											1.00
	p											--

Location 06 – Stebrišče												
		Cond.	**HCO_3^-**	**Ca^{2+}**	**pH**	**Mg^{2+}**	**$\delta^{13}C_{DIC}$**	***p*CO_2 air**	**$\delta^{13}C_{air}$**	***p*CO_2 (aq)**	**I_{sat}**	**Drip rate**
Cond.	R	1.00	0.65	-0.02	-0.22	0.66	0.73	-0.11	0.26	0.21	-0.20	0.24
	p	--	0.24	0.97	0.67	0.23	0.16	0.84	0.67	0.68	0.70	0.65
HCO_3^-	R		1.00	0.58	-0.78	0.85	0.74	0.10	-0.13	0.67	-0.76	0.11
	p		--	0.23	0.12	0.03	0.09	0.87	0.80	0.22	0.13	0.84
Ca^{2+}	R			1.00	-0.78	0.26	-0.11	0.83	-0.76	0.73	-0.91	0.31
	p			--	0.12	0.62	0.83	0.08	0.08	0.16	0.03	0.55
pH	R				1.00	-0.80	-0.32	-0.76	0.56	-0.95	0.97	0.24
	p				--	0.10	0.60	0.08	0.33	0.00	0.00	0.64
Mg^{2+}	R					1.00	0.78	0.12	0.00	0.77	-0.67	0.12
	p					--	0.07	0.85	0.99	0.12	0.21	0.82
$\delta^{13}C_{DIC}$	R						1.00	-0.50	0.52	0.21	-0.21	-0.10
	p						--	0.39	0.29	0.73	0.74	0.85
***p*CO_2 air**	R							1.00	-0.94	0.76	-0.79	0.04
	p							--	0.02	0.08	0.06	0.94
$\delta^{13}C_{air}$	R								1.00	-0.58	0.71	-0.05
	p								--	0.30	0.18	0.92
***p*CO_2 (aq)**	R									1.00	-0.88	-0.20
	p									--	0.02	0.71
I_{sat}	R										1.00	0.31
	p										--	0.55
Drip rate	R											1.00
	p											--
Location 07 – Čarobni vrt												
		Cond.	**HCO_3^-**	**Ca^{2+}**	**pH**	**Mg^{2+}**	**$\delta^{13}C_{DIC}$**	***p*CO_2 air**	**$\delta^{13}C_{air}$**	***p*CO_2 (aq)**	**I_{sat}**	**Drip rate**
Cond.	R	1.00	-0.85	-0.06	0.18	0.28	-0.71	-0.16	-0.09	-0.25	-0.14	-0.04
	p	--	0.07	0.92	0.73	0.64	0.18	0.76	0.89	0.63	0.79	0.93
HCO_3^-	R		1.00	0.33	-0.39	-0.63	0.25	0.31	-0.16	0.50	-0.10	0.13
	p		--	0.52	0.51	0.18	0.63	0.61	0.77	0.39	0.88	0.81
Ca^{2+}	R			1.00	-0.94	-0.74	0.19	0.97	-0.86	0.97	-0.79	-0.55
	p			--	0.02	0.09	0.72	0.01	0.03	0.01	0.11	0.26
pH	R				1.00	0.68	-0.15	-0.99	0.98	-0.96	0.92	0.32
	p				--	0.21	0.81	0.00	0.00	0.00	0.01	0.53
Mg^{2+}	R					1.00	-0.49	-0.66	0.57	-0.81	0.46	0.33
	p					--	0.32	0.23	0.23	0.10	0.44	0.52
$\delta^{13}C_{DIC}$	R						1.00	0.16	-0.04	0.37	0.26	-0.29
	p						--	0.80	0.95	0.55	0.67	0.57
***p*CO_2 air**	R							1.00	-0.97	0.94	-0.90	-0.44
	p							--	0.01	0.00	0.01	0.38
$\delta^{13}C_{air}$	R								1.00	-0.91	0.98	0.15
	p								--	0.03	0.00	0.78
***p*CO_2 (aq)**	R									1.00	-0.81	-0.39
	p									--	0.05	0.44
I_{sat}	R										1.00	0.15
	p										--	0.78
Drip rate	R											1.00
	p											--

Location 08 – Vrh Velike gore												
		Cond.	**HCO_3^-**	**Ca^{2+}**	**pH**	**Mg^{2+}**	**$\delta^{13}C_{DIC}$**	***p*CO_2 air**	**$\delta^{13}C_{air}$**	***p*CO_2 (aq)**	**I_{sat}**	**Drip rate**
Cond.	R	1.00	0.96	0.12	0.01	0.66	-0.81	-0.04	-0.08	0.25	0.21	0.69
	p	--	0.01	0.85	0.98	0.22	0.19	0.94	0.90	0.63	0.69	0.13
HCO_3^-	R		1.00	0.30	0.16	0.66	-0.63	-0.13	0.18	0.27	0.41	0.55
	p		--	0.56	0.80	0.15	0.25	0.83	0.73	0.66	0.50	0.26
Ca^{2+}	R			1.00	0.81	0.61	0.52	-0.41	0.60	-0.32	0.96	-0.42
	p			--	0.10	0.20	0.37	0.49	0.21	0.60	0.01	0.41
pH	R				1.00	0.10	0.58	-0.89	0.93	-0.85	0.92	-0.15
	p				--	0.87	0.42	0.02	0.02	0.03	0.01	0.78
Mg^{2+}	R					1.00	-0.09	0.25	0.01	0.46	0.48	0.15
	p					--	0.89	0.69	0.99	0.44	0.42	0.78
$\delta^{13}C_{DIC}$	R						1.00	-0.32	0.42	-0.65	0.44	-0.77
	p						--	0.68	0.48	0.35	0.56	0.13
***p*CO_2 air**	R							1.00	-0.94	0.93	-0.69	-0.15
	p							--	0.02	0.01	0.13	0.77
$\delta^{13}C_{air}$	R								1.00	-0.88	0.80	-0.07
	p								--	0.05	0.11	0.90
***p*CO_2 (aq)**	R									1.00	-0.59	0.01
	p									--	0.22	0.99
I_{sat}	R										1.00	-0.18
	p										--	0.73
Drip rate	R											1.00
	p											--
Location 09 – Zgornji Tartar												
		Cond.	**HCO_3^-**	**Ca^{2+}**	**pH**	**Mg^{2+}**	**$\delta^{13}C_{DIC}$**	***p*CO_2 air**	**$\delta^{13}C_{air}$**	***p*CO_2 (aq)**	**I_{sat}**	**Drip rate**
Cond.	R	1.00	0.38	0.35	0.23	0.03	-0.71	-0.16	-0.82	-0.01	0.27	0.41
	p	--	0.52	0.57	0.66	0.96	0.18	0.76	0.09	0.98	0.61	0.42
HCO_3^-	R		1.00	-0.13	0.31	0.79	-0.43	0.53	-0.33	-0.26	0.26	0.62
	p		--	0.80	0.61	0.06	0.40	0.36	0.53	0.68	0.67	0.19
Ca^{2+}	R			1.00	-0.70	-0.17	0.12	0.46	-0.48	0.67	-0.60	0.04
	p			--	0.19	0.74	0.82	0.44	0.34	0.22	0.28	0.95
pH	R				1.00	0.61	-0.57	-0.64	0.61	-0.95	0.90	0.34
	p				--	0.27	0.32	0.17	0.28	0.00	0.01	0.51
Mg^{2+}	R					1.00	-0.31	0.04	0.23	-0.50	0.70	0.55
	p					--	0.55	0.94	0.66	0.39	0.19	0.26
$\delta^{13}C_{DIC}$	R						1.00	0.00	0.29	0.71	-0.19	-0.66
	p						--	1.00	0.58	0.18	0.76	0.15
***p*CO_2 air**	R							1.00	-0.89	0.57	-0.69	0.33
	p							--	0.04	0.24	0.13	0.52
$\delta^{13}C_{air}$	R								1.00	-0.48	0.82	-0.36
	p								--	0.41	0.09	0.48
***p*CO_2 (aq)**	R									1.00	-0.74	-0.35
	p									--	0.09	0.49
I_{sat}	R										1.00	0.15
	p										--	0.78
Drip rate	R											1.00
	p											--

Location 10 – Pivka River inside											
		Cond.	**HCO_3^-**	**Ca^{2+}**	**pH**	**Mg^{2+}**	**$\delta^{13}C_{DIC}$**	***p*CO_2 air**	**$\delta^{13}C_{air}$**	***p*CO_2 (aq)**	**I_{sat}**
Cond.	R	1.00	0.83	0.98	0.88	0.95	1.00	-0.69	0.82	-0.73	0.99
	p	--	0.38	0.13	0.12	0.20	0.03	0.31	0.39	0.48	0.08
HCO_3^-	R		1.00	0.86	1.00	0.94	0.48	-0.99	0.99	-0.20	1.00
	p		--	0.14	0.01	0.06	0.52	0.10	0.01	0.80	--
Ca^{2+}	R			1.00	0.92	0.81	0.20	-0.86	0.81	-0.13	1.00
	p			--	0.26	0.19	0.80	0.34	0.19	0.87	--
pH	R				1.00	0.96	0.84	-0.73	1.00	-0.20	1.00
	p				--	0.19	0.36	0.27	0.00	0.87	0.06
Mg^{2+}	R					1.00	0.71	-0.91	0.95	-0.52	1.00
	p					--	0.29	0.27	0.05	0.48	--
$\delta^{13}C_{DIC}$	R						1.00	-0.76	0.55	-0.88	1.00
	p						--	0.45	0.45	0.12	--
***p*CO_2 air**	R							1.00	-0.99	0.07	-0.71
	p							--	0.08	0.95	0.50
$\delta^{13}C_{air}$	R								1.00	-0.26	1.00
	p								--	0.74	--
***p*CO_2 (aq)**	R									1.00	1.00
	p									--	--
I_{sat}	R										1.00
	p										--

Location 11 – Pivka River outside											
		Cond.	**HCO_3^-**	**Ca^{2+}**	**pH**	**Mg^{2+}**	**$\delta^{13}C_{DIC}$**	***p*CO_2 air**	**$\delta^{13}C_{air}$**	***p*CO_2 (aq)**	**I_{sat}**
Cond.	R	1.00	0.26	0.79	0.46	-0.24	0.77	0.45	0.62	-0.44	0.46
	p	--	0.67	0.11	0.36	0.69	0.23	0.37	0.19	0.39	0.36
HCO_3^-	R		1.00	-0.15	0.82	0.41	0.26	0.14	0.63	-0.71	0.80
	p		--	0.77	0.09	0.42	0.68	0.82	0.25	0.18	0.10
Ca^{2+}	R			1.00	0.37	-0.45	0.13	0.55	-0.53	-0.57	0.27
	p			--	0.54	0.37	0.83	0.33	0.36	0.31	0.66
pH	R				1.00	0.27	0.94	0.60	0.18	-0.94	0.96
	p				--	0.66	0.06	0.21	0.74	0.01	0.00
Mg^{2+}	R					1.00	0.46	0.11	0.85	-0.03	0.32
	p					--	0.43	0.86	0.07	0.96	0.59
$\delta^{13}C_{DIC}$	R						1.00	0.86	0.50	-0.91	0.90
	p						--	0.14	0.50	0.09	0.10
***p*CO_2 air**	R							1.00	0.44	-0.47	0.74
	p							--	0.39	0.35	0.09
$\delta^{13}C_{air}$	R								1.00	0.10	0.38
	p								--	0.85	0.46
***p*CO_2 (aq)**	R									1.00	-0.81
	p									--	0.05
I_{sat}	R										1.00
	p										--

Table A.7 Oxygen isotope composition of precipitation at sampling locations: Postojna, Zalog pri Postojni and Ljubljana.Mean value and standard deviation is calculated.

Date month/year	$\delta^{18}O_p$ (‰, VSMOW)		
	Postojna[a]	Zalog pri Postojni[b]	Ljubljana[c]
03/2010	-	-7.93	-11.60
04/2010	-	-9.92	-8.60
05/2010	-	-5.66	-5.05
06/2010	-7.61	-7.61	-7.38
07/2010	-	-6.58	-7.55
08/2010	-6.31	-5.56	-6.26
09/2010	-5.86	-6.83	-6.97
10/2010	-	-8.27	-7.51
11/2010	-	-11.01	-12.71
12/2010	-9.24	-8.68	-11.01
01/2011	-	-	-9.95
02/2011	-7.91	-	-11.00
03/2011	-	-	-5.70
04/2011	-	-	-6.67
05/2011	-	-	-8.24
06/2011	-	-	-5.72
Mean	-7.40	-7.81	-8.25
St. Dev.	1.34	1.76	2.34

[a]this thesis
[b]Data from dr. Sonja Lojen (Jožef Stefan Institute, Ljubljana)
[c]Data from dr. Polona Vreča (Jožef Stefan Institute, Ljubljana)

Table A.8 Stable carbon $\delta^{13}C$ and oxygen $\delta^{18}O$ composition of soda straw samples. Length and mass of each sample is given.

Sample	**$\delta^{13}C$** (‰, VPDB)	**$\delta^{18}O$** (‰, VPDB)	**Length** (cm)	**Mass** (g)
Location 01 – Slonova glava				
1-1-a	-8.92	-5.84	2.9	3.608
1-1-b	-8.57	-5.38	2.5	1.249
1-1-c	-7.94	-5.21	2.1	1.301
1-1-d	-9.05	-6.61	1.6	0.700
1-2-a	-8.98	-5.14	1.8	0.779
1-2-b	-9.54	-5.17	1.7	0.695
1-2-c	-7.84	-5.01	1.7	0.626
1-2-d	-9.36	-6.17	1.5	0.584
1-3-a	-9.72	-5.64	1.3	0.479
1-3-b	-8.83	-5.06	1.2	0.572
1-3-c	-9.22	-6.87	1.2	0.374
1-3-d	-9.99	-4.84	1.2	0.435
Location 02 – Biospeleološka postaja				
2-1	-3.94	-7.82	1.0	0.176
2-2	-8.84	-6.42	1.8	0.259
2-3	-8.61	-5.90	2.5	2.166
2-4	-9.08	-5.78	2.4	0.874
2-5	-10.12	-6.43	Small pieces	1.860
Location 03 – Vodopad				
3-1	-10.58	-4.96	1.6	0.731
3-2	-10.58	-5.80	1.2	0.571
3-3	-9.98	-5.28	1.3	0.821
3-4	-9.35	-5.54	1.0	0.487
Location 06 – Stebrišče				
6-3	-8.86	-6.44	1.6	0.214
6-4	-9.58	-7.84	1.2	0.335
Location 07 – Čarobni vrt				
7	-9.71	-6.40	10.5	2.910
Location 08 – Vrh Velike gore				
8-1	-8.60	-7.03	1.9	0.443
8-2	-8.88	-6.17	3.0	0.367
Location 09 – Zgornji Tartar				
9	-9.36	-6.02	-	-

Table A.9 Stable carbon $\delta^{13}C$ and oxygen $\delta^{18}O$ composition of carbonates of peculiar growth type.

Sample	$\delta^{13}C$ (‰, VPDB)	$\delta^{18}O$ (‰, VPDB)	Description
Location 01 – Slonova glava			
1a	-4.27	-4.39	white part from inside
1b	-5.23	-3.99	rounded part
1c	-4.65	-4.10	outer unsymmetrical part
Location 09 – Zgornji Tartar			
9OH1-U	-5.78	-6.53	Smallest part from inside
9OH2-U	-5.57	-7.09	Largest part from inside
9OH3-U	-5.52	-6.95	Middle part from inside
9OH1-V	-6.18	-6.69	Smallest part from outside
9OH2-V	-6.23	-6.83	Largest part from outside
9OH3-V	-7.50	-6.76	Middle part from outside

Table A.10 Stable isotope composition $\delta^{13}C$ and $\delta^{18}O$ of modern carbonate precipitated on watch glasses.

Location	Sample no.	$\delta^{13}C$ (‰, VPDB)	$\delta^{18}O$ (‰, VPDB)
01 – Slonova glava	1	-12.37	-3.07
02 – Biospeleološka postaja	2	-12.03	-3.56
03 – Vodopad	3	-12.21	-3.56
04 – Kongresna dvorana	4	-11.86	-4.67
05 – Podrti kapnik	5	-9.95	-3.81
06 – Stebrišče	6	-12.04	-3.16
09 – Zgornji Tartar	9	-12.34	-3.38

Precipitation plates /watch glasses at locations 07 – Čarobni vrt and 08 – Vrh Velike gore were moved away from the initial position by strong drip rate and there was not enough precipitated carbonate for analysis.

Table A.11 Stable isotope composition $\delta^{13}C$ and $\delta^{18}O$ of old samples with description of each layer.

Sample	$\delta^{13}C$ (‰, VPDB)	$\delta^{18}O$ (‰, VPDB)	Description
Location 02 – Biospeleološka postaja – stalactite			
ST2-1-1	-3.65	-6.24	Inner part
ST2-1-2	-3.80	-4.97	gray
ST2-1-3	-5.84	-10.35	yellow
ST2-1-4	-6.91	-6.41	Outer part
ST2-1-5	-6.95	-5.58	Surface
ST2-2-1	-5.14	-6.39	Inner part
ST2-2-2	-5.01	-6.08	
ST2-2-3	-4.79	-5.85	
ST2-2-4	-7.33	-6.24	Outer part
Location 04 – Kongresna dvorana – stalactite 1			
4b	-2.76	-4.33	Outer part
Location 04 – Kongresna dvorana – stalactite 2			
4-1-1	-5.36	-4.23	The most inner part
4-1-2	-2.23	-4.67	
4-1-3	-3.74	-4.53	
4-1-4	-1.15	-5.52	
4-1-5	-1.35	-4.65	
4-1-6	-2.25	-4.92	The most outer part
Location 04 – Kongresna dvorana – flowstone			
4-2-1	-6.99	-4.82	The most outer part
4-2-2	-3.02	-4.21	
4-2-3	-2.49	-6.66	
4-2-4	-0.78	-5.80	
4-2-5	-1.51	-5.18	The most inner part
Location 05 – Podrti kapnik – flowstone			
5-1	-7.95	-6.35	Yellow/ inner part
5-2	-7.58	-4.97	Intense yellow
5-3	-6.27	-5.19	yellow
5-4	-4.68	-5.62	whitish
5-5	-5.88	-5.10	white
5-6	-4.48	-4.60	white yellow
5-7	-3.97	-5.42	Gray/ outer part
5-S	-6.04	-5.46	Cleaned surface

Sample	$\delta^{13}C$ (‰, VPDB)	$\delta^{18}O$ (‰, VPDB)	Description
Location 06 – Stebrišče – flowstone			
6-1r	-5.34	-5.41	Lower part/ down to earth
6-2r	-3.57	-6.01	gray
6-3r	-6.25	-5.49	orange
6-4r	-2.02	-4.48	Gray, more lines visible
6-5r	-3.79	-4.21	Gray, more lines visible
6-6r	-4.39	-4.40	orange
6-7r	-2.46	-4.13	orange
6-8r	-3.74	-3.38	Dominant gray
6-9r	-5.80	-4.08	Top yellow
6-Sr	-6.20	-4.34	Cleaned surface
Location 09 – Zgornji Tartar – stalactite			
9S-1a	-8.78	-4.92	Inside
9S-1b	-7.77	-4.09	First white circle
9S-2	-9.91	-5.16	First gray layer
9S-3	-2.46	-4.20	White layer
9S-4	-1.52	-4.15	At the surface of stalagmite
9S-5S	-5.16	-4.89	Surface of stalagmite

Table A.12 Stable isotope composition $\delta^{13}C$ and $\delta^{18}O$ of drilled cores from stalagmites with description of each layer.

Sample	$\delta^{13}C$ (‰, VPDB)	$\delta^{18}O$ (‰, VPDB)	Depth (mm)	Description
Location 06 – Stebrišče – drilled core, stalagmite				
6-1a	-5.49	-6.37	4	Uniform gray, (top)
6-1b	-4.33	-5.64	25	Uniform gray, (middle)
6-1c	-2.01	-5.94	63	Uniform gray, (bottom)
6-2-1	-2.72	-5.46	90	Gray, ≈ l-5 mm
6-2-2-a	-2.64	-5.23	93	Light gray, ≈ l-10 mm (top)
6-2-2-b	-3.78	-5.22	96	Light gray, (middle)
6-2-2-c	-4.41	-4.71	100	Light gray, (bottom)
6-2-3	-3.53	-5.42	103	Light gray, ≈ l-7 mm (top)
6-2-3-b	-4.43	-5.81	106	Light gray, ≈ l-7 mm (middle)
6-2-3-c	-4.27	-5.67	109	Light gray, ≈ l-7 mm (bottom)
6-2-4	-7.45	-6.38	143	≈ l-15 mm; orange part; hiatus??
6-2-5	-8.08	-6.48	146	≈ l-11 mm, darker orange part
6-2-6	-5.13	-5.76	149	≈ l-1.5 mm; orange white part
6-2-7	-4.96	-7.30	150	≈ l-2 mm; white
6-2-8a	-5.28	-7.18	155	Orange part containing holes, ≈ l-12 mm (top)
6-2-8b	-6.05	-4.72	160	Orange part containing holes, ≈ l-12 mm (bottom)
6-2-9	-4.24	-6.80	162	White, ≈ l-7 mm
6-2-10a	-5.74	-6.84	167	Orange part , ≈ l-20 mm (top)
6-2-10b	-6.86	-6.55	175	Orange part , ≈ l-20 mm (bottom)
6-2-11	-5.18	-6.67	185	≈ l-4 mm; dark orange
6-2-12	-4.67	-6.13	183	≈ l-5 mm; lighter
6-2-13	-4.12	-7.35	192	≈ l-10 mm
6-2-14	-5.36	-6.65	204	≈ l-10 mm; white part soft
6-2-15	-6.32	-8.86	215	≈ l-5 mm
6-3-1	-8.55	-6.44	290	Upper gray part, ≈ l-1.5 mm
6-3-2	-2.05	-6.08	302	White yellow layer, ≈ l-10 mm
6-3-3	-1.65	-4.34	307	White layer, ≈ l-5 mm
6-3-4	-1.71	-5.69	315	White layer, ≈ l-4 mm
6-3-5	-4.31	-6.87	322	White circled layer, 2r≈10 mm
6-3-6	-5.53	-5.98	340	Gray “irregular” layer, ≈ l-7 mm
6-3-7a	-5.95	-7.35	373	Dark gray, ≈ l-15 mm (top)
6-3-7b	-7.28	-7.08	417	Dark gray, ≈ l-15 mm (bottom)
6-3-8a	-7.03	-12.11	423	Gray, ≈ l-15 mm (top)
6-3-8b	-7.53	-6.93	425	Gray, ≈ l-15 mm (upper middle)
6-3-8c	-7.95	-8.76	430	Gray, ≈ l-15 mm (lower middle)
6-3-8d	-8.41	-6.73	435	Gray, ≈ l-15 mm (bottom)

Sample	$\delta^{13}C$ (‰, VPDB)	$\delta^{18}O$ (‰, VPDB)	Depth (mm)	Description
Location 07 – Čarobni vrt – drilled core, stalagmite				
7-1	-9.67	-5.38	3	Upper orange part, ≈ l-0.4 mm
7-2	-8.52	-5.19	4	Orange-gray part, ≈ l-0.4 mm (top)
7-2a	-4.54	-4.54	7	Orange-gray part, ≈ l-0.4 mm (bottom)
7-3a	-5.51	-5.34	12	Orange and dark red part, ≈ l-2 mm (top)
7-3b	-5.95	-5.38	13	Orange and dark red part, ≈ l-2 mm (bottom)
7-4	-6.61	-3.77	15	Orange no homogeneous part, ≈ l-3 mm
7-5	-6.24	-4.30	18	Dark orange, ≈ l-2 mm
7-6	-6.01	-4.10	20	Light orange, ≈ l-2 mm
7-7	-6.81	-4.54	24	Dark orange, ≈ l-5 mm
7-8	-7.63	-4.41	28	Light orange, ≈ l-3 mm
7-9a	-7.04	-4.76	30	Dark orange, ≈ l-9 mm (top)
7-9b	-6.54	-4.98	34	Dark orange, ≈ l-9 mm (middle)
7-9c	-5.87	-4.42	38	Dark orange, ≈ l-9 mm (bottom)
7-10	-6.51	-4.61	42	Upper lighter part (≈ l-10 mm) before “strange” growth
7-11a	-8.19	-4.71	61	“Strange” growth, ≈ l-30 mm (top)
7-11b	-7.62	-4.20	98	“Strange” growth, ≈ l-30 mm (middle)
7-11c	-8.46	-4.47	163	“Strange” growth, ≈ l-30 mm (bottom)
7-12a	-9.63	-4.91	269	Very thin layers, ≈ l-10 mm (top)
7-12b	-9.28	-4.61	277	Very thin layers, ≈ l-10 mm (bottom)
7-13a	-8.60	-4.25	291	“Strange” growth, ≈ l-80 mm (top)
7-13b	-9.12	-6.91	346	“Strange” growth, ≈ l-80 mm (bottom)
Location 08 – Vrh Velike gore – drilled core, stalagmite				
8-1a	-5.85	-4.08	3	Grey upper part (≈ l-3cm) with white inclusions (top)
8-1b	-5.35	-4.92	14	Grey upper part (≈ l-3cm) with white inclusions (middle)
8-1c	-5.83	-4.98	23.5	Grey upper part (≈ l-3cm) with white inclusions (bottom)
8-2	-3.90	-4.56	29	Gray layer ≈ l-5 mm
8-3	-4.34	-6.29	32.5	3 upper very thin layers
8-4	-3.43	-4.90	34	3 lower very thin layers
8-5	-3.73	-5.72	37	Gray layer ≈ l-3 mm
8-6	-1.79	-5.99	39	White layer ≈ l-1 mm. Possible minimal sample mixing with 8-5
8-7	-4.06	-3.84	41	Orange part with a lot of pores. ≈ l-4 mm; layer is between two dominant orange layers
8-8	-3.88	-4.03	43	Orange- lighter layer, homogeneous ≈ l-1.5 mm
8-9	-4.38	-4.52	45	Orange- darker layer, homogeny ≈ l-2 mm
8-10a	-5.88	-5.23	46	Light orange layer (lighter part, ≈ l-2 mm)
8-10b	-6.76	-5.70	48	Light orange layer (darker part, ≈ l-2.5 mm)
8-11a	-6.19	-5.02	49	Thin lighter and darker lines, ≈ l-10 mm (top, darker)
8-11b	-5.49	-5.43	51	Thin lighter and darker lines, ≈ l-10 mm (upper middle, lighter)
8-11c	-5.62	-5.43	55	Thin lighter and darker lines, ≈ l-10 mm (lower middle, darker)
8-11d	-5.23	-6.60	56.5	Thin lighter and darker lines,

				≈ l-10 mm (bottom, dominant white stripe)
8-12a	-4.93	-5.05	60	Gray-orange part, ≈ l-7 mm (top)
8-12b	-4.93	-4.37	63	Gray-orange part, ≈ l-7 mm (bottom)
8-13	-5.73	-3.90	67	≈ l-7 mm
8-14	-6.40	-4.41	73	≈ l-4 mm
8-15	-6.99	-4.47	80	≈ l-7 mm
8-16	-6.88	-4.36	84.5	≈ l-2 mm
8-17a	-8.02	-4.27	91.5	Possible precrystallization, ≈ l-70 mm (top)
8-17b	-8.34	-4.54	121	Possible precrystallization, ≈ l-70 mm (middle)
8-17c	-8.05	-4.15	155	Possible precrystallization, ≈ l-70 mm (bottom)
8-18a	-8.71	-3.59	164	Mixture of orange brighter and darker stripes, ≈ l-20 mm (top)
8-18b	-8.60	-4.97	171.5	Mixture of orange brighter and darker stripes, ≈ l-20 mm (middle)
8-18c	-9.41	-4.13	173.5	Mixture of orange brighter and darker stripes, ≈ l-20 mm (bottom)
8-19	-9.56	-4.39	181	Dark layer
8-20	-8.42	-4.82	183	white yellow layer

Institut "Jožef Stefan", Ljubljana, Slovenija
1001 Ljubljana, Jamova cesta 39, p. p. 3000 / Tel.: 01 477 3900/ Fax: 01 251 93 85 / www.ijs.si

datum: 11. november 2011

Magda Mandić
Physics Department, University of Rijeka
Omladinska 14
51000 Rijeka

CROATIA

Zadeva: Podatki o izotopski sestavi kisika v padavinah

Spoštovani,

V skladu z vašo prošnjo, poslano po e-mailu 18.10.2011, vam v prilogi pošiljamo razpoložljive podatke o izotopski sestavi kisika v padavinah v Ljubljani in Postojni za obdobje marec 2010 – junij 2011, ki jih lahko uporabite v vaši doktorski disertaciji z naslovom »Determination of equilibrium conditions of carbonate precipitation in Postojna Cave by comparison of isotopic composition of carbon ^{13}C and oxygen ^{18}O in carbonates and drip water and their possible applications to paleoclimatology«.

Vse analize so bile opravljene na Odseku za znanosti o okolju Instituta »Jožef Stefan«. Izotopsko sestavo kisika v vodi ($\delta^{18}O$) smo določili z masnim spektrometrom s kontinuirnim pretokom IsoPrime (GV Instruments) s preparativnim nastavkom MultiFlow Bio po ekvilibraciji vode s CO_2.

Ker podatki še niso bili objavljeni, jih lahko uporabite zgolj za navedeni namen. V nalogi navedite, da so bile analize opravljene na Odseku za znanosti o okolju Instituta »Jožef Stefan« v okviru programa P1-0143 »Kroženje snovi v okolju, snovna bilanca in modeliranje okoljskih procesov ter ocena tveganja« (v angleščini: »Cycling of substances in the environment, mass balances, modelling of environmental processes and risk assessment«), financiranega iz strani Javne agencije za raziskovalno dejavnost Republike Slovenije (v angleščini: Slovenian Research Agency). Prosimo, da nam ob zaključku doktorata posredujete kopijo vaše disertacije.

V kolikor nameravate podatke uporabili tudi za pripravo drugih publikacij in prezentacij, smo pri pripravi le teh pripravljeni sodelovati kot soavtorji.

S pozdravi,

Dr. Polona Vreča

Priloga:
- Tabela s podatki o izotopski sestavi padavin ($\delta^{18}O$ v ‰)

1 / 2

Institut "Jožef Stefan", Ljubljana, Slovenija
1001 Ljubljana, Jamova cesta 39, p. p. 3000 / Tel.: 01 477 3900/ Fax: 01 251 93 85 / www.ijs.si

Tabela s podatki o izotopski sestavi padavin ($\delta^{18}O$ v ‰)

	Zalog pri Postojni[1]	Ljubljana[2] (Reaktorski center Podgorica)
mar.10	-7,93	-11,60
apr.10	-9,92	-8,60
maj.10	-5,66	-5,05
jun.10	-7,61	-7,38
jul.10	-6,58	-7,55
avg.10	-5,56	-6,26
sep.10	-6,83	-6,97
okt.10	-8,27	-7,51
nov.10	-11,01	-12,71
dec.10	-8,68	-11,01
jan.11		-9,95
feb.11		-11,00
mar.11		-5,70
apr.11		-6,67
maj.11		-8,24
jun.11		-5,72

Opombe:
1 – v primeru uporabe podatkov navajati kot avtorico dr. Sonjo Lojen
2 – v primeru uporabe podatkov navajati kot avtorico dr. Polono Vreča

2 / 2

Figure A.1 Letter with $\delta^{18}O_p$ in precipitation from Ljubljana (dr. Polona Vreča) and Zalog pri Postojni (dr. Sonja Lojen) and permission for use.

ZNANSTVENORAZISKOVALNI CENTER
SLOVENSKE AKADEMIJE ZNANOSTI IN UMETNOSTI

Inštitut za raziskovanje krasa
Znanstvenoraziskovalni center Slovenske akademije znanosti in umetnosti
Titov trg 2, 6230 Postojna, Slovenija
T. 05 700 19 00, F. 05 700 19 99, E. izrk@zrc-sazu.si, www.zrc-sazu.si/www/izrk/izrk-s.htm

45/80-3/10
4.5.2010

Martina Stupar
ZVKDS OE Nova gorica
Delpinova ulica 16
5000 Nova gorica

Prošnja za jemanje vzorcev sige v Postojnski jami

Prosimo za dovoljenje za vzorčevanje sige v Postojnski jami. Sige bomo potrebovali za analize stabilnih izotopov kisika in ogljika za ugotavljanje vplivov jamske klime na rast kapnikov v jami, ugotavljanje sprememb rasti sige v času in človekovih vplivov na jamsko klimo. Raziskava poteka v okviru proučevanja starosti sedimentov v Postojnskem jamskem sistemu.

Odlaganje sige v Postojnski jami je odvisno tudi od klimatskih pogojev, ki vladajo v sami jami. Ti pa se v različnih delih jame zelo različni, odvisni predvsem od bližine vhodov ter od zračne cirkulacije. Nihanje temperatur ali razlika med temperaturo zraka in skale lahko povzroča v jami kondenzacijo zračne vlage ali pa tudi sezonsko izsuševanje jamskih sten in tudi že odložene sige. Posledica tega so morfološko zelo različni kapniki, opazno hrapavi in s prahom potemnjeni kapniki v Velikem domu, Stari jami, beli kapniki in tanke sigove prevleke v Biospeleološki postaji in v Zgornjem Tartarju, svetlosivi kapniki in sigove prevleke na Veliki gori, gladki kristalasti kapniki v Čarobnem vrtu in Pisanem rovu.

Zaradi sprememb klime v preteklosti ter zaradi odpiranja ali zasipavanja nekaterih jamskih vhodov so se klimatski pogoji v jami v času spreminjali, te spremembe pa so ostale zapisane v sigi. Najlepše se vidijo v jami v usekih ob turističnih poteh in železniški progi kot spreminjanje barve in strukture v plasteh sige.

V jami opažamo tudi recentne spremembe v odlaganju sige, kar bi lahko bilo posledica posegov v jamo zaradi turizma, predvsem večje prevetrenosti jame in močnejšega izsuševanja jame zaradi umetno odprtih vhodov v jamski sistem.

Nekatere od starejših sprememb v rasti sige so bile v preteklosti datirane z U/Th metodo, neodgovorjeno pa je ostalo vprašanje, ali se te spremembe odražajo tudi v izotopski sestavi stabilnih izotopov kisika in ogljika oziroma ali lahko s temi metodami ugotovimo vplive jamske klime na odlaganje sige. Ti odgovori nam lahko dajo tudi zelo koristne praktične napotke v zvezi s turističnim upravljanjem jame.

Za izotopske analize se potrebuje praviloma do nekaj gramov sige, zato bodo vzorci zelo majhni. Sige nameravamo vzorčevati v dostopnih profilih, ki so jih razgalili pri izravnavanju jamskih tal ob poteh ali pa z izvrtavanjem jeder premera 4 cm. To je minimalna debelina jedra, ki ohrani plastovitost oziroma se ne zdrobi pri vrtanju. Pri tem bomo pazili, da vrtine ne bodo na vidnih mestih, ter da napravimo čim manjše posege v sigo.

Potrebovali bi tudi nekaj sigovih skorij ali manjših stalaktitov, vendar so to lahko že odlomljeni koščki, ki jih je povsod po jami dovolj.

Jamo smo si že ogledali, ter določili mesta, kjer so ustrezne sige in je vzorčevanje možno zaradi minimalnega posega v jamo. Vzorce sige bi vzeli pred biospeleološko postajo v Rovu novih podpisov, nekaj vzorcev sige od tu pa hranimo še od časa, ko so preurejali turistično pot. Vzorčevali bi sigo na dveh mestih ob progi pred Kongresno dvorano, ter ob progi v Stari jami pred končno postajo železnice. Potrebovali bi tri vzorce sige iz usekov poti na Veliki gori ter v Čarobnem vrtu. Vzorec sige bi vzeli tudi v zgornjem Tartarju in v vhodni dvorani v Črni jami.

Vzorce, kose sige ali jedra vrtin bomo prerezali in polovico shranili na Inštitut za raziskovanje krasa v Postojna, ostali del vzorca pa se bo uporabil za izvrtavanje podvzorcev. Analize bo opravila mag. Magda Mandič z Oddelka za Fiziko, Univerze na Reki v okviru svojega doktorskega študija, laboratorijske analize pa bodo narejene na Joanneum research centru, Institute of Water Resources Management Hydrology and Geophysics, Graz.

V pričakovanju ugodnega odgovora, s spoštovanjem,

dr. Andrej Mihevc

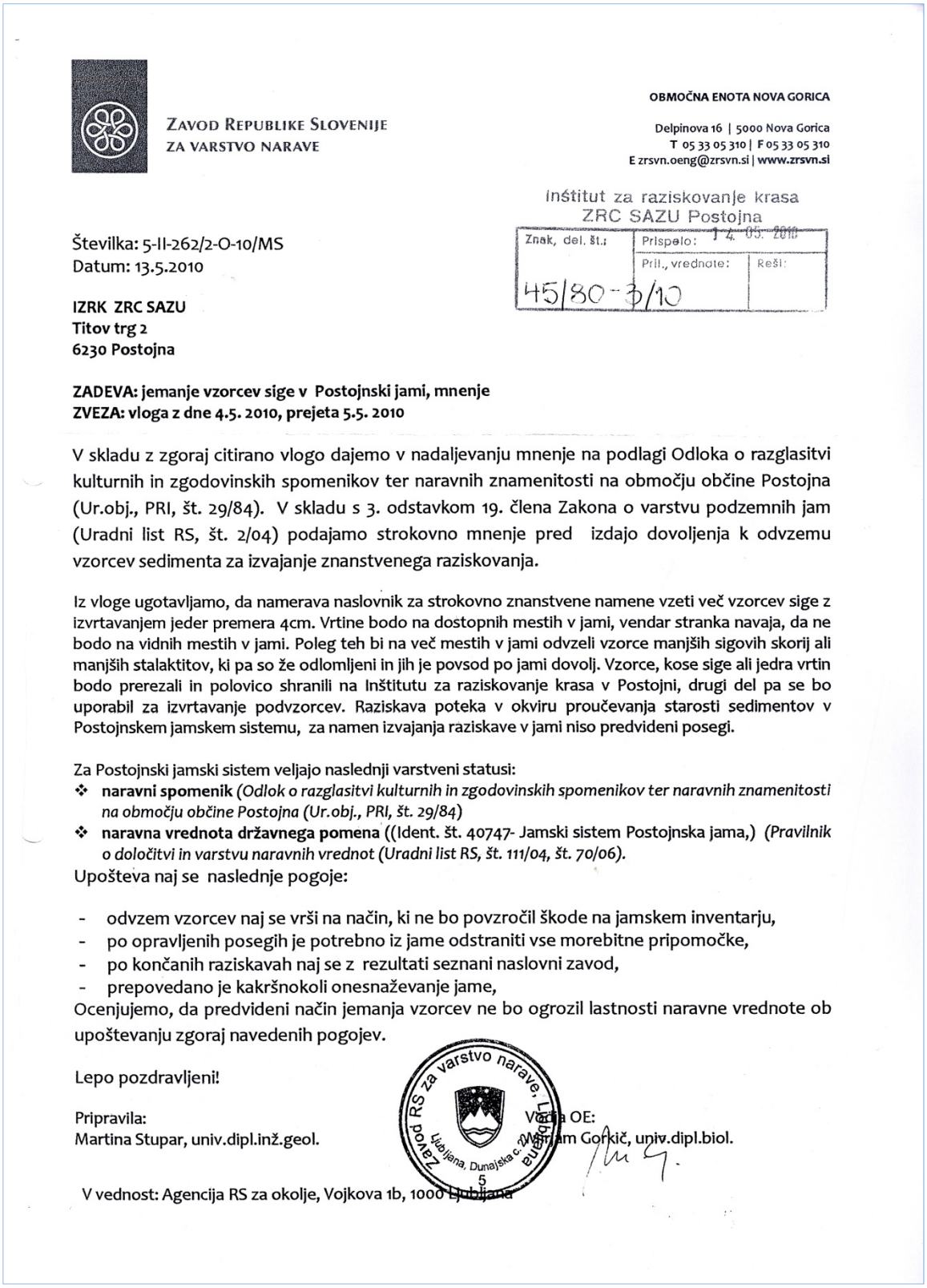

ZAVOD REPUBLIKE SLOVENIJE
ZA VARSTVO NARAVE

OBMOČNA ENOTA NOVA GORICA

Delpinova 16 | 5000 Nova Gorica
T 05 33 05 310 | F 05 33 05 310
E zrsvn.oeng@zrsvn.si | www.zrsvn.si

Inštitut za raziskovanje krasa
ZRC SAZU Postojna

Znak, del. št.:	Prispelo: 14. 05. 2010	
45/80-3/10	Pril., vrednote:	Rešl:

Številka: 5-II-262/2-O-10/MS
Datum: 13.5.2010

IZRK ZRC SAZU
Titov trg 2
6230 Postojna

ZADEVA: jemanje vzorcev sige v Postojnski jami, mnenje
ZVEZA: vloga z dne 4.5. 2010, prejeta 5.5. 2010

V skladu z zgoraj citirano vlogo dajemo v nadaljevanju mnenje na podlagi Odloka o razglasitvi kulturnih in zgodovinskih spomenikov ter naravnih znamenitosti na območju občine Postojna (Ur.obj., PRI, št. 29/84). V skladu s 3. odstavkom 19. člena Zakona o varstvu podzemnih jam (Uradni list RS, št. 2/04) podajamo strokovno mnenje pred izdajo dovoljenja k odvzemu vzorcev sedimenta za izvajanje znanstvenega raziskovanja.

Iz vloge ugotavljamo, da namerava naslovnik za strokovno znanstvene namene vzeti več vzorcev sige z izvrtavanjem jeder premera 4cm. Vrtine bodo na dostopnih mestih v jami, vendar stranka navaja, da ne bodo na vidnih mestih v jami. Poleg teh bi na več mestih v jami odvzeli vzorce manjših sigovih skorij ali manjših stalaktitov, ki pa so že odlomljeni in jih je povsod po jami dovolj. Vzorce, kose sige ali jedra vrtin bodo prerezali in polovico shranili na Inštitutu za raziskovanje krasa v Postojni, drugi del pa se bo uporabil za izvrtavanje podvzorcev. Raziskava poteka v okviru proučevanja starosti sedimentov v Postojnskem jamskem sistemu, za namen izvajanja raziskave v jami niso predvideni posegi.

Za Postojnski jamski sistem veljajo naslednji varstveni statusi:

- **naravni spomenik** *(Odlok o razglasitvi kulturnih in zgodovinskih spomenikov ter naravnih znamenitosti na območju občine Postojna (Ur.obj., PRI, št. 29/84)*
- **naravna vrednota državnega pomena** ((Ident. št. 40747- Jamski sistem Postojnska jama,) *(Pravilnik o določitvi in varstvu naravnih vrednot (Uradni list RS, št. 111/04, št. 70/06).*

Upošteva naj se naslednje pogoje:

- odvzem vzorcev naj se vrši na način, ki ne bo povzročil škode na jamskem inventarju,
- po opravljenih posegih je potrebno iz jame odstraniti vse morebitne pripomočke,
- po končanih raziskavah naj se z rezultati seznani naslovni zavod,
- prepovedano je kakršnokoli onesnaževanje jame,

Ocenjujemo, da predvideni način jemanja vzorcev ne bo ogrozil lastnosti naravne vrednote ob upoštevanju zgoraj navedenih pogojev.

Lepo pozdravljeni!

Pripravila:
Martina Stupar, univ.dipl.inž.geol.

Vodja OE:
Miriam Gorkič, univ.dipl.biol.

Zavod RS za varstvo narave, Ljubljana, Dunajska c. 5

V vednost: Agencija RS za okolje, Vojkova 1b, 1000 Ljubljana

Figure A.2 Request for sampling in Postojna Cave and permission obtained from Slovenian Ministry of Environment, the Institute of the Republic of Slovenia for Nature Conservation.

B. Appendix II

Photographs of investigated locations and sampling

Location 01 – Slonova glava	Lokacija 01 – Slonova glava

Figure B.1 Ceiling from where soda straw samples were taken

Slika B.1 Svod s kojega su uzeti uzorci slamčica

Figure B.2 Railway passes near the sampling place

Slika B.2 Tračnice turističkog vlaka u blizini lokacije uzorkovanja

Figure B.3 Sampling of a drip water and measurement of field parameters

Slika B.3 Skupljanje prokapne vode i mjerenje okolišnih uvjeta

Location 02 – Biospeleološka postaja

Lokacija 02 – Biospeleološka postaja

Figure B.4 Collection of drip water in narrow neck HDPE bottle

Slika B.4 Skupljanje vode u plastičnu HDPE bočicu uskog grla

Figure B.5 Sampling of drip water and measurement of field parameters. Logging of field data into sampling diary

Slika B.5 Sakupljanje prokapne vode i bilježenje uvjeta okoliša u dnevnik uzorkovanja

Figure B.6 Measurement of field parameters

Slika B.6 Mjerenje okolišnih uvjeta

Location 03 – Vodopad	Lokacija 03 – Vodopad

Figure B.7 Wind velocity measurement

Slika B 7 Mjerenje brzine vjetra

Figure B.8 Sampling of drip water and measurement of field parameters.

Slika B.8 Skupljanje prokapne vode i mjerenje okolišnih uvjeta

.

Location 04 – Kongresna dvorana	Lokacija 04 – Kongresna dvorana

Figure B.9 Location where a part of a stalactite has been sampled

Slika B.9 Mjesto na kojem je uzorkovan stalaktit

Location 05 – Podrti kapnik Lokacija 05 – Podrti kapnik

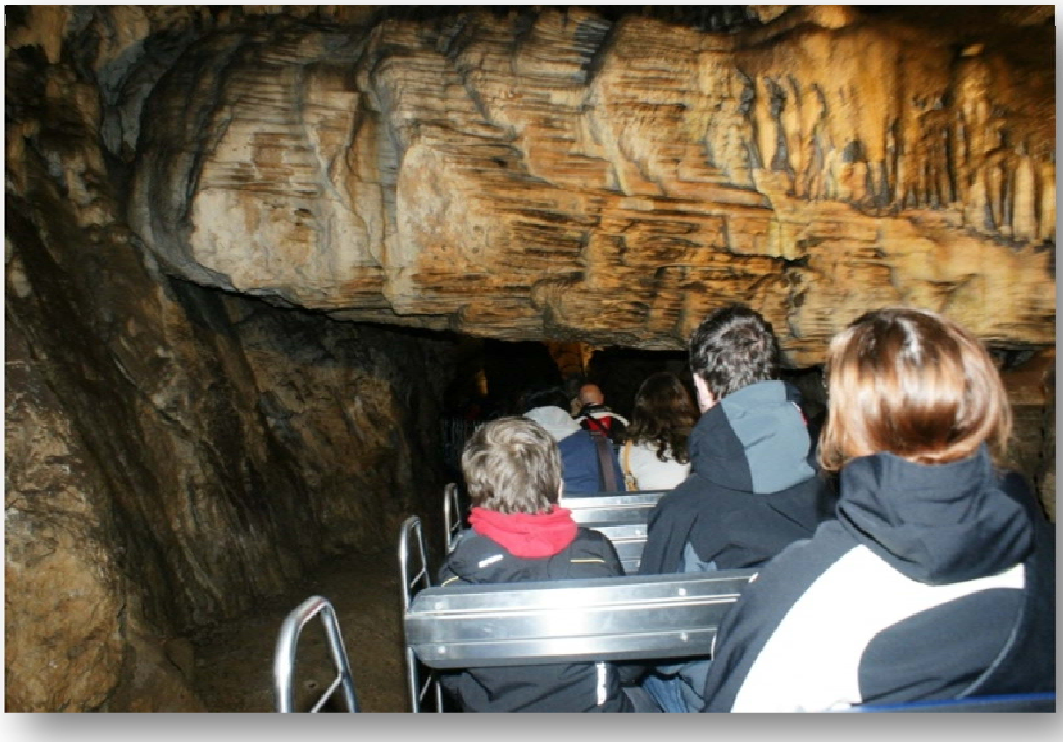

Figure B.10 Broken stalagmite location (view from the touristic train)

Slika B.10 Lokacija slomljeni stalagmit (pogled iz turističkog vlaka)

Figure B.11 Flowstone under which drip water has been collected (upper and left photo)

Slika B.11 Sigovina ispod koje je sakupljana prokapna voda (slika gore i desno)

Location 06 – Stebrišče	Lokacija 06 – Stebrišče

Figure B.12 Sampling location is isolated from direct air flow current

Slika B.12 Mjesto uzorkovanja je zaklonjeno od strujanja zraka

Figure B.13 Sampling of drip water

Slika B.13 Uzorkovanje prokapne vode

Location 07 – Čarobni vrt | Lokacija 07 – Čarobni vrt

Figure B.14 Steep entrance from the main passage in Velika Gora to Čarobni vrt

Slika B.14 Strmi put u Čarobni vrt

Figure B.15 Sampling of drip water for stable isotope analysis

Slika B.15 Uzorkovanje prokapne vode za izotopnu analizu

Figure B.16 In Čarobni vrt each stone is covered with precipitated carbonate

Slika B.16 U Čarobnom vrtu svaki kamen prekriven je istaloženim karbonatom

Location 07 – Čarobni vrt | Lokacija 07 – Čarobni vrt

Figure B.17 View to the Velika Gora from Čarobni vrt

Slika B.17 Pogled prema Velikoj Gori iz Čarobnog vrta

Figure B.18 From the sampling site in Čarobni vrt, going uphill, ceiling can be reached

Slika B.18 Krećući se od lokacije uzorkovanja uzbrdo možemo doći do dijela gdje se spajaju pod i strop

Location 08 – Vrh Velike gore | Lokacija 08 – Vrh Velike gore

Figure B.19 Sampling location on the top of the highest flowstone

Slika B.19 Lokacija uzorkovanja na vrhu najviše sigovine

Figure B.20 Drip water sampling. The cave wall is furred with precipitated carbonate

Slika B.20 Skupljanje prokapne vode. Vidljivo je da su zidovi lokacije obloženi nataloženim karbonatom

Figure B.21 Sampling of drip water for stable isotope analysis

Slika B.21 Uzorkovanje prokapne vode za analizu stabilnih izotopa

Location 09 – Zgornji Tartar

Lokacija 09 – Zgornji Tartar

Figure B.22 Broken ceiling, due to the Pivka River former flow

Slika B.22 Dio stropa se srušio zbog toka rijeke Pivke koji je u prošlosti bio drugačiji od današnjeg

Figure B.23 Ceiling is rich with stalactites and the floor is covered by precipitated carbonate

Slika B.23 Na stropu se nalaze stalaktiti, dok je pod prekriven istaloženim karbonatom

Location 10 - Pivka River inside

Lokacija 10 - Rijeka Pivka unutra

Figure B.24 From Tartar main passage to sampling location Pivka River inside

Slika B.24 Prolaz iz glavnog rova u Tartaru prema lokaciji Rijeka Pivka unutra

Location 11 - Pivka River outside	Lokacija 11 - Rijeka Pivka vani

Figure B.25 Sampling of Pivka River outside. Measurement of chemical parameters

Slika B.25 Uzorkovanje rijeke Pivke vani. Mjerenje kemijskih parametara

Cave surface cover and cave entrance	Tlo iznad špilje i ulaz u špilju

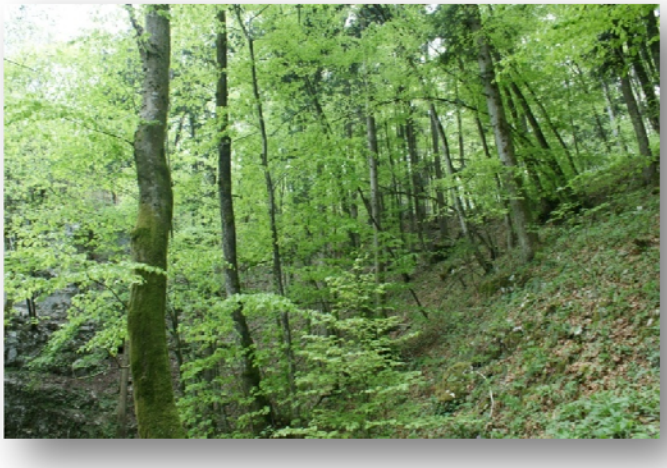

Figure B.26 Surface above the Postojna Cave is covered by forest

Slika B.26 Površina iznad Postojnske jame prekrivena je šumom

Figure B.27 Today's main entrance into the Postojna Cave

Slika B.27 Današnji glavni ulaz u Postojnsku jamu

Biography

Magda (born Lipovac) Mandić was born on 17th September 1975 in Postojna, Slovenia. She attended elementary and high school in Čabar, Croatia. In 1994 she started her study in the Faculty of Education at the University of Rijeka, direction - a professor of mathematics and physics. The study was completed 1999 by receiving the title of professor of mathematics and physics (the institution had been renamed into the Faculty of Arts). That same year she started working in primary and secondary schools in the Primorsko-goranska County. In 2004 she started to work at the Department of Physics, Faculty of Medicine, University of Rijeka, where she was assistant teacher. She worked at the newly established Laboratory for measurement of stable isotope. Scientific training and fellowship completed in the following laboratories:

- in Germany Umweltforschungzentrum Leipzig-Halle GmbH (UFG), where under the guidance of dr. Stefan Weise's learned about mass spectrometry and stable isotopes. Work with peripheral unit Gas bench. The training lasted one month.
- in Slovenia at the Jozef Stefan Institute, under the supervision of dr. Polona Vreča she learned basics of samples preparation for mass spectroscopy analysis.
- Accomplished two times two-week trainings in 2005 and 2007 in Austria Joanneum Research (2004), under the mentorship of dr. Albrecht Leis. The week-long visit to the lab. Learns about operational work in LIMS database.
- In Croatia, the Ruđer Bošković Institute (2004). The two-week visit. Learns about the radioactive isotopes and preparation of samples for their measurement.
- In Germany, Bremen, in Thermo Electron corporation. A week-long training (2006) about the use and maintaining of mass spectrometers
- In Austria, Vienna, (2007) Hydrological Laboratory in the IAEA under the mentorship of Dr. Manfred Gröning. Training on the use of mass spectroscopy and HDO equilibration unit lasted a month.
- Two-week training course organized by IAEA in Budva on the use of isotope techniques in hydrology (2007)
- Austria (2008) in the IAEA Hydrological laboratory under the mentorship of Dr. Manfred Gröning. Training on the use of mass spectroscopy and laser techniques in the determination of the concentration of stable isotopes
- In Postojna (2008, 2010, 2012), International School of karst, each in a period of one week.

In 2004 started post-graduate study of atomic and molecular physics and astrophysics at the Faculty of Science in Zagreb. From 2010 she has been employed at the Department of Physics at the University of Rijeka. She is married and mother of two sons.

Životopis

Magda (rođena Lipovac) Mandić rođena je 17. rujna 1975. godine u Postojni, Slovenija. Osnovnu školu i opću gimnaziju pohađala je u Čabru. Godine 1994. upisuje tadašnji Pedagoški fakultet Sveučilišta u Rijeci, smjer - professor matematike i fizike. Studij završava 1999. godine (institucija je u međuvremenu preimenovana u Filozofski fakultet) i stječe titulu profesora matematike i fizike. Iste godine počinje raditi u osnovnim i srednjim školama na području Primorsko-goranske županije. Godine 2004. zapošljava se na katedri za fiziku Medicinskog fakulteta Sveučilišta u Rijeci, gdje obavlja poslove asistenta i radi u novoosnovanom Laboratoriju za mjerenje stabilnih izotopa SILab. Znanstveno se usavršava u laboratorijima:

- u Njemačkoj na Umweltforschungzentrum Leipzig-Halle GmbH (UFZ), gdje pod vodstvom dr. Stefana Weise-a uči o spektrometriji masa stabilnih izotopa i radu s perifernom jedinicom Gas bench. Usavršavanje je trajalo mjesec dana.
- u Sloveniji na Institutu Jožef Štefan, pod mentorstvom dr. Polona Vreča uči osnove pripreme uzoraka za spektroskopiju masa. Dvotjedna usavršavanja 2005. i 2007. Godine.
- u Austriji na Joanneum Research (2004), pod mentorstvom dr. Albrechta Leisa. U jednotjednoj posjeti laboratoriju uči operativno raditi u LIMS bazi podataka.
- U Hrvatskoj na Institutu Ruđer Bošković (2004). u dvotjednom posjetu uči o radioaktivnim izotopima i pripremi uzoraka za njihovo mjerenje.
- U Njemačkoj u kompaniji koja proizvodi spektrometre masa Thermo Scientific. Jednotjedno usavršavanje (2006) o uporabi i održavaju spektrometara mase
- U Austriji (2007) u IAEA Hidrološkom laboratoriju pod mentorstvom dr. Manfreda Groeniga. Usavršavanje na temu spektroskopija masa i uporaba HDO jedinice za ekvilibraciju vode trajalo je mjesec dana.
- Dvotjedni tečaj pod organizacijom IAEA o uporabi izotopnih tehnika u hidrologiji (2007)
- U Austriji (2008) u IAEA Hidrološkom laboratoriju pod mentorstvom dr. Manfreda Groeniga. Usavršavanje na temu spektroskopija masa i uporabu laserskih tehnika u određivanju koncentracije stabilnih izotopa
- U Postojni (2008, 2010, 2012) Međunarodne škole krša, u trajanju od jednog tjedna

Godine 2004. upisuje poslijediplomski studij Atomske i molekularne fizike i astrofizike na Prirodoslovno-matematičkom fakultetu u Zagrebu. Od 2010. godine zaposlena je na Odjelu za fiziku Sveučilišta u Rijeci. Udana je i majka dvojice sinova.

Bibliography (from CROSBI)/ Bibliografija (iz CROSBI-ja)

Magda Mandić

(262141)

Chapter in book / Poglavlja u knjizi

1. Roller-Lutz, Zvjezdana; Mandić, Magda; Bojić, Diana; Lutz, Hans Otto; Kapelj, Sanja. Stable isotopes in Gacka river catchment: Installation of a laboratory for stable isotope analysis in Croatia // *Advances in Isotope Hydrology and its Role in Sustainable Water Resources Management (IHS-2007)* / IAEA (ur.). Beč : IAEA, 2007.. Str. 625-631.

Textbooks / Udžbenici i skripta

1. Dresto-Alač, Branka; Bojić, Diana; Cvejanović, Slobodan; Lekić, Andrica; Mandić, Magda; Žauhar, Gordana. Praktikum fizikalnih mjeranja . Rijeka : Medicinski fakultet, 2007..

Original scientific and review papers in CC journals / Izvorni znanstveni i pregledni radovi u CC časopisima

1. Surić, Maša; Roller-Lutz, Zvjezdana; Mandić, Magda; Krajcar Bronić, Ines; Juračić, Mladen. Modern C, O, and H isotope composition of speleothem and dripwater from Modrič Cave, eastern Adriatic coast (Croatia). // *International Journal of Speleology*. **39** (2010) , 2; 91-97

2. Mandić, Magda; Bojić, Diana; Roller-Lutz, Zvjezdana; Lutz, Hans O.; Krajcar Bronić, Ines. Note on the spring region of Gacka River (Croatia). // *Isotopes in Environmental and Health Studies*. **44** (2008) , 2; 201-208

3. Borojević Šoštarić, S., Palinkaš, A.L., Neubauer, F., Hurai, V., Cvetković, V., Roller-Lutz Z., Mandić, M, Genser, J.: Silver-base metal epithermal vein and listwanite hosted deposit Crnac, Rogozna Mts., Kosovo, Part II: A link between magmatic rocks and epithermal mineralization, structural and genetic ; Ore geology review. **50** (2013), 98–117

Under review:

Mandić, M., Mihevc, A., Leis, A., Krajcar Bronić, I.: Concentration of CO_2 and its $\delta^{13}C$ in cave air of Postojnska jama Cave, Slovenia," International Journal of Speleology; DOI: http://scholarcommons.usf.edu/cgi/editor.cgi xxxarticle

Scientific papers in other journals / Znanstveni radovi u drugim časopisima

1. Roller-Lutz, Zvjezdana; Mandić, Magda; Lutz, Hans Otto. Involving GLOBE Schools in Study of the Stable Isotope Composition of Precipitation in Croatia. // *Water & Enviroment News*. **24** (2008.) ; 18-19

Conference reports (abstracts) in other journals / Kongresno priopćenje (sažeci) u ostalim časopisima

1. Mandic, Magda; Takac, Danijela; Lutz, Hans Otto; Roller-Lutz, Zvjezdana. Stable isotope composition of precipitation in Croatia // *Geophysical Research Abstracts*. EGU General Assembly, 2008.

Other refereed conference papers / Drugi radovi u zbornicima skupova s recenzijom

1. Mandić, Magda; Bojić, Diana; Lutz, Hans Otto; Kapelj, Sanja; Roller-Lutz, Zvjezdana. Hrvatski laboratorij za analizu izotopnih omjera lakih elemenata (H, O, C, _) // *Hrvatske vode i Europska unija: izazovi i mogućnosti: zbornik radova (Croatian water and European Union: chalenges and possibilities : proceedings)* / Dragutin Gereš (ur.). Zagreb : Sveučilišna tiskara, 2007. 745-750

Abstracts in conference proceedings / Sažeci u zbornicima skupova

1. Mandić, Magda; Mihevc, Andrej; Leis, A.; Krajcar Bronić, I. Geochemical and stable isotope characterisation of drip water and modern carbonate from Postojna Cave, Slovenia // *daphne DFG-Forschergruppe 4th Workshop*, Abstract volume / Mangini, A. ; Spoetl, Ch. ; Scholtz, D. ; Immerhauser, A. (ur.). Heidelberg, Njemačka : daphne, 2012. 65-66

2. Mandić, Magda; Mihevc, Andrej; Leis, Albrecht; Krajcar Bronić, Ines. APPRAISAL OF ENVIRONMENTAL CONDITIONS IN POSTOJNA CAVE, SLOVENIA // *Karst forms and processes* / Mihevc, Andrej ; Gabovšek, Franci (ur.). Postojna : Karst Research Institute, Scientific Reasrch Centre of the Slovenian Academy of Science and Arts, 2012. 59-59

3. Mandić, Magda; Krajcar Bronić, Ines; Mihevc, Andrej; Leis, Albrecht. Isotopic signals from speleothems of Postojna cave, Slovenia // *18th international Karstological school "Classical Karst"* / Mihevc, Andrej ; Prelovšek, Mitja ; Zupan Hajna, Nadja (ur.). Postojna : Karst Reasrch Institute, Scientific Reasrch centre of Slovenian Academy of science and Arts, 2010. 44-44

4. Mandić, Magda; Krajcar Bronić, Ines; Mihevc, Andrej; Leis, Albrecht; Mandić, Luka. Influence of different physical conditions on stable isotopes of water and carbonates in Postojna Cave, Slovenia // *3rd daphne workshop*. Innsbruck, 2010. 70-70

5. Barešić, Jadranka; Horvatinčić, Nada; Roller-Lutz, Zvjezdana; Mandić, Magda. Delta 13C values of dissolved inorganic carbon in the Plitvice Lakes // *X Isotope Workshop of the European Society for the Isotope Research : Abstract Book*. Wroclaw : European Society for the Isotope Research and Laboratory of Isotope Geology and Geoecology, Institute of Geological Sciences, University of Wroclaw, 2009. 77-78

6. Borojević Šoštarić, Sibila; Palinkaš, Ladislav; Mandić, Magda; Roller-Lutz, Zvjezdana. Stable isotope study on carbonates of the epithermal Pb-Zn-Ag deposit Crnac, Kosovo // *X Isotope Workshop of the European Society for the Isotope Research : Abstract Book.*

Wroclaw : European Society for the Isotope Research and Laboratory of Isotope Geology and Geoecology, Institute of Geological Sciences, University of Wroclaw, 2009..2009. 83-84

7. Hunjak, Tamara; Mance, Diana; Mandić, Magda; Lutz, Hans O.; Roller-Lutz, Zvjezdana. Mjeriti delta δ^2H i $\delta^{18}O$ magnetskom ili laserskom spektroskopijom? // *Knjiga sažetaka 6. Znanstvenog sastanka Hrvatskog fizikalnog društva*. Zagreb, 2009. 172-172

8. Roller-Lutz, Zvjezdana; Lutz, Hans O.; Mance, Diana; Mandić, Magda; Hunjak, Tamara. Stable Isotope Composition of Precipitation in Croatia // *X Isotope Workshop of the European Society for the Isotope Research : Abstract Book*, Wroclaw: European Society for the Isotope Research and Laboratory of Isotope Geology and Geoecology, Institute of Geological Sciences, University of Wroclaw , 2009.. Zlotniki Lubanskie, Poljska, 2009. 119-120

9. Strmić Palinkaš, Sabina; Palinkaš, Ladislav; Mandić, Magda; Roller-Lutz, Zvjezdana; Maliqi, Gani. Oxygen and carbon isotope study of the Pb-Zn-Ag hydrothermal-replacement and skarn deposit Trepča, Kosovo // *X Isotope Workshop of the European Society for the Isotope Research : Abstract Book*, Wroclaw : European Society for the Isotope Research and Laboratory of Isotope Geology and Geoecology, Institute of Geological Sciences, University of Wroclaw , 2009..Zlotniki Lubanskie, Poljska, 2009. 125-126

10. Surić, Maša; Roller-Lutz, Zvjezdana; Mandić, Magda; Hoffmann, Dirk; Juračić, Mladen. Stable isotope records from Modrič Cave (Croatia) // *The Fifth International Conference Climate Change: The Karst Records, Abstract Volume* / Li, Hong-Chun (ur.). Chonqing, Kina : School of Geographical Sciences, Southwest University, Chongqing, 2008. 56

11. Bojić, Diana; Mandić, Magda; Roller-Lutz, Zvjezdana; Lutz, Hans O: Kapelj, Sanja; Horvatinčić, Nada; Krajcar Bronić, Ines; Sironić, Andreja. Isotopic composition of spring waters from Croatian karst regions: Gacka River area // *Proceedings of the European Society for Isotope Research : ESIR IX* / Tamas, Tudor (ur.). Cluj-Napoca : Cluj University Press, 2007. 9-9

12. Mandić, Magda; Roller-Lutz, Zvjezdana; Lutz, Hans Otto. Stimulating student's awareness of environmental matters through a new physics tool in the GLOBE program // *GIREP-EPEC Conference Frontiers of Physics Education : Abstracts*. Rijeka : Sveučilišna knjižnica, 2007. 90-90

13. Roller-Lutz, Zvjezdana; Mandić, Magda; Bojić, Diana; Lutz, Hans Otto; Kapelj, Sanja. Installation of a laboratory for stable isotope analysis in Croatia // *International Symposium on Advaces in Isotope Hydrology and its Role in Sustainable Water Resources Management : IHS-2007 : Book of Abstracts* / IAEA (ur.). Beč, 2007. 151/46-151/46